

ENERGY SYSTEMS AND CONTROL

BOOK OF PROJECTS | SPRING 2020

Abstract

We are extremely proud to present the book or projects for "Energy Systems and Controls". This course pursues an aggressive objective. It introduces fundamentals of systems & control and optimization within the context of energy systems applications.

The course content includes: (i) mathematical models, (ii) state estimation, (iii) optimization, (iv) machine learning, and (v) optimal control (e.g. dynamic programming).

The students engage in team projects, in which they must apply one or more fundamental areas to an energy systems application.

We organized this project book into thematic areas. We wish you a pleasant reading.

Prof. Scott Moura & Josh Bass

smoura@berkeley.edu, josh_bass@berkeley.edu

Table of Contents

Part I: Clean Energy Markets

- Optimization of the UAE energy portfolio - Team 2
(p. 3 – 25)
- Optimization of Microgrid Design for the Puerto Rico San Juan International Airport - Team 3
(p. 26 – 45)
- Optimal Sizing and Bids Scheduling of a Price-Maker Battery on a Nodal Wholesale Market - Team 4
(p. 46 – 63)
- Hybrid Plant Economic Dispatch - Team 6
(p. 64 – 82)
- Decarbonizing Port Ecosystems: Optimizing Energy Transitions - Team 8
(p. 83 – 127)
- Environmental and Economic Implications of Energy Storage in California - Team 10
(p. 128 – 153)

Part II: Electric Vehicles

- Total Cost of Ownership Optimization for Fleet Transformation from ICE to EV - Team 1
(p.154 – 199)
- Optimizing EV Charging Times to Minimize GHG Emissions & Ensure Distribution Grid Stability - Team 7
(p. 200 – 229)
- Optimal Location of EV Charging Stations - Team 9
(p. 230 – 273)
- Electrification Potential of Bus Routes in Boston - Team 11
(p. 274 – 291)
- Total Cost of Ownership Optimization for Fleet Transformation from ICE to EV - Team 12
(p. 292 – 327)

Part III: Building Energy

- The Design of a Model Predictive Control Algorithm for Smart Thermostats in Residential Buildings - Team 14
(p. 328 – 359)
- Energy Modeling for Early-stage Net Zero Energy House - Team 15
(p. 360 – 388)

Optimization of the UAE energy portfolio

Omar Alzaabi, Dyami Andrews, Luis Fernández, Priyaj Mehta, Xingyue Sun

1. Abstract

This project aimed to understand the impact of a carbon tax on the United Arab Emirates' energy portfolio in the year 2050 by developing a model separate from the current POLES model used in the UAE National Energy Strategy 2050. In this way, the model could give UAE officials greater insight into their options for affecting change in the country, with one of them being a carbon tax perhaps implemented in a fashion similar to that of the Baker-Schultz Plan. To do this, a model of the effect of a carbon tax on power generation resources according to their operational carbon emissions was developed in order to incentivize the development of a cleaner energy portfolio that balanced the UAE's economic needs as an oil-producing country and the world's need for carbon reduction. A convex optimization algorithm using CVX was then used to minimize the total cost of the system while taking into account economic constraints and current resources. The implementation of a carbon tax was found to be effective for high carbon taxes. Below the threshold of 137 \$/usd, a carbon tax was found to be ineffective.

2. Introduction

2.1 Motivation & Background

The United Arab Emirates Ministry of Energy and Industry recently published UAE national Energy Strategy 2050 [9], which indicates that the carbon emission will be reduced by 70% from the power generating process. In their energy portfolio of 2050 based on the POLES model [9], 44% power would be generated from renewable energy, 38% from gas, 12% from clean fossil and 6% from nuclear energy. However, this POLES model uses GDP as an input without a result as to how GDP would change based on the new energy portfolio. At the same time, this model lacks analysis on carbon pricing, falling oil production and technology innovation. Especially for a country whose economy depends so much on its ability to produce, use, and export oil, this presents quite a limitation to the efficacy of the POLES model in determining what might be an "optimal" power generation portfolio.

We therefore saw value in creating a separate model, built from different principles, with the goal of informing UAE energy strategy by showing the effect of applying a carbon tax at various strengths. In this way, we hope to empower UAE leadership to take stronger action towards decarbonization through the implementation of a carbon tax, with the recommendation that it be leveraged in a manner similar to a Baker-Schultz plan [5]. A key benefit that this approach would offer is some insight into risk asymmetry, that is, how the UAE's actions expose it to risk depending on world events and circumstances beyond its control. If, for example, the UAE fails to plan a path towards decarbonization and is forced to rapidly decarbonize without time to

prepare, we would expect the cost of this would be greater than the cost of planning for decarbonization more aggressively than is actually needed. Having a model that can accurately predict the costs incurred in these situations could have a profound effect on the degree to which UAE leaders push to decarbonize the nation's power generation portfolio.

2.2 Relevant Literature

The UAE's energy portfolio for now is mostly natural gas (56%), and heat oil (27%), with renewable electricity counting for 15% and coal for 2% of the mix [6]. Other energy sources are in their early stages of deployment. By 2050, the UAE aims to achieve 50% of energy mix from clean energy sources. Among all the different kinds of clean energy sources, solar is the most promising one, because UAE has some of the world's best solar resources. Hence, solar energy would be considered as one of the representatives of clean energy in this study [1]. Besides solar, other energy sources such as nuclear energy and wind will also play an important role in decarbonizing the energy portfolio. Nuclear power especially must be considered since the UAE is currently constructing new nuclear power plants and these are designed to be used for several decades, meaning they'll still be running in 2050 [6, 7].

The United Arab Emirates Ministry of Energy and Industry published the 2050 total energy demand projection in the MOEI 2019 Energy Report [3]. Electricity demand is changing with seasons. There is a high demand increasing between May and November, and a peak in August. Seasonal changes of power demand were analyzed in Abu Dhabi Water & Electricity Company (ADWEC) Statistical Report 2008-2012 (2013) [4]. This huge demand of electricity mainly is met by natural gas right now. Therefore, when there is carbon tax implementation on natural gas, this huge increase might encourage the development of clean energy [1].

Meanwhile, the cost of those energy sources is the main factor to consider when the policy is being made. In order to compare different energy sources of unequal life spans, project size, different capital cost, risk, return, and capacities, levelized cost of energy (LCOE) is considered as the unit cost for each technology [2]. The LCOE for various conventional and renewable energy generation technologies are analyzed in the Lazard's levelized cost energy analysis — version 13. 2019 [2]. It is worth noting that we use LCOE as a first approximation to the question of portfolio optimization, since it considers the entire lifetime of a project and does not meaningfully distinguish technologies with large capital expenses or operational expenses. We discuss this in greater depth in the discussion of our results.

The data for the LCOE of the considered technologies was found in studies that modeled the change in price of these technologies considering various publications and methods till the year 2050. This data had considerable variations in different publications because of the drastically evolving technologies and their significant price differences in a short period of time. These

different starting points used in the studies including different methods used resulted in the wide range of projections for the year 2050. Ultimately, projections published by government entities such as NREL were used wherever available. [10, 11, 12]

Research to find the ramp rates for the various technologies considered was conducted by looking through articles to find data of ramp rates with the units MW/hr. After looking through a significant number of sources it was apparent that this data was not easily available online. A reason this may be is due to “the confidential bidding processes of various market players” that do not disclose these values [13]. Data for the ramp rate of only Hydrogen Storage was found in an NREL study [14]. However, data for the response times of these technologies, with a unit of time were found relatively easily [15, 16]. Response time is the time required for a technology to react to a change in demand. Due to the non-availability of definitive ramp rate data, as a very crude assumption, it was assumed that the ramp rates for the technologies be adjusted relative to the available response time data considering the ramp rate for Hydrogen Storage as a reference.

2.3 Focus of This Study

In this study, UAE energy portfolio is optimized based on projected demand, energy sources and storage, and assumed carbon tax, using a convex programming model to minimize total cost (Including carbon tax). According to this optimization, policy could be made regarding a lower carbon emission and cost energy portfolio.

3. Technical Description

3.1 Methodology

In this study, the objective is to minimize the total cost of the energy portfolio, subject to a few constraints. Therefore, it is a typical optimization problem. Because the objective function is convex and all the constraints are convex, which results in a feasible convex set, it is reasonable to choose convex programming to solve this problem. Convex programming (using CVX) is very convenient to use in an optimization problem because it allows the user to obtain the global minimum results when there exists the local minimum. It is a unique minimum value.

A convex optimization problem has the form

$$\begin{aligned} & \text{Minimize } f(x) \\ & \text{Subject to } g_i(x) \leq 0, i = 1, \dots, m \\ & \quad a_j^T x = b_j, j = 1, \dots, l \end{aligned}$$

To be a convex problem, objective function must be convex. The inequality constraint functions must be convex for all $i=1, \dots, m$, the equality constraint functions must be affine for all $j=1, \dots, l$.

The proposed methodology of determining an optimized energy production portfolio requires an accurate modeling of economic power dispatch for a set of known and unknown parameters.

This section includes a discussion on the validity of the parameters and assumptions used, as well as important dynamics that are not included in the model.

The projected demand in the year 2050 was estimated by the Ministry of Energy and Industry to be 100 GW. This value may be taken at face value as the authors are presenting a critical analysis of the public energy strategy. The hourly power demand for the UAE could not be found online or in the literature. Instead the hourly demand for Saudi Arabia was used [17], due to its similar climate and consumer lifestyle. The power curve resembles a double-hump shape, a result of higher HVAC demand as the temperature rises which is then followed by a second, slightly smaller peak in the early evening. Ultimately, only the hourly demand data for Friday was used in this study as it showed the highest demand. The seasonal variation in demand in the Emirate of Abu Dhabi is dramatic. Peak loads in the coldest winter months are about half of the peak in the summer. This motivated the inclusion of compressed hydrogen due to recent analysis predicting it to likely become the first viable seasonal storage capability. Due to the availability of monthly demand data, the optimization can be run for the whole year of 2050, in order to capture seasonal dynamics.

3.2 Models

The objective function used in the optimization contains the LCOE or Levelized Cost of Storage (LCOS) for each power generation and storage method. Levelized cost is used to account for both capital and variable costs at once. Values from Lazard were used except for nuclear technology in which the following method was used to calculate LCOE [18].

$$LCOE_{nuclear} = \sum_{t=1}^n \left(\frac{I_t + M_t + F_t}{(1+r)^t} \right) / \sum_{t=1}^n \left(\frac{E_t^1}{(1+r)^t} \right)$$

Where M_t , are the maintenance costs per kW per year, F_t are the fuel costs per kW per year, I_t is the capital cost, r is the discount rate, n is the lifetime of the reactor, t is the year, and E_t^1 is the capacity factor. The top sum is split into two, the first being a sum of only capital costs during the construction period. All cost components used to calculate the LCOE of a current generation light water reactor (LWR) were taken from Lazard save for the capital cost, which is actually known in this case from cost figures of the four Barakah units recently completed or nearing completion in Abu Dhabi. The sixty-year lifetime of LWRs mean that the Korean-designed Barakah units are likely to still be in operation in 2050, and therefore were hard-coded into the optimal mix. The construction cost of the Barakah power plants is reported to be \$24.4 billion USD, however other reports indicate a cost of \$32 billion USD, which is used in this analysis as a conservative estimate. Both are considerably lower than Lazard capital cost estimates, which seems to be an indication that the positive Korean learning rate has carried over into the UAE project. Most nuclear enterprises around the world have exhibited negative learning [19]. Cost assumptions can be found in Table 1.

Table 1. Nuclear LCOE cost assumptions.

	M_t	F_t	I_t	E_t^1	r	n	Construction time
Barakah (LWR)	155.44	0.009	5714	0.9	3%	65	5 years
UC Berkeley Mk1 FHR (Advanced Nuclear) [20]	155.44	0.0135	4507	0.9	2%	65	5 years

The UC Berkeley Mk1 fluoride-salt-cooled high temperature reactor (UCB Mk1 FHR) was chosen as a candidate advanced nuclear reactor technology [20]. Salt-cooled reactors are advantageous due to layers of passive safety mechanisms. The construction cost of twelve 100 MW FHR units is estimated to be \$5,408,877,325 USD. A slightly lower discount rate was assumed to crudely account for the improved economics of smaller unit sizes compared to 1000 MW LWRs. This is a result of the technology risk reduction for subsequent units once the first unit has been constructed and demonstrated successfully. The cost of fuel is assumed to be 1.5 times the cost of conventional fuel due to higher enrichment and the use of a novel form of pebble fuel. Decommissioning costs were not accounted for in this study.

In this study, the model is a compact convex program as follows.

$$\text{minimize } f(g, e) = \sum_i \sum_j (Cg_i + Ctax_i) * g_{i,j} + \gamma * emiss_{i,j} + \sum_i Cs_i * max_j(e_{i,j})$$

s.t.

$$\begin{aligned}
p_j &\geq D_j \\
p_j &\leq \sum_i g_{i,j} a_{i,j} + \sum_i Id_{i,j} - \sum_i Ic_{i,j} \\
e_{i,j} &= e_{i,j-1} + Ic_{i,j} - Id_{i,j} \\
|g_{i,j} - g_{i,j-1}| &\leq Rg_i \\
|Ic_{i,j} - Ic_{i,j-1}| &\leq Rs_i \\
|Id_{i,j} - Id_{i,j-1}| &\leq Rs_i \\
e_{i,j} &\geq 0, \quad Id_{i,j} \geq 0, \quad Ic_{i,j} \geq 0, \quad g_{i,j} \geq 0 \\
e_{i,1} &= 0, \quad Id_{i,1} = Ic_{i,1} = 0
\end{aligned}$$

Variable Definitions:

i index indicates the energy system type, j index indicates the time step.

C_g : leveled cost of energy for each generation source

C_{tax} : carbon tax associated with each energy source

C_s : leveled cost of energy for each storage type

g : individual generation for each power source

e : energy stored in each storage type

γ : weighting term for emissions

$emiss$: emissions from each power source

p : total power generation.

D : energy demand.

a : indicates the availability for each power source.

I_d : energy discharged from storage for each storage type

I_c : energy charged into storage for each storage type

R_g : ramping capacity of each generation source

R_s : ramping capacity of each storage source

In order to simplify the model and also because getting data for the existing transmission network in the UAE proved to be quite difficult, the grid was treated as a lossless, one-node system where the only concern was meeting load. While we recognize that this approach limits the applicability of this model's results to actual policy decisions, we believe it is a reasonable concession given our position without full access to data such as would be necessary to intelligently model the grid. Despite this limitation, we believe the overall model still gives enough insight into the effects of a carbon tax to be of some use.

The carbon tax model is a simple linear relation that applies a cost based on how much carbon is emitted by a given source. For simplicity, a power source's carbon emissions in tonnes per kWh of energy are first found from our sources, then combined with the carbon tax value to give an effective tax cost for each source in \$/kWh. In this way each resource is acted upon by the carbon tax in proportion to its carbon output while still giving us a convenient way to write a cost function for the purposes of optimization. Mathematically, we represent the hourly cost of this carbon tax as

$$Cost_{carbon}(\frac{\$}{hr}) = T_{rate}(\frac{\$}{tonne}) * E_{carbon}(\frac{tonne}{kWh}) * s_{gen}(kW),$$

where T_{rate} is the carbon tax rate set by the user, E_{carbon} is the equivalent amount of CO₂ emitted per kWh of energy generated by a resource, and s_{gen} is the apparent power generated by a resource in kW during that time interval of one hour.

We also considered ramping rates by imposing constraints on each generation/storage resource that it could only change production by some maximum magnitude, in MW/hour, between time steps either due to natural constraints of the technology (mechanical wear, reaction rate limits, etc) or due to industry-imposed ramping rates that are put in place to help maintain grid stability (such as for solar power). Initially this was attempted with a linear relation between ramping rate

and installed power capacity, such that aggregate ramping rate across the entire UAE grid would vary based on the total installed capacity.

$$R_i(\max_j(g_{i,j})) = \beta_i * \max_j(g_{i,j})$$

Unfortunately we were not able to reconcile this common-sense approach with CVX's requirements, so we simplified the ramping rate to just a constant value.

$$R_i = \beta_i$$

3.3 Results

Plots of our results are presented here with some explanation of their significance, for further discussion and explanation of the trends seen in the next section of this report. In Figures 1 and 2, we get a look at the response of the energy mix as carbon tax increases through its full range of values. We see that the market does not respond effectively to the carbon tax until a threshold is met, at which point emissions decrease sharply and costs begin to level off.

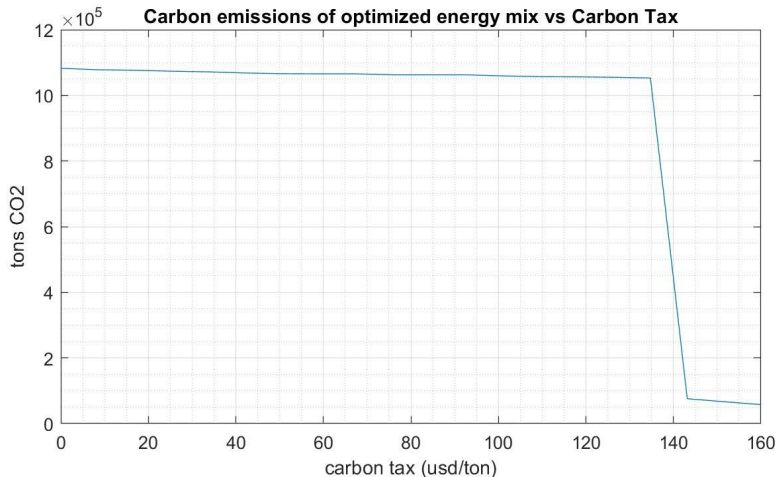


Figure 1. Carbon emissions of optimized energy mix vs. carbon tax.

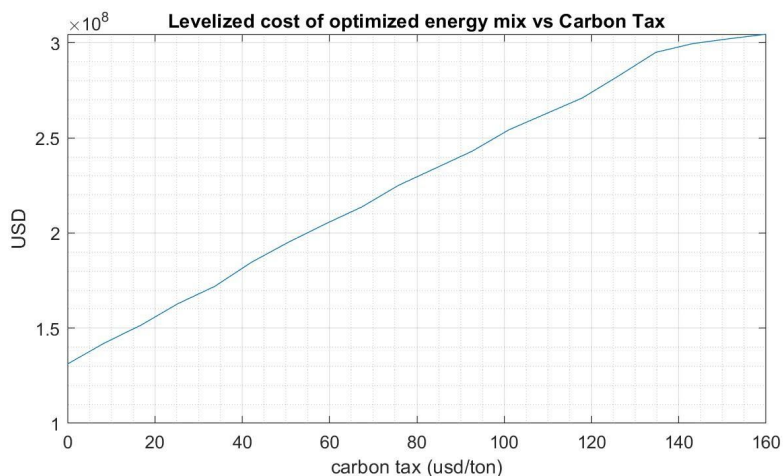


Figure 2. Levelized cost of optimized energy mix vs carbon tax.

Figures 3 and 4 present the same data as Figures 1 and 2 but zoomed in to give a better idea of the small-scale responses of both carbon emissions and total cost. Here we see that cost (Figure 4) does not behave quite as linearly as it seemed to in Figure 2.

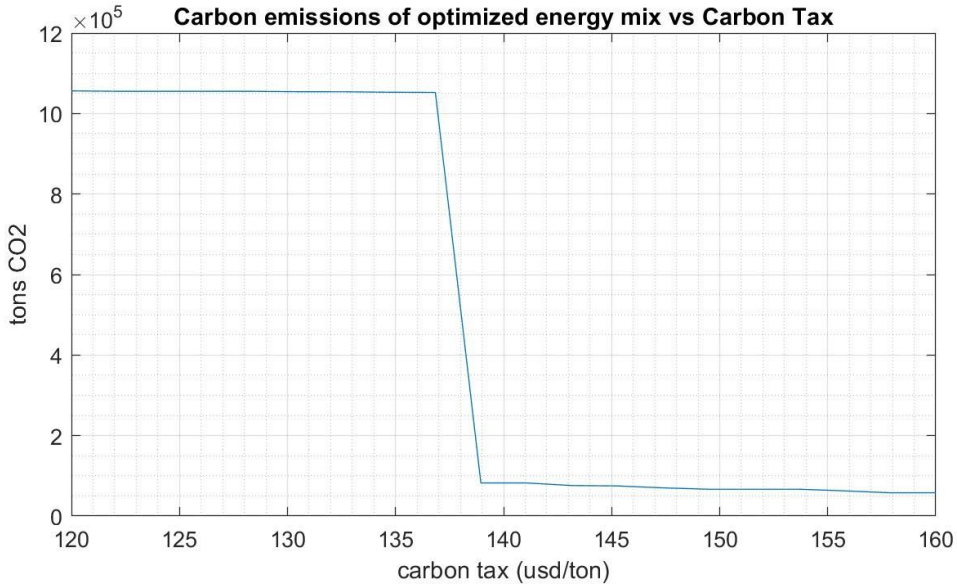


Figure 3. Carbon emissions of optimized energy mix vs carbon tax (zoomed in version).

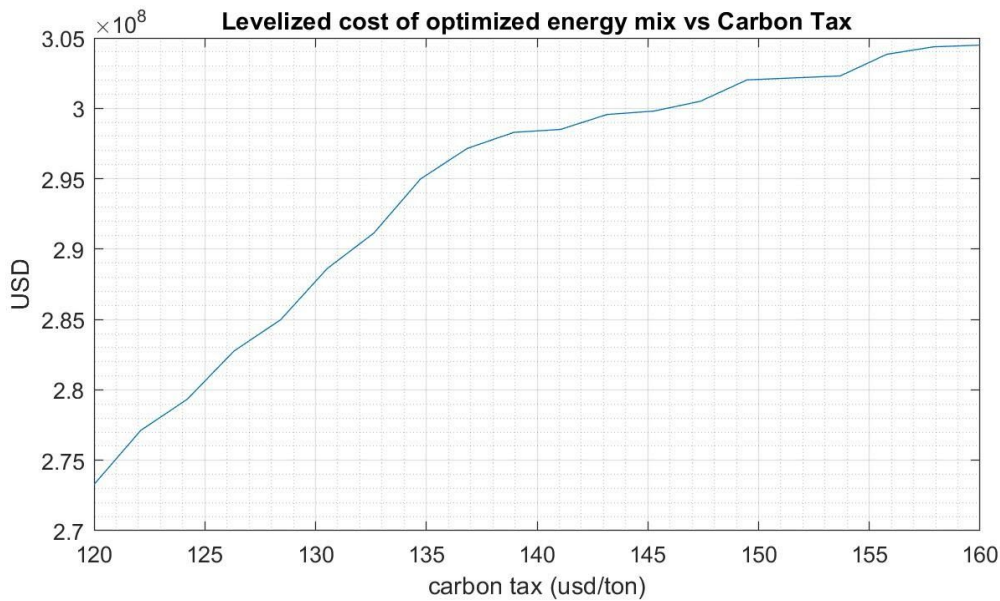


Figure 4. Levelized cost of optimized energy mix vs carbon tax (zoomed in version).

Figures 5-12 show the various generation and storage mixes that arise at different carbon tax intensities. Figures 5 & 6 show the results that would likely occur under no taxation, Figures 7 & 8 show the results that would occur just *before* the threshold at which the tax becomes truly effective, Figures 9 & 10 show the results right after this threshold, and Figures 11 & 12 help to illustrate the diminishing returns on the effect of the carbon tax past this point by applying an astronomical 200 \$/ton tax.

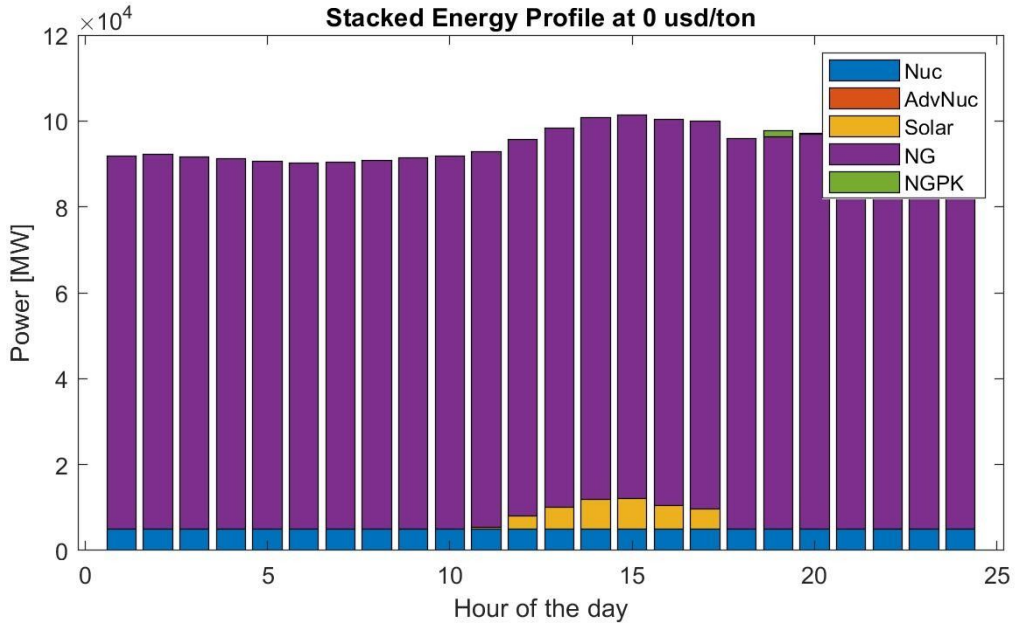


Figure 5. Energy portfolio without carbon tax.

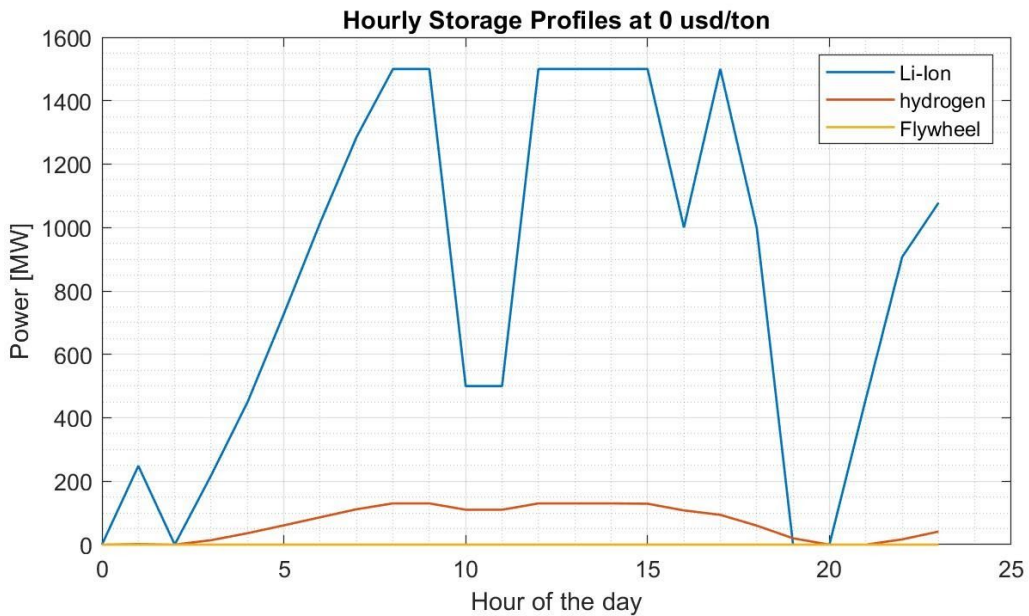


Figure 6. Hourly storage in a day without carbon tax.

Here we see that storage has increased by roughly two orders of magnitude, but our power generation mix is still largely natural gas.

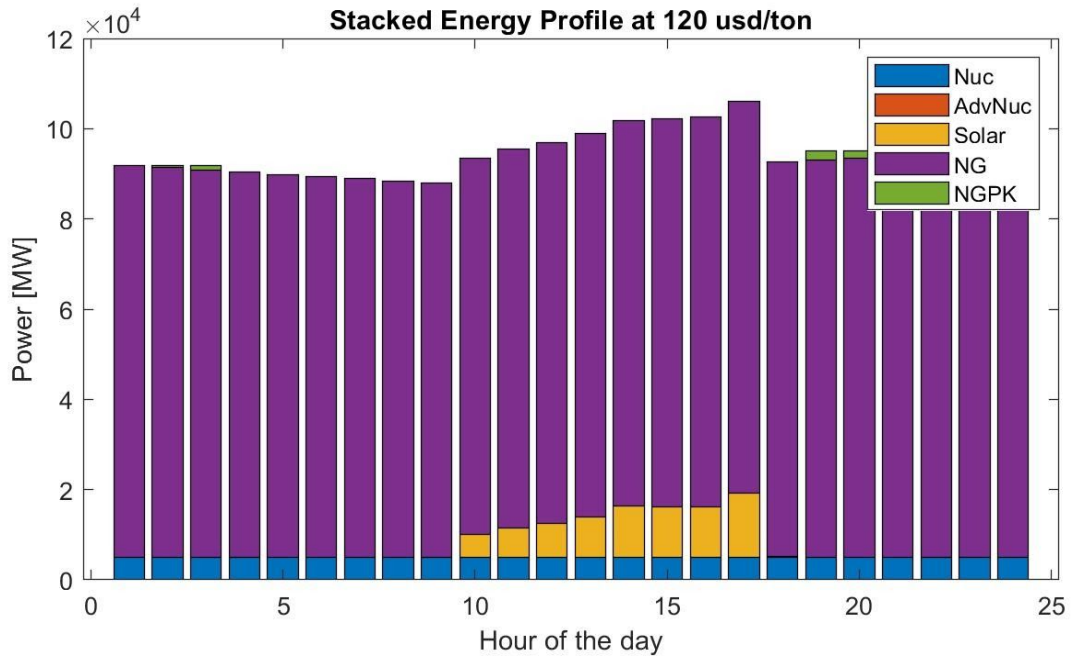


Figure 7. Energy portfolio with \$120/ton carbon tax.

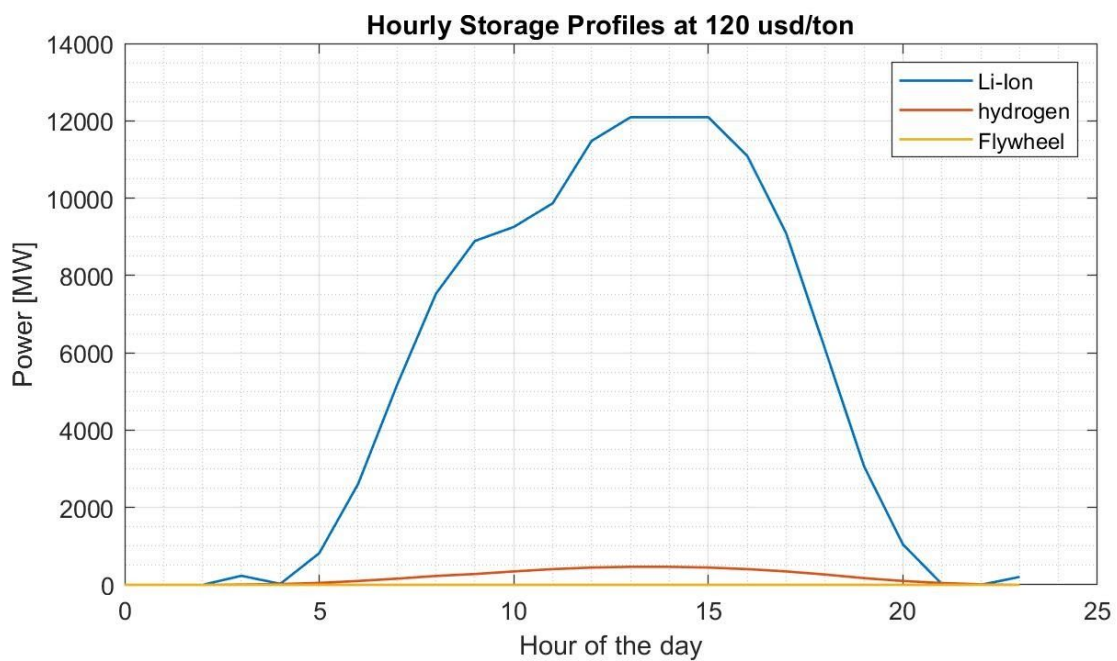


Figure 8. Hourly storage in a day with \$120/ton carbon tax.

Here storage has not changed very much when compared to the last profile, but the generation portfolio underwent a drastic change in composition, with Advanced Nuclear now taking the lead in power generation.

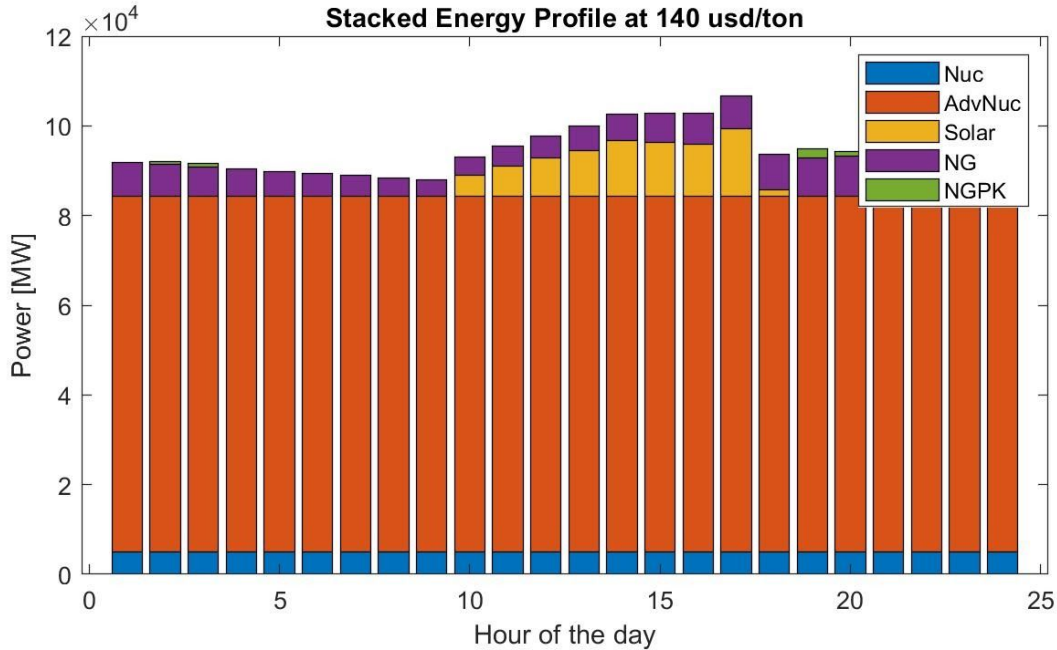


Figure 9. Energy portfolio with \$140/ton carbon tax.

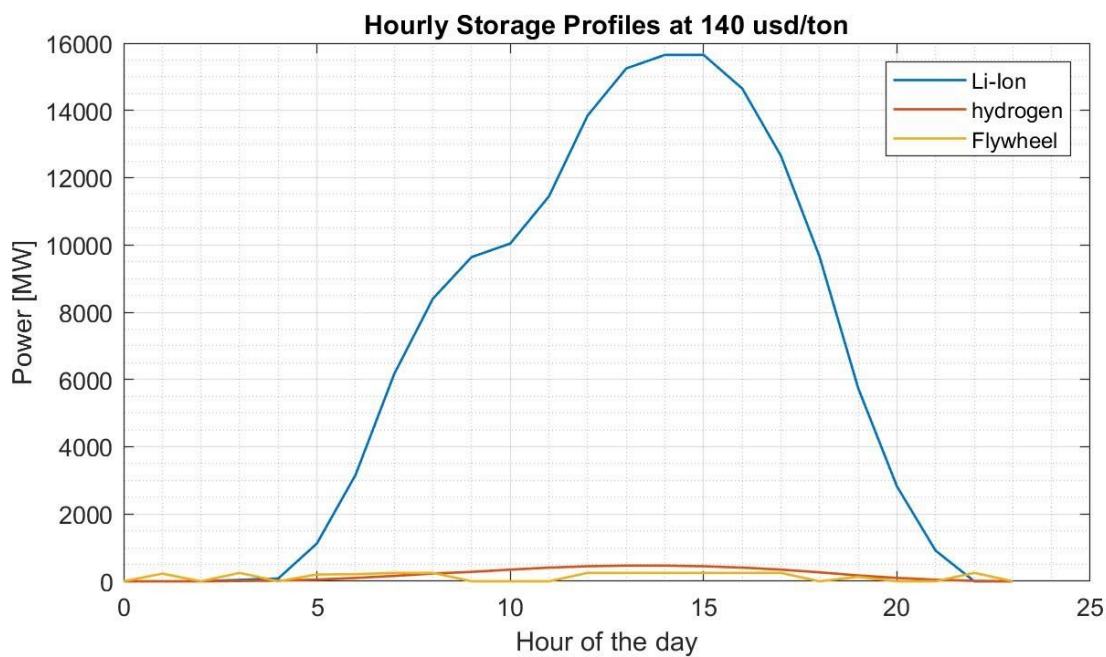


Figure 10. Hourly storage in a day with \$140/ton carbon tax.

Here we see some decrease in the amount of natural gas peakers and in overall natural gas power generation which is supplanted by a sizable increase of about 30-35% in the power capacity of the storage portfolio.

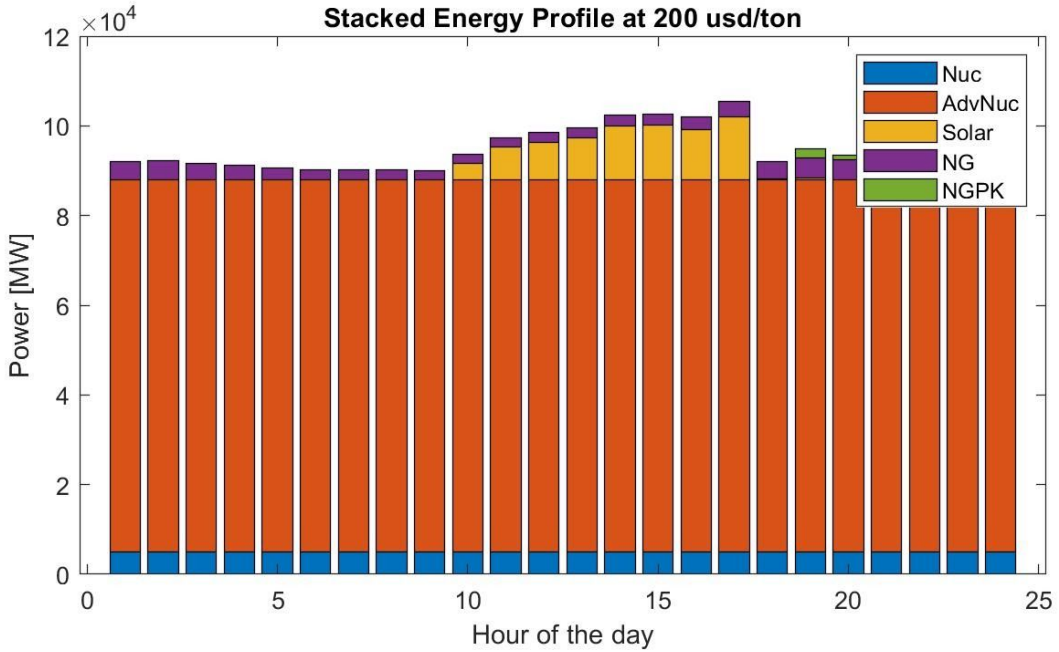


Figure 11. Energy portfolio with \$200/ton carbon tax.

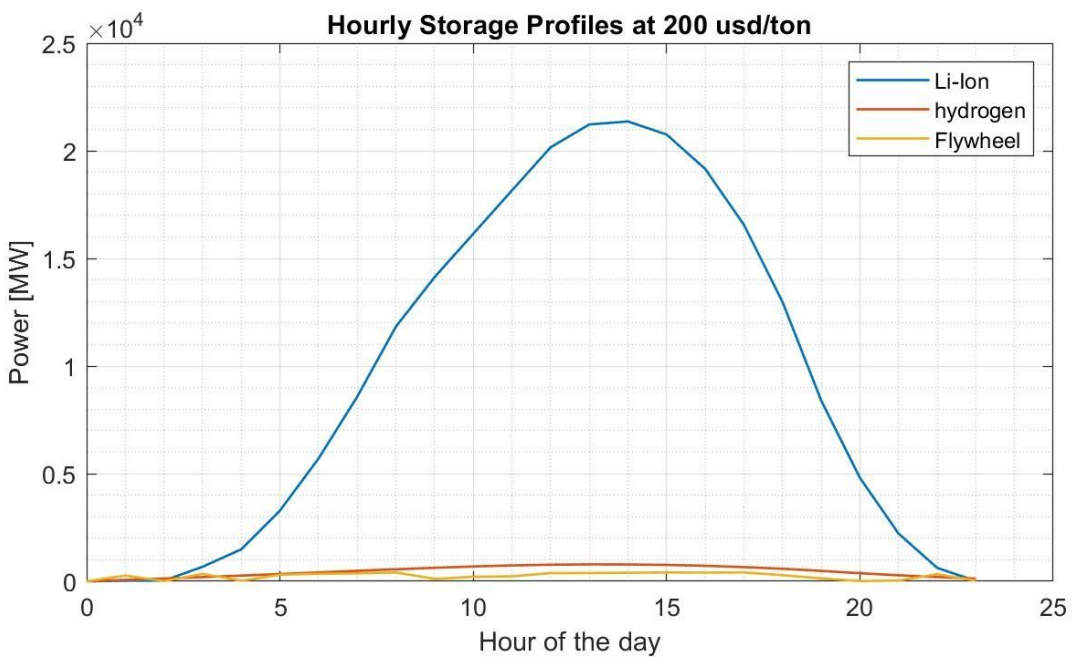


Figure 12. Hourly storage in a day with \$200/ton carbon tax.

4. Discussion

This project aimed to create a program to simulate the effects of a carbon tax through considering a series of cost-optimized energy mixes for the UAE. Our results effectively show the variation of energy sourcing based on different carbon tax scenarios. Ultimately, introducing a carbon tax less than 137 \$/ton (figures 1 & 3), we do not see shifts away from the use of natural gas generation. Figures 3 and 4 show the high resolution changes of cost and carbon production as carbon tax is varied. At a carbon tax of around 137 \$/ton, there is an abrupt shift to prioritizing advanced nuclear power. Past the 137 \$/ton point, we do not see much shift in carbon emissions, and the price has a reduced slope. While the 137 \$/ton point might not be perfectly accurate, there is likely a point at which a carbon tax will punish emissions enough to influence a drastic shift in energy production. Compared to today's norms of a 20 \$/ton carbon tax, a near 7 times increase in carbon tax might seem outlandish. To provide some perspective, at the calculated shifting point, the total price is increased by 225% by the carbon tax (Figure 1). An interesting outcome of the drastic shift in energy generation that we see at the 137 \$/ton point is that a low commitment carbon tax will have little to no effect on carbon output. The only means of creating large impacts is to commit fully to the incentive, otherwise the only effect will be to increase the cost of electricity.

While these initial results are slightly discouraging, we must also consider the potential changes in the energy market in the coming 30 years. We did consider the developing technology of advanced nuclear power, but aside from that most of our values were based in today's technology. It is entirely possible that in three decades, the price of solar further decreases, or other unforeseen technological developments occur. Additionally, changes in global opinion on the importance of climate change could influence what a 'reasonable' carbon tax is. Through tariffs or other means, the UAE could see an increased operational cost associated with their use even if they do not directly tax their combined cycle plants. Further investigation must be undertaken to determine a price ceiling beyond which natural gas is unfavorable.

Our approach to energy storage was effective but inherently flawed. We know that the energy storage portfolio optimization works because it initially chose to allocate most of the storage capacity to the resource with the lowest LCOE: Hydrogen storage. While hydrogen storage may indeed have a low LCOE compared to the other storage strategies we considered, Lithium-Ion batteries and Flywheels, it is a technology that is very expensive for short-term storage durations and needs longer storage durations to actually become economically viable. As we were working with a day-scale for our optimization, we artificially imposed a restricted ramping rate on hydrogen storage to produce more realistic results.

Ramping rates were actually implemented effectively as exponential rates due to the structure of the constraints as can be seen in the optimization model. These constraints are not necessarily

incorrect however ramping rate data is usually available as linear rates, while the results of the optimization showed generally expected trends, the actual values are unlikely to represent accurate results. The ramping rate constraints should be corrected in order to more easily be used. Further, typically such storage devices also have some lag or response time before they can start discharging or charging power. This model assumes a perfect prediction of and execution of power demands.

Storage cost information was especially challenging to find. The candidate power storage devices included in the optimization are lithium ion batteries, flywheels, and compressed hydrogen. The expected dynamics were to see a minimal and significant contribution from flywheels and lithium batteries observed at an hourly resolution and compressed hydrogen storage charged during the winter months and discharged over the summer. Incomplete and inaccurate data most likely prevented these trends to manifest themselves for a one-day simulation. Therefore, a year-long optimization was not attempted.

Future improvement of this model should also consider a broader range of realistic power generation and energy storage technologies. For example, geothermal energy and biomass are promising clean energy to investigate in the future. Furthermore, sensitivity analyses should be performed on the different variables, like carbon tax, to see their impact on the convex programming model and give policymakers a better idea of what levers they can pull to affect change. Also, it would be better to include the price variability of those energy technologies because the oil market is relatively turbulent. The price in the energy market changes as the economy changes with time. In the long run, the energy portfolio should be able to keep the total cost as stable as possible in order to provide people a consistent power supply. The relationship between carbon credit and Gross Domestic Product (GDP) could be done in a more specific analysis, which requires more data on the existing economic phenomena.

5. Table of Responsibilities

Team Member	Contribution
Omar Alzaabi	<ul style="list-style-type: none"> -Team Leader -Development of optimization algorithm -Obtaining demand data from UAE agencies -Obtaining UAE energy proposals
Dyami Andrews	<ul style="list-style-type: none"> -Research into lifetime carbon emissions and leveled costs of technologies considered -Development of optimization algorithm
Luis Fernández	<ul style="list-style-type: none"> -Development of carbon tax cost model

	-Research into lifetime carbon emissions and leveled costs of technologies considered
Priyaj Mehta	-Development of optimization algorithm -Research into the ramping rates and response times of technologies considered
Xingyue Sun	-Development of optimization algorithm -Research into the integration of ramping rates in optimization

6. Summary

In summary, This project aimed to determine the effects that a carbon tax would have on the energy mix in the UAE. Through this analysis we hoped to gain insights on optimal carbon tax values, and GDP effects. While the GDP effects remain nebulous and difficult to calculate, this project was successful in producing results regarding suggested carbon taxes. Our results show that without a decently high carbon tax (137 \$/ton), the optimal choice will include a majority of natural gas combined cycle generation. This results in essence condemns low commitment carbon taxes as having little effect other than increasing the cost of energy generation. There is more investigation to be done, regarding more nuanced ramping rates, and consideration of other generation sources, but this project shows interesting results despite these areas of improvement.

References

- [1] Mongird, K.; Viswanathan, V.; Balducci, P.; Alam, J.; Fotedar, V.; Koritarov, V.; Hadjerioua, B. Energy Storage Technology and Cost Characterization Report. July 2019.
- [2] "Lazard's Levelized Cost of Energy Analysis," Version 13. Nov 2019.
- [3] MOEI 2019 Energy Report
- [4] Abu Dhabi Water & Electricity Company. (2013). ADWEC Statistical Report 2008-2012.
- [5] "Our Plan," Climate Leadership Council. [Online]. Available: <https://clcouncil.org/our-plan/>
- [6] "UAE State of Energy Report 2019," United Arab Emirates Ministry of Energy and Technology. Technical Report.
- [7] Mahmoud Habboush, "Arab World's First Nuclear Reactor Cleared for Startup," Bloomberg Business. Feb 2020. [Online]. Available: <https://www.bloomberg.com/news/articles/2020-02-17/atomic-arabia-u-a-e-reactor-passes-final-hurdle-to-startup>
- [8] "Renewable Energy Prospects: United Arab Emirates," International Renewable Energy Agency. Technical Report. Apr 2015.
- [9] "UAE National Energy Strategy 2050," United Arab Emirates Ministry of Energy and Industry. Presentation slide deck.
- [10] Cole, Wesley, and A. Will Frazier. 2019. Cost Projections for Utility-Scale Battery Storage. Golden, CO: National Renewable Energy Laboratory. NREL/TP-6A20-73222. <https://www.nrel.gov/docs/fy19osti/73222.pdf>.
- [11] D. Steward, G. Saur, M. Penev, and T. Ramsden. Life Cycle Cost Analysis of Hydrogen Versus Other Technologies for Electrical Energy Storage. NREL/TP-560-46719 November 2009. [Online]. Available: <http://www.osti.gov/bridge>
- [12] Oliver Schmidt^{1,2,5,*}, Sylvain Melchior³, Adam Hawkes⁴ and Iain Staffell. Projecting the Future Levelized Cost of Electricity Storage Technologies. January 2019. [Online]. Available: <https://doi.org/10.1016/j.joule.2018.12.008>
- [13] ResearchGate Forum: What is the typical MW/minute ramping capability for each type of reserve? Accessed May 2020. [Online] Available: https://www.researchgate.net/post/What_is_the_typical_MW_minute_ramping_capability_for_each_type_of_reserve
- [14] J. Eichman, K. Harrison, and M. Peters, National Renewable Energy Laboratory. Novel Electrolyzer Applications: Providing More Than Just Hydrogen. NREL/TP-5400-61758 September 2014.
- [15] U.S. Department of Energy, Office of Electricity Delivery and Energy Reliability. Electric Power Industry Needs for Grid-Scale Storage Applications. Accessed May 2020. [Online]. Available: https://www.energy.gov/sites/prod/files/oeprod/DocumentsandMedia/Utility_12-30-10_FINAL_lowres.pdf
- [16] Mustafa E. Amiryar * and Keith R. Pullen *, A Review of Flywheel Energy Storage System

Technologies and Their Applications. MDPI. March 2017

[17] Alshahrani, Jubran, and Peter Boait. "Reducing High Energy Demand Associated with Air-Conditioning Needs in Saudi Arabia." *Energies* 12.1 (2019): 87.

[18] Ray, D. "Lazard's Levelized Cost of Energy Analysis—Version 13.0." *Lazard: New York, NY, USA* (2019): 20.

[19] Lovering, Jessica R., Arthur Yip, and Ted Nordhaus. "Historical construction costs of global nuclear power reactors." *Energy Policy* 91 (2016): 371-382.

[20] Andreades, C., and P. F. Peterson. "Mk1 Pebble-Bed Fluoride-Salt-Cooled High-Temperature Reactor Capital Cost Estimation." *Transactions of the American Nuclear Society* 113 (2015).

Appendix

1 Main Code

```
1 %% CE 295 - Energy Systems and Control
2 % Final Project: Group 2
3 % Team Leader: Omar Ashraf Alzaabi
4 % Prof. Scott Moura
5
6 clear all
7 close all
8 fs = 15; % Font Size for plots
9 %% CALCULATIONS
10 consumption_2017=129539; % GWh assume 100% combined cycle natural
    gas
11 demand_2017=consumption_2017/24/365;
12 demand_2050=100; % GW according to MOEI 2019 Energy Report
13
14 % seasonal changes of power demand [GWh]
15 seasonal_abudhabi={[1:12],...
16     [1600 1500 1800 2250 2550 2600 3100 3100 3000 2750 2200 2000]};
17 seasonal_normalized=seasonal_abudhabi;
18 % normalize seasonal variation curve
19 seasonal_normalized{2}=seasonal_abudhabi{2}/max(seasonal_abudhabi
    {2});
20 %Abu Dhabi Water & Electricity Company. (2013). ADWEC Statistical
    Report 2008-2012.
21
22 hourly_demand_summer_ksa={[0:23],...
23     [51 51 51 50 50 48 46 46 47.5 50 52 53 54 55.5 55.5 54.5 54 ...
24     52.5 54.5 54.5 53.5 52.5 51.5 51]}; 
25
26 hourly_demand_winter_ksa={[0:23],...
27     [28 27 26 25.5 25 25 26.5 25.5 24.5 25.5 26.5 27 27.5 28 28 ...
28     28.5 28.3 29 32 31 31 30.5 30 29]}; 
29 hourly_summer_shape=hourly_demand_summer_ksa{2}/max(
    hourly_demand_summer_ksa{2});
30 hourly_winter_shape=hourly_demand_winter_ksa{2}/max(
    hourly_demand_winter_ksa{2});
31 %% DATA
32 current_load=demand_2017;% GW assume all natural gas combined cycle
33 future_load=100; % GW
34 future_seasonal_load={[1:12],seasonal_normalized{2}*future_load}; %
    GW
35 nuclear_supply=5.600; %GW
36 summer_hourly_load=hourly_summer_shape*future_load;
37 winter_hourly_load=hourly_summer_shape*future_load/2;
```

```

38
39 %%Parameters
40
41
42
43 % l_j^S: Apparent power consumption [MVA]
44 l_S = summer_hourly_load*1000; %convert GW to MW
45
46 % c_j: Marginal generation cost [USD/MW]
47 cg = [168.7 % Conventional nuclear
48       120.3 % Advanced nuclear
49       40 % Solar
50       50 % Combined Cycle NG
51       200 % Gas Peaking
52     ];
53
54 % cost of storage
55 cs = [150 %li-ion
56       100 % hydrogen (seasonal storage)
57       500]; %flywheel
58
59 co2permwh=[0, 0, 0, 0.51,0.81]; %c02 emissions tons/per mwh,
60 rampdc = [500
61           10
62           5000000];
63 rampc = rampdc;
64
65 capacity = ones(24,length(cg));
66 capacity(:,3) =
67   [0,0,0,0,0,0,0.1,0.2,0.3,0.6,0.8,0.9,1,0.9,0.8,0.6,0.3, ...
68    0.2,0.1,0,0,0,0]; %hourly solar capacity
69
70 ramp = [0,0,120000,500,2100];%
71 % s_j,max: Maximal generating power [MW]
72 s_max = ones(24,length(cg))*max(l_S);
73
74 %% Problem 1
75
76 %% Plot active and reactive power consumption
77 figure(1);
78 bar(0:length(l_S)-1, [l_S]);
79 legend('UAE daily power consumption in the year 2050 [MW]', ...
80        'Location', 'southoutside')
81 xlabel('hour of day')
82 ylim([min(l_S)-1000 max(l_S)])
83 %% Problem 2
84
85 %% Assumptions:
86 %% - Disregard the entire network diagram
87 %% - Balance supply and demand, without any network considerations
88 %% - Goal is to minimize generation costs, given by c^T s
89 mult = linspace(6,8,20);
90 [trash,len] = size(mult);
91 count=1;
92 totalcosthourly=zeros(len,24);
93 totalcost=zeros(len,1);
94 totalemissionshourly=zeros(len,24);

```

```

94 totalemissions=zeros(len,1);
95 tt=0:23;
96 % Solve with CVX
97 countf = 1
98
99 for iii = 1:+1:len
100 ct = 20*mult(iii); % carbon tax usd/ton
101 %ct = ctlbs * 2.205/2000 %convert to usd/kg
102 carbon_tax= co2permwh*ct; %[0, 0, 0, 80, 140];
103
104 for gamma=0
105 cvx_begin
106     variables p(24) s(24,length(cg)) k(24,length(cs)) l(24,
length(cs)) e(24,length(cs))% declare your optimization
variables here
107         minimize(sum(cg' * s' +carbon_tax*s'+gamma*(co2permwh*s'))+
sum(cs'* max(e)')) % objective function here
108         subject to % constraints
109             % k: discharge
110             % l: charge
111             % e: energy stored
112             % Loop over each node
113             % remember to change objective fn . cs*max(e)
114             for jj = 1:length(l_S)
115                 for ii = 1:length(cg)
116                     % Balance power generation with power
consumption
117                     p(jj) >= l_S(jj)
118                     p(jj) <= sum(s(jj,:).*capacity(jj,:)) + sum(k(
jj,:)) - sum(l(jj,:))
119
120                     %e(jj) == sum(l(1:jj,:))-sum(k(1:jj,:));
121                     if jj >1
122                         e(jj,:) == e(jj-1,:) + l(jj,:) - k(jj,:)
123                     else
124                         e(1,:) == 0
125                         k(1,:) == 0
126                     end
127
128                     k(2,:) == 0
129
130
131                     k(jj,:) >= 0
132                     l(jj,:) >= 0
133 %                     k(jj,:) <= rampdc.*sum(e)/24
134 %                     l(jj,:) <= rampc.*sum(e)/24
135
136                     e(jj,:) >= 0
137 % Non-negative power generation
138                     p(jj) >= 0
139 % Non-negative power production
140                     s(jj,1:5) >= 0
141
142                     s(jj,1) >= 5600*0.9
143                     s(jj,4) >= max(s(:,4))*0.4
144
145                     if capacity(jj,3) == 0

```

```

146         s(jj,3) == 0
147     end
148
149         %restrict absolute change
150     end
151     if jj > 1
152         - rampdc <= k(jj,:)-k(jj-1,:) <= rampdc
153
154         - rampc <= l(jj,:)-l(jj-1,:) <= rampc
155
156         - ramp <= s(jj,:)-s(jj-1,:) <= ramp
157
158     end
159 end
160
161         % Apparent Power Limits
162 s <= s_max
163
164 cvx_end
165 figure(countf)
166 %bar(s,'stacked')
167 title(['Stacked Energy Profile at ',num2str(mult(count)*20),' usd/ton'])
168 xlabel('Hour of the day')
169 ylabel('Power [MW]')
170 legend('Nuc','AdvNuc','Solar','NG','NGPK','Demand')
171 totalcosthourly(count,:)=cg'*s'+cs'*e' + carbon_tax*s';
172 totalcost(count)=sum(totalcosthourly(count,:));
173 totalemissionshourly(count,:)=co2permwh*s';
174 totalemissions(count)=sum(totalemissionshourly(count,:));
175
176
177 figure(countf+1)
178 %plot(tt,e,'LineWidth',1)
179 title(['Hourly Storage Profiles at ',num2str(mult(count)*20),' usd/ton'])
180 xlabel('Hour of the day')
181 ylabel('Power [MW]')
182
183 grid on
184 grid minor
185 legend('Li-Ion','hydrogen','Flywheel')
186 countf = countf+2
187 count=count+1;
188 end
189
190 % Output Results
191 fprintf(1,'----- PROBLEM 2 -----\\n');
192 fprintf(1,'-----\\n');
193 fprintf(1,'Minimum Generating Cost : %4.2f USD\\n',cvx_optval);
194 %fprintf(1,'Gen Power : p = %1.3f MW | s = %1.3f MW\\n',p,s);
195 fprintf(1,'\\n');
196 fprintf(1,'Total apparent power : %1.3f MW consumed | %1.3f MW
generated\\n',sum(l_S),sum(sum(s)));
197 s;
198 totalcost;
199 totalemissions;

```

```

200 %p
201 end
202
203 %% plotting
204
205 figure(17)
206 plot(mult.*20,totalemissions)
207 xlabel('carbon tax (usd/ton)')
208 ylabel('tons CO2')
209 title('Carbon emissions of optimized energy mix vs Carbon Tax')
210 grid on
211 grid minor
212 figure(18)
213 plot(mult.*20,totalcost)
214 xlabel('carbon tax (usd/ton)')
215 ylabel('USD')
216 title('Levelized cost of optimized energy mix vs Carbon Tax')
217 grid on
218 grid minor
219
220 figure(count+2)
221 plot(tt,s,'LineWidth',1)
222 title('Hourly Generation Profiles')
223 xlabel('Hour of the day')
224 ylabel('Power [MW]')
225 title('Levelized cost of optimized energy mix vs Carbon Tax')
226
227 hold on
228 % plot(tt,e,'LineWidth',1)
229 plot(tt,l_S, 'black','LineWidth',1)
230 % plot(tt,sum(s,2)+sum(k,2)-sum(l,2),'r--','LineWidth',1)
231 % plot(tt,sum(s,2),'g--','LineWidth',1)
232 grid on
233 grid minor
234 legend('Nuc','AdvNuc','Solar','NG','NGPK','Demand')
235
236 figure(count+3)
237 plot(tt,e,'LineWidth',1)
238 title('Hourly Storage Profiles')
239 xlabel('Hour of the day')
240 ylabel('Power [MW]')
241
242 grid on
243 grid minor
244 legend('Li-Ion','hydrogen','Flywheel')
245
246 % figure(4)
247 % plot(tt,k,'LineWidth',1)
248 % grid on
249 % grid minor
250 % legend('li+','hydrogen','flywheel')
251 %
252 % figure(5)
253 % plot(tt,l,'LineWidth',1)
254 % grid on
255 % grid minor

```

```
256 %% legend('li+','hydrogen','flywheel')
```

Listing 1: Convex Optimization Code

2 Helper Code

```
1 %% CALCULATIONS
2 consumption_2017=129539; % GWh assume 100% combined cycle natural
3   gas
4 demand_2017=consumption_2017/24/365;
5 demand_2050=100; % GW according to MOEI 2019 Energy Report
6
7 %% seasonal changes of power demand [GWh]
8 seasonal_abudhabi={[1:12],...
9   [1600 1500 1800 2250 2550 2600 3100 3100 3000 2750 2200 2000]};
10 seasonal_normalized=seasonal_abudhabi;
11 % normalize seasonal variation curve
12 seasonal_normalized{2}=seasonal_abudhabi{2}/max(seasonal_abudhabi
13   {2});
14 %Abu Dhabi Water & Electricity Company. (2013). ADWEC Statistical
15   Report 2008-2012.
16
17 hourly_demand_summer_ksa={[0:23],...
18   [51 51 51 50 50 48 46 46 47.5 50 52 53 54 55.5 55.5 54.5 54 ...
19   52.5 54.5 54.5 53.5 52.5 51.5 51]}; 
20
21 hourly_demand_winter_ksa={[0:23],...
22   [28 27 26 25.5 25 25 26.5 25.5 24.5 25.5 26.5 27 27.5 28 28 ...
23   28.5 28.3 29 32 31 31 30.5 30 29]};
24 hourly_summer_shape=hourly_demand_summer_ksa{2}/max(
25   hourly_demand_summer_ksa{2});
26 hourly_winter_shape=hourly_demand_winter_ksa{2}/max(
27   hourly_demand_winter_ksa{2});
28 %% DATA
29 current_load=demand_2017;% GW assume all natural gas combined cycle
30 future_load=100; % GW
31 future_seasonal_load={[1:12],seasonal_normalized{2}*future_load}; %
32   GW
33 nuclear_supply=5.600; %GW
34 summer_hourly_load=hourly_summer_shape*future_load;
35 winter_hourly_load=hourly_winter_shape*future_load/2;
```

Listing 2: Demand Load Data from UAE

Listings

1	Convex Optimization Code	1
2	Demand Load Data from UAE	6

Optimization of Microgrid Design for the Puerto Rico San Juan International Airport

Sarah Barr Engel, Rohan Datta, Lucas Duffy, Fangxing Liu, Phong Ly, Joshua Romo

I. Abstract

Equatorial islands like Puerto Rico are particularly vulnerable to natural disasters and climate change. To demonstrate increased resiliency and renewable energy integration, the San Juan Luis Munoz Marin International Airport (SJU) has been proposed as a pilot project to install a microgrid. This study determines the optimal generation for a microgrid at SJU that incorporates solar, wind, battery storage and existing diesel generation. The optimization program minimizes capital expenditures, operating costs, and greenhouse gas emissions under two scenarios: fully grid-connected and fully isolated (“island” mode). The optimization program is further improved with a new set of battery dynamic equations that incorporate battery power loss. Results from the optimization program indicate that the necessary microgrid would include wind energy and battery storage in addition to some of the existing diesel generators. The airport would be powered by wind and the existing grid when fully connected and by wind and diesel during an outage. The improved battery dynamics decreased the daily cost of the microgrid by \$2000 and \$2600 during normal operation and an outage, respectively.

II. Introduction

Motivation & Background

As the growing threat of climate change meets global electrification, the electric power sector faces a massive challenge. A clean energy transition is essential to meeting the UN sustainable development goals and limiting global climate change. Microgrids (MGs) are locally-controlled electrical generation and distribution systems that can function both connected to traditional grid infrastructure and as electrical “islands”. Interest in MG systems has increased due to the wide range of potential benefits they offer including improved energy efficiency, local energy generation, reliability of supply, and lower environmental impact. In addition, MGs enable electrification in places unable to connect to a centralized grid. MGs are seen to improve everything from grid resilience in industrialized countries to rural electrification in developing countries.

In 2017, Hurricanes Irma and Maria devastated the U.S. Territory Puerto Rico, causing nearly 3,000 deaths (Newkirk, 2018), \$43 billion in economic losses (Rivera, 2018), and leaving people without electricity for months. As of 2019, Puerto Rico has increased its Renewable Portfolio Standard (RPS) with the goal of 100% renewable electricity by 2050 (Gheorgiu, 2019). Puerto Rico’s governor, Ricardo Rossello, stated that the broad energy reform is motivated by high energy prices from importing fossil fuels as well as the need for improved resilience from extreme weather events. The newest RPS has placed responsibility on Puerto Rico to increase resiliency through distributed energy resources (DER) and microgrids, where the need for DER is critical due to Puerto Rico’s vulnerable transmission towers and power lines crossing through central mountains and forests. Our team has proposed a microgrid design for the San Juan Airport due to its role as critical infrastructure. During an extreme weather event that may compromise the integrity of the electricity grid, it is estimated that the San Juan Airport could require over 120,000 kW as its critical demand (Jeffers et al. 2018).

Despite their benefits, MG systems can be extremely complex both technically and politically, often requiring participation from multiple stakeholders and new regulations to maximize benefits. A microgrid supports multiple distributed generation technologies as well as energy storage and demand response systems. Deciding whether to implement specific technologies while also maintaining optimal operational efficiency is a challenge that requires dynamical systems modeling.

Relevant Literature

Talebi et al. is one of the few sources of literature that has focused on designing renewable microgrids using optimization. The paper relies on linear multi-objective optimization to minimize two objective functions. The primary objective minimizes the capital and operating costs of a system with solar, wind, and diesel resources over a 15-year lifespan. The second minimizes the emissions from diesel generators and electricity purchased from the grid. However, the article neglects embodied emissions from wind and solar. In addition, the incorporation of two separate objective functions means the program is non-convex and cannot be solved with CVX.

The standard battery dynamics equations used in convex optimization programs rely on the calculation of the battery's state-of-charge (SOC) from the SOC values at previous timesteps and charging/discharging power. Though the optimization program used by *Hu et al.* focuses on sizing, charging, and on-road power management of plug-in hybrid electric vehicles, the battery dynamics equations used are an improvement to current industry practice and can be applied to other lithium-ion battery systems. This paper models the vehicle's battery pack as strings connected in parallel, with each cell modeled as an open circuit voltage (OCV) in series with a resistor. An affine approximation of the OCV function was used and determined by fitting experimental lithium-iron-phosphate cell data, with a reasonable accuracy when the SOC is between 20-80%.

Anderson et al. developed an algorithm for the optimization of solar photovoltaic (PV) and energy storage capacity of small community microgrids for rural electrification by minimizing installation costs and LCOE and solving an economic dispatch problem using anticipated load and generation. The authors' first optimization formulation focuses on maximization of profit obtained from energy sales and constrains the operation of system based on power balance, limits of power dispatched from or absorbed by the energy storage, and power flow through DC-AC and DC-DC converters. Their next objective is to minimize the installation costs. A steady-state simulator was used to model the behavior of each system configuration and determine time-varying price of energy from PV and energy storage systems.

Li et al. provides a good background on the applications of microgrids and the methods that have been proposed to resolve issues that arise from the intermittent nature of distributed generation and uncertain power exchange between the loads and sources. They focus on the optimal day-ahead scheduling for isolated microgrids, using chance-constrained programming, transforming the model into a solvable mixed-integer linear program in GAMS, and applying the CPLEX solver. Their approach helps balance reliability with economic feasibility.

Focus of this Study

This project seeks to model the design and operation of a microgrid for the San Juan International Airport under different outage scenarios. The model incorporates the installation of and generation from solar panels, wind turbines, and battery storage and utilizes existing on-site diesel generators to meet hourly demand. Convex programming is used to minimize operating and

capital costs as well as greenhouse gas emissions. Robust battery dynamic equations are used in the optimization program to improve the accuracy of battery modeling.

III. Technical Description

Our team estimated SJU's load profile using airport data from South Korea's Incheon International Airport (Baek et al. 2016). The load profile, which provides an hourly demand based on a 365-day average, was scaled down to account for the difference in peak demand (60MW for Incheon airport and 13.5MW for SJU). Figure 1 shows the load profile used in the optimization program.

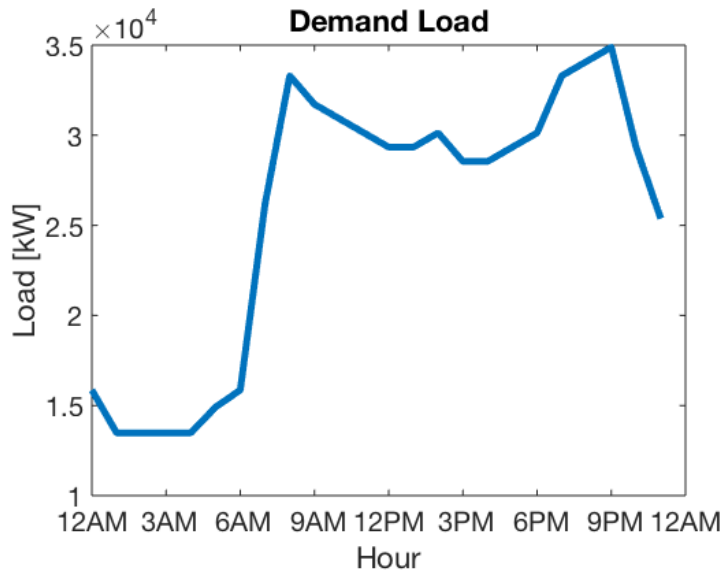


Figure 1: Load Profile of SJU

Solar

Solar irradiation data was retrieved from National Solar Radiation Data Base (NSRDB 2010). We took the average of the data on the first day of each month in 2010. The solar irradiation at time t , along with solar panel parameters, were used to describe the solar power generated at time t and were adapted from (Sufyan et al. 2019):

$$g_{\text{solar}}(t) = n_{\text{solar}} P_{\text{PV}, \text{rated}} \frac{I}{I_{\text{ref}}} \left(1 + k_t (T_{\text{amb}} + 0.0256 I) - T_{\text{ref}} \right)$$

We chose the SunPower X-series X-21-345 (SunPower) as the preferred panel and used its specifications in our model. SunPower has been ranked as one of the top solar panel producers based on panel performance, quality, durability, and warranties (Energy Sage). SunPower has also been named one of the top 3 sustainable solar panel manufacturers based on emissions, water use, conflict materials, and worker's rights, health and safety (Silicon Valley Toxics Coalition). The specific model was chosen due to its high efficiency and designation as a panel for commercial scale projects.

Wind

Though horizontal wind turbines tend to have higher efficiencies, federal aviation guidelines prevent installation of these turbines due to their height and flight path restrictions (Barret et al., 2018). However, vertical axis wind turbines have successfully been deployed at airports, including the Detroit Metropolitan Airport (Dib, 2009). Thus, SunSurf's WT3 Vertical Axis Wind Turbine, a VAWT model that is commercially available with a rated output of 50 kW, has been selected for this optimization program (SolarStore). The wind speed at the San Juan airport was retrieved from the National Centers for Environmental Information (NOAA). We took the average of the data over five days in January. The following equation describes how wind power is calculated from the actual wind speed, rated cut-in speed, and rated cut-out speed:

$$P_{w,h} = \begin{cases} 0, & v_h \leq v_{ci} \text{ or } v_h \geq v_{co} \\ P_{w,max} \frac{v_h - v_{ci}}{v_{rt} - v_{ci}}, & v_{ci} \leq v_h \leq v_{rt} \\ P_{w,max}, & v_{rt} \leq v_h \leq v_{co} \end{cases}$$

Diesel

The diesel generators were modeled based on the existing 1200 kW MTU diesel generators at SJU and serve as a secondary power generation source alongside battery storage, given by the equation:

$$g_{diesel} = n_{diesel} P_{diesel}$$

Battery

Battery parameters were taken from a Saft Intensium Max battery container (Saft Batteries) fitted with 2,436 Saft VL 45 E Li-ion cells (Custom Power). Each cell has a rated storage capacity of 0.16 kWh, and each battery unit has a rated storage capacity of 388 kWh and a footprint of 14.77 m².

Formulation of Optimization Program

Our team designed a linear optimization problem to determine the optimum capacity of solar generation, wind generation, battery energy storage, diesel generation, and grid electricity. To consider both the capital expenditures (CAPEX), operating expenditures (OPEX), and lifecycle emissions of each energy resource, a social cost of carbon was used to convert the lifecycle emissions into monetary units. Appendix A describes key inputs and variables, with the variables in **blue** text indicating the optimization variables. We formulated two versions of the microgrid design and control optimization program: one using industry standard battery dynamics and one using improved, convex battery dynamics incorporated from Hu et al, 2016.

The optimization program using the standard industry battery dynamics is presented below:

$$\begin{aligned}
 & \text{minimize} && c_b \sum_{t=1}^{24} B_c + c_s \sum_{t=1}^{24} g_s s + c_w \sum_{t=1}^{24} g_w w + c_d \sum_{t=1}^{24} D + 0.001 b \\
 & && + c_{grid} \sum_{t=1}^{24} E + CO2_b \sum_{t=1}^{24} B_c + CO2_s \sum_{t=1}^{24} g_s s + CO2_w \sum_{t=1}^{24} g_w w \\
 & && + CO2_d \sum_{t=1}^{24} D + CO2_G \sum_{t=1}^{24} E \\
 \text{subject} & \quad SOC(i+1) = SOC(i) + \gamma B_c(i) - \frac{1}{\gamma} B_d(i) && \text{Battery Dynamics} \quad (2) \\
 \text{to:} & \quad 0 \leq B_c(i) \leq b B_0; && \text{Battery Charging/} \quad (3) \\
 & \quad 0 \leq B_d(i) \leq b B_0 && \text{Discharging} \\
 & \quad s * g_{solar}(i) + w * g_{wind}(i) + D(i) + B_d(i) && \text{Load Constraint} \quad (4) \\
 & \quad - B_c(i) + E(i) = L(i) && \\
 W_{battery} b + W_{solar} s + W_{wind} w & \leq A_{max} && \text{Area Constraint} \quad (5) \\
 0 \leq D(i) \leq (1 - Z)n_{diesel}P_{diesel} & && \text{Diesel Constraint} \quad (6) \\
 SOC_{min} \leq SOC(i) \leq SOC_{max} & && \text{Min/max allowable} \\
 & && \text{cell energy levels} \quad (7) \\
 SOC(t=1) = 0 & && \text{SOC Boundary} \\
 & && \text{Condition} \quad (8) \\
 s_{min} \leq s \leq s_{max} & && \text{Solar scaling} \\
 & && \text{constraint} \quad (9) \\
 b_{min} \leq b \leq b_{max} & && \text{Battery scaling} \\
 & && \text{constraint} \quad (10) \\
 w_{min} \leq w \leq w_{max} & && \text{Wind scaling} \\
 & && \text{constraint} \quad (11) \\
 0 \leq \sum_{t=1}^{24} E \leq \sum E_{grid} Z & && \text{Grid Constraints} \quad (12)
 \end{aligned}$$

The objective function in Equation (1) minimizes the CAPEX and OPEX of the battery, solar, wind, and diesel generator units. To assign a cost to the emissions from each energy resource, we assumed a social cost of carbon of \$50/ton of CO₂eq. The costs of solar, wind, diesel, and battery are based on the levelized cost of energy (LCOE) over an expected lifetime of 20 years. The equation was relaxed to an inequality constraint to preserve convexity. Constraint (2) describes the industry battery dynamics, with Constraint (3) describing the battery charging and discharging limits. Constraint (4) describes the supply and demand balance, indicating that the microgrid must balance the power flow at each time step. Constraint (5) ensures the sum of the area of each resource does not exceed the total available area. Constraint (6) maintains that the diesel generation is less than the total capacity, where $Z \in [0, 1]$ represents a given outage scenario.

To accurately model battery dynamics using either the standard or improved convex formulation, the battery state of charge (SOC) must be zeroed at one point during the day to avoid modeling the battery as an infinite power sink. In this case, SOC was zeroed at the first timestep to serve as a boundary condition (i.e. $SOC(t=1)=0$) in Constraint (8). Constraints (9)-(11) constrain the number of units of each generation resource to minimums and maximums, which were determined by the airport's available area. Finally, Constraint (12) restricts the purchased electricity based on the available capacity from the grid.

Instead of relying on the industry standard the battery dynamics, we employed the battery dynamics from (Hu et al. 2016), described below by updated Constraints (2*), (3*), (4*), and (8*) in addition to the new Constraints (13)-(15).

$\frac{\ P\ _2}{1000} c_b + c_s \sum_{t=1}^{24} g_s s + c_w \sum_{t=1}^{24} g_w w$ $+ c_d \sum_{t=1}^{24} D + 0.01n$ $+ c_{grid} \sum_{t=1}^{24} E + CO2_b \frac{\ P\ _2}{1000} + CO2_s \sum_{t=1}^{24} g_s s$ $+ CO2_w \sum_{t=1}^{24} g_w w + CO2_d \sum_{t=1}^{24} D$ $+ CO2_g \sum_{t=1}^{24} E$ $SOC(i+1) = SOC(i) - P(i)$ $P(i) - P_c(i) + \frac{R * C * P_c(i)^2}{2 * SOC(i) + C * n * U_0^2} \leq 0$ $sg_{solar}(i) + wg_{wind} + D(i) + E(i) + \frac{P(i)}{1000} = L(i)$ $SOC(t=11) = 0$ $P(i)_{min} \leq P(i) \leq 0 \in M_c$ $i_{min} \sqrt{n(\frac{2}{C}SOC(i) + U_0^2 n)} \leq P_c(i) \leq i_{max} \sqrt{n(\frac{2}{C}SOC(i) + U_0^2 n)} \in M_d$ $n \geq 0$	<i>Modified Objective Function</i> (1*)
	<i>Battery Dynamics</i> (2*)
	<i>Electrochemical to Electric Battery Power Conversion</i> (3*)
	<i>New Supply/Demand Constraint</i> (4*)
	<i>SOC Boundary Condition</i> (8*)
	<i>Electrical Battery Power Constraints</i> (13)
	<i>Electrochemical Battery Power Constraints</i> (14)
	<i>Non-negative number of battery cells</i> (15)

The current industry standard battery equations rely on battery charging/ discharging efficiency and models a battery at a macro scale, where the efficiency serves as a proxy for modeling at the cell level. Using the battery dynamics described in Hu et al, Constraint (3*) was determined using an affine approximation by fitting experimental battery data (accurate within the 20-80% SOC window) and attaining the current as a function of the electrochemical battery power and the battery energy. It has been shown in Hu et al. that Constraint (3*) is active at the optimal solution, incurring zero error while still maintaining convexity. Because the program is still convex, computation time is not expected to increase. In Hu et al., the battery power constraints are based on predetermined charging and discharging time zones. Thus, we set M_c in Constraint (13) to be between 15:00 and 18:00 according to the results using industry standard battery equations. To minimize costs by allowing the battery to discharge as slowly as possible, SOC was zeroed at 11:00. Constraint (14) constrains the electrical battery power. Constraint (15) ensures a non-negative number of batteries are included.

With the new battery dynamics, the battery electric power can be both positive and negative. Positive power indicates discharging and negative power indicates charging. We modified the objective function so that the battery cost is based on the two-norm of the battery electrical power rather than the summation of the charging power. In the modified objective function, n refers to the number of battery cells rather than the number of battery units. The battery parameters such as state capacity and footprint were updated accordingly.

For each formulation, we ran the optimization program at both $Z = 1$, when there is full availability of electricity from the grid, and at $Z = 0$, when there is an outage, and no electricity from the grid can be used. The expected value of grid generation is the amount of generation available from the grid each time step multiplied by the outage parameter, as described in Constraint (12). Tuning Z allows the resulting microgrid to be designed according to the level of resilience expected from it: a microgrid designed for a Z -value of 0 is capable of meeting 100% of load for the Airport at all times; a microgrid designed for a Z -value of 1 will minimize costs by taking advantage of the low LCOE for renewable generation while relying on the grid to supply the majority of the load.

IV. Results

We used CVX in Matlab to run our optimization programs and recorded generation curves, battery dynamics, and emissions for each of the four cases: 1) optimization with industry standard battery equations run with $Z = 1$, a fully connected grid, 2) optimization with industry standard battery equations run with $Z = 0$, a fully islanded grid, 3) optimization with improved battery dynamics run with $Z = 1$, a fully connected grid, 4) optimization with improved battery dynamics run with $Z = 0$, a fully islanded grid. A summary of all results can be found in Appendix B.

The hourly demand and the generation contribution of each resource for Case 1 are plotted in Figure 2. Load peaks around 08:00 and 21:30. Wind energy provides the necessary generation from 10:00 to 18:00 when the wind speeds are most optimal for wind generation. Wind slightly overproduces during this time, charging the battery, which is then discharged when wind generation decreases, as seen in Figure 2. The rest of the needed electricity is imported from the grid, peaking during main operating hours on either side of the wind generation distribution when wind generation would be too low to be cost effective. In this outage scenario, solar generation is not cost effective and therefore does not contribute.

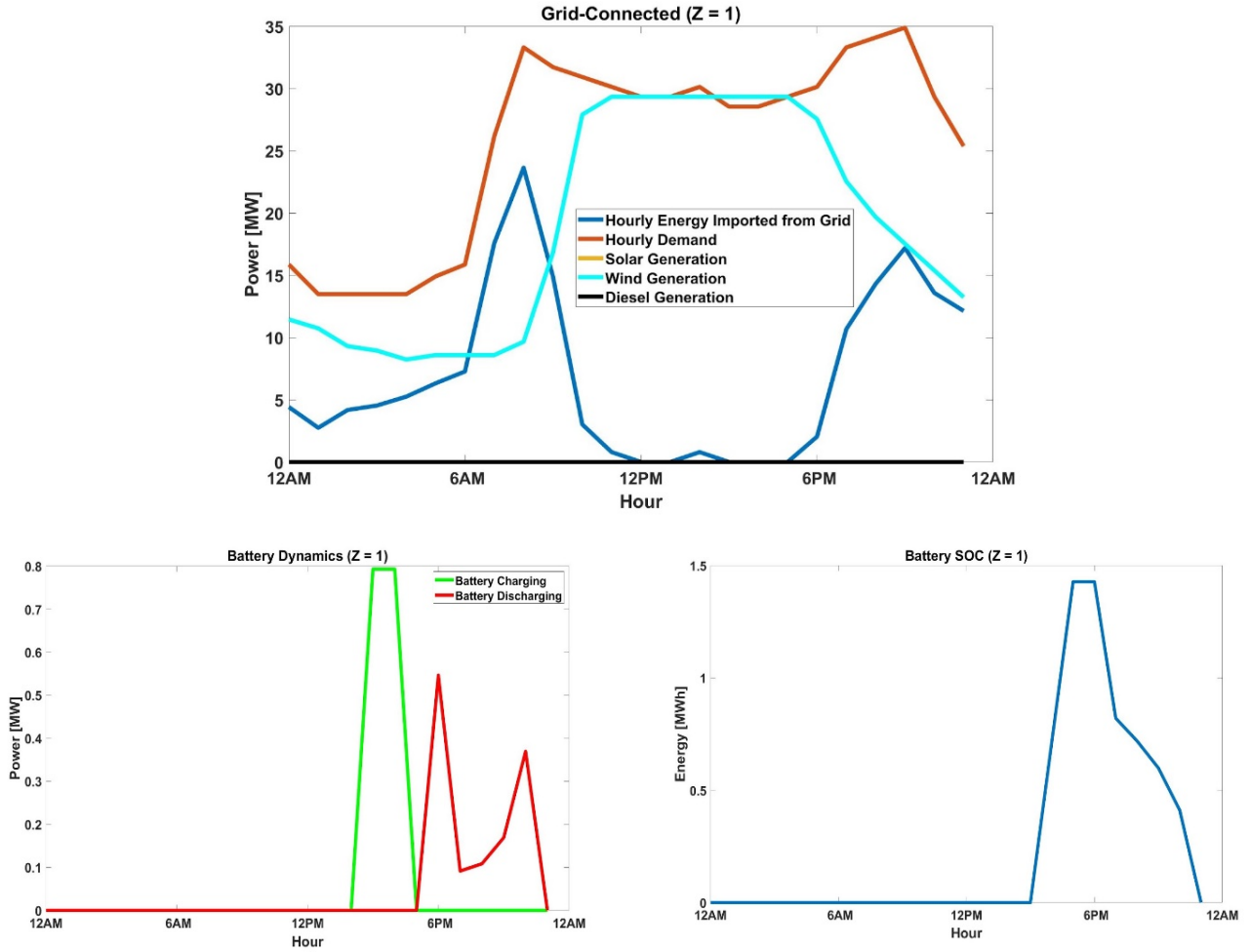


Figure 2: Hourly Generation of Each Resource & Industry Standard Battery Dynamics for Z = 1 (Case 1)

Battery charging corresponds to the time of day with the peak wind source, from 14:30 until 18:00. The battery discharges gradually from 17:30 to 23:30, with two discrete peaks of discharge occurring at 18:00 and 23:00 respectively. Even with access to reliable power from the central grid, the optimal microgrid scheme relies heavily on batteries in order to minimize costs and emissions.

Figure 3 displays the required microgrid generation for Case 2, where the grid is completely unavailable to meet demand.

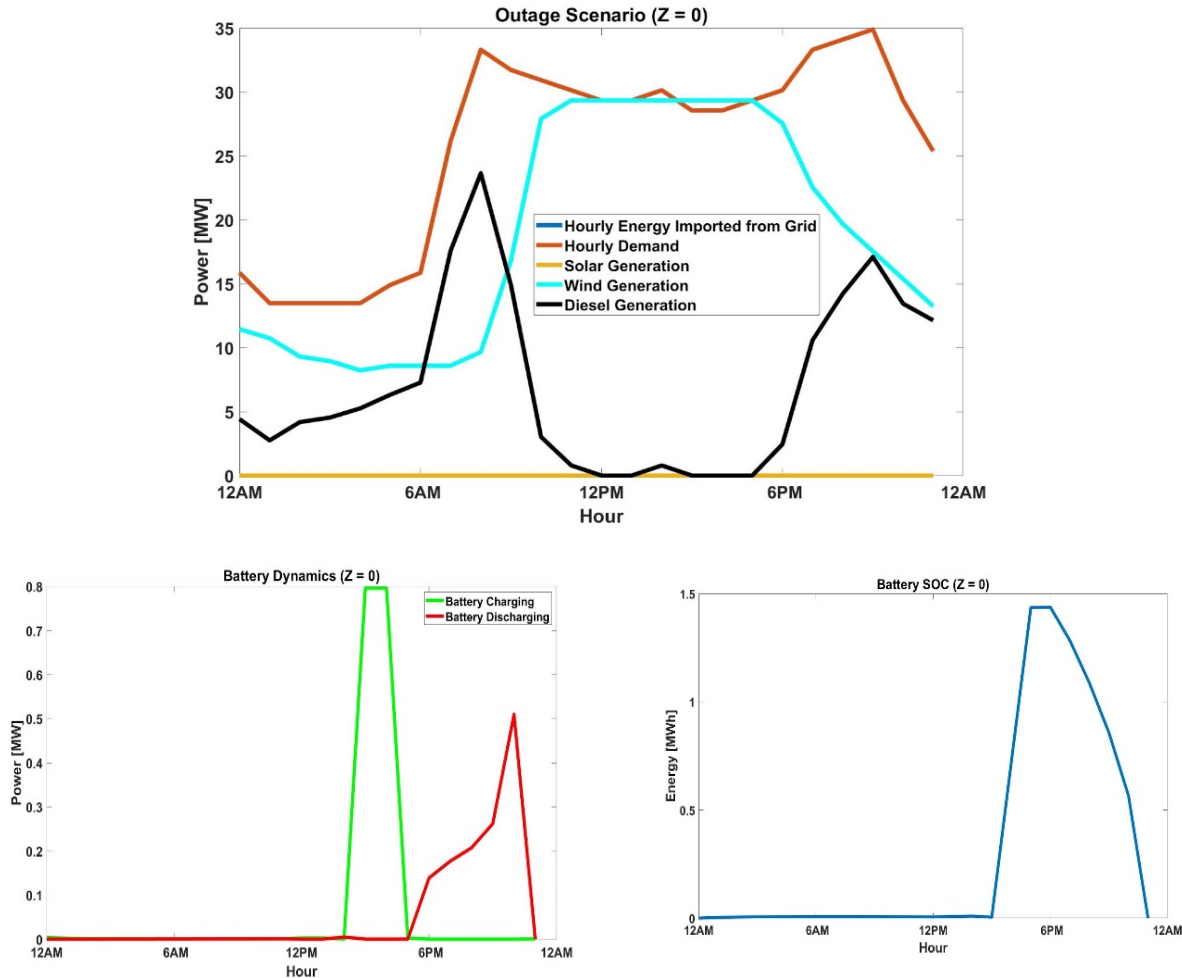


Figure 3: Hourly Generation of Each Resource & Industry Battery Dynamics for $Z = 0$ (Case 2)

Solar is still not competitive with wind generation or storage potential, and the microgrid relies on diesel generation to satisfy the load demand that can no longer be supplied by the grid. The battery charging again corresponds to the time of day with the peak wind source, from 14:30 until 18:00. The battery discharges gradually from 17:30 to 23:30, but contrary to the $Z = 1$ scenario, the discharge cycle has one discrete peak rather than two, occurring around 21:30. Without access to reliable power from the main grid, the optimal microgrid relies heavily on batteries to minimize costs and emissions. Battery SOC for this scenario is similar to the battery SOC in Case 1.

With the battery model reformulated using Hu et al. battery dynamics, we re-ran the optimization program. Results for Case 3, where there is full grid availability, are plotted in Figure 4.

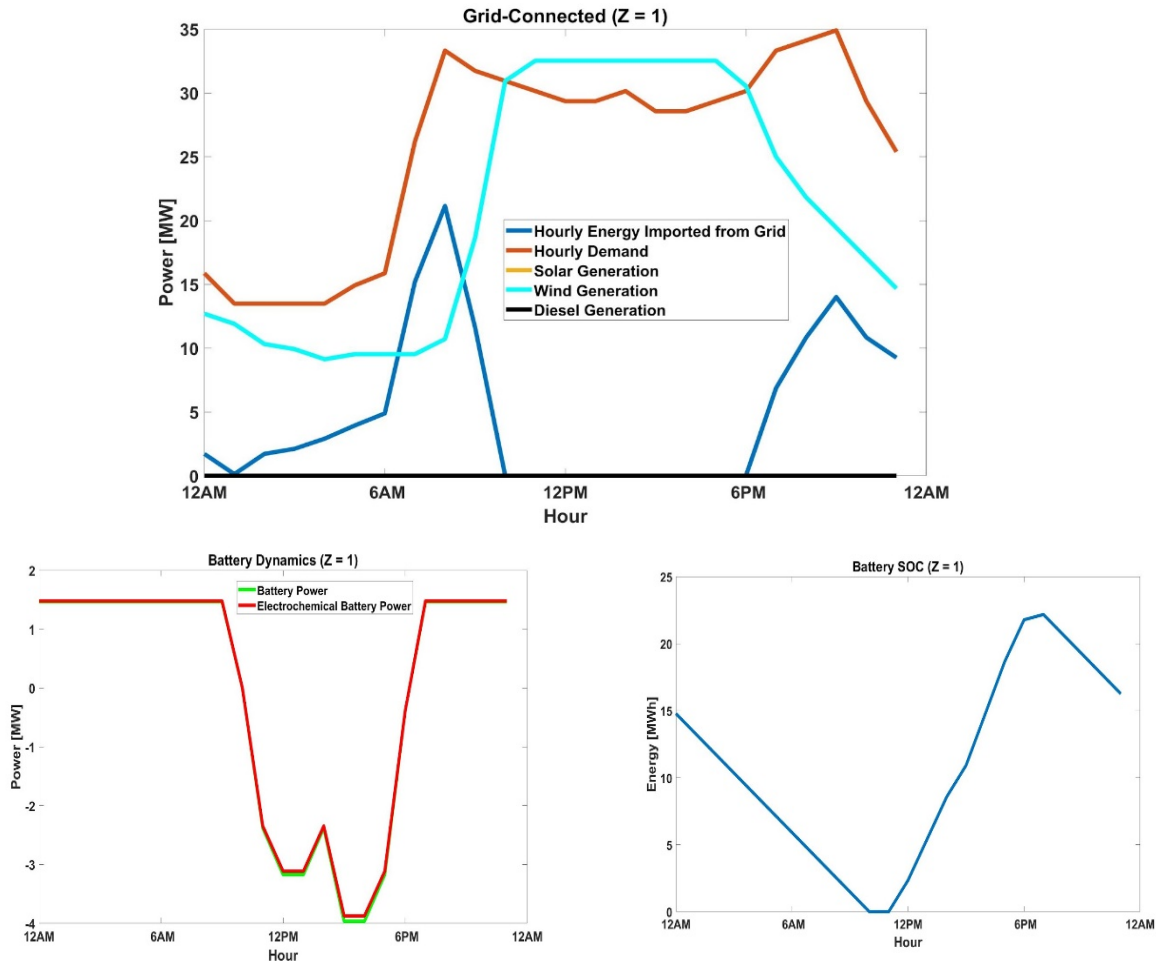


Figure 4: Hourly Generation of Each Resource & Hu et al. Battery Dynamics for $Z = 1$ (Case 3)

With the improved battery dynamics incorporated for $Z = 1$, more energy is generated from the wind turbines during peak wind resource hours. Solar energy remains cost prohibitive. Peak energy from the grid is imported at the same time as in Case 1, but with lower electricity usage, potentially due to the improved storage dynamics that allow for more efficient allocation of the available distributed energy resources. The battery is still required to fully discharge at 11:00 and begins charging much earlier than in the industry standard formulation: around 12:00 as opposed to 15:00. Battery dynamics confirm electrochemical cell behavior, with electrochemical battery power slightly greater in magnitude than battery power at each timestep.

Figure 5 shows the battery dynamics for Case 4, when no grid power is available to meet demand. Significantly less diesel generation is required compared to Case 2, the outage scenario with the standard dynamics, suggesting that incorporating more accurate battery dynamics leads to more efficient use of distributed energy resources. The battery dynamics differ slightly from Case 3, with a small dip in battery power occurring at 02:00.

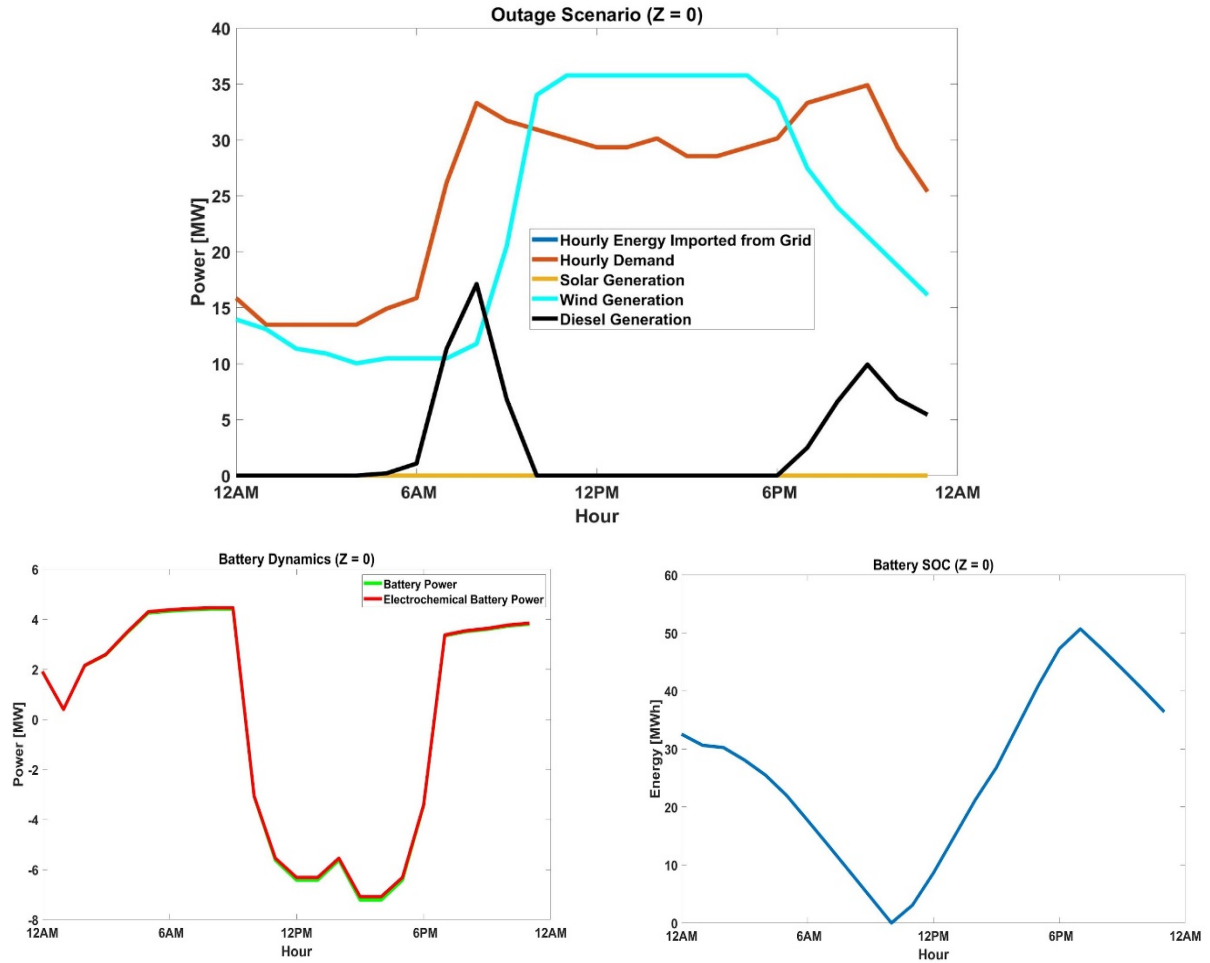


Figure 5: Hourly Generation of Each Resource & Hu et al. Battery Dynamics at $Z = 0$ (Case 4)

The results from Case 4 are used to appropriately size the microgrid needed to satisfy the load of the airport. This would require installing 716 wind turbines, at a rated capacity of 50 kW, and 146 battery units, each rated for 388 kWh. Using the capital costs of each of these technologies, it would cost \$115.55 million to build the microgrid. Based on the optimization program, which accounts for operating costs, and the increasing frequency and severity of natural disasters, this would be a financially prudent investment.

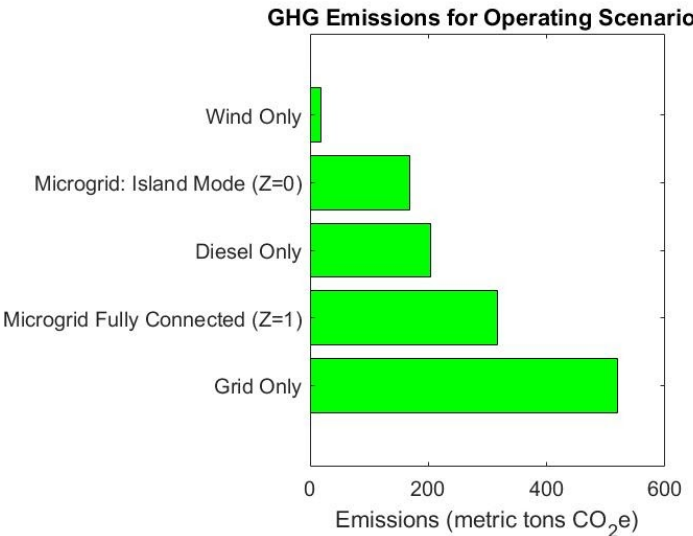


Figure 6: Emissions from each scenario using industry standard battery dynamics

Figure 6 displays the emissions reductions from transitioning to the proposed microgrid. Adding a microgrid to the airport reduces the greenhouse gas emissions associated with its electricity use. In the $Z = 1$ case, transitioning from 100% grid electricity to a mix of grid electricity and wind reduces the daily CO₂e emission by 39%, because it reduces the use of the petroleum and natural gas-reliant grid. In the $Z = 0$ case, where a blackout is assumed, switching from only backup diesel generators to the microgrid reduces the daily CO₂e emissions by 17%. The reason this switch yields a smaller reduction is due to the life cycle emissions of the batteries.

V. Discussion

The global electricity sector needs to decarbonize rapidly to keep warming below the 1.5°C threshold set by the Paris Climate Accord. Solar energy is an established player in the commercial energy space, but smaller-scale wind is not very common. This analysis will hopefully spur more research into locations and loads that pair well with wind energy, especially from smaller capacity turbines like the vertical-axis design chosen for this study. In addition, the fact that the optimal generation incorporated battery storage with renewables, even when grid electricity was a viable option, is a promising result. There has been much debate over the cost of storage and whether it is viable to pair storage with renewable energy projects, especially when the intermittency of renewables can be addressed through energy storage. While the feasibility of added storage will vary with different electricity generation mixes and prices, as well as different state and local incentives, our results show that this is important research to continue as the world pursues more sustainable energy systems.

Sensitivity Analysis

Our current input data and parameters heavily favor wind generation, due to the lower LCOE value and higher power capacity of the selected wind turbine relative to the solar panel. This also may be based on the specific wind data used, which was only for the month of January. Generator diversity is beneficial when relying on intermittent fuel sources to meet demand, so we ran an alternative scenario to understand how dispatch changes when there is no wind to harness.

The optimal dispatch on a no-wind day is shown in Figure 7 for both the isolated and grid-connected microgrids.

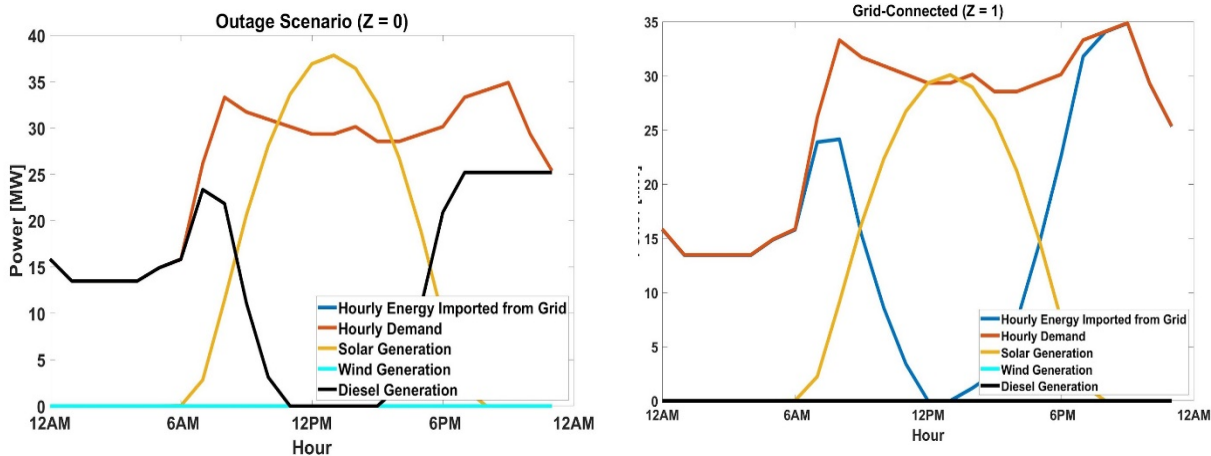


Figure 7: Optimal generation for a no-wind day at SJU microgrid in island (left) and grid-connected mode (right)

Without available wind, the grid-connected microgrid required power from about 104,000 solar panels and stored excess energy in 3 battery units. As was true with the original data, the optimal solution dispatches diesel generators to meet demand during an outage. However, diesel generators are expensive to operate, so the stand-alone microgrid also requires power from an additional 27,000 solar panels and 84 battery units.

Because Puerto Rico has recently updated its RPS to eliminate coal by 2028 and to have 100% renewable power by 2050, we conducted a sensitivity analysis to determine how the dispatch of microgrid resources may change as a result of a cleaner central grid. Using energy portfolio projections prepared for PREPA, the portfolio projections for 2038 detailed in the report were modified to reflect the new policy updates (PREPA 2019). For 2038, we assume natural gas still provides 21% of the total energy, wind provides 5%, solar provides 52%, and battery storage provides 22% for a lifecycle grid emission factor of 281 g CO₂/ kWh. For the 100% renewable target in 2050, we assume natural gas is eliminated, wind provides 10%, solar provides 60%, and battery storage provides 30% of total energy for a life cycle emission factor of 178.3. Using these two emission factors for 2038 and 2050, the number of units of each generation resource were determined at Z = 1. The generation profiles for 2038 and 2050 are presented below:

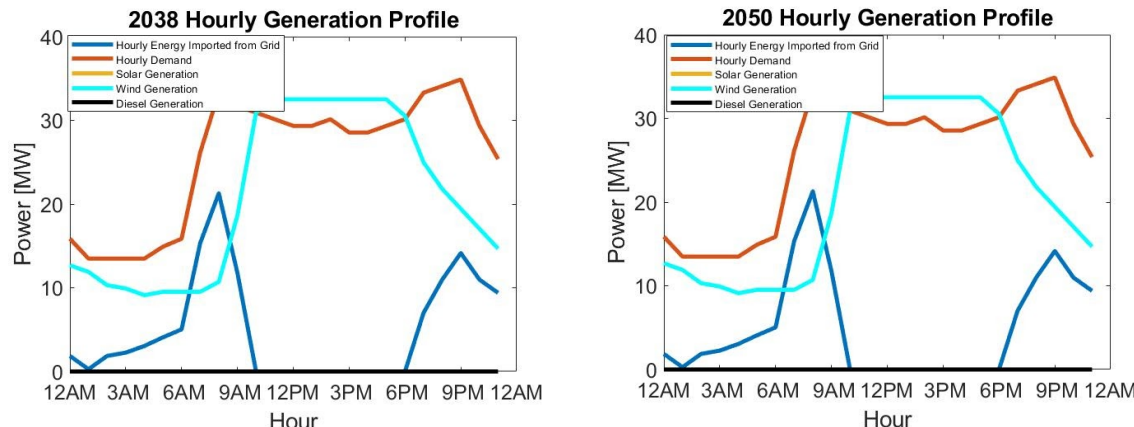


Figure 8: Hourly generation profiles based on the updated 2050 RPS target

As seen in Figure 8, generation profiles are similar between the two scenarios, with electricity providing slightly more of the hourly demand in the 2050 RPS scenario due to its lower lifecycle emission factors. However, both still require the use of 650 turbine units. From 2038 to the 2050 scenario, the number of battery units decreased from 12 to 11 units. The emissions also decrease by 20% due to the cleaner central grid.

Limitations & Future Work

The optimization algorithm described in this paper can be generalized and adapted to optimize the sizing of MGs for many applications outside of aviation. However, there were limitations when applied to the context of SJU. The first major limitation was the lack of the airport's actual load data. Because PREPA did not have available load data for SJU, scaled load data from South Korea's Incheon International airport was used instead. However, the load profile and characteristics may be significantly different, which could lead to different sizing characteristics of various generators. Another limitation encountered was the use of constant electricity prices rather than time-of-use (ToU) electricity prices due to the lack of availability, which would have provided the program motivation to minimize importing electricity during times of high ToU prices. Including local and federal renewable energy incentives would also improve our cost estimates.

While the sensitivity analysis starts to address the intermittency of renewables, future improvements of this program involve collecting annual solar irradiance, wind speed, and load data distributions to determine the expected value and standard deviation of each resource and the electricity demand. Using these distributions, the power generation and load profile can be rewritten as chance constraints that need to be satisfied a minimum percentage of the time. This stochastic program could then be rewritten into a second-order cone program using the inverse cumulative distribution function for the Gaussian distribution.

VI. Summary

Puerto Rico's newest RPS seeks to increase resiliency through distributed energy resources (DER) and microgrids, and our team has proposed a microgrid design for the San Juan Airport due to its role as critical infrastructure. This study determines the optimal generation for a microgrid at SJU that incorporates solar, wind, battery storage and existing diesel generation. The optimization program minimizes capital expenditures, operating costs, and greenhouse gas emissions under two scenarios: fully grid-connected and fully islanded. The optimization program is further improved with a new set of battery dynamic equations that incorporate battery power loss. Results from the optimization program indicate that the microgrid needed to satisfy the load of the airport would include 716 wind turbines, at a rated capacity of 50 kW, and 146 battery units, each rated for 388 kWh. It would cost \$115.55 million to build the microgrid; based on the optimization program, which accounts for operating costs, and the increasing frequency and severity of natural disasters, this would be a financially prudent investment. The airport would be powered by wind and the existing grid when fully connected and by wind and diesel during an outage. Transitioning from 100% grid electricity to a mix of grid electricity and wind reduces the daily CO₂e emission by 39%. Switching from only backup diesel generators to the microgrid reduces the daily CO₂e emissions by 17%. Our results show that more research into microgrid with wind energy and battery storage will be important as the world pursues more sustainable energy systems.

VII. Table of Responsibilities

Team Member	Responsibilities
Rohan Datta	Data Collection, Coding Logistics
Lucas Duffy	Collected data for leveled cost of energy, identified CE295 reference paper, helped troubleshoot optimization program, wrote up results and managed references
Sarah Barr Engel	Determined solar, wind, diesel modules and found/calculated their associated parameters, added calculation of CO2 emissions to program, helped troubleshoot optimization program, worked on discussion and analysis of results
Fangxing Liu	Collected data for load demand, solar irradiance and wind speed, helped formulate the optimization program, incorporated new battery dynamics and generated results
Phong Ly	Collected temperature data to predict solar generation; helped formulate optimization program, helped troubleshoot optimization programs, helped conduct sensitivity analysis, finalized report formatting
Joshua Romo	Collected battery parameters for both sets of battery dynamic equations; helped conduct sensitivity analysis; helped organize presentation and final report
Linnan Cao	Assisted in researching project financial feasibility

Acknowledgements

We would like to thank Dr. Scott Moura for his mentorship and the scope development of this project. Finally, we thank Graduate Student Instructor Aaron Kandel for his assistance during this course and promoting an interactive learning environment to address the mitigation and adaptation challenges of energy systems to climate change.

VIII. References

- A. Anderson, S. Suryanarayanan and R. Podmore. (2017). Capacity optimization of a community microgrid for rural electrification. IEEE PES PowerAfrica, Accra, 2017, pp. 423-428.
- Americas Generators. (2020). 1200 kW MTU Diesel Generator Set - UL2200. Retrieved from: americasgenerators.com/1200-kW-MTU-Diesel-Generator-Set-UL2200.aspx
- Asmus, P., Forni, A., & Vogel, L. (2018). Microgrid Analysis and Case Studies Report. California Energy Commission. Retrieved from: <https://www.energy.ca.gov/2018publications/CEC-500-2018-022/CEC-500-2018-022.pdf>
- Baek, S., Kim, H., & Chang, J. (2016). Optimal Hybrid Renewable Airport Power System: Empirical Study on Incheon International Airport, South Korea. *Sustainability*, 8, 562; doi:10.3390/su8060562
- Barret, S., DeVita, P., & Miller, R. (2018). Technical Guidance for Evaluating Selected Solar Technologies on Airports. Federal Aviation Administration.
- Chen, C., Wang, J., Qiu, F., & Zhao, D. (2015). Resilient Distribution System by Microgrids Formation After Natural Disasters. *IEEE Transactions on Smart Grid*. Retrieved from: <https://ieeexplore.ieee.org/document/7127029>
- Clean Energy Authority. (2015). Puerto Rico - Renewable Energy Portfolio Standard - Solar Rebates And Incentives. *Clean Energy Authority*, 5 May 2015. www.cleanenergyauthority.com, <https://www.cleanenergyauthority.com/solar-rebates-and-incentives/puerto-rico/puerto-rico-renewable-energy-portfolio-standard>.
- Cole, Wesley, and A. Will Frazier. (2019). Cost Projections for Utility-Scale Battery Storage. Golden, CO: National Renewable Energy Laboratory. NREL/TP-6A20-73222. <https://www.nrel.gov/docs/fy19osti/73222.pdf>.
- Dib, Ali. (2009). Metro Airport Explores Wind Power. GreeningDetroit. Retrieved April 8, 2020 from <https://www.greeningdetroit.com/2009/11/21/metro-airport-explores-wind-power/>
- EIA. (2020). Puerto Rico Territory Energy Profile. Retrieved May 07, 2020, from <https://www.eia.gov/state/print.php?sid=RQ>
- Gheorghiu, I. (2019, March 26). Puerto Rico passes 100% renewable energy bill as it aims for storm resilience. Retrieved March 31, 2020, from <https://www.utilitydive.com/news/puerto-rico-passes-100-renewable-energy-bill-as-it-aims-for-storm-resilien/551303/>
- Horvath, A., UC Berkeley. 2019. CEE 268E Lecture Notes 13
- International District Energy Association. (2018). Microgrids as Resilient Energy Infrastructure. Utility Dive. Retrieved from: [https://www.utilitydive.com/spons/microgrids-as-resilient-energy-infrastructure/519251/”](https://www.utilitydive.com/spons/microgrids-as-resilient-energy-infrastructure/519251/)
- Jeffers, R., Baca, M., Wachtel, A., DeRosa, S., Staid, A., Fogelman, W., ... Currie, F. (2018). Analysis of Microgrid Locations Benefiting Community Resilience for Puerto Rico. Livermore, CA: Sandia National Laboratories.

- Lazard. (2018). Levelized Cost of Energy Analysis (LCOE 12.0). Retrieved from:
<https://www.lazard.com/perspective/levelized-cost-of-energy-and-levelized-cost-of-storage-2018/>
- Li, Y., Yang, Z., Li, G., Zhao, D., Tian, W. (2018). Optimal Scheduling of an Isolated Microgrid with Battery Storage Considering Load and Renewable Generation Uncertainties." IEEE Transactions on Industrial Electronics. Retrieved from:
https://www.researchgate.net/publication/325522247_Optimal_Scheduling_of_an_Isolated_Microgrid_With_Battery_Storage_Considering_Load_and_Renewable_Generation_Uncertainties.
- National Academies of Sciences, Engineering, and Medicine. (2015). Renewable Energy as an Airport Revenue Source. Washington, DC: The National Academies Press.
<https://doi.org/10.17226/22139>.
- National Renewable Energy Laboratory. (2010). National Solar Radiation Data Base: 1991-2010 Update. Retrieved ____ from https://rredc.nrel.gov/solar/old_data/nsrdb/1991-2010/
- National Renewable Energy Laboratory. (2015). Energy Transition Initiative: Island Energy Snapshot - Puerto Rico (Fact Sheet). Retrieved from
<https://www.nrel.gov/docs/fy15osti/62708.pdf>
- Newkirk, V. (2018). A Year After Hurricane Maria, Puerto Rico Finally Knows How Many People Died. The Atlantic. Retrieved from:
<https://www.theatlantic.com/politics/archive/2018/08/puerto-rico-death-toll-hurricane-maria/568822/>
- NOAA. (2020). Climate Data Online: Dataset Discovery. Retrieved from:
<https://www.ncdc.noaa.gov/cdo-web/datasets>
- Puerto Rico Electric Power Authority. (2019). 2019 Fiscal Plan for the Puerto Rico Electric Power Authority. https://aeepr.com/es-pr/Documents/Exhibit%201%20-%202019%20Fiscal_Plan_for_PREPA_Certified_FOMB%20on_June_27_2019.pdf
- Rivera, D. (2018). Puerto Rico lost \$43 billion after Hurricane Maria, according to govt. Report. NBC News. <https://www.nbcnews.com/news/latino/puerto-rico-lost-43-billion-after-hurricane-maria-according-govt-n943441>
- Saft Batteries. (2005, March). High Energy Lithium-ion Cell: VL 45 E cell. Retrieved May 7, 2020, from <https://www.custompower.com/documents/VL45E.pdf>
- Saft Batteries. (2019, December 17). Intensium® Max, the megawatt energy storage system. Retrieved from <https://www.saftbatteries.com/products-solutions/products/intensium®-max-megawatt-energy-storage-system>
- Siemens Industry. (2019). Puerto Rico Integrated Resource Plan 2018-2019 (Rep.). Schenectady, NY: Siemens. doi:<https://energia.pr.gov/wp-content/uploads/2019/02/PREPA-Ex.-1.0-IRP-2019-PREPA-IRP-Report.pdf>
- SolarStore. (2020). SunSurfs WT3 Vertical Axis Wind Turbine 50,000W. Retrieved April 7, 2020 from https://www.solarstore.co/SunSurfs-WT3-Vertical-Axis-Wind-Turbine-50000W-50KW-_p_68.html

- SolarStore.co (2020). SunSurfs WT3 Vertical Axis Wind Turbine 50,000W. Retrieved March 31, 2020, from https://www.solarstore.co/SunSurfs-WT3-Vertical-Axis-Wind-Turbine-50000W-50KW-_p_68.html
- SunPower Corporation. (2016). Module Datasheets: SunPower X-Series Residential Solar Panels. Retrieved April 7, 2020 from <https://us.sunpower.com/sites/default/files/media-library/data-sheets/ds-x21-series-335-345-residential-solar-panels.pdf>.
- SunPower® (2016). X-Series Residential Solar Panels | X21-335-BLK | X21-345. Retrieved March 31, 2020, from <https://us.sunpower.com/sites/default/files/media-library/data-sheets/ds-x21-series-335-345-residential-solar-panels.pdf>
- Valibeigi, A. & R. A. de Callafon. (2019). Cooperative Energy Scheduling for Microgrids under Peak Demand Energy Plans. IEEE Conference on Decision and Control. Retrieved from: <https://arxiv.org/abs/2001.11983>

[Appendix A]: Comprehensive List of Variables and Parameters Used

Variable Name	Units	Value	Description
s	n/a	varies	No. of solar panels
b	n/a	varies	No. of battery units
w	n/a	varies	No. of turbines
S _{min} , S _{max}	n/a	[0,2656]	Solar scaling limits
B _{min} , B _{max}	n/a	[0,100000]	Battery scaling limits
W _{min} , W _{max}	n/a	[0,112000]	Wind scaling limits
SOC _{min} , SOC _{max}	kWh	0.15B ₀ ; 0.95B ₀	
S ₀	kW	0.345	Rated Power of Solar Panel (SunPower, 2016)
W ₀	kW	50	Rated Power of Wind Turbine (SolarStore, 2020)
D ₀	kW	1200	Generation Power of Diesel
B ₀	kWh	1000	Rated Battery Capacity (Saft Batteries, 2005)
L	kWh	varies	Hourly Load Demand (adapted Baek, 2016)
E _{grid}	kWh	varies	Energy from Grid
Z	[0,1]	varies	Outage Parameter
I	W/m ²	varies	Solar Irradiance (NREL, 2020)
n _{solar}	n/a	144	Number of Solar Panels
K _t	n/a	-0.0029	Temperature Coefficient
T _{ref}	Celsius	25	Reference Temperature
I _{ref}	W/m ²	1000	Reference Irradiance
c _s	\$/kWh	0.1255	LCOE of Solar (Lazard, 2018)
W _{solar}	m ²	1.63	Footprint of Panel (SunPower, 2016)
V	m/s	varies	Wind Speed (NOAA, 2020)
A	m ²	254.5	Swept Area of Turbine (SolarStore, 2020)
v _{ci}	m/s	1.8	Cut in Wind Speed (SolarStore, 2020)
v _{co}	m/s	28	Cut out Wind Speed (SolarStore, 2020)
v _{rt}	m/s	10	Rated Wind Speed (SolarStore, 2020)
n _{turbines}	n/a	1	Number of Turbines
c _w	\$/kWh	0.038	Turbine Cost per kWh Generated (Lazard, 2018)
n _{diesel}	n/a	21	Number of Diesel Generators
c _d	\$/kWh	0.239	Cost of Diesel per kWh Generated (Lazard, 2018)

W _{diesel}	m ²	14.7	Diesel Footprint (Americas Generators, 2020)
U ₀	V	3.3	Coefficient in Open-Circuit-Voltage (Hu et al. 2016)
C	Farads	51782	Equivalent Cell Capacitance (Hu et al. 2016)
R	Ohms	0.01	Cell Resistance (Hu et al. 2016)
W _{battery}	m ²	14.86	Footprint of Each Cell (Saft Batteries, 2005)
g _{battery cost}	\$/kWh	0.7	LCOE of Battery (Saft Batteries, 2005)
γ	n/a	0.9	Battery Charge/ Discharge Efficiency
CO _{2b}	ton CO ₂ /kWh	456E-6	Battery LCA Values of CO ₂ Emissions (Horvath, 2019)
CO _{2s}	ton CO ₂ /kWh	64E-7	Solar LCA Values of CO ₂ Emissions (Horvath, 2019)
CO _{2w}	ton CO ₂ /kWh	31E-8	Wind LCA Values of CO ₂ Emissions (Horvath, 2019)
CO _{2d}	ton CO ₂ /kWh	331.2E-9	Diesel LCA Values of CO ₂ Emissions (Horvath, 2019)
CO _{2G}	ton CO ₂ /kWh	844.86E-10	Grid LCA Values of CO ₂ Emissions (Horvath, 2019)
A _{max}	m ²	627465.2	Total Area Available (Google Earth)

[Appendix B]: Cost and Emissions Values

Model Dynamics	Daily Cost (\$)	No. of Solar Panels	No. of Wind Turbines	No. of Batteries	Daily Carbon Emissions (ton)
Simple Battery (Normal)	59007.4	0	587	2	153.7
Complex Battery (Normal)	57031.81	0	650	63	184.6
Simple Battery (Outage)	61326.7	0	587	21695	78.6
Complex Battery (Outage)	58711.06	0	716	145	200.6

Optimal Sizing and Bids Scheduling of a Price-Maker Battery on a Nodal Wholesale Market

CE295 Class Project Report

May 11, 2020

Guillaume Goujard*, Kieran Janin†, Salomé Schwarz‡, Charles Garnot§ and Ramdane Bessaid¶

Department of Civil and Environmental Engineering, UC Berkeley

*Email: guillaume_goujard@berkeley.edu

†Email: kieran.janin@berkeley.edu

‡Email: salome_schwarz@berkeley.edu

§Email: charles.garnot@berkeley.edu

¶Email: ramdane_bessaid@berkeley.edu

Abstract—The market for battery storage is set to boom in the coming years. This trend may be explained by a combination of reasons ranging from a falling cost of technology to a growing need to address uncertain and unflexible renewable energy generation. It is well known that the costs and constraints remain too high for a large-scale lithium-ion battery storage to be profitable solely by arbitrating a wholesale market. However, in this report, we show that by carefully selecting its location and its size with respect to its influence on the prices and on the congestions, a battery storage can still be profitable on a nodal wholesale market. To that end, we develop a price-maker mixed-integer optimization framework that maximizes a depreciated battery storage revenue. This program can be used to yield the optimal location and size of a battery storage. Furthermore, it can be used to optimize the bidding schedule of a battery storage in a nodal transmission-constrained wholesale market. We conducted multiple simulations to illustrate and confirm the need for such an approach. Namely, we compared the price-maker results with price-taker program results on actual data from the New Zealand nodal wholesale market of September 2, 2019.

Index Terms—Local Marginal Price, Nodal Network, Wholesale Market, MILP Optimization, Battery Storage optimization

NOMENCLATURE

β	Dual variable of the line constraints
γ	System marginal cost
λ	Local marginal prices
\mathcal{N}	Set of nodes ranging from 1 to n
ω	Element of the set of dual variables
σ^g	Dual variables of the generator bids
σ^u	Dual variables of the battery bids
a	Generator bid prices
B	Amortized cost of 1 MWh of battery capacity
c	Battery bid prices
d	Nodal demand
g	Generator power injection
H	Shift-factor matrix
h	Line capacity

i_b	Battery storage location
L	Fixed large number
l	Number of transmission lines
M_g	Producer-Node adjacency matrix
M_u	Battery-node adjacency matrix
p	Nodal power injection
P^{max}	Generator bid volumes
P^{min}	Generator minimum bid volumes
q	Battery bid volumes
$r^{\beta, \sigma_g, \sigma_u}$	Auxiliary binary variables for slack constraints
r^c	Auxiliary binary variable for battery bids
T	Horizon of the battery scheduling problem
u	Battery power injection
z	Storage charge level (SOC)
z^{cap}	Battery capacity

I. INTRODUCTION

A. Background & Motivation

Battery Energy Storage Systems (BESS) are expected to skyrocket in energy markets. In the United States alone, prospective studies suggest that installed capacity will increase by 3.8 GW by 2023 [1] [2]. Different factors explain this trend: the falling cost of this technology, more adapted market rules, new regulations requesting storage, and the increase in penetration of renewable energies in the electricity mix. Indeed, BESS represent an opportunity to transition to a low-carbon energy mix. While wind and solar generation emit little carbon, they are fundamentally uncertain and inflexible. BESS demonstrate major strengths to address these shortcomings. First, these systems can balance demand and supply at transmission or distribution levels and on a short time frame. They can also adapt to the needs of loads and generators: storing the surplus of generation during the day and releasing it for the evening ramp-up. Finally, BESS improve the grid reliability by participating in ancillary and regulation markets [3] [4].

While many of the existing batteries earn the majority of their revenues from ancillary and regulation markets [5] [6], the competition is fierce, and the market limited. As an example, the Hornsdale Power Reserve – 100 MW/129 MWh, the largest battery in the world – has taken up to 55% share of the South Australian Frequency Control Ancillary Service (FCAS) and lowered price by 90% since its entry [7] as shown in [Figure 1](#)). Frequency Regulation markets' signals are also

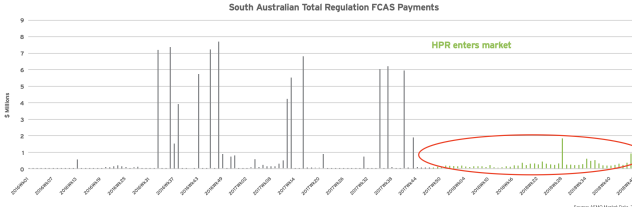


[Fig. 1: South Australian Total Regulation FCAS Payments, 2016-2018 \[8\]](#)

power-intensive and therefore require the battery to operate short-time cycles. These cycles rapidly lead to the battery degradation. Besides, a recent finding [9] showed that a battery with an expected lifetime of 90 months could last for only 56 by aggressively cycling.

Therefore, a company seeking to install a battery on a nodal network should seek to amortize its investment on the wholesale market rather than solely on the ancillary and regulation markets. In fact, despite getting most of its revenue from FCAS, the Hornsdale Power Reserve still offers 119 MWh of its capacity directly into the wholesale market for energy arbitrage [10] [11]. In light of new regulations about energy storage, utilities will have no choice but to plan to deploy large-scale battery units, putting the depreciation of the investment second to the operational aspects. For instance, the California Public Utilities Commission adopted a 1.325 GW procurement mandate for electricity storage by 2020. These entities need to plan and participate in the existing wholesale market. To that end, the BESS challenge will not only consist of finding the best capacity and location, but also following an optimal bidding schedule. It means that the battery operator will aim at maximizing the multiplication of the nodal clearing prices by the clearing volumes over a time horizon. Clearing prices are referred to as Locational Marginal Prices (LMP) λ .

When bidding on the wholesale market, there are two different approaches: considering the new battery as a *price-taker* or as a *price-maker*.

On the one hand, saying that a new actor is a *price-taker* means that their entry into the market will not influence the market's behavior in any way. They will only *take* whatever price the market has cleared. In this case, the LMPs are exogenous to the Optimal Battery Scheduling Program (OBSP). We generally make this assumption for small volumes offered to the market. Despite this, while a battery certainly has a more limited capacity than a power plant, its financial interest is to take advantage of and resolve congestions. Indeed, congestions

on a wholesale market isolate part of the market and, therefore, the volumes offered are no longer negligible in the congested area. We will illustrate this in the results.

On the other hand, assuming an agent to be *price-maker* means that their bids will move the clearing price and/or the cleared volume of the battery. In that regard, the LMP is endogenous to the OBSP.

To visualize these two approaches, a simplified example of economic dispatch is introduced: one node, one trading period, and unlimited available energy. It will illustrate how taking into account the endogeneity of LMPs λ can lead to a better strategy. [Figure 2](#) illustrates the economic dispatch for our very simple example. Without the battery, the clearing price is \$50.

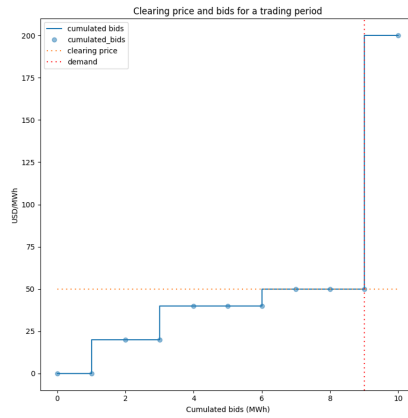


[Fig. 2: Clearing price and bids without the battery](#)

The red bids of [Figure 3](#) show the battery bids in three different set-ups. In the left plot of [Figure 3](#), the clearing price has been dramatically reduced by the battery's market entry (\$20 instead of \$50). This scenario shows that the battery is *price-maker*. In the middle, to improve the gains, the battery bids at the LMP (\$50). However, in this case, while the battery did not impact the clearing price that remained at \$50, the cleared volume U is now low. Finally, on the right hand side, a mixed approach is taken. The product $\lambda \times U$ is optimized. The entire battery volume is cleared and a better profit is earned compared to the other two bidding examples.

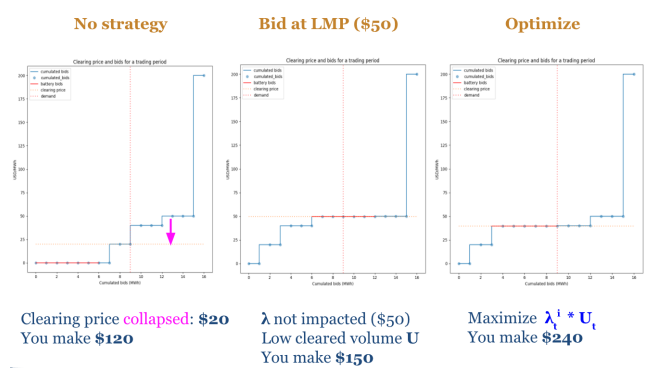


[Fig. 3: Battery bidding strategy and profit](#)

B. Relevant Literature

There are three different ways to position BESS on the grid: on the distribution network near the load center, co-located with variable renewable energy generators (solar, wind) or on the transmission network [12]. We can broadly classify the literature pertaining to the optimization of the operation and sizing of a BESS in the three mentioned groups. The first set of articles takes the Independent System Operator's (ISO) perspective having the duty to optimize system reliability and reduce cost of transmission [13]. The second set of articles focuses on finding the best operation of a battery jointly operating with other resources such as solar [14] [15], wind [16] or both [17], and increasingly with electric vehicles. Finally, the last set deals with the optimization of a standalone storage system from a merchant operator point of view and at a transmission level. We will focus on that last group.

As previously explained, a widespread approach to generate an optimal bidding schedule for a battery storage is to assume that the storage will be *price-taker* and as a result devise an optimization program with exogenous market prices. Some articles have looked into finding an optimal sizing and operation but under exogenous real-time price [18]. Others, have focused on finding the optimal dispatch over multi-markets (day-ahead market, reserve and regulation market) [19]. Other articles have focused on devising an optimization program taking storage degradation into consideration [20]. On nodal markets, feasibility studies concerning implementation of battery storage has been conducted but always under the *price-taker* assumption [21] [22]. Mohsenian et al. laid a framework for a price-maker large-scale battery storage program over a nodal-wholesale market [23]. However, they considered large-scale battery storage and did not provide with a comparative price-taker approach to illustrate the importance of the endogenous assumption. In our work, we also used the linearization techniques introduced in [24] and the clear formulation of the E.D dispatch in [25].

C. Focus of this Study and contribution

Since BESS are to become an important piece of the power grid, how can a utility still plan a long-term investment when the BESS impact on the market can be so strong that prices eventually collapse? A utility should therefore take into account, for its planning, that the BESS may shift the prices when it enters a market.

In this report, we develop and linearize a mathematical program under equilibrium constraints. We finally illustrate our program by comparing it to a *price-taker* program for the New Zealand wholesale market and with the data of September 2, 2019.

II. PROBLEM NOTATIONS AND FORMULATION

A. Key challenges

The following table presents the key assumptions made before stating our problem.

Challenges	Solution (S) / Assumption (A)
Uncertainty over bids & demand	Perfect information (A)
Spatial heterogeneity (e.g NZ has 300 nodes)	DC power flow for Economic Dispatch (S)
Multi-temporal dimension	Battery State Of Charge equations as a constraint (S)
Endogenous (LMP) : Non-linear objective function	Linearized Mathematical Program under Equilibrium Constraints (S)

B. Battery storage problem

We consider a standalone battery storage located at the transmission level and bidding solely on a nodal wholesale market. The topology of the network is assumed to have a set of nodes \mathcal{N} numerated from 1 to n and we assume that the battery pack is located at node $i_b \in \mathcal{N}$, with capacity z^{cap} . The time horizon of our optimization problem is T , typically one day. The operator bids a price c_t and volume q_t at each trading period t . We recall that we want to devise an optimization program with three purposes :

- 1) Find the best location of the battery on the network,
- 2) Find the best capacity,
- 3) Find the best bidding schedule to optimize revenues.

We will devise an optimization program for $z^{cap}, (c, q)$. The best location will be found by iterating the optimization program over the nodes of the network.

1) *State of Charge (SOC) Constraints:* Denote $u \in \mathbb{R}^T$, the storage power injection vector. $u_t > 0$ (resp. $u_t < 0$) if the battery is injecting (resp. withdrawing) energy to the grid at time period t . Denote $z \in \mathbb{R}^T$, the SOC profile of the battery. The SOC profile is constrained by the capacity and some minimum level that we set to zero in this article (see equation (1)). The power injection vector is bounded by an upward and downward charging rate constraint to limit short and deep cycles (see equation (2)). We use an ideal linear model for the SOC profile with an assumed efficiency of 1, hence equation (3). To prevent a bias in the revenues of the battery, we impose the first SOC to be equal to the last (see equation (4)).

$$0 \leq z \leq z^{cap} \quad \text{SOC constraint} \quad (1)$$

$$u^{min} \leq u \leq u^{max} \quad \text{Charging rate constraint} \quad (2)$$

$$z_{t+1} = z_t - u_t \quad \text{SOC update equation} \quad (3)$$

$$z_{T+1} = z_1 \quad \text{SOC boundary conditions} \quad (4)$$

Note that z can fully be expressed as a function of u : $z = z_1 + Lu$. L is a sub-triangular matrix filled with -1 . These 4 equations can be rewritten under compact form and as a function of u in the following way :

$$\tilde{L}u \leq \bar{u} + z^{cap}e \quad \text{Battery Power Injection Feasibility} \quad (5)$$

Where we have :

$$\begin{aligned}\tilde{L} &= [L \quad -L \quad I \quad -I]^T \\ \bar{u} &= [-z_1 1_{T-1} \quad 0 \quad -z_1 1_{T-1} \quad 0 \quad u^{max} \quad u^{min}]^T \\ e &= [1^{T-1} \quad 0]^T\end{aligned}$$

Since the demand will be assumed as inelastic in the Economic Dispatch problem (8), we need to draw a distinction between our selling bids $q_t^u > 0$ and the supplement of demand occurring from charging the battery $q_t^u < 0$. In the last case, to remove the battery contribution to the economic dispatch bids, we need to set $c_t = 0$ (more explanations at (II-C5)). We add the binary variable $r^c \in \{0, 1\}^T$ and the two following constraints :

$$\begin{aligned}(r^c - 1)L &\leq q^u \\ c_t &\leq r^c L\end{aligned}$$

With this formulation if $q^u < 0$ then $c_t = 0$, if $q^u \geq 0$, c_t is unconstrained.

2) *Optimization problem:* Let $\lambda_t \in \mathbb{R}^n$ be the local marginal prices (LMP) for time period t . At each period, we earn or pay (depending on the sign of u_t), $\lambda_t^{ib} \cdot u_t$, where λ_t^{ib} is the LMP of the node where the battery is installed. Since the battery charging cycles implies dynamic arbitrage, our program will be multi-periodic from $t = 1$ to $t = T$, hence the denomination of "bidding schedule". To obtain the optimal size, we need to account for the cost for installing a battery. If one MWh of battery costs b USD and the battery is depreciating in y years, then to be profitable, our battery's profits must exceed $B = \frac{b \cdot T}{365 \cdot 24 \cdot y}$ (see the results for values). This quantity is going to appear as a linear penalty on z^{cap} in the battery program.

We will now devise two programs : one under the *price-taker* framework and the other under the *price-maker* framework. Both frameworks will be compared in an offline setup in the results section (III). We used the blue color to highlight optimization variables.

3) *Price-taker framework:* Under the price-taker framework, the LMPs are exogenous and the battery is self-scheduling. Therefore, our bidding strategy will be a succession of self-schedule volumes sent to the market operator.

$$\begin{aligned}\max_{z^{cap}, u} \quad & \left(\sum_{t=1}^T \lambda_t^{ib} u_t \right) - B \cdot z^{cap} \\ \text{subject to} \quad & \tilde{L}u \leq \bar{u} + z^{cap}e\end{aligned}\tag{6}$$

4) *Price-maker framework:* Under the price-maker framework, both the LMPs and the storage power injection are the results of the market clearing operation denoted as E.D

and introduced in (8). Hence $(\lambda_t, u_t) \in \text{E.D}_t(c_t^u, q_t^u)$, and our bidding strategy (c^u, q^u) over the next T periods is:

$$\begin{aligned}\max_{z^{cap}, c^u, q^u} \quad & \left(\sum_{t=1}^T \lambda_t^{ib} \cdot u_t \right) - B \cdot z^{cap} \\ \text{subject to} \quad & \tilde{L}u \leq \bar{u} + z^{cap}e \\ & (\lambda_t, u_t) \in \text{E.D}_t(c_t^u, q_t^u)\end{aligned}\tag{7}$$

C. Nodal Wholesale Market

1) *Topology of the network and DC Power flow equations:* We denote $p_t \in \mathbb{R}^n$ as the nodal power injection vector. The l transmission lines have capacity h_i for each of them. To obtain conditions on the feasibility of p_t , we use the DC Power Flow equations. First, these equations imply that the power is balanced over the grid and there is no loss : $1^T p_t = 0$. Second, the flows over the lines are reactive and are linear in the voltage angles. If i is the line between node k and j , the flow over i is $b_i(\delta_k - \delta_j)$. Denoting $H \in \mathbb{R}^{g, 2l}$ the shift-factor matrix, we can link the line flows to the nodal power injections p_t and finally obtain that $Hp_t \leq h$.

2) *Time Frame of the market:* We consider the bids and constraints of market participants in a general multi-periodic setting : $\mathcal{T} = \{1, \dots, T\}$. We do not consider multiple-time blocks of energy.

3) *Demand:* We consider that demand is fixed and known. At each time step, we are given $d_t \in \mathbb{R}_+^n$

4) *Producer:* Let $g_t \in \mathbb{R}_+^g$ be the generation vector dispatched by the market. More precisely, $g_{t,i}$ is the generation dispatch by the market operator to the unit i and at time step t . In this report, we are considering a simple Wholesale market with one bidding band per generator and per time-step to simplify our notations. A generalization to multiple bands is straightforward by multiplying the dimension of the generation vector by the number of bands. Denote $P_t^{min}, P_t^{max}, a_t \in \mathbb{R}_+^g$, the minimum, maximum capacity and bid price of all the units at time period t . More precisely, at each time period t , each producer sends three information to the operator :

- $P_{t,i}^{min}$, its must-run capacity which is self-scheduled,
- $P_{t,i}^{max}$, the maximum capacity it is willing to offer in the market,
- $a_{t,i}$, the bidding price associated to the volume $P_{t,i}^{max} - P_{t,i}^{min}$

It follows that the cost for the dispatch of g_t is $a_t^T g_t$. With g_t feasible if and only if : $I_t^g g_t \leq q_t^g$.

$$I_g = \begin{bmatrix} I \\ -I \end{bmatrix}; \quad q_t^g = \begin{bmatrix} P_t^{max} \\ P_t^{min} \end{bmatrix}$$

Since we may have multiple generators on the same network node, we denote $M_g \in \mathbb{R}^{n,g}$, the producer-node adjacency matrix. $M_{g,i,j} = 1$ if and only if producer j belongs to node i , with $i \in \{1, \dots, g\}$ and $j \in \mathcal{N}$. Otherwise $M_{g,i,j} = 0$.

5) *Battery :* Our battery can buy on the wholesale market at the clearing price. In that case the bid volume is negative q_t^u , u will be negative and it will act as a supplement of demand.

Both bidding volume and self-scheduled demand are taken into account with the following constraint :

$$u_t \leq q_t^u$$

Indeed, if $q_t^u < 0$, $c_t = 0$ by construction (see (II-B1)). To minimize the objective function, $u_t^* = q_t^u$. Otherwise, if $\epsilon = q_t^u - u_t^*$ is an extra MWh of demand that has to be met by a generator, therefore increasing the cost.

Finally, like for the generators, we define $M_u \in \mathbb{R}^n$, the battery-node adjacency matrix, all its elements are zero except for :

$$M_{ui_b} = 1$$

D. Economic Dispatch

At a time period t , the market operator dispatches the generation g_t and the storage u_t in order to minimize the cost for the network while at the same time respecting the power balance, line constraints and bids constraints:

$$\begin{aligned} \min_{p_t, g_t, u_t} \quad & a_t^T g_t + c_t \cdot u_t \\ \text{subject to} \quad & \gamma : 1^T p_t = 0 \\ & \lambda : p_t = M_n g_t + M_u u_t - d_t \\ & \beta : H p_t \leq h \\ & \sigma_g : I_g g_t \leq q_t^g \\ & \sigma_u : u_t \leq q_t^u \end{aligned} \quad (8)$$

E. Mathematical Program under Equilibrium Constraint

As shown in program (7), λ and u are solutions of the Economic Dispatch. In other words, they must satisfy the KKT conditions of the LP program (8). Let us first devise the Lagrangian of the Economic Dispatch and its dual function before formalizing and linearizing the KKT conditions.

1) *Lagrangian and dual function:* We define the Lagrangian of the problem as $\mathcal{L}(p_t, g_t, u_t, \omega)$. $\omega = (\gamma, \lambda, \beta, \sigma^g, \sigma^u)$ belongs to the set of dual variables Ω . We define $\Omega = \mathbb{R} \times \mathbb{R}^n \times \mathbb{R}_+^{2l} \times \mathbb{R}_+^g \times \mathbb{R}_+$. For the clarity of the notations, since we have fixed the time period on which we are working, we dropped the dependency of the optimization variables, primal and dual, in t . However, we kept the dependence in t of the exogenous input.

$$p = \min_{p, g, u} \max_{\omega \in \Omega} \mathcal{L}(p, g, u, \omega)$$

$$\begin{aligned} \mathcal{L}(p, g, u, \omega) = & a_t^T g + c_t \cdot u + \gamma 1^T p + \beta^T (H p - h) \\ & + \lambda^T (d_t + p - M_g g - M_u u) \\ & + \sigma_g^T (I_g g - q_t^g) + \sigma_u (u - q_t^u) \\ = & (a_t^T - \lambda^T M_g + \sigma_g^T I_g) g \\ & + (c_t - \lambda^T M_u + \sigma_u) u \\ & + (\gamma 1^T + \beta^T H + \lambda^T) p \\ & - \beta^T h + \lambda^T d_t - \sigma_g^T q_t^g - \sigma_u q_t^u \end{aligned}$$

We define \mathcal{A} s.t :

$$\begin{aligned} \mathcal{A} = \{ & \omega \in \Omega, a_t^T - \lambda^T M_n + \sigma_g^T I_g \geq 0; \\ & c_t - \lambda^T M_u + \sigma_u \geq 0; \\ & \gamma 1^T + \beta^T H + \lambda^T \geq 0 \} \end{aligned}$$

Then, we can devise the dual of the problem under a closed-form expression:

$$g(\omega) = \min_{p, g, u} \mathcal{L}(p, g, u, \omega)$$

$$g(\omega) = \begin{cases} \lambda^T d_t - \beta^T h - \sigma_g^T q_t^g - \sigma_u q_t^u & \text{if } \omega \in \mathcal{A} \\ -\infty & \text{otherwise} \end{cases}$$

Since the problem is a linear optimization problem, it is convex. Furthermore, we assume that the primal problem is well posed, i.e, there exists a feasible point into the set. Therefore, Slater's condition is satisfied, and strong duality holds:

$$a_t^T g^* + c_t u^* = d_t^T \lambda^* - h^T \beta^* - q_t^g \sigma_g^* - q_t^u \sigma_u^* \quad (9)$$

2) *KKT Conditions for the Economic Dispatch:* Here we devise the KKT conditions to obtain a set of constraints \mathcal{C} such that if there exists $(p, g, u, \omega) \in \mathcal{C}$ then $\lambda, u = E.Q_t(c_t, q_t^u)$. Let (p, g, u, ω) satisfies the KKT conditions, they are optimal and verify:

- **Stationary conditions** for the Lagrangian

$$\nabla_p L = \gamma 1 + H^T \beta + \lambda = 0 \quad (10)$$

$$\nabla_g L = a_t - M_g \lambda + I_g^T \sigma_g = 0 \quad (11)$$

$$\nabla_u L = c_t - M_u \lambda + \sigma_u = 0 \quad (12)$$

- **Complementary Slackness conditions**

$$\beta^T (H p_t - h) = 0 \quad (13)$$

$$\sigma_g^T (I_g g - q_t^g) = 0 \quad (14)$$

$$\sigma_u (u - q_t^u) = 0 \quad (15)$$

- **Primal Constraints**

All the other constraints present in program (8) must be satisfied at the optimum.

F. Linearization of the program

The KKT conditions cannot be re-injected as such into our battery program (7).

a) *Slack constraints:* Indeed, the 5 equations of complementary slackness are not affine and must be linearized using integers. The complementary constraints can be linearized using the Fortuny-Amat and McCarl linearization [24]. To do that, we must add a new set of integer variables : $r^\beta \in \{0, 1\}^{2l}$, $r^{\sigma_g} \in \{0, 1\}^{2g}$, $r^{\sigma_u} \in \{0, 1\}$. If we choose L to be sufficiently large and to satisfy the following linear

constraints, we will satisfy the complementary slackness conditions.

$$\beta \leq (1 - r^\beta)L \quad (16)$$

$$H p_t - h \leq r^\beta L \quad (17)$$

$$\sigma_g \leq (1 - r^{\sigma_g})L \quad (18)$$

$$(I_g g - q_t^g) \leq r^{\sigma_g} L \quad (19)$$

$$\sigma_u \leq (1 - r^{\sigma_u})L \quad (20)$$

$$(u - q_t^u) \leq r^{\sigma_u} L \quad (21)$$

b) *Objective function:* The objective function of the battery program is not linear and must be transformed as well.

Here, we use equality (12), (15) and finally strong duality (9) to recover a linear objective function.

First, by multiplying (12) by u :

$$c_t u - M_u \lambda u + \sigma_u u = 0$$

Then from the complementary slackness condition (15) :

$$\sigma_u u = \sigma_u q_t^u$$

Finally from strong duality (9) :

$$-c_t u = a_t^T g_t + \beta^T h + \sigma_g^T q_t^g + \sigma_u q_t^u - \lambda^T d_t$$

The resulting objective function is :

$$\begin{aligned} \lambda^T u &= -c_t u - \sigma_u u && \text{(from (12))} \\ &= -c_t u - \sigma_u q_t^u && \text{(from (15))} \\ &= a_t^T g + \beta^T h + \sigma_g^T q_t^g + \sigma_u q_t^u - \lambda^T d_t && \text{(from (9))} \\ &= a_t^T g + h^T \beta + q_t^g \sigma_g - d_t^T \lambda \end{aligned}$$

Note that we now have an objective function which is a linear function in the variables : $g, \beta, \lambda, \sigma_g$

c) *Illustration of the objective function linearization for a single-node wholesale market:* For a single node wholesale market, the one-time profit made by the battery $\lambda \cdot u$ can be expressed as the difference between what was paid by the load $\lambda \cdot d$, which is linear in λ and what was paid to the other generators : $\sum_{i \leq g} \lambda \cdot g_i$. The geometrical nature of the decomposition is highlighted by figure (4). Applying, the stationary equation (11) and for one node, we have

$$c_i - \lambda + \sigma_i^{\max} P_i^{\max} - \sigma_i^{\min} P_i^{\min} = 0, \quad \forall i \leq g$$

The slack constraints impose that $\sigma_i^{\max} P_i^{\max} = \sigma_i^{\max} g_i$ and $\sigma_i^{\min} P_i^{\min} = g_i$. Thus, we can further subdivide each generator's profit $\lambda \cdot g_i = c_i g_i + \sigma_i^{\max} P_i^{\max} - \sigma_i^{\min} P_i^{\min}$. This new formulation is linear in $g_i, \sigma_i^{\max}, \sigma_i^{\min}$. As a result, the objective function is linear :

$$\lambda \cdot u = \lambda \cdot d - \sum_{i=1}^g c_i g_i + \sigma_i^{\max} P_i^{\max} - \sigma_i^{\min} P_i^{\min}$$

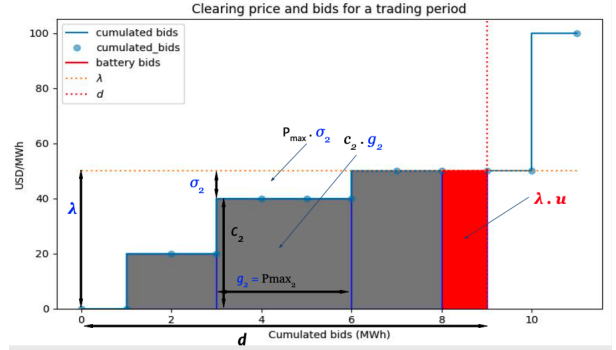


Fig. 4: Linearization of objective function for single-node wholesale market

G. MILP program

We reintroduce the subscript relative to the time period as we are now devising the multi-period optimization program for the battery. The optimization variables are now :

$$z^{cap}, q^u, r^c, g, p, u, \gamma, \beta, \lambda, \sigma^g, \sigma^u, r^{\sigma_g}, r^\beta, r^{\sigma_u}$$

We finally devise the price-maker optimal sizing and bid scheduling program as a mixed-integer linear program.

$$\begin{array}{ll} \min & \left(\sum_{t=1}^T d_t^T \lambda_t - (a_t^T g_t + h^T \beta_t + q_t^g \sigma_t^g) \right) - B z^{cap} \\ \text{s.t.} & \tilde{L} u \leq \bar{u} + z^{cap} e \\ & (r_t^c - 1)L \leq q_t^u \quad \forall t \leq T \\ & c_t \leq r_t^c L \quad \forall t \leq T \\ & 1^T p_t = 0 \quad \forall t \leq T \\ & H p_t \leq h \quad \forall t \leq T \\ & I_g g_t \leq q_t^g \quad \forall t \leq T \\ & u_t \leq q_t^u \quad \forall t \leq T \\ & p_t = M_n g_t + M_u u_t - d_t \quad \forall t \leq T \\ & \gamma_t 1 + H^T \beta_t - \lambda_t = 0 \quad \forall t \leq T \\ & a_t + M_n \lambda_t + I_g^T \sigma_t^g = 0 \quad \forall t \leq T \\ & c_t + M_u \lambda_t + \sigma_t^u = 0 \quad \forall t \leq T \\ & \beta_t \leq (1 - r_t^\beta) L \quad \forall t \leq T \\ & H p_t - h \leq r_t^\beta L \quad \forall t \leq T \\ & \sigma_t^g \leq (1 - r_t^{\sigma_g}) L \quad \forall t \leq T \\ & (I_g g_t - q_t^g) \leq r_t^{\sigma_g} L \quad \forall t \leq T \\ & \sigma_t^u \leq (1 - r_t^{\sigma_u}) L \quad \forall t \leq T \\ & (u_t - q_t^u) \leq r_t^{\sigma_u} L \quad \forall t \leq T \end{array}$$

III. RESULTS & DISCUSSION

A. Case Study: New Zealand

1) *Why New Zealand?*: New Zealand's Energy Market (NZEM) offers a comfortable application of our subject matter. New Zealand's daily wholesale market operates over 48 trading periods of 30 minutes, whereas standard energy markets operate on an hourly basis [26]. The clearing economic dispatch algorithm used to dispatch generation is called "Scheduling, Pricing and Dispatch" (or SPD) and uses DC powerflow equations which matches our assumptions [27].

2) *Data and simulation sources*: The Electrical Authority gives open access to a number of interesting data resources regarding the NZEM, including the loads, bids and network characteristics directly in csv format for ease of use. To make this reproducible as well as give a base for such research on the NZ market, all the source code can be found at the following link: https://github.com/GuillaumeGoujard/LMP_NZ

B. Presentation of the Baseline Testing Scenario

First, we present the scenario on which we obtained our results. We arbitrarily decided to work the 2nd day of September 2019. On this day, 80 generators offered bids on the market. While we based our tests on real data, we multiplied the loads by a factor of 1.3 to favor congestion and added a fuel generator on node 10 of fixed marginal cost of \$100 to demonstrate the well-functioning behavior of our program II-G, prevent infeasible situations and ease the interpretation of results. We explain and precise our choices in the following subsection.

- **Topology** The NZ network is comprised of 182 nodes ([subsection A-A](#)). We aggregated these nodes in 19 nodes and we connected them with transmission lines as per [28] ([subsection A-A](#)). A swing node (0) was set between the two islands. This reduces the dimension of the problem and makes the testing faster to perform. We will only refer to those 19 nodes indexed from 1 to 19 in the following. We additionally had to aggregate the generators which were not referenced in that article (see [B](#)).

- **Loads** The load curves of the simplified network come from aggregating demand at the considered nodes. We multiplied the load at node 10 by 12, so that for some hours, the demand exceeds the capacity of the single line connecting 10 to 2 ([subsection A-B](#)). For the rest of the nodes, we applied a factor of 1.3 to the curves.

- **Bids** We simplified the bidding data for each generator. For each generator and each trading period, P_{min} was taken as the volume bid at \$0. P_{max} was taken as the maximum of the cumulative volume offered to the market. Finally a was taken as the weighted average of the bidding prices for bids over \$0. ([subsection A-C](#))

- **Gamma prices and congestion charge** We ran an economic dispatch to report on the system constants before applying the battery program. In this regard, an important metric to keep track of is the system marginal cost,

γ , which gives the marginal cost of the last dispatched generator under the merit order and without considering congestion. Congestion charge on the other hand is reported as the difference between λ , the LMP and γ . We can see the evolution of these metrics for the baseline scenario in [subsection A-D](#). We can confirm that the node 10 is highly congested.

C. Result for price-maker battery

We run the price-maker optimization program ([II-G](#)) over the scenario. The price-maker optimization framework determines which node, capacity and strategy is best to adopt to maximize profits. We set the investment period of the battery arbitrary for 4.5 years, to favor investment in the capacity and prevent a large capacity biased by the one-day scenario. This yields a B of 137 USD/MWh for one day and we run the program over each node of the network storing the profits and the optimal capacity.

We present the results in [Table I](#). We see that for most of the nodes of the network, the battery operator has difficulty paying for the initial investment in capital. The cost of the battery is too important to hope paying it with arbitrage alone. Furthermore, as we would expect, the congested node of index 10, presents a z^{cap} of 17 MWh and positive returns. We will focus on this example in the rest of the discussion. Maybe counter-intuitively, our program suggests that nodes 18, 19 could be home to 55 MWh battery. This is surely because of the negative congestion charges as shown on [subsection A-D](#).

Node index	Depreciated profits [in \$]	Arbitrage only [in \$]	z^{cap} [in MWh]
1, 2, 5, 6, 7, 8, 9, 13, 14, 15, 17	-3.547	889.878	6.522
3, 12	128.674	2468.163	17.078
4	-136.986	0	1.000
10	93.850	2433.338	17.078
11	-77.563	815.862	6.522
16	180.643	4477.674	31.368
18, 19	361.085	7912.833	55.128

TABLE I: Nodal profits and z^{cap}

D. Node 10 - Comparison with price-taker program

We chose to discuss the results over the Node 10, since this is the node that we tweaked in our test-case. Its isolated location makes it easy to interpret the results. We implemented a price-taker program following Program 6 with the baseline LMPs. The results are shown in [Figure 5](#). In black, (in green resp.), can be seen the cumulated profits and the SOC of the battery operated with the price-maker program (price-taker resp.). In red can be seen the expected revenues of the price-taker program. This is what the operator would earn, if the price-taker assumption would hold. As we can see, the actual revenues are way below.

[Figure 6](#) confirms that the prices moved. λ_{pm} stands for prices under the price-maker assumption (the same as the baseline) and λ_{pt} stands for prices under the price-taker

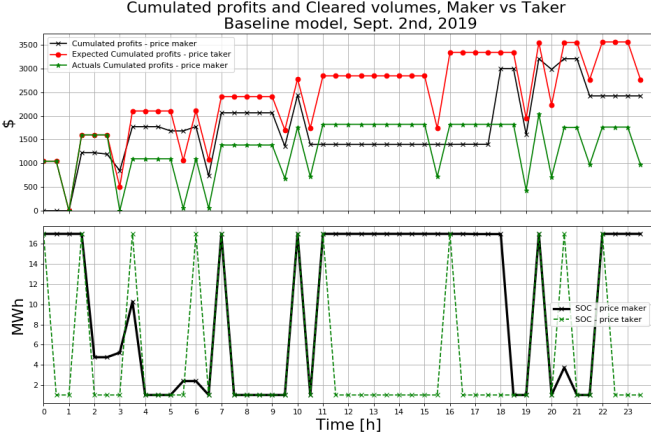


Fig. 5: Cumulated profits and SOC for price taker vs price maker program

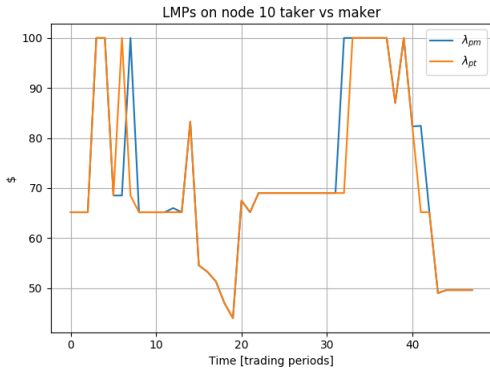


Fig. 6: LMP comparison at node 10 for base situation, price-maker case, price-taker case

assumption. The congestion are solved or created at the worst moment by the price-taker operated battery.

Finally, the norm-2 deviation from the baseline prices for the price-taker and the price maker program, for the node 10 and as a function of the battery capacity are presented in Figure 7. The price-taker assumption is contradicted even for a small capacity at node 10 before stabilizing for greater capacities. We deduce from this figure that as soon as a congestion occurs on node 10, the price-taker assumption cannot hold.

IV. SUMMARY

In this report, we developed a mixed-integer linear program maximizing the depreciated revenue of a battery operator over a nodal wholesale market and under the constraint that the cleared price and volumes are endogenous to the program. To express these constraints, we formulated and then exploited the KKT conditions of the Nodal Economic Dispatch. We linearized the slack constraints at the cost of adding a set of auxiliary binary variables. Furthermore, we linearized the objective function using results from strong duality.

Finally, we tested our program against a simpler price-taker algorithm and on a real-world example set-up. We accessed the

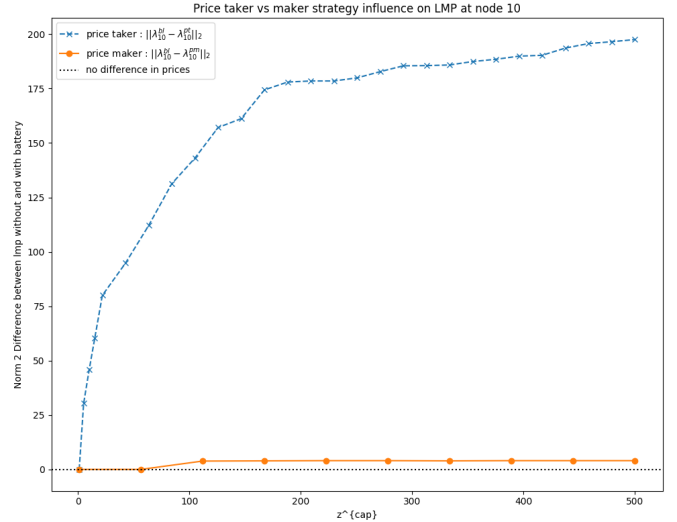


Fig. 7: $\|\lambda_p - \lambda\|^2$ as a function of z_{cap}

loads and bids data of the New Zealand wholesale market, on September 2, 2019. We created a baseline scenario by congesting node MDN. The results of the simulation confirm the soundness of the approach, with a price-maker making a better profit but also the price-taker earning actual revenues way below what was expected. The price-maker program will make sure it never completely solves the congestion as to benefit from its price-maker position over the congested area. A price-taker program, on the other hand, does not take the topology into consideration. Its brutal injection and withdrawing either creates or solves congestion, it ends up paying a higher price for this strategy. While these results hold for our simulation and for a specific setup of congestion, further work should look into characterizing the influence of a battery bidding strategy on the clearing prices and on the consumer and producer surplus of the market. If even a small battery can use its price-maker position over a congested area to benefit from high-price, this anti-competitive behavior when operated by larger-scale battery could impact the social welfare and should be studied in more details.

Further work should be conducted to further validate these first results namely :

- Validating our approximation of the Economic Dispatch program of the New-Zealand market with GAMS vSPD algorithm: <https://github.com/ElectricityAuthority/vSPD>,
- Validating our approximation of the bids of the New-Zealand market by comparing the predicted to the actual LMPs.
- Testing the program over a whole year,
- Taking into account the stochastic nature of the demand, of the generator bids into the optimization framework (robust optimization),
- Developing an online setup, using machine learning to predict the actors bidding strategy and the loads,

ACKNOWLEDGMENT

We'd like to thank Bertrand Travacca, Mathilde Badoual for their input on the project, as well as Pr. Moura for his advice during this semester!

V. TABLE OF RESPONSIBILITIES

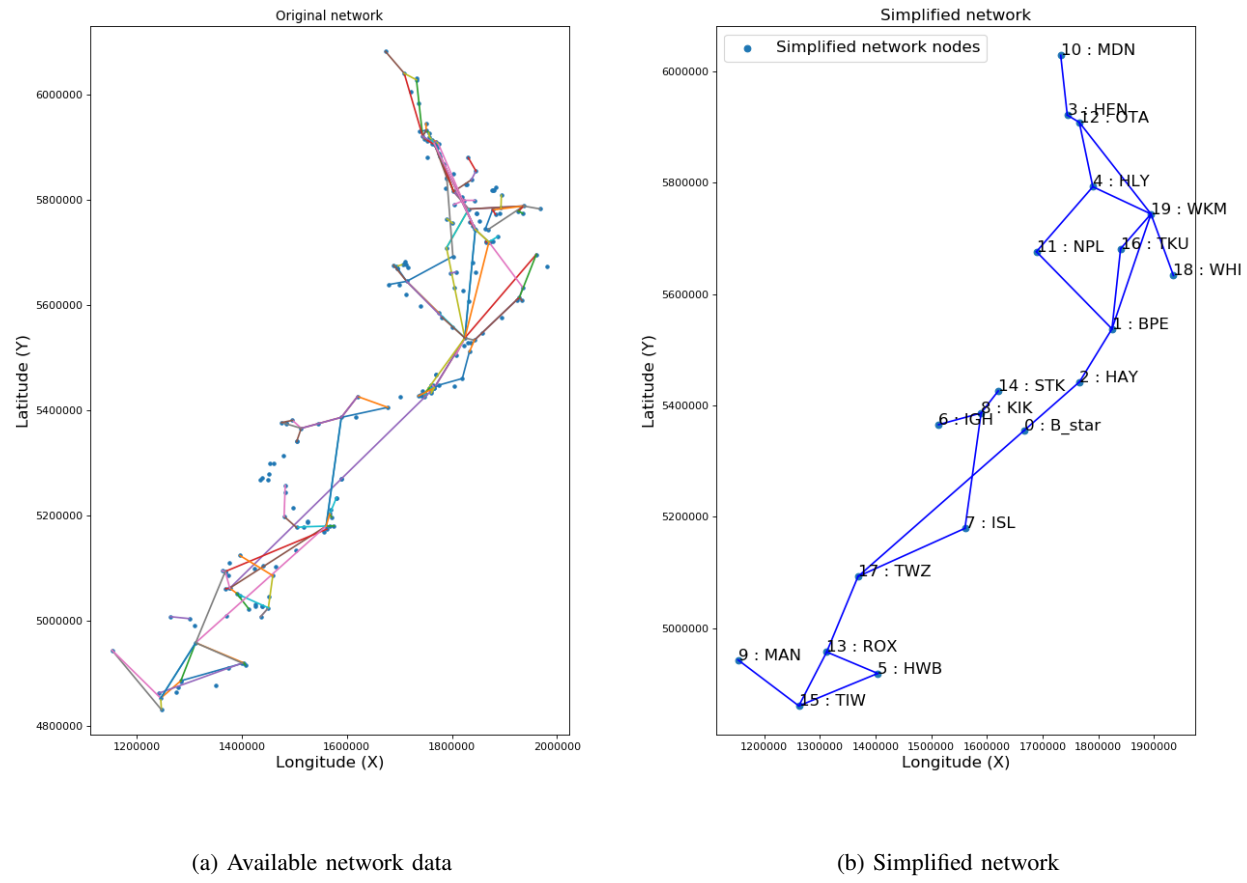
Salomé	<ul style="list-style-type: none"> 1. Literature review on bids and offers in the NZ wholesale market 2. Python program to generate bidding curves 3. Created the generator adjacency matrix in a json dictionary format 4. Power Point design with Kieran & Guillaume 5. Report's introduction, design & review
Charles	<ul style="list-style-type: none"> 1. Literature review on bids and offers in the NZ wholesale market 2. Literature review on the marginal costs of hydro and gas generators
Guillaume	<ul style="list-style-type: none"> 1. Theoretical development of the battery program 2. Python programs of the price-maker, price-taker Economic Dispatch program 3. Literature review on Bidding Optimization over Wholesale Markets
Kieran	<ul style="list-style-type: none"> 1. Literature review on Economic Dispatch in NZ 2. Presentation, Article python code for visualization 3. Python program for the topology of NZ 4. Design of the test-case and discussion of the results
Ramdane	<ul style="list-style-type: none"> 1. Literature review on Economic Dispatch in NZ

REFERENCES

- [1] E. Gimon, "How market rules are holding back energy storage," 2019. [Online]. Available: <https://www.greentechmedia.com/articles/read/energy-storage-wholesale-market-rules>
- [2] "Global grid-scale battery market size, market share, application analysis, regional outlook, growth trends, key players, competitive strategies and forecasts, 2019 to 2027," 2020.
- [3] "Technology roadmap - energy storage," 2014. [Online]. Available: <https://www.iea.org/reports/technology-roadmap-energy-storage>
- [4] P. L. Joskow, "Challenges for wholesale electricity markets with intermittent renewable generation at scale: the us experience," *Oxford Review of Economic Policy*, vol. 35, no. 2, pp. 291–331, 2019.
- [5] M. Petkovic, "Tesla big battery at hornsdale earns record revenue in september 2019," 2019. [Online]. Available: <https://reneweconomy.com.au/tesla-big-battery-at-hornsdale-earns-record-revenue-in-september-2019/>
- [6] A. S. Sidhu, M. G. Pollitt, and K. L. Anaya, "A social cost benefit analysis of grid-scale electrical energy storage projects: A case study," *Applied energy*, vol. 212, pp. 881–894, 2018.
- [7] S. V. . G. Parkinson, "The stunning numbers behind success of tesla big battery," 2018. [Online]. Available: <https://reneweconomy.com.au/the-stunning-numbers-behind-success-of-tesla-big-battery-63917/>
- [8] Aurecon, "Aurecon hornsdale power reserve impact study 2018," 2018. [Online]. Available: <https://www.aurecongroup.com/-/media/files/downloads/library/thought-leadership/aurecon-hornsdale-power-reserve-impact-study-2018.pdf>
- [9] Y. Du, R. Jain, and S. M. Lukic, "Effects of battery degradation on economic viability of energy storage systems participating in regulation markets," in *2017 IEEE Power & Energy Society General Meeting*. IEEE, 2017, pp. 1–5.
- [10] AEMO, "Hornsdale wind farm 2 fcas trial," 2018.
- [11] "Noen hornsdale wind farm fcas trial report," 2018.
- [12] P. D. N. Thomas Bowen, Ilya Chernyakhovskiy, "Grid-scale battery storage: Frequently asked questions," 2017. [Online]. Available: <https://www.nrel.gov/docs/fy19osti/74426.pdf>
- [13] K. Divya and J. Østergaard, "Battery energy storage technology for power systems—an overview," *Electric power systems research*, vol. 79, no. 4, pp. 511–520, 2009.
- [14] F. Cucchiella, I. D'adamo, and M. Gastaldi, "Photovoltaic energy systems with battery storage for residential areas: an economic analysis," *Journal of Cleaner Production*, vol. 131, pp. 460–474, 2016.
- [15] A. Nottrott, J. Kleissl, and B. Washom, "Energy dispatch schedule optimization and cost benefit analysis for grid-connected, photovoltaic-battery storage systems," *Renewable Energy*, vol. 55, pp. 230–240, 2013.
- [16] X. Wang, D. M. Vilathgamuwa, and S. S. Choi, "Determination of battery storage capacity in energy buffer for wind farm," *IEEE Transactions on Energy Conversion*, vol. 23, no. 3, pp. 868–878, 2008.
- [17] A. R. Prasad and E. Natarajan, "Optimization of integrated photovoltaic-wind power generation systems with battery storage," *Energy*, vol. 31, no. 12, pp. 1943–1954, 2006.
- [18] R. Dufo-López, "Optimisation of size and control of grid-connected storage under real time electricity pricing conditions," *Applied Energy*, vol. 140, pp. 395–408, 2015.
- [19] M. Kazemi, H. Zareipour, N. Amjadi, W. D. Rosehart, and M. Ehsan, "Operation scheduling of battery storage systems in joint energy and ancillary services markets," *IEEE Transactions on Sustainable Energy*, vol. 8, no. 4, pp. 1726–1735, 2017.
- [20] G. He, Q. Chen, C. Kang, P. Pinson, and Q. Xia, "Optimal bidding strategy of battery storage in power markets considering performance-based regulation and battery cycle life," *IEEE Transactions on Smart Grid*, vol. 7, no. 5, pp. 2359–2367, 2015.
- [21] M. B. Salles, J. Huang, M. J. Aziz, and W. W. Hogan, "Potential arbitrage revenue of energy storage systems in pjm," *Energies*, vol. 10, no. 8, p. 1100, 2017.
- [22] R. H. Byrne, T. A. Nguyen, D. A. Copp, R. J. Concepcion, B. R. Chalamala, and I. Gyuk, "Opportunities for energy storage in caiso: Day-ahead and real-time market arbitrage," in *2018 International Symposium on Power Electronics, Electrical Drives, Automation and Motion (SPEEDAM)*. IEEE, 2018, pp. 63–68.
- [23] H. Mohsenian-Rad, "Coordinated price-maker operation of large energy storage units in nodal energy markets," *IEEE Transactions on Power Systems*, vol. 31, no. 1, pp. 786–797, 2015.
- [24] S. A. Gabriel, A. J. Conejo, J. D. Fuller, B. F. Hobbs, and C. Ruiz, *Complementarity modeling in energy markets*. Springer Science & Business Media, 2012, vol. 180.
- [25] J. W. Mather, "Market design and analysis for uncertain, flexible, and decentralized power systems," Ph.D. dissertation, UC Berkeley, 2018.
- [26] A. J. Conejo, M. Carrión, J. M. Morales *et al.*, *Decision making under uncertainty in electricity markets*. Springer, 2010, vol. 1.
- [27] T. Alvey, D. Goodwin, X. Ma, D. Streiffert, and D. Sun, "A security-constrained bid-clearing system for the new zealand wholesale electricity market," *IEEE Transactions on power systems*, vol. 13, no. 2, pp. 340–346, 1998.
- [28] V. Mathiesen, "Mapping of selected markets with nodal pricing or similar systems australia, new zealand and north american power markets," 2011.

APPENDIX A
CASE STUDY : NEW ZEALAND

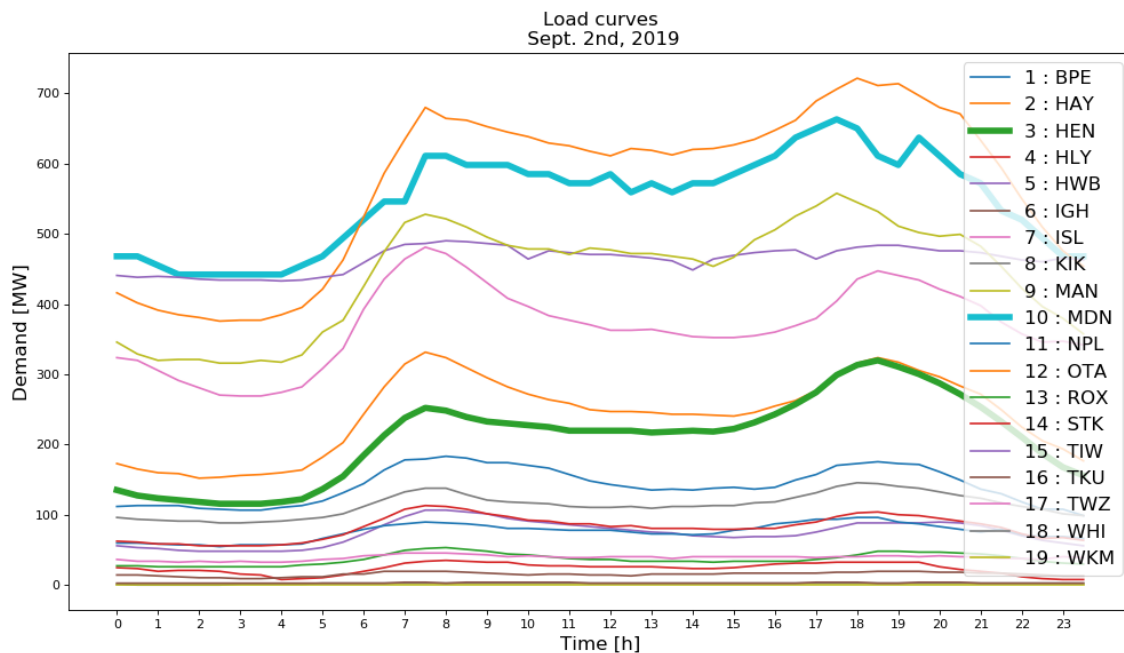
A. New Zealand Topology



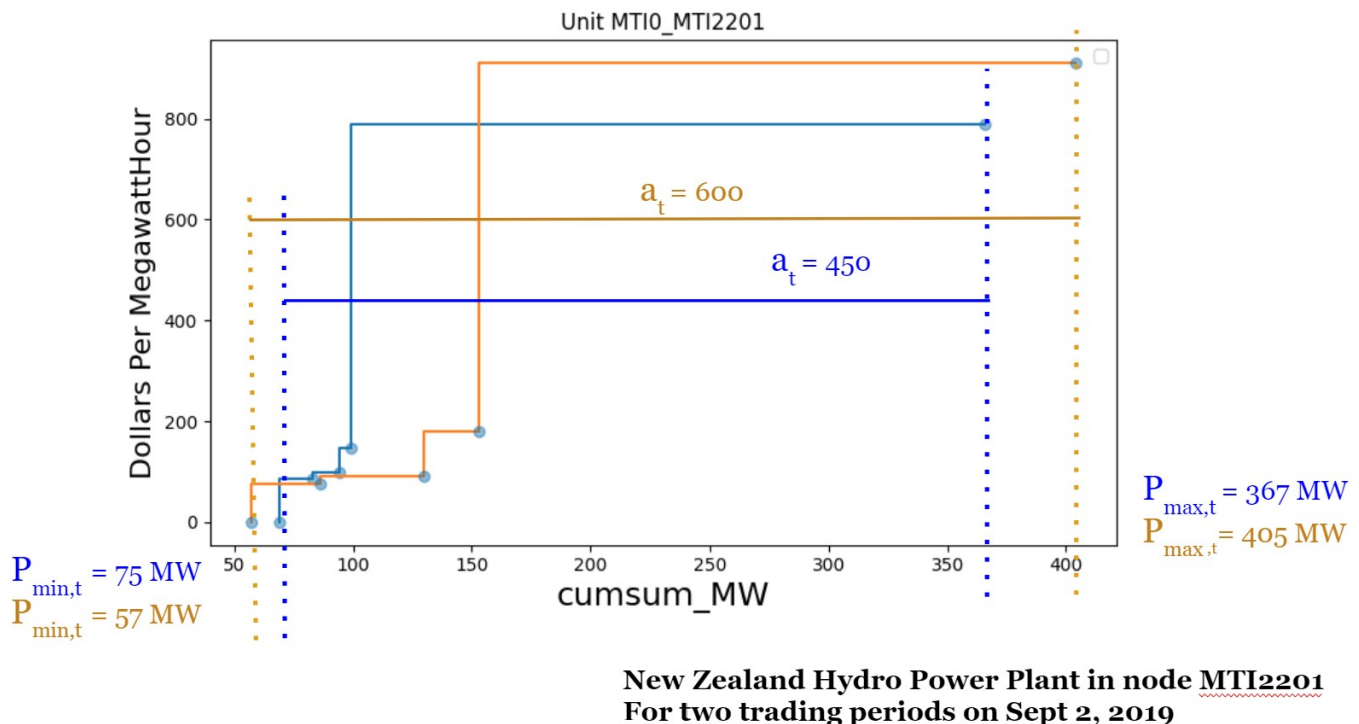
(a) Available network data

(b) Simplified network

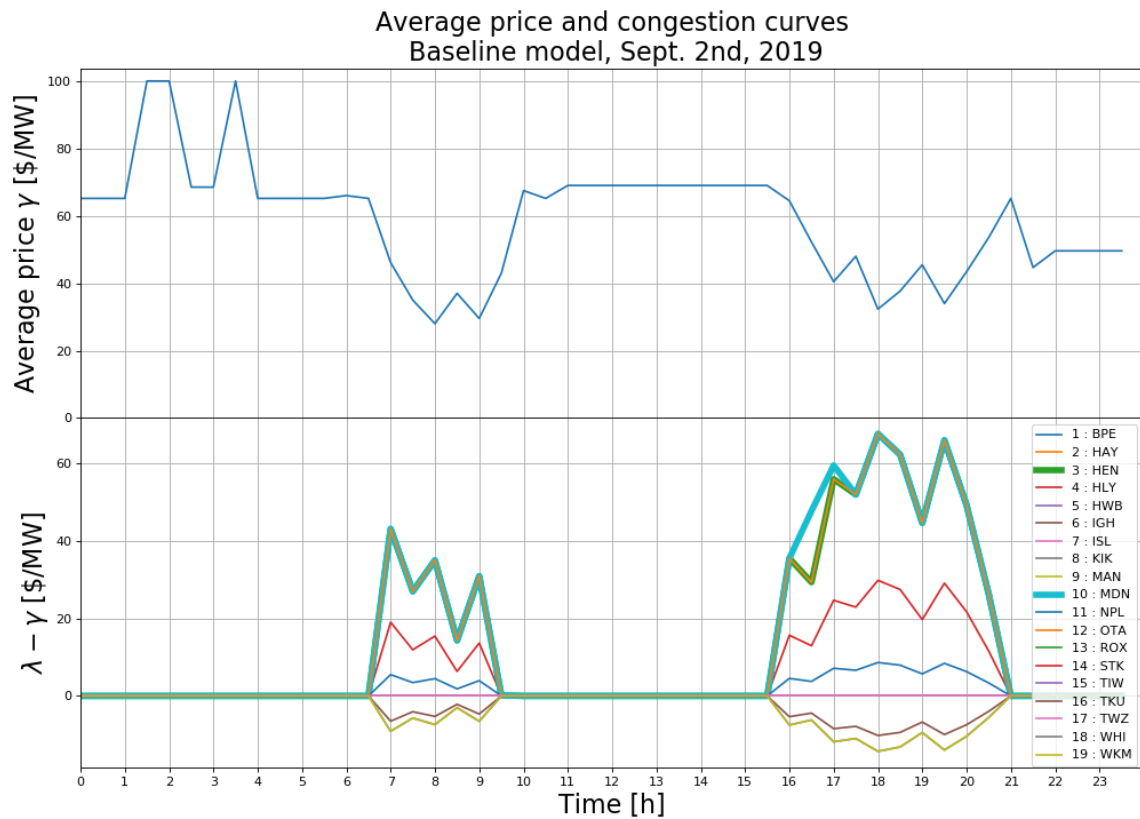
B. Load Curves



C. Example of bid curves



D. Gamma price and congestion curves for the baseline scenario



APPENDIX B
NODE AGGREGATIONS PER THE 19 NODES

Simplified node	Original nodes
MDN	BRB DAR KEN KOE KTA MDN MPE MTO WEL
HEN	ALB HEN HEP HPI SVL
OTA	BOB GLN MER MNG OTA PAK PEN ROS TAK WIR SWN
HLY	HLY TMN TWH
WKM	CBG EDG HAM HIN HTI KAW KIN KMO KPU LFD MAT MTI MTM NAP OKI OKE OWH ROT TGA TKH TMI TMU TRK WAI WHU WKM WKO WRK THI PPI ARA WPA ATI OHK ARI KPO
NPL	CST HUI HWA MIN MRA NPL OPK SFD WVY MKE KPA
TKU	TKU RPO
WHI	FHL GIS RDF TUI WHI WHI WRA WTU
BPE	BPE BRK DVK LTN MGM MHO MTN MTR NPK OKN ONG TNG TWC WDV WGN WPW
HAY	CPK GFD GYT HAY KWA MLG MST PNI PRM TKR UHT WIL WWD
STK	ARG BLN MOT MPI STK
KIK	KIK MCH
IGH	DOB GYM HKK KUM IGH WMG WPT ORO RFN ATU
ISL	ABY ADD APS ASB ASY BRY CLH COL CUL HOR ISL KAI KKA MLN OTI PAP SBK SPN SPN TIM TKA TMK WPR WPR
TWZ	BDP BPT NSY OAM STU TWZ WTK AVI BEN OHA OHB OHC TKB
ROX	CML CYD FKN ROX
HWB	BAL BWK HWB PAL PAL SDN TMH
TIW	BDE EDN GOR INV NMA TWI
MAN	MAN

APPENDIX C
ALL FIGURES FROM THE PAPER

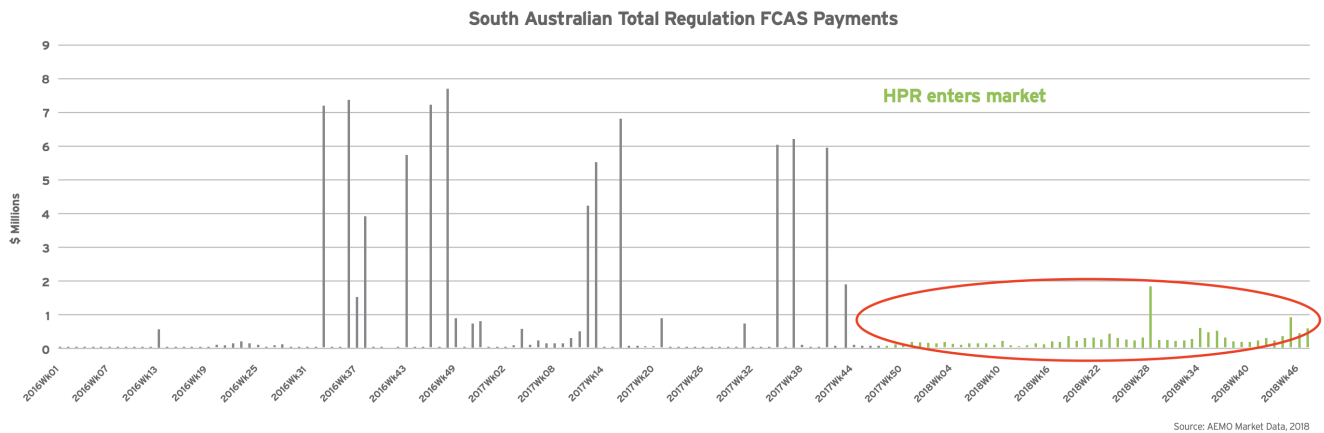


Fig. 1: South Australian Total Regulation FCAS Payments, 2016-2018 [8]

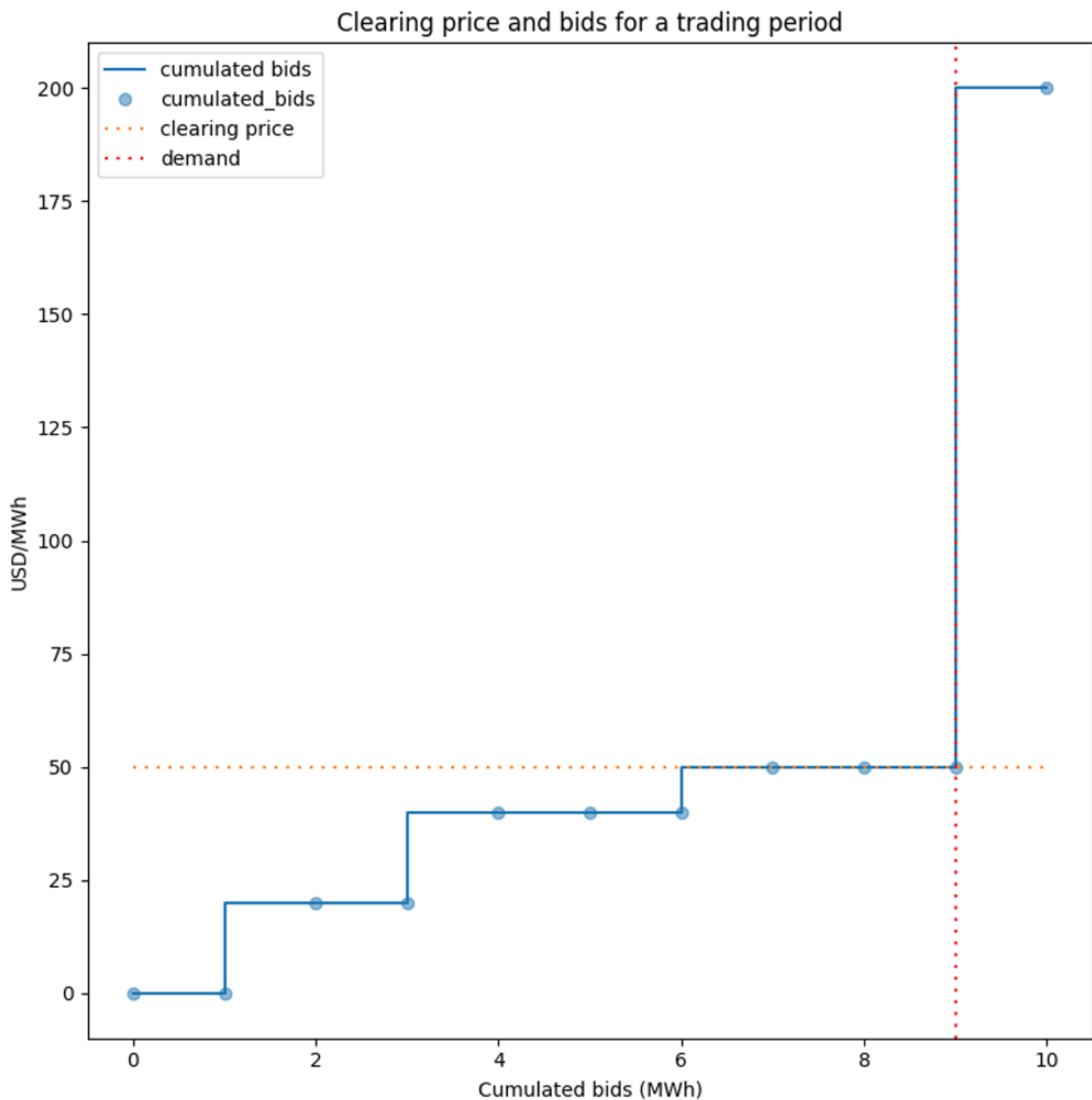
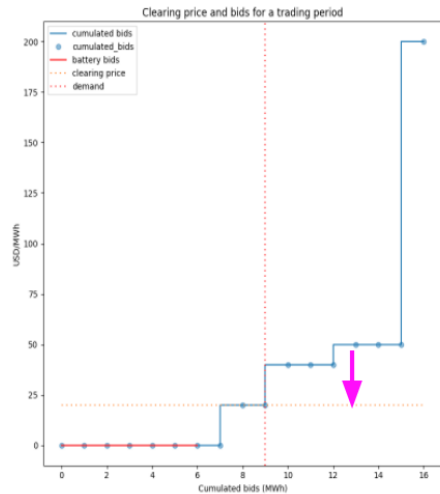


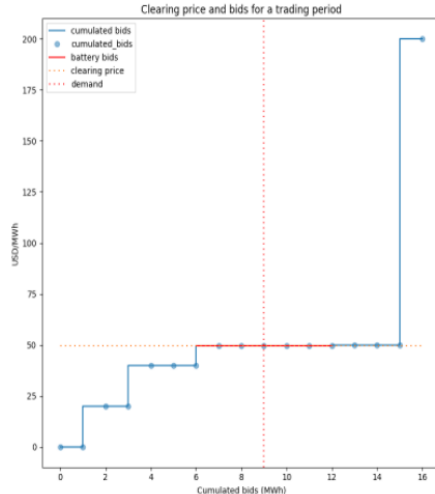
Fig. 2: Clearing price and bids without the battery

No strategy



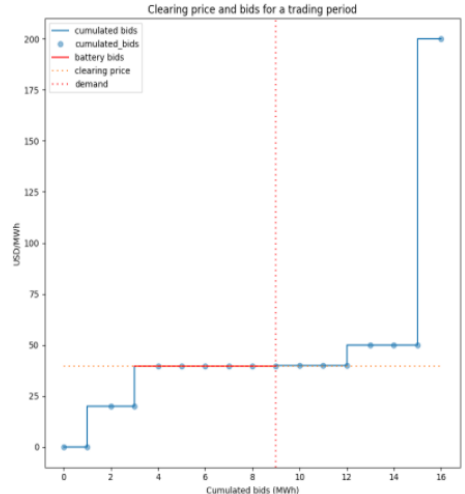
Clearing price collapsed: **\$20**
You make **\$120**

Bid at LMP (\$50)



λ not impacted (\$50)
Low cleared volume \mathbf{U}
You make **\$150**

Optimize



Maximize $\lambda_t^i * \mathbf{U}_t$
You make **\$240**

Fig. 3: Implementation challenges

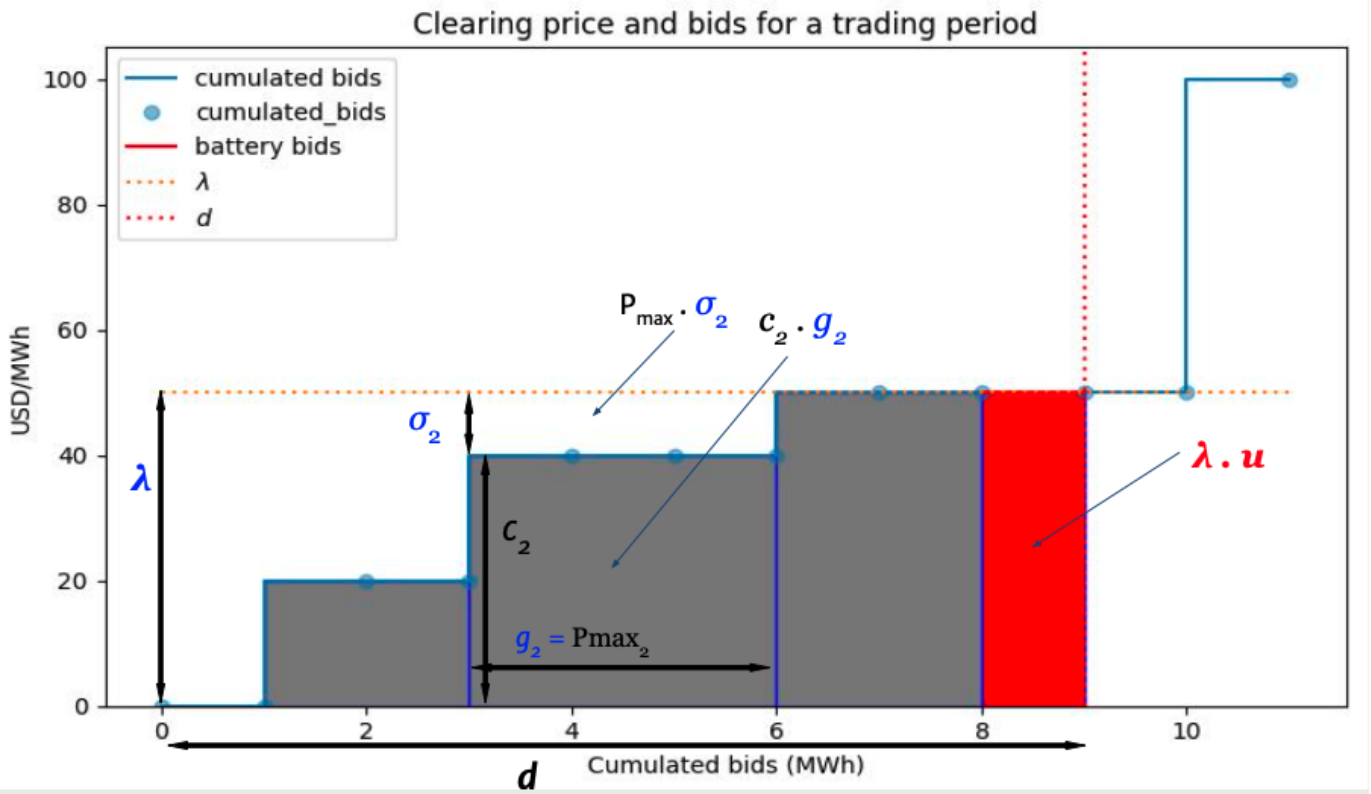


Fig. 4: Linearization of objective function for single-node wholesale market

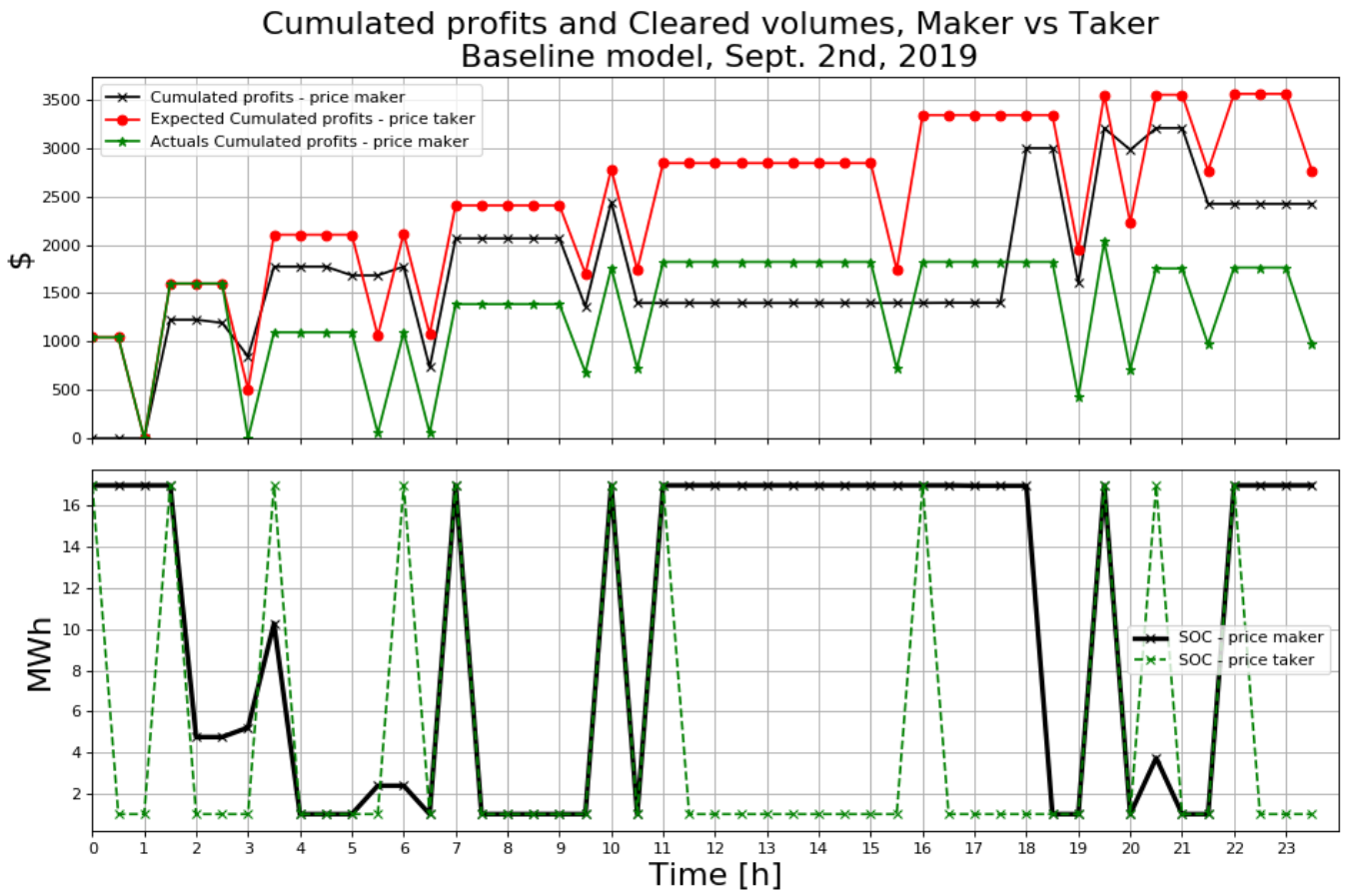


Fig. 5: Cumulated profits and SOC for price taker vs price maker program

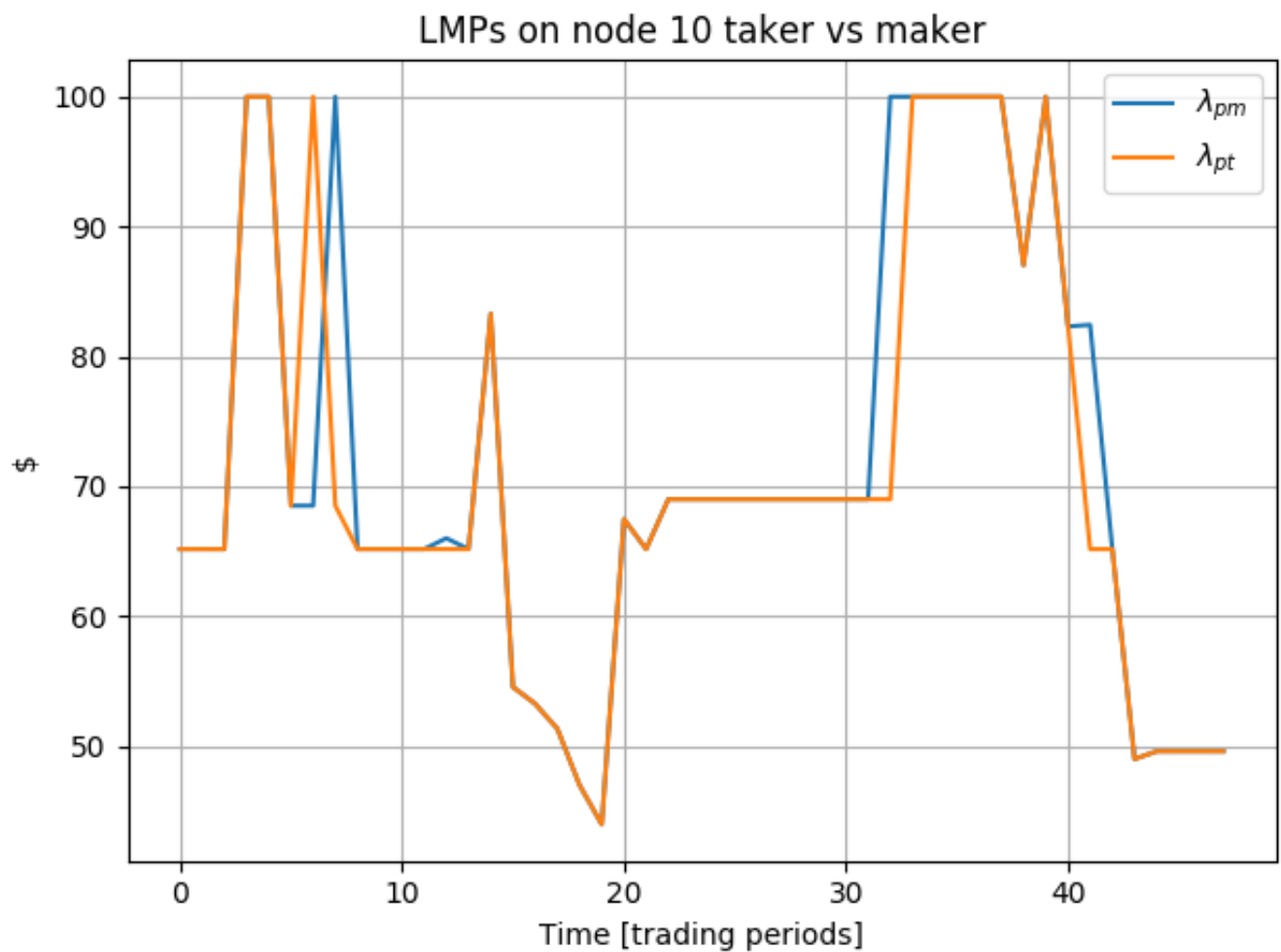


Fig. 6: LMP comparison at node 10 for base situation, price-maker case, price-taker case

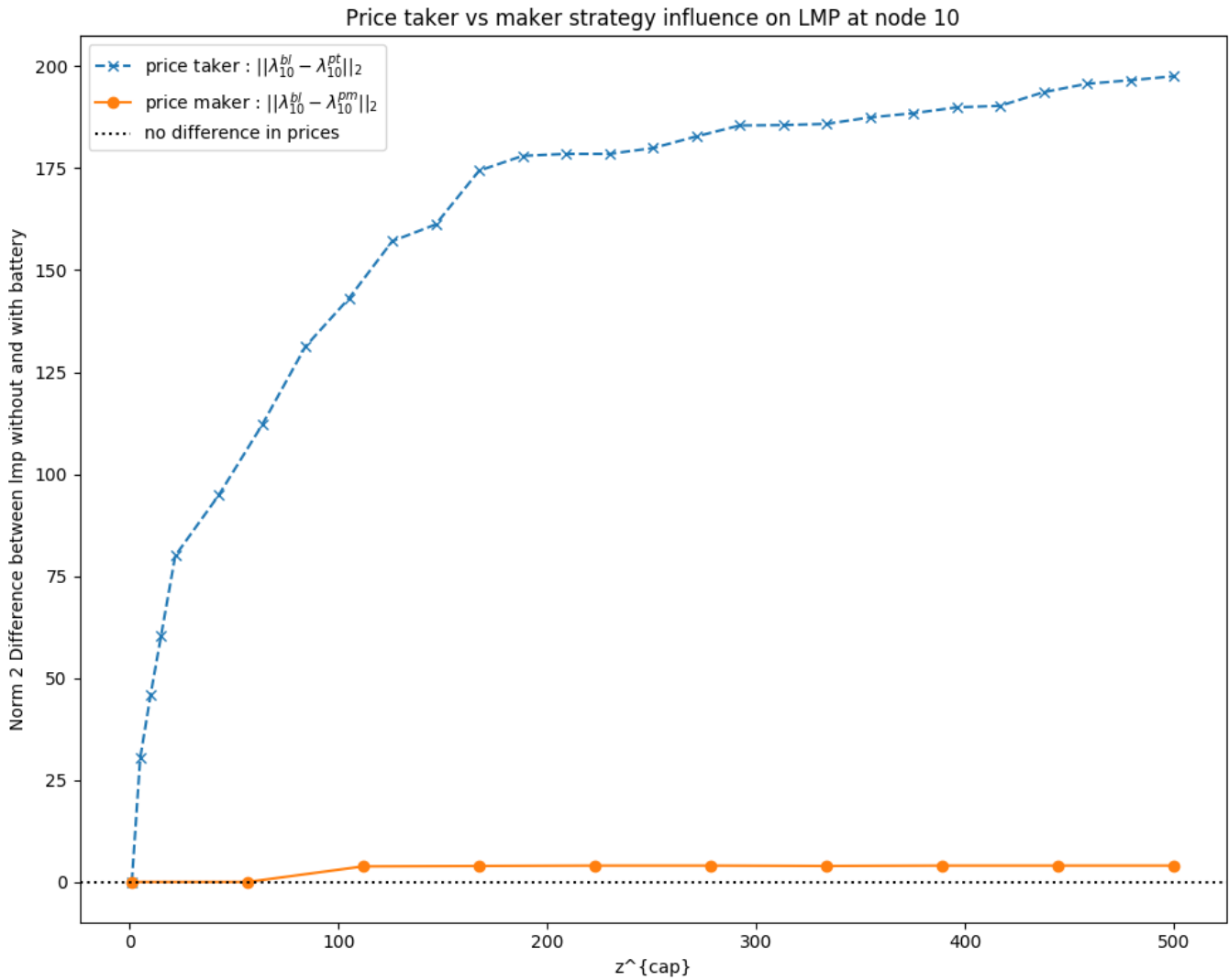


Fig. 7: $\|\lambda_p - \lambda\|^2$ as a function of z_cap

Hybrid plant economic dispatch

Margaret McCall, Will Gorman, Jess Carney
Cristina Crespo, Nick Clarke, Guangxuan Zeng

May 8, 2020

Abstract

Unlike conventional generation resources, solar power output fluctuates due to stochastic changes in weather. Batteries could mitigate variability, and project developers have an increased interest in hybrid projects, where a generator is co-located with a battery resource. In this project, we use electricity market prices in ERCOT to predict an optimal bidding strategy for a solar-plus-storage hybrid project in the wholesale energy and ancillary services market. First, we created an optimization program which maximizes wholesale market net revenue under both perfect foresight and a variety of system plant designs. We found that net revenue is most sensitive to the power size of the battery. Next, we develop three machine learning algorithms to predict the prices of regulation down market products: (1) Markov Chains, (2) Random Forest, and (3) Auto Regressive with Exogenous Inputs (ARX). These were compared against a persistence model as a baseline. We found ARX to be the most performant in forecasting price spikes, while the persistence model provided highest revenue. Finally, we ran multiple uncertainty cases with our optimization involving chance constraints as well as use of the machine learning price predictions and found a 2-5% reduction in net revenue from our perfect foresight case.

1 Introduction

1.1 Motivation and Background

Deployment of variable renewable energy (VRE) technologies such as wind and solar is growing rapidly in the United States. This growth is, in part, fueled by the rapid decrease in the cost of VREs over the last decade but also due to policy support and improving technology efficiencies. Average annual VRE penetration levels in the U.S. reached 9% in 2018, with independent system operators (ISOs) in California (CAISO) and the Plains region (SPP) reaching VRE penetration levels of 16% and 20%, respectively [1–3]. Certain regions have seen instantaneous VRE penetration levels higher than 60% [4].

Unlike conventional generation resources (e.g., fossil and nuclear power plants), VRE power output fluctuates due to stochastic weather patterns [5, 6]. Due to this variability and uncertainty, these technologies are more challenging to control on the power system. Many researchers have studied the impact of VRE technologies on the grid and found that renewables can be integrated at low penetration levels by taking advantage of balancing area cooperation, sub-hourly scheduling, regulation reserves, and transmission investment [7, 8].

However, research has also shown that as more VRE is integrated in wholesale markets, the value of those resources declines because VREs induce a price-suppression effect in wholesale markets during times of concentrated production [9–11]. Sometimes, this effect leads to negative prices at some locations, which increases VRE curtailment. Learning how to integrate these higher levels of VRE, though, is of practical importance; 11 states plus Washington D.C. have already adopted policies to mandate greater than 50% of their energy to come from carbon free energy, and 4 of those have mandated 80-100% clean energy standards [12].

Storage technologies could mitigate VRE variability and value degradation concerns, thereby facilitating larger penetrations of VRE on the system [13, 14]. While many types of storage technologies exist, the recent decline of battery storage costs has furthered interest in integrating battery technology onto the grid as a system asset [15, 16]. Additionally, project developers have an increased interest in the design of so-called hybrid projects, where a generator is physically co-located and paired with a battery resource at the point of interconnection (see Figure 10 in appendix) [17]. Though batteries and VRE do not need to be physically coupled to mitigate intermittency concerns, a developer's financial incentive to hedge against wholesale risk is motivating the growing interest in hybrid projects. Considering this increased interest in pairing batteries with VRE technology, this project aims to understand hybrid project dispatch in wholesale markets.

1.2 Relevant Literature

There has been a significant amount of literature surrounding the optimal dispatch of storage technologies in wholesale electricity markets. Early work focused on linear programming optimization techniques [18], while more recent strategies have explored dynamic programming techniques [19], and included more sophisticated modeling of battery life cycle and its effect on bidding in different markets (day-ahead energy, spinning reserve, and regulation markets) [20, 21]. We will rely on formulations described in this work but also engage with a growing literature on hybrid projects. This literature is much more nascent but has focused on applying the above techniques to the new hybrid project context [22]. Whilst the provision of ancillary services has historically been reserved to conventional dispatchable power plants, recent studies have shown how renewables have the technical capacity to offer AS, namely solar PV [23].

Similarly, much work has gone into developing machine learning techniques. In our project, reinforcement learning is suitable to analyze the dynamic behavior and constraints of a complex system with uncertainties [24], which is widely used in assessment of market power in day-ahead markets [25] and the incomplete information market [26] to design bidding mechanisms. We plan to apply these techniques in a new context to help understand how uncertainty in ancillary service prices affects battery management in a hybrid project.

To that end, research incorporating uncertainty in residential solar+battery energy management for building loads [27] will also be informative in our work.

1.3 Focus of the study

Considering this increased interest in pairing batteries with renewables, our project aims to develop optimization algorithms to determine an ideal dispatch strategy for hybrid projects across wholesale energy and ancillary service markets. We develop machine learning techniques to predict market prices and study how the resulting uncertainty of market prices affects the net revenue of our dispatch strategy in the new battery + solar context.

2 Methods

2.1 General modeling approach

Figure 1 shows how the two key elements of our project, prediction of AS prices and optimization of hybrid dispatch, are connected to each other. Overall, the prediction exercise serves as a data input to our optimization model. The battery dynamics in our hybrid plant are modeled in an AC-coupled configuration, and we ignore battery degradation costs in our implementation of the battery constraints (discussed in greater detail below). The optimization objective is to obtain the storage dispatch which maximizes net revenue in hourly energy and regulation down real-time markets. We assume that the hybrid system can either charge from the grid (full flexibility) or be limited to charge from solar plant only (due to the financial incentives of the investment tax credit).

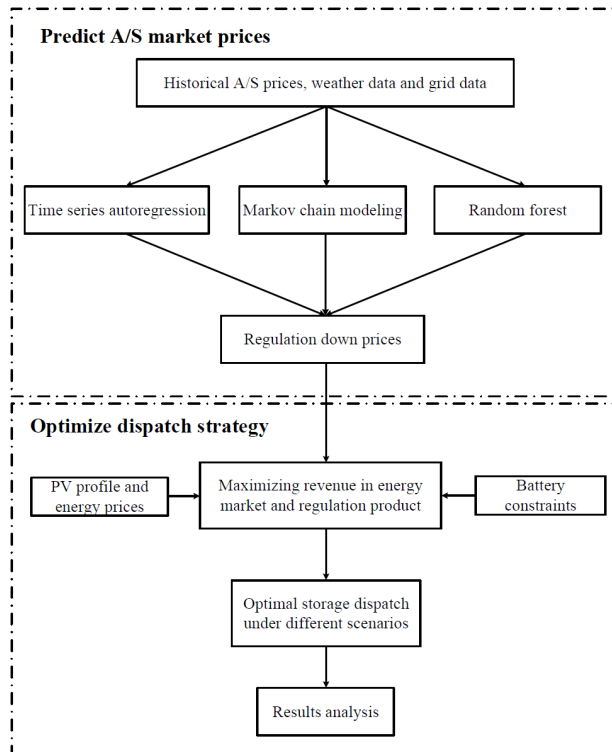


Figure 1: Project structure showing relationship between machine learning and optimization components

Key input data

1. Ancillary Service prices from ERCOT (actual 2018 and predicted 2018 discussed below)
2. Energy prices from West Hub in ERCOT (2018)
3. PV profiles modeled from weather data in west Texas

2.2 Machine Learning Implementation

2.2.1 Overview of approach

We compared several different machine learning approaches to predict regulation down prices, with the aim of generating a more realistic price prediction to feed into the optimization model. The data we collected to include in our model is as follows. All data is specific to ERCOT and is reported hourly:

1. Ancillary service bids, 2010-2019 (source: ERCOT)
2. Ancillary service procurement plan, 2014-2019 (source: ERCOT)
3. Ancillary service day-ahead (DAH) market prices and volumes, 2008-2018 (source: ABB)
4. Energy prices (DAH and hourly average realtime) by load zone, 2014-2018 (source: ABB)
5. Generation by source, load, and ramping requirements, 2010-2018 (source: CEMS and ERCOT)
6. Forecasted temperature by load zone, 2014-2019 (source: ERCOT)
7. Forecasted short-term wind power production, 2014-2019

For models incorporating all seven data sources (e.g., random forest), we used data from 2014-2017 as training data and from 2018 as test data. For models incorporating only regulation down prices, we were able to train on more historical data, from 2008-2017, and still use 2018 as our test data.

To evaluate our models, we opted against using a standard metric such as RMSE—instead, we evaluated the fraction of the time that the model correctly predicted that an hour would have a price spike. Here we have defined a price spike as a 90th-percentile regulation down price, based on data from 2014-2017; with this definition, an hourly regulation down price of greater than \$13.2/MWh constitutes a price spike. We used this cutoff to classify regulation down prices as either ‘spike’ or ‘regular’ hours. We decided to evaluate our models this way because storage plays an arbitrage role in the energy market, meaning that predicting which hours will have price spikes, and bidding in those hours, is more important than predicting the exact price. The spiky nature of A/S price data means that even a model that correctly predicted a price spike, but incorrectly predicted the magnitude (e.g., predicted \$100/MWh on real data of \$500/MWh), would have a misleadingly inflated RMSE even if the model performed well in the market.

For models that explicitly predict a categorical value (i.e., hours classified as ‘spike’ or ‘regular’) rather than a continuous price, such as the random forest model, we translated those categories into a continuous price to feed into the optimization program in the following way: for ‘regular’ hours, we assigned them the average regulation down price at that hour from 2014-2017. For ‘spike’ hours, we assigned them the average hourly price of ‘spike’ hours from 2014-2017 (\$25.6/MWh). Iteration with the optimization program could help determine the most useful way to conduct this translation.

2.2.2 Baseline scenario: Persistence model

We used a 24-hour lagged persistence model as our baseline for comparison of our other time-series forecasts. In this model, the regulation down price at time $t - 24$ was used as the predicted regulation down price at time t . For the random forest model, where we explored using 48-hour lagged data and omitting 24-hour lagged data, we built a 48-hour lagged persistence model for comparison.

Our decision to use multiples of 24-hour lags, both for our baseline scenario and our three main machine learning models, was based on our observation of significant auto-correlation at 24-hour intervals in the regulation down price data.

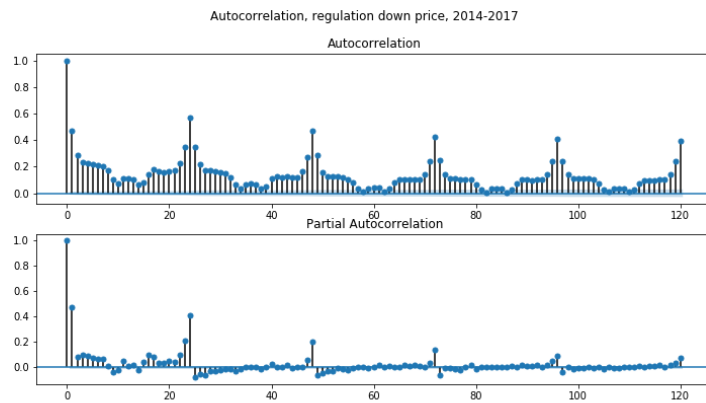


Figure 2: Autocorrelation and partial autocorrelation in the regulation down historical price data, indicating autocorrelation at 24-hour intervals

2.2.3 Approach #1: Markov chain model

We first programmed a Markov chain model to use historical patterns in regulation down prices to predict future prices probabilistically. Markov chain models calculate the probability of transitioning from one state to another between time steps. In our model, a state represents a given price bin (e.g., \$0-5/MWh). We decided to pursue the Markov chain model on the hope that it would recreate the spikes present in our data. Based on the auto-correlation present in the data with a period of 24 hours, we structured our Markov model to have 24 layers, one for the probabilities at each hour of the day.

To train the Markov chain model, we used hourly regulation down price data from 2008-2017. We cross-validated the model using the TimeSeriesSplit module from the Python package scikit-learn. In contrast to other cross-validation approaches, TimeSeriesSplit creates training and testing data that are faithful to the progression of time (i.e., training data always comes temporally before testing data). We cross-validated ($k=5$) the model to select the optimal number of price bins (40). (It should be noted that our Markov chain model produces continuous, not categorical, outputs; the output is processed into categories for purposes of evaluation.)

We implemented the Markov chain model using historical regulation down prices from 2008-2017 to build a Markov chain model that predicts regulation down prices for the entirety of 2018 at once. This approach assumes that a wealth of historical data will make the best model. However, were we to expand on this work, we could build a rolling model that uses the most recent 180 days' worth of historical regulation down prices to predict several days' worth of price data at a time. This would explore the competing hypothesis

that recent data will be a better predictor of prices.

We made two adjustments to our model to improve performance: first, we manually implemented an outlier cutoff for the top 0.5% of price spikes, setting those values to the cutoff values (\$54.6/MWh) instead, to curtail the model's frequent excursions to the \$500/MWh range. Second, instead of modeling all of 2018 at once (which, in a Markov chain model, entails inputting the first hour of a time series and probabilistically calculating the subsequent 8759 hours), we modeled it a week at a time to "reset" with real data and try to get the price spikes to line up more consistently.

2.2.4 Approach #2: Random forest model

Because predicting the exact hourly regulation down price with such spiky data tended to produce large errors, we decided to explore the possibilities of a classification model to explicitly predict whether a given hour constituted a price spike or not. We implemented a random forest classifier model to perform this classification. We settled on random forest after exploring several types of decision trees; random forest performed better than others in early testing, and to keep computational burden low with our large dataset, we decided to narrow our focus. However, future work could reincorporate different classification models.

To construct our random forest (RF) model, we classified hours as either 'spikes' or 'regular' depending on whether they were above or below the 90th-percentile regulation down price, as explained in section 2.2.1. This acted as our target variable.

We processed our feature variables by splitting our features into those that needed to be lagged (e.g., A/S price and generation data for hour t) and those that could be used synchronously with the hours they were meant to predict (e.g., wind production forecasts and weather forecasts for hour t). For features that needed to be lagged, we lagged them by 24, 48, and 72 hours. Finally, we engineered several features that would ordinarily only be included as lagged variables—namely, load, net load, coal generation, and NGCC generation at time t . Due to the relatively high correlation between these features and regulation down price seen in our exploratory data analysis (.17-.33—weak to low moderate correlation, but stronger than most others), we hypothesized that predicting values for these four variables and including them synchronously could improve the model. We used a RF regressor model with all the same features (lagged and synchronous) to predict these four variables, and then incorporated them as features into our main RF model. (RF outperformed OLS and Ridge substantially in these predictions, with an RMSE on the order of 500 compared to 2000.) Our full training dataset had 43814 observations and 225 features.

We then followed a three-stage approach in constructing our RF model. We first built a RF model with 168 features, dropping by hand several redundant features (e.g., temperatures and energy prices from each ERCOT region). Next, we added our 4 engineered features. Finally, we reviewed the feature importance to downselect to the 20 most important features. Our 4 engineered features were among the most important. (Although a preferred method of downselecting to the most important features would have been to recursively eliminate features to determine those with the greatest impact on model performance, the size of our dataset and computing/time limitations led us to use scikit-learn's built-in feature importance metrics as a proxy.) We built a new RF model with this subset of features, which led to substantial improvements in runtime and improvements in spike prediction accuracy. We attempted to tune the hyperparameters of this model, but could not achieve greater accuracy than with the default hyperparameters.

The graph below shows sequential improvements in validation set spike prediction with each step. We pursued this process twice: once for a model including the 24-hour-lagged data, and once without the 24-hour-lagged data. The latter model is likely to be more faithful to real-world data availability.

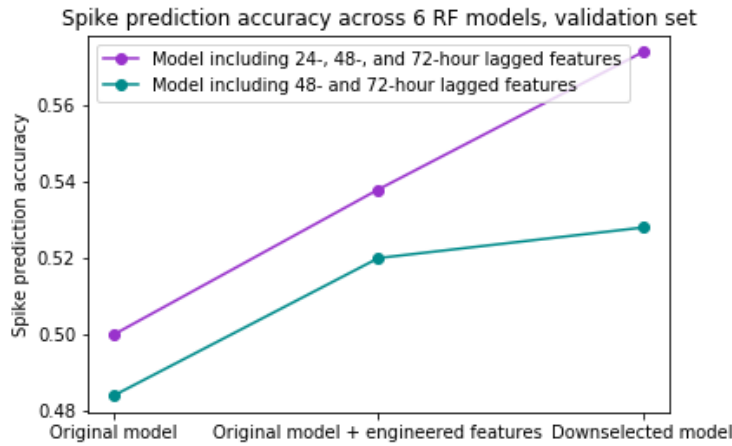


Figure 3: Sequential improvement in validation set accuracy for 2 main models (one with 24-, 48-, and 72-hour lagged features; another with only 48- and 72-hour lagged features) each with 3 sub-models.

2.2.5 Approach #3: Auto-regression model

The final machine learning model we implemented was an auto-regressive model with exogenous inputs (ARX), which estimates the next value in a time series as a function of the previous values and some external variables. We chose to use this model because of its simplicity and since it would allow us to clearly see which variables have the most impact on price.

The first step was to divide the full time series (2014-2018) into training (2014-2017) and testing (2018) data. Over 60 exogenous variables were available for use in the model, so the next step was to streamline these variables. This was done with a simple correlation analysis to see which variables had the greatest correlation with price. Any variables with an absolute value of correlation below 0.15 were removed, leaving 23 exogenous variables. We found bid price and quantity, the amount of ancillary services required, system load, and renewable and natural gas generation had higher levels of correlation with ancillary service price than temperature, ramping rates, and hydroelectric, nuclear, and coal generation.

Next, we created a 24, 48, and 72 hour lag matrix of both endogenous and exogenous variables padded with hour on each side, and split into training and testing data. This fed into a standard ARX model, using AutoReg method of Statsmodels, a well-known python package for time series forecasting. From this fitted model we extracted a vector of predictions for 2018 to be fed back into the optimization.

While this had initial promising results, its overall performance in the optimization was found wanting. However, the model could likely be improved upon by a more rigorous selection of exogenous inputs using different cost functions, such as Lasso or Ridge. Furthermore, additional feature engineering should be performed, such as lags reaching back one or more years, rolling averages, etc.

2.3 Optimization Implementation

2.3.1 Baseline scenario: Deterministic Linear Program Formulation

The results from the above section flowed into the optimization program we developed to maximize the hybrid project's net revenue. We outline the objective function (1a), optimization variables, and constraints (1b-1j) of our deterministic linear program below. The objective function maximizes the net revenue from energy prices (P_E) and regulation down prices (P_R) which our hybrid plant receives by both providing energy

services in MWh (G_E) as well as regulation down reserves in MW (G_R). Most of the constraints in our problem involve making sure the battery is balanced. Constraints 1b through 1f ensure that none of the limits of the battery are exceeded. The energy limits are linearly modeled with the state of charge at a given timestep (SOC(k)), and the discharge (B_d) and charge (B_c) limits cannot exceed the power capacity of the battery (C).

Constraint 1g describes the linear energy balance equation which is driven by: (1) the prior SOC, (2) the battery charge or discharge in a given hour, (3) the efficiency of the discharge (η), and (4) the accounting of energy due to regulation down services ($\epsilon * G_R(k)$). We assume that when our battery provides regulation, it will be called in real-time 20% of the time, which is implemented with the ϵ term. This term is positive in our formulation because regulation down effectively involves ramping down the power output of the hybrid system, thus increasing the available energy for the next time step.

Our final three constraints (1h-1j) involve modeling the amount of regulation product and energy service our hybrid plant can provide. The regulation product is constrained by the amount that our power plant can ramp down in a given hour, which at a maximum is driven by the batteries ability to charge (C) and the amount of energy it is currently discharging in a given timestep (B_D). However, if the battery is already charging, it is limited in how much regulation it can provide, thus the negative value of B_C . The energy service has to equal the amount of exogenous solar generation ($S(k)$) and whether the battery is charging or discharging in a given hour. Finally, constraint 1i limits the energy output to be less than our interconnection limit (S_{max}) and whether we allow for grid charging via an indicator variable I_g .

$$G_E, G_R, B_c, B_d, SOC \underset{\text{minimize}}{\sum_{k=1}^{8760}} -(P_E G_E(k) + P_R G_R(k)) \quad (1a)$$

$$\text{subject to} \quad 0 \leq SOC(k) \leq Y \quad k = 0, \dots, 8760, \quad (1b)$$

$$0 \leq B_c(k) \leq C, \quad (1c)$$

$$0 \leq B_d(k) \leq C, \quad (1d)$$

$$B_d(k) + B_c(k) \leq C, \quad (1e)$$

$$SOC(0) = 0, \quad (1f)$$

$$SOC(k+1) = SOC(k) + \eta B_c(k) - \frac{B_d(k)}{\eta} + \epsilon G_R(k), \quad (1g)$$

$$G_R(k) \leq C + B_d(k) - B_c(k), \quad (1h)$$

$$-I_g C \leq G_E(k) \leq S_{max}, \quad (1i)$$

$$G_E(k) = S(k) + B_d(k) - B_c(k) \quad (1j)$$

In this formulation, the machine learning team provides predictions for the P_R price.

2.3.2 Modelling under uncertainty: Chance constraints formulation

We now discuss modeling of the solar uncertainty via chance constraints. Prior to this section, we have considered a deterministic timeseries for the solar resource. To model the variability of solar, we will use a reformulation of the grid balance constraint (1j) to convert our deterministic problem into a Chance Constraints problem. That is, we will consider that the solar power $S(k)$ is the product of a constant solar plant size (100MW) and a random variable that models the capacity factor: $S(k) = sCF(k)$

$$S(k) \sim \mathcal{N}(\bar{S}(k), \sigma_s^2) \quad (2)$$

Since we cannot solve our optimization using random variables (shown in red) we will solve in expectation. In order to do so, we will relax the grid balance rule into chance constraints (3i,3j), allowing for them to be

violated a percentage of the timesteps. In practice, this means changing the grid balance *equality* constraint to two *inequality* constraints. The probability of the constraints being satisfied is coded by $\alpha = 5\%$, which means that 95% of the time we are respecting the constraints.

Linear Program 3 shows the implementation of chance constraints, under the hypothesis that the distribution of the solar capacity factors is normal. The distribution has been centered and normalized to Gaussian distribution $\mathcal{N}(0, 1)$. In this case, the grid constraint becomes second order cone constraints.

$$G_R, B_c, B_d, SOC \underset{k=1}{\text{minimize}} \sum^{8760} -(P_E(B_d(k) - B_c(k) + \bar{S}(k)) + P_R G_R(k)) \quad (3a)$$

$$\text{subject to } 0 \leq SOC(k) \leq Y \quad k = 0, \dots, 8760, \quad (3b)$$

$$0 \leq B_c(k) \leq C, \quad (3c)$$

$$0 \leq B_d(k) \leq C, \quad (3d)$$

$$B_d(k) + B_c(k) \leq C, \quad (3e)$$

$$SOC(0) = 0, \quad (3f)$$

$$SOC(k+1) = SOC(k) + \eta B_c(k) - \frac{B_d(k)}{\eta} + \epsilon G_R(k), \quad (3g)$$

$$G_R(k) \leq C + B_d(k) - B_c(k), \quad (3h)$$

$$\sigma_s \leq \frac{1}{\Phi^{-1}(1-\alpha)} [-B_c(k) + B_d(k) + \bar{S}(k) + I_g C], \quad (3i)$$

$$\sigma_s \leq \frac{1}{\Phi^{-1}(1-\alpha)} [B_c(k) - B_d(k) - \bar{S}(k) + S_{max}] \quad (3j)$$

To refine our model, we will modify these chance constraints by using the inverse of the cumulative distribution function of our solar capacity factor datasets, over four years (2015-2018), instead of supposing a specific distribution function as we did with the Gaussian distribution above (optimization program 3). In this case, we will again use a random variable for the capacity factor, which will model though the inverse of its cumulative distribution function (cdf) $F(x)$. That is: $S(k) \sim sF(u)$, where the u variable are the solar capacity values and s is the parameter for the solar plant size ($s = 100MW$). CDF graphs can be found in the Appendix.

We rearrange optimization program 3, by changing the objective function and the chance constraints as follows:

$$G_R, B_c, B_d, SOC \underset{k=1}{\text{minimize}} \sum^{8760} -(P_E[B_d(k) - B_c(k) + sF^{-1}(1-\alpha)] + P_R G_R(k)) \quad (4a)$$

$$\text{subject to } -I_g C \leq -B_c(k) + B_d(k) + sF^{-1}(1-\alpha), \quad (4b)$$

$$-S_{max} \leq B_c(k) - B_d(k) - sF^{-1}(1-\alpha) \quad (4c)$$

All scenarios' inverse cdfs timeseries values were calculated at $\alpha = 5\%$. We can summarize the scenarios we created for the chance constraints in the optimization programs 3 and 4 in the following way:

1. *CC normal dist*: We used the constant value of the inverse of a centered and normalized Gaussian distribution, and calculated the average and standard deviation of the distribution that resulted from taking the average of each hour across the years 2015-2018
2. *CC hist cte*: We used a constant value of the inverse of the cdf that resulted from taking the average of each hour across the years 2015-2018 (black line on Figure 11b).

3. *CC hist TWD*: We created an hourly Typical Weather Day timeseries by sampling the cdf of each hour that resulted from stacking all values of capacity factors over the period 2015-2018 (Figure 11a). We repeated this typical day (24 timepoints) throughout the optimization timesteps
4. *CC hist TWSD*: We created an hourly Typical Weather *Seasonal* Days timeseries by sampling the cdf of each hour that resulted from stacking all values of capacity factors over the period 2015-2018, grouping by seasons (three month periods), to account for seasonal variations in solar resource and daylight savings. We repeated this typical day (24 timepoints) throughout the optimization timesteps

3 Results

3.1 Machine Learning: price prediction results

Model	Spike prediction accuracy	Overall prediction accuracy
Persistence model (24 hrs ahead)	.541	.950
Persistence model (48 hrs ahead)	.458	.942
Markov chain	.174	.767
Random forest (24 hrs ahead)	.467	.955
Random forest (48 hrs ahead)	.461	.956
ARX	.860	.800

Table 1: Test accuracy for each model (test data: 2018)

Only the ARX model significantly outperformed the persistence model (86.0% spike prediction accuracy compared to 54.1%), although the 48-hour ahead random forest model slightly outperformed the 48-hour ahead persistence model (46.1% spike prediction accuracy compared to 45.8%). Due to the random nature of this model, more runs would need to be performed to determine if this outperformance persists on average.

Below are selected visualizations of predicted and test data.

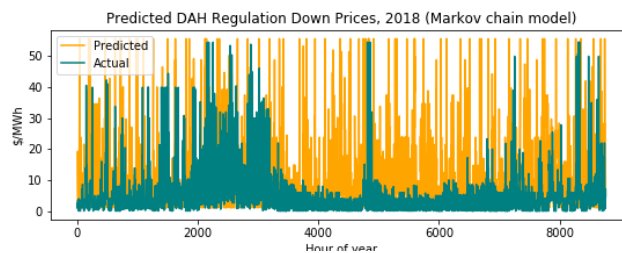


Figure 4: Markov chain model, predicted prices versus actual prices

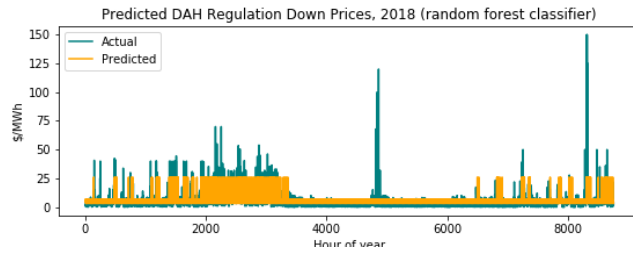


Figure 5: Random forest model (48 hours ahead), predicted prices versus actual prices

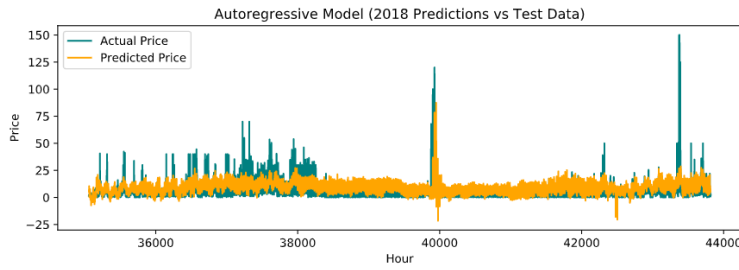


Figure 6: Auto-regressive with Exogenous Inputs model, predicted prices versus actual prices

3.2 Optimization: results analysis

3.2.1 Sensitivity analysis

First, we present the results of our base case perfect foresight optimization. We validated our model by plotting two optimization variables: (1) the hybrid power plant output and (2) the storage charging. Figure 7 shows these results for each season of our analysis averaged over the hour. Overall, the battery is serving to shift solar generation from time periods of low prices to time periods of high prices, as we would expect. The next result we analyzed was a sensitivity analysis of a variety of the design specifications of our hybrid power plant. Figure 8 shows how the revenue our power plant generates changes as we adjust the various parameters. The key parameters we varied were storage duration, efficiency, power output, solar plant size, and interconnection limits. Storage power output had the biggest affect on revenues while the interconnection limit had a non-linear interaction with revenues. Storage duration appeared to have the least effect, suggesting that costs can be saved upfront by limiting the total amount of energy capacity of the battery.

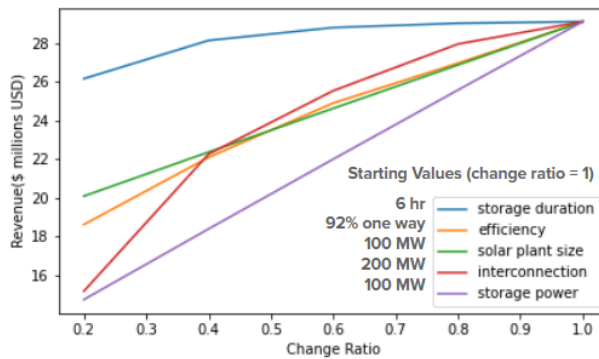


Figure 8: Sensitivity analysis of parameter space against net revenues

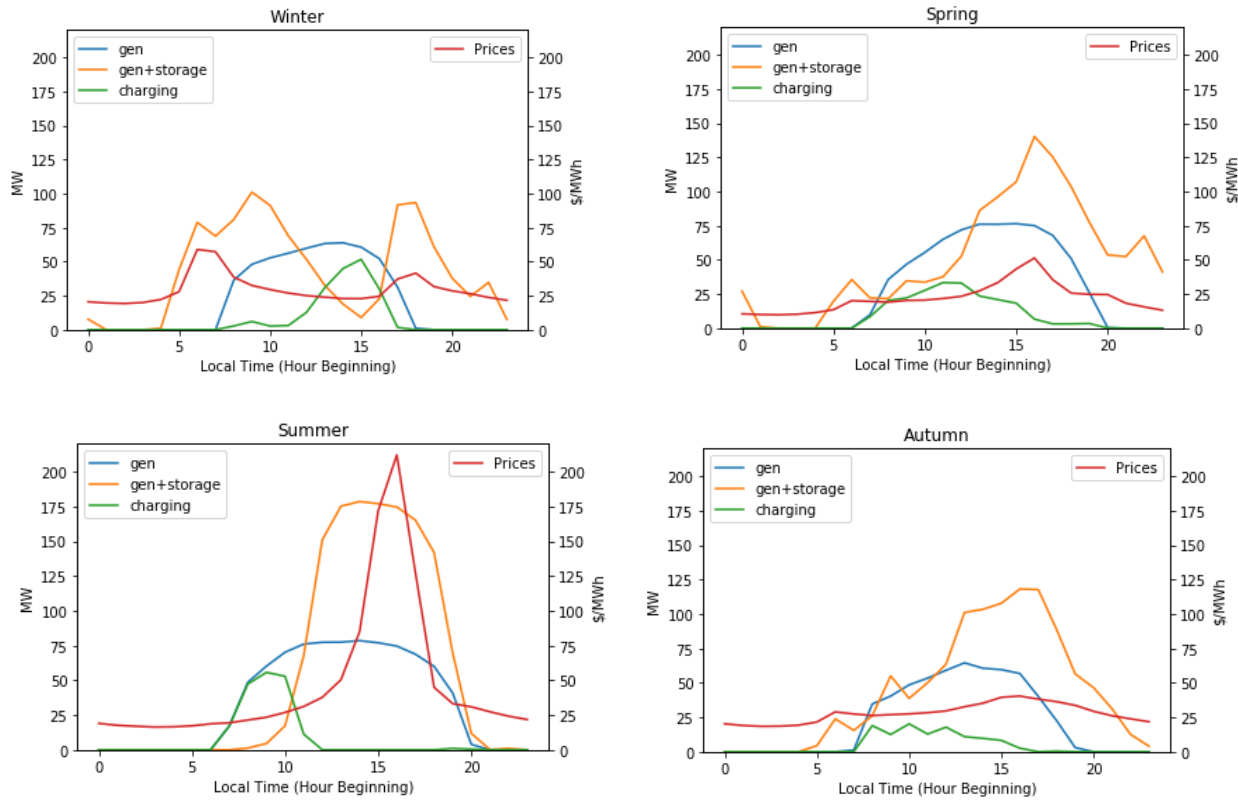


Figure 7: Optimization results by season

3.2.2 Scenario comparison

We now present the comparison of the optimization results from our base case (deterministic, perfect foresight) to the different chance constraints scenarios presented in Section 2.3.2 (to model solar resource uncertainty) and the machine learning forecasts models presented in Section 2.2.2 (predicting ERCOT down regulation market prices).

Figure 9 shows the results for all scenarios, with triangles showing solar uncertainty (chance constraints) scenarios and circles showing AS market forecast (machine learning) scenarios. These sets of results were produced by performing a two step approach. First, we run our optimization with the stochastic solar distribution or the forecast prices (depending on the scenarios) to retrieve the the optimization variables that resulted, that is, the scheduling of the hybrid plant. Next, we recalculated the actual net revenue that the hybrid plant would receive by operating under the optimized schedule, but with the true values of solar resource and market prices.

As we can see from 9, we consistently get higher net revenue when allowing the hybrid plant to charge the batteries from both onsite solar and the grid (*Grid charging allowed*) in comparison to only charging the batteries from onsite solar generation (*Only onsite charging*). This is an expected result since the hybrid plant has a greater opportunity to generate revenues in this case, charging from the grid at moments of low energy market prices and selling to the grid when energy market prices are high. The only scenario that is an exception to this overall trend is the chance constraint scenario using only a unique value of the inverse cdf as a proxy for the capacity factor at all hours, which is our least refined chance constraint. This supports the idea that further refinement of the chance constraint helps us improve our bidding, ultimately resulting

in similar expected revenues in comparison to the perfect foresight case.

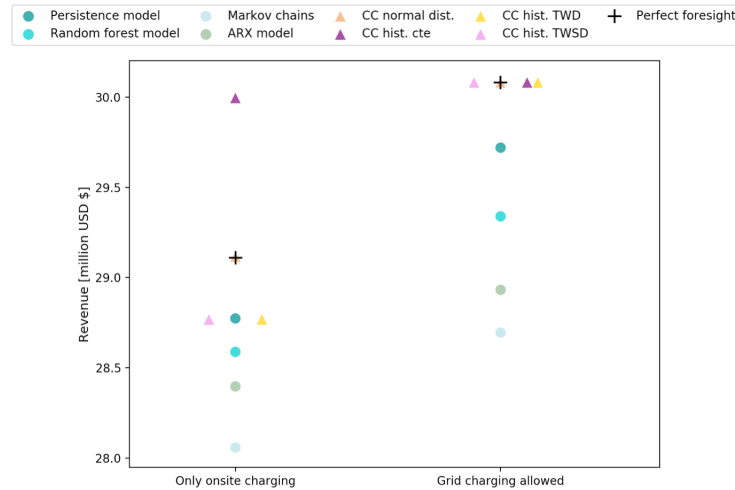


Figure 9: Revenue with forecasts of down regulation prices and chance constraints against perfect foresight

Contrary to the above observation, we can also see that the use of a *unique typical weather day* approach to the chance constraint optimization yields very similar results to the use of *seasonal typical weather days*, suggesting the *unique typical weather day* modelling strategy is sufficient. Indeed, the second order cone constraints program, which assumes a normal distribution of the solar capacity factor cdfs (optimization program 3), performs the best out of all scenarios in the case where we can only charge from onsite solar generation.

Interestingly, all chance constraints output the same net revenue when the batteries are allowed to charge from the grid. This suggests that the grid balance constraints limiting values are being reached at exactly the same timesteps.

With regards to the scenarios that forecast down regulation prices, we can see that the simpler persistence model outperforms all other approaches, both when the hybrid plant is allowed to charge from the grid and when it is not. This is a surprising result given that the accuracy of the ARX model was higher than all other machine learning approaches. We also observe a greater spread in the net revenue values for the machine learning scenarios when grid charging is allowed since the algorithm more frequently incurs in forecast errors

4 Discussion

Having analysed the results of our project in Section 3, we devote the following section to comment the limitation of our methods, pose open questions and delineate natural next steps for the work presented.

Optimization methodology

In conceptualizing our co-optimization model we assumed that that our hybrid plant would only provide down regulation in the AS markets, and simplified its tradeoff with the energy wholesale market exclusively through a percentage of battery capacity that had to be reserved for the provision of such service, at all time-steps. This, however, does not correctly model the actual dynamics of the interaction of the energy and AS markets. Further work should explore more complex couplings of the markets in the co-optimised

dispatch programs, and address the non-convexities of the resulting constraints.

As regards to the uncertainty modelling, we created several scenarios using chance constraints derived from the cdf of historic capacity factor data. The way in which we sample from these cdfs could be improved; for example, we could group our samples per hour and month, instead of seasonally. An open question remains whether we should be sampling from the cdf that results from taking the average from a multi-year dataset of capacity factor values (black line on Figure 11b), or whether we should sample from the larger dataset composed of all values for each hour from the historic datasets (red line on Figure 11b); in our modeling we used the former approach.

Next steps in the uncertainty scenario analysis would include performing Monte Carlo simulations to validate that the chance-constrained optimization solutions actually satisfy the grid limit constraints with probability 95%. The idea in this case would be to sample randomly the cumulative distribution function for solar capacity factors to check that the grid balancing constraints were satisfied (3i, 3j for the normal distribution assumption; 4b, 4c for the solar capacity factor historic distributions). A nuance to take into account when following this approach is that, in order to perform the random sampling from the *actual historic capacity factor* cdf chance constraints, we should use bootstrapping techniques to resample from our data since our sample size is relatively small. However, when assuming the centered and normalized Gaussian distribution of capacity factors we could use Monte Carlo directly to generate data based on the Gaussian $\mathcal{N}(0, 1)$.

Moreover, the use of a two-step approach explained in Section 3.2.2 to compare the perfect foresight case to the stochastic scenarios should be validated by ensuring that the resulting battery scheduling in the optimization is feasible with the actual solar resource.

Machine Learning models

In addition to the comments offered within the methodology section about how to improve specific modeling approaches, following are more general takeaways from our machine learning models.

Real-world application was a driving factor in our modeling. Our decision to incorporate 48-hour lagged data instead of 24-hour (or less) lagged data in our models was based on applicability. According to our industry partner, 48-hour lagged models are likely more useful than 24-hour lagged models, based on real-world data availability and bid timing. However, even data that is technically available 48 hours ahead of time (e.g., bid data) may not actually be public or accessible to forecasting teams. Thus, validating model performance under actual prediction conditions is important; this is especially so in situations where there may be a short turnaround time between getting key data and making bids, given that our random forest model runs quite slowly. Finally, to make the model more useful, we could explore the role of over-predicting price spikes (i.e., sacrificing overall prediction accuracy for spike prediction accuracy)—does this hurt revenue?

We have several reflections on model performance. First is the most surprising and unexplained aspect of our modeling: that the ARX model substantially outperformed all others in terms of spike prediction accuracy but underperformed them in terms of revenue generated. This suggests that spike prediction accuracy, despite its seeming relevance to bidding strategies, may not be the best metric with which to compare our models. Evaluating bid performance relative to the highest value hours may help clarify this further. However, it is equally possible there is some fault in our implementation. Also notable was that natural gas prices were strong predictors in the ARX model. Next, the Markov chain model may need further troubleshooting—it has a tendency to predict lots of spikes, which seems out of line with the training data. It could benefit from assessment of performance over time, since 2014 was a very spiky year and could have an outsize influence on the predictions.

Finally, for the random forest model, it was surprising that classification could at best barely equal the persistence model, given that we trained it with the same data used for the prediction model, and much more in addition to that. Given more time, we could have built models with different subsets of the available data to determine if some of it was muddying the prediction, or if random forests are simply not well-suited to this prediction problem. In the RF model, it was also surprising that the engineered features performed so strongly: the top 5 most important features in the 48-hour lagged model were, in order, the 48-hour lagged price, engineered NGCC generation, the 72-hour lagged price, engineered net load, and regulation down quantity. Bid data, interestingly, had no important impact on prices, despite the logical connection between bids and clearing price. We could potentially make better use of bid data by making a non-machine-learning-based market model. That could help us better understand how energy and A/S prices are co-optimized, as the black box of machine learning isn't drawing a strong connection.

5 Table of responsibilities

Team Member	Responsibilities
Will Gorman	Optimization: Deterministic constraints, AS modeling
Cristina Crespo	Optimization: Chance constraints modeling, Scenario analysis
Guangxuan Zeng	Optimization: Parameter sensitivity analysis, visualization
Margaret McCall	Machine Learning: Data acquisition/cleaning, Markov Chains, Random Forest
Jess Carney	Machine Learning: Results analysis, ARX
Nick Clarke	Machine Learning: Data cleaning, ARX, abandoned models (ARX+,RNN)

6 Summary

Battery technologies could mitigate renewable variability, and project developers have an increased interest in physically pairing batteries and renewables at the point of interconnection. In this project, we developed an algorithm for optimally dispatching “hybrid” projects, which co-locate solar and batteries, into the wholesale market of Texas using ML-backed forecasts of ancillary service prices. Overall, we found that the persistence model, where the optimization algorithm uses prices a day or two before as a predictor for today’s prices, performed best with our optimization algorithm. Across our range of ML-methods applied, net-revenue of our hybrid project only decreased by 2-5% as compared to our perfect foresight case. Though this impact is small, we believe there is much room for improvement via additional ML-methods. Furthermore, while our model focused on predicting ancillary service prices, it could be the case that predicting energy prices is more important. We relied on a perfect foresight of energy prices and look forward to implementing similar ML-methods to further refine our optimal dispatch strategy.

All python code for this project can be found in GitHub [click below]



github.com/nickolasclarke/anciML

7 Appendix

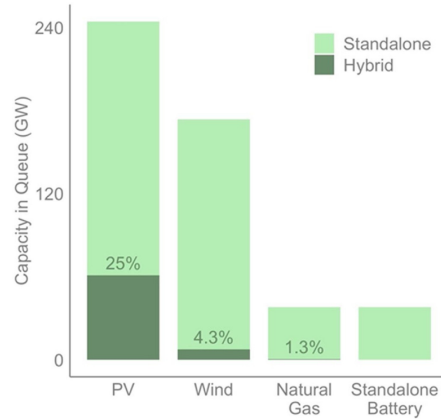


Figure 10: Percentage of projects pairing with batteries (i.e. “Hybrids”) in interconnection queues

Parameter baseline assumptions

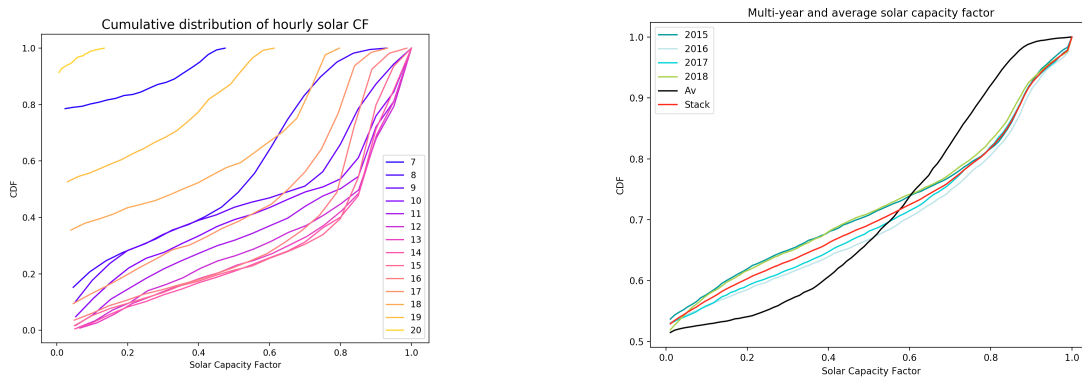
Table 2 below shows the system specifications and parameters implemented in our baseline battery model. We solve our optimization using the pyomo package within Python.

Parameter	Value
Storage duration	6h
Single trip battery efficiency	92%
Solar plant size	100MW
Interconnection AC limit	200MW
Storage power size	100MW

Table 2: System parameters for baseline case

CDF Modelling

Below are the figures plotting our cumulative distribution functions discussed in section 2.3.2.



(a) CF per hour for the period 2015-2018

(b) CF data for the period 2015-2018

Figure 11: Cumulative distribution functions (cdf) of solar hourly capacity factors (CF)

References

- [1] Ryan Wiser, Mark Bolinger, Galen Barbose, Naim Darghouth, Ben Hoen, Andrew Mills, Joe Rand, Dev Millstein, Seongeun Jeong, Kevin Porter, Nicholas Disanti, and Frank Oteri. 2018 Wind Technologies Market Report. page 103, 2018.
- [2] Mark Bolinger, Joachim Seel, and Dana Robson. Utility-Scale Solar: Empirical Trends in Project Technology, Cost, Performance, and PPA Pricing in the United States - 2019 Edition. Technical report, Lawrence Berkeley National Lab, December 2019.
- [3] EIA. Annual Energy Outlook 2019 with projections to 2050. Technical report, US Energy Information Administration, January 2019. URL <https://www.eia.gov/outlooks/aeo/pdf/aeo2019.pdf>.
- [4] Christian Roselund. California blows through solar power, renewable energy output records. *pv magazine*, page 16, May 2018. URL <https://www.pv-magazine.com/2018/05/01/california-blows-through-solar-power>.
- [5] Anne Sjoerd Brouwer, Machteld van den Broek, Ad Seebregts, and André Faaij. Impacts of large-scale Intermittent Renewable Energy Sources on electricity systems, and how these can be modeled. *Renewable and Sustainable Energy Reviews*, 33:443–466, May 2014. ISSN 13640321. doi: 10.1016/j.rser.2014.01.076. URL <https://linkinghub.elsevier.com/retrieve/pii/S1364032114000987>.
- [6] Kolbjørn Engeland, Marco Borga, Jean-Dominique Creutin, Baptiste François, Maria-Helena Ramos, and Jean-Philippe Vidal. Space-time variability of climate variables and intermittent renewable electricity production – a review. *Renewable and Sustainable Energy Reviews*, 79:600 – 617, 2017. ISSN 1364-0321. doi: <https://doi.org/10.1016/j.rser.2017.05.046>. URL <http://www.sciencedirect.com/science/article/pii/S1364032117306822>.
- [7] Aaron Bloom, Aaron Townsend, David Palchak, Joshua Novacheck, Jack King, Clayton Barrows, Eduardo Ibanez, Matthew O’Connell, Gary Jordan, Billy Roberts, Caroline Draxl, Kenny Gruchalla, RePPAE LLC, Wexford, PA (United States), and GE Energy, Denver, CO (United States). Eastern Renewable Generation Integration Study. Technical Report NREL/TP-6A20-64472, 1318192, August 2016. URL <http://www.osti.gov/servlets/purl/1318192/>.
- [8] GE Energy. Western Wind and Solar Integration Study. Technical Report NREL/SR-550-47434, 981991, May 2010. URL <http://www.osti.gov/servlets/purl/981991-FaFbxN/>.
- [9] Andrew D. Mills and Ryan H. Wiser. Changes in the Economic Value of Photovoltaic Generation at High Penetration Levels: A Pilot Case Study of California. *IEEE Journal of Photovoltaics*, 3(4): 1394–1402, October 2013. ISSN 2156-3381, 2156-3403. doi: 10.1109/JPHOTOV.2013.2263984. URL <http://ieeexplore.ieee.org/document/6541950/>.
- [10] A.D. Mills and R.H. Wiser. Changes in the economic value of wind energy and flexible resources at increasing penetration levels in the Rocky Mountain Power Area: Changes in the economic value of wind with increasing penetration. *Wind Energy*, 17(11):1711–1726, November 2014. ISSN 10954244. doi: 10.1002/we.1663. URL <http://doi.wiley.com/10.1002/we.1663>.
- [11] Lion Hirth, Falko Ueckerdt, and Ottmar Edenhofer. Integration costs revisited – An economic framework for wind and solar variability. *Renewable Energy*, 74:925–939, February 2015. ISSN 09601481. doi: 10.1016/j.renene.2014.08.065. URL <https://linkinghub.elsevier.com/retrieve/pii/S0960148114005357>.
- [12] Galen Barbose. U.S. Renewables Portfolio Standards: 2019 Annual Status Update. *Lawrence Berkeley National Laboratory*, page 48, July 2019.

- [13] Paul L Denholm, Jacob Nunemaker, Wesley J Cole, and Pieter J Gagnon. The Potential for Battery Energy Storage to Provide Peaking Capacity in the United States. Technical Report NREL/TP-6A20-74184, 1530173, June 2019. URL <http://www.osti.gov/servlets/purl/1530173/>.
- [14] William A. Braff, Joshua M. Mueller, and Jessika E. Trancik. Value of storage technologies for wind and solar energy. *Nature Climate Change*, 6(10):964–969, October 2016. ISSN 1758-678X, 1758-6798. doi: 10.1038/nclimate3045. URL <http://www.nature.com/articles/nclimate3045>.
- [15] Noah Kittner, Felix Lill, and Daniel M. Kammen. Energy storage deployment and innovation for the clean energy transition. *Nature Energy*, 2(9):17125, September 2017. ISSN 2058-7546. doi: 10.1038/nenergy.2017.125. URL <http://www.nature.com/articles/nenergy2017125>.
- [16] Wesley J Cole and Allister Frazier. Cost Projections for Utility-Scale Battery Storage. Technical Report NREL/TP-6A20-73222, 1529218, June 2019. URL <http://www.osti.gov/servlets/purl/1529218/>.
- [17] Will Gorman, Andrew Mills, Mark Bolinger, Ryan Wiser, Nikita G. Singhal, Erik Ela, and Eric O’Shaughnessy. Motivations and options for deploying hybrid generator-plus-battery projects within the bulk power system. *The Electricity Journal*, 33(5):106739, June 2020. ISSN 10406190. doi: 10.1016/j.tej.2020.106739. URL <https://linkinghub.elsevier.com/retrieve/pii/S1040619020300312>.
- [18] Dylan McConnell, Tim Forcey, and Mike Sandiford. Estimating the value of electricity storage in an energy-only wholesale market. *Applied Energy*, 159:422–432, December 2015. ISSN 03062619. doi: 10.1016/j.apenergy.2015.09.006. URL <https://linkinghub.elsevier.com/retrieve/pii/S0306261915010740>.
- [19] Hao Wang and Baosen Zhang. Energy Storage Arbitrage in Real-Time Markets via Reinforcement Learning. In *2018 IEEE Power & Energy Society General Meeting (PESGM)*, pages 1–5, Portland, OR, August 2018. IEEE. ISBN 978-1-5386-7703-2. doi: 10.1109/PESGM.2018.8586321. URL <https://ieeexplore.ieee.org/document/8586321/>.
- [20] P. Zou, Q. Chen, Q. Xia, G. He, and C. Kang. Evaluating the contribution of energy storages to support large-scale renewable generation in joint energy and ancillary service markets. *IEEE Transactions on Sustainable Energy*, 7(2):808–818, 2016.
- [21] Guannan He, Qixin Chen, Chongqing Kang, Pierre Pinson, and Qing Xia. Optimal Bidding Strategy of Battery Storage in Power Markets Considering Performance-Based Regulation and Battery Cycle Life. *IEEE Transactions on Smart Grid*, 7(5):2359–2367, September 2016. ISSN 1949-3053, 1949-3061. doi: 10.1109/TSG.2015.2424314. URL <https://ieeexplore.ieee.org/document/7106509/>.
- [22] Thomas Carriere, Christophe Vernay, Sebastien Pitaval, Francois-Pascal Neirac, and George Karinotakis. Strategies for combined operation of PV/storage systems integrated into electricity markets. *IET Renewable Power Generation*, 14(1):71–79, January 2020. ISSN 1752-1416, 1752-1424. doi: 10.1049/iet-rpg.2019.0375. URL <https://digital-library.theiet.org/content/journals/10.1049/iet-rpg.2019.0375>.
- [23] A. F. Hoke, M. Shirazi, S. Chakraborty, E. Muljadi, and D. Maksimovic. Rapid active power control of photovoltaic systems for grid frequency support. *IEEE Journal of Emerging and Selected Topics in Power Electronics*, 5(3):1154–1163, 2017.
- [24] Lefeng Cheng and Tao Yu. A new generation of ai: A review and perspective on machine learning technologies applied to smart energy and electric power systems. *International Journal of Energy Research*, 43(6):1928–1973, 2019. doi: 10.1002/er.4333. URL <https://onlinelibrary.wiley.com/doi/abs/10.1002/er.4333>.

- [25] V. Nanduri and T. K. Das. A reinforcement learning model to assess market power under auction-based energy pricing. *IEEE Transactions on Power Systems*, 22(1):85–95, 2007.
- [26] T. Bach, J. Yao, and S. Yang. Fuzzy q – learning for uniform price wholesale power markets. In *2013 International Conference on Communication Systems and Network Technologies*, pages 578–582, 2013.
- [27] Chao Sun, Fengchun Sun, and Scott Moura. Nonlinear predictive energy management of residential buildings with photovoltaics batteries. *Journal of Power Sources*, 325:723–731, 09 2016. doi: 10.1016/j.jpowsour.2016.06.076.

Decarbonizing Port Ecosystems: Optimizing Energy Transitions

Jennifer Conde, Louise Elzvik, Serena Patel, Laura Raigosa, T.G. Roberts,
Jash Vora

Abstract

California ports support the U.S. economy but are also some of the worst points of concentrated emissions affecting underserved communities. Our project used a techno-economic analysis of reducing port emissions by transitioning infrastructure to cleaner energy alternatives like hydrogen fuel and electricity through solar power purchase agreements (PPA). We created our own model of a port based on data from the Ports of Oakland and Long Beach. To simultaneously optimize for both cost and lifecycle emissions, we used an objective function incorporating a trade-off between cost and emissions. From there we created a pareto frontier that visually explains the trade offs between our two variables.

Our analysis found that diesel is the best option for minimizing cost, hydrogen is the best option for minimizing emissions, and electrified equipment with a PPA presents a middle-ground solution. Additionally, we analyzed how a carbon tax would impact the economic feasibility of decarbonized port cargo handling equipment. We found that a carbon tax over \$2,000 is needed to decarbonize some equipment types we studied, which is politically infeasible. However, a combination of policies such as a carbon tax paired with equipment subsidies could make decarbonization achievable. Our results show that it is feasible for ports to reduce their emissions by up to 97% with decarbonized equipment.

Introduction

Motivation & Background

Ports are at the heart of the U.S. economy, handling both imports and exports around the world and generating \$128 billion annually in direct business [1]. Ports are particularly crucial in California, which is the fifth largest economy in the world, and three of the ten largest U.S. ports are located in California: Port of Los Angeles (#1), Port of Long Beach (#2), and Port of Oakland (#10) [2]. However, ports are a major consumer of energy and are particularly reliant on fossil fuel-based technologies. This makes ports and their surrounding communities vulnerable to hazardous pollutants, disproportionately impacting low-income, marginalized, disadvantaged communities. Decarbonizing ports in California and implementing cleaner infrastructure can pave the way for similar changes at ports around the world, including several planned mega-development projects in emerging economies that will inevitably burden marginalized groups and disrupt ecosystems. One of the challenges in decarbonizing ports involves financing

the new infrastructure, including electric ship-to-shore and gantry cranes, zero-emissions trucks, and electric vehicle chargers and/or hydrogen refueling stations.

The Seaport Air Quality 2020 and Beyond Plan [3] from the Port of Oakland shows there has been roughly an 80% decrease in emissions since 2005 through initiatives such as mandating shore-power (incoming ships plug into the grid instead of idling in the bay on their own oil) and electrifying large cranes. We chose to focus on Cargo Handling Equipment (CHE) because it was the second largest source of emissions [4] at the Port of Oakland in 2017 and contributes over 60% of the Diesel PM and PM_{2.5}, which have major health effects on the surrounding marginalized communities. We did not choose ocean going vessels or ships (the largest source of emissions) because they are not as close to where people live and don't have as many supportive policies.

Literature Review

Our study expands on previous techno-economic studies of port infrastructure decarbonization by creating a mathematical model that demonstrates the trade-off between port emissions and cost, in order to decarbonize while prioritizing environmental justice. The Environmental Protection Agency highlights the environmental impact of ports as being a major challenge area [5]. The California Air Resources Board (CARB) also plays an instrumental role in port decarbonization, both by setting regulations on point-source emissions and by implementing financing incentives such as green equipment subsidies.

Three ports were used as key case studies: Port of Long Beach [6], Port of Los Angeles [7] and Port of Savannah [8]. These ports have each developed outlines for infrastructure decarbonization, which provide cost estimates for electrified and hydrogen-powered equipment, emissions data, and timelines to achieve various emissions reduction goals. These outlines were helpful in determining the status-quo of current U.S. port decarbonization plans and to identify areas for improvement. The Port of Los Angeles developed an interesting project in which a fleet of experimental hydrogen trucks replaced a portion of their diesel trucks in June of 2019 [7]. Researching their experience helped us understand key challenges hydrogen trucks face, as well as approximate costs and fleet size associated with them. The Port of Savannah, on the other hand, had a hybrid diesel-electric rubber-tired gantry crane (RTG) program put in place in 2012. They observed that electric RTGs helped decrease operational costs, as electricity was cheaper than diesel fuel [8]. Furthermore, the RTGs were designed to capture energy lost when lowering containers, increasing energy efficiency and leading to savings of \$10 million dollars every year [8]. Finally, the Port of Long Beach had some interesting infrastructure modernization projects such as the Middle Harbor Redevelopment Program and the Pier B On-Dock Rail Support Facility which reduced emissions from trucking by expanding rail lines for shipping [6].

Another important reference was the Port of Oakland's 30 year plan for CHE decarbonization, which included the number of each type of equipment considered and some cost estimates for electrification and diesel options [9]. Although studies have been focused on electrification of entire terminals to justify electrical infrastructure upgrades, interviews with the Port of Oakland utility manager Jared Carpenter indicated that there is a need for understanding how hydrogen can play a role in port decarbonization: the port's power demands are increasing, and there is an opportunity to harness the methane being flared at the nearby EBMUD wastewater treatment facility for hydrogen fuel production.

Hydrogen-powered fuel cells for the equipment we analyzed are not currently in the commercial phase, but we found feasibility studies [10] and conservative hydrogen fuel cost projections [11] from the Port of Long Beach, California Fuel Cell Partnership [12], and the U.S. Department of Energy hydrogen at ports research [13] that we incorporated into our model.

Local environmental impact from port pollution is clearly a major issue for surrounding communities. The West Oakland Environmental Indicators Project has filed a complaint describing the injustices that the Port of Oakland has inflicted on the nearby, historically black community of West Oakland [14]. In the “Owning Our Air West Oakland Community Action Plan,” data is shown clearly demonstrating that the Port of Oakland releases diesel particulate matter and PM2.5 (cancer-causing agents) into the surrounding community to a disproportionate degree [15]. A UC Berkeley policy group is pushing CARB for comprehensive regulatory requirements, community engagement, and emissions data for the hotspot of West Oakland [16].

Focus of this Study

Ports are highly energy-intensive, have high capital costs for equipment, and are long-term operations that occur all over the world, so we hope that our project can serve as a model for decarbonization of ports globally. The focus of this study is to analyze the trade-offs between cost and emissions associated with transforming one port based on data from the Ports of Oakland and Long Beach, by shifting from fossil-fuel based technologies to lower emission technologies: specifically hydrogen and electric-powered equipment. We decided to include a focus on environmental justice because ports produce highly concentrated emissions and are often close to underserved communities [7]. These emissions can have detrimental effects on the surrounding communities, so lowering emissions was a priority, both for the environment and to protect these marginalized communities.

We are looking for the optimal, most cost-effective mix of low-carbon energy sources (hydrogen, solar PPAs) to decarbonize high-emission port infrastructure such as reefers, forklifts, RTGs, top handlers, and on-dock and off-dock yard tractors, subject to constraints from each technology’s daily energy consumption, total cost of ownership, budget considerations, and emission reduction mandates. This cost optimization includes trade-offs with emissions, as explained in the objective function. A second optimization problem also focuses on adding a carbon tax, which introduces a price on carbon and changes the emissions consideration to a strict emissions cap (constraint), as well as including purchase subsidies for low-carbon equipment.

Technical Description

Equipment & Fuel Types

For this study, we identified six of the most energy-intensive cargo handling equipment used at ports, namely:

1. Refrigerated containers (commonly known as “Reefers”)
2. Rubber Tire Gantry Cranes (RTGs)

3. Top-picks (or top-handlers)
4. Forklifts
5. On-dock yard tractors
6. Off-dock yard tractors

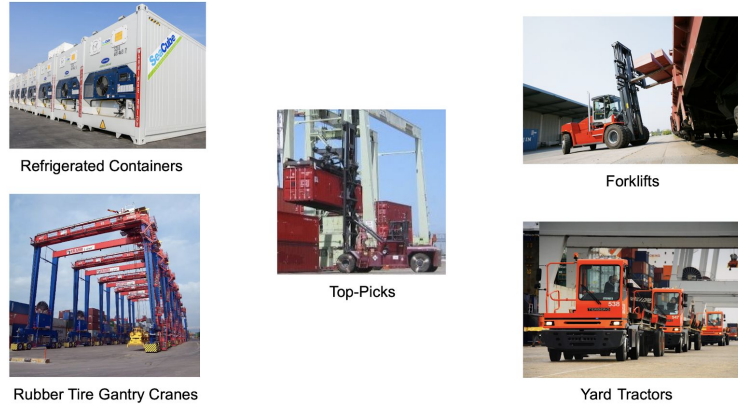


Figure 1: Visual of the listed equipments

Having finalized the machinery, we decided to explore three different fuel scenarios:

- (i) Diesel-powered machinery: In this scenario, we evaluated emissions, fuel usage, and operating costs of the machinery currently used by the Port of Oakland. Diesel-powered equipment is also the current industry standard.
- (ii) Electric-powered machinery with electricity supplied via a solar + storage power purchase agreement (PPA): In this scenario, we assumed that all the equipment was powered by electricity. This electricity would be supplied by a solar plus storage PPA signed by the port authority with a local developer. Thus, electricity would be available at all times of day.
- (iii) Hydrogen-powered machinery: In this scenario, we assumed that all the equipment was powered by hydrogen and used relevant purchase prices for hydrogen fuel and operating costs.

These fuel technologies were selected to reflect the status quo and projected future of port machinery. While electric-powered machinery is still in its nascent phase, it is relatively more mature than hydrogen-powered technology. However, the amount of publicly available information about machinery-associated costs (purchase costs, warranty, maintenance costs) was very limited. Despite reaching out to multiple vendors, we were unable to obtain specific values for most machinery. Thus, many of the price inputs in the model are ranges taken from research papers and available estimates online.

Objective Functions

Our objective function aims to minimize the cost and emissions of port equipment by optimizing the fuel consumed by each type of port equipment. In this function, each type of equipment and each type of fuel is considered, with a Pareto variable, lambda (λ), that can vary the weight and importance of cost versus emissions. A conceptual outline of our objective function is:

$$\min_x [(1-\lambda) \cdot (c_{cap} + c_{op}) + \lambda \cdot e] \cdot x$$

In this function, our decision variable x represents the number of each type of equipment of a certain fuel scenario that should optimally be installed. Each value x_{ij} refers to the number of each equipment type to install, for each technology i and each fuel source j . Since there are six equipment types and three fuels, the x vector consists of 18 decision variables. Operating and capital costs are also 18-variable vectors, each taking into account a discount rate of 5% and a gradual increase in operating hours of 1.2% each year [9]. Capital cost c_{cap} covers the up-front purchase price of equipment, while operating cost c_{op} factors in the continuing cost of fuel and maintenance. The emissions vector e values were based upon operating hours and life-cycle carbon dioxide emissions associated with each technology and fuel type. These are outlined below, where r is the annual discount rate, g is the rate of growth in operating hours, and n is the year in which the cost is applied.

$$c_{cap} = c_{initial\ purchase} + c_{future\ purchase} * \frac{1}{(1+r)^n}$$

$$c_{op,ij} = \sum_{n=1}^{20} \left(\frac{\$ cost\ of\ fuel}{unit\ fuel} * \frac{unit\ fuel}{operating\ hour} * \frac{operating\ hours}{year} + \frac{\$ maintenance\ cost}{operating\ hour} * \frac{operating\ hours}{year} \right) * \frac{1}{(1+r)^n} * (1+g)^{n-1}$$

$$e_{ij} = \frac{kgCO2(e)}{operating\ hour} * \frac{operating\ hours}{year} * 20\ years$$

Capital cost incorporates a year-one purchase price, as well as future purchase prices with a discount rate included. Operating cost depends on operating hours, which increase by rate g each year, and the discount rate r .

The system is also subject to certain constraints: the number of each type of equipment cannot be negative, and there is a required total number of each equipment type, for all fuels. The equipment totals are based on Port of Oakland data for all terminals at the port. Mathematically,

$$-x_{ij} \leq 0, \quad \forall (i,j) \quad [\text{non-negativity}]$$

$$\sum_{j=1}^3 x_{ij} \leq x_{i,total} \quad \forall \quad [\text{equipment total numbers}]$$

In essence, for a series of values of λ between 0 and 1, this function optimizes the fuel mix of six types of port operating equipment, given total required equipment numbers, costs, and carbon dioxide emissions.

In order to deepen our analysis to help favor greener alternatives, we explored the possibilities of implementing a carbon tax or subsidies for our less-carbon-intensive fuel options, electricity and hydrogen. These factors account for emissions within the cost: a carbon tax includes emissions within operating costs, while subsidies include emissions within capital costs. Therefore, the Pareto trade-off was no longer necessary. The new objective function and its components are outlined below.

$$\min (c_{cap} + c_{op}) \cdot x$$

$$c_{cap} = (c_{initial\ purchase} + c_{future\ purchases}) * (1 - subsidy)$$

$$c_{op} = \frac{\$ cost\ of\ fuel}{unit\ fuel} * \frac{unit\ fuel}{op.\ hour} * \frac{op.\ hours}{year} + \frac{\$ maintenance\ cost}{op.\ hour} * \frac{op.\ hours}{year} + \frac{\$ carbon\ tax}{kgCO2(e)} * \frac{kgCO2(e)}{op.\ hour} * \frac{op.\ hours}{year}$$

In these formulas, the subsidy is expressed as a percentage, and the carbon tax is selected in units of \$/ton CO₂e. Different subsidies and carbon taxes can be considered to determine the sensitivity of our final fuel mix, and to find the break-even point at which a subsidy or carbon tax is high enough to incentivize ports to decarbonize.

Results & Discussion

An overview of the results can be captured by a Pareto frontier, shown in Figure 2. The value of lambda was varied from 0 and 1, and the resulting cost and emissions are shown. On the left, when lambda is one, the emissions are minimized at 17,200 tons of CO₂e over 20 years, but the project would be extremely expensive, costing more than \$720 million dollars. When lambda is zero, on the far right, the cost is minimized at around \$328 million dollars, but the emissions would be as high as 528,400 tons of CO₂e. The Pareto curve shows the clear tradeoff between prioritizing emissions reduction or cost.

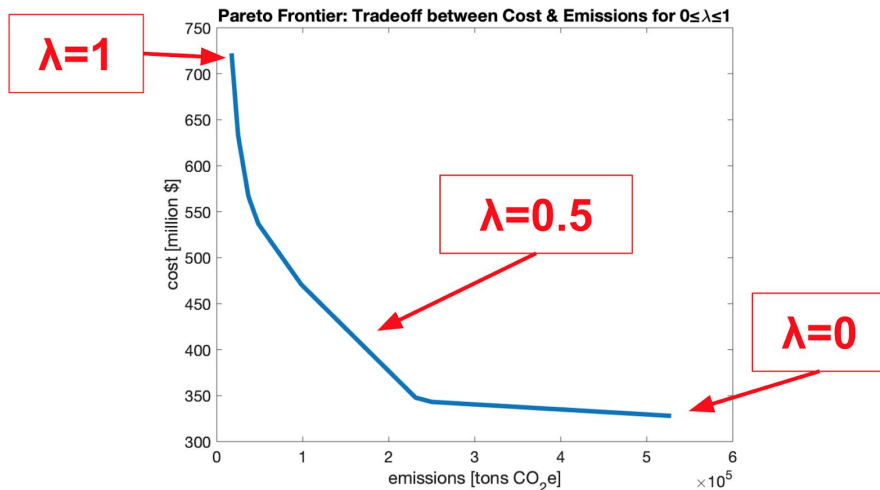


Figure 2: Pareto curve for the optimization program, where the trade-off between cost and emissions as a function of can be observed

With the inherent trade-off in mind, we can determine the optimal fuel mix of our CHE fleet. We vary lambda from 0 to 1 and obtain the results for an “unconstrained” case. In this context, “unconstrained” means there are no constraints for budget or total emissions. The results are shown in Figure 3. Blue represents diesel, red represents electric under a solar PPA agreement, and yellow represents hydrogen fuel from electrolysis. The results are consistent: when emissions are prioritized, hydrogen is always chosen except for forklifts. When cost is prioritized, diesel is chosen on all equipment except reefers. For forklifts, hydrogen is never the optimal fuel choice because their energy consumption patterns indicate fewer emissions using electricity than hydrogen. For reefers, diesel is not preferred due to the high upfront cost. We assume that ports have an appropriate number of plugs for all reefers to plug into the grid for power, which means no capital cost is needed for electrification. However, the ports would have to purchase generators to power the reefers on diesel. This means that electrified reefers are always cheaper than diesel.

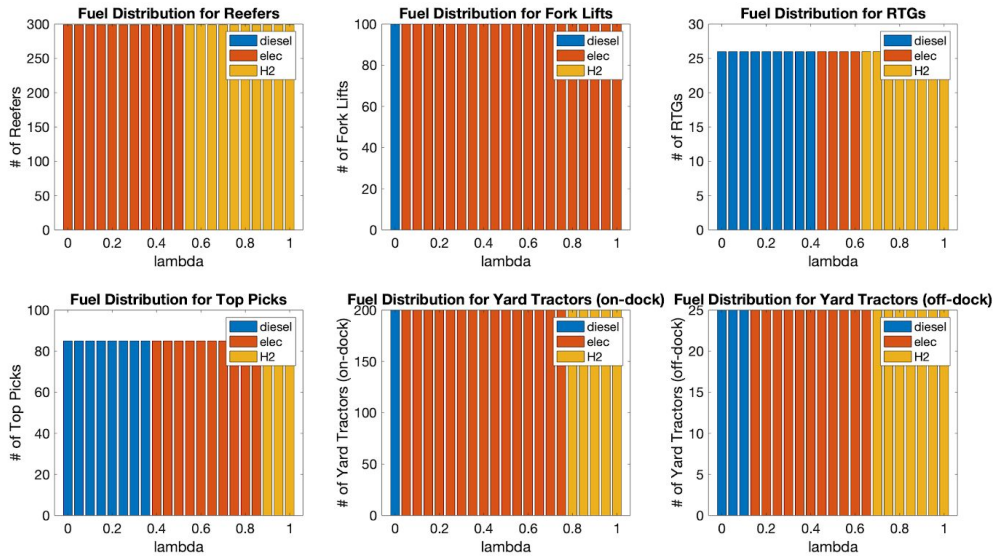


Figure 3: Results of optimization program with no emissions cap or budget constraint

Realistically, we would expect port operators to implement a budget in their electrification efforts, or for policymakers to implement a cap on the total number of emissions. We ran both these scenarios as well, and the results are in Figure 4. Interestingly, our optimization indicates that electric equipment is the optimal fuel for most lambda values. The

main exception is for RTGs, which we have consistently found to be difficult to decarbonize.

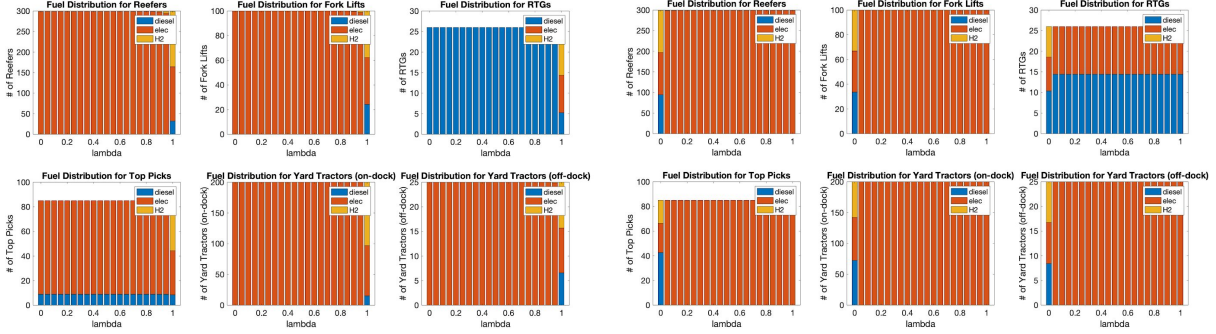


Figure 4: Results of optimization program with an emissions constraint of 100,000 tons (left) and results of optimization program with a budget constraint of \$500 million (right)

We additionally run a scenario with both budget and emissions constraints. With both of these constraints in place, Figure 5 indicates that a mix of all fuel types is optimal. Some of the equipment types do have dominating fuels, such as electric top picks, electric on-dock yard tractors, and diesel RTGs.

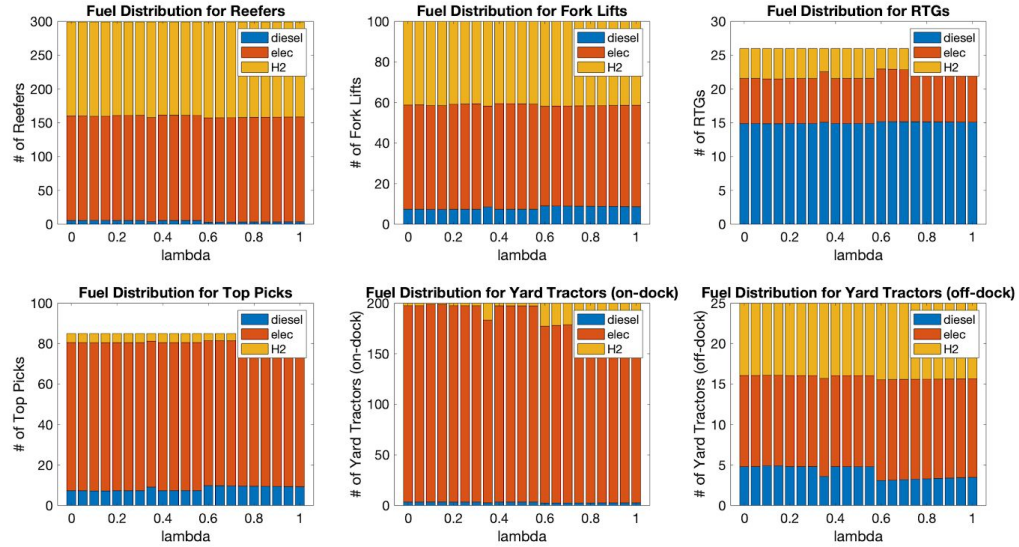


Figure 5: Results of optimization with an emissions constraint of 100,000 tons and a budget constraint of \$500 million

Another scenario we analyzed was the effect of carbon tax. In this scenario, instead of varying lambda from 0 to 1, we implemented different values of carbon taxes and examined how high a carbon tax would have to be to make decarbonized CHE economically feasible. The results were discouraging: when only cost was considered, an extremely high carbon tax would be required to push the adoption of electric over diesel. Yard tractors (on-dock) and forklifts would be the easiest to switch, at a carbon tax of \$125 per ton CO₂e. This would be followed by

off-dock yard tractors at a price of \$500 per ton CO₂e. However, top-picks would require a carbon tax of \$1,625, while RTG would require \$2,250.

These high prices show how difficult it is to decarbonize port CHE under reasonable economic considerations. These prices of carbon are clearly unfeasible, as the current carbon price in California is around \$15, and even the most rigid carbon pricing programs are rarely above \$100 per ton of CO₂e [17].

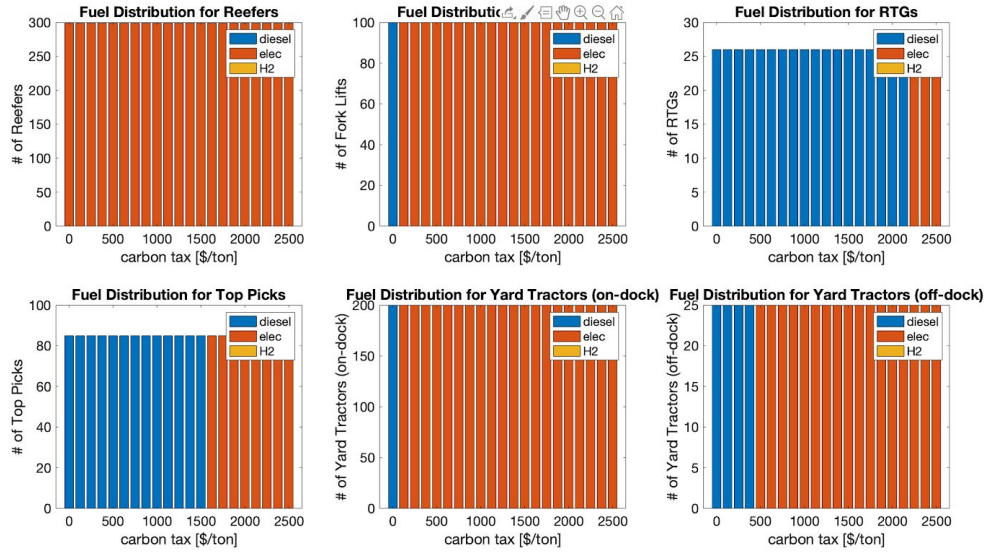


Figure 6: Fuel distribution for a variety of carbon taxes, from 0 to \$2,500 dollars

The use of subsidies could be considered to complement a carbon tax and make decarbonizing port CHE more economically feasible. As shown in Figure 7, even a 25% subsidy for port equipment can significantly reduce the carbon tax required to make decarbonized equipment economically feasible. Most notably, the carbon tax for RTGs is reduced from \$2,250 to \$1,625, a 27.8% decrease. The carbon tax for top picks is reduced from \$1,625 to \$1,125, a 30.8% decrease. Although the carbon taxes are still infeasible, adding the equipment subsidy does help overcome the upfront costs, which pose as a significant barrier to decarbonization.

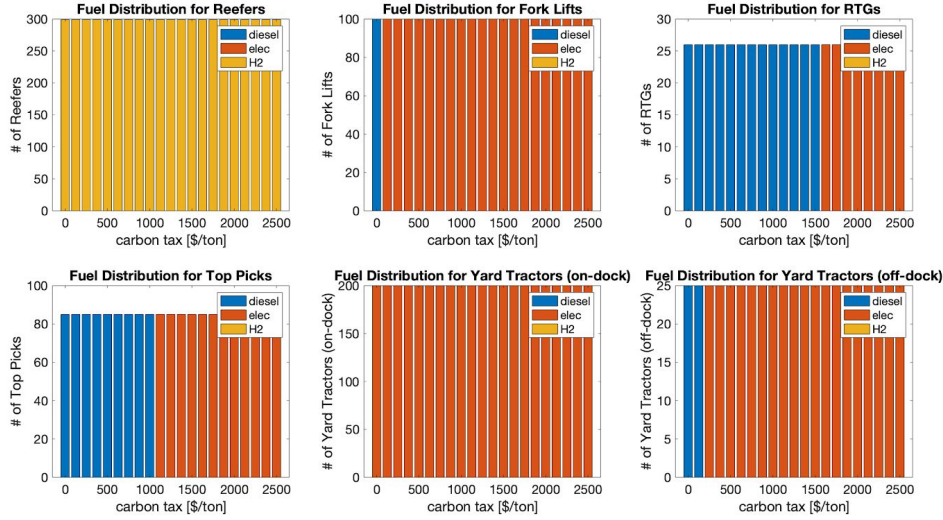


Figure 7: Results of optimization with a 25% equipment subsidy for various carbon taxes

Our optimization scenarios have demonstrated the unique challenges that ports face when trying to decarbonize. We have shown that diesel CHE, which is typically the standard in today's ports, is ideal for minimizing port costs, while decarbonized equipment is significantly more expensive due to upfront equipment costs. It is important to note that while the upfront costs of electric and hydrogen-powered equipment are more than their diesel counterparts, the maintenance costs and equivalent fuel costs have the potential to be cheaper for electric and hydrogen equipment (see Appendix A for a full list of all costs we used in our model). When optimizing for emissions and ignoring cost, hydrogen was the optimal fuel most often; however, not even a carbon tax of \$2,500 with a 25% equipment subsidy makes transitioning to hydrogen economically feasible for most equipment types.

Our work shows that economics alone will not galvanize ports to decarbonize. The economics do not work favorably to encourage the transition to clean energy since extremely high carbon prices are required to make electric and hydrogen CHE economically feasible, but policymakers can still make this transition possible through mandates. The combination of mandates, subsidies, and a carbon price can force ports to decarbonize, thus lessening the impact of harmful pollutants on surrounding communities, while also easing the economic burden to terminal operators that own the CHE. While ports' overall costs might increase, there is a greater benefit in lessening the environmental impacts with respect to both climate change and the disadvantaged communities around the ports. The key takeaways from our optimizations are that CHE at ports are extremely difficult to decarbonize and a combination of policy strategies will be needed to accomplish the transition to cleaner fuels.

Although our analysis synthesized a great deal of information from past research and relevant stakeholders and ran several optimization scenarios, there are still several next steps that we would like to see implemented in our optimization formulation and results.

First, our optimization currently does not allow for a phase-in of different fuel types for CHE. Our model requires that all equipment be purchased in year 1 and the same fuel source is used for all 20 years. This might not be realistic, and ports might consider implementing decarbonization in phases, starting with a smaller number of decarbonized CHE rather than transitioning their entire fleet upfront and allowing for feasibility studies. A revised optimization model would allow such a phase-in to occur.

Second, we currently do not consider the infrastructure upgrades required to support decarbonized fleets. For instance, an electrified fleet would require the installation of charging stations and distribution system upgrades to accommodate the increased electrical load. As one example, in a phone interview with Mike Marrs, the Vice President of Sales at Cal-Lift, he indicated that the upfront cost of an electric top pick in our model is currently \$1.6 million, but this number could increase up to \$2 million when accounting for infrastructure upgrades. These costs would fall on various port stakeholders, particularly terminal operators. Likewise, transitioning to a hydrogen fleet would require hydrogen storage tanks and refueling stations, which we did not take into account in our current cost setup.

Finally, we would like to incorporate uncertainty for both equipment costs and fuel costs into our model. Many decarbonized CHE types are not commercially available and so the cost of these equipment can be estimated but is not certain. More data on this will be known as R&D increases and as ports go through pilot programs with hydrogen and electric equipment. Additionally, fuel costs into the future are uncertain. The price of diesel over time will likely change from what it is today, and the Energy Information Administration gives estimates for lower and upper bounds of what the price could be 20 to 30 years from now [18]. Similarly, the cost to produce hydrogen could change over time as technology advances. Incorporating the uncertainties of both upfront costs and fuel costs like a Markowitz Portfolio Optimization would allow us to penalize cost variability, making more cost-stable options favorable.

Although there are many improvements that could be made to our model, we are hoping that our optimization results can help advance sustainability at ports by informing policymakers and port operators of the challenges in decarbonization and their responsibilities, thus spurring them to take impactful action.

Responsibilities

Task	Teammates Responsible
Port of Long Beach, Fenix Marine Terminal Contact	Louise
Port of Long Beach, Southern California Edison Contact	Jenny

Port of Oakland Contact, UCB Port of Oakland policy research Contact	Serena
Diesel Scenario: research fixed and operational costs, construct cost function, analyze impacts of a carbon tax	Jenny
Solar PPA + Battery Scenario: research fixed and operational costs, construct cost function	T.G. & Jash
Hydrogen Scenario: research fixed and operational costs, construct cost function	Serena & Laura
Determine optimization model, input and state variables	Everyone
Code model skeleton in MATLAB	Louise
Implement model and sensitivity scenarios (carbon tax, equipment subsidies) and create all figures in MATLAB	Jenny
Write presentation script	T.G. & Serena
Edit presentation script	Everyone
Record presentation	Everyone
Edit presentation video	T.G.
Project Proposal, Final Report	Everyone

Summary

The aim of our project was to analyze cost-effective strategies for reducing the emissions at a port terminal. The port was heavily modeled off the Ports of Oakland and Port of Long Beach, which are situated near marginalized communities that bear the brunt of these emissions and the associated health risks. We considered switching cargo handling equipment (CHE) and reefers from diesel power to electricity from a solar PPA and/or hydrogen fuel cells.

We find that using diesel minimizes cost over our 20 year study, whereas hydrogen minimizes emissions, and the electrified equipment with a PPA acts as a middle-ground solution. A carbon tax of over \$2,000 is needed to decarbonize some CHE we studied. However, pairing an equipment subsidy could reduce this tax by over 30% for RTGs and top-picks. Our results show that maximum investment can reduce the port emissions from CHE and reefers by up to 97%. As a result of our findings, we strongly urge policymakers to support the transition to emission-free port equipment by subsidizing the upfront costs. We encourage port operators and policymakers to prioritize feasibility studies of decarbonized technologies especially for

hydrogen, which have yet to reach commercial stages but offer an exciting opportunity unique to large ports like the Port of Oakland.

References

- [1] S. Brickman, "Seaports Need a Lot of Energy, But Electrification Can Reduce Pollution and Costs", *Alliance to Save Energy*, 2018. [Online]. Available: <https://www.ase.org/blog/seaports-need-lot-energy-electrification-can-reduce-pollution-and-costs>. [Accessed: 09- Feb- 2020].
- [2] P. Burnson, "Top 30 U.S. Ports 2019", *Logistics Management*, 2019. [Online]. Available: https://www.logisticsmgmt.com/article/top_30_u.s._ports_trade_tensions_determine_where_cargo_goes_next. [Accessed: 11- Feb- 2020].
- [3]"Ports Primer: 2.2 Current Port Industry Challenges | US EPA", *US EPA*, 2020. [Online]. Available:<https://www.epa.gov/community-port-collaboration-and-capacity-building/ports-primer-22-current-port-industry-challenges>. [Accessed: 11- Feb- 2020].
- [4]"Port of Oakland 2017 Seaport Air Emissions Inventory", *Portofoakland.com*, 2018. [Online]. Available: https://www.portofoakland.com/files/PDF/Port_Oakland_2017_Emissions_Inventory.pdf. [Accessed: 09- Feb- 2020].
- [5]"Ports Primer: 2.2 Current Port Industry Challenges | US EPA", *US EPA*, 2020. [Online]. Available:<https://www.epa.gov/community-port-collaboration-and-capacity-building/ports-primer-22-current-port-industry-challenges>. [Accessed: 11- Feb- 2020].
- [6]"Port of Long Beach Middle Harbor Redevelopment Project,", *Ship Technology*, 2020. [Online]. Available:<https://www.ship-technology.com/projects/port-of-long-beach-middle-harbor-redevelopment-project-california/>. [Accessed: 12- Feb- 2020].
- [7]"Community Group Alleges Civil Rights Violations by the City and Port of Oakland in Complaint to Federal Government", *Earth Justice*, 2017. [Online]. Available: <https://earthjustice.org/news/press/2017/community-group-alleges-civil-rights-violations-by-the-city-and-port-of-oakland-in-complaint-to-federal>. [Accessed: 09- Feb- 2020].
- [8]E. Gilmore, "Eye On Infrastructure: Electrifying Ports Saves Fuel, Money, And Public Health," *Alliance to Save Energy*, 2017. [Online]. Available: <https://www.ase.org/blog/eye-infrastructure-electrifying-ports-saves-fuel-money-and-public-health>

- [9] "Zero-Emission Cargo-Handling Equipment Feasibility Assessment", *AECOM*, 2019. [Online]. Available:
<https://www.portofoakland.com/files/PDF/AECOM%20Zero%20emission%20CHE%20feasibility%20assessment%20Nov%202019.pdf>. [Accessed: 08- May- 2020].
- [10] "Our Zero Emissions Future", *Port of Long Beach*, 2018. [Online]. Available:
<https://www.polb.com/environment/our-zero-emissions-future/#program-details>. [Accessed: 08- May- 2020].
- [11] "Manufacturing Cost Analysis of 100 and 250 kW Fuel Cell Systems for Primary Power and Combined Heat and Power Applications", *Batelle; U.S. Department of Energy*, 2016. [Online]. Available:
https://www.energy.gov/sites/prod/files/2016/07/f33/fcto_battelle_mfg_cost_analysis_pp_chp_fc_systems.pdf. [Accessed: 08- May- 2020].
- [12] "Cost to Refill", *California Fuel Cell Partnership*, 2015. [Online]. Available:
<https://cafcp.org/content/cost-refill>. [Accessed: 08- May- 2020].
- [13] L. Steele and C. Meyers, "Hydrogen Fuel Cell Applications in Ports: Feasibility Study at Multiple U.S. Ports," *Pacific Northwest National Laboratory; Oak Ridge National Laboratory*, 2019. [Online]. Available:
<https://www.energy.gov/sites/prod/files/2019/10/f68/fcto-h2-at-ports-workshop-2019-viii3-steele.pdf>. [Accessed: 08- May- 2020].
- [14] "Community Group Alleges Civil Rights Violations by the City and Port of Oakland in Complaint to Federal Government," *Earthjustice*, 2017. [Online]. Available:
<https://earthjustice.org/news/press/2017/community-group-alleges-civil-rights-violations-by-the-city-and-port-of-oakland-in-complaint-to-federal>. [Accessed: 08- May- 2020].
- [15] "The West Oakland Community Action Plan, Volume 2", *Bay Area Air Quality Management District*, 2019. [Online]. Available:
<https://www.baaqmd.gov/community-health/community-health-protection-program/west-oakland-community-action-plan>. [Accessed: 08- May- 2020].
- [16] N. Helme, S. Davis, S. Reed, N.G. Helme, M. Levinson and D. Wooley, "Advancing Environmental Justice: A New State Regulatory Framework to Abate Community-Level Air Pollution Hotspots and Improve Health Outcomes", *Goldman School of Public Policy*, 2017. [Online]. Available: https://gspp.berkeley.edu/assets/uploads/page/CEPP_Report_09.7.17.pdf. [Accessed: 08- May- 2020].

- [17] M. Carr and S. Hasto, “Here’s How Carbon Gets Priced Around the World”, *Bloomberg*, 2018. [Online]. Available: <https://www.bloomberg.com/graphics/2018-carbon-pricing/>. [Accessed: 08- May- 2020].
- [18] “Annual Energy Outlook 2020”, *Environmental Protection Agency*, 2020. [Online]. Available: https://www.eia.gov/outlooks/aoe/tables_ref.php. [Accessed: 08- May- 2020].
- [19] “Electric Refrigerated Container Racks: Technical Analysis”, *Electric Power Research Institute*, 2010. [Online]. Available: https://www.massport.com/capitalprogramsattachments/M495-D1/M495-D1%20Appendix%20A-%20EPRI%20Elec.%20Reefer%20Rack%20Technical%20Analysis_Dec2010.pdf. [Accessed: 08- May- 2020].
- [20] “Technology Assessment: Mobile Cargo Handling Equipment”, *California Environmental Protection Agency Air and Resources Board*, 2015. [Online]. Available: https://ww3.arb.ca.gov/msprog/tech/techreport/che_tech_report.pdf. [Accessed: 08- May- 2020].
- [21] “Table 6. Carbon Intensity Lookup Table for Gasoline and Fuels that Substitute for Gasoline”, *California Air and Resources Board*. [Online]. Available: https://ww3.arb.ca.gov/fuels/lcfs/121409lcfs_lutables.pdf. [Accessed: 08- May- 2020].
- [22] P. Denholm and G. Kulcinski, “Net Energy Balance and Greenhouse Gas Emissions from Renewable Energy Storage Systems,” *Fusion Technology Institute University of Wisconsin-Madison*, 2003. [Online]. Available: <http://fti.neep.wisc.edu/pdf/fdm1261.pdf>. [Accessed: 08- May- 2020].
- [23] M/ Pehl, A. Arvesen, F. Humpenoder, A. Popp, E. Hertwich and G. Luderer, “Understanding future emissions from low-carbon power systems by integration of life-cycle assessment and integrated energy modelling,” *Nature Energy*, 2017. [Online]. Available: <https://www.nature.com/articles/s41560-017-0032-9>. [Accessed: 08- May- 2020].
- [24] “CA-GREET3.0 Lookup Table Pathways - Technical Support Documentation,” *California Air and Resources Board*, 2018. [Online]. Available: <https://ww3.arb.ca.gov/fuels/lcfs/ca-greet/lut-doc.pdf>. [Accessed: 08- May- 2020].
- [25] “Kalmar DCG50-90 5-9 ton capacity,” *Kalmar*. [Online]. Available: https://www.kalmarglobal.com/globalassets/equipment/forklift-trucks/forklift-trucks-5-9-ton/sb-ltg9-en-ww_lr.pdf. [Accessed: 08- May- 2020].

- [26] “Loaded Container Handler Engine Replacement,” *CSX Intermodal Terminals*, 2014. [Online]. Available: https://files.nc.gov/ncdeq/Air%20Quality/motor/grants/files/CSX_Intermodal_Terminals_Charlotte-Loaded_Container_Handler_Engine_Replacement.pdf. [Accessed: 08- May- 2020].
- [27] “Cummins 15kW Diesel Generator,” *Gen Pro*, 2020. [Online]. Available: <https://aagenpro.com/store/product/cummins-15kw-diesel-generator/>. [Accessed: 08- May- 2020].
- [28] “Path to slashing zero-emissions costs to California ports proposed,” *JOC*, 2017. [Online]. Available: https://www.joc.com/port-news/us-ports/port-los-angeles/path-slashing-zero-emissions-costs-california-ports-proposed_20170803.html. [Accessed: 08- May- 2020].
- [29] “Electric Forklifts vs LP Forklifts – Reduce Operating Costs,” *Warehouse IQ*, 2011. [Online]. Available: <https://www.warehouseiq.com/electric-forklifts-vs-lp-forklifts-reduce-operating-costs/>. [Accessed: 08- May- 2020].
- [30] V. Papaioannou, S. Pietrosanti, W. Holderbaum, V. M. Becerra and R. Mayer, “Analysis of Energy Usage for RTG Cranes,” *ResearchGate*, 2017. [Online]. Available: https://www.researchgate.net/publication/314250201_Analysis_of_energy_usage_for_RTG_cranes. [Accessed: 08- May- 2020].
- [31] M. Bolinger, J. Seel and D. Robson, “Utility-Scale Solar - Empirical Trends in Project Technology, Cost, Performance and PPA Pricing in the United States,” *Lawrence Berkeley National Laboratory*, 2019. [Online]. Available: https://emp.lbl.gov/sites/default/files/lbln_utility_scale_solar_2019_edition_final.pdf. [Accessed: 08- May- 2020].
- [32] “Charging Ahead: The Port Community Electric Vehicle Blueprint,” *Port of Long Beach; California Energy Commission*, 2019.
- [33] D. Peterson, J. Vickers, D. DeSantis “DOE Hydrogen and Fuel Cells Program Record,” *Department of Energy United States of America*, Feb 2020. [Online]. Available: https://www.hydrogen.energy.gov/pdfs/19009_h2_production_cost_pem_electrolysis_2019.pdf

- [34] G. Thomas, “Energy Density (LHV) for fuels in liquid state,” *Sandia National Laboratories*, 2003. [Online]. Available: https://www1.eere.energy.gov/hydrogenandfuelcells/pdfs/bulk_hydrogen_stor_pres_sandia.pdf
- [35] T. Ramsden, “An Evaluation of the Total Cost of Ownership of Fuel CellPowered Material Handling Equipment,” *National Renewable Energy Laboratory*, 2013. [Online]. Available: <https://www.nrel.gov/docs/fy13osti/56408.pdf>

Appendices

Appendix A: Defining the Cost Functions

Note for all tables: The number in brackets next to each equipment indicates the source for each value in the table, respectively. Multiple sources used to find the same number are indicated with an “&”. For example, in Table 1, Reefers have [19] and [*] as the citations. This means that source 19 was used for the first column and the asterisked source was used for the second column.

Table 1: Quantities to keep consistent regardless of fuel type. These include the number of operating hours per year and the total number of each equipment type at the port. These numbers are based mainly on data from the Port of Oakland.

Qualities Across All Fuels	Hours Run / year	Total Quantity
Reefer [19], [*]	3000	299
Forklift [20], [*]	720	100
RTG [9], [9]	1200	26
Toppicks [20], [9]	1028	85
Yard Tractors (on dock) [9], [9]	1600	200
Yard Tractors (off dock) [9], [9]	1000	25

* Interview with Jared Carpenter, Utility Business Administrator at Port of Oakland

Table 2: Lifetime carbon dioxide emissions for each fuel type. For the electric scenario, we considered lifetime emissions for both solar and lead-acid batteries. Lead-acid batteries are currently the most-used batteries for port CHE although there is a trend towards lithium-ion batteries [*].

CO2 Emissions	Diesel [kgCO2/gallon]	Electric [kgCO2/kWh]	Hydrogen [kgCO2/kgH2]
Reefer [21], [22] & [23], [24]	13.3388	0.0261	1.3768
Forklift [21], [22] & [23], [24]	13.3388	0.0261	1.3768
RTG [21], [22] & [23], [24]	13.3388	0.0261	1.3768
Toppicks [21], [22] & [23], [24]	13.3388	0.0261	1.3768
Yard Tractors (on dock) [21], [22] & [23], [24]	13.3388	0.0261	1.3768
Yard Tractors (off dock) [21], [22] & [23], [24]	13.3388	0.0261	1.3768

* Phone Call with David Mills, Account Manager at Toyota Material Handling

Table 3: Energy consumption for each fuel type

Energy Consumption	Diesel [gallons/h]	Electric [kWh/hour]	Hydrogen [kgH2/day]
Reefer [19], [19], [19]	0.735	2.8875	0.7120575071
Forklift [25], [29], [33]	1.5	3.572	5
RTG [9], [30], [33]	6	600	45
Toppicks [26], [34], [33]	5	206.3888	33
Yard Tractors (on dock) [9], [34], [33]	2.5	103.1944	21
Yard Tractors (off dock) [9], [34], [33]	2.5	103.19441	13.125

Table 4: Cost of each fuel type. Note that these prices are likely to experience uncertainty over a 20-year timeframe. We would like to account for this uncertainty in the next iteration of this project.

Fuel Cost	Diesel [\$/gal]	Electric [\$/kWh]	Hydrogen [\$/kgH2]
Reefer [9], [31], [34]	\$3.50	\$0.04	\$13.99
Forklift [9], [31], [34]	\$3.50	\$0.04	\$13.99
RTG [9], [31], [34]	\$3.50	\$0.04	\$13.99
Toppicks [9], [31], [34]	\$3.50	\$0.04	\$13.99
Yard Tractors (on dock) [9], [31], [34]	\$3.50	\$0.04	\$13.99
Yard Tractors (off dock) [9], [31], [34]	\$3.50	\$0.04	\$13.99

Table 5: Cost of maintenance. We had some trouble finding concrete numbers for the electric and hydrogen costs per operating hour. This is because electric and hydrogen equipment types are rarely deployed or still in the R&D stages, so even terminal operators and equipment manufacturers are uncertain of the true values. However, it is safe to assume that the maintenance cost of electric is cheaper than diesel, and the maintenance cost of hydrogen is cheaper than electric [35].

Maintenance Cost	Diesel [\$/operating hour]	Electric [\$/operating hour]	Hydrogen [\$/operating hour]
Reefer [*], no source assumed same as Forklift, no source assumed 80% of electric cost	\$5	\$4.75	\$3.80
Forklift [*], [**], no source assumed 80% of electric cost	\$5	\$4.75	\$3.80
RTG [*], no source assumed 80% of diesel cost, no source assumed 80% of electric cost	\$10	\$8.00	\$6.40
Toppicks [*], no source assumed 80% of diesel	\$10	\$8.00	\$6.40

cost, no source assumed 80% of electric cost			
Yard Tractors (on dock) [9], [9], no source assumed 80% of electric cost	\$30	\$20	\$16
Yard Tractors (off dock) [9], [9], no source assumed 80% of electric cost	\$25	\$17	\$14

* Phone Call with Mike Marrs, Vice President of Sales at Cal-Lift

** Phone Call with Mika Perez at North Bay Warehouse Equipment Co.

Table 6: Price to purchase equipment upfront in year 1. We assume that all equipment is purchased at the start of year one and thus is not discounted. These upfront costs are estimates since many of these equipment types are still in either R&D or testing phases.

Capital (Upfront) Cost	Diesel [\$]	Electric[\$]	Hydrogen [\$]
Reefer [27], assume plugs already exist at ports so no additional cost, [11]	\$13,900	0	\$23,105
Forklift [20], [32] [32]	\$40,000	\$45,000	\$70,000
RTG [9], [28], [28]	\$2,000,000	\$2,500,000	\$3,500,000
Toppicks [28], [28], [32]	\$560,000	\$1,600,000	\$2,520,000
Yard Tractors (on dock) [9], [28], [28]	\$129,000	\$250,000	\$385,000
Yard Tractors (off dock) [9], [9] [28]	\$129,000	\$274,000	\$385,000

Table 7: Lifetime of equipment before replacement is needed. Diesel lifetimes had the most known values for equipment lifetimes. Similar to other variables, this is because electric and hydrogen equipment has not been deployed yet, so terminal operators and equipment manufacturers do not know how long the equipment lasts.

Equipment Lifetime	Diesel [years]	Electric [years]	Hydrogen [years]
Reefer [*], assume electric and hydrogen equipments replaced as often as diesel	20	20	20
Forklift [*], [**], assume hydrogen equipments replaced as often as diesel	20	14	20
RTG [9], assume electric and hydrogen equipments replaced as often as diesel	20	20	20
Toppicks [*], assume electric and hydrogen equipments replaced as often as diesel	20	20	20
Yard Tractors (on dock) [9], assume electric and hydrogen equipments replaced as often as diesel	8	8	8
Yard Tractors (off dock) [9], assume electric and hydrogen equipments replaced as often as diesel	12.8	12	12.8

* Phone Call with Mike Marrs, Vice President of Sales at Cal-Lift

** Phone Call with Mika Perez at North Bay Warehouse Equipment Co.

Table 8: Lifetimes and costs of individual components in equipment. These components often need to be replaced more often than the entire equipment.

Component Replacement	Lead-Acid Batteries: Lifetime [years]	Lead-Acid Batteries: Cost	Fuel Cells: Lifetime	Fuel Cells: Cost [\$/kW]
Reefer [N/A], [N/A], [33], [33]	N/A	N/A	Replace 42% every 7 years	\$100
Forklift [**], [**], [33], [33]	5	\$5,000	Replace 42% every 7 years	\$100
RTG [*], [*], [33], [33]	10	\$10,000	Replace 42% every 7 years	\$100
Toppicks [*], [*], [33], [33]	10	\$10,000	Replace 42% every 7 years	\$100
Yard Tractors (on-dock) [*], [*], [33], [33]	10	\$10,000	Replace 42% every 7 years	\$100
Yard Tractors (off-dock) [*], [*], [33], [33]	10	\$10,000	Replace 42% every 7 years	\$100

* Phone Call with Mike Marrs, Vice President of Sales at Cal-Lift

** Phone Call with Mika Perez at North Bay Warehouse Equipment Co.

Appendix B: MATLAB Code

MATLAB Code 1: Port_Model_2.m published as a PDF

- Includes Pareto frontier optimization scenarios with varying lambda values to balance costs and emissions
- Can also use this code to implement additional budget and emissions constraints
- Note that the output from the cvx optimization has been excluded to reduce the page length of this appendix

MATLAB Code 2: Port_Model_ctax.m published as a PDF

- Includes economic optimization for equipment distribution among fuel types based on varying levels of carbon tax
- Incorporated a 25% subsidy as well, but this can easily be changed using the “subsidy” variable
- Note that the output from the cvx optimization has been excluded to reduce the page length of this appendix

MATLAB Code 3: Port_Model_subsidy published as a PDF

- Includes economic optimization for equipment distribution among fuel types based on equipment subsidies only
- Subsidies vary from 0% to 100%
- Note that the output from the cvx optimization has been excluded to reduce the page length of this appendix

Port_Model_2.m

Table of Contents

.....	1
Our System	1
Setting Up Constraints	1
Set Up Cost (for Objective Function)	2
CVX Optimization	5
Plotting	28

```
clear; close all;
fs = 15; % Font Size for plots
```

Our System

```
% objective function: minimize cost * number of units for each
technology,
% summed up
% We want to be able to change hours operated/year, fuel prices,
carbon
% tax, subsidies for buying the equipment (i.e. reducing capital cost
of
% low carbon technology),

% x vector: discrete number of each type of technology. (eg: reefer
BAU,
% reefer electric, reefer hydrogen, then: forklift, rtg, toppick, yard
tractors
% on dock, and yard tractors off dock)

% constraints:

%INEQUALITY
% 1. capping emissions of all the equipment together
% 2.

%EQUALITY
% 1. total number of each type of unit
```

Setting Up Constraints

```
horizon = 20;

% Hours Each Unit is Run (hours) each year
h_rf = 3000;
h_fl = 720;
h_rtg = 1200;
h_tp = 1030;
h_yt_on = 1600;
h_yt_off = 1000;
operating_hours = [h_rf; h_fl; h_rtg; h_tp; h_yt_on; h_yt_off];
```

```

% Emissions from each technology [kgCO2(e)/gallon, kgCO2(e)/kWh,
% kgCO2(e)/kgH2].
% bau, electric, hydrogen
co2_energy = [13.34, 0.006 + 0.020125, 1.38];

% Total number of each type of unit (#)
num_rf = 299;
num_fl = 100;
num_rtg = 26;
num_tp = 85;
num_yt_on = 200;
num_yt_off = 25;

```

Set Up Cost (for Objective Function)

```

% Fuel Costs (feel free to change these unit, this is just my first
guess)
% BAU: $/gallon diesel
% Electricity: $/kWh electricity
% Hydrogen: $/kg hydrogen
c_fuel = [3.5, 0.04, 13.99; 3.5, 0.04, 13.99; 3.5, 0.04, 13.99;
3.5, 0.04, 13.99; 3.5, 0.04, 13.99; 3.5, 0.04, 13.99];

% Maintenance Costs
% BAU: $/operating hour
% Electricity: $/operating hour
% Hydrogen: $/operating hour
c_maintenance = [5, 4.75, 3.80; 5, 4.75, 3.80; 10, 8, 6.40; 10,
8, 6.40; 30, 20, 16; 25, 17, 14];

% Energy Consumption
% BAU: gallons of diesel/operating hour
% Electricity: kWh of electricity/hour
% Hydrogen: kg of hydrogen/hour
energy_consumption = [0.735, 2.8875, 0.029669; 1.5, 3.572, 0.208333;
6, 600, 1.875; 5, 206.4, 1.375; 2.5, 103.2, 0.875; 2.5, 103.2,
0.546875];

% Upfront Costs, [$/unit]
% For reefers, only the cost of the generator is considered (not
% plug), so electric capital cost = 0
c_upfront = [13900, 0, 23100; 40000, 45000, 70000; 2000000,
2500000, 3500000; 560000, 1600000, 2520000; 129000, 250000,
385000; 129000, 274000, 385000];
% Lifetime of equipment [years]
lifetimes = [20, 20, 13.333; 20, 20, 55.5; 20, 20, 33.333; 20,
20, 38.89159; 8, 8, 25; 13, 13, 40]; % maximum 20

growth_rate = 0.012;
discount_rate = 0.05;

% Total Emissions (kgCO2(e)) over 1 year, gives a 6x3

```

```

co2_year1 = (co2_energy .* energy_consumption) .* operating_hours;
co2 = zeros(6,3);
for i = 1:horizon
    co2 = co2 + (co2_energy .* energy_consumption) .* 
    (operating_hours*(1+growth_rate)^(i-1));
end
% Remember to flatten this in the rows and not the columns!!
% Also make sure they're all normalized to years rather than hours or
days

% Variable Cost ($) over 20 years
c_var = zeros(6,3);

for equipment = 1:6
    for fuel = 1:3
        annual_cost = operating_hours(equipment) *
        (c_maintenance(equipment,fuel) + c_fuel(equipment,
        fuel)*energy_consumption(equipment, fuel));
        for year = 1:20
            growth = (1+growth_rate)^(year-1);
            discount = 1/(1+discount_rate)^(year);
            c_var(equipment, fuel) = c_var(equipment, fuel) +
            annual_cost * growth*discount;
        end
    end
end

%Fixed Cost ($) Over 20 Years (rows=equipment, cols=years)
% upfront costs in year "0"
% replacement costs in year 1-20 (columns 1-21)
fixed_bau = [zeros(6,21)];
fixed_elec = [c_upfront(:,2), zeros(6,20)];
fixed_h2 = [c_upfront(:,3), zeros(6,20)];

%Add in the costs for any replacements in the following rows
% (referencing lifetimes)
% whatever year equipment would be replaced in, add 1 because of the
shift
% due to year 0
fixed_bau(5,9+1) = 129000; fixed_bau(5,18+1) = 129000;
fixed_bau(6,14+1) = 129000;

% Electric Battery Replacements
fixed_elec(2,6+1) = 5000; % replace forklift battery only
fixed_elec(:,11+1) = [5000, 10000, 10000, 10000, 10000, 10000]; %
replace all batteries
fixed_elec(2,16+1) = 5000; % replace forklift battery only
% Electric Equipment Replacements
fixed_elec(2,15+1) = 45000; % forklift
fixed_elec(5,9+1) = 250000; % yard tractor on-dock
fixed_elec(5,18+1) = 250000; % yard tractor on-dock
fixed_elec(6,13+1) = 274000; % yard tractor off-dock

fc_cost = 100; % per kW

```

```

% fixed_h2(1,14+1) = 23100;
% fixed_h2(2,11+1) = 70000;
% fixed_h2(3,11+1) = 3500000;
% fixed_h2(4,11+1) = 2520000;
% fixed_h2(5,11+1) = 350000;
% fixed_h2(6,11+1) = 350000;

% replace 42% of fuel cell stack every 7 years
fc_repl_rate = 0.42;
fixed_h2(1,14+1) = 23100; % machine replacement
fixed_h2(1,7+1) = 1*fc_cost*fc_repl_rate;
fixed_h2(2, 7+1) = 6.94*fc_cost*fc_repl_rate; fixed_h2(2, 15+1) =
6.94*fc_cost*fc_repl_rate;
fixed_h2(3, 7+1) = 62.49*fc_cost*fc_repl_rate; fixed_h2(3, 15+1) =
62.49*fc_cost*fc_repl_rate;
fixed_h2(4, 7+1) = 45.83*fc_cost*fc_repl_rate; fixed_h2(4, 15+1) =
45.83*fc_cost*fc_repl_rate;
fixed_h2(5, 9+1) = 350000; fixed_h2(5, 18+1) = 350000; % machine
replacement
fixed_h2(6, 13+1) = 350000; % machine replacement
fixed_h2(6, 7+1) = 29.16*fc_cost*fc_repl_rate; fixed_h2(6, 15+1) =
29.16*fc_cost*fc_repl_rate;

% fixed_h2(2, 6+1) = 6.94*fc_cost; fixed_h2(2, 12+1) = 6.94*fc_cost;
fixed_h2(2, 18+1) = 6.94*fc_cost;
% fixed_h2(3, 4+1) = 62.49*fc_cost; fixed_h2(3, 8+1) = 62.49*fc_cost;
% fixed_h2(3, 12+1) = 62.49*fc_cost; fixed_h2(3, 16+1) =
62.49*fc_cost;
% fixed_h2(4, 4+1) = 45.83*fc_cost; fixed_h2(4, 8+1) = 45.83*fc_cost;
% fixed_h2(4, 12+1) = 45.83*fc_cost; fixed_h2(4, 16+1) =
45.83*fc_cost;
% fixed_h2(5, 3+1) = 29.16*fc_cost; fixed_h2(5, 6+1) = 29.16*fc_cost;
% fixed_h2(5, 9+1) = 29.16*fc_cost; fixed_h2(5, 12+1) = 29.16*fc_cost;
% fixed_h2(5, 15+1) = 29.16*fc_cost; fixed_h2(5, 18+1) =
29.16*fc_cost;
% fixed_h2(6, 5+1) = 29.16*fc_cost; fixed_h2(6, 10+1) = 29.16*fc_cost;
% fixed_h2(6, 15+1) = 29.16*fc_cost; fixed_h2(6, 20+1) =
29.16*fc_cost;

%Interest rates each year
discount = zeros(21,1);
for years = 1:size(discount,1)
    discount(years) = 1/(1+discount_rate)^(years-1);
end

c_fixed = [fixed_bau*discount, fixed_elec*discount,
fixed_h2*discount];

%Reshape to 1x18, in row order
total_emissions = reshape(co2.', 1, 18);
total_cost = reshape((c_var + c_fixed).',1,18);

```

CVX Optimization

normalize values

```
lambda = 0:0.05:1;
total_cost_norm = total_cost./max(total_cost);
total_emissions_norm = total_emissions./max(total_emissions);
x_opt = zeros(18,size(lambda,2));
emissions_lambda = zeros(size(lambda,2),1);
costs_lambda = zeros(size(lambda,2),1);

for i = 1:size(lambda,2)
    cvx_begin
        variables x(18); % declare your optimization variables here
        minimize((1-lambda(i))*total_cost_norm*x +
lambda(i)*total_emissions_norm*x) % objective function here
        subject to % constraints

            % Number of each type of unit
            sum(x(1:3)) == num_rf;
            sum(x(4:6)) == num_fl;
            sum(x(7:9)) == num_rtg;
            sum(x(10:12)) == num_tp;
            sum(x(13:15)) == num_yt_on;
            sum(x(16:18)) == num_yt_off;
            x(1) >= 0;
            x(2) >= 0;
            x(3) >= 0;
            x(4) >= 0;
            x(5) >= 0;
            x(6) >= 0;
            x(7) >= 0;
            x(8) >= 0;
            x(9) >= 0;
            x(10) >= 0;
            x(11) >= 0;
            x(12) >= 0;
            x(13) >= 0;
            x(14) >= 0;
            x(15) >= 0;
            x(16) >= 0;
            x(17) >= 0;
            x(18) >= 0;

            %
            % total_emissions*x < 1E5*907.185;
            %
            % total_cost*x < 5000000000;

    cvx_end
    emissions_lambda(i) = total_emissions*x;
    costs_lambda(i) = total_cost*x;
    x_opt(:,i) = x;
```

```

0|0.000|0.000|8.1e+00|1.5e+01|8.4e+04|-2.671708e+03  0.000000e+00|
0:0:00| chol  1  1
1|1.000|1.000|2.8e-06|3.0e-01|5.4e+03|-2.048378e+02 -5.493724e+03|
0:0:00| chol  1  1
2|1.000|0.953|1.2e-07|4.3e-02|2.6e+02|-2.127467e+02 -4.495183e+02|
0:0:00| chol  1  1
3|1.000|1.000|1.3e-08|3.0e-03|9.2e+01|-2.874658e+02 -3.777378e+02|
0:0:00| chol  1  1
4|0.994|0.884|1.6e-08|6.1e-04|1.1e+01|-3.011192e+02 -3.113791e+02|
0:0:00| chol  1  1
5|0.967|0.912|2.2e-09|8.1e-05|1.3e+00|-3.051906e+02 -3.064339e+02|
0:0:00| chol  1  1
6|0.952|0.943|1.6e-10|7.4e-06|1.7e-01|-3.058207e+02 -3.059852e+02|
0:0:00| chol  1  1
7|0.977|0.979|8.5e-12|4.5e-07|3.9e-03|-3.059148e+02 -3.059185e+02|
0:0:00| chol  1  1
8|0.989|0.989|1.5e-13|5.0e-09|4.5e-05|-3.059171e+02 -3.059172e+02|
0:0:00| chol  1  1
9|0.989|0.989|1.9e-15|5.6e-11|4.9e-07|-3.059171e+02 -3.059171e+02|
0:0:00|
stop: max(relative gap, infeasibilities) < 1.49e-08
-----
number of iterations      =   9
primal objective value  = -3.05917145e+02
dual    objective value  = -3.05917146e+02
gap := trace(XZ)          = 4.90e-07
relative gap              = 8.00e-10
actual relative gap       = 7.54e-10
rel. primal infeas (scaled problem) = 1.90e-15
rel. dual      "      "      "      = 5.64e-11
rel. primal infeas (unscaled problem) = 0.00e+00
rel. dual      "      "      "      = 0.00e+00
norm(X), norm(Y), norm(Z) = 3.8e+02, 1.4e+00, 1.4e+00
norm(A), norm(b), norm(C) = 5.2e+00, 3.9e+02, 2.9e+00
Total CPU time (secs)   = 0.15
CPU time per iteration  = 0.02
termination code         = 0
DIMACS: 2.4e-15  0.0e+00  8.2e-11  0.0e+00  7.5e-10  8.0e-10
-----
Status: Solved
Optimal value (cvx_optval): +7.24188

```

Plotting

```

opt_rf = zeros(3,21); opt_fl = zeros(3,21); opt_rtg = zeros(3,21); opt_tp = zeros(3,21); opt_yt_on = ze-
ros(3,21); opt_yt_off = zeros(3,21);

for i = 1:3 opt_rf(i,:) = x_opt(i,:); opt_fl(i,:) = x_opt(i+3,:); opt_rtg(i,:) = x_opt(i+6,:); opt_tp(i,:) = x_opt(i
+9,:); opt_yt_on(i,:) = x_opt(i+12,:); opt_yt_off(i,:) = x_opt(i+15,:); end

```

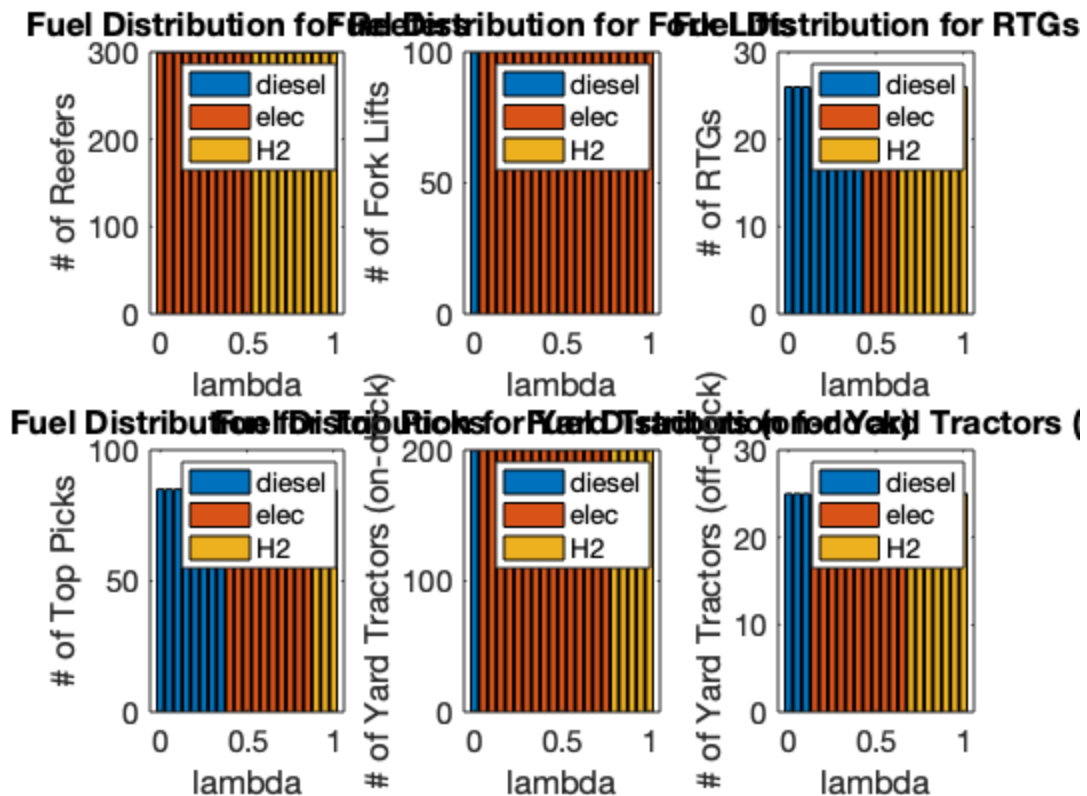
```

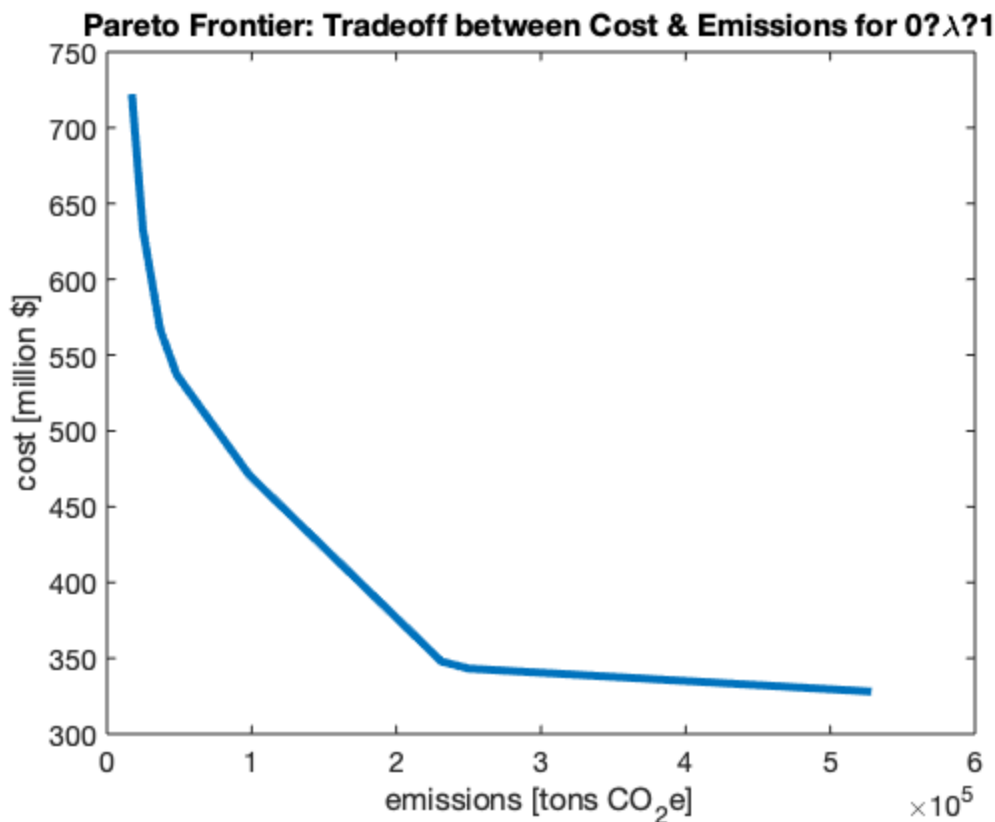
equipment_types = {'Reefers', 'Fork Lifts', 'RTGs', 'Top Picks', 'Yard Tractors (on-dock)', 'Yard Tractors (off-dock)'};

for i = 1:6
    subplot(2, 3, i);
    x_plot = x_opt(3*i-2:3*i,:);
    bar(lambda, x_plot, 'stacked');
    legend('diesel', 'elec', 'H2');
    xlabel('lambda');
    ylabel(strcat('# of', equipment_types(i)));
    title(strcat('Fuel Distribution for', equipment_types(i)));
    set(gca, 'FontSize', 15);
end

figure();
plot(emissions_lambda./907.185, costs_lambda./10^6, 'LineWidth', 4);
xlabel('emissions [tons CO_2e]');
ylabel('cost [million $]');
title('Pareto Frontier: Tradeoff between Cost & Emissions for 0?
\lambda=0');
% ta = annotation('textarrow', [0.86, 0.86], [0.28, 0.18], 'String',
% '\lambda=0', 'FontSize', 18);
set(gca, 'FontSize', 14);

```





Published with MATLAB® R2019b

Port_Model_ctax.m

Table of Contents

.....	1
Our System	1
Setting Up Constraints	1
Set Up Cost (for Objective Function)	2
CVX Optimization	4
Plotting	28

```
clear; close all;
fs = 15; % Font Size for plots
```

Our System

```
% objective function: minimize cost * number of units for each
% technology,
% summed up
% We want to be able to change hours operated/year, fuel prices,
% carbon
% tax, subsidies for buying the equipment (i.e. reducing capital cost
% of
% low carbon technology),

% x vector: discrete number of each type of technology. (eg: reefer
% BAU,
% reefer electric, reefer hydrogen, then: forklift, rtg, toppick, yard
% tractors
% on dock, and yard tractors off dock)

% constraints:

%INEQUALITY
% 1. capping emissions of all the equipment together
% 2.

%EQUALITY
% 1. total number of each type of unit
```

Setting Up Constraints

```
horizon = 20;

% Hours Each Unit is Run (hours) each year
h_rf = 3000;
h_fl = 720;
h_rtg = 1200;
h_tp = 1030;
h_yt_on = 1600;
h_yt_off = 1000;
```

```

operating_hours = [h_rf; h_fl; h_rtg; h_tp; h_yt_on; h_yt_off];

% Emissions from each technology [kgCO2(e)/gallon, kgCO2(e)/kWh,
% kgCO2(e)/kgH2].
% bau, electric, hydrogen
co2_energy = [13.34, 0.006 + 0.020125, 1.38];

% Total number of each type of unit (#)
num_rf = 299;
num_fl = 100;
num_rtg = 26;
num_tp = 85;
num_yt_on = 200;
num_yt_off = 25;

conv_fctr = co2_energy./907.185; % convert from kg CO2 to ton CO2

```

Set Up Cost (for Objective Function)

```

% Fuel Costs (feel free to change these unit, this is just my first
guess)
% BAU: $/gallon diesel
% Electricity: $/kWh electricity
% Hydrogen: $/kg hydrogen
c_fuel = [3.5, 0.04, 13.99; 3.5, 0.04, 13.99; 3.5, 0.04, 13.99;
3.5, 0.04, 13.99; 3.5, 0.04, 13.99; 3.5, 0.04, 13.99];

% Maintenance Costs
% BAU: $/operating hour
% Electricity: $/operating hour
% Hydrogen: $/operating hour
c_maintenance = [5, 4.75, 3.80; 5, 4.75, 3.80; 10, 8, 6.40; 10,
8, 6.40; 30, 20, 16; 25, 17, 14];

% Energy Consumption
% BAU: gallons of diesel/operating hour
% Electricity: kWh of electricity/hour
% Hydrogen: kg of hydrogen/hour
energy_consumption = [0.735, 2.8875, 0.029669; 1.5, 3.572, 0.208333;
6, 600, 1.875; 5, 206.4, 1.375; 2.5, 103.2, 0.875; 2.5, 103.2,
0.546875];

% Upfront Costs, [$/unit]
% For reefers, only the cost of the generator is considered (not
% plug), so electric capital cost = 0
c_upfront = [13900, 0, 23100; 40000, 45000, 70000; 2000000,
2500000, 3500000; 560000, 1600000, 2520000; 129000, 250000,
385000; 129000, 274000, 385000];
% Lifetime of equipment [years]
lifetimes = [20, 20, 13.333; 20, 20, 55.5; 20, 20, 33.333; 20,
20, 38.89159; 8, 8, 25; 13, 13, 40]; % maximum 20

growth_rate = 0.012;

```

```

discount_rate = 0.05;

% Total Emissions (kgCO2(e)) over 20 years, gives a 6x3
co2 = zeros(6,3);
for i = 1:horizon
    co2 = co2 + (co2_energy .* energy_consumption) .* 
    (operating_hours*(1+growth_rate)^(i-1));
end
% Remember to flatten this in the rows and not the columns!!
% Also make sure they're all normalized to years rather than hours or
days

%Fixed Cost ($) Over 20 Years (rows=equipment, cols=years)
% upfront costs in year "0"
% replacement costs in year 1-20 (columns 1-21)
fixed_bau = [zeros(6,21)];
fixed_elec = [c_upfront(:,2), zeros(6,20)];
fixed_h2 = [c_upfront(:,3), zeros(6,20)];

%Add in the costs for any replacements in the following rows
% (referencing lifetimes)
% whatever year equipment would be replaced in, add 1 because of the
shift
% due to year 0
fixed_bau(5,9+1) = 129000; fixed_bau(5,18+1) = 129000;
fixed_bau(6,14+1) = 129000;

% Electric Battery Replacements
fixed_elec(2,6+1) = 5000; % replace forklift battery only
fixed_elec(:,11+1) = [5000, 10000, 10000, 10000, 10000, 10000]; %
replace all batteries
fixed_elec(2,16+1) = 5000; % replace forklift battery only
% Electric Equipment Replacements
fixed_elec(2,15+1) = 45000; % forklift
fixed_elec(5,9+1) = 250000; % yard tractor on-dock
fixed_elec(5,18+1) = 250000; % yard tractor on-dock
fixed_elec(6,13+1) = 274000; % yard tractor off-dock

fc_cost = 100; % per kW
% fixed_h2(1,14+1) = 23100;
% fixed_h2(2,11+1) = 70000;
% fixed_h2(3,11+1) = 3500000;
% fixed_h2(4,11+1) = 2520000;
% fixed_h2(5,11+1) = 350000;
% fixed_h2(6,11+1) = 350000;

% replace 42% of fuel cell stack every 7 years
fc_repl_rate = 0.42;
fixed_h2(1,14+1) = 23100; % machine replacement
fixed_h2(1,7+1) = 1*fc_cost*fc_repl_rate;
fixed_h2(2, 7+1) = 6.94*fc_cost*fc_repl_rate; fixed_h2(2, 15+1) =
6.94*fc_cost*fc_repl_rate;
fixed_h2(3, 7+1) = 62.49*fc_cost*fc_repl_rate; fixed_h2(3, 15+1) =
62.49*fc_cost*fc_repl_rate;

```

```

fixed_h2(4, 7+1) = 45.83*fc_cost*fc_repl_rate; fixed_h2(4, 15+1) =
45.83*fc_cost*fc_repl_rate;
fixed_h2(5, 9+1) = 350000; fixed_h2(5, 18+1) = 350000; % machine
replacement
fixed_h2(6, 13+1) = 350000; % machine replacement
fixed_h2(6, 7+1) = 29.16*fc_cost*fc_repl_rate; fixed_h2(6, 15+1) =
29.16*fc_cost*fc_repl_rate;

% fixed_h2(2, 6+1) = 6.94*fc_cost; fixed_h2(2, 12+1) = 6.94*fc_cost;
fixed_h2(2, 18+1) = 6.94*fc_cost;
% fixed_h2(3, 4+1) = 62.49*fc_cost; fixed_h2(3, 8+1) = 62.49*fc_cost;
% fixed_h2(3, 12+1) = 62.49*fc_cost; fixed_h2(3, 16+1) =
62.49*fc_cost;
% fixed_h2(4, 4+1) = 45.83*fc_cost; fixed_h2(4, 8+1) = 45.83*fc_cost;
% fixed_h2(4, 12+1) = 45.83*fc_cost; fixed_h2(4, 16+1) =
45.83*fc_cost;
% fixed_h2(5, 3+1) = 29.16*fc_cost; fixed_h2(5, 6+1) = 29.16*fc_cost;
% fixed_h2(5, 9+1) = 29.16*fc_cost; fixed_h2(5, 12+1) = 29.16*fc_cost;
% fixed_h2(5, 15+1) = 29.16*fc_cost; fixed_h2(5, 18+1) =
29.16*fc_cost;
% fixed_h2(6, 5+1) = 29.16*fc_cost; fixed_h2(6, 10+1) = 29.16*fc_cost;
% fixed_h2(6, 15+1) = 29.16*fc_cost; fixed_h2(6, 20+1) =
29.16*fc_cost;

%Interest rates each year
discount = zeros(21,1);
for years = 1:size(discount,1)
    discount(years) = 1/(1+discount_rate)^(years-1);
end

subsidy = 0.25;
c_fixed = [fixed_bau*discount, fixed_elec*(1-subsidy)*discount,
fixed_h2*(1-subsidy)*discount];

%Reshape to 1x18, in row order
total_emissions = reshape(co2.', 1, 18);

```

CVX Optimization

```

normalize values lambda=0:0.05:1; total_cost_norm=total_cost./max(total_cost); total_emissions_norm
=total_emissions./max(total_emissions);

c_tax = 0:125:2500; % [$/ton CO2]
x_opt = zeros(18,size(c_tax,2));

for i = 1:size(c_tax,2)
    % Variable Cost ($) over 20 years
    c_var = zeros(6,3);

    for equipment = 1:6
        for fuel = 1:3

```

```

        annual_cost = operating_hours(equipment)
* (c_maintenance(equipment,fuel) + (c_fuel(equipment,
fuel)+c_tax(i)*conv_fctr(fuel))*energy_consumption(equipment, fuel));
    for year = 1:20
        growth = (1+growth_rate)^(year-1);
        discount = 1/(1+discount_rate)^(year);
        c_var(equipment, fuel) = c_var(equipment, fuel) +
annual_cost * growth*discount;
    end
end
total_cost = reshape((c_var + c_fixed).',1,18);

cvx_begin
    variables x(18); % declare your optimization variables here
    minimize(total_cost*x) % objective function here
    subject to % constraints

        % Number of each type of unit
        sum(x(1:3)) == num_rf;
        sum(x(4:6)) == num_fl;
        sum(x(7:9)) == num_rtg;
        sum(x(10:12)) == num_tp;
        sum(x(13:15)) == num_yt_on;
        sum(x(16:18)) == num_yt_off;
        x(1) >= 0;
        x(2) >= 0;
        x(3) >= 0;
        x(4) >= 0;
        x(5) >= 0;
        x(6) >= 0;
        x(7) >= 0;
        x(8) >= 0;
        x(9) >= 0;
        x(10) >= 0;
        x(11) >= 0;
        x(12) >= 0;
        x(13) >= 0;
        x(14) >= 0;
        x(15) >= 0;
        x(16) >= 0;
        x(17) >= 0;
        x(18) >= 0;

        % total_emissions*x < 1E5*907.185;

        % total_cost*x < 3000000000;

cvx_end

x_opt(:,i) = x;

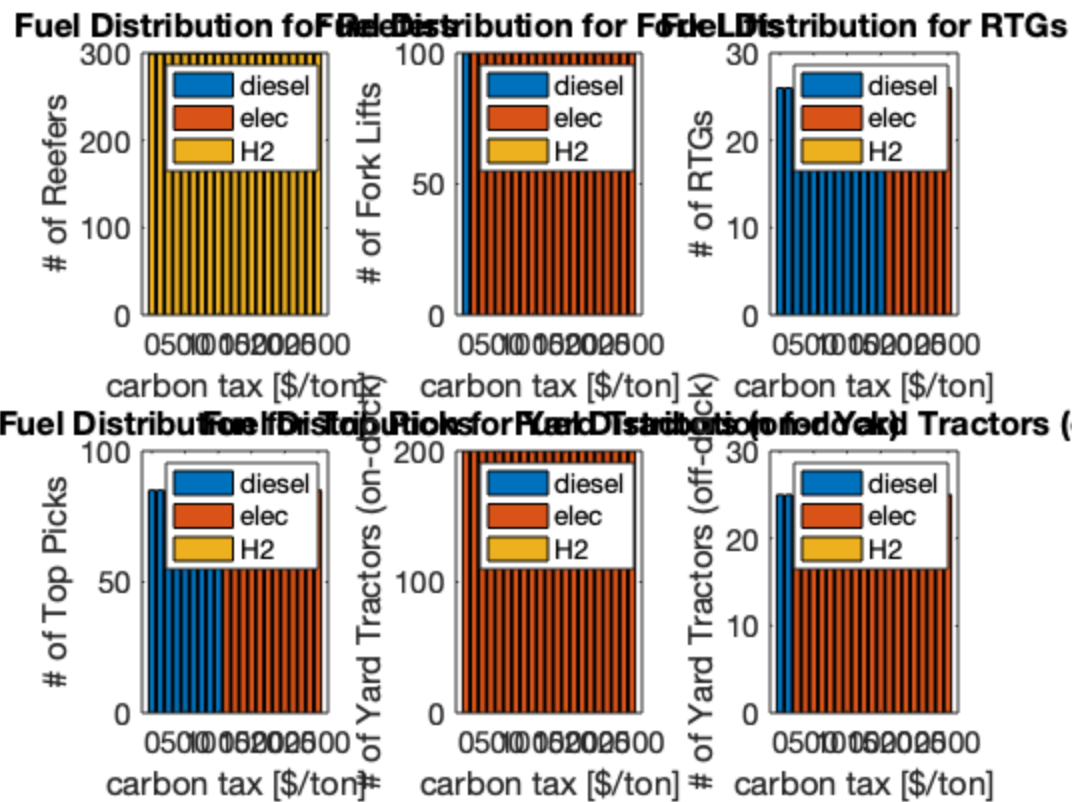
end

```

```
--  
Status: Solved  
Optimal value (cvx_optval): +5.27402e+08
```

Plotting

```
opt_rf = zeros(3,21); opt_fl = zeros(3,21); opt_rtg = zeros(3,21); opt_tp = zeros(3,21); opt_yt_on = zeros(3,21); opt_yt_off = zeros(3,21);  
  
for i = 1:3 opt_rf(i,:) = x_opt(i,:); opt_fl(i,:) = x_opt(i+3,:); opt_rtg(i,:) = x_opt(i+6,:); opt_tp(i,:) = x_opt(i+9,:); opt_yt_on(i,:) = x_opt(i+12,:); opt_yt_off(i,:) = x_opt(i+15,:); end  
  
equipment_types = {'Reefers', 'Fork Lifts', 'RTGs', 'Top Picks', 'Yard Tractors (on-dock)', 'Yard Tractors (off-dock)' };  
  
for i = 1:6  
    subplot(2, 3, i);  
    x_plot = x_opt(3*i-2:3*i,:);  
    bar(c_tax, x_plot', 'stacked');  
    legend('diesel', 'elec', 'H2');  
    xlabel('carbon tax [$/ton]');  
    ylabel(strcat('# of', equipment_types(i)));  
    title(strcat('Fuel Distribution for', equipment_types(i)));  
    xticks([0, 500, 1000, 1500, 2000, 2500]);  
    set(gca, 'Fontsize', 15);  
end
```



Published with MATLAB® R2019b

Port_Model_subsidy.m

Table of Contents

.....	1
Our System	1
Setting Up Constraints	1
Set Up Cost (for Objective Function)	2
CVX Optimization	5
Plotting	28

```
clear; close all;
fs = 15; % Font Size for plots
```

Our System

```
% objective function: minimize cost * number of units for each
technology,
% summed up
% We want to be able to change hours operated/year, fuel prices,
carbon
% tax, subsidies for buying the equipment (i.e. reducing capital cost
of
% low carbon technology),

% x vector: discrete number of each type of technology. (eg: reefer
BAU,
% reefer electric, reefer hydrogen, then: forklift, rtg, toppick, yard
tractors
% on dock, and yard tractors off dock)

% constraints:

%INEQUALITY
% 1. capping emissions of all the equipment together
% 2.

%EQUALITY
% 1. total number of each type of unit
```

Setting Up Constraints

```
horizon = 20;

% Hours Each Unit is Run (hours) each year
h_rf = 3000;
h_fl = 720;
h_rtg = 1200;
h_tp = 1030;
h_yt_on = 1600;
h_yt_off = 1000;
operating_hours = [h_rf; h_fl; h_rtg; h_tp; h_yt_on; h_yt_off];
```

```

% Emissions from each technology [kgCO2(e)/gallon, kgCO2(e)/kWh,
% kgCO2(e)/kgH2].
% bau, electric, hydrogen
co2_energy = [13.34, 0.006 + 0.020125, 1.38];

% Total number of each type of unit (#)
num_rf = 299;
num_fl = 100;
num_rtg = 26;
num_tp = 85;
num_yt_on = 200;
num_yt_off = 25;

```

Set Up Cost (for Objective Function)

```

% Fuel Costs (feel free to change these unit, this is just my first
guess)
% BAU: $/gallon diesel
% Electricity: $/kWh electricity
% Hydrogen: $/kg hydrogen
c_fuel = [3.5, 0.04, 13.99; 3.5, 0.04, 13.99; 3.5, 0.04, 13.99;
3.5, 0.04, 13.99; 3.5, 0.04, 13.99; 3.5, 0.04, 13.99];

% Maintenance Costs
% BAU: $/operating hour
% Electricity: $/operating hour
% Hydrogen: $/operating hour
c_maintenance = [5, 4.75, 3.80; 5, 4.75, 3.80; 10, 8, 6.40; 10,
8, 6.40; 30, 20, 16; 25, 17, 14];

% Energy Consumption
% BAU: gallons of diesel/operating hour
% Electricity: kWh of electricity/hour
% Hydrogen: kg of hydrogen/hour
energy_consumption = [0.735, 2.8875, 0.029669; 1.5, 3.572, 0.208333;
6, 600, 1.875; 5, 206.4, 1.375; 2.5, 103.2, 0.875; 2.5, 103.2,
0.546875];

% Upfront Costs, [$/unit]
% For reefers, only the cost of the generator is considered (not
% plug), so electric capital cost = 0
c_upfront = [13900, 0, 23100; 40000, 45000, 70000; 2000000,
2500000, 3500000; 560000, 1600000, 2520000; 129000, 250000,
385000; 129000, 274000, 385000];
% Lifetime of equipment [years]
lifetimes = [20, 20, 13.333; 20, 20, 55.5; 20, 20, 33.333; 20,
20, 38.89159; 8, 8, 25; 13, 13, 40]; % maximum 20

growth_rate = 0.012;
discount_rate = 0.05;

% Total Emissions (kgCO2(e)) over 20 years, gives a 6x3

```

```

co2 = zeros(6,3);
for i = 1:horizon
    co2 = co2 + (co2_energy .* energy_consumption) .*
    (operating_hours*(1+growth_rate)^(i-1));
end
% Remember to flatten this in the rows and not the columns!!
% Also make sure they're all normalized to years rather than hours or
days

% Variable Cost ($) over 20 years
c_var = zeros(6,3);

for equipment = 1:6
    for fuel = 1:3
        annual_cost = operating_hours(equipment) *
        (c_maintenance(equipment,fuel) + c_fuel(equipment,
        fuel)*energy_consumption(equipment, fuel));
        for year = 1:20
            growth = (1+growth_rate)^(year-1);
            discount = 1/(1+discount_rate)^(year);
            c_var(equipment, fuel) = c_var(equipment, fuel) +
            annual_cost * growth*discount;
        end
    end
end

%Fixed Cost ($) Over 20 Years (rows=equipment, cols=years)
% upfront costs in year "0"
% replacement costs in year 1-20 (columns 1-21)
fixed_bau = [zeros(6,21)];
fixed_elec = [c_upfront(:,2), zeros(6,20)];
fixed_h2 = [c_upfront(:,3), zeros(6,20)];

%Add in the costs for any replacements in the following rows
% (referencing lifetimes)
% whatever year equipment would be replaced in, add 1 because of the
shift
% due to year 0
fixed_bau(5,9+1) = 129000; fixed_bau(5,18+1) = 129000;
fixed_bau(6,14+1) = 129000;

% Electric Battery Replacements
fixed_elec(2,6+1) = 5000; % replace forklift battery only
fixed_elec(:,11+1) = [5000, 10000, 10000, 10000, 10000, 10000]; %
replace all batteries
fixed_elec(2,16+1) = 5000; % replace forklift battery only
% Electric Equipment Replacements
fixed_elec(2,15+1) = 45000; % forklift
fixed_elec(5,9+1) = 250000; % yard tractor on-dock
fixed_elec(5,18+1) = 250000; % yard tractor on-dock
fixed_elec(6,13+1) = 274000; % yard tractor off-dock

fc_cost = 100; % per kW
% fixed_h2(1,14+1) = 23100;

```

```

% fixed_h2(2,11+1) = 70000;
% fixed_h2(3,11+1) = 3500000;
% fixed_h2(4,11+1) = 2520000;
% fixed_h2(5,11+1) = 350000;
% fixed_h2(6,11+1) = 350000;

% replace 42% of fuel cell stack every 7 years
fc_repl_rate = 0.42;
fixed_h2(1,14+1) = 23100; % machine replacement
fixed_h2(1,7+1) = 1*fc_cost*fc_repl_rate;
fixed_h2(2, 7+1) = 6.94*fc_cost*fc_repl_rate; fixed_h2(2, 15+1) =
6.94*fc_cost*fc_repl_rate;
fixed_h2(3, 7+1) = 62.49*fc_cost*fc_repl_rate; fixed_h2(3, 15+1) =
62.49*fc_cost*fc_repl_rate;
fixed_h2(4, 7+1) = 45.83*fc_cost*fc_repl_rate; fixed_h2(4, 15+1) =
45.83*fc_cost*fc_repl_rate;
fixed_h2(5, 9+1) = 350000; fixed_h2(5, 18+1) = 350000; % machine
replacement
fixed_h2(6, 13+1) = 350000; % machine replacement
fixed_h2(6, 7+1) = 29.16*fc_cost*fc_repl_rate; fixed_h2(6, 15+1) =
29.16*fc_cost*fc_repl_rate;

% fixed_h2(2, 6+1) = 6.94*fc_cost; fixed_h2(2, 12+1) = 6.94*fc_cost;
fixed_h2(2, 18+1) = 6.94*fc_cost;
% fixed_h2(3, 4+1) = 62.49*fc_cost; fixed_h2(3, 8+1) = 62.49*fc_cost;
% fixed_h2(3, 12+1) = 62.49*fc_cost; fixed_h2(3, 16+1) =
62.49*fc_cost;
% fixed_h2(4, 4+1) = 45.83*fc_cost; fixed_h2(4, 8+1) = 45.83*fc_cost;
% fixed_h2(4, 12+1) = 45.83*fc_cost; fixed_h2(4, 16+1) =
45.83*fc_cost;
% fixed_h2(5, 3+1) = 29.16*fc_cost; fixed_h2(5, 6+1) = 29.16*fc_cost;
% fixed_h2(5, 9+1) = 29.16*fc_cost; fixed_h2(5, 12+1) = 29.16*fc_cost;
% fixed_h2(5, 15+1) = 29.16*fc_cost; fixed_h2(5, 18+1) =
29.16*fc_cost;
% fixed_h2(6, 5+1) = 29.16*fc_cost; fixed_h2(6, 10+1) = 29.16*fc_cost;
% fixed_h2(6, 15+1) = 29.16*fc_cost; fixed_h2(6, 20+1) =
29.16*fc_cost;

%Interest rates each year
discount = zeros(21,1);
for years = 1:size(discount,1)
    discount(years) = 1/(1+discount_rate)^(years-1);
end

% c_fixed = [fixed_bau*discount, fixed_elec*discount,
fixed_h2*discount];

%Reshape to 1x18, in row order
total_emissions = reshape(co2.', 1, 18);
% total_cost = reshape((c_var + c_fixed).',1,18);

```

CVX Optimization

normalize values

```
subsidy = 0:0.05:1;
x_opt = zeros(18,size(subsidy,2));

for i = 1:size(subsidy,2)
    c_fixed = [fixed_bau*discount, fixed_elec*(1-subsidy(i))*discount,
    fixed_h2*(1-subsidy(i))*discount];
    total_cost = reshape((c_var + c_fixed).',1,18);
    cvx_begin
        variables x(18); % declare your optimization variables here
        minimize(total_cost*x) % objective function here
        subject to % constraints

            % Number of each type of unit
            sum(x(1:3)) == num_rf;
            sum(x(4:6)) == num_fl;
            sum(x(7:9)) == num_rtg;
            sum(x(10:12)) == num_tp;
            sum(x(13:15)) == num_yt_on;
            sum(x(16:18)) == num_yt_off;
            x(1) >= 0;
            x(2) >= 0;
            x(3) >= 0;
            x(4) >= 0;
            x(5) >= 0;
            x(6) >= 0;
            x(7) >= 0;
            x(8) >= 0;
            x(9) >= 0;
            x(10) >= 0;
            x(11) >= 0;
            x(12) >= 0;
            x(13) >= 0;
            x(14) >= 0;
            x(15) >= 0;
            x(16) >= 0;
            x(17) >= 0;
            x(18) >= 0;

            % total_emissions*x < 1E5*907.185;

            % total_cost*x < 500000000;

    cvx_end
    x_opt(:,i) = x;

end
```

```

7|0.988|0.988|3.8e-10|2.0e-10|2.3e+02|-1.576735e+08 -1.576737e+08|
0:0:00| chol 1 1
8|0.989|0.989|1.3e-10|7.7e-11|2.5e+00|-1.576737e+08 -1.576737e+08|
0:0:00|
stop: max(relative gap, infeasibilities) < 1.49e-08
-----
number of iterations      =  8
primal objective value = -1.57673658e+08
dual   objective value = -1.57673660e+08
gap := trace(XZ)          = 2.49e+00
relative gap              = 7.88e-09
actual relative gap       = 7.89e-09
rel. primal infeas (scaled problem) = 1.26e-10
rel. dual    "        "        "        = 7.74e-11
rel. primal infeas (unscaled problem) = 0.00e+00
rel. dual    "        "        "        = 0.00e+00
norm(X), norm(y), norm(Z) = 3.8e+02, 5.6e+05, 5.8e+05
norm(A), norm(b), norm(C) = 5.2e+00, 3.9e+02, 7.2e+05
Total CPU time (secs)   = 0.06
CPU time per iteration = 0.01
termination code         = 0
DIMACS: 1.6e-10  0.0e+00  1.2e-10  0.0e+00  7.9e-09  7.9e-09
-----
-----
Status: Solved
Optimal value (cvx_optval): +2.02762e+08

```

Plotting

```

opt_rf = zeros(3,21); opt_fl = zeros(3,21); opt_rtg = zeros(3,21); opt_tp = zeros(3,21); opt_yt_on = zeros(3,21); opt_yt_off = zeros(3,21);

for i = 1:3 opt_rf(i,:) = x_opt(i,:); opt_fl(i,:) = x_opt(i+3,:); opt_rtg(i,:) = x_opt(i+6,:); opt_tp(i,:) = x_opt(i+9,:); opt_yt_on(i,:) = x_opt(i+12,:); opt_yt_off(i,:) = x_opt(i+15,:); end

equipment_types = {'Reefers', 'Fork Lifts', 'RTGs', 'Top Picks', 'Yard Tractors (on-dock)', 'Yard Tractors (off-dock)'};

for i = 1:6
    subplot(2, 3, i);
    x_plot = x_opt(3*i-2:3*i,:);
    bar(subsidy.*100, x_plot, 'stacked');
    legend('diesel', 'elec', 'H2');
    xlabel('equipment subsidy (%)');
    ylabel(strcat('# of ', equipment_types(i)));
    title(strcat('Fuel Distribution for ', equipment_types(i)));
    set(gca, 'FontSize', 15);
end

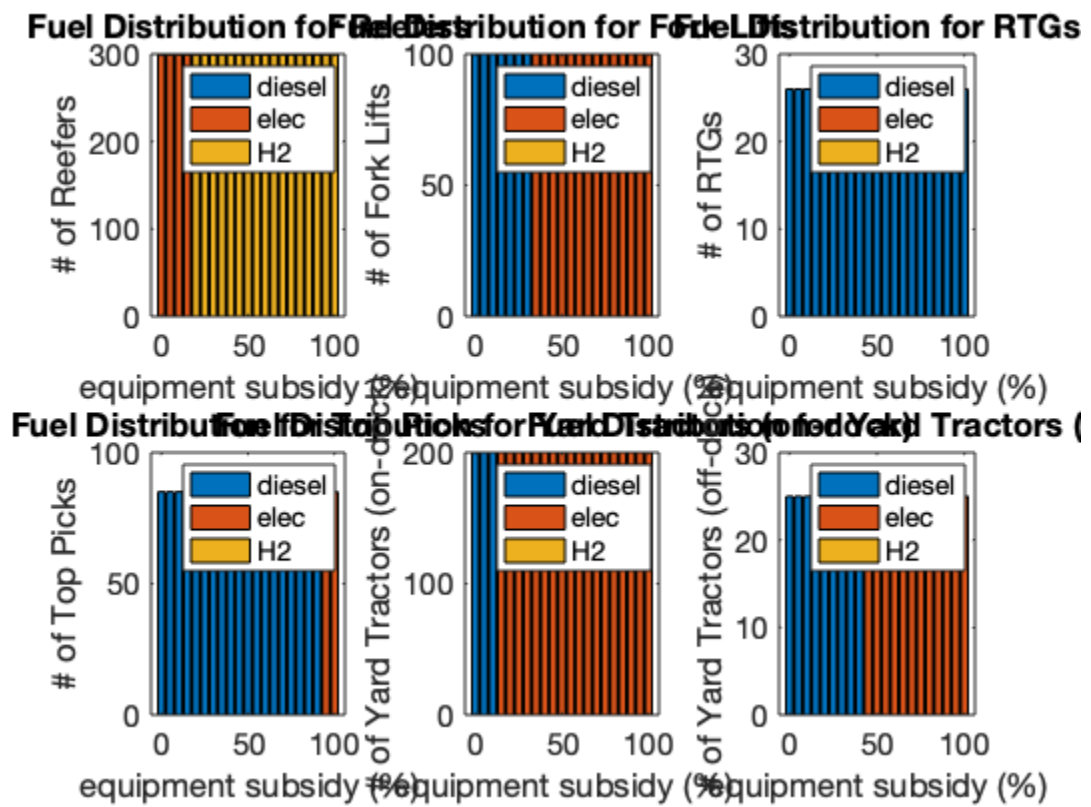
% figure();
% plot(emissions_lambda./907.185, cost_lambda./10^6, 'LineWidth', 4);
% xlabel('emissions [tons CO2e]');

```

```

% ylabel('cost [million $]');
% title('Pareto Frontier: Tradeoff between Cost & Emissions for 0?
\lambda?1');
% % ta = annotation('textarrow', [0.86, 0.86], [0.28, 0.18], 'String',
'\\lambda=0', 'FontSize', 18);
% set(gca, 'Fontsize', 14);

```



Published with MATLAB® R2019b

Environmental and Economic Implications of Energy Storage in California

Sarah Cook, Rachel Hursh, Sarah Nordahl, Natalia Pascual,
Jason Porzio, Pietro Vannucci

University of California, Berkeley
CEE 295: Energy Systems and Control
May 8, 2020

Abstract

Energy storage is an underutilized, emerging technology with potential to revolutionize and help decarbonize the electricity sector. This study seeks to determine the profit maximizing amount of Li-ion battery capacity for energy arbitrage in the California electricity market between 2020 and 2050. We accounted for variability in future outcomes by analyzing results of scenarios with differing capital costs, electricity prices, and energy policy adherence. Each of these scenarios was analyzed through the lens of profit maximization as well as environmental benefits maximization. In the profit maximizing optimization model, we found that under a majority of the market conditions there are no incentives to increase the total battery energy storage system (BESS) capacity in California past the initial capacity existing in 2020. High construction cost of Li-ion BESS facilities is the main barrier to their profitability and implementation. These results suggest a likely need for subsidies to develop this industry in order to overcome high construction costs. In the environmental benefit maximizing optimization model, we found that avoided emissions are greater when GHG policy adherence is low and lesser when policy adherence is high, and produced larger increases in BESS capacity than in the profit maximizing scenario. This shows that Li-ion batteries provide an environmental service that should be considered when setting energy storage targets. Finally, the “optimal” quantity of lithium ion BESS facilities is highly dependent on the global setting as factors like electricity prices, energy demand, and electricity mix greatly impact results and are highly uncertain. For now, all we can conclusively say is that *broadly*, across many scenarios, increasing lithium ion BESS capacity has positive profits and benefits.

Introduction

Motivation and Background

Electricity has always been a particularly challenging form of energy to manage, primarily due to the inherent complications of storage. Matching electrical power production with its consumption has been the key constraint dictating its use. This is not only due to the fact that electricity is difficult to store efficiently, but also because electricity demand is highly time-dependent. One way that spikes in demand have been met in the past is through the use of highly-inefficient and costly (both monetarily and environmentally) “peaker plants”. These plants, typically powered by natural gas, are set to go online every evening after most users return home and solar power production decreases. While this method provides needed power during this time, there are several drawbacks. The rapid ramping of natural gas combustion has obvious pollutant emissions associated with it and the cost of running these expensive plants combined with the surge in demand only serves to drive up electricity prices for everyone. One way to reduce these negative side-effects, is to devise a way to better store energy throughout the day. Battery Energy Storage System (BESS) are a promising alternative to surmount this obstacle and bolster the energy grid in a reliable way. They provide opportunities to leverage the extra energy produced from renewables and deliver that energy when demand is highest, thus reducing our reliance on peaker plants.

In the past, battery storage ventures have failed to entice investors who were primarily worried about the upfront costs of constructing a BESS facility. Due to the lack of projects of sufficiently large scope to learn from, uncertainties still remain in projecting expenditures. Therefore, our project hopes to address this concern by exploring the profitability of BESS. We are interested in figuring out what quantity of storage the state of California needs in order to meet demand while still being profitable, excluding any ancillary services that BESS might otherwise provide. The environmental benefit of electricity storage is important, but we understand that industries are unlikely to invest in solutions that are not also economically attractive. Therefore, our goal is to outline a system through which energy storage could be profitable while establishing independence from fossil fuels. This study will show whether increasing storage has the capability to financially satisfy investors while also reducing overall emissions. To be comprehensive in our assessment, we are basing emissions off of life-cycle assessment numbers and we include the environmental burden of producing the batteries required for the energy storage we recommend. Finding solutions to this problem has immense applications for California’s energy grid and beyond.

To aid in our analysis, we will utilize financial analysis techniques we’ve learned in MBA 212: Energy and Environmental Markets, as well as grid infrastructure analysis we are learning in ENERES 254: Electric Power Systems.

Problem Statement

Our goal is to determine optimal BESS capacity and associated profits along with the corresponding GHG emission savings for the years 2020-2050 in California. The focus of this study is to determine the profit maximizing and social benefit maximizing amount of Li-ion energy storage for arbitrage in the California energy market through an optimization model over a variety of price and policy scenarios. Additionally, we will identify environmental impacts of these scenarios.

Relevant Literature and Data Collection

Although energy storage systems have existed for many decades, there has been a recent boom in popularity and research regarding lithium-ion energy storage. Spurred by the growth of electric vehicles and changing electricity portfolios, lithium-ion technology and market trends are rapidly changing, and their influence on existing electric power systems is quickly growing. Luckily, there is a wealth of scientific resources describing the current setting and challenges in the fields of BESS and the infrastructure they enhance.

Many papers give a “techno-economic” review of the functions and basic physics of BESS to help describe how batteries work and the role they could fill in our current electric infrastructure. Ahlen et al. (2019) provides a good representation of this, as it presents these topics and defines many of the key terminologies, uses, and market trends of batteries, specifically Li-ion and flow batteries. The report goes in depth on the many use cases of batteries and the concept of value stacking - the ability for batteries to perform multiple functions at once. In particular, Ahlen et al. breaks down the uses into peak reduction services, reliability services, energy arbitrage, frequency regulation, microgrid/offgrid services, renewable services, and transmission / distribution system deferral. Our report focuses only on the description of energy arbitrage and how batteries behave while performing this function. Additionally, Ahlen et al. introduced cost components of batteries and forecasts of battery prices into the future. The report also displayed a steeply decreasing price trend for the capital costs of Li-ion batteries that inspired us to investigate when and if arbitrage services could be profitable and beneficial in California.

One of the most influential factors on determining profitability and benefit of BESS is capital costs. To get more detailed forecasts of Li-ion battery capital costs into the future, we utilized values from Cole and Frazier (2019). This NREL synthesis of data collected capital cost projections for Li-ion batteries from existing literature and compiled these results into three trends (low, medium, and high) out to 2050. These three trends all predict a sharp drop in Li-ion BESS capital costs that will eventually level out. The values from these three pathways were used directly as the low, medium, and high capital cost scenarios for our objective functions (see Table 1). Cole and Frazier (2019) also mentioned how almost all past capital cost projections were gross over-estimates compared to actual historic trends. Ultimately, they stated there was a high degree of uncertainty in cost trends. However, price trends for ancillary technologies, such as solar panels, may be used as a point of comparison. Li-ion BESS technology could see large-scale adoption and the emergence of a well-developed supply chain, similar to the growth of solar panels. Given that the Li-ion BESS supply chain spans many regions, there are many potential sources of uncertainty that may affect future pricing.

In addition to capital costs, operation and maintenance (O&M) of BESS facilities were considered. Feldman et al. (2019) provides a detailed breakdown of the costs associated with a Li-ion BESS from which we used the annual O&M value in our objective functions. Feldman et al. also provides detailed values of capital cost, breaking it down into money spent on the battery pack itself, the electrical and structural balance of systems, the engineering procurement and construction, and more.

We also explored relevant literature on the environmental impacts of the use phase of BESS, ultimately finding that this was a very complex field. The environmental impacts associated with BESS use is heavily dependent on when the batteries are charged/discharged and the electricity mix sourcing the batteries. Kern (2019) discusses how the multiple services provided by energy storage cause differing environmental impacts that can be compiled similar to value stacking. Additionally, Kern explores the possibility of optimizing the hourly capacity dedicated to a variety of functions in order to maximize

positive environmental impacts. We focused mainly on Kern's discussion of the environmental impact of energy arbitrage given the scope of our project, but it was interesting to observe how some services result in positive environmental impacts, while others result in negative environmental impacts. In the future, decisions will have to be made on how to best optimize the use of BESS, and compromises will have to be made between environmental responsibility, grid functionality, and industry profit.

Given that our study focuses on California, we needed to collect data on regional electricity prices, demand, and supply. A base year of price data was created by averaging discounted prices from 2017, 2018, and 2019 data available through EIA's website. We generated three electricity price forecasts: a low 1% annual price increase, a medium 2% annual price increase, and a high 5% annual price increase. The price increases were applied to the base year to create our future forecasts. Base years of supply and demand data were also generated in a similar manner. Demand values were averaged over the last three years to generate a demand base year, and using the assumption that electricity supply equals demand, we set the supply base year equal to the demand base year. However, when trends regarding supply and demand were pulled from the EIA, it was observed that supply and demand was stable year to year in California since roughly 2008. Further research was done to determine how supply and demand should be modeled into the future. Some sources predicted that yearly supply and demand would resume increasing due to increased electrification in many sectors, particularly transportation (Kavalec 2018). However, many sources predicted that the electricity usage trend would remain stable or even decrease due to the increased availability of energy efficient technologies countering increased electrification from other sectors (McGinty 2019; Davis 2020). Ultimately, due to unprecedented global events that resulted in decreased electricity usage across all sectors (Dewan 2020) and historic evidence of yearly demand stability, we felt it was appropriate to forecast supply and demand as unchanging year to year. It still remains unclear how electricity supply and demand trends will change in the future, and it will be interesting to see if electricity usage or pricing is significantly altered as a result of current events.

Methodology

Our analysis began by clearly delineating the system boundaries and temporal scope. We decided we would focus on the state of California for the time period of 2020 to 2050 to account for profits within the lifetime of a battery and to include long term clean energy policy goals. To simplify our analysis, we did not take network constraints into account (i.e. transmission and distribution complications) and we assumed that our theoretical interaction with the grid would have a negligible effect on its overall operation and economics. Making these assumptions allowed us to simply focus on the given supply and demand at every point in time in terms of the price of electricity and the fuel mix used to generate it.

As such, the next step was to construct the objective function. We wanted a function that would weigh the potential profit of using BESS for energy arbitrage against the cost of procuring, installing, and maintaining the system. To account for variability in these costs, we created scenarios for varying forecasted electricity prices and construction costs throughout our time horizon (Table 2) Therefore, by optimizing for profitability we were able to find the amount of BESS capacity for which installation is economically incentivized. Consequently, the environmental impact of this could then be derived as a function of the optimized capacity. The resulting objective function is shown as Equation 1:

$$\max_Q \sum_{k=2020}^{2050} (\sum_{i=1}^{365} \sum_{j=0}^{23} P_{ijk} (q_{ijk} - r_{ijk})) - C_k (Q_k - Q_{k-1}) - M_k Q_k \quad (1)$$

The first term of this equation, P_{ijk} , represents the price of electricity at a specific hour, day, and year. These values were calculated by extrapolating CAISO data from 2017-2019. First, an average hourly price for a standard year was derived from two representative days in each month in order to represent the diurnal and seasonal variability. Secondly, this price was extrapolated into the future based on forecasted electricity prices (EIA 2020). P_{ijk} is then multiplied by energy entering or leaving BESS at a given time, given by the term $(q_{ijk} - r_{ijk})$, to find the sales revenue or purchasing costs for that hour, reflecting the cash flow at each point in time as a function of whether we are storing or dispensing electricity. The next variable, C_k , represents the capital costs of installing additional units of battery storage and is taken from Cole and Frazier (2019). The capital cost is multiplied by the change in total amount of energy storage capacity in a given year, which is represented by $Q_k - Q_{k-1}$. The variable, M_k , then takes into account the expected maintenance costs as a function of total capacity and was estimated from Fu et al. (2018). In order to account for differences in prices over our timeframe, the net present value (NPV) of every datapoint was calculated based on 2020 US dollars. The objective function combines all these terms in order to weigh the potential revenue of expanding capacity against capital and maintenance costs over a 30 year time horizon. This objective function was constrained by the following guidelines:

$$Z_{ijk} = Z_{i(j-1)k} + \eta r_{ijk} - \frac{1}{\eta} q_{ijk} \quad (2)$$

$$0 \leq Z_{ijk} \leq Q_k \quad (3)$$

$$0 \leq q_{ijk} \leq \frac{1}{4} Q_k \quad (4)$$

$$0 \leq r_{ijk} \leq \frac{1}{4} Q_k \quad (5)$$

$$r_{ijk} \leq 0.05 * D_{ijk} \quad (6)$$

$$q_{ijk} \leq 0.05 * D_{ijk} \quad (7)$$

Equation 2 represents the constraint on charge dynamics for the battery system. Energy losses from the BESS as a result of charging from and discharging to the grid are accounted for with the efficiency term η , assuming there are losses from the transfer in both directions. Equations 3-5 simply establish the physical limit on the amount of energy that can enter or leave the battery. Equation 3 restricts the state of charge to be between 0 (empty) and Q_k (full). The total capacity was modeled as a single battery with a traditional four hour charging cycle, which is represented by Equations 4 and 5 limiting the total hourly charge/discharge to $\frac{1}{4}$ of the total capacity. Finally, in order to ensure that grid stability remained unaffected by our additional BESS capacity, we limited the possible charging or discharging at any given time to be 5% of the total grid demand. This is taken into consideration in Equations 6 and 7. Total grid demand was calculated from the average demand at each hour of two representative days per month, similarly to the hourly price forecasting, in years 2017-2019 as reported by EIA (2020). The above objective function and constraints allow the program to solve for the optimal amount of battery capacity in California each year for the next 30 years, strictly in terms of the economic benefits.

Once the optimal level of BESS capacity was determined from the objective function, we then wanted to determine the subsequent environmental impact. To do so, we first needed to forecast the hourly energy mix of the California grid through 2050. We accomplished this similarly to how we calculated the average hourly price. We sampled two representative days in each month from CAISO data in years 2017-2019 to determine a 2020 baseline. To extrapolate into the future, we began by considering California Senate Bill 100, which states that 100% renewable energy usage (which we considered as the sources in green in Table 1) should be met by 2045. We determined the GHG impacts of optimal BESS capacity based on three scenarios that represent different levels of adherence to the SB100 goal (High = 100% achievement, Medium = 70% progress, and Low = 30% progress). A complete list of these scenarios can be found in Table 3. To calculate the carbon intensity, we took a weighted average of the emissions factors for each energy source. The carbon intensity without BESS was then compared to the new carbon intensity with optimal BESS capacity to identify the potential benefit of utilizing battery technology to support the grid. Table 1 shows the various energy sources in the grid and their respective carbon intensities.

Table 1: Carbon Intensities of CA Grid Suppliers

Source (CAISO Designation)	Emission Factor (kg CO ₂ e/MWh)	Assumptions/Sources
Geothermal	38	Horvath 2019
Biomass	56	Horvath 2019
Biogas	-58	Russel et al. 2019
Small Hydro	55	Horvath 2019
Wind	31	Horvath 2019
Solar PV	64	Horvath 2019
Solar Thermal	27	Bruckner et al. 2019
Hydro	55	Horvath 2019
NGCC	696	Horvath 2019
Nuclear	17	Horvath 2019
Imports	603	Avg. mix of equal parts coal, NGCC, and hydro for CA electricity imports; Horvath 2019

We then used these High, Medium, and Low targets to linearly forecast the changes in our energy mixes and gradually increased the fraction of renewable sources as a function of their 2020 baseline. In turn, these values can be used to calculate the carbon intensity of the grid for a given hour, day and year. Appendix A shows the average annual carbon intensity over the study time horizon for each of these policy scenarios. Equation 8 shows the exact calculation as a function of the energy absorbed from and discharged to the grid at any given point in time. This captures the need to account for the difference between carbon intensity from purchased electricity and the carbon intensity of the grid at the time that the electricity is discharged, producing the net offset in GHG emissions. This equation was calculated for each of the three scenarios described above (High, Medium, Low), and specified by the subscript “S”:

$$Total\ Avoided\ Emissions_S = \sum_{k=2020}^{2050} \sum_{i=1}^{365} \sum_{j=0}^{23} (q_{ijk} - r_{ijk}) * CI_{ijk,S} \quad (8)$$

Thus, the lifetime avoided emissions from a given BESS capacity is calculated for each scenario which we can then use to determine the societal benefits of these avoided GHGs. By using an estimated Social Cost of Carbon (SCC) as calculated by the EPA (2017) we can attribute economic benefit to each scenario. The following equation reflects the incorporation of SCC, where SCC_k is the social cost of carbon discounted for every year from 2020 to 2050. Equation 9 is similar to Equation 1 but also includes a term for this potential societal benefit:

$$\max_Q \sum_{k=2020}^{2050} \left(\sum_{i=1}^{365} \sum_{j=0}^{23} P_{ijk} (q_{ijk} - r_{ijk}) \right) - C_k(Q_k - Q_{k-1}) - M_k Q_k + SCC_k CI_{ijk,S} (r_{ijk} - q_{ijk}) \quad (9)$$

By putting the societal benefit of avoided GHG emissions in terms of US dollars, we can directly compare this benefit to the profits and costs of running BESS. This new objective function, operating with the same constraints as listed in Equations 2-7, elucidates whether the environmental benefits contribute to the profitability of BESS. By conducting our analysis through this lens as well, we were able to see exactly how including the SCC affects our results and whether that should be a worthwhile consideration that affects BESS adoption.

Table 2: List of 9 Profit Maximization Scenarios included in Equation 1

1% Yearly Price Increase	Low Construction Costs
	Medium Construction Costs
	High Construction Costs
2% Yearly Price Increase	Low Construction Costs
	Medium Construction Costs
	High Construction Costs
5% Yearly Price Increase	Low Construction Costs
	Medium Construction Costs
	High Construction Costs

Table 3: List of 27 Benefit Maximizing Scenarios included in Equation 9

1% Yearly Price Increase Or 2% Yearly Price Increase Or 5% Yearly Price Increase	Low Construction Costs	Low GHG Policy Strength
		Medium GHG Policy Strength
		High GHG Policy Strength
2% Yearly Price Increase Or 5% Yearly Price Increase	Medium Construction Costs	Low GHG Policy Strength
		Medium GHG Policy Strength
		High GHG Policy Strength
5% Yearly Price Increase	High Construction Costs	Low GHG Policy Strength
		Medium GHG Policy Strength
		High GHG Policy Strength

Results

Maximizing Profits

We found that under a majority of the market conditions explored, a profit-maximizing objective does not call for increases in the total BESS capacity in California past the initial capacity existing in 2020 (Figure 1.1). Only when construction costs are low and price increases are low to medium did capacity increase over the study time horizon of 30 years. Low construction costs allow for increases in annual capacity when forecasted prices increase by 1% and 2%, but high prices can negate the benefit of low construction costs as seen by the 5% increase scenario where optimal capacity growth is zero (Figure 1.1). These results suggest a likely need for subsidies to develop this industry in order to overcome high construction costs. Figure 1.2 shows that there is potential for higher profits due to increasing BESS capacity if the construction costs are low enough. The highest potential cumulative profit over 30 years was \$319 million while the lowest cumulative profit was \$32 million (under high price conditions).

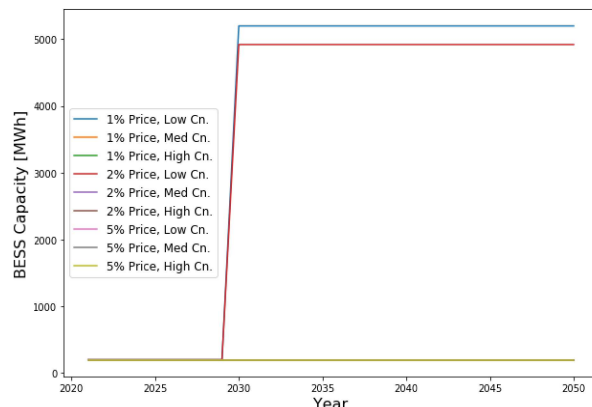


Figure 1.1: Annual BESS Capacity from Equation 1

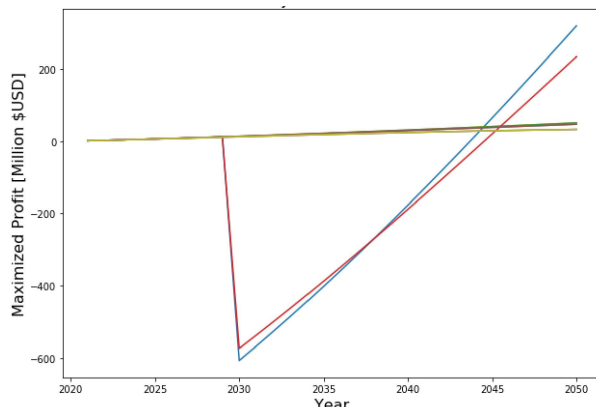


Figure 1.2: Annual Profits from Equation 1

The highest GHG emissions savings correspond to the scenarios with high optimal capacity for BESS, low to medium prices and low construction costs, as shown by Figure 2. Higher capacity allows for more storage and subsequent displacement of energy having higher carbon intensity. Due to constant capacity over the time horizon under most electricity price and construction cost conditions, the avoided emissions are the same for all remaining scenarios.

Figure 2 also indicates that avoided emissions are greater when GHG policy adherence is low and lesser when policy adherence is high. This is expected because high policy adherence means high renewable penetration. As dirty sources of energy gradually leave the grid, BESS' potential to displace emissions decreases. This trend is observable in the annual changes in avoided emissions included in Appendix B (Figures A2-A6); over time, as more renewables are integrated into the mix, the emission savings decrease.

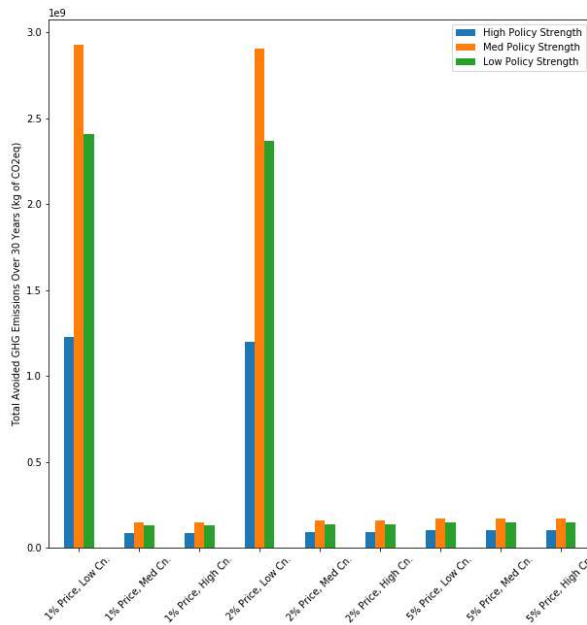


Figure 2: Cumulative Avoided GHG Emissions with Equation 1

Maximizing Total Benefit

When integrating the benefits of avoided emissions into our objective function, we get a wide range of results. Instead of 9 scenarios like in the profit maximizing optimization, we now have 27 scenarios since there are 3 greenhouse gas policy strengths for each original 9 scenarios. Figure 3.1 shows the annual optimal BESS capacity for each scenario. One of the main takeaways from this figure is that there is a slightly greater portion of scenarios that see changes in capacity than in the profit maximizing objective function. Some stay at the initial capacity, some immediately jump to 6-8 GWh, and some increase capacity to around 5 GWh at the year 2030. There is no strong trend in how the scenarios affect the decision to increase capacity.

Additionally, Figure 3.2 shows the cumulative profit resulting from the battery behavior in all scenarios. The highest cumulative profit was found to be \$1.4 billion, while the lowest cumulative profit was found to be negative \$923 million. It is clear that there is a higher variability of cumulative profit in

the benefit maximizing behavior than in the profit maximizing behavior. This is because the benefit maximizing behavior is attempting to find the optimal combination of electricity sales (which contribute to profit) and avoided emissions (which do not contribute to profit). Therefore, a scenario may see low profits but high avoided emissions and still have a high benefit, potentially even resulting in a negative cumulative profit.

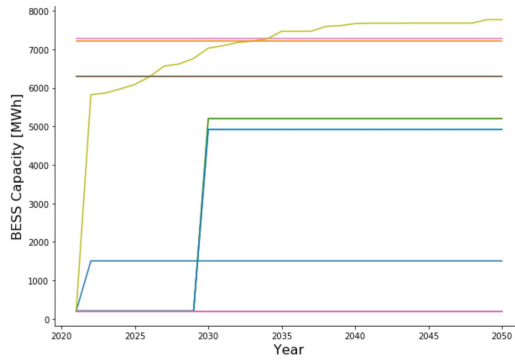


Figure 3.1: Annual BESS Capacity from Equation 9

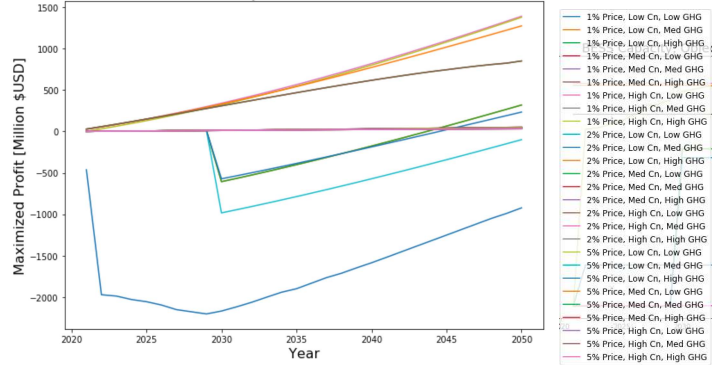


Figure 3.2: Cumulative Yearly Profits from Equation 9

Additionally, Figure 4 represents the emission reductions associated with the benefit maximizing behavior. Similar to the profit maximizing behavior, we see large increases in avoided emissions if there is a large increase in BESS capacity. Due to the higher variability in capacity changes, there is a less clear trend on which scenarios see greater emission reductions. However, the logic still applies that if the electricity mix is less carbon intensive there are less emissions available to be avoided.

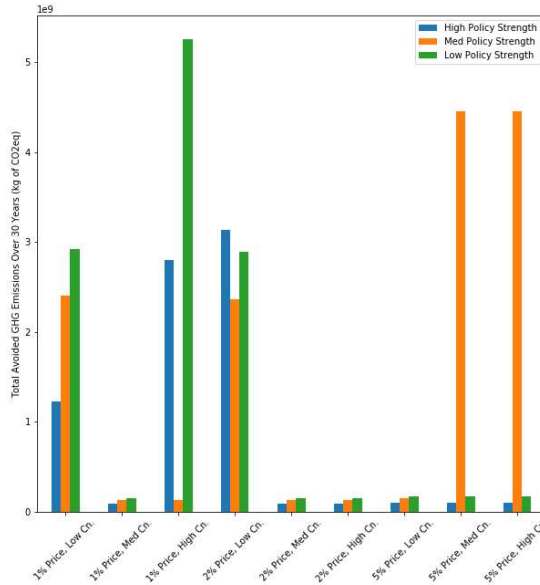


Figure 4: Cumulative Avoided GHG Emissions with Equation 9

Finally, Figure 5 shows the average yearly profits for the profit maximizing behavior and the benefit maximizing behavior. Here it appears that the benefit maximizing behavior may choose to

increase capacity nearly immediately or in 2030. As a result, the yearly profits for the benefit maximizing behavior generally are higher, except for the initial spike. The average cumulative profit for the profit maximizing behavior is \$94 million, and the average cumulative profit for the benefit maximizing behavior is \$234 million.

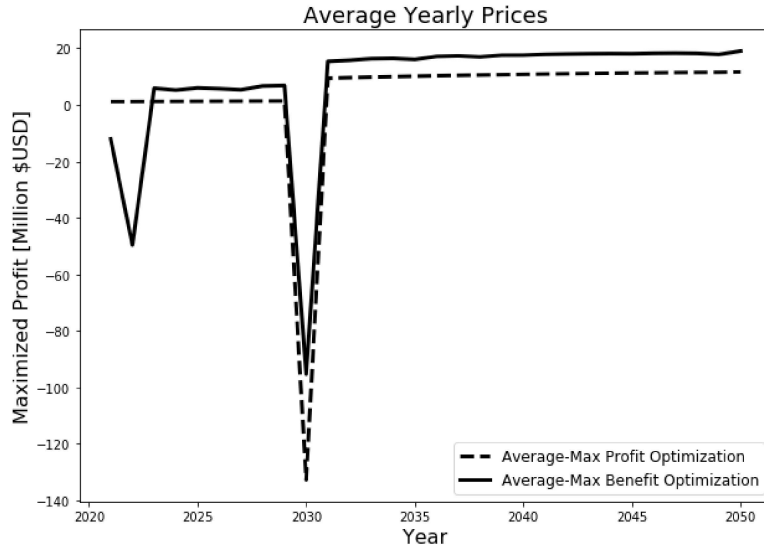


Figure 5: Average Profits for each Optimization Objective

Discussion

From these results, several main takeaways should be noted. First, as is clearly seen in the profit maximizing optimization, the high construction cost of lithium ion BESS facilities is the main barrier to their profitability and implementation. The only scenarios that saw an increase in capacity were those with low construction costs. In most scenarios, the high cost of construction outweighed the potential profits of expanding capacity. Even though this trend is less clear with the benefit maximizing behavior, it likely still holds.

Second, when considering the societal benefits of avoided emissions in the optimization function, more scenarios resulted in both higher capacity overall and earlier addition of capacity than in the profit maximizing scenario. Therefore, it is clear that lithium ion batteries provide an environmental service that should be considered when setting energy storage targets.

Third, across both behaviors, the environmental benefits of BESS facilities decrease as the electricity mix is decarbonized. Therefore, to maximize environmental benefit, BESS facilities that will be operating in arbitrage or peak shaving/emission reduction should be built in a time horizon where the grid still has a significant portion of fossil based electricity generation. However, this does not consider how batteries may play an essential role in renewable integration. This was outside the scope of our project.

Fourth, average yearly and cumulative profits of the benefit maximizing behavior were higher than the profit maximizing behavior. This result is counterintuitive and not fully understood. At the moment, we believe this is the result of there being greater incentives to add more capacity in the benefit maximizing behavior due to the added value of avoiding emissions that naturally occurs when

participating in arbitrage. This means that by considering total benefit, one would be motivated to make more capacity, and therefore more profits. However, this goes against the logic of the term “profit maximizing,” since if more profits could be made by increasing capacity, the capacity should be increased. We are puzzled by this contradiction but did not have the time to investigate it further.

Finally, it is clear the “optimal” quantity of lithium ion BESS facilities is highly dependent on the global setting. Factors like electricity prices, energy demand, electricity mix, and more play a role in our results; and all of these factors are highly uncertain. In an attempt to capture this variability through comparing possible scenarios, we found that the optimal quantity of Li-ion battery energy storage is truly an uncertain value that exists within a range and depends on highly variable factors. In order to more conclusively say whether or not lithium ion BESS is an investment worth making, the likelihoods of the used scenarios should be determined and used to weigh different investment decisions. For now, all we can conclusively say is that *broadly*, across many scenarios, increasing lithium ion BESS capacity has positive profits and benefits.

In conclusion, we have found that BESS have immense potential to revolutionize the electricity industry. Across the various scenarios that we analyzed for this report, a general trend we observed is that BESS significantly aid in reducing GHG emissions across the board. Though the extent of their influence depends heavily on policy adherence over time and grid energy mix, the net impact is always a positive one. This reduction in GHG emissions is also reflected in the financial benefit associated with the social cost of carbon described previously. However, it is important to note that the profit from electricity arbitrage vastly overshadowed this revenue. This is shown in Figure A16 in Appendix B. As such, it is important to note that BESS profitability will be mostly a question of private and not public benefit. Though BESS can prove itself to be an important component of our fight towards 100% renewable energy, it is difficult to make a purely economic argument for its public benefit. This is because it depends on many uncertain variables such as: carbon pricing/taxes to make alternatives less attractive, infrastructure investments, and the progression of other renewable energy sources.

Limitations & Future Considerations

While we made efforts to incorporate all key components in our approach, we made some limiting assumptions and exclusions in order to simplify our model. In particular, we made assumptions that span the grid interaction dynamics, forecasting, economics, and technology of BESS. As mentioned previously, we did not include any network constraints or distribution and transmission complications in our grid interaction dynamics. On top of this, we took on a price taker assumption that BESS integration in the grid would not change the price of electricity.. Lastly, we did not consider the ancillary services that BESS provides to the grid in terms of grid stability or reliability from intermittent generation sources. From a forecasting perspective, most of our projections out to 2050 followed a linear extrapolation model for electricity prices, demand, and GHG policy adherence. In addition, we only utilized data for 24 days to represent the entire year. This may not be accurate, especially if the particular day that was chosen was abnormal for some reason. However, abnormalities were hopefully reduced by generating base years that consisted of average values across three years. There is large variation throughout the literature for demand forecasting, some predicting slight decreases due to energy efficiency gains while others projecting increases due to transportation electrification. Unfortunately, it is simply too complex to accurately predict future demand and as such we made the assumption that demand remained constant

throughout our time horizon. From an economic perspective, we acknowledge that it is infeasible to purchase thousands of MWh of capacity in a single year, as our model recommends. These unrealistic budget constraints should be taken into consideration when interpreting the results. Finally, the assumptions we made on battery technology were to simplify complex internal dynamics. We assumed a constant efficiency of installed batteries even though efficiency may decrease over time. Second, state of charge dynamics were simplified to be represented by a linear equation. As we've seen in literature and throughout CE 295, BESS have nonlinear dynamics. Lastly, we ignored the disruption that could be caused by entrance of new technologies into the market over the next 30 years. We assumed that all future battery storage capacity would be fulfilled by existing or improved Li-ion battery technology.

With these limitations addressed, future models and research would benefit from better forecasting to improve the accuracy of estimates in future years. In this sense, our research provides a framework which can evolve to accept more sophisticated inputs for modeling data.

Summary

Energy storage is an underutilized, emerging technology with potential to revolutionize and decarbonize the electricity sector. This study seeks to determine the profit maximizing amount of Li-ion battery capacity for energy arbitrage in the California electricity market between 2020 and 2050. We accounted for variability in future outcomes by analyzing results of scenarios with differing capital costs, electricity prices, and energy policy adherence. Each of these scenarios was analyzed through the lens of profit maximization as well as total benefits maximization.

In the profit maximizing optimization model, we found that under a majority of the market conditions there are no incentives to increase the total BESS capacity in California past the initial capacity existing in 2020. Only scenarios with low construction costs and relatively low prices result in an increase in optimal BESS capacity over the 30 year time horizon. These results suggest a likely need for subsidies to develop this industry in order to overcome high construction costs. High construction cost of Li-ion BESS facilities is the main barrier to their profitability and implementation. Additionally, we found that avoided emissions are greater when GHG policy adherence is low and lesser when policy adherence is high. This is expected, as high policy adherence means high renewable penetration, decreasing the potential for displacing “dirty” sources thus decreasing avoided emissions.

In the total benefit maximizing optimization model, there was a larger increase in BESS capacity than in the profit maximizing scenarios showing that Li-ion batteries provide an environmental service that should be considered when setting energy storage targets; however, as mentioned the environmental benefits decrease as the carbon intensity of the grid decreases. Additionally, the cumulative profits were higher in the total benefit maximizing case; however, this result is counterintuitive and not fully understood. One possible explanation is that by considering total benefit, there would be increased motivation to make more capacity, though this needs to be investigated further.

Finally, our model’s optimal quantity of Li-ion BESS capacity is highly dependent on factors like electricity prices, energy demand, and electricity mix which are all highly uncertain. Even with multiple scenarios established to capture this variability, results are still largely inconclusive. In order to more definitively say whether or not Li-ion BESS is an investment worth making, the likelihoods of the scenarios should be determined and used to weigh different investment decisions. For now, all we can conclusively say is that broadly, across many scenarios, increasing Li-ion BESS capacity has positive profits and environmental benefits. To determine more substantial conclusions, future versions of the model should be adapted to include more characteristics of battery behavior, consider a wider range of scenarios, and take into account BESS impacts on market conditions and mix.

Table of Responsibilities

Data Collection and Cleaning	
Electricity Demand Forecasts	Jason
Marginal Construction Cost Projections of BESS	Jason
Operation and Maintenance Cost of BESS	Jason & Pietro
Energy Storage Efficiency	Jason
Energy Mix Data for 2017, 2018, 2019	Sarah N., Rachel, Jason
Carbon Intensities By Source	Pietro, Natalia
Electricity Pricing	Rachel, Natalia
Data Cleaning	Sarah C., Rachel, Sarah N.
Scenario Development	
Price Forecasts	Natalia, Rachel, Jason
Varied Marginal Construction Cost Projections of BESS (Sensitivity Analysis)	Sarah C.
Energy Mix for CA Electricity Forecasts	Sarah N.
Carbon Intensity of Electricity by Source	
Optimization Modeling	
Optimization Formulation; Constraints and Parameter Definition	All
Coding/Debugging Optimization Models	Sarah C.
Report and Presentation	
Progress Report	All
Presentation Slides	All
Presentation Speakers	Jason, Pietro, Sarah C.
Final Report: Motivation and Background	Pietro
Final Report: Problem Statement	All
Final Report: Relevant Literature	Jason
Final Report: Methodology	Pietro, Sarah C., Sarah N.
Final Report: Results	Jason, Sarah N.
Final Report: Discussion	Pietro, Natalia
Final Report: Summary	Natalia
Final Report: Abstract	Natalia
Final Report: Proofreading/Editing	All

Appendix A: Methodology Supplement

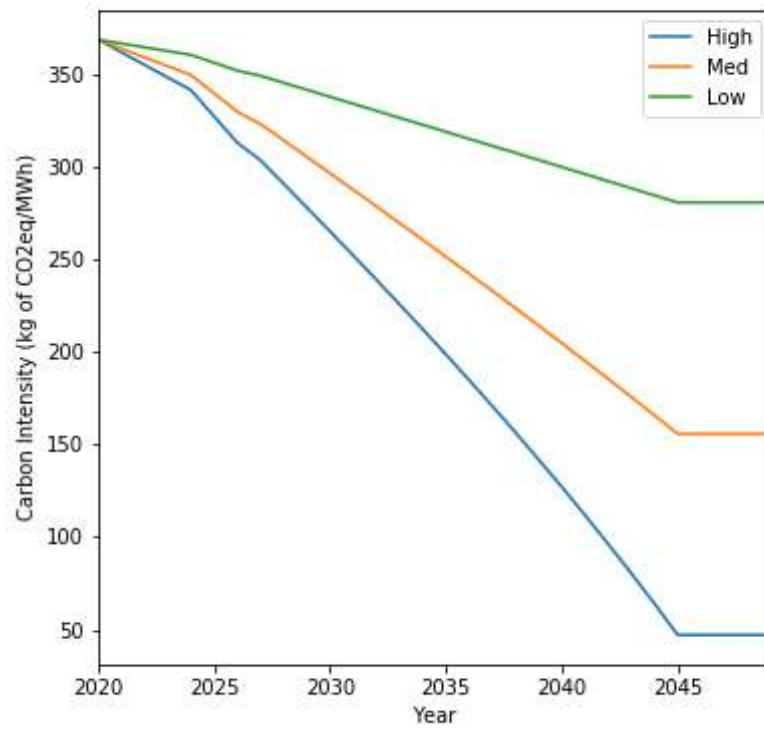


Figure A1: Average Annual Carbon Intensity of CA Grid

Note: Legend corresponds to GHG policy strength.

Appendix B: Additional Result Figures

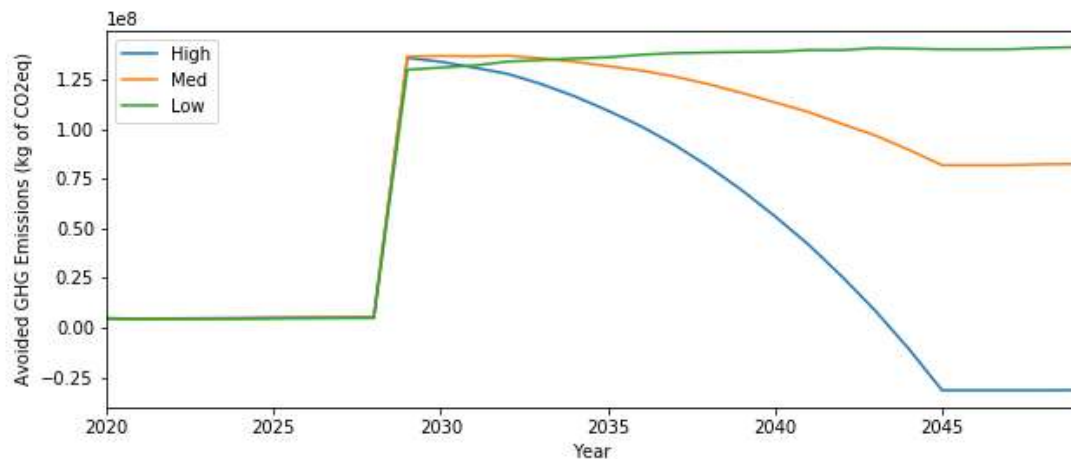


Figure A2: Annual Avoided GHG Emissions w/ Profit Maximization (1% Price, Low Cn.)

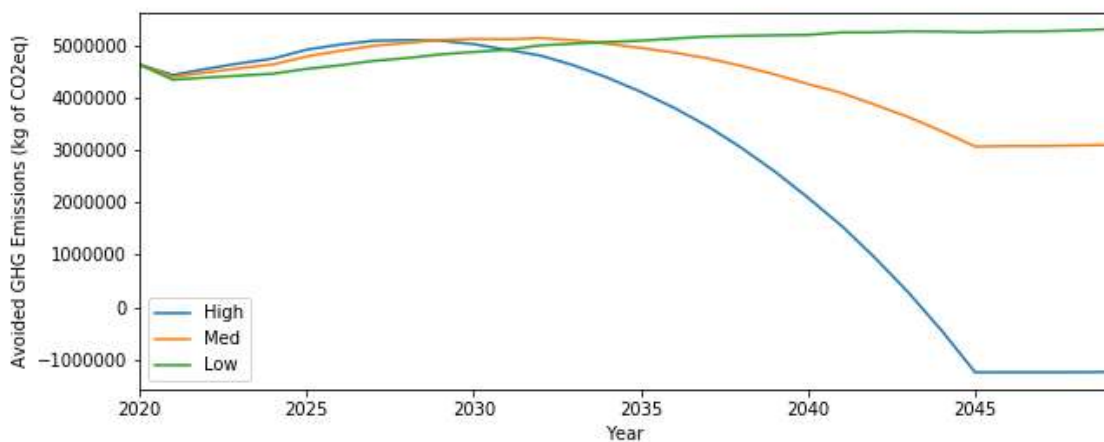


Figure A3: Annual Avoided GHG Emissions w/ Profit Maximization(1% Price, Med or High Cn.)

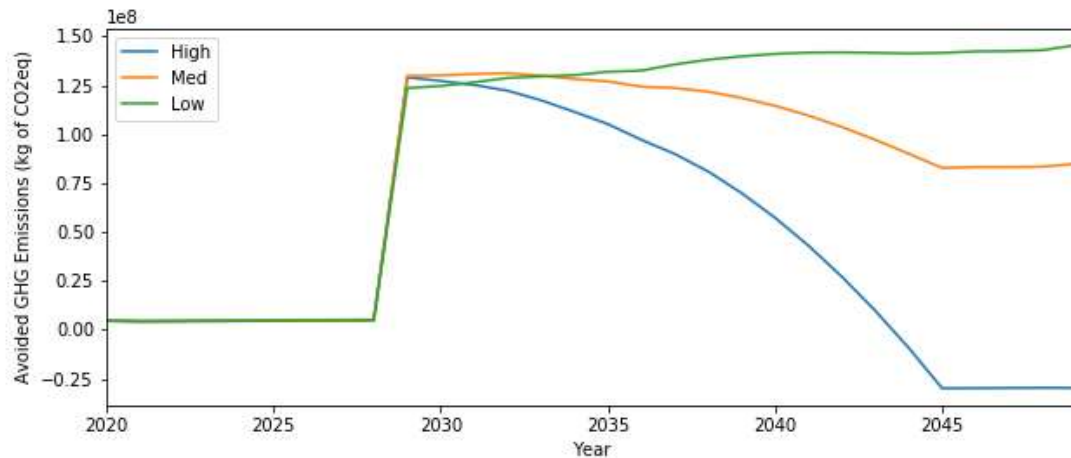


Figure A4: Annual Avoided GHG Emissions w/ Profit Maximization (2% Price, Low Cn.)

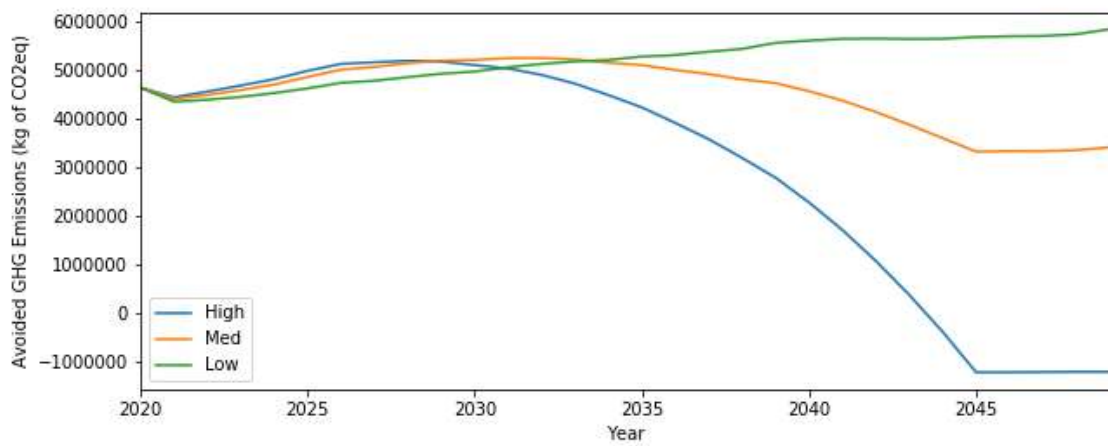


Figure A5: Annual Avoided GHG Emissions w/ Profit Maximization (2% Price, Med or High Cn.)

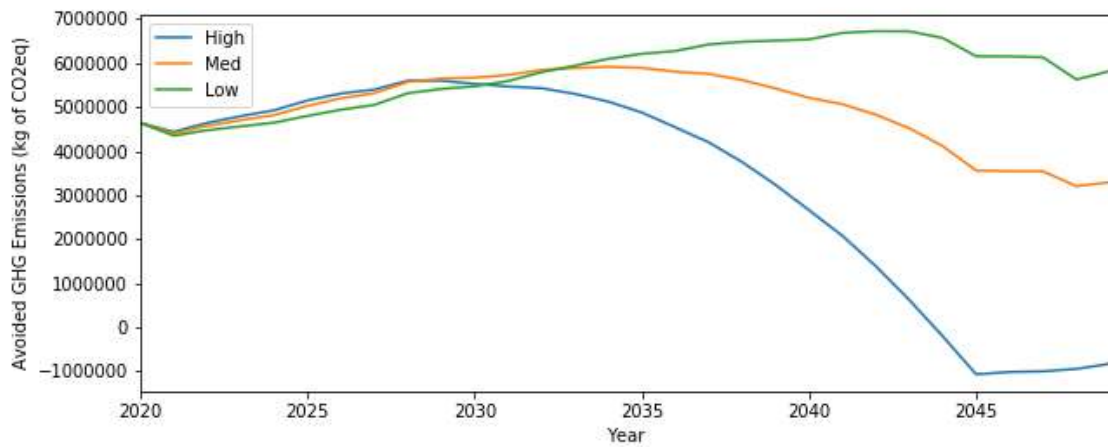


Figure A6: Annual Avoided GHG Emissions w/ Profit Maximization (5% Price; Low, Med or High Cn.)

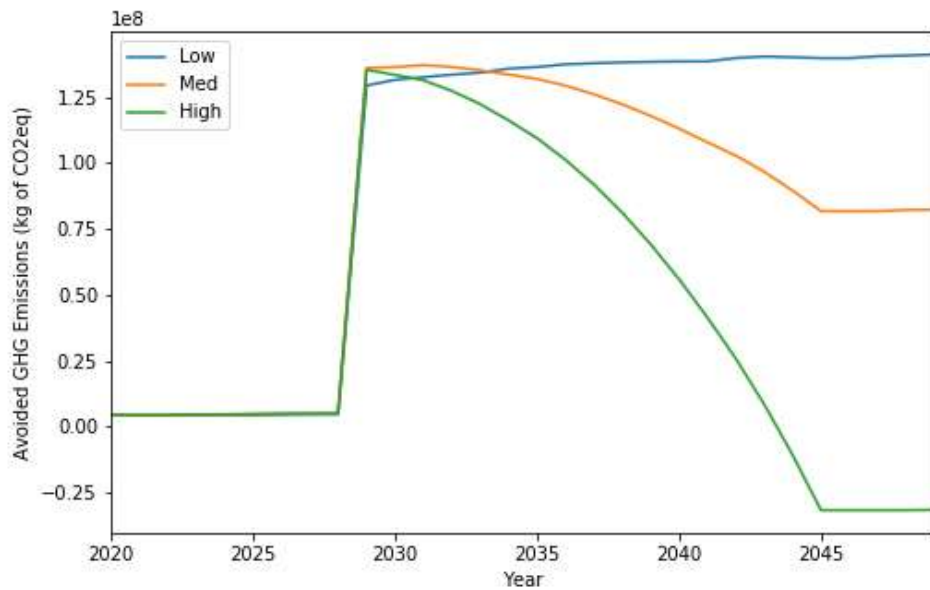


Figure A7: Annual Avoided GHG Emissions w/ Total Benefit Maximization (1% Price; Low Cn.)

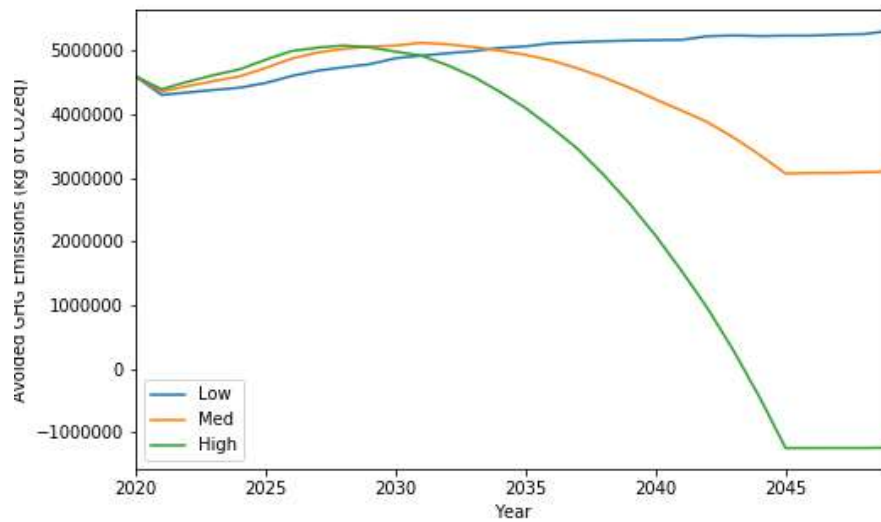


Figure A8: Annual Avoided GHG Emissions w/ Total Benefit Maximization (1% Price; Med Cn.)

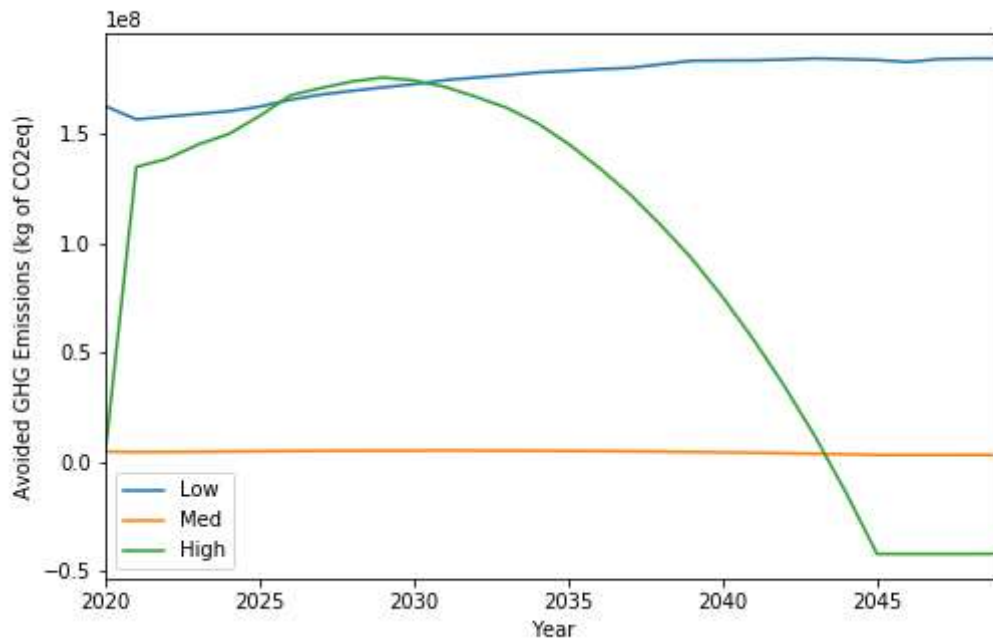


Figure A9: Annual Avoided GHG Emissions w/ Total Benefit Maximization(1% Price; High Cn.)

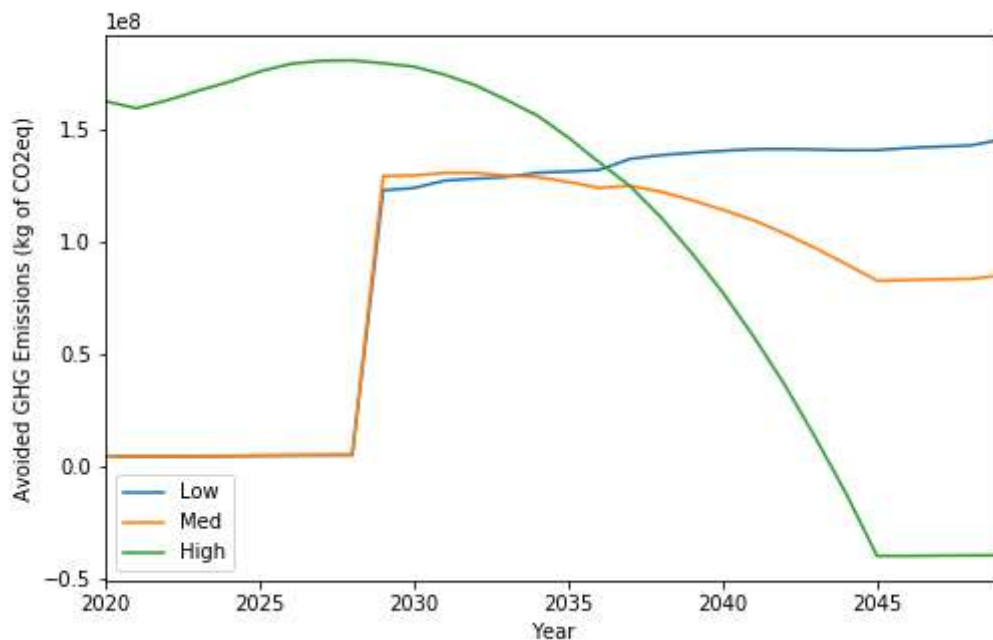


Figure A10: Annual Avoided GHG Emissions w/ Total Benefit Maximization (2% Price; Low Cn.)

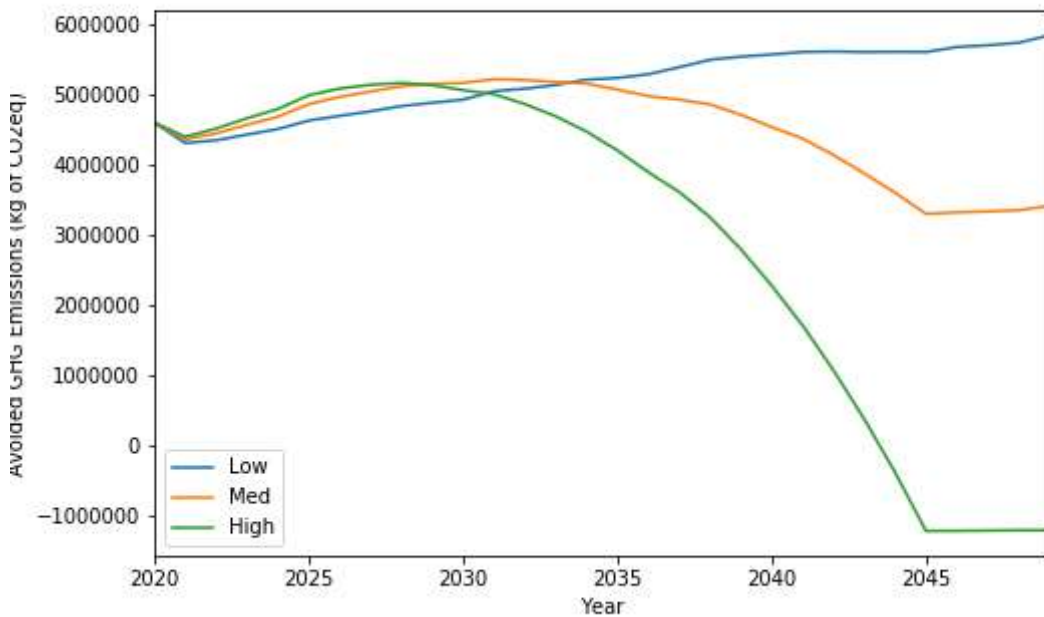


Figure A11: Annual Avoided GHG Emissions w/ Total Benefit Maximization (2% Price; Med Cn.)

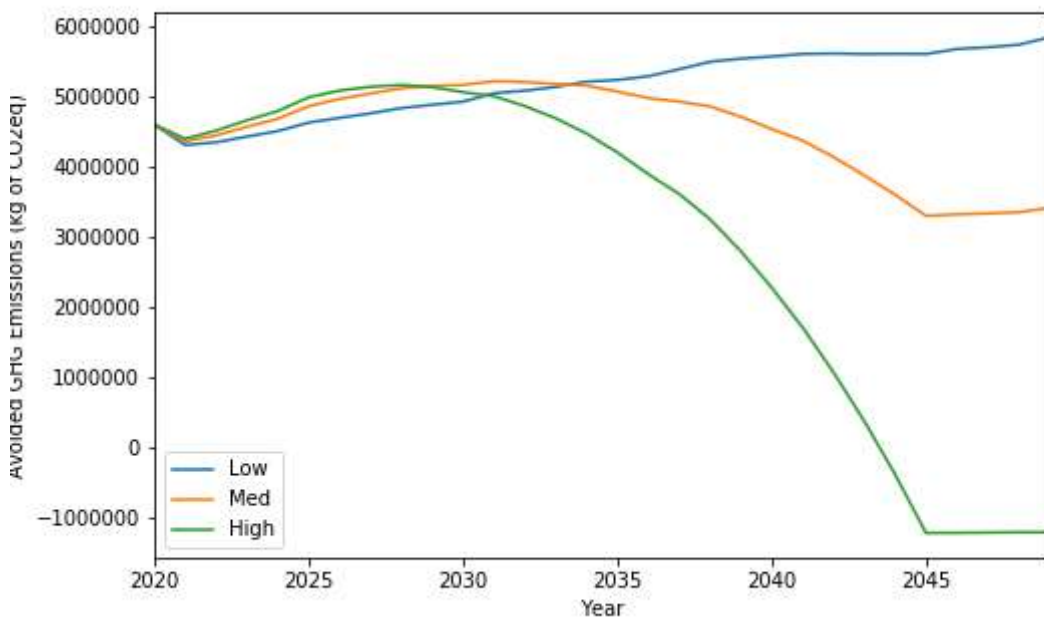


Figure A12: Annual Avoided GHG Emissions w/ Total Benefit Maximization (2% Price; High Cn.)

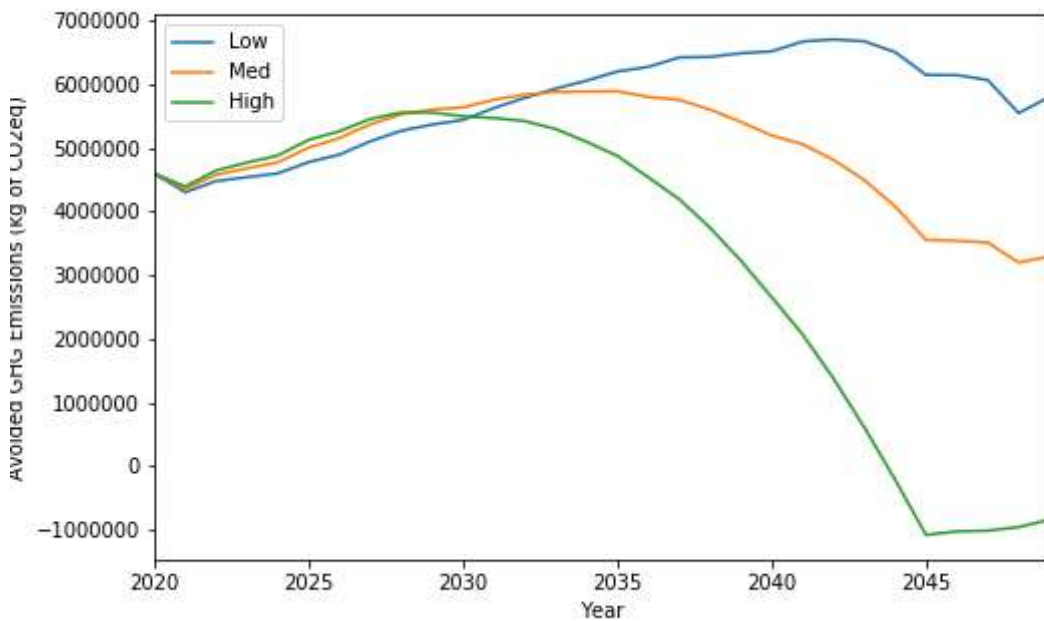


Figure A13: Annual Avoided GHG Emissions w/ Total Benefit Maximization (5% Price; Low Cn.)

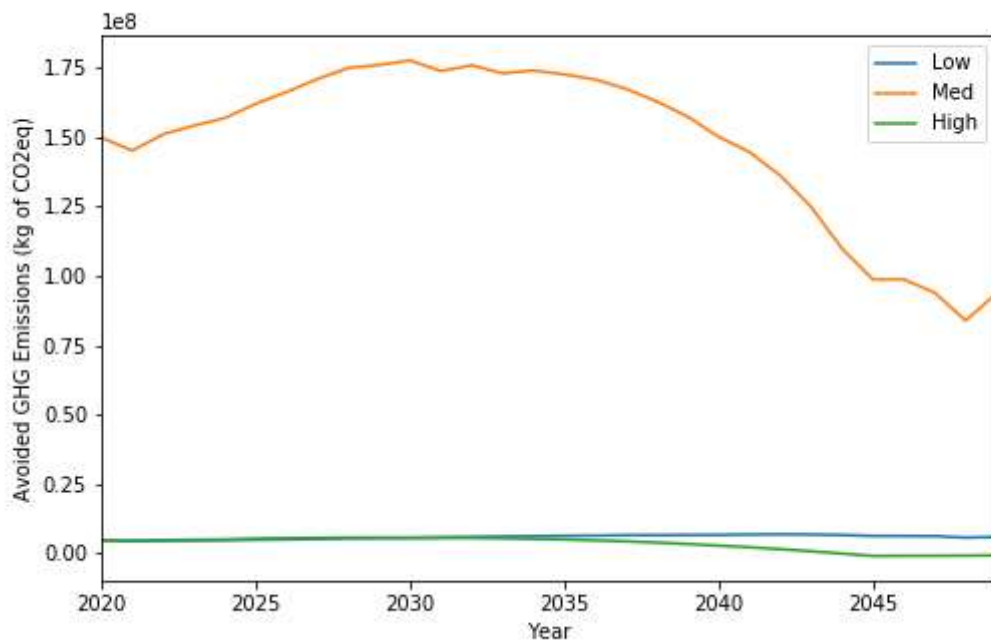


Figure A14: Annual Avoided GHG Emissions w/ Total Benefit Maximization (5% Price; Med Cn.)

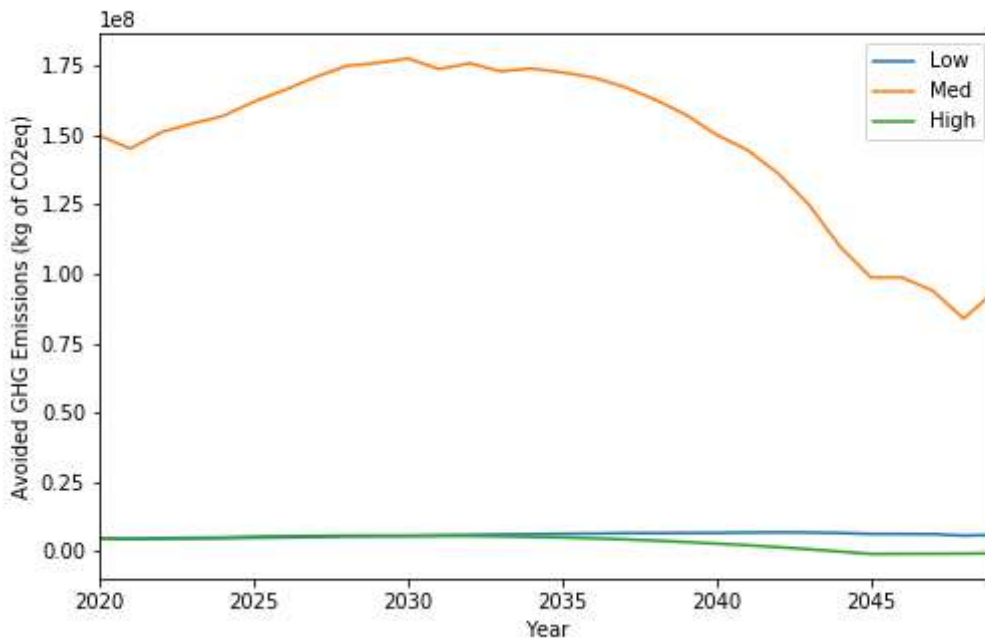


Figure A15: Annual Avoided GHG Emissions w/ Total Benefit Maximization (5% Price; High Cn.)

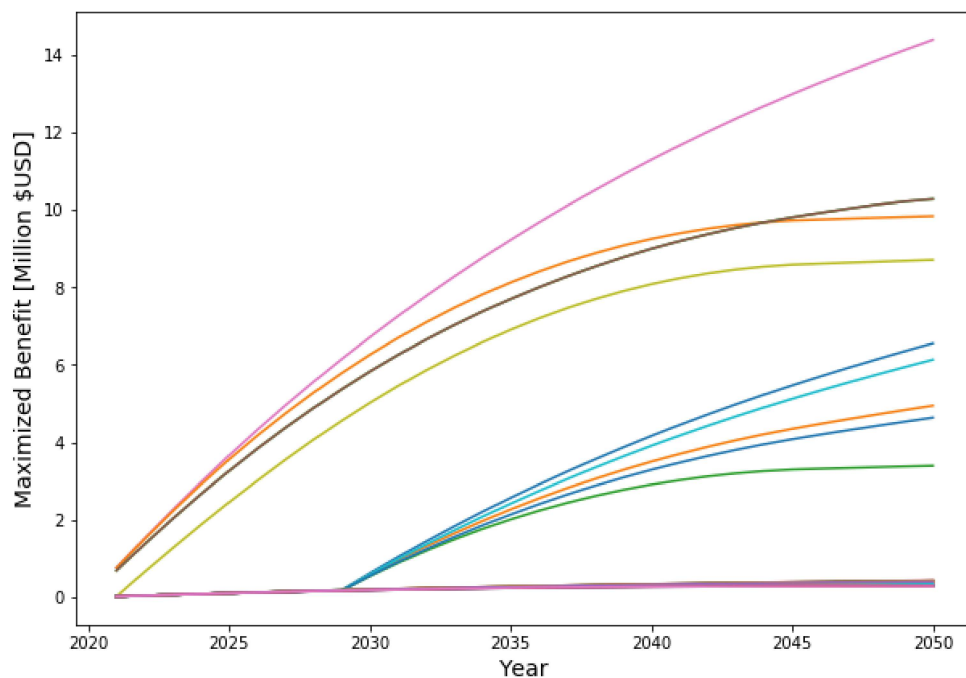


Figure A16: Cumulative Social Cost of Carbon Benefit for 27 Scenarios

Appendix C: Optimization Model Code Sample

Objective Function Formulation: Maximizing Profit Equation 1

```

i=2*12 #2 days per month * 12 months per year
j=24    # 24 hours in a day
k=30    # 30 years
Q_init = np.array([200])

Pp = P1*15 # <--- Changes for different scenarios
Dp = demand
Ckp = Ck.loc[1:,'Low'] # <--- Changes for different scenarios
Mkp = Mk[1:] # Maintenance Costs

Z = Variable((i*j*k), nonneg=True) #2days*12months*24hours*30years
Q_s1 = Variable(k, nonneg=True) #30 years
deltaQ_s1 = Variable(k, nonneg=True) #30 years
q_s1 = Variable((i*j*k), nonneg=True) #2days*12mon*24hours*30years
r_s1 = Variable((i*j*k), nonneg=True)

fxn = -(q_s1-r_s1)*Pp + Ckp.values.T*deltaQ_s1 + Mkp.values.T*Q_s1

constraints = [deltaQ_s1[0] == Q_s1[0] - Q_init]
constraints += [Z[0] == 0,
                 Z[i*j*k-1] == 0]

for ijk_idx in np.arange(1,i*j*k):
    constraints += [Z[ijk_idx] == Z[ijk_idx-1] - q_s1[ijk_idx]/eta +
                    r_s1[ijk_idx]*eta]

for k_idx in np.arange(k):
    constraints += [r_s1[i*j*k_idx:i*j*(k_idx+1)] <= Dp*0.05,
                    q_s1[i*j*k_idx:i*j*(k_idx+1)] <= Dp*0.05,
                    Z[i*j*k_idx:i*j*(k_idx+1)] <= Q_s1[k_idx],
                    q_s1[i*j*k_idx:i*j*(k_idx+1)] <=
0.25*Q_s1[k_idx],
                    r_s1[i*j*k_idx:i*j*(k_idx+1)] <=
0.25*Q_s1[k_idx]]

    if k_idx > 0:
        constraints += [deltaQ_s1[k_idx] == Q_s1[k_idx] -
Q_s1[k_idx-1]]

scenario1 = Problem(Minimize(fxn), constraints)
profit = np.append(profit, scenario1.solve())

```

Objective Function Formulation: Maximizing Benefit Equation 9

```

i=2*12 # 2 days per month * 12 months per year
j=24   # 24 hours in a day
k=30   # 30 years
Q_init = np.array([200])

Pp = P1*15 # <--- Changes for different scenarios
Dp = demand
Ckp = Ck.loc[1:,'Low'] # <--- Changes for different scenarios
Mkp = Mk[1:] # Maintenance Costs
CI = CI_low # <--- Changes for different scenarios

Z = Variable((i*j*k), nonneg=True)      #2days*12months*24hours*30years
Q_s1 = Variable(k, nonneg=True)          #30 years
deltaQ_s1 = Variable(k, nonneg=True)    #30 years
q_s1 = Variable((i*j*k), nonneg=True)  #2days*12mon*24hours*30years
r_s1 = Variable((i*j*k), nonneg=True)  #2days*12mon*24hours*30years

fxn = -(q_s1-r_s1)*Pp + Ckp.values.T*deltaQ_s1 + Mkp.values.T*Q_s1 +
SCC[1:].values.T@CI.values@(r_s1 - q_s1)

constraints = [deltaQ_s1[0] == Q_s1[0] - Q_init]
constraints += [Z[0] == 0,
                 Z[i*j*k-1] == 0]

for ijk_idx in np.arange(1,i*j*k):
    constraints += [Z[ijk_idx] == Z[ijk_idx-1] - q_s1[ijk_idx]/eta +
r_s1[ijk_idx]*eta]

for k_idx in np.arange(k):
    constraints += [r_s1[i*j*k_idx:i*j*(k_idx+1)] <= Dp*0.05,
                    q_s1[i*j*k_idx:i*j*(k_idx+1)] <= Dp*0.05,
                    Z[i*j*k_idx:i*j*(k_idx+1)] <= Q_s1[k_idx],
                    q_s1[i*j*k_idx:i*j*(k_idx+1)]<=0.25*Q_s1[k_idx],
                    r_s1[i*j*k_idx:i*j*(k_idx+1)]<=0.25*Q_s1[k_idx]]

    if k_idx > 0:
        constraints += [deltaQ_s1[k_idx]==Q_s1[k_idx]-Q_s1[k_idx-1]]

scenario1 = Problem(Minimize(fxn), constraints)
profit_scc = np.append(profit_scc, scenario1.solve())

```

Total Cost of Ownership Optimization for Fleet

Transformation from ICE to EV

Bianca Acosta
Dayu Apoji
Emin Burak Onat
Alp Cinar
Harry Lam
Greg Turk



1. Abstract

This report presents an optimization study to determine the minimum battery size for incorporation into the TCO of an EV fleet. The study was conducted by the following core steps: define the Representative Case Example, characterize the truck energy consumption, develop battery degradation models, build tools to calculate TCO for some route based on models of truck energy and battery degradation, and demonstrate the tool on the Representative Example. Results of the analysis show that, while the different battery degradation models result in slightly different TCO curves, the optimal battery capacity and minimum feasible TCO are virtually identical. The optimal battery capacity for the Case is approximately 233 kW.hrs. The EV option is price-competitive with ICE trucks at battery unit prices of approximately 150 \$/kW.hr. Sensitivity studies of some major variables were also performed to highlight pathways towards deployment of EV trucks. The sensitivity studies show 'Breakeven Battery Unit Price' – the battery unit price at which $TCO_{EV} = TCO_{ICE}$ over a range of diesel and electricity prices at constant discount rate, and IRR – the discount rate at which $TCO_{EV} = TCO_{ICE}$ – over the same range of diesel and electricity prices, at a constant battery price.

2. Introduction

Motivation & Background

There has been immense interest in decarbonizing the transportation sector, the largest greenhouse gases (GHG) contributor in the U.S. in 2018 according to the Environmental Protection Agency (EPA), accounting for more than 36% [1]. One of the major discussion points spurred by Elon Musk's TED talk on the future of sustainable transportation was the revolution of the trucking industry [2]. Medium- and heavy-duty Vehicles (MHDVs) play an important role in the U.S. economy in addition to the trucking industry. These vehicles are also the second largest energy consumer and GHG emissions producers in the sector while representing around one twentieth in the entire U.S. vehicle fleet [3].

In view of the emerging success in electric drive light-duty vehicles (LDV), researchers seek to capture the huge energy and economic improvement opportunity per truck, in particular the higher overall battery-to-wheel efficiency and reduced roadside air pollution assured by electrifying truck fleets. The electrification will no doubt be critical to meeting states and national climate goals but range-payload tradeoff and limited cost

competitiveness have not yet been fully resolved to achieve broad market adoption. One study by Sripad et al. [6] proposed that the trucking industry may have to resort to batteries beyond Li-ion to enable driving range longer than 600 mi (see Figure 1) and more efforts are underway to bridge the research gaps as to which performance metrics to consider.

While there is obvious progress and achievement in electrification of transit buses across the globe, several differences in other MHDVs are prohibiting viable project development. Some examples include diverse sets of duty cycles based upon vocational purposes. The varying daily route parameters and the increasing per-mile energy demands as a function of gross vehicle weight for Classes 3-8 MHDVs result in a wide array of required battery sizes. Moultsak, et al. identified batteries to be the largest cost element for electric vehicles, together with annual mileage and vehicle lifetime determines the cost parity to conventional fuel vehicles [4]. With a more than 80% drastic fall in the prices since 2010 for Li-ion battery packs over the past decade to \$176/ kWh, it is attractive to assess the economic feasibility for electrification of vehicle fleet subject to effective strategies to lower the associated costs of vehicle charging for charging infrastructure and electricity demand charges. As one can imagine, the financial case would need to be evaluated on a life-cycle basis to determine the cost parity of such comparison with conventional fleet.

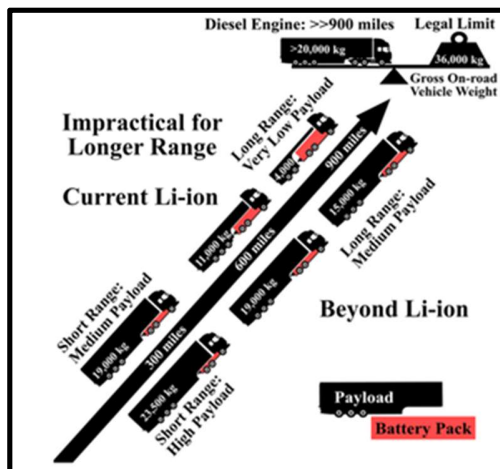


Figure 1. Summary of a comparison between current and beyond Li-ion batteries for electrifying semi trucks.

Given a multitude of factors affecting the assessment of technical and financial feasibility of a transition to zero emission freight fleets, our team is intrigued to address the following two research questions :

1. Can we make an economic case for electric versus diesel trucks based on total and capital costs over their lifetimes?
2. What are the major factors that affect the cost-effectiveness of a transition from conventional ICE fleet to electrified fleet?

Unlike purchase decisions on private passenger vehicles, which are heavily influenced by emotional factors, the primary considerations for a commercial fleet operation are to achieve desired job deliverables and cost-effectiveness. To take into account the characteristics specific to individual business cases, we adopted an analysis of total cost of ownership (TCO) to guide the comparison, which includes both the capital expenditure (CAPEX) to purchase the vehicles as well as the operating costs (OPEX) over the entire vehicle lifetime. Here, we are seeking to optimize the TCO for fleet transformation from ICE fleet to EV fleet for a given project life, CAPEX, OPEX and time value of money and create a tool which fleet managers can use to assess the economic viability for electrifying fleet.

Relevant Literature

There has been considerable research in the electrification of MHDVs. We studied journal papers on fuel consumption modeling for trucks, impact of hybrid fuel trucks on fuel consumption, total cost of ownership for vehicle fleets, battery degradation modeling. We highlight the key literatures that have motivated our study below by their topics.

Total Cost of Ownership: Moultsak et al. compared the TCO and greenhouse gas emissions (GHG) for three regions, namely China, Europe and the U.S. [4] The research suggested that batteries are the largest cost element for EV and fuel costs yield the largest cost savings for EV but utility demand charges complicate electricity price projects. Vehicle annual mileage and vehicle lifetime are key determinants of cost parity to conventional fuel vehicles. When considering tradeoff between battery capacity and payback, TCO calculation suggests that duty cycles with shorter trips and frequent stops are suitable for electrification, given opportunities for regenerative braking, engine-off at idle and extended time for charging. Findings from this report motivated us to consider optimizing for a minimum battery capacity and defining trip parameters for scoping our project.

Other papers also found that base case estimates of TCO are higher for the battery electric trucks (BET) than the diesel trucks. [6-7] Reason attributed to the difference in the upfront

purchase cost of the two vehicles. BET has the advantage of lower fuel cost while at the same expected to require costly battery and electric vehicle supply equipment. Paper summarizes that for the BET, the total cost of ownership is a function of vehicle price, annual vehicle kilometers traveled, maintenance cost, salvage value, battery cost, the battery replacement cost and the cost of electric vehicle supply equipment (charging infrastructure) including installation.

Vehicle Dynamics Model: Sripad et al. provides vehicle dynamics and cost models that justifies the investment of HD commercial fleet electrification. [6,9] For a relatively short payback period to be viable, the authors suggested that drag coefficient has to be reduced to allow for lowering battery pack size while meeting payload requirement, further reductions are needed for electricity and battery pack prices, and battery cycle life to be long enough for less than 50% battery pack replacement for a fleet over their lifetime. W

Battery Degradation Model: Wang et al. provides a very simple Li-ion battery degradation model that we incorporated besides the advanced battery degradation model given in Schmalstieg et al. [8,10] Also, Xu et al. formulates a semi-empirical Li-ion battery degradation model to assess cell life loss and hence the aging cost. [11] These literatures were helpful for defining our battery degradation model.

Focus of this Study

The goal of this research is to develop optimization models to find minimum battery size given some route distance, payload, and economic scenario (discount rate, fuel/equipment costs, project life) for incorporation into the TCO of an EV fleet. Besides, this work aims to assess TCO of the EV truck relative to ICE alternatives, including a sensitivity analysis on major variables, namely battery cost, diesel price, electricity price.

3. Technical Description

Brief Methodology

As previously discussed, the main goal of this project is to analyze and optimize the total cost of ownership (TCO) for fleet (i.e. truck) transformation to electric vehicle (EV). We chose to study a 'Representative Example', described in detail later, to ground our work

in a somewhat realistic application. In general, the study consisted of the following core steps:

1. Define the Representative Example
2. Characterize the underlying physics of truck energy (power) consumption based on first-principle modeling. This is necessary to determine the battery capacity required to complete the route defined in the Representative Example.
3. Develop a simple and advanced model for battery degradation. Understanding battery lifetime and replacement cycles is critical to projecting the CAPEX of EV trucks.
4. Build tool to calculate TCO for some route based on models of truck energy and battery degradation, as well as TCO for ICE equivalent.
5. Demonstrate tool on Representative Example. Calculate optimal battery capacity and associated TCO.
6. Finally, perform sensitivity studies of some major variables to highlight pathways towards deployment of EV trucks.

The analysis was conducted using general programming language Python. This allows us to perform multiple-loop algorithms effectively and manage the data frames efficiently. However, as requested by the industry partner (Allison Transmission) we also prepare the spreadsheet for easy referencing and input parameter alteration. It should be noted that the more advanced model is not captured in the spreadsheet.

Representative Case Example

The Duff Beer Co is a beer distributor located in Reno, Nevada that stocks eight Save Mart Supermarkets in the greater Reno area. The company delivery truck was recently totalled in a collision with a black bear, and Duff's CFO is evaluating replacement options. The CEO is an EV enthusiast, and has requested that the CFO consider buying an EV truck. The distribution of Save Marts is shown below, as is the daily route that Duff Beer Co uses to serve them.

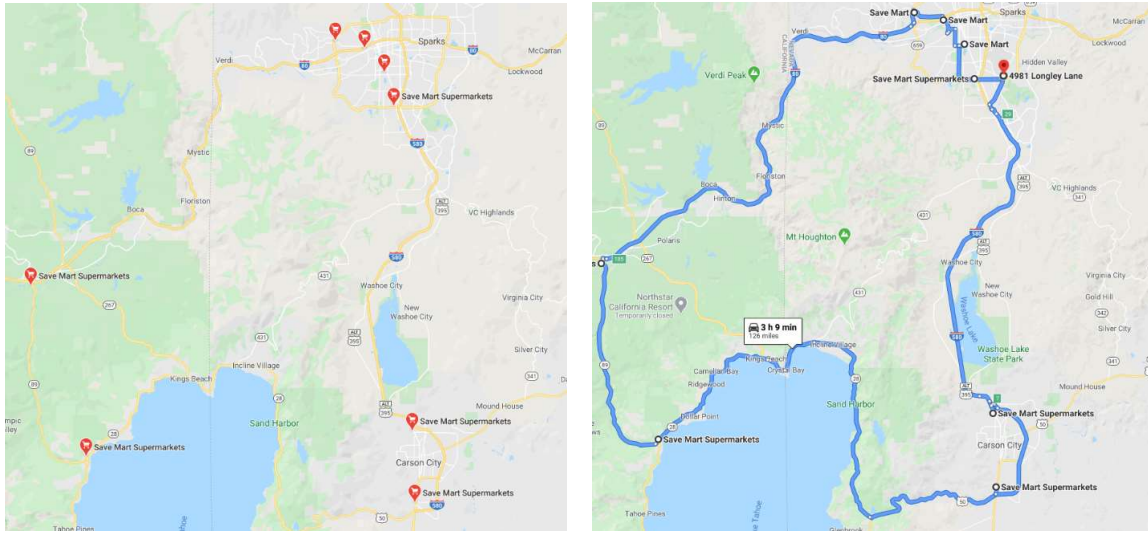


Figure 2. Duff Beer Co beer distribution daily route

In the Reno area, beer is only consumed from 12 oz cans, and beer is only purchased in 30 packs. Each Save Mart sells ~60 cases of beer per day. Each can weighs 360 grams, and hence each case 10.8 kg. The distance and weight of each leg of the trip is summarized in Table 1.

Table 1. Trip Parameters for Duff Beer Daily Distribution

Stop	Payload, cases	Payload, kg	Distance (mi)	Distance (km)	Avg Speed (km/hr)	Average Grade (%)
Reno 1	480	5184	1.9	3.06	30	0
Reno 2	420	4536	3.3	5.21	40	0
Reno 3	360	3888	3.4	5.47	30	0
Reno 4	300	3240	2.4	3.86	30	2.7
Truckee	240	2592	31.1	50.05	85	0.6
Tahoe City	180	1944	13.5	21.73	70	0.5
Carson City 1	120	1296	37.6	60.51	65	-0.7
Carson City 2	60	648	8.8	14.16	65	-0.12
Warehouse	0	0	24	38.62	85	-0.26

A single beverage delivery truck is used to complete the route. It is a Durastar International Beverage 4300 (picture in **Appendix B**). The International Durastar is a Class 6 truck. It is limited to a Gross Vehicle Weight (GVW, total weight including payload) of 26,000 lb or 11,793.4 kg. We estimate that the chassis + cab weigh + prospective electric drivetrain weigh ~4250 kg, leaving 7543.4 kg available for battery + payload.

Simplifying Assumptions:

- The route is mostly highway, and Duff Beer Co drivers LOVE cruise control. Assume constant velocity (different velocities at each different section of the route).
- Following the black bear incident, Duff Beer Co has rigorously trained its drivers to accelerate at a constant rate of 1 mph/s (the new company mantra is "0-60 in... 60!") for safety purposes. Assume constant acceleration.
- Duff Beer Co drivers are terrible at decelerating by coasting, and nearly all deceleration is accomplished by the brakes. Assume instantaneous deceleration with no energy recovery.
- The CEO has already installed a 50 kW CHAdeMO charger at the warehouse for his 'company' Tesla. Assume no charger investment will be required, nor any additional demand charges.
- Assume batteries will be replaced when the route consumes 95% of battery capacity.
- Assume the Durastar 4300 is available as an EV with the option to custom size the battery pack

A complete list of assumptions/parameter values used in evaluating the Representative Example can be found in the **Appendix B**.

Underlying Physics and Energy Requirement

Our first approach was to minimize the work done by the wheels of a given truck that is required to complete a specified distance (route). The initial method in our optimization model was to assume the given truck will travel at constant velocity ($a=0$). In this approach, we have the battery size (in kWh) as the optimization variable, given the values of route distance, and mass of vehicle (the base mass of vehicle plus the added battery mass). Then, we consider the sum of the forces on the system;

$$m \cdot \frac{dv}{dt} = F_T - k_1 v^2 - k_2 - k_3$$

Where:

- F_T is the traction force exerted by the wheels
- $k_1 = \frac{1}{2} \rho C_D A$ is the air drag term; ρ = air density, C_D = coefficient of drag, A = frontal (cross-sectional) area of truck [m^2].
- $k_2 = C_r \cdot m \cdot g$ is the friction term

- $k_3 = m \cdot g \cdot \sin(\theta)$
- v is the truck's velocity [m/s]

More comprehensive explanation on the equations and the derivation can be found in **Appendix C**. The analysis has been performed using a variation of battery size (Figure 3.a). We can see that in the given case, the battery size has to be above 180 kWh to provide adequate required power to the EV truck, considering no margin capacity of the battery. If we specify 95% margin of capacity, as discussed in the previous subsection, then the battery size has to be at least 190 kWh. Further discussion on the battery and its degradation model is discussed below.

Battery Degradation - Simplified Model

The battery must maintain sufficient capacity to complete the given route. However, the battery will decay over time and discharge cycles. The battery must be replaced if it degrades below a specified level, in this case, required power / β (where β is the specified battery capacity margin). Unfortunately, battery degradation models are incredibly complex, and are typically empirical fits for multiple degradation pathways (temperature aging, cycle aging, etc.). For the first analysis, we simplified the battery degradation model using an approximation based on Wang et al. [10]:

$$Q (\% \text{ loss}) = \alpha \times Ah^{0.55}$$

Where:

- Ah is the number of cycles multiplied by the depth of discharge, and
- α is temperature dependent (at 25 deg C, α is ~ 0.15).

Figure 3.a illustrates the relationship between battery capacity, required power, and replacement power. Figure 3.b models battery degradation based on the simplified model. Each color corresponds to a different initial battery capacity (the y-intercept). If too small a battery is purchased, it will require replacement at some point over a 15 year project life (this appears in the chart as a spike back to the initial capacity).

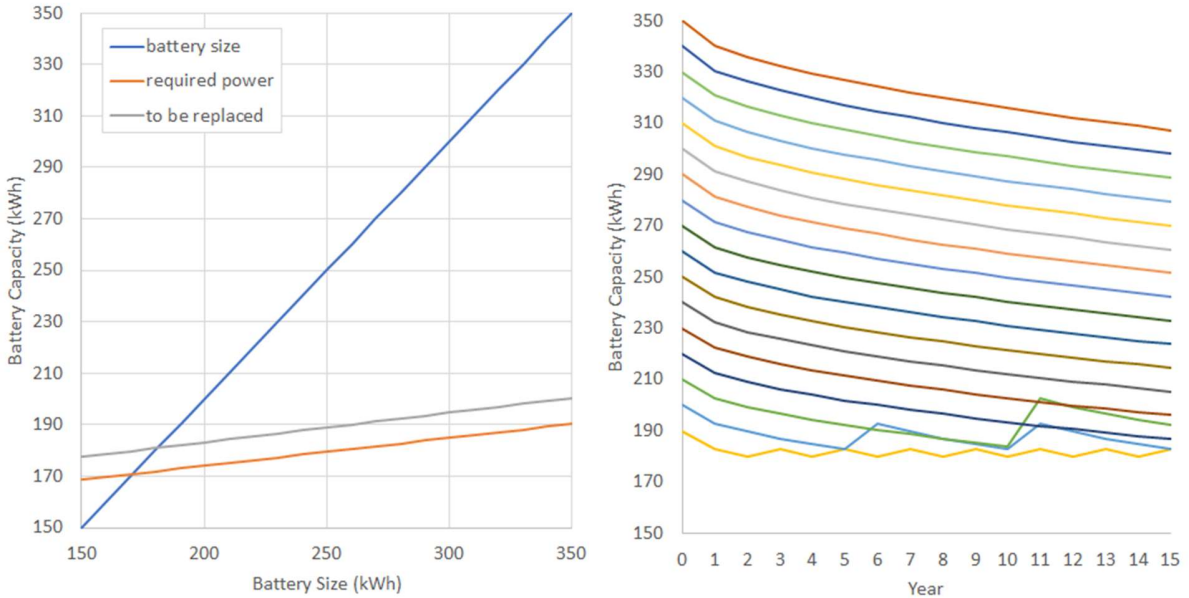


Figure 3. (a) left: required power for each battery size, (b) right: estimated battery degradation based on the simplified model (the battery capacity is kept to be above the required power).

Battery Degradation - Advanced Model

For an aging prediction a lot of different aging factors have to be considered. These factors are e.g. temperature, storage voltage and time for calendar aging and in addition cycle depth, SOC range, current rate and charge throughput for cycle aging. Schmalstieg J. et al. tested to analyze more than 60 cells of the same type under different impact factors in [7]. The tested battery was the Sanyo UR18650E, an 18650 round cell which is manufacturer rated with 2.05 Ah minimum and 2.15 Ah typically. An OCV curve of the cell is shown in Figure 4.

In this degradation model, we incorporated hourly ambient temperature and voltage change of the battery. As the battery discharges, the voltage it can provide decreases with a nonlinear behavior. The author considered that the minimum and maximum battery required is 1.1 to 1.5 times the battery required to complete the given route, respectively. Therefore, we simulated the batteries for depth of discharge between the range 67% and 90%. As seen from the below plot, after 3 hours of drive the selected batteries' voltage throughput decreases to 3.78 and 3.6 respectively for depth of discharge rates of 67% and 90%.

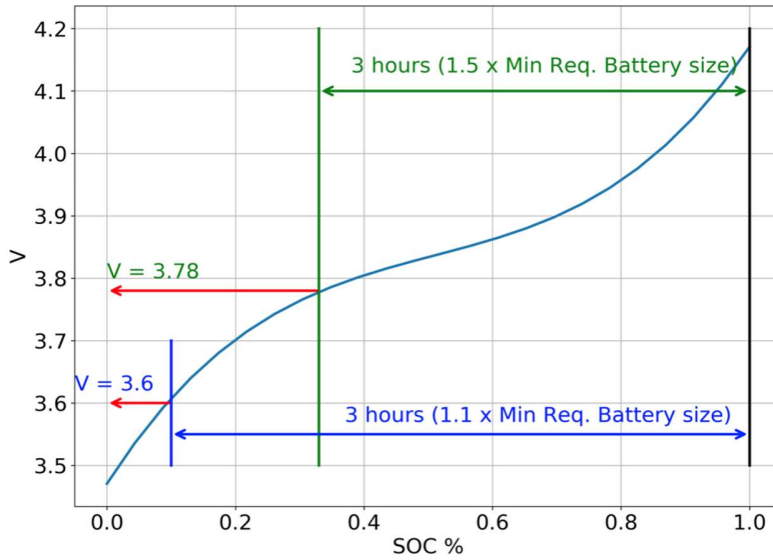


Figure 4. OCV curve of Sanyo UR18650E EV battery

As stated in [7], first aging factor depending on voltage and temperature is

$$\alpha_{cap}(T, V) = (7.543 * V - 23.75) * 10^6 * e^{-6976/T}$$

Where voltage V in volts and an absolute temperature T in kelvins.

Second aging factor depends on average voltage and depth of discharge (DoD)

$$\beta_{cap}(V_{avg}, DoD) = 7.348 * 10^{-3} * (V_{avg} - 3.667)^2 + 7.600 * 10^{-4} + 4.081 * 10^{-3} * DoD$$

From above aging factors, battery aging function can be calculated as

$$C = 1 - \alpha_{cap} * t^{0.75} - \beta_{cap} * \sqrt{Q}$$

Where Q is charge throughput in ampere-hour.

For this model, the trucks are assumed to be used everyday for 15 years. The one-year temperature and voltage change during each discharge is used for the simulation input.

Comparison of Battery Degradation Models

Figure 5 compares the two battery degradation models over 20 years of daily operation and a range of depth-of-discharges. The models are considerably different, both in magnitude/trajectory of degradation, and, surprisingly, the impact of depth-of-discharge. In the simple model, depth-of-discharge and rate of degradation are correlated (as is obvious from the equation). In the complex model, they are inversely correlated, because

degradation is a function of voltage, and batteries operating at higher depth-of-discharge operate at a lower time-averaged voltage.

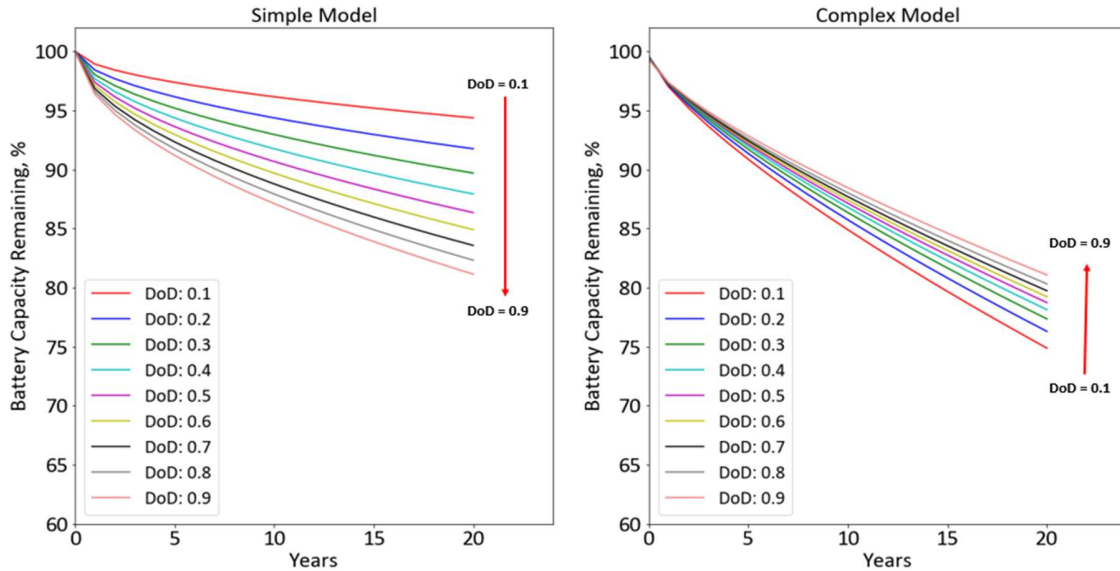


Figure 5. Comparison of two battery degradation models

We have no real basis for trusting either model. Both require major simplifying assumptions, and the complex model employs compounding layers of unverifiable (with our resources) assumptions. For the purposes of this report, we will consider results from both models. However, the excel tool will be developed with the simple model, as the complex model would largely defeat the purpose of using Excel for simplicity.

Total Cost of Ownership (TCO) Calculation

We seek to determine the lowest possible TCO for an EV that can meet the requirements of Duff Beer Co, and compare that figure to the TCO of an equivalent ICE. The following components must be considered to calculate TCO:

- CAPEX: Initial truck purchase and any associated charging infrastructure, as well as any battery replacement
- OPEX: Annual energy and maintenance
- Tax benefits of depreciation/terminal write-off value

For the Representative Example, we assumed a 15 year project life, 5 year straight-line depreciation, WACC = 10%, a tax rate of 21%. The formula for TCO is hence:

$$TCO = CAPEX_0 + \sum_{n=1}^{15} \frac{CAPEX_n + OPEX_n - 0.21 * DEP_n}{1.10^n} - \frac{0.21 * WriteOff}{1.10^{15}}$$

$$DEP_n = \sum_{i=n-5}^{n-1} 0.2 * CAPEX_i$$

$$WriteOff = \sum_{n=1}^{15} CAPEX_n - \sum_{n=1}^{15} DEP_n$$

This calculation is illustrated in the **Appendix D** as 'Discounted Cash Flow'. A complication of the TCO calculation is that battery capacity must be evaluated each year (using the battery degradation model) to determine if the battery must be replaced. This can be accomplished in a variety of ways, but it renders the TCO equation very difficult to implement as a traditional optimization function.

Implementation

While formal minimization of the TCO equation exceeds our capabilities, brute force iteration is perfectly viable. We use the following method:

- Calculate TCO of an ICE truck
- Calculate the bare minimum battery capacity b' , defined as capacity which will complete the route once (no buffer for degradation)
- Define the range of battery capacity to study. We set the lower bound at $1.1*b'$, and the upper bound at the minimum of $[1.5*b', (\text{Class 6 weight limit} - \text{mass_truck} - \text{mass_payload_max})]$
- Calculate TCO for an EV truck for discrete battery sizes (at a 1 kW.hr resolution) over this interval

Due to extreme uncertainty in battery unit price, we performed this analysis over a range of battery prices - a mini sensitivity analysis.

Results: Representative Example

Applying this methodology to the Representative Example yields the following curves for TCO as a function of installed battery capacity and battery unit price. While the different battery degradation models result in slightly different TCO curves (as a function of installed capacity), the optimal battery capacity and minimum feasible TCO are virtually identical. The optimal battery capacity for Duff Beer Co's application is approximately 233

kW.hrs. The EV option is price-competitive with ICE trucks at battery unit prices of approximately 150 \$/kW.hr.

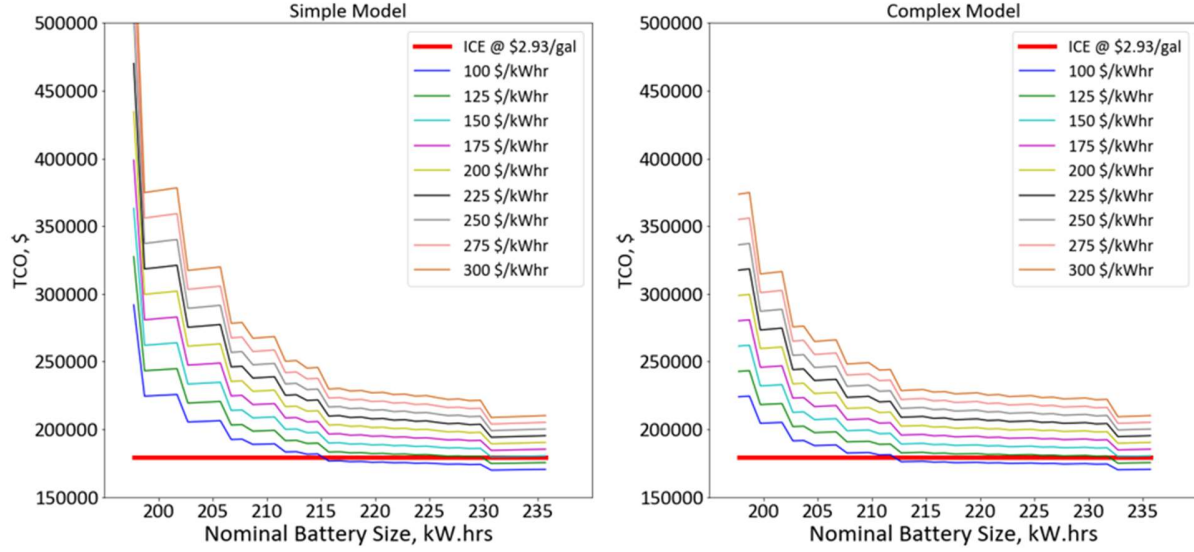


Figure 6. TCO as a function of battery pack size with varying prices in simple degradation model (6a, left) and complex degradation model(6b, right)

Results: Sensitivity Analysis

The most important input variables in the TCO calculation are: WACC, diesel price, electricity price, and battery price. We performed a sensitivity analysis to highlight for Duff Beer Co management the combinations of these variables that would result in an economically viable EV truck. Results of the sensitivity analysis are split into two tables. The first table shows ‘Break-even Battery Unit Price’ – the battery unit price at which $TCO_{EV} = TCO_{ICE}$ over a range of diesel and electricity prices, at a constant WACC of 10%:

Electricity Price, \$/kW.hr	Sensitivity Analysis: Break-even Battery Unit Price, at WACC = 10%																				
	Diesel Price, \$/kW.hr																				
\$ 0.02	\$ 284.9	\$ 298.5	\$ 312.1	\$ 325.6	\$ 339.2	\$ 352.8	\$ 366.4	\$ 379.9	\$ 393.5	\$ 407.1	\$ 420.6	\$ 434.2	\$ 447.8	\$ 461.4	\$ 474.9	\$ 488.5	\$ 502.1	\$ 515.6	\$ 529.2	\$ 542.8	\$ 556.4
\$ 0.04	\$ 232.4	\$ 245.9	\$ 259.5	\$ 273.1	\$ 286.6	\$ 300.2	\$ 313.8	\$ 327.4	\$ 340.9	\$ 354.5	\$ 368.1	\$ 381.6	\$ 395.2	\$ 408.8	\$ 422.4	\$ 435.9	\$ 449.5	\$ 463.1	\$ 476.6	\$ 490.2	\$ 503.8
\$ 0.06	\$ 179.8	\$ 193.3	\$ 206.9	\$ 220.5	\$ 234.1	\$ 247.6	\$ 261.2	\$ 274.8	\$ 288.4	\$ 301.9	\$ 315.5	\$ 329.1	\$ 342.6	\$ 356.2	\$ 369.8	\$ 383.4	\$ 396.9	\$ 410.5	\$ 424.1	\$ 437.6	\$ 451.2
\$ 0.08	\$ 127.2	\$ 140.8	\$ 154.3	\$ 167.9	\$ 181.5	\$ 195.1	\$ 208.6	\$ 222.2	\$ 235.8	\$ 249.4	\$ 262.9	\$ 276.5	\$ 290.1	\$ 303.6	\$ 317.2	\$ 330.8	\$ 344.4	\$ 357.9	\$ 371.5	\$ 385.1	\$ 398.6
\$ 0.10	\$ 74.6	\$ 88.2	\$ 101.8	\$ 115.3	\$ 128.9	\$ 142.5	\$ 156.1	\$ 169.6	\$ 183.2	\$ 196.8	\$ 210.3	\$ 223.9	\$ 237.5	\$ 251.1	\$ 264.6	\$ 278.2	\$ 291.8	\$ 305.4	\$ 318.9	\$ 332.5	\$ 346.1
\$ 0.12	\$ 22.1	\$ 35.6	\$ 49.2	\$ 62.8	\$ 76.3	\$ 89.9	\$ 103.5	\$ 117.1	\$ 130.6	\$ 144.2	\$ 157.8	\$ 171.3	\$ 184.9	\$ 198.5	\$ 212.1	\$ 225.6	\$ 239.2	\$ 252.8	\$ 266.4	\$ 279.9	\$ 293.5
\$ 0.14	\$ (6.0)	\$ (2.5)	\$ 1.1	\$ 10.2	\$ 23.8	\$ 37.3	\$ 50.9	\$ 64.5	\$ 78.1	\$ 91.6	\$ 105.2	\$ 118.8	\$ 132.3	\$ 145.9	\$ 159.5	\$ 173.1	\$ 186.6	\$ 200.2	\$ 213.8	\$ 227.3	\$ 240.9
\$ 0.16	\$ (19.5)	\$ (15.9)	\$ (12.4)	\$ (8.9)	\$ (5.3)	\$ (1.8)	\$ 2.6	\$ 11.9	\$ 25.5	\$ 39.1	\$ 52.6	\$ 66.2	\$ 79.8	\$ 93.3	\$ 106.9	\$ 120.5	\$ 134.1	\$ 147.6	\$ 161.2	\$ 174.8	\$ 188.3
\$ 0.18	\$ (32.9)	\$ (29.4)	\$ (25.8)	\$ (22.3)	\$ (18.7)	\$ (15.2)	\$ (11.7)	\$ (8.1)	\$ (4.6)	\$ (1.0)	\$ 3.9	\$ 13.6	\$ 27.2	\$ 40.8	\$ 54.3	\$ 67.9	\$ 81.5	\$ 95.1	\$ 108.6	\$ 122.2	\$ 135.8
\$ 0.20	\$ (46.3)	\$ (42.8)	\$ (39.2)	\$ (35.7)	\$ (32.2)	\$ (28.6)	\$ (25.1)	\$ (21.6)	\$ (18.0)	\$ (14.5)	\$ (11.0)	\$ (7.4)	\$ (3.9)	\$ (0.3)	\$ 5.6	\$ 15.3	\$ 28.9	\$ 42.5	\$ 56.1	\$ 69.6	\$ 83.2

Figure 7. Sensitivity analysis results. Higher resolution version in [Appendix E](#)

The second table shows IRR – the discount rate at which $TCO_{EV} = TCO_{ICE}$ – over the same range of diesel and electricity prices, at a constant battery price of \$175/kW.hr (based on literature, a reasonable near-term estimate for EV battery prices when manufactured at efficient scale):

		Sensitivity Analysis: IRR, at Battery Price of \$175/kW.hr																				
		Diesel Price, \$/kW.hr																				
Electricity Price, \$/kW.hr		\$ 2.00	\$ 2.10	\$ 2.20	\$ 2.30	\$ 2.40	\$ 2.50	\$ 2.60	\$ 2.70	\$ 2.80	\$ 2.90	\$ 3.00	\$ 3.10	\$ 3.20	\$ 3.30	\$ 3.40	\$ 3.50	\$ 3.60	\$ 3.70	\$ 3.80	\$ 3.90	\$ 4.00
		\$ 0.02	19.1%	20.2%	21.1%	22.2%	23.2%	24.2%	25.2%	26.1%	27.0%	28.1%	29.0%	30.1%	31.2%	32.2%	33.3%	34.3%	35.4%	36.4%	37.4%	38.4%
\$ 0.04		14.9%	16.1%	17.2%	18.2%	19.3%	20.3%	21.3%	22.3%	23.3%	24.3%	25.3%	26.2%	27.2%	28.2%	29.2%	30.3%	31.3%	32.4%	33.4%	34.5%	35.5%
\$ 0.06		10.4%	11.6%	12.8%	14.0%	15.1%	16.2%	17.3%	18.3%	19.4%	20.4%	21.4%	22.5%	23.5%	24.4%	25.4%	26.3%	27.3%	28.3%	29.3%	30.4%	31.5%
\$ 0.08		5.3%	6.7%	8.0%	9.3%	10.6%	11.8%	13.0%	14.1%	15.2%	16.3%	17.4%	18.4%	19.5%	20.6%	21.5%	22.6%	23.6%	24.6%	25.5%	26.5%	27.4%
\$ 0.10		-1.2%	0.6%	2.4%	3.9%	5.4%	6.8%	8.2%	9.4%	10.7%	12.0%	13.1%	14.2%	15.4%	16.5%	17.6%	18.6%	19.7%	20.7%	21.7%	22.7%	23.7%
\$ 0.12		-127.5%	-8.3%	-5.4%	-3.1%	-1.0%	0.9%	2.6%	4.1%	5.6%	7.0%	8.4%	9.6%	10.9%	12.1%	13.3%	14.4%	15.5%	16.6%	17.7%	18.7%	19.8%
\$ 0.14		N/A	N/A	N/A	-199.9%	-121.2%	-7.9%	-5.1%	-2.8%	-0.8%	1.1%	2.8%	4.3%	5.7%	7.2%	8.5%	9.8%	11.0%	12.3%	13.4%	14.5%	15.7%
\$ 0.16		N/A	N/A	N/A	N/A	N/A	N/A	-178.0%	-115.3%	-7.6%	-4.8%	-2.5%	-0.5%	1.2%	3.0%	4.5%	5.5%	7.4%	8.7%	9.9%	11.2%	
\$ 0.18		N/A	N/A	N/A	N/A	N/A	N/A	N/A	N/A	N/A	N/A	-167.5%	-109.8%	-7.2%	-4.5%	-2.3%	-0.3%	1.5%	3.1%	4.7%	6.1%	
\$ 0.20		N/A	N/A	N/A	N/A	N/A	N/A	N/A	N/A	N/A	N/A	N/A	N/A	N/A	N/A	N/A	-157.9%	-104.7%	-6.8%	-4.2%	-2.0%	-0.1%

Figure 8. Sensitivity analysis result. Higher resolution version in [Appendix E](#)

4. Discussion

Our results are generally as expected/found in the literature:

- The Representative Example confirms that electrification of EV trucks is not economically competitive under ‘normal’ conditions. Government incentives, price of carbon, or unusual circumstances (very cheap electricity, very expensive diesel) could result in some viable scenarios, but in general, battery unit prices of ~150 - 175 \$/kW.hr are required.
- The Representative Example, a SWAG at a scenario that might make sense for electrification, landed almost exactly on the practical route limitation of Class 6 EVs at Lithium-Ion energy densities (200 km with initial payload of 5000 kg). Longer routes would require either mid-route charging or a Class 8 truck. Heavier payloads will require a Class 8 Truck.
- We agonized over the battery degradation model and spent the time to build two versions, only for both to converge on the same answer - oversize the battery by ~33% (relative to the minimum battery size that can complete the route). The general rule of thumb for EV battery life is 80% of initial capacity (25% oversized), so our results essentially confirm that rule of thumb.
- We were able to consolidate our calculations into an Excel file, but it is very unwieldy. It would benefit from additional efforts to abstract complexity and simplify the user interface.
- The Representative Example did not include costs of charging infrastructure. This functionality was built into the Python script, and must be considered for real applications. Both charger CAPEX and demand charges could be significant, particularly for small fleets with minimal economy of scale. Had charging been included in the scope of the Representative Example, the EV TCO would have been up to \$100,000 higher (\$40k for charging infrastructure, ~\$60k present value of lifetime demand charges at 50 kW and 12.5 \$/kW.month). However, it would be

perfectly reasonable to split a single CHAdeMO charger, and its costs, between 4 - 6 fleet vehicles. Future efforts could identify the optimal fleet size for deployment of EV trucks, which is likely to be discontinuous due to the benefit of amortizing chargers across multiple EVs.

- We have no crystal ball on the trajectory of battery prices, but the breakeven prices we calculate seem feasible on the 5-10 year time horizon. Continued R&D efforts in the EV trucking space is justified.
- This project was not a great application of our coursework. It would be better suited for an engineering economics or applied engineering course. That said, it was unquestionably industrially relevant, and representative of work real engineers do (scoping, techno-economic evaluation).

5. Summary

In this study, we have developed optimization models to find the minimum battery size given some route distance, payload, and economic scenario for incorporation into the TCO of an EV fleet. We have also assessed TCO of the EV truck relative to ICE alternatives, including a sensitivity analysis on major variables. Briefly, the study consisted of the following core steps: (1) define the Representative Example to ground our work in a somewhat realistic application, (2) characterize the underlying physics of truck energy consumption based on first-principle modeling, (3) develop a simple and advanced model for battery degradation, (4) build tool to calculate TCO for some route based on models of truck energy and battery degradation, as well as TCO for ICE equivalent, (5) demonstrate tool on Representative Example to calculate optimal battery capacity and associated TCO, and finally (7) perform sensitivity studies of some major variables to highlight pathways towards deployment of EV trucks.

Results of the analysis show that, while the different battery degradation models result in slightly different TCO curves (as a function of installed capacity), the optimal battery capacity and minimum feasible TCO are virtually identical. The optimal battery capacity for Duff Beer Co's application is approximately 233 kW.hrs. The EV option is price-competitive with ICE trucks at battery unit prices of approximately 150 \$/kW.hr. The sensitivity analysis shows 'Breakeven Battery Unit Price' – the battery unit price at which $TCO_{EV} = TCO_{ICE}$ over a range of diesel and electricity prices, at a constant WACC of 10%. A second sensitivity analysis gives IRR over the same range of diesel and electricity prices, at a constant battery price of \$175/kW.hr.

References

- [1] "Inventory of U.S. Greenhouse Gas Emissions and Sinks", EPA, 2020. Retrieved May 6, 2020 from <https://www.epa.gov/ghgemissions/inventory-us-greenhouse-gas-emissions-and-sinks>
- [2] Musk, E. (2017). The future we're building -- and boring. Retrieved May 6, 2020 from https://www.ted.com/talks/elon_musk_the_future_we_re_building_and_boring
- [3] Trucking Industry Revenues Top \$796 Billion in 2018. (2019). Retrieved May 6, 2020 from <https://www.trucking.org/news-insights/trucking-industry-revenues-top-796-billion-2018>
- [4] Moultsak, M., Lutsey, N., & Hall, D. (2017). Transitioning to zero-emission heavy-duty freight vehicles. *Int. Counc. Clean Transp.*
- [5] A Behind the Scenes Take on Lithium-ion Battery Prices. (2019, March 5). Retrieved May 6, 2020, from <https://about.bnef.com/blog/behind-scenes-take-lithium-ion-battery-prices/>
- [6] Sripad, S., & Viswanathan, V. (2018). Quantifying the economic case for electric semi-trucks. *ACS Energy Letters*, 4(1), 149-155. doi.org/10.1021/acsenergylett.8b02146
- [7] Zhou, T., Roorda, M. J., MacLean, H. L., & Luk, J. (2017). Life cycle GHG emissions and lifetime costs of medium-duty diesel and battery electric trucks in Toronto, Canada. *Transportation Research Part D: Transport and Environment*, 55, 91-98.
- [8] Johannes Schmalstieg, Stefan Käbitz, Madeleine Ecker, Dirk Uwe Sauer, (2014). A holistic aging model for Li(NiMnCo)O₂ based 18650 lithium-ion batteries, *Journal of Power Sources*, Volume 257, Pages 325-334, ISSN 0378-7753, <https://doi.org/10.1016/j.jpowsour.2014.02.012>.
- [9] Sripad, S., & Viswanathan, V. (2017). Performance Metrics Required of Next-Generation Batteries to Make a Practical Electric Semi Truck. *ACS Energy Letters*, 2(7), 1669–1673. doi: 10.1021/acsenergylett.7b00432
- [10] Wang, J., Liu, P., Hicks-Garner, J., Sherman, E., Soukiazian, S., Verbrugge, M., ... Finamore, P. (2011). Cycle-life model for graphite-LiFePO₄ cells. *Journal of Power Sources*, 196(8), 3942–3948. doi: 10.1016/j.jpowsour.2010.11.134
- [11] Xu, B., Oudalov, A., Ulbig, A., Andersson, G., & Kirschen, D. S. (2018). Modeling of Lithium-Ion Battery Degradation for Cell Life Assessment. *IEEE Transactions on Smart Grid*, 9(2), 1131–1140. doi: 10.1109/tsg.2016.2578950

[12] EIA. Table 12. Petroleum and Other Liquids Prices. Annual Energy Outlook 2020 (2020). Retrieved May 6, 2020 from https://www.eia.gov/outlooks/aoe/tables_ref.php.

[13] Lee, D.-Y., Thomas, V. M., & Brown, M. A. (2013). Electric Urban Delivery Trucks: Energy Use, Greenhouse Gas Emissions, and Cost-Effectiveness. *Environmental Science & Technology*, 47(14), 8022–8030. doi: 10.1021/es400179w

Appendix

Appendix A: Table of Responsibilities

Task	Team Members
Conceptualization	Bianca, Emin, Alp, Dayu, Greg, Harry
Literature Review & characterization of primary variables: <ul style="list-style-type: none">● Input variables and representative scenario● Battery cost● O&M costs● Vehicle efficiency	Bianca, Emin, Alp, Greg, Harry
Energy consumption analysis (from first principle modeling)	Greg, Emin, Dayu, Harry
Battery degradation models	Greg, Emin, Dayu
TCO analysis	Emin, Greg, Harry, Dayu
Sensitivity analysis	Greg, Dayu
Visualization & Software	Greg, Emin, Dayu
Writing - Draft, Review & Editing	Bianca, Emin, Alp, Dayu, Greg, Harry

Appendix B - Assumptions Used in the Representative Example

EV:

- $\text{rho_air} = 1.22 \text{ [kg/m}^3]$
- $\text{Coeff_drag} = 0.75 [-]$
- $\text{Area_cab} = 7 \text{ [m}^2]$
- $\text{Coeff_friction} = 0.015 [-]$
- $\text{Eff_drivetrain} = 0.9 [-]$
- $\text{Eff_powertrain} = 0.95 [-]$
- safety factor = 0.95 [-]
- acceleration = 0.448 [m/s^2]
- alpha_degradation = 0.15 [-]
- battery_e_density = 0.1
[kW.hr/kg]
- chassis_weight = 4250 [kg]
- maintenance = 0.022 [\$/km]

ICE:

- $\text{rho_air} = 1.22 \text{ [kg/m}^3]$
- $\text{Coeff_drag} = 0.75 [-]$
- $\text{Area_cab} = 7 \text{ [m}^2]$
- $\text{Coeff_friction} = 0.015 [-]$
- $\text{Eff_drivetrain} = 0.9 [-]$
- $\text{Eff_powertrain} = 0.4 [-]$
- safety factor = 0.95 [-]
- acceleration = 0.448 [m/s^2]
- diesel_e_density = 38
[kW.hr/gal]
- chassis_weight = 4250 [kg]
- engine_weight = 1200 [lb]
- maintenance = 0.045 [\$/km]

Financial

- Truck base cost = 91000 [\$]
- WACC = 10 [%]
- project life = 15 [years]
- tax rate = 21 [%]
- 5 yr straight-line depreciation
- Electricity price = 0.12
[\$/kW.hr]
- Diesel price = 2.93 [\$/gal]
- WACC is nominal; all price components inflate at same rate

Referenced from [6, 9, 10, 13]

Picture of the Durastar International Beverage 4300



Appendix C - Underlying Physics

- Optimization variable:
 - Battery size = x [kWh]
 - Given values:
 - Distance of route = d
 - Mass of vehicle = $m(x) = m_0 + \alpha x$
 - Where m_0 is the base mass of the vehicle and αx is the added battery mass
 - Then, we first consider the sum of forces on the system:
- $$m \cdot \frac{dv}{dt} = F_T - k_1 v^2 - k_2 - k_3$$
- Where:
 - F_T is the traction force exerted by the wheels
 - $k_1 = \frac{1}{2} \rho C_D A$ is the air drag term; ρ = air density, C_D = coefficient of drag, A = frontal (cross-sectional) area of truck [m^2].
 - $k_2 = C_r \cdot m \cdot g$ is the friction term
 - $k_3 = m \cdot g \cdot \sin(\theta)$
 - v is the truck's velocity [m/s]
 - Assuming, then, that the velocity is constant ($\frac{dv}{dt} = 0$), we can solve for the traction force exerted by the wheels:

$$F_T = (\frac{1}{2} \rho C_D A) v^2 + m \cdot g \cdot (C_r + \sin(\theta))$$

- Next, we use the formulation for work to compute the work done at the wheels:

$$Work = W = F_T \cdot d = [(\frac{1}{2} \rho C_D A) v^2 + m \cdot g \cdot (C_r + \sin(\theta))] \frac{d}{\eta}$$

- Where η is the energy efficiency term.

Above equations can be written for an application with multiple segments, n:

- m_n = (mass of truck chassis + cab) + (mass drivetrain) + (m_b) + (payload_n)
- m_b is battery mass
- $m_n = [m_1, m_2, \dots, m_n]$
- $d_n = [d_1, d_2, \dots, d_n]$
- $v_n = [v_1, v_2, \dots, v_n]$
- $\theta_n = [\theta_1, \theta_2, \dots, \theta_n]$

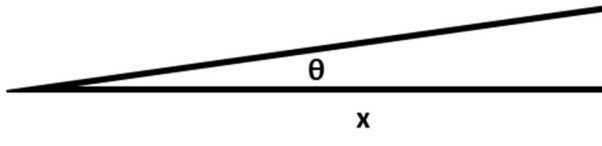
- $X [kW.hrs] = \sum_{n=1}^n Work_n = \left(\frac{1}{2} \rho_a * C_d * A_{cab} * v_n^2 + m * g(C_r + \sin(\theta)) \right) * \left(\frac{1}{Eff_d} \right) * d_n^T * \left(\frac{1 kJ}{1000 J} \right) * \left(\frac{1 hr}{3600 s} \right)$

Constraint:

- $\frac{m_b * ED_b}{\beta} \geq X$

Where ED_b is battery energy density [kWhr/kg] and β is some safety factor

Calculating θ [deg] from Grade [%]:



- $Grade = 100 * \frac{y}{x}$
- $\tan(\theta) = \frac{y}{x}$
- $\left(\frac{Grade}{100} \right)$

Constant Acceleration: $dv/dt = \alpha$

- (1) $m * \frac{dv}{dt} = F_T - \frac{1}{2} \rho_a * C_d * A_{cab} * v^2 - C_r * m * g - m * g * \sin(\theta)$
- (2) $F_{acc} = m * \frac{dv}{dt} + \frac{1}{2} \rho_a * C_d * A_{cab} * v^2 + C_r * m * g + m * g * \sin(\theta)$
- (3) $W_{acc} = \int_0^x F_{acc} * dx$
- (4) $W_{acc} = \int_0^x \left[m * \alpha + \frac{1}{2} \rho_a * C_d * A_{cab} * v(x)^2 + C_r * m * g + m * g * \sin(\theta) \right] * dx$
- (5) $v = \frac{dx}{dt} = \int_0^t \alpha * dt = \alpha * t$
- (6) $t = v/\alpha$
- (7) $x = \int_0^t v * dt = \int_0^t \alpha * t * dt = \frac{1}{2} \alpha * t^2 = \frac{1}{2} \alpha * \frac{v^2}{\alpha^2} = \frac{v^2}{2\alpha}$
- (8) $v(x)^2 = 2 * \alpha * x$
- (9) $W_{acc} = \int_0^x \left[m * \alpha + \frac{1}{2} \rho_a * C_d * A_{cab} * 2 * \alpha * x + C_r * m * g + m * g * \sin(\theta) \right] * dx$
- (10) $W_{acc} = \frac{1}{2} \rho_a * C_d * A_{cab} * \alpha * x^2 + x * (m * \alpha + C_r * m * g + m * g * \sin(\theta))$

Combined:

- (1) Constant velocity, v_e
- (2) Constant acceleration, α
- (3) Total distance, x_{net}
- (4) $x_{acc} = \frac{v_e^2}{2*\alpha}$
- (5) $x_{ss} = x_{net} - x_{acc}$

$$(6) \quad X_{net} = (W_{acc} + W_{ss}) * \left(\frac{1}{Eff_d} \right) * \left(\frac{1 \text{ kJ}}{1000 \text{ J}} \right) * \left(\frac{1 \text{ hr}}{3600 \text{ s}} \right)$$

$$(7) \quad W_{acc} = \left[\frac{1}{2} \rho_a * C_d * A_{cab} * \alpha * x_{acc} + m * \alpha + C_r * m * g + m * g * \sin(\theta) \right] * x_{acc}$$

$$(8) \quad W_{ss} = \left(\frac{1}{2} \rho_a * C_d * A_{cab} * v^2 + m * g (C_r + \sin(\theta)) \right) * x_{ss}$$

$$(9) \quad \frac{m_b * ED_b}{\beta} \geq X$$

Appendix D - Discounted Cash Flow

t	Battery Capacity	CAPEX	Depreciation	Book Value	Tax Benefit	OPEX, Maint	OPEX, Electricity	Cost	Cost, PV	TCO, net
[years]	[kW.hrs]	[\$]	[\$]	[\$]	[\$]	[\$]	[\$]	[\$]	[\$]	[\$]
0	221	\$129,685	\$ -	\$ 129,685	\$ -	\$ -	\$ -	\$129,685	\$129,685	\$129,685
1	213.36	\$ -	\$ 25,937	\$ 103,748	\$ 5,447	\$ 1,627	\$ 8,068	\$ 4,249	\$ 3,862	\$133,547
2	209.79	\$ -	\$ 25,937	\$ 77,811	\$ 5,447	\$ 1,627	\$ 8,068	\$ 4,249	\$ 3,511	\$137,058
3	206.97	\$ -	\$ 25,937	\$ 51,874	\$ 5,447	\$ 1,627	\$ 8,068	\$ 4,249	\$ 3,192	\$140,250
4	204.56	\$ -	\$ 25,937	\$ 25,937	\$ 5,447	\$ 1,627	\$ 8,068	\$ 4,249	\$ 2,902	\$143,152
5	202.40	\$ -	\$ 25,937	\$ -	\$ 5,447	\$ 1,627	\$ 8,068	\$ 4,249	\$ 2,638	\$145,790
6	200.44	\$ -	\$ -	\$ -	\$ -	\$ 1,627	\$ 8,068	\$ 9,695	\$ 5,473	\$151,263
7	198.61	\$ -	\$ -	\$ -	\$ -	\$ 1,627	\$ 8,068	\$ 9,695	\$ 4,975	\$156,238
8	196.90	\$ -	\$ -	\$ -	\$ -	\$ 1,627	\$ 8,068	\$ 9,695	\$ 4,523	\$160,761
9	195.28	\$ -	\$ -	\$ -	\$ -	\$ 1,627	\$ 8,068	\$ 9,695	\$ 4,112	\$164,873
10	221	\$ 38,685	\$ -	\$ 38,685	\$ -	\$ 1,627	\$ 8,068	\$ 48,380	\$ 18,653	\$183,525
11	213.36	\$ -	\$ 7,737	\$ 30,948	\$ 1,625	\$ 1,627	\$ 8,068	\$ 8,071	\$ 2,829	\$186,354
12	209.79	\$ -	\$ 7,737	\$ 23,211	\$ 1,625	\$ 1,627	\$ 8,068	\$ 8,071	\$ 2,572	\$188,926
13	206.97	\$ -	\$ 7,737	\$ 15,474	\$ 1,625	\$ 1,627	\$ 8,068	\$ 8,071	\$ 2,338	\$191,263
14	204.56	\$ -	\$ 7,737	\$ 7,737	\$ 1,625	\$ 1,627	\$ 8,068	\$ 8,071	\$ 2,125	\$193,389
15	202.40	\$ -	\$ 7,737	\$ -	\$ 1,625	\$ 1,627	\$ 8,068	\$ 8,071	\$ 1,932	\$195,321

Appendix E - Python Code (TCO Calculations) 097

Define Engineering Constants

```
In [41]: 1 mass_truck = 4250          # mass of truck chassis and cab (excludes engine and battery)
2 mass_engine = 1200/2.2       # engine weighs 1200 lbs
3 rho_air = 1.22             # air density in kg/m3
4 C_d = 0.75                 # coefficient of drag
5 A_cab = 7                  # truck cab frontal surface area, m2
6 C_r = 0.015                # coefficient of rolling resistance
7 g = 9.8                    # gravitational constant
8 E_d_ev = 0.83              # aggregate efficiency of EV drivetrain
9 E_d_ice = 0.36              # aggregate efficiency of ICE drivetrain
10 ED_b = 0.1                 # battery energy density, kW.hr/kg
11 ED_diesel = 38             # kW.hrs/gal of diesel, based on Lower Heating Value
12 beta = 0.95                # safety factor - replace battery when the route depletes 95% of its capacity
13 a = 0.448                  # constant acceleration in m/s^2
14 k_deg = 0.15               # for battery degradation model
15 max_weight = 11793.4       # max weight of class 6 truck
```

Battery Degradation Models

```

: M 1 ## Simple model
2
3 def deg(P_t0, cycles, dod):
4     Q = k_deg*((cycles*dod)**0.55)
5     P_avail = P_t0*(100-Q)/100
6     return P_avail

: M 1 ## complicated model
2 p_0 = 3.4707;
3 p_1 = 1.6112;
4 p_2 = -2.6287;
5 p_3 = 1.7175;
6 z_vec = np.linspace(0,1,24)
7 OCV = lambda z_vec: p_0 + p_1*z_vec + p_2*z_vec**2 + p_3*z_vec**3
8
9 temp_data = pd.read_csv('C:/Users/gturm/Dropbox/Haas/Spring 2020/Systems Control/Project/2107761.csv')
10 temp_data = temp_data.loc[:,['DATE','HLY-TEMP-NORMAL']].groupby('DATE').mean().reset_index()
11 temp_data['HLY-TEMP-NORMAL'] = temp_data['HLY-TEMP-NORMAL']+273.15
12 temp_data = temp_data.iloc[23:].reset_index(drop=True)
13
14 idx=[]
15 hours_of_work = 9 #hours daily
16 for i in 6*np.arange(1,len(temp_data)/6,4,dtype=int):
17     idx.append(list(range(i,i+hours_of_work+1)))
18 idx = np.ndarray.flatten(np.array(idx)).astype(int).tolist()
19 temp_data = temp_data[temp_data.index.isin(idx)].reset_index()
20 T = temp_data['HLY-TEMP-NORMAL']

21
22
23
24 def battery_degradation(DoD,number_of_years):
25
26
27
28 SOC = np.linspace(1,1-DoD,hours_of_work)
29
30 V = list(OCV(SOC))
31 V.insert(0,4.2)
32 V1 = [V for i in range(52*7)]
33 V1 = np.ndarray.flatten(np.array(V1)).astype(float).tolist()
34 #temp_data['V'] = V1
35 Q = 2.15 #Ah
36
37 def alpha_cap(V,T):
38     alpha = (7.543*np.array(V)-23.75)*10**6*np.exp(-6976/np.array(T))
39     return np.mean(alpha)
40
41 def beta_cap(V,DoD):
42     return np.mean(7.346*10**(-3)*(np.mean(V)-3.667)**2 + 7.6*10**(-4) + 4.081*10**(-3)*DoD)
43
44 capacity_left = 1 - alpha_cap(V1,T)*(365*number_of_years)**0.75 - beta_cap(V1,DoD)*np.sqrt(Q)
45
46 return capacity_left

```

Define Economic Constants

```
[1]: ┌─ wacc = 0.10          # cost of capital (discount rate)
  ┌─ project_life = 15      # years
  ┌─ price_maint_ev = 0.022 # cost of maintenance for EV, $/km
  ┌─ price_maint_ice = 0.045 # cost of maintenance for ICE, $/km
  ┌─ price_elect = 0.12      # electricity price, $/kW.hr
  ┌─ price_diesel = 2.93     # $/gal
  ┌─ rate_tax = 0.21         # tax rate, fraction
  ┌─ price_chassis = 91000   # cost of ICE truck. Assumed an EV pays the same price for just the chassis + cab
  ┌─ demand_charge = 10      # $/kW, assessed monthly
  ┌─ n_chargers = 0          # number of chargers to add
  ┌─ charger_P = 50          # charger operating power, kW
  ┌─ price_charger = 40000    # charger unit cost, $ per unit
  ┌─ number_of_trucks = 1     # quantity of trucks across which to amortize charging expenses
  ┌─
  ┌─ #set of battery prices to consider, $/kW.hr
  ┌─ price_battery = [100,125,150,175,200,225,250,275,300]
```

Define Route

```
[4]: ┌─ # distances of each segment
  ┌─ # defined in km and converted to m
  ┌─ d_n_km = np.array([3.06, 5.21, 5.47, 3.86, 50.05, 21.73, 60.51, 14.16, 38.62])
  ┌─ d_n = d_n_km*1000
  ┌─
  ┌─ # average/constant velocities of each segment
  ┌─ # defined in km/hr and converted to m/s
  ┌─ v_n_kmph = np.array([30, 40, 30, 30, 85, 70, 65, 65, 85])
  ┌─ v_n = v_n_kmph*1000/3600
  ┌─ # calculate x_acc for each segment
  ┌─ x_acc_n = (v_n**2)*0.5*(1/a)
  ┌─ x_ss_n = d_n - x_acc_n
  ┌─
  ┌─ # Payload of each segment
  ┌─ payload_n = np.array([5184, 4536, 3888, 3240, 2592, 1944, 1296, 648, 0])
  ┌─
  ┌─ # grade of each segment
  ┌─ # converted to theta, in degrees
  ┌─ grade_n = np.array([0, 0, 0, 2.7, 0.6, 0.5, -0.7, -0.12, -0.26])
  ┌─ theta = np.arctan(grade_n/100)
```

Calculate TCO of ICE Truck

```
[1]: # Calculate energy consumption per day
[2]
[3] m_n = payload_n + mass_truck + mass_engine
[4] F_acc = 0.5*rho_air*C_d*A_cab*a*x_acc_n + m_n*a + C_r*m_n*g + m_n*g*np.sin(theta)
[5] F_ss = 0.5*rho_air*C_d*A_cab*(v_n**2) + m_n*g*(C_r + np.sin(theta))
[6]
[7] P_acc = np.dot(F_acc, x_acc_n)
[8] P_ss = np.dot(F_ss, x_ss_n)
[9]
[10] P_req = (P_acc + P_ss) *(1/E_d_ice) * (1/1000) * (1/3600)
[11]
[12] print('Energy Consumed Per Day: ', round(P_req, 1), ' kW.hrs')
[13]
```

Energy Consumed Per Day: 363.9 kW.hrs

```
[1]: # Calculate TCO
[2] filepath= 'C:/Users/gturk/Dropbox/Haas/Spring 2020/Systems Control/Project/model runs/'
[3]
[4] # initial capex is cost of chassis. all other years = 0
[5] CAPEX = [round((price_chassis),2)]
[6] for yr in np.arange(1,project_life+1, 1):
[7]     CAPEX.append(0)
[8]
[9] #calculate depreciation assuming 5 yr straight Line
[10] DEP = [0]
[11] for yr in np.arange(1,project_life+1, 1):
[12]     d_t = 0
[13]     for z in range(1,min(6, yr+1)):
[14]         d_t += 0.2 * CAPEX[yr-z]
[15]     DEP.append(d_t)
[16]
[17] #calculate book value(t)
[18] BOOKVAL = [CAPEX[0]]
[19] for yr in np.arange(1,project_life+1, 1):
[20]     BOOKVAL.append(sum(CAPEX[:yr+1]) - sum(DEP[:yr+1]) )
[21]
[22] #calculate tax benefit of depreciation / write-off at end of project
[23] TAXBEN = [0]
[24] for yr in np.arange(1,project_life, 1):
[25]     TAXBEN.append(DEP[yr]*rate_tax)
[26] TAXBEN.append((BOOKVAL[-1]*DEP[-1])*rate_tax)
[27]
[28] #calculate OPEX due to maintenance
[29] OPEX_maint = [0]
[30] for yr in np.arange(1,project_life+1, 1):
[31]     OPEX_maint.append(365 * d_n_kn.sum() * price_maint_ice)
[32]
[33] #calculate OPEX cost of electricity
[34] OPEX_elect = [0]
[35] for yr in np.arange(1,project_life+1, 1):
[36]     OPEX_elect.append(365 * P_req * (1/ED_diesel) * price_diesel)
[37]
[38]
[39] # Consolidate into dataframe
[40] fin_b = pd.DataFrame(index=np.arange(0,project_life+1, 1))
[41] fin_b['CAPEX'] = CAPEX
[42] fin_b['Depreciation'] = DEP
[43] fin_b['Book Value'] = BOOKVAL
[44] fin_b['Tax Benefit'] = TAXBEN
[45] fin_b['OPEX, Maintenance'] = OPEX_maint
[46] fin_b['OPEX, Electricity'] = OPEX_elect
[47] fin_b['Cost'] = fin_b['CAPEX'] + fin_b['OPEX, Maintenance'] + fin_b['OPEX, Electricity'] - fin_b['Tax Benefit']
[48]
[49] for i in fin_b.index.tolist():
[50]     fin_b.at[i, 'Cost, PV'] = fin_b.at[i, 'Cost'] / ((1+wacc)**i)
[51]     if i == 0:
[52]         fin_b.at[i, 'TCO, net'] = fin_b.at[i, 'Cost, PV']
[53]     else:
[54]         fin_b.at[i, 'TCO, net'] = fin_b.at[i-1, 'TCO, net'] + fin_b.at[i, 'Cost, PV']
[55]
[56] print('TCO: ', str(fin_b.at[project_life, 'TCO, net']))
[57] fin_b.to_csv(filepath+'ICE.csv')
[58]
[59] fin_b
[60]
[61] tco_ice = fin_b.at[project_life, 'TCO, net']
[62]
```

TCO: 179733.89889409303

Calculate TCO for EV: Simple Battery Degradation Model

Calculate Minimum Battery Size

```
55]: M
 1 # Guess Battery Size
 2 m_b_guess = 2000
 3
 4 # iterate until calculated battery mass is within 0.01% of guessed battery size
 5 check = False
 6 count = 0
 7
 8 while check == False and count < 100:
 9
10     m_n = payload_n + mass_truck + m_b_guess
11
12     F_acc = 0.5*rho_air*C_d*A_cab*a*x_acc_n + m_n*a + C_r*m_n*g + m_n*g*np.sin(theta)
13     F_ss = 0.5*rho_air*C_d*A_cab*(v_n**2) + m_n*g*(C_r + np.sin(theta))
14
15     P_acc = np.dot(F_acc, x_acc_n)
16     P_ss = np.dot(F_ss, x_ss_n)
17
18     P_req = (P_acc + P_ss) * (1/E_d_ev) * (1/1000) * (1/3600) * (1/beta)
19
20     m_b_req = P_req / ED_b
21
22     err = np.abs(m_b_guess - m_b_req)/m_b_req
23     if err <= 0.0001:
24         check = True
25     else:
26         m_b_guess = m_b_req
27
28
29     count+=1
30
31 print('Required Battery Rating: ', round(P_req, 1), ' kW.hrs')
32 print('Required Battery Mass: ', round(m_b_guess, 0), ' kg')
33
```

Required Battery Rating: 179.7 kW.hrs
Required Battery Mass: 1797.0 kg

Calculate Economics for a Variety of Battery Sizes

```

]: M 1 filepath= 'C:/Users/gturk/Dropbox/Haas/Spring 2020/Systems Control/Project/model runs/'
2
3 battery_min = 1.10 * P_req
4 # battery + truck chassis + payload cannot exceed Class 6 weight limits
5 battery_max = (max_weight - payload_n.max() - mass_truck)*ED_b
6 battery_sizes = np.arange(battery_min, battery_max, 1)
7 #battery_sizes = [170.8*1.15]
8 case_num = 1
9 TCO_list_of_lists=[]
10
11 for p in price_battery:
12     TCOS = []
13     for b in battery_sizes:
14
15         #calculate P_req_b for battery size
16         m_n = payload_n + mass_truck + b / ED_b
17         F_acc = 0.5*rho_air*C_d*A_cab*a*x_acc_n + m_n*a + C_r*m_n*g + m_n*g*np.sin(theta)
18         F_ss = 0.5*rho_air*C_d*A_cab*(v_n**2) + m_n*g*(C_r + np.sin(theta))
19         P_acc = np.dot(F_acc, x_acc_n)
20         P_ss = np.dot(F_ss, x_ss_n)
21         P_req_b = (P_acc + P_ss) *(1/E_d_ev) * (1/1000) * (1/3600) * (1/beta)
22
23         #iterate through years to determine CAPEX requirements
24         #initial capex is cost of chassis + battery + chargers
25         CAPEX = [round((price_chassis + b*p + n_chargers*price_charger/number_of_trucks),2)]
26         #track battery capacities through the years
27         X_t = [b]
28         #calculate Depth_of_Discharge
29         DoD = P_req_b / b
30         # age_battery will track the age of the battery through replacement cycles
31         age_battery = 0
32         # calculate replacement capacity
33         X_replace = P_req_b / beta
34
35         for yr in np.arange(1,project_life+1, 1):
36             X_yr_end = deg(b, 365*(age_battery+1), DoD)
37             # Determine if battery must be replaced
38             if X_yr_end <= X_replace:
39                 CAPEX.append(round(b*p,2))
40                 age_battery = 0
41                 X_t.append(round(b,2))
42             else:
43                 CAPEX.append(0)
44                 age_battery+=1
45                 X_t.append(round(X_yr_end,2))
46
47         #calculate depreciation assuming 5 yr straight Line
48         DEP = [0]
49         for yr in np.arange(1,project_life+1, 1):
50             d_t = 0
51             for z in range(1,min(6, yr+1)):
52                 d_t += 0.2 * CAPEX[yr-z]
53             DEP.append(d_t)
54
55         #calculate book value(t)
56         BOOKVAL = [CAPEX[0]]
57         for yr in np.arange(1,project_life+1, 1):
58             BOOKVAL.append(sum(CAPEX[:yr+1]) - sum(DEP[:yr+1]) )
59
60         #calculate tax benefit of depreciation / write-off at end of project
61         TAXBEN = [0]
62         for yr in np.arange(1,project_life, 1):
63             TAXBEN.append(DEP[yr]*rate_tax)
64             TAXBEN.append((BOOKVAL[-1]+DEP[-1])*rate_tax)
65
66         #calculate OPEX due to maintenance
67         OPEX_maint = [0]
68         for yr in np.arange(1,project_life+1, 1):
69             OPEX_maint.append(365 * d_n_km.sum() * price_maint_ev)
70
71         #calculate OPEX cost of electricity
72         #cost is electricity consumption + demand charge
73         OPEX_elect = [0]
74         for yr in np.arange(1,project_life+1, 1):
75             OPEX_elect.append(365 * P_req_b * price_elect + 12*demand_charge*n_chargers*charger_P/number_of_trucks)
76

```

```

77
78     # Consolidate into dataframe
79     fin_b = pd.DataFrame(index=np.arange(0,project_life+1, 1))
80     fin_b['X(t), kW.hrs'] = X_t
81     fin_b['CAPEX'] = CAPEX
82     fin_b['Depreciation'] = DEP
83     fin_b['Book Value'] = BOOKVAL
84     fin_b['Tax Benefit'] = TAXBEN
85     fin_b['OPEX, Maintenance'] = OPEX_maint
86     fin_b['OPEX, Electricity'] = OPEX_elect
87     fin_b['Cost'] = fin_b['CAPEX'] + fin_b['OPEX, Maintenance'] + fin_b['OPEX, Electricity'] - fin_b['Tax Benefit']
88
89     for i in fin_b.index.tolist():
90         fin_b.at[i, 'Cost, PV'] = fin_b.at[i, 'Cost'] / ((1+wacc)**i)
91         if i == 0:
92             fin_b.at[i, 'TCO, net'] = fin_b.at[i, 'Cost, PV']
93         else:
94             fin_b.at[i, 'TCO, net'] = fin_b.at[i-1, 'TCO, net'] + fin_b.at[i, 'Cost, PV']
95
96     TCOs.append(fin_b.at[project_life, 'TCO, net'])
97     fin_b.to_csv(filepath+'tco_case#_'+str(case_num)+'.csv')
98     case_num+=1
99     TCO_list_of_lists.append(TCOs)
100
101
102
103 print('done')

```

done

```

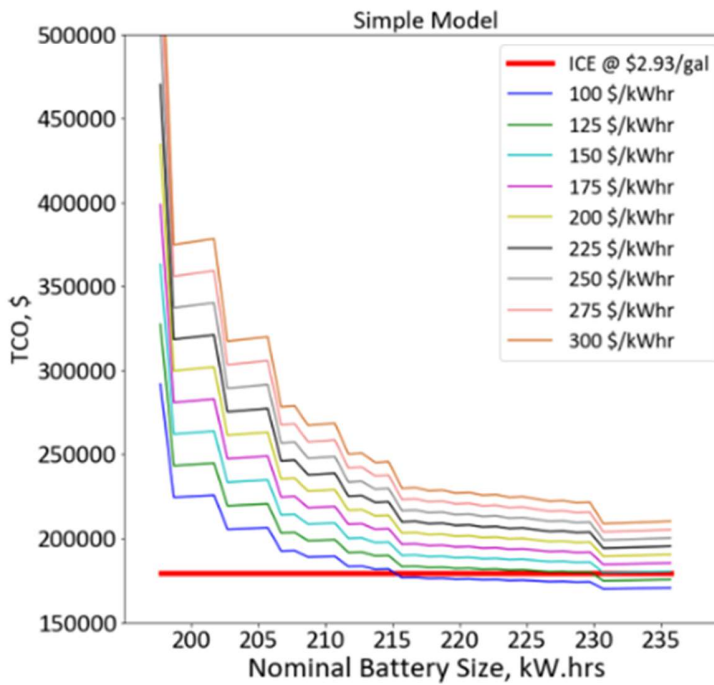
In [82]: M
1 figure = plt.figure(figsize=(10,10))
2 ax = figure.add_subplot(111)
3 plt.rcParams["font.family"] = "calibri"
4
5 TCO_ice = []
6 for i in battery_sizes:
7     TCO_ice.append(tco_ice)
8
9 ax.plot(battery_sizes,TCO_ice, color=colors[0], label = 'ICE @ $2.93/gal', linewidth=5 )
10 for x in range(0, len(TCO_list_of_lists)):
11     TCOs = TCO_list_of_lists[x]
12     ax.plot(battery_sizes, TCOs, color= colors[x+1], label=(str(price_battery[x])+' $/kWhr'))
13
14 ax.set_title('Simple Model', fontsize=24)
15 ax.set_ylim(150000,500000)
16 #ax.set_xlim(1800,2000)
17 ax.set_xlabel('Nominal Battery Size, kW.hrs', fontsize=24)
18 ax.set_ylabel('TCO, $', fontsize = 24)
19 ax.tick_params(labelsize=24)
20 ax.legend(fontsize=20)
21 #ax.set_xlim(0,241)
22 ax.set_xlim(195,248)
23 ax.set_xticks(np.arange(200,236,5))

```

```

Out[82]: [<matplotlib.axis.XTick at 0x1de38b1f588>,
<matplotlib.axis.XTick at 0x1de389ece08>,
<matplotlib.axis.XTick at 0x1de38b1f7c8>,
<matplotlib.axis.XTick at 0x1de38732cc8>,
<matplotlib.axis.XTick at 0x1de38732948>,
<matplotlib.axis.XTick at 0x1de38757888>,
<matplotlib.axis.XTick at 0x1de387303c8>,
<matplotlib.axis.XTick at 0x1de38730e88>]

```



Calculate TCO for EV: Complex Battery Degradation Model

Calculate Minimum Battery Size

```
n [83]: M
1 # Guess Battery Size
2 m_b_guess = 2000
3
4 # iterate until calculated battery mass is within 0.01% of guessed battery size
5 check = False
6 count = 0
7
8 while check == False and count < 100:
9
10     m_n = payload_n + mass_truck + m_b_guess
11
12     F_acc = 0.5*rho_air*C_d*A_cab*a*x_acc_n + m_n*a + C_r*m_n*g + m_n*g*np.sin(theta)
13     F_ss = 0.5*rho_air*C_d*A_cab*(v_n**2) + m_n*g*(C_r + np.sin(theta))
14
15     P_acc = np.dot(F_acc, x_acc_n)
16     P_ss = np.dot(F_ss, x_ss_n)
17
18     P_req = (P_acc + P_ss)*(1/E_d_ev)*(1/1000)*(1/3600)*(1/beta)
19
20     m_b_req = P_req / ED_b
21
22     err = np.abs(m_b_guess - m_b_req)/m_b_req
23     if err <= 0.0001:
24         check = True
25     else:
26         m_b_guess = m_b_req
27
28
29     count+=1
30
31 print('Required Battery Rating: ', round(P_req, 1), ' kW.hrs')
32 print('Required Battery Mass: ', round(m_b_guess, 0), ' kg')
33
```

Required Battery Rating: 179.7 kW.hrs

Required Battery Mass: 1797.0 kg

Calculate Economics for a Variety of Battery Sizes

```
[4]: M 1 filepath= 'C:/Users/gturm/Dropbox/Haas/Spring 2020/Systems Control/Project/model runs/'
2
3 battery_min = 1.10 * P_req
4 # battery + truck chassis + payload cannot exceed Class 6 weight limits
5 battery_max = (max_weight - payload_n.max() - mass_truck)*ED_b
6 battery_sizes = np.arange(battery_min, battery_max, 1)
7 #battery_sizes = [170.8*1.15]
8 case_num = 1
9 TCO_list_of_lists=[]
10
11 for p in price_battery:
12     TCOs = []
13     for b in battery_sizes:
14
15         #calculate P_req_b for battery size
16         m_n = payload_n + mass_truck + b / ED_b
17         F_acc = 0.5*rho_air*C_d*A_cab*a*x_acc_n + m_n*a + C_r*m_n*g + m_n*g*np.sin(theta)
18         F_ss = 0.5*rho_air*C_d*A_cab*(v_n**2) + m_n*g*(C_r + np.sin(theta))
19         P_acc = np.dot(F_acc, x_acc_n)
20         P_ss = np.dot(F_ss, x_ss_n)
21         P_req_b = (P_acc + P_ss) *(1/E_d_ev) * (1/1000) * (1/3600) * (1/beta)
22
23         #iterate through years to determine CAPEX requirements
24         #initial capex is cost of chassis + battery + chargers
25         CAPEX = [round((price_chassis + b*p + n_chargers*price_charger/number_of_trucks),2)]
26         #track battery capacities through the years
27         X_t = [b]
28         #calculate Depth_of_Discharge
29         DoD = P_req_b / b
30         #age_battery will track the age of the battery through replacement cycles
31         age_battery = 0
32         # calculate replacement capacity
33         X_replace = P_req_b / beta
34
35         for yr in np.arange(1,project_life+1, 1):
36             X_yr_end = b * battery_degradation(DoD, (age_battery+1))
37             # Determine if battery must be replaced
38             if X_yr_end <= X_replace:
39                 CAPEX.append(round(b*p,2))
40                 age_battery = 0
41                 X_t.append(round(b,2))
42             else:
43                 CAPEX.append(0)
44                 age_battery+=1
45                 X_t.append(round(X_yr_end,2))
46
47         #calculate depreciation assuming 5 yr straight line
48         DEP = [0]
49         for yr in np.arange(1,project_life+1, 1):
50             d_t = 0
51             for z in range(1,min(6, yr+1)):
52                 d_t += 0.2 * CAPEX[yr-z]
53             DEP.append(d_t)
54
55         #calculate book value(t)
56         BOOKVAL = [CAPEX[0]]
57         for yr in np.arange(1,project_life+1, 1):
58             BOOKVAL.append(sum(CAPEX[:yr+1]) - sum(DEP[:yr+1]) )
59
60         #calculate tax benefit of depreciation / write-off at end of project
61         TAXBEN = [0]
62         for yr in np.arange(1,project_life, 1):
63             TAXBEN.append(DEP[yr]*rate_tax)
64             TAXBEN.append((BOOKVAL[-1]+DEP[-1])*rate_tax)
65
66         #calculate OPEX due to maintenance
67         OPEX_maint = [0]
68         for yr in np.arange(1,project_life+1, 1):
69             OPEX_maint.append(365 * d_n_kn.sum() * price_maint_ev)
70
71         #calculate OPEX cost of electricity
72         #cost is electricity consumption + demand charge
73         OPEX_elect = [0]
74         for yr in np.arange(1,project_life+1, 1):
75             OPEX_elect.append(365 * P_req_b * price_elect + 12*demand_charge*n_chargers*charger_P/number_of_trucks)
```

```

77
78
79     # Consolidate intp dataframe
80     fin_b = pd.DataFrame(index=np.arange(0,project_life+1, 1))
81     fin_b['X(t), kW.hrs'] = X_t
82     fin_b['CAPEX'] = CAPEX
83     fin_b['Depreciation'] = DEP
84     fin_b['Book Value'] = BOOKVAL
85     fin_b['Tax Benefit'] = TAXBEN
86     fin_b['OPEX, Maintenance'] = OPEX_maint
87     fin_b['OPEX, Electricity'] = OPEX_elect
88     fin_b['Cost'] = fin_b['CAPEX'] + fin_b['OPEX, Maintenance'] + fin_b['OPEX, Electricity'] - fin_b['Tax Benefit']
89
90     for i in fin_b.index.tolist():
91         fin_b.at[i, 'Cost, PV'] = fin_b.at[i, 'Cost'] / ((1+wacc)**i)
92         if i == 0:
93             fin_b.at[i, 'TCO, net'] = fin_b.at[i, 'Cost, PV']
94         else:
95             fin_b.at[i, 'TCO, net'] = fin_b.at[i-1, 'TCO, net'] + fin_b.at[i, 'Cost, PV']
96
97     TCOs.append(fin_b.at[project_life, 'TCO, net'])
98     fin_b.to_csv(filepath+'tco_case#_'+str(case_num)+'.csv')
99     case_num+=1
100 TCO_list_of_lists.append(TCOs)
101
102
103
104 print('done')

```

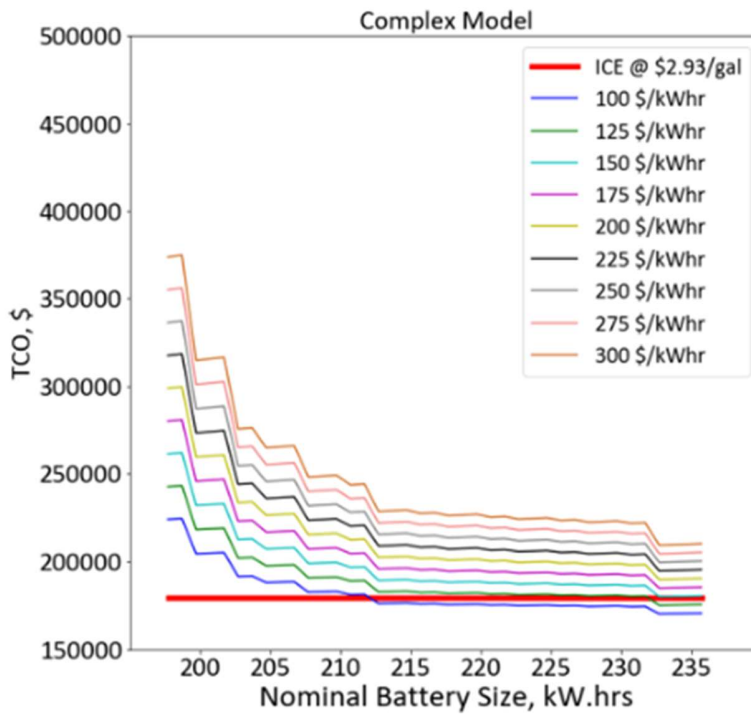
done

```

[85]: M
  1 figure = plt.figure(figsize=(10,10))
  2 ax = figure.add_subplot(111)
  3 plt.rcParams["font.family"] = "calibri"
  4
  5 TCO_ice = []
  6 for i in battery_sizes:
  7     TCO_ice.append(tco_ice)
  8
  9 ax.plot(battery_sizes,TCO_ice, color=colors[0], label = 'ICE @ $2.93/gal', linewidth=5 )
10 for x in range(0, len(TCO_list_of_lists)):
11     TCOs = TCO_list_of_lists[x]
12     ax.plot(battery_sizes, TCOs, color= colors[x+1], label=(str(price_battery[x])+' $/kWhr'))
13
14 ax.set_title('Complex Model', fontsize=24)
15 ax.set_xlim(150000,500000)
16 #ax.set_xlim(1000,2000)
17 ax.set_xlabel('Nominal Battery Size, kW.hrs', fontsize=28)
18 ax.set_ylabel('TCO, $', fontsize = 24)
19 ax.tick_params(labelsize=24)
20 ax.legend(fontsize=20)
21 #ax.set_xlim(0,24.1)
22 ax.set_xlim(195,248)
23 ax.set_xticks(np.arange(200,236,5))

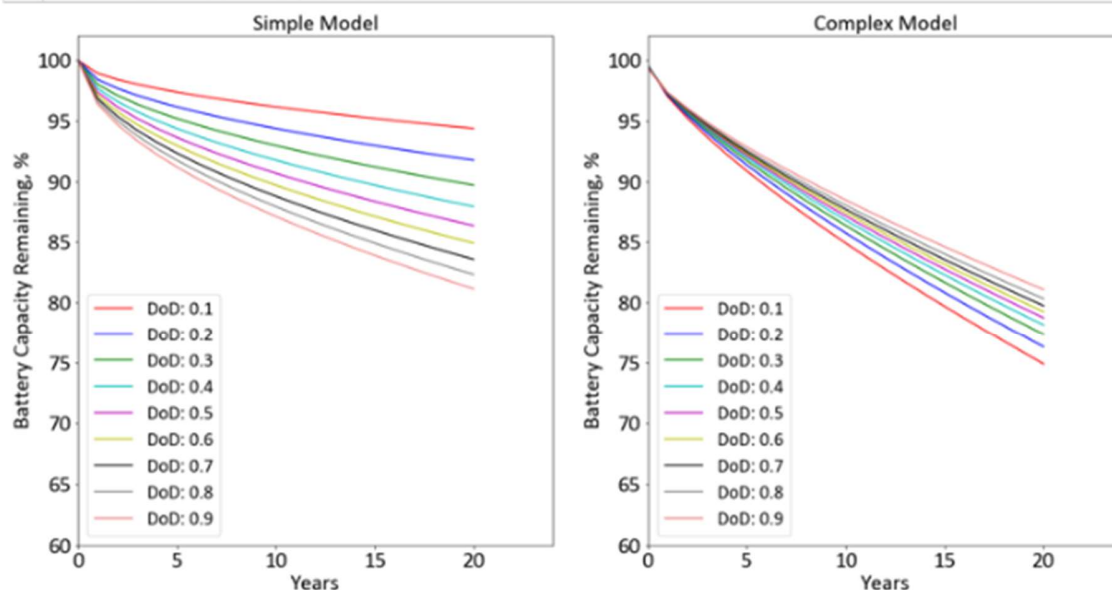
```

Out[85]: [`<matplotlib.axis.XTick at 0x1de38991ec8>`, `<matplotlib.axis.XTick at 0x1de390ecd08>`, `<matplotlib.axis.XTick at 0x1de3898d108>`, `<matplotlib.axis.XTick at 0x1de3930a188>`, `<matplotlib.axis.XTick at 0x1de3930a7c8>`, `<matplotlib.axis.XTick at 0x1de3930f2c8>`, `<matplotlib.axis.XTick at 0x1de3930fd48>`, `<matplotlib.axis.XTick at 0x1de39313848>`]



Compare Battery Degradation Models

```
[]: M
  1 k_deg = 0.15
  2 yrs = np.arange(0,21,1)
  3 dods = np.arange(0.1,1,0.1)
  4 simple = []
  5 robust = []
  6
  7 for dod in dods:
  8     s = []
  9     r = []
 10    for y in yrs:
 11        s.append(deg(100, 365*y, dod))
 12        r.append(100*battery_degradation(dod, y))
 13    simple.append(s)
 14    robust.append(r)
 15
 16 figure = plt.figure(figsize=(20,10))
 17 plt.rcParams["font.family"] = "calibri"
 18 ax1 = figure.add_subplot(121)
 19 ax2 = figure.add_subplot(122)
 20
 21 for x in range(0, len(dods)):
 22     dod = dods[x]
 23     s = simple[x]
 24     r = robust[x]
 25     ax1.plot(yrs, s, color = colors[x], label="DoD: "+str(round(dod,1)))
 26     ax2.plot(yrs, r, color = colors[x], label="DoD: "+str(round(dod,1)))
 27
 28 ax1.set_title('Simple Model', fontsize = 24)
 29 ax2.set_title('Complex Model', fontsize = 24)
 30 for ax in (ax1, ax2):
 31     ax.set_ylim(60,102)
 32     ax.set_xlim(0,24)
 33     ax.set_xlabel('Years', fontsize=24)
 34     ax.set_ylabel('Battery Capacity Remaining, %', fontsize = 24)
 35     ax.tick_params(labelsize=24)
 36     ax.legend(fontsize=20, loc='lower left')
 37     ax.set_xticks(np.arange(0,24,5))
 38     ax.set_yticks(np.arange(60,101,5))
```



Appendix F - Python Code (Sensitivity Analysis)

```
In [1]: 1 import numpy as np
2 import pandas as pd
3 from matplotlib import pyplot as plt
4
5 %matplotlib inline
6 colors = ['r', 'b', 'g', 'c', 'm', 'y', 'k', 'grey', 'lightcoral', 'chocolate', 'orange', 'gold', 'lime', 'teal', 'deepslategray']
7
8
9
10
11
12
13
14
15
16
17
18
19
20
21
```

Constant Variables

```
In [2]: 1 mass_truck = 4250      # mass of truck chassis and cab (excludes engine and battery)
2 mass_engine = 1200/2.2    # engine weighs 1200 Lbs
3 rho_air = 1.22          # air density in kg/m3
4 C_d = 0.75              # coefficient of drag
5 A_cab = 7                # truck cab frontal surface area, m2
6 C_r = 0.015             # coefficient of rolling resistance
7 g = 9.8                 # gravitational constant
8 E_d_ev = 0.83           # aggregate efficiency of EV drivetrain
9 E_d_ice = 0.36           # aggregate efficiency of ICE drivetrain
10 ED_b = 0.1               # battery energy desnity, kW.hr/kg
11 ED_diesel = 38          # kJ.hrs/gal of diesel, based on Lower Heating Value
12 beta = 0.95              # safety factor - replace battery when the route depletes 95% of its capacity
13 a = 0.448                # constant acceleration in m/s^2
14 k_deg = 0.15             # for battery degradation model
15 max_weight = 11793.4     # max weight of class 6 truck
16
17 project_life = 15        # years
18 price_maint_ev = 0.022   # cost of maintenance for EV, $/km
19 price_maint_ice = 0.045   # cost of maintenance for ICE, $/km
20 rate_tax = 0.21           # tax rate, fraction
21 price_chassis = 91000     # cost of ICE truck. Assumed an EV pays the same price for just the chassis + cab
```

Battery Degradation Model

```
In [3]: M
1 ## complicated model
2 p_0 = 3.4707;
3 p_1 = 1.6112;
4 p_2 = -2.6287;
5 p_3 = 1.7175;
6 z_vec = np.linspace(0,1,24)
7 OCV = lambda z_vec: p_0 + p_1*z_vec + p_2*z_vec**2 + p_3*z_vec**3
8
9 temp_data = pd.read_csv('C:/Users/gturm/Dropbox/Haas/Spring 2020/Systems Control/Project/2107761.csv')
10 temp_data = temp_data.loc[:,['DATE','HLY-TEMP-NORMAL']].groupby('DATE').mean().reset_index()
11 temp_data['HLY-TEMP-NORMAL'] = temp_data['HLY-TEMP-NORMAL']+273.15
12 temp_data = temp_data.iloc[23:].reset_index(drop=True)
13
14 idx=[]
15 hours_of_work = 9 #hours daily
16 for i in 6*np.arange(1,len(temp_data)/6,4,dtype=int):
17     idx.append(list(range(i,i*hours_of_work+1)))
18 idx = np.ndarray.flatten(np.array(idx)).astype(int).tolist()
19 temp_data = temp_data[temp_data.index.isin(idx)].reset_index()
20 T = temp_data['HLY-TEMP-NORMAL']
21
22
23
24 def battery_degradation(DoD,number_of_years):
25
26
27
28 SOC = np.linspace(1,1-DoD,hours_of_work)
29
30 V = list(OCV(SOC))
31 V.insert(0,4.2)
32 V1 = [V for i in range(52*7)]
33 V1 = np.ndarray.flatten(np.array(V1)).astype(float).tolist()
34 #temp_data['V'] = V1
35 Q = 2.15 #Ah
36
37 def alpha_cap(V,T):
38     alpha = (7.543*np.array(V)-23.75)*10**6*np.exp(-6976/np.array(T))
39     return np.mean(alpha)
40
41 def beta_cap(V,DoD):
42     return np.mean(7.346*10**(-3)*(np.mean(V)-3.667)**2 + 7.6*10**(-4) + 4.081*10**(-3)*DoD)
43
44 capacity_left = 1 - alpha_cap(V1,T)*(365*number_of_years)**0.75 - beta_cap(V1,DoD)*np.sqrt(Q)
45
46 return capacity_left
```

Define Route

```
In [4]: 1 # distances of each segment
2 # defined in km and converted to m
3 d_n_km = np.array([3.06, 5.21, 5.47, 3.86, 50.05, 21.73, 60.51, 14.16, 38.62])
4 d_n = d_n_km*1000
5
6 # average/constant velocities of each segment
7 # defined in km/hr and converted to m/s
8 v_n_kmph = np.array([30, 40, 30, 30, 85, 70, 65, 65, 85])
9 v_n = v_n_kmph*1000/3600
10 # calculate x_acc for each segment
11 x_acc_n = (v_n**2)*0.5*(1/a)
12 x_ss_n = d_n - x_acc_n
13
14 # Payload of each segment
15 payload_n = np.array([5184, 4536, 3888, 3240, 2592, 1944, 1296, 648, 0])
16
17 # grade of each segment
18 # converted to theta, in degrees
19 grade_n = np.array([0, 0, 0, 2.7, 0.6, 0.5, -0.7, -0.12, -0.26])
20 theta = np.arctan(grade_n/100)
```

Define battery sizes to consider

```
In [17]: 1 # calculate minimum battery size
2 # Guess Battery Size
3 m_b_guess = 2000
4 # iterate until calculated battery mass is within 0.01% of guessed battery size
5 check = False
6 count = 0
7 while check == False and count < 100:
8     m_n = payload_n + mass_truck + m_b_guess
9     F_acc = 0.5*rho_air*c_d*A_cab*a*x_acc_n + m_n*a + C_r*m_n*g + m_n*g*np.sin(theta)
10    F_ss = 0.5*rho_air*c_d*A_cab*(v_n**2) + m_n*g*(C_r + np.sin(theta))
11    P_acc = np.dot(F_acc, x_acc_n)
12    P_ss = np.dot(F_ss, x_ss_n)
13    P_req = (P_acc + P_ss)*(1/E_d_ev) * (1/1000) * (1/3600) * (1/beta)
14    m_b_req = P_req / ED_b
15    err = np.abs(m_b_guess - m_b_req)/m_b_req
16    if err <= 0.0001:
17        check = True
18    else:
19        m_b_guess = m_b_req
20    count+=1
21
22 print('Required Battery Rating: ', round(P_req, 1), ' kw.hrs')
23 print('Required Battery Mass: ', round(m_b_guess,0), ' kg')
24
25 battery_min = 1.10 * P_req
26 battery_max = (max_weight - payload_n.max() - mass_truck)*ED_b
27 battery_sizes = np.arange(round(battery_min,0), round(battery_max,0), 1)
28 print(battery_sizes)
```

Required Battery Rating: 179.7 kw.hrs
Required Battery Mass: 1797.0 kg
[198. 199. 200. 201. 202. 203. 204. 205. 206. 207. 208. 209. 210. 211.
212. 213. 214. 215. 216. 217. 218. 219. 220. 221. 222. 223. 224. 225.
226. 227. 228. 229. 230. 231. 232. 233. 234. 235.]

Function to calculate TCO of ICE

```
In [6]: def calc_tco_ice(p_diesel, r):
    wacc = r
    price_diesel = p_diesel

    # Calculate energy consumption per day
    m_n = payload_n + mass_truck + mass_engine
    F_acc = 0.5*rho_air*C_d*A_cab*a*x_acc_n + m_n*a + C_r*m_n*g + m_n*g*np.sin(theta)
    F_ss = 0.5*rho_air*C_d*A_cab*(v_n**2) + m_n*g*(C_r + np.sin(theta))
    P_acc = np.dot(F_acc, x_acc_n)
    P_ss = np.dot(F_ss, x_ss_n)
    P_req_ice = (P_acc + P_ss) * (1/E_d_ice) * (1/1000) * (1/3600)

    # initial capex is cost of chassis. all other years = 0
    CAPEX = [round((price_chassis),2)]
    for yr in np.arange(1,project_life+1, 1):
        CAPEX.append(0)
    #calculate depreciation assuming 5 yr straight Line
    DEP = [0]
    for yr in np.arange(1,project_life+1, 1):
        d_t = 0
        for z in range(1,min(6, yr+1)):
            d_t += 0.2 * CAPEX[yr-z]
        DEP.append(d_t)
    #calculate book value(t)
    BOOKVAL = [CAPEX[0]]
    for yr in np.arange(1,project_life+1, 1):
        BOOKVAL.append(sum(CAPEX[:yr+1]) - sum(DEP[:yr+1]))
    #calculate tax benefit of depreciation / write-off at end of project
    TAXBEN = [0]
    for yr in np.arange(1,project_life, 1):
        TAXBEN.append(DEP[yr]*rate_tax)
    TAXBEN.append((BOOKVAL[-1]*DEP[-1])*rate_tax)
    #calculate OPEX due to maintenance
    OPEX_maint = [0]
    for yr in np.arange(1,project_life+1, 1):
        OPEX_maint.append(365 * d_n_km.sum() * price_maint_ice)
    #calculate OPEX cost of electricity
    OPEX_elect = [0]
    for yr in np.arange(1,project_life+1, 1):
        OPEX_elect.append(365 * P_req_ice * (1/ED_diesel) * price_diesel)
    # Consolidate into dataframe
    fin_b = pd.DataFrame(index=np.arange(0,project_life+1, 1))
    fin_b['CAPEX'] = CAPEX
    fin_b['Depreciation'] = DEP
    fin_b['Book Value'] = BOOKVAL
    fin_b['Tax Benefit'] = TAXBEN
    fin_b['OPEX, Maintenance'] = OPEX_maint
    fin_b['OPEX, Electricity'] = OPEX_elect
    fin_b['Cost'] = fin_b['CAPEX'] + fin_b['OPEX, Maintenance'] + fin_b['OPEX, Electricity'] - fin_b['Tax Benefit']
    for i in fin_b.index.tolist():
        fin_b.at[i, 'Cost, PV'] = fin_b.at[i, 'Cost'] / ((1+wacc)**i)
        if i == 0:
            fin_b.at[i, 'TCO, net'] = fin_b.at[i, 'Cost, PV']
        else:
            fin_b.at[i, 'TCO, net'] = fin_b.at[i-1, 'TCO, net'] + fin_b.at[i, 'Cost, PV']

    tco_ice = fin_b.at[project_life, 'TCO, net']

    return tco_ice
```

Function to calculate optimal TCO of EV, given some input conditions

```

18: M 1 def calc_tco_ev(p_elect, p_bat):
2     # define local variables
3     wacc = r
4     price_elect = p_elect
5     price_battery = p_bat
6
7     # need to iterate over acceptable range of battery sizes, and select lowest TCO
8     tcos = []
9     for b in battery_sizes:
10        #calculate P_req_b for battery size
11        m_n = payload_n * mass_truck * b / ED_b
12        F_acc = 0.5*rho_air*C_d*A_cab*a*x_acc_n + n_n*a + C_r*m_n*g + m_n*g*np.sin(theta)
13        F_ss = 0.5*rho_air*C_d*A_cab*(v_n**2) + n_n*g*(C_r + np.sin(theta))
14        P_acc = np.dot(F_acc, x_acc_n)
15        P_ss = np.dot(F_ss, x_ss_n)
16        P_req_b = (P_acc + P_ss)*(1/E_d_ev) * (1/1000) * (1/3600) * (1/beta)
17
18        #iterate through years to determine CAPEX requirements
19        #initial capex is cost of chassis + battery
20        CAPEX = [round((price_chassis + b*price_battery),2)]
21        #track battery capacities through the years
22        X_t = [b]
23        #calculate Depth_of_Discharge
24        DoD = P_req_b / b
25        # age_battery will track the age of the battery through replacement cycles
26        age_battery = 0
27        # calculate replacement capacity
28        X_replace = P_req_b / beta
29
30        for yr in np.arange(1,project_life+1, 1):
31            X_yr_end = b * battery_degradation(DoD, (age_battery+1))
32            # Determine if battery must be replaced
33            if X_yr_end < X_replace:
34                CAPEX.append(round((price_battery),2))
35                age_battery = 0
36                X_t.append(round(b,2))
37            else:
38                CAPEX.append(0)
39                age_battery+=1
40                X_t.append(round(X_yr_end,2))
41
42        #calculate depreciation assuming 5 yr straight line
43        DEP = [0]
44        for yr in np.arange(1,project_life+1, 1):
45            d_t = 0
46            for z in range(1,min(6, yr+1)):
47                d_t += 0.2 * CAPEX[yr-z]
48            DEP.append(d_t)
49
50        #calculate book value(t)
51        BOOKVAL = [CAPEX[0]]
52        for yr in np.arange(1,project_life+1, 1):
53            BOOKVAL.append(sum(CAPEX[:yr+1]) - sum(DEP[:yr+1]))
54
55        #calculate tax benefit of depreciation / write-off at end of project
56        TAXBEN = [0]
57        for yr in np.arange(1,project_life, 1):
58            TAXBEN.append(DEP[yr]*rate_tax)
59        TAXBEN.append((BOOKVAL[-1]+DEP[-1])*rate_tax)
60
61        #calculate OPEX due to maintenance
62        OPEX_maint = [0]
63        for yr in np.arange(1,project_life+1, 1):
64            OPEX_maint.append(365 * d_n_km.sum() * price_maint_ev)
65
66        #calculate OPEX cost of electricity
67        OPEX_elect = [0]
68        for yr in np.arange(1,project_life+1, 1):
69            OPEX_elect.append(365 * P_req_b * price_elect)
70
71        # Consolidate into DataFrame
72        fin_b = pd.DataFrame(index=np.arange(0,project_life+1, 1))
73        fin_b['X(t, Kw.hrs)'] = X_t
74        fin_b['CAPEX'] = CAPEX
75        fin_b['Depreciation'] = DEP
76        fin_b['Book Value'] = BOOKVAL
77        fin_b['Tax Benefit'] = TAXBEN
78        fin_b['OPEX, Maintenance'] = OPEX_maint
79        fin_b['OPEX, Electricity'] = OPEX_elect
80        fin_b['Cost'] = fin_b['CAPEX'] + fin_b['OPEX, Maintenance'] + fin_b['OPEX, Electricity'] - fin_b['Tax Benefit']
81
82        for i in fin_b.index.tolist():
83            fin_b.at[i, 'Cost, PV'] = fin_b.at[i, 'Cost'] / ((1+wacc)**i)
84            if i == 0:
85                fin_b.at[i, 'TCO, net'] = fin_b.at[i, 'Cost, PV']
86            else:
87                fin_b.at[i, 'TCO, net'] = fin_b.at[i-1, 'TCO, net'] + fin_b.at[i, 'Cost, PV']
88
89        tcos.append(fin_b.at[project_life, 'TCO, net'])
90
91        #determine min tco, and battery size
92        tco_star = tcos[0]
93        battery_size_star = battery_sizes[0]
94        for x in range(1, len(battery_sizes)):
95            if tcos[x] < tco_star:
96                tco_star = tcos[x]
97                battery_size_star = battery_sizes[x]
98
99    return tco_star, battery_size_star

```

Sensitivity Analysis: Battery Breakeven Price

```
|: M 1 d_ps = np.arange(2.0,4.01, 0.1)
2 e_ps = np.arange(0.02, 0.21, 0.02)
3
4 #clean into rounded numbers
5 diesel_prices = []
6 elect_prices = []
7 for x in range(0,len(d_ps)):
8     diesel_prices.append(round(d_ps[x],2))
9 for x in range(0, len(e_ps)):
10    elect_prices.append(round(e_ps[x],2))
11
12
13 sens_bat_price = pd.DataFrame(index=elect_prices, columns=diesel_prices)
14
15 wacc = 0.10
16 count = 1
17
18 for e in elect_prices:
19     for d in diesel_prices:
20
21         print(count)
22         count += 1
23         # update sensitivity variables
24         price_elect = e
25         price_diesel = d
26
27         # calculate TCO_ice
28         tco_ice = calc_tco_ice(d, wacc)
29
30         # iterate on battery prices until tco_ev = tco_ice
31         p_guess = 400
32         check = False
33         while check == False:
34             tco_ev, bat_cap = calc_tco_ev(wacc, e, p_guess)
35             if abs(tco_ev-tco_ice)/tco_ice <= 0.001:
36                 check = True
37             else:
38                 tco_ev_alpha, batcap = calc_tco_ev(wacc, e, p_guess-1)
39                 m = (tco_ev - tco_ev_alpha)
40                 b = tco_ev - m*p_guess
41                 p_guess = (tco_ice - b)/m
42
43         sens_bat_price.at[e, d] = p_guess
44
45 print('done')
```

Sensitivity Analysis: IRR

```
42]: M 1 d_ps = np.arange(2.0,4.01, 0.1)
2 e_ps = np.arange(0.02, 0.21, 0.02)
3
4 #clean into rounded numbers
5 diesel_prices = []
6 elect_prices = []
7 for x in range(0,len(d_ps)):
8     diesel_prices.append(round(d_ps[x],2))
9 for x in range(0, len(e_ps)):
10    elect_prices.append(round(e_ps[x],2))
11
12
13 sens_irr = pd.DataFrame(index=elect_prices, columns=diesel_prices)
14
15 price_battery = 175
16 count = 1
17
18 for e in elect_prices:
19     for d in diesel_prices:
20
21         print(count)
22         count += 1
23         # update sensitivity variables
24         price_elect = e
25         price_diesel = d
26
27         # iterate on battery prices until tco_ev = tco_ice
28         r_guess = 0.20
29         check = False
30         bail = False
31         while check == False and bail == False:
32             # calculate TCO_ice
33             tco_ice = calc_tco_ice(d, r_guess)
34             #calculate TCO_ev
35             tco_ev, bat_cap = calc_tco_ev(r_guess, e, price_battery)
36
37             #print progress, if desired
38             #print(d, e, tco_ice, tco_ev, r_guess)
39
40             #check for convergence
41             if abs(tco_ev-tco_ice)/tco_ice <= 0.001:
42                 check = True
43             # update wacc based on slope
44             else:
45                 tco_ev_alpha, batcap = calc_tco_ev(r_guess-0.002, e, price_battery)
46                 tco_ice_alpha = calc_tco_ice(d, r_guess-0.002)
47                 delta = tco_ev - tco_ice
48                 delta_alpha = tco_ev_alpha - tco_ice_alpha
49                 m = (delta - delta_alpha)/(0.002)
50                 b = delta - m*r_guess
51                 r_guess = -b/m
52
53                 if abs(r_guess) > 10:
54                     bail = True
55
56             if check == True:
57                 sens_irr.at[e, d] = r_guess
58             else:
59                 sens_irr.at[e, d] = 'BAD'
60
61 print('done')
```

Appendix G - Sensitivity Analysis Results

Sensitivity Analysis: Break-even Battery Unit Price, at WACC=10%												
Diesel Price, \$/kW.hr												
Electricity Price, \$/kW.hr	\$ 2.00	\$ 2.10	\$ 2.20	\$ 2.30	\$ 2.40	\$ 2.50	\$ 2.60	\$ 2.70	\$ 2.80	\$ 2.90	\$ 3.00	\$ 3.10
\$ 0.02	\$ 284.9	\$ 298.5	\$ 312.1	\$ 325.6	\$ 339.2	\$ 352.8	\$ 366.4	\$ 379.9	\$ 393.5	\$ 407.1	\$ 420.6	\$ 434.2
\$ 0.04	\$ 232.4	\$ 245.9	\$ 259.5	\$ 273.1	\$ 286.6	\$ 300.2	\$ 313.8	\$ 327.4	\$ 340.9	\$ 354.5	\$ 368.1	\$ 381.6
\$ 0.06	\$ 179.8	\$ 193.3	\$ 206.9	\$ 220.5	\$ 234.1	\$ 247.6	\$ 261.2	\$ 274.8	\$ 288.4	\$ 301.9	\$ 315.5	\$ 329.1
\$ 0.08	\$ 127.2	\$ 140.8	\$ 154.3	\$ 167.9	\$ 181.5	\$ 195.1	\$ 208.6	\$ 222.2	\$ 235.8	\$ 249.4	\$ 262.9	\$ 276.5
\$ 0.10	\$ 74.6	\$ 88.2	\$ 101.8	\$ 115.3	\$ 128.9	\$ 142.5	\$ 156.1	\$ 169.6	\$ 183.2	\$ 196.8	\$ 210.3	\$ 223.9
\$ 0.12	\$ 22.1	\$ 35.6	\$ 49.2	\$ 62.8	\$ 76.3	\$ 89.9	\$ 103.5	\$ 117.1	\$ 130.6	\$ 144.2	\$ 157.8	\$ 171.3
\$ 0.14	\$ (6.0)	\$ (2.5)	\$ 1.1	\$ 10.2	\$ 23.8	\$ 37.3	\$ 50.9	\$ 64.5	\$ 78.1	\$ 91.6	\$ 105.2	\$ 118.8
\$ 0.16	\$ (19.5)	\$ (15.9)	\$ (12.4)	\$ (8.9)	\$ (5.3)	\$ (1.8)	\$ 2.6	\$ 11.9	\$ 25.5	\$ 39.1	\$ 52.6	\$ 66.2
\$ 0.18	\$ (32.9)	\$ (29.4)	\$ (25.8)	\$ (22.3)	\$ (18.7)	\$ (15.2)	\$ (11.7)	\$ (8.1)	\$ (4.6)	\$ (1.0)	\$ 3.9	\$ 13.6
\$ 0.20	\$ (46.3)	\$ (42.8)	\$ (39.2)	\$ (35.7)	\$ (32.2)	\$ (28.6)	\$ (25.1)	\$ (21.6)	\$ (18.0)	\$ (14.5)	\$ (11.0)	\$ (7.4)

Sensitivity Analysis: IRR, at Battery Price of \$175/kW.hr												
Electricity Price, \$/kW.hr	\$ 2.00	\$ 2.10	\$ 2.20	\$ 2.30	\$ 2.40	\$ 2.50	\$ 2.60	\$ 2.70	\$ 2.80	\$ 2.90	\$ 3.00	\$ 3.10
\$ 0.02	19.1%	20.2%	21.1%	22.2%	23.2%	24.2%	25.2%	26.1%	27.0%	28.1%	29.0%	30.1%
\$ 0.04	14.9%	16.1%	17.2%	18.2%	19.3%	20.3%	21.3%	22.3%	23.3%	24.3%	25.3%	26.3%
\$ 0.06	10.4%	11.6%	12.8%	14.0%	15.1%	16.2%	17.3%	18.3%	19.4%	20.4%	21.4%	22.5%
\$ 0.08	5.3%	6.7%	8.0%	9.3%	10.6%	11.8%	13.0%	14.1%	15.2%	16.3%	17.4%	18.4%
\$ 0.10	-1.2%	0.6%	2.4%	3.9%	5.4%	6.8%	8.2%	9.4%	10.7%	12.0%	13.1%	14.2%
\$ 0.12	-17.5%	-8.3%	-5.4%	-3.1%	-1.0%	0.9%	2.6%	4.1%	5.6%	7.0%	8.4%	9.6%
\$ 0.14	N/A											
\$ 0.16	N/A											
\$ 0.18	N/A											
\$ 0.20	N/A											

Acknowledgement

We would like to thank Professor Scott Moura and Dr. Andrej Ivanco from Allison Transmission for all of their guidance and advice on this project. The team also thanks our GSI Aaron Kandel for all of his assistance during the entire course and to the rest of the CE 295 class for constructive feedback.

Optimizing EV Charging Times to Minimize GHG Emissions & Ensure Distribution Grid Stability

Christina Ismailos, Ahana Mukherjee, Ayse Ozturk, Nicholas Pesta, Emily Rogers, Daniel Tutt

Abstract

Electrification of the transportation sector through increased usage of electric vehicles (EVs) will be a critical step in reducing greenhouse gas emissions to combat climate change. However, EV sustainability relies heavily on the carbon intensity of the electricity grid. Additionally, increased grid penetration by electric vehicles and distributed generation can have consequences of voltage stability on the distribution grid. The purpose of this project is to develop an algorithm that will identify optimal charging times for EVs to minimize greenhouse gas (GHG) emissions while leveraging the capabilities of four-quadrant inverters in EV chargers to provide local voltage regulation to ensure distribution grid voltages remain within a specified threshold. The project tested several scenarios of the EV penetration on the IEEE 13-node distribution test feeder while utilizing typical summer and winter electric grid carbon intensity data from CAISO. Results indicated that the optimal charging algorithm resulted in up to 40% savings in carbon dioxide emissions. Moreover, local voltage control was integral to regulating voltage magnitudes as EV penetration on the grid increased. This algorithmic approach has broad impacts for the environment by minimizing GHG emissions; the utility provider by running distributed volt-var control; and the consumer through cost reductions in charging infrastructure.

1. Introduction

1.1. Motivation and Background

Electrification of transportation is an instrumental step towards decarbonizing our society. California, in specific, has mandated the sale of 5 million electric vehicles on the road by 2030 along with 250,000 electric vehicle charging stations by 2025 [1]. The electric grid has been called upon to accommodate this increased demand for electrified transportation. However, this can have several consequences, especially burdening current distribution grids. These networks, designed to deliver bulk power from the transmission network to homes and businesses, must now accommodate sudden large loads from EV charging. These new loads can cause erratic and reversing power flows through distribution networks, threatening the power quality delivered to customers. Thus, in order to ensure electrified transportation demands are being met in addition to typical household and commercial loads, an effective way to control power quality, particularly with respect to voltage magnitude along distribution networks (which, in the US, should deliver within 5% of 120V), must be determined.

In addition to concerns regarding power quality, there are additional concerns regarding long term climate impacts. Currently, electric vehicle charging times often coincide with electricity demand peaks in the morning and late evening hours as illustrated by Figure 1. During these times, the electric grid typically has the highest carbon emissions due to higher usage of fossil fuels for electricity generation, also shown on Figure 1. This is particularly problematic for decarbonizing the transportation sector. Renewable energy production, especially solar, typically peaks during the daytime. However, electric vehicles

seldom maximize use of this renewable resource. Instead, current electric vehicle charging trends demonstrate that EVs often draw power from the grid when it has the highest emissions.

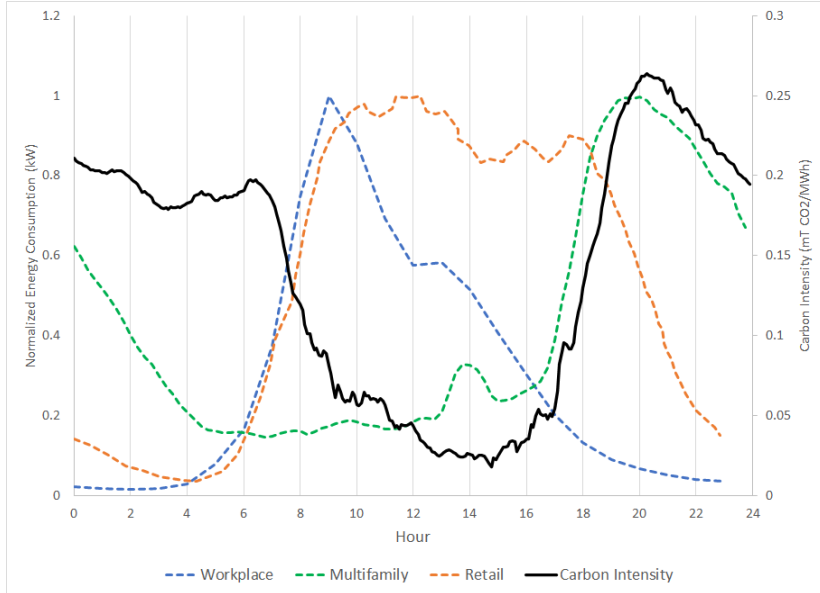


Figure 1 - Electrical Vehicle Charging Demand & Carbon Intensity of California's Electric Grid

In order to mitigate overloading and backfeed on distribution grids along with minimizing greenhouse gas (GHG) emissions from EV charging, optimal control of EV charging is warranted. Consequently, this project aims to develop an algorithm that will minimize GHG emissions by developing optimal charging times while simultaneously correcting voltage magnitude through reactive compensation at the distribution level by leveraging the battery inverters in EVs. This level of grid stability and charging time synchronicity will have a wide range of benefits across multiple stakeholders such as the utility provider and the customer.

1.2. Focus of this Study

This study will develop an optimal control scheme for coordinated electric chargers on a distribution feeder with the dual tasks of 1) minimizing GHG emissions by adjusting the times when electric vehicles are charging and 2) maintaining voltage magnitudes on the feeder within an acceptable range. The control scheme will be tested on the IEEE 13-node feeder model.

2. Literature Review

Existing literature and studies have examined the impact of electric vehicles on grid stability and other related phenomena. These will provide the necessary background information as well as inform underlying assumptions in order to carry out the project objective. Additionally, literature on optimization programming for electric vehicle charging will serve to inform development of the project's objective function and related mathematical modeling.

Current studies in the smart charging realm have varied aims such as regulating voltage and frequency [2,5,16], forecasting electricity demand [5,16], minimizing CO₂ emissions and maximizing profits [12]. Several studies have focused on the regulation and modeling of voltage magnitudes in distribution networks with high EV and distributed energy resources (DER) penetration [3,4,16]. In particular, Arnold

et. al. details an approximate linear power flow model for an unbalanced distribution feeder along with a method for optimizing voltage magnitude with reactive compensation [3]. Meanwhile, Li et. al. examined methods for real-time and decentralized voltage control in distribution networks cautioning that simple controls may be insufficient [4]. Le Floch et. al. also developed control models for EVs that take into account user and grid constraints and aim to balance generation and voltage control objectives [17]. The aforementioned studies were integral to developing the models used within this project.

Most commonly employed techniques for optimization are Convex Optimization [15,13], Dynamic Programming [10,14] and Game Theoretical Frameworks [12]. Driver arrival behavior is critical to model for the project objective. Markov Chains [7,10,13] and Queuing Theory [23,24] is frequently used in modelling the charging time patterns. Yang, et. al [13] presented a two-stage stochastic linear program which was used to optimize between the cost and mismatch in predictions in schedule decisions. Ma. et al. [12] modeled PEV charging as a non-cooperative game and suggested that Nash Equilibrium provided optimal results where communication with and among PEVs is not possible.

Literature on current electric vehicle charging behavior as well as modeling distribution grids was critical to developing scenarios for testing. Hardman et al ranked the location in which electric vehicle charging events typically occur, with residential charging comprising 50-80% of the total events followed by workplace charging and lastly public charging infrastructure, which made up 10% of all charging events [18]. Hardman's study along with data availability steered the project aim towards focusing on residential charging. Additionally, distribution network topology and EV charger penetration scenario development was motivated by the study conducted by Ahoura et al [19]. The study distributed 1,000 homes along the IEEE 13-node distribution test feeder and simulated a residential distribution grid using five different EV penetration rates [19].

3. Technical Description

3.1. Model Inputs and Data

CAISO Winter and Summer Carbon Intensity

The California electrical grid is managed almost entirely by the California Independent System Operator, or CAISO. There are multiple ISOs in the United States, and each manages the flow of electricity in their territory, but CAISO is the only institution that is responsible for a single state. This colocation of state boundaries and ISO territory allows for a relatively straightforward process to determine the characteristics of the electricity used in California.

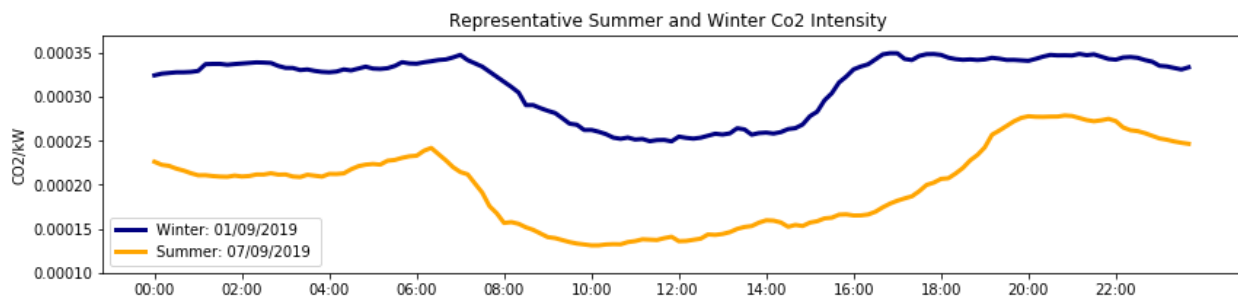


Figure 2 - Representative seasonal grid CO2 intensity

One of the critical characteristics for this project was the carbon intensity of the electricity. This variable is embedded in the objective function of the optimization model, and therefore having accurate

information was critical for ensuring a legitimate result. The carbon intensity data was calculated using two data sources available from CAISO - the hourly GHG emissions and the hourly electrical supply. The emissions were divided by the supply to give an emissions per megawatt value that could be applied to discrete units of electrical demand. In order to capture the seasonal variation in electrical sources and demand behavior, these data sources were collected for the entirety of two days - January 9, 2019 and July 9, 2019. These days were compared to neighboring days to ensure they were generally representative samples and did not exhibit any outlier tendencies.

NREL Residential Electricity Demand & Charging Profiles

The project requires developing EV charging profiles based on existing demands. Moreover, in order to understand how increased EV loads combined with other standard electricity demands affect distribution grid stability, existing residential demands data will be required. Residential electricity consumption among 200 randomly selected households in the Midwest along with electric vehicle charging profiles were obtained from the National Renewable Energy Laboratory (NREL) database [20]. This project primarily utilized level-2 charger data which had a maximum power output of 6,600 W. The charging profile data was utilized in conjunction with EV arrival modeling and predictive modeling in the supervisory control level of the algorithm. Charging profile data indicated that time of the day was a significant variable in predicting charging behavior. Variability in the charging profile based on day of the week (i.e. weekday vs. weekend charging) was not included this study. The IEEE 13-node test feeder served as the primary test model for the distribution grid. Standard IEEE loads (i.e. real and reactive power) at each of the nodes were used in conjunction with the NREL charging profile data to accurately model a distribution network.

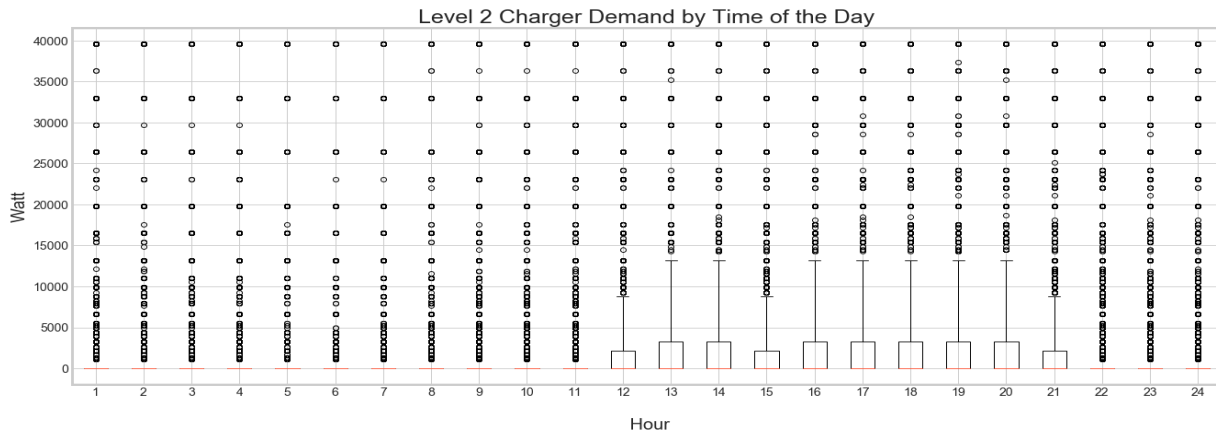


Figure 3 - Dynamic charger demand during one typical day

3.2. Modeling the Grid

Power Flow Solver

The grid, like other physical systems, can be characterized mathematically. However, the electrical characteristics of the grid over time, such as the voltage magnitude, are determined by a nonlinear system of equations with the overall power demand as variables and the network characteristics as parameters. These nonlinear systems of equations cannot be solved algebraically, and generally require the use of a numerical method like gradient descent. Power flow solvers are programs written to solve these nonlinear systems quickly, and various versions are available. The distribution feeder for our project is simulated on the OpenDSS power flow solver [21] maintained by the Electric Power Research Institute. The software

is open source and can be managed with a Python plugin [22]. In addition, Python programs are available which can read standard files characterizing a network and the loads on that network, and input it into the OpenDSS power flow solver. Together, the OpenDSS power flow solver and these Python programs can simulate any distribution feeder and set of loads described in a standard file. In Python, the programs are also flexible enough to allow for internal control loops, like the local control described below.

3.3. Modeling EV Charging

Electric Vehicle Arrivals & Departures to Chargers

In order to schedule EV charging optimally, it is necessary to model EV arrival, departure, and energy demand. An EV charging event consists of two successive events. First, is arrival to the charging facility which is a discrete event. This is followed by a continuous charging event then ends with departure. Queuing theory is a common approach in modeling EV charging times [23,24]. A queuing system consists of three processes: arrival to queue, waiting and service time. In a residential charging event, modeling waiting times is not necessary. Therefore, we developed a queuing model that captures non-homogeneity and self-serve nature of residential charging using M_t/M/inf queuing systems.

This desired state of charge is the energy demand component of the EV demand modeling. The demand of each car depends on many factors, such as level of charge at arrival, battery capacity, stay duration and individual habits. Since this information is not always available, the demand can be predicted using black-box models. The decision tree predictive model ultimately deployed used only time of day and duration variables and resulted in 76% accuracy.

The EV modeling is performed consecutively. First, we modeled the arrival and departure times by utilizing the queuing theory. Then, using the time of the day and charging duration values from the simulations we predicted the energy consumption using decision trees.

Arrival Distribution

Arrival time is the time that an EV is first present at a charger. This can be approximated by Poisson distribution. Figure 4 illustrates the arrival distribution of 200 independent chargers for each time frame. Given the arrival histogram, we decided to use a non-homogeneous Poisson process to capture the time variant property of EV arrivals.

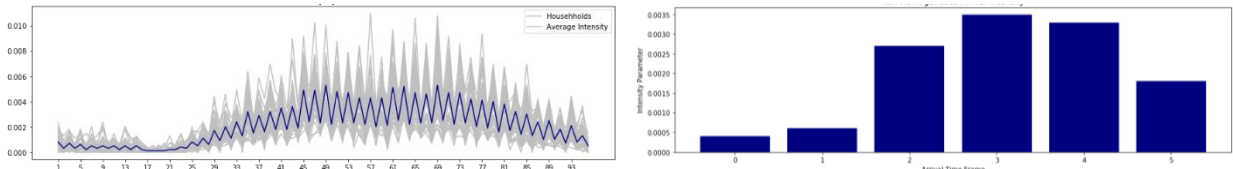


Figure 4 - Average daily arrival rate of non-homogeneous Poisson Model

The NREL data is collected with 15 min intervals so we assumed that the arrival rate is constant throughout each interval. Let $\lambda(k)$ be the arrival rate of EV during the time interval $\{(k-1)\Delta t, k\Delta t\}$ where k is a discrete integer. Then; $\lambda(\hat{k}) = \frac{N(k)}{\Delta t}$. We take the average of this value for 365 days. Since the $\lambda(k)$ does not show significant variation in 15 min intervals we binned the parameters values in 6 intervals as

seen above. We used these 6 time frames when simulating the EVs. The average time between successive arrivals ignoring the non-homogeneity is found to be 8.6 hours.

Charging Duration Distribution

The mean charging duration is 36 mins. However, the curve is skewed towards the right. Exponential distribution is adopted in several papers to model the duration times. However, with an exponential model, 0 min charging duration has the highest probability which is not realistic based on our dataset. Rather than using exponential distribution we capture the EV charging duration via fitting a gamma distribution. Figure 5 shows how the histogram and the gamma distribution matches.

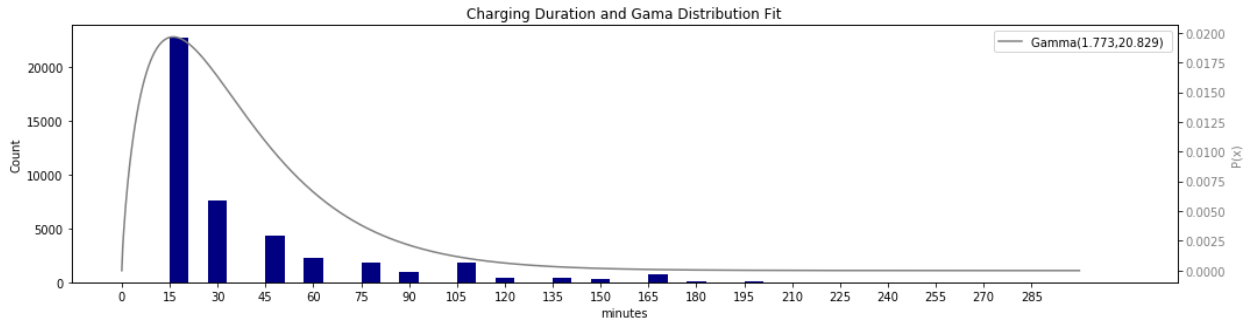


Figure 5 - Charging duration counts and estimated PDF

Simulation Results

Arrival and service distributions are used to simulate EV charging sessions in various scenarios. We performed simulations based on the number of chargers. Each charger is assumed to have the same arrival and duration distributions. Each charger can serve multiple EVs per day; one charging event is called a charging session. Each charging session also has an associated energy demand that has to be met within the span of plug-in and plug-out time. Figure 6 shows a comparison of real data and simulated data.

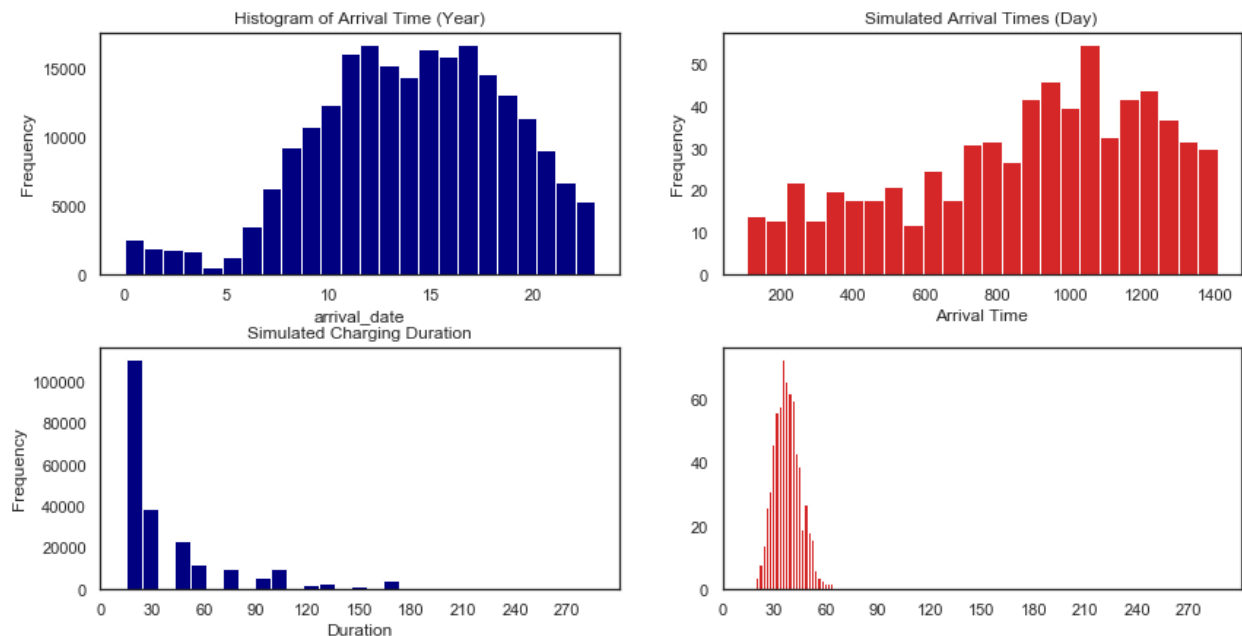


Figure 6 - Real and simulated arrival times

There is a slight difference between the durations of the simulated data and the real data. We believe this difference is caused by using aggregated data to generate the model. In the simulations, the arrival times and durations are continuous which reflects reality. The rest of the simulations are in Appendix B.

Energy Demand Prediction Model

To predict the energy demand of each charging session we trained a decision tree model with features ‘arrival time’, ‘departure time’ and ‘duration’. The resulting model predicts energy consumption with 76% accuracy on the test data.

3.4. Two-Level Control

In order to minimize carbon emission while ensuring grid stability a two-level control scheme is developed. The variable names are listed in Appendix C.

Supervisory Control Optimization

A convex optimization problem is formulated to minimize the carbon emissions arising from uncontrolled charging of the electric vehicles. The model solves for an optimal charging schedule across 144 time steps for N many chargers. All chargers are assumed to be residential level 2 chargers with a maximum of 7.2 kW power output. Electric vehicle presence at charger i is represented in matrix Z_i . The dimensions of the Z_i is a j by 144 matrix where j is the number of charging events at the charger station i. The model represents the minimum carbon scenario by allowing discharging from EV to grid. We also ran the model a second time without discharging, where was restricted to [0,1]. These no-discharge scenarios were not simulated, but they represent cases with smaller power swings and less overall charging utilization making local control simpler and more effective.

Objective Function:

$$\min_{\sigma_t^i} \sum_{i=1}^N \sum_{t=0}^{144} C_t \sigma_t^i P_{max} \quad \text{carbon minimization (1)}$$

$$\text{st.} \quad P_{max} Z_i \sigma^i = D_i \quad \text{for} \quad \forall i \in \{1, 2, \dots, N\} \quad \text{demand constraint (2)}$$

$$\sigma_t^i \geq -1 \quad \text{power output coefficient (3)}$$

$$\sigma_t^i \leq +1 \quad \text{power output coefficient (4)}$$

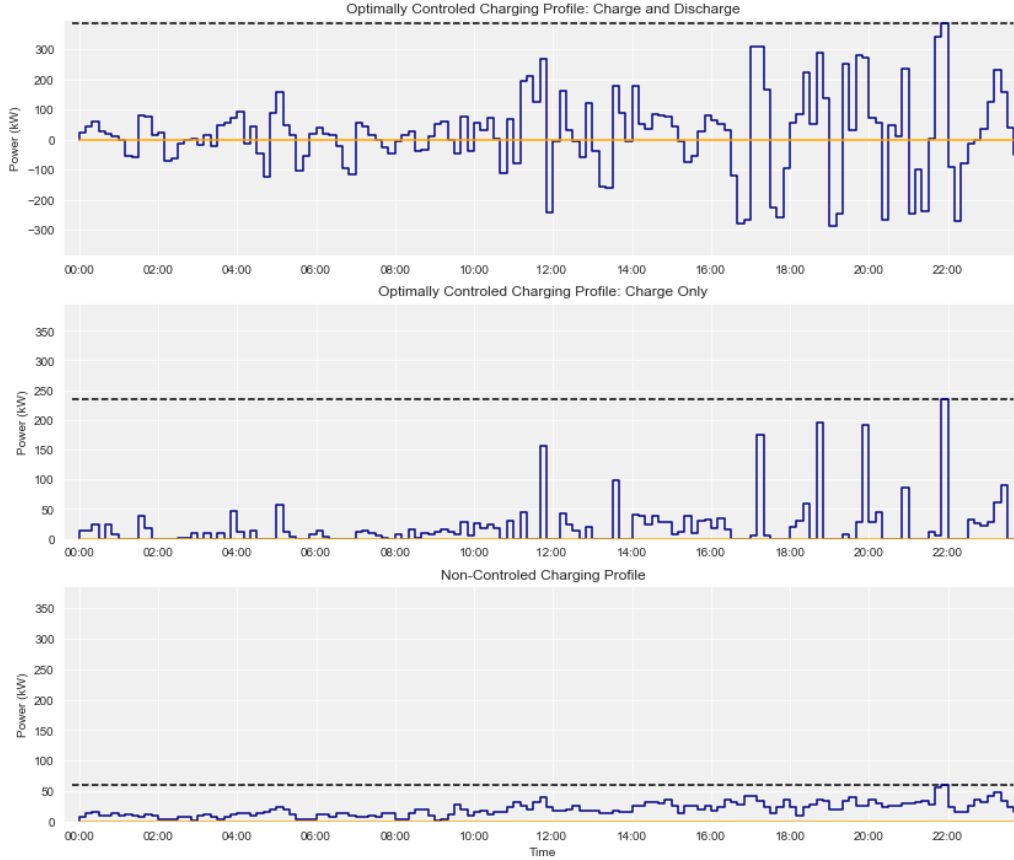


Figure 7 – Optimized and Not Optimized Charging Profiles

Local Control & Power Flow

The local controller was developed from the paper by Li et. al. on real-time decentralized voltage control [4]. Effectively, it is an integral controller with an acceptable range rather than a single target, described by the equations below. If the local voltage is above or below the set limits, the controller begins adjusting reactive power accordingly until the voltage has returned within the set bounds.

Local Controller Functions:

$$q_i(t) = q_i(t - 1) - \epsilon d_i(v_i(t))$$

where

$$d_i(v_i(t)) \equiv \max(0, v_i - v_{max}) - \max(0, v_{min} - v_i)$$

In addition to these fundamental equations, the local control needs to balance voltage regulation with vehicle charging. The controller first reduces the charging power and then provides reactive compensation so that together they do not exceed its maximum power level, according to the following constraint:

$$S_{i,max}(t)^2 \geq P_{i,opt}(t)^2 + q_i(t)^2$$

Finally, the controller needs a method for reducing its reactive compensation when no longer necessary. With a single target, an integral controller would automatically adjust to continually meet said target, but

with a target range it no longer adjusts within the acceptable range. This is problematic; for example, when responding to a very low voltage, the controller would continue to neglect charging and devote itself entirely to reactive compensation even after the voltage had returned to the acceptable range, and would not readjust its compensation until the voltage rose above the maximum limit. To prevent this outcome, the controller also checks the voltage levels and if it is not within proximity of the voltage limits, it reduces the reactive compensation. The sensitivity of this adjustment can be varied, but if too sensitive it can lead to oscillations.

3.5. Model Integration

The individual models described above need to be connected in order to arrive at a complete solution to the problem posed in this project. The vehicle charging optimization model creates a schedule predicting when chargers should be deployed to achieve optimal carbon reductions but does not incorporate the grid requirements during this development. Model connections were developed to create the larger model structure shown in Figure 8, which shows how the predicted schedule developed by the Supervisory Control is assigned to nodes and then fed to the Local Control. The Local Control then works with the Power Flow Solver to utilize the charger activity schedule to provide reactive power when needed to ensure voltage stability in the grid.

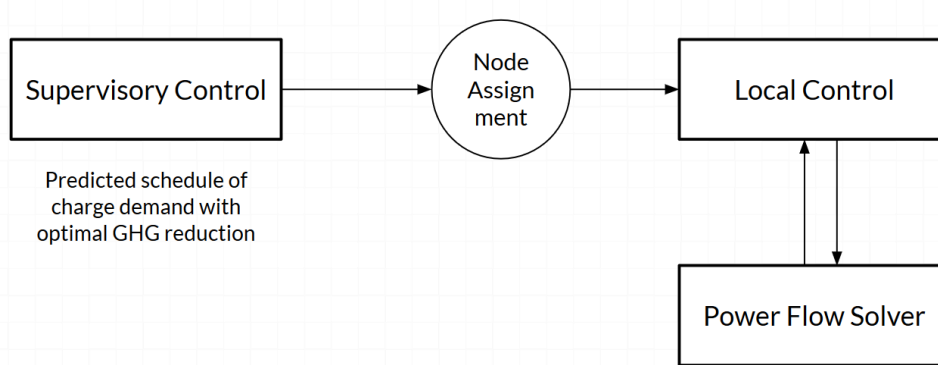


Figure 8 - Overall Model Structure

The key transition between the models is merging the individual chargers that are being optimized by the supervisory model into the nodes that comprise the IEEE Distribution Feeder, shown in Figure 8 as the Node Assignment circle. This transition is necessary because the different models need to interact with the electrical grid at different scales. The interaction between vehicles and chargers needs to be modelled individually in order to capture the characteristics that drive charging behavior and create robust arrival and departure schedules. The voltage stability model, on the other hand, has to work at the smallest discrete level of the distribution circuit, which is a node, in order to calculate the voltage requirements.

This transition was made by aggregating chargers onto nodes based on various testing scenarios. The testing scenario would prescribe how many total chargers were present on the circuit, and how many electric vehicles were out interacting with those chargers. The distribution of chargers on the grid was set up to correspond to the approximate number of households on each node or the grid. Figure 9 demonstrates how these breakdowns might occur.

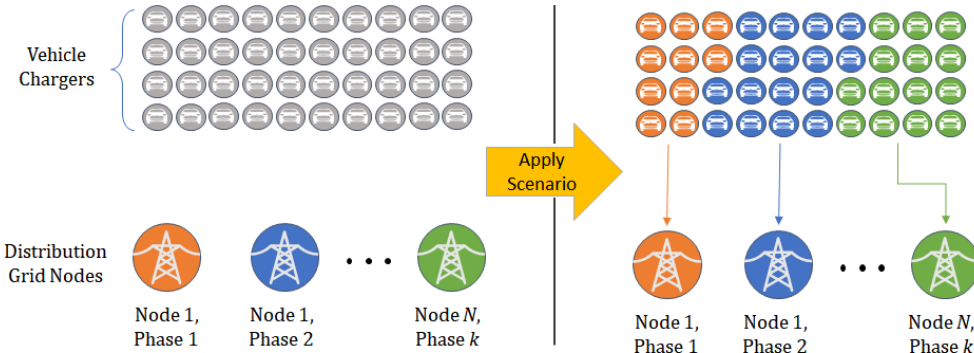


Figure 9 - Load breakdown schematic

3.6. Scenario Testing

Twenty different modeling scenarios were examined to illustrate the impact that varying key input parameters would have on the results. These parameters are grid carbon intensity, number of EV chargers in the network, and arrival intensity of the chargers (how often they are charging). Each is described briefly below and illustrated in a table in Appendix D.

- a) Grid carbon intensity:
 - i. Higher carbon intensity was represented by the California grid during winter months using CAISO data from January 9, 2019.
 - ii. Lower carbon intensity was represented for summer months using CAISO data from July 9, 2019.
- b) Total number of chargers:
 - i. The hypothetical maximum EV penetration was assumed to be 1 EV for each of 1052 households (i.e. 1052 chargers). This case was not modeled but served as a point of reference for deciding the modeling scenarios.
 - ii. Baseline Case of no chargers was used to initialize the model such that we could observe the grid stability before any EV loads were added.
 - iii. Low EV Case included 100 chargers in the network. This was based on the assumption that roughly 10% of the maximum 1052 households were charging an EV.
 - iv. Medium EV Case included 200 chargers, based on roughly 20% of maximum penetration.
 - v. High EV Case included 520 chargers based on roughly 50% of maximum penetration.
- c) Arrival Intensity:
 - i. Low Frequency is based on an arrival intensity corresponding with charging arrival every 8 hours. This is the base rate.
 - ii. Medium Frequency is a 50% increase above the base rate (roughly every 6 hours).
 - iii. High Frequency is a 100% increase above the base rate (roughly every 4 hours).

3.7. Results

Carbon Reductions

Optimizing charging times produced significant carbon reductions, particularly when EVs were allowed to discharge onto the grid. The results are summarized in Figure 10 and Figure 11 below.

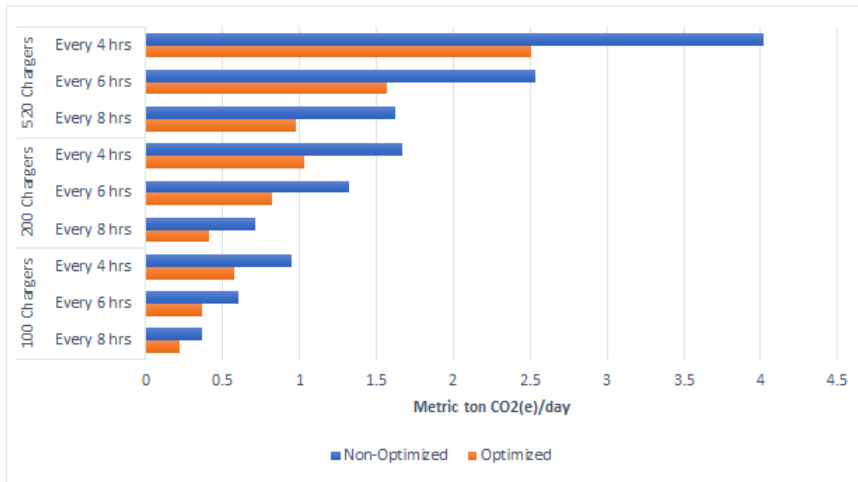


Figure 10 - Winter Electric Grid - Carbon Emissions of EV Penetration & Arrival Intensity Scenarios



Figure 11 - Summer Electric Grid - Carbon Emissions of EV Penetration & Arrival Intensity Scenarios

Voltage Stability

One of the main premises of this project was that as more EVs and distributed generation (e.g. solar) are added to a distribution feeder, voltage instability would increase. This instability can be further increased when EVs discharge to the grid or optimize their charging. However, EV chargers are capable of providing reactive power compensation to the grid. They could manage the voltage stability of the grid by taking advantage of this capability and become an asset rather than a hindrance.

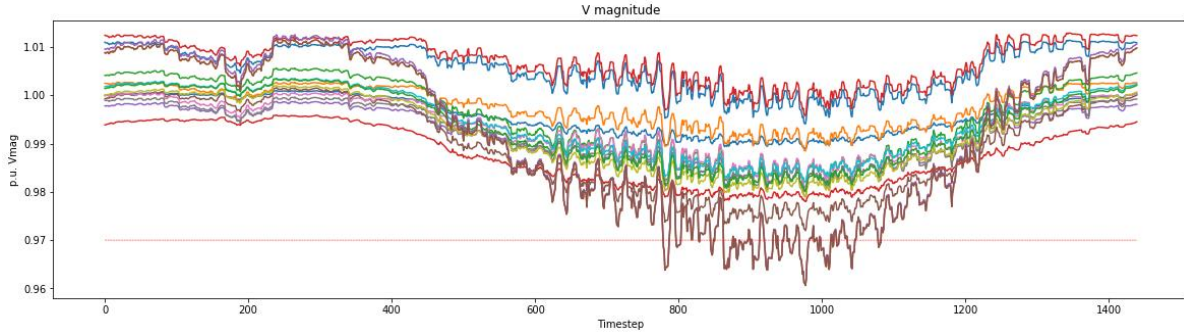


Figure 12 - Voltage magnitude for all nodes on network over time, no chargers, winter day.

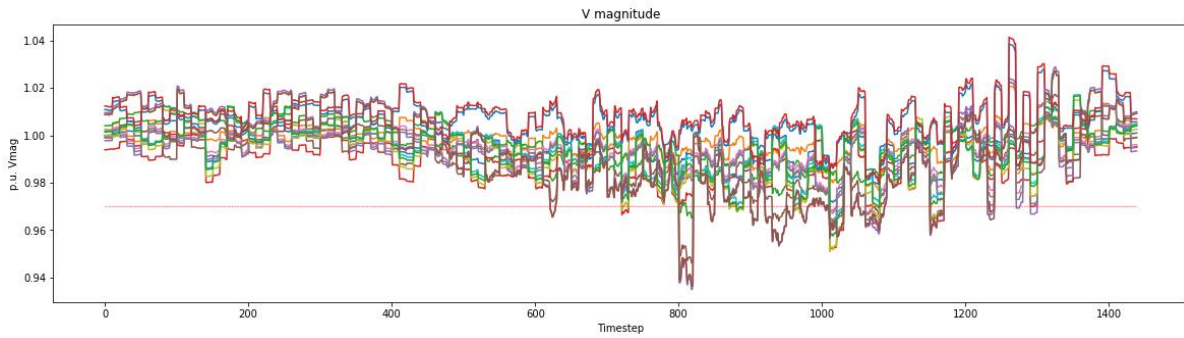


Figure 13 - Voltage magnitude for all nodes on network over time, optimized chargers, high EV and high frequency of charging, winter day.

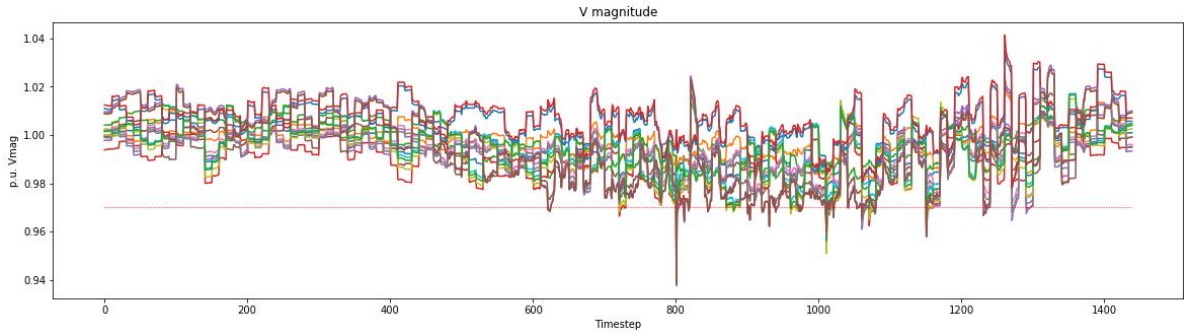


Figure 14 - Voltage magnitude for all nodes on network over time, optimized chargers and local control, high EV and high frequency of charging, winter day.

Simulations on the IEEE 13-node feeder supported this premise. Comparing Figures 12 and 13, it is clear that many EV chargers charging and discharging in tandem can create large swings in the grid voltage magnitude. Comparing Figures 13 and 14, it is clear that the local control is capable of returning grid voltage to within set limits. Because the local control functions like an integral controller, we expect to see the momentary deviations followed by quick returns to the limit, as in Figure 14. All the scenarios were tested using the grid simulation coupled with local control. Refer to Appendix E for all the results showing voltage magnitudes over time.

Although particularly effective in scenarios with many EVs, the local control occasionally slows or prevents vehicle charging, and does not always maintain the voltages within set limits. There are potential

conflicts between charging EVs optimally and maintaining voltage stability, and voltage control has limited effectiveness when few EVs are charging.

In order to evaluate the extent of this conflict, two measures were used. First, the percent of time during which charging was at all affected by local control was measured. Even though these effects may be minimal, it serves as a good check to ensure that local control is working as expected. Second, the percent of time during which charging is prevented because of the local control was measured. This means that the local control is doing all it can to maintain voltage stability, delivering no power to the vehicle. In addition, it means that the voltage level continues to exceed the set limits, or at best is right on the margin.

All scenarios were run with per-unit voltage limited to the range [0.97, 1.03], which required occasional control intervention. For the US power grid, voltage limits are typically set at [0.95, 1.05], but these limits only required very minimal intervention in our scenarios based on the network and load profile. In order to test the local control more rigorously, we introduced stricter limits. Consequently, all the high and low penetration scenarios were run again under ‘Strict Voltage Limits’, with voltage limited to the range [0.98, 1.02], which required significantly more control intervention (see Tables 1 and 2 below). The results show that, as the number of chargers and frequency of charging increases, the local control becomes more effective and conflicts less with vehicle charging.

Table 1 - Percent of time charging is affected by Local Control, for all scenarios

Winter, Standard Voltage Limits				
Frequency of use:	Low	Med	High	
Number of Chargers:	100	3.88%	3.42%	3.64%
Chargers:	200	4.78%	3.68%	3.99%
	520	3.24%	3.36%	3.78%

Winter, Strict Voltage Limits			
Frequency of use:	Low	High	
Number of Chargers:	100	11.89%	13.43%
Chargers:	200	14.31%	12.94%
	520	12.88%	9.60%

Summer, Standard Voltage Limits				
Frequency of use:	Low	Med	High	
Number of Chargers:	100	3.43%	5.04%	3.40%
Chargers:	200	3.75%	3.75%	3.85%
	520	3.24%	3.36%	2.83%

Summer, Strict Voltage Limits			
Frequency of use:	Low	High	
Number of Chargers:	100	11.70%	13.52%
Chargers:	200	13.08%	10.99%
	520	12.88%	6.45%

Table 2 - Percent of time Local Control prevents charging, for all scenarios

Winter, Standard Voltage Limits			
Frequency of use:	Low	Med	
Number of Chargers:	100	1.60%	2.09%
Chargers:	200	1.60%	0.49%
	520	0.42%	0.12%

Winter, Strict Voltage Limits			
Frequency of use:	Low	High	
Number of Chargers:	100	8.67%	4.87%
Chargers:	200	7.71%	2.57%
	520	3.27%	0.45%

Summer, Standard Voltage Limits			
Frequency of use:	Low	Med	
Number of Chargers:	100	1.77%	0.94%
Chargers:	200	1.32%	1.17%
	520	0.42%	0.12%

Summer, Strict Voltage Limits			
Frequency of use:	Low	High	
Number of Chargers:	100	9.04%	6.17%
Chargers:	200	7.30%	4.37%
	520	3.27%	0.48%

4. Discussion

4.1. Relevance of the Results

This project demonstrates tangible benefits for environmental sustainability, utility providers, and electricity customers. By using two-level control, this modeling strategy not only maximizes carbon savings from EV uptake, it also progresses towards a promising solution for grid instability.

Replacing internal combustion engine (ICE) vehicles with EVs is a critical part of California's strategy for GHG mitigation. Greater carbon savings can be realized by also optimizing charging time to correspond to the carbon intensity of the electric grid. Smarter charging algorithms will be particularly important as more EVs are adopted in California and charging infrastructure is expanded to offices, retail, and public spaces. Considering a high EV uptake scenario with optimal charging instead of current charging trends, an additional approximately 2 metric tons of CO₂ per 1000 vehicles would be saved during a summer day, and approximately 3 metric tons per 1000 vehicles during a winter day. Extending these savings across the 5 million EVs mandated by the California state government, this is roughly equivalent to taking nearly 1 million ICE passenger vehicles off the roads (a typical passenger vehicle emits 4.6 metric tons CO₂/year) [25]. Optimized charging could contribute significantly to statewide efforts to curtail GHG emissions.

However, the prospect of adding 5 million EVs to the grid presents a significant obstacle for stability due to sudden voltage swings. Our model demonstrates that higher charging rates can contribute to a solution instead of being a hindrance by using reactive power compensation to manage voltage stability. Both utility providers and customers reap additional benefits from greater grid stability resulting from distributed volt-var control. By better managing EV loads on the existing grid, utilities may also avoid costs to upgrade the grid. This also benefits customers who will experience more consistent and reliable electricity access, in addition to lower costs from avoided maintenance fees and the value of carbon emission mitigation.

4.2. Limitations

This study specifically utilizes California's abundance of low carbon intensity solar generation to reduce carbon emissions by shifting EV charging. As a result, application and extrapolation of this study to electricity grids with lower penetration of solar or renewables may be limiting. Another limitation of this study is its extension to DC fast charging. This optimization used Level 2 charging and on-board EV inverters for volt-var compensation. Further research is required to adjust this approach for DC fast charging station-based inverters. In the future, more complex battery control and degradation models could be implemented to analyze the effects of volt-var compensation on battery health. Lastly, a limitation to the premise of the presented model is the usage of EV owner charging inputs of desired state of charge, starting and ending charging times as opposed to optimizing when EV owners should charge. A future model could develop optimized EV charging times regardless of EV owner preferences and dynamically communicate them to EV owners through demand response events.

4.3. Next Steps

This project used a simple 13-node model to demonstrate the concept of combined carbon reduction and improved grid stability. The promising preliminary results indicate that future scenarios should be tested to extrapolate the methodology to more complex and realistic demand profiles as well as distribution networks. Adding commercial demand could be accomplished by developing a residential and commercial load split within the 13-node model based on a topographical reference in California.

Similarly, future models could vary the load profiles used to simulate how the system might interact with higher PV penetration, other less predictable renewable sources, or sudden load variations. This could be valuable for jurisdictions using higher quantities of wind or other renewables and would test the robustness of the grid stability approach.

A more advanced control algorithm could be added such that the system could track and adjust for a single problematic node. By adding connected controls, chargers could more efficiently react to and accommodate high point loads and more uneven distributions of demand across the grid. This could be especially beneficial for accommodating polarized adoption behaviors where certain neighborhoods or regions have significantly higher EV uptake than adjacent areas. Each of these steps would further evaluate the efficacy of the modeling approach and create a strategy that is more robust and widely applicable for California's EV strategy.

5. Summary

Electrifying transportation presents an exciting opportunity to decarbonize the transportation sector. However, the impact of these new electrical loads on distribution grids is still unclear. This project developed a model to optimize the scheduling of EV charging while ensuring distribution grid stability. Utilizing the IEEE 13-node distribution test feeder, a total of 1,042 residential loads were modeled with several scenarios of EV charger penetration (i.e. 10%, 20%, 50%) along with vehicle arrival intensity subject to typical winter and summer carbon intensities of the electric grid. Results indicated that if sufficient EVs in a distribution network can coordinate charging times, significant carbon savings, up to 40%, can be achieved. Local voltage control was integral to regulating voltage magnitudes as EV penetration on the grid increased. However, this level of optimal control is rendered ineffective if there is low penetration of EV charging on the grid. These results are critical for motivating increased EV adoption. Moreover, optimal control schemes have a wide range of benefits for utility providers as costly upgrades to charging infrastructure or the electric grid can be eliminated. Overall, the effectiveness of this type of local control increases as EV penetration increases allowing EVs to provide ancillary services to the grid instead of burdening grid functionality. The effectiveness of this type of optimal control algorithm will be further understood when modeled under more realistic assumptions including a larger distribution feeder. Nevertheless, optimal charging coupled with local control even on a distributed scale has overarching grid and consumer benefits.

References:

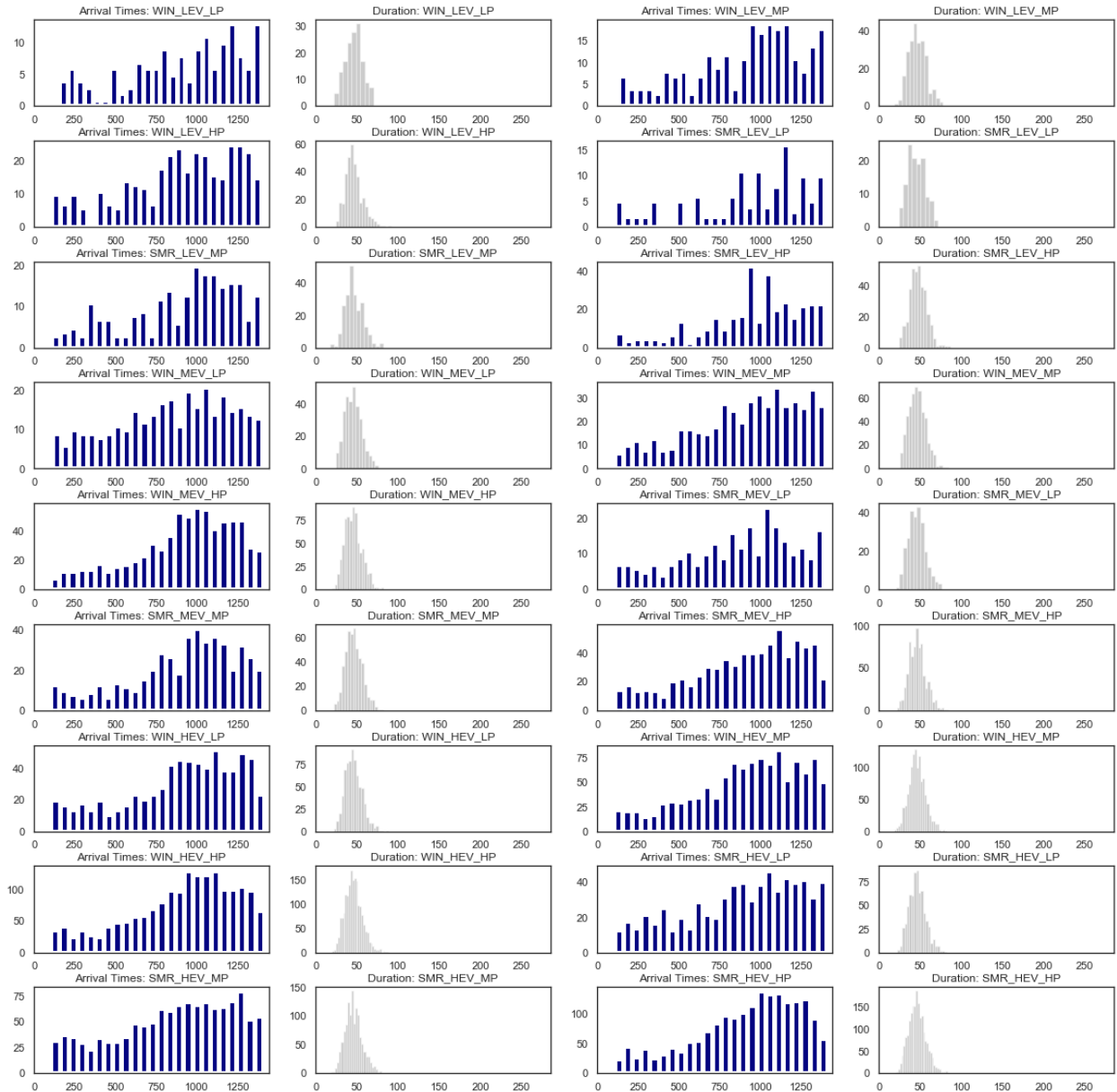
1. Zero Emission Vehicles (2020). California Public Utilities Commission. <https://www.cpuc.ca.gov/zev/>.
2. Han, S., Han, S., and Sezaki, K. (2010). Development of an Optimal Vehicle-to-Grid Aggregator for Frequency Regulation. *IEEE Transactions on Smart Grid*. 1:1, 65-72. doi: 10.1109/TSG.2010.2045163
3. Arnold, D.B., Sankur, M., Roel, D., Brady, K., Callaway, D.S., and von Meier, A. (2016). Optimal Dispatch of Reactive Power for Voltage Regulation and Balancing in Unbalanced Distribution Systems. UC Berkeley: Center for Information Technology Research in the Interest of Society (CITRIS). Retrieved from <https://escholarship.org/uc/item/9qq066hw>
4. N. Li, G. Qu and M. Dahleh (2014). "Real-time decentralized voltage control in distribution networks," 2014 52nd Annual Allerton Conference on Communication, Control, and Computing (Allerton), Monticello, IL, pp. 582-588, doi: 10.1109/ALLERTON.2014.7028508
5. Lopes, J.A., Soares, F., Almeida, P., and Moreira da Silva, M. (2009). Smart Charging Strategies for Electric Vehicles: Enhancing Grid Performance and Maximizing the Use of Variable Renewable Energy Resources. EVS24 International Battery, Hybrid and Fuel Cell Electric Vehicle Symposium.
6. K. Clement, E. Haesen and J. Driesen. (2009). Coordinated charging of multiple plug-in hybrid electric vehicles in residential distribution grids. 2009 IEEE/PES Power Systems Conference and Exposition, Seattle, WA, pp. 1-7, doi: 10.1109/PSCE.2009.4839973.
7. Wang, B., Hu, B., Qiu, C., Chu, Pe., and Gadh, R. EV Charging Algorithm Implementation with User Price Preference. UC California Institute of Energy Efficiency and Environment with the Unified Integration of Inverter Fed Resources to Power Grid Project. University of California, Los Angeles. Department of Mechanical Engineering.
8. Sokorai, P., Fleischhacker, A., Lettner, G. and Auer, H. (2018). Stochastic Modeling of the Charging Behavior of Electromobility. *World Electric Vehicle Journal*. 9: 44. doi: 10.3390/wevj9030044.
9. McLaren, J., Miller, J., O'Shaughnessy, E., Wood, E., and Shapiro, E. (2016). Emissions Associated with Electric Vehicle Charging: Impact of Electricity Generation Mix, Charging Infrastructure Availability, and Vehicle Type. National Renewable Energy Laboratory. NREL/TP-6A20-64852.
10. Iversen, E.B., Morales, J.M. and Madsen, H., 2014. Optimal charging of an electric vehicle using a Markov decision process. *Applied Energy*, 123, pp.1-12.
11. Xu, Y., Çolak, S., Kara, E.C., Moura, S.J. and González, M.C., 2018. Planning for electric vehicle needs by coupling charging profiles with urban mobility. *Nature Energy*, 3(6), pp.484-493.
12. Ma, Z., Callaway, D.S. and Hiskens, I.A., 2011. Decentralized charging control of large populations of plug-in electric vehicles. *IEEE Transactions on control systems technology*, 21(1), pp.67-78.
13. L. Yang, J. Zhang and H. V. Poor, Risk-Aware Day-Ahead Scheduling and Real-time Dispatch for Electric Vehicle Charging. *IEEE Transactions on Smart Grid*, vol. 5, no. 2, pp. 693-702, March 2014.
14. X. Wu, X. Hu, X. Yin and S. J. Moura, Stochastic Optimal Energy Management of Smart Home With PEV Energy Storage. *IEEE Transactions on Smart Grid*, vol. 9, no. 3, pp. 2065-2075, May 2018.

15. Y. He, B. Venkatesh and L. Guan, Optimal Scheduling for Charging and Discharging of Electric Vehicles. *IEEE Transactions on Smart Grid*, vol. 3, no. 3, pp. 1095-1105, Sept. 2012.
16. Luo, X., Xia, S. and Chan, K.W., 2014. A decentralized charging control strategy for plug-in electric vehicles to mitigate wind farm intermittency and enhance frequency regulation. *Journal of power sources*, 248, pp.604-614.
17. C. Le Floch, S. Bansal, C. J. Tomlin, S. J. Moura and M. N. Zeilinger. (2019). Plug-and-Play Model Predictive Control for Load Shaping and Voltage Control in Smart Grids. *IEEE Transactions on Smart Grid*, vol. 10, no. 3, pp. 2334-2344.
18. Hardman, S. et al (2018). A review of consumer preferences of and interactions with electric vehicle charging infrastructure. *Transportation Research Part D*. 62, 508-523. doi: 10.1016/j.trd.2018.04.002.
19. Ahourai, F., Huang, I., Al Faruque, A. (. Modeling and Simulation of the EV Charging in a Residential Distribution Power Grid. Center for Embedded Computer Systems. UC Irvine. Department of Electrical Engineering and Computer Science.
20. Muratori, Matteo (2017): Impact of uncoordinated plug-in electric vehicle charging on residential power demand - supplementary data. National Renewable Energy Laboratory.
<https://dx.doi.org/10.7799/1363870>.
21. Electric Power Research Institute. <https://smartgrid.epri.com/SimulationTool.aspx>
22. OpenDSS. <https://pypi.org/project/OpenDSSDirect.py/>
23. X. Zhang and S. Grijalva, "An advanced data driven model for residential electric vehicle charging demand," 2015 IEEE Power & Energy Society General Meeting, Denver, CO, 2015, pp. 1-5, doi: 10.1109/PESGM.2015.7286396.
24. P. Han, J. Wang, Y. Han and Q. Zhao, "A Novel Coordinative Resident Electric Vehicle Charging Mechanism," 2012 Asia-Pacific Power and Energy Engineering Conference, Shanghai, 2012, pp. 1-4, doi: 10.1109/APPEEC.2012.6307227.
25. Green Vehicle Guide (2018). U.S. Environmental Protection Agency.
<https://www.epa.gov/greenvehicles/greenhouse-gas-emissions-typical-passenger-vehicle>.

Appendix A: Table of Responsibilities

Task	Member Responsible
Conduct literature review and background research	All
Determine electricity grid mix, generation and load profiles, and distribution feeder layout	Dani, Ahana, Nick, Christina, Emily
Access and clean necessary input data from relevant sources	Ahana, Emily, Nick, Christina
Identify EV charging topology and modeling scenarios from EV charging data and grid distribution profile.	Christina, Nick
Combine load profiles, charger locations, charging times, grid topology, and Power Flow solver into a simulation program	Dani
Develop optimal control program for reactive power supply from EV chargers	Dani, Tugba
Develop suitable optimization model to determine optimal charging times with lowest carbon emissions, given user and grid constraints	Tugba, Nick
Connect three components and run simulations: 1) supervisory optimization of carbon, 2) local optimization of voltage magnitude and 3) model of the grid.	Tugba, Dani
Synthesize, analyze, and present results	All

Appendix B: Arrival-Duration Simulation of Scenarios



Appendix C: Variables for two-level control scheme

List of Variables		
Variable	Units	Description
N	-	Number of chargers for each scenario
J_i	-	Number of charging sessions at charger i
\sigma^i	-	t x 1 vector of power coefficient for charger i
Z_i	-	J_i x 144 matrix representing EV presence for each session
C_t	CO2/kW	Carbon intensity of the grid at time t
P_max	[kW]	Maximum power output of charger
D_i	[kWh]	J_i x 1 vector representing demands for each session
q_i	kW	Reactive power produced by the local control at location i. Corresponding to a single phase and node
E	kW	Integrator gain term.
d_i	Per unit	Divergence of voltage outside of range
v_i	Per unit	Voltage magnitude at location i, corresponding to a single phase and node
v_max	Per unit	maximum voltage limit
v_min	Per unit	minimum voltage limit
S_i,max	kW	maximum power all chargers can deliver at location i, corresponding to a single phase and node
P_i,opt	kW	optimal power demanded by all chargers at location i, corresponding to a single phase and node

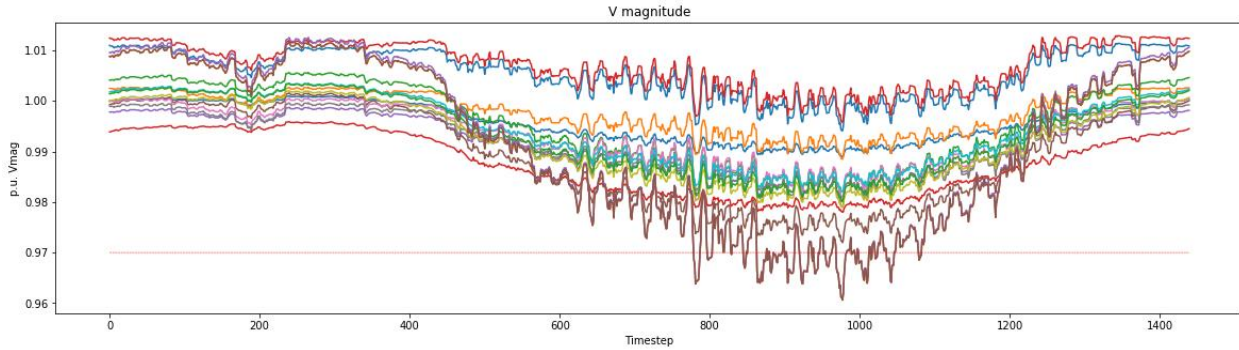
Appendix D: Modeling Scenario Matrix

	Scenario Name	Grid Carbon Intensity	Total Number of Chargers	Frequency of Charging (Arrival Intensity)
1	No EV Case (Baseline)	High (Winter)	0	N/A
2	No EV Case (Baseline)	Low (Summer)	0	N/A
3	Low EV Case - Low Freq	High (Winter)	100	Base
4	Low EV Case - Med Freq	High (Winter)	100	50% increase
5	Low EV Case - High Freq	High (Winter)	100	100% increase
6	Low EV Case - Low Freq	Low (Summer)	100	Base
7	Low EV Case - Med Freq	Low (Summer)	100	50% increase
8	Low EV Case - High Freq	Low (Summer)	100	100% increase
9	Med EV Case - Low Freq	High (Winter)	200	Base
10	Med EV Case - Med Freq	High (Winter)	200	50% increase
11	Med EV Case - High Freq	High (Winter)	200	100% increase
12	Med EV Case - Low Freq	Low (Summer)	200	Base
13	Med EV Case - Med Freq	Low (Summer)	200	50% increase
14	Med EV Case - High Freq	Low (Summer)	200	100% increase
15	High EV Case - Low Freq	High (Winter)	520	Base
16	High EV Case - Med Freq	High (Winter)	520	50% increase
17	High EV Case - High Freq	High (Winter)	520	100% increase
18	High EV Case - Low Freq	Low (Summer)	520	Base
19	High EV Case - Med Freq	Low (Summer)	520	50% increase
20	High EV Case - High Freq	Low (Summer)	520	100% increase

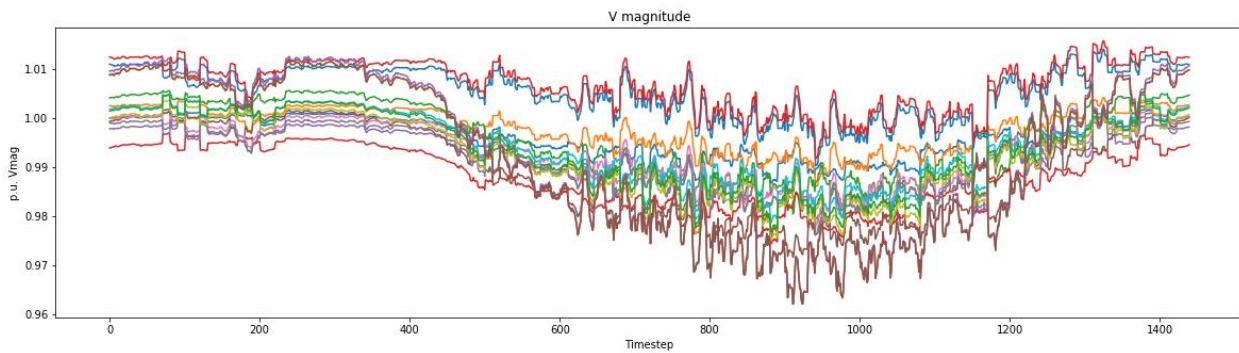
Appendix E: Graphs of voltage magnitudes for all scenarios

Graphs are labeled by the scenario number from the table in Appendix D, as well as whether standard or strict voltage limits were used. ([0.97, 1.03] or [0.98, 1.02])

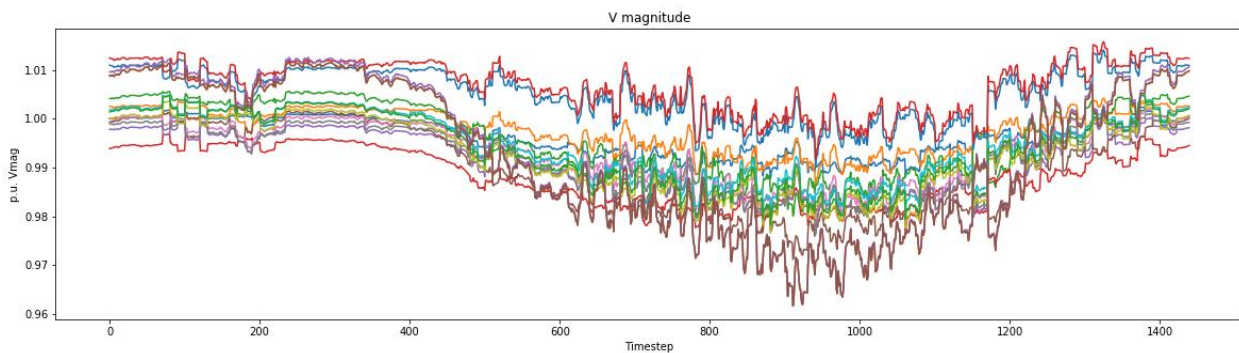
1-2 – Baseline



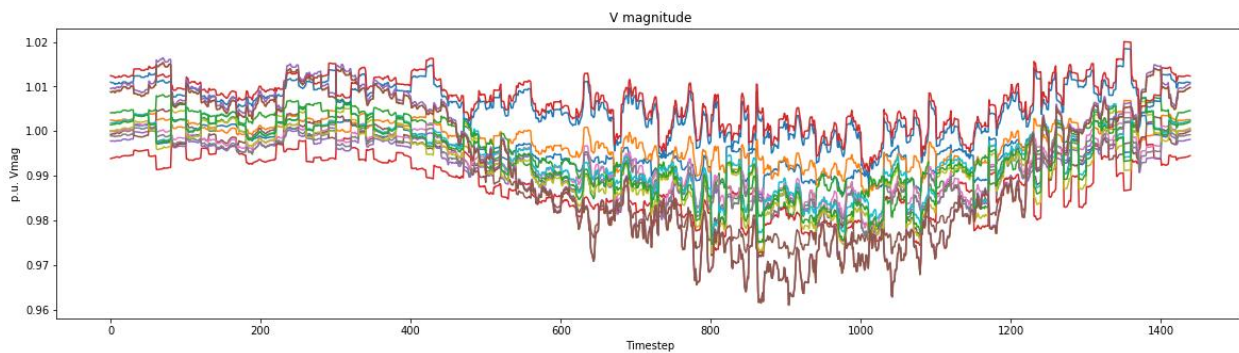
3 - Standard



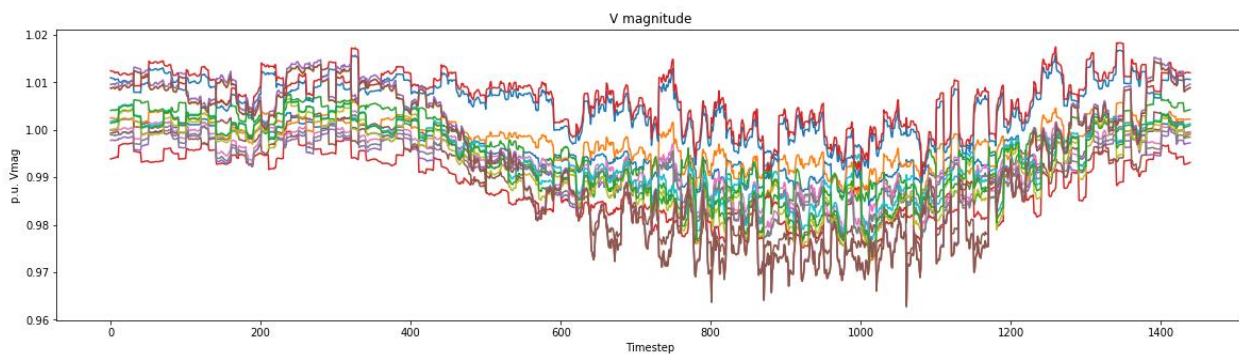
3 – Strict



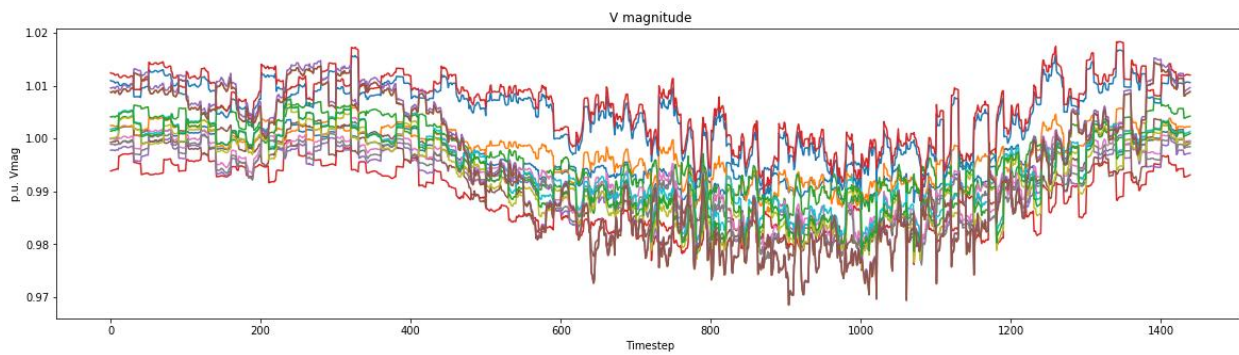
4 - Standard



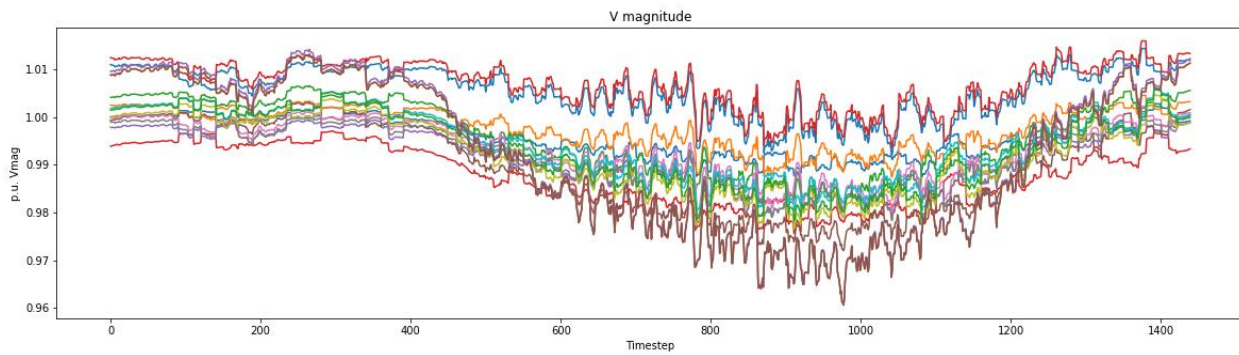
5 - Standard



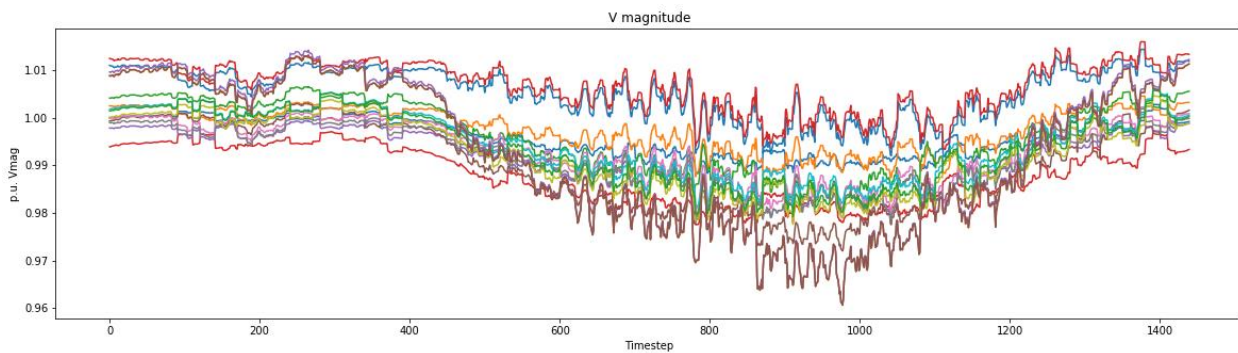
5 - Strict



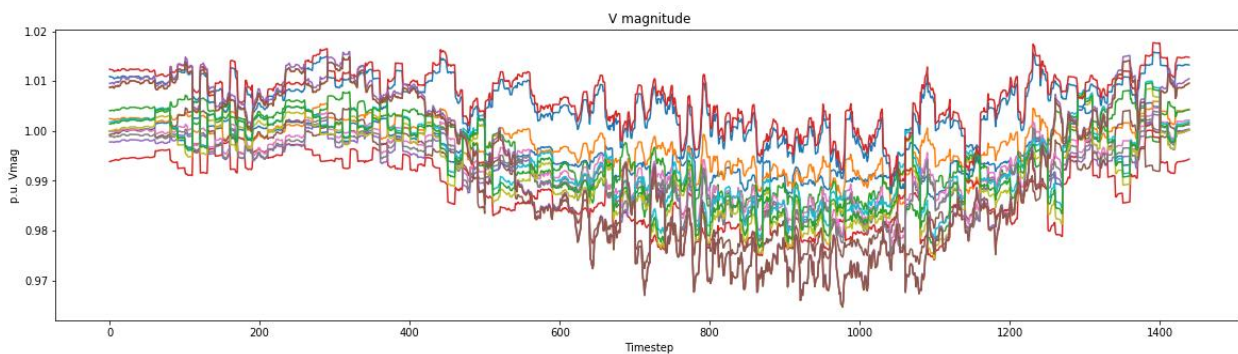
6 - Standard



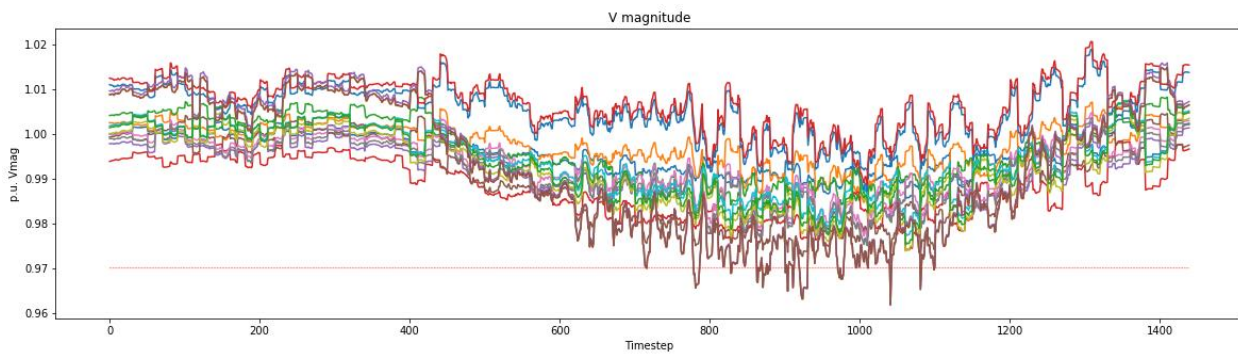
6 - Strict



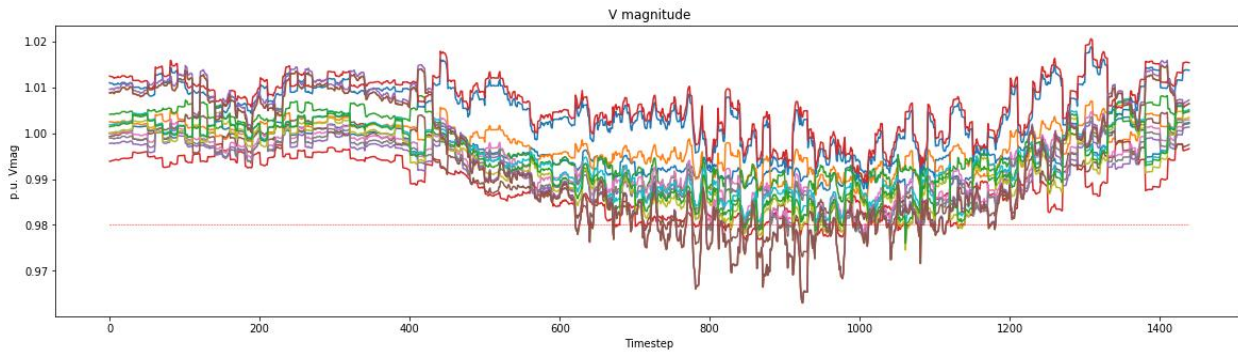
7 - Standard



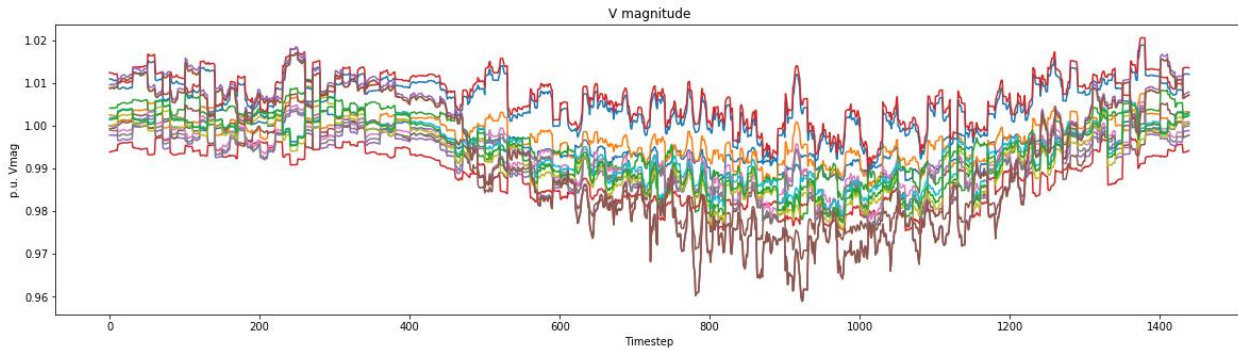
8 - Standard



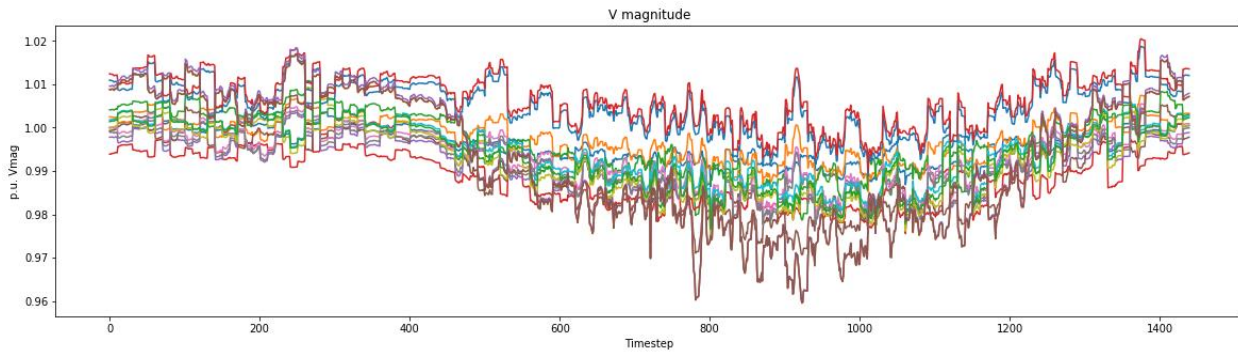
8 - Strict



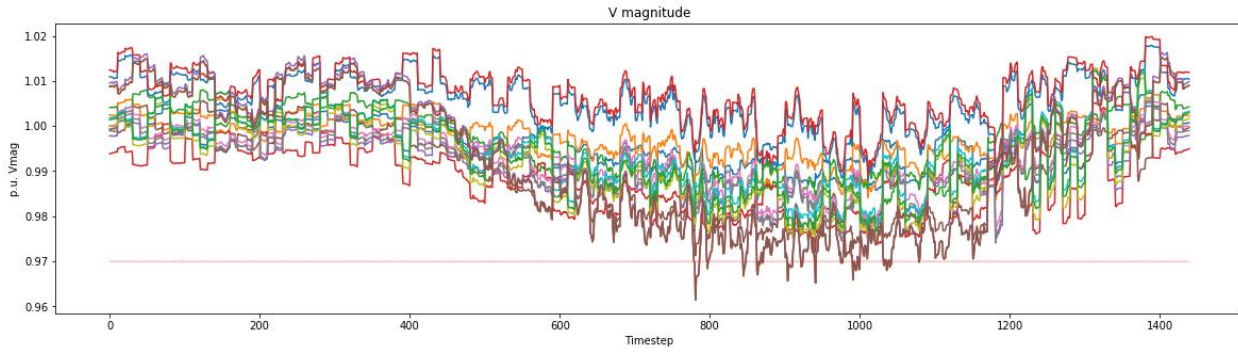
9 - Standard



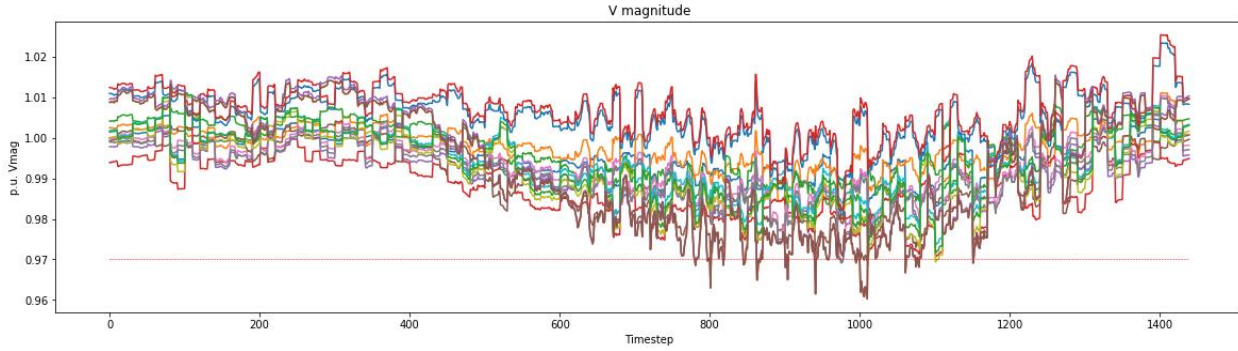
9 - Strict



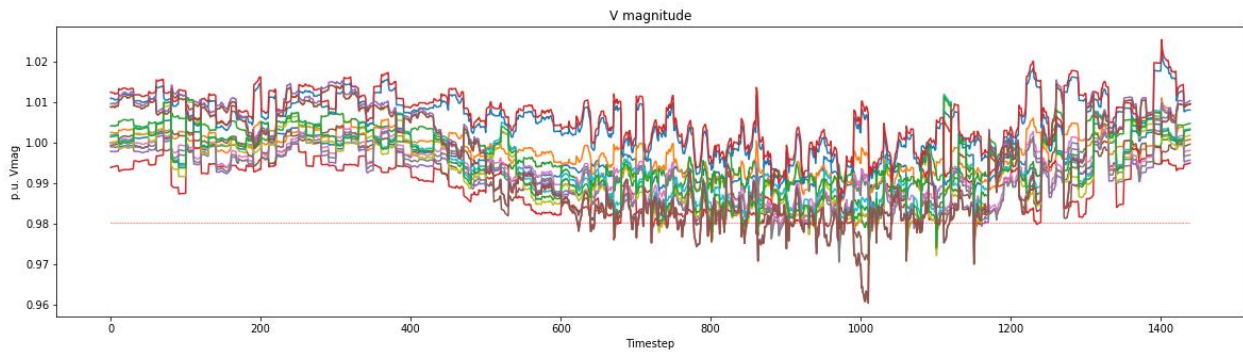
10 - Standard



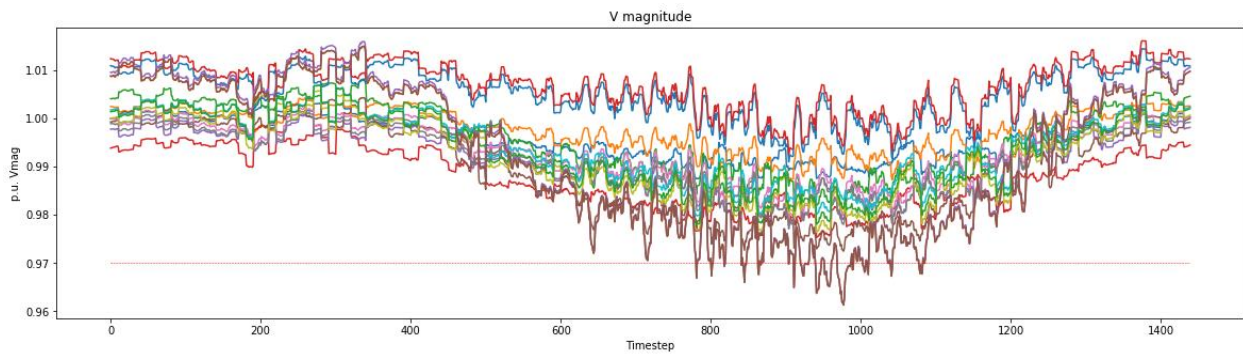
11 - Standard



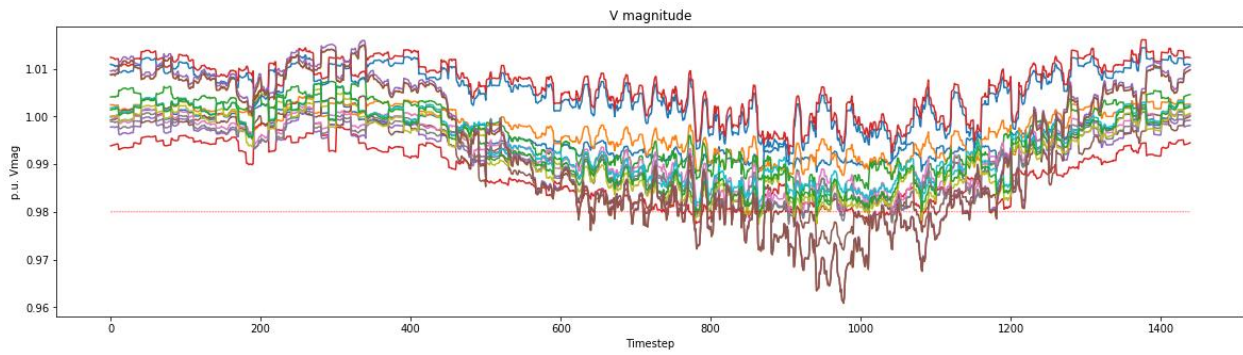
11 - Strict



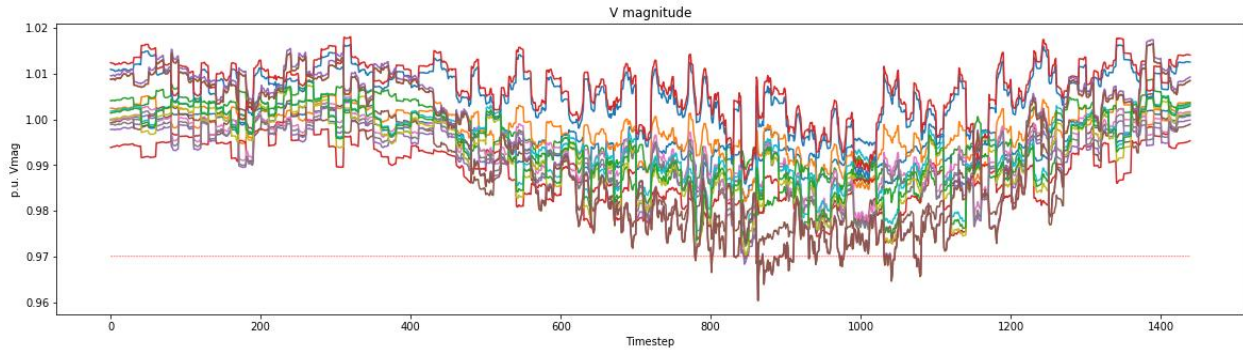
12 - Standard



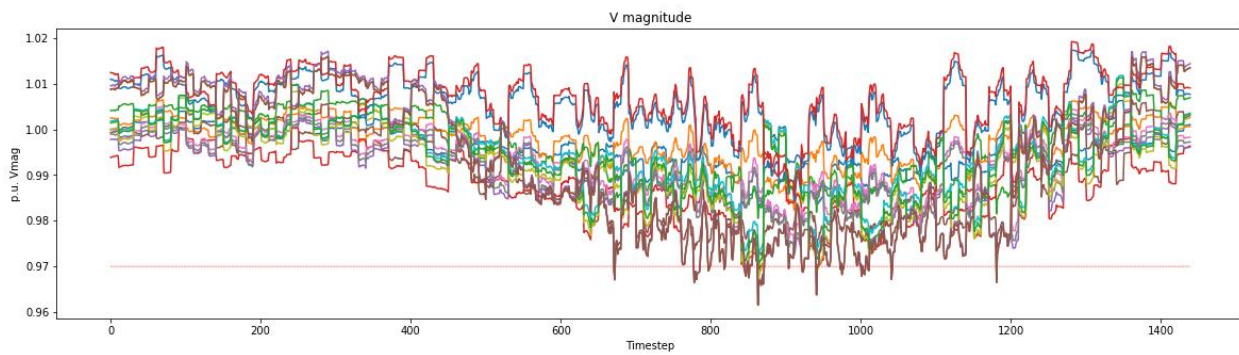
12 - Strict



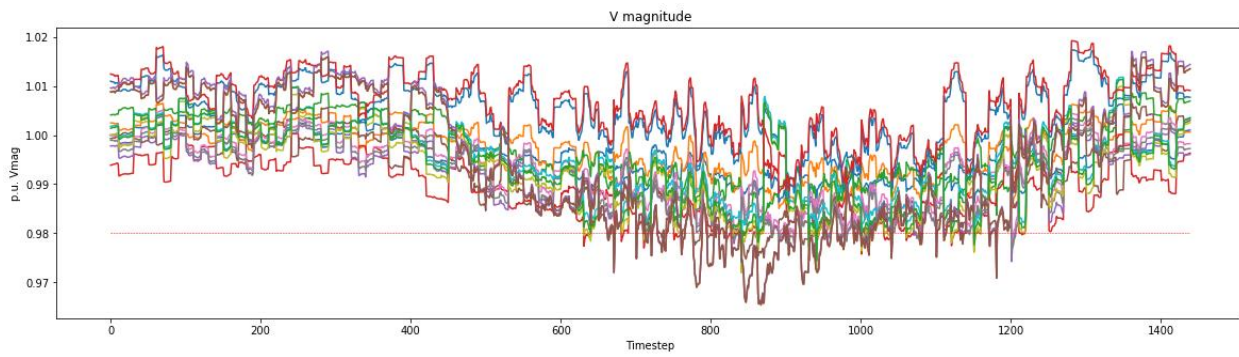
13 - Standard



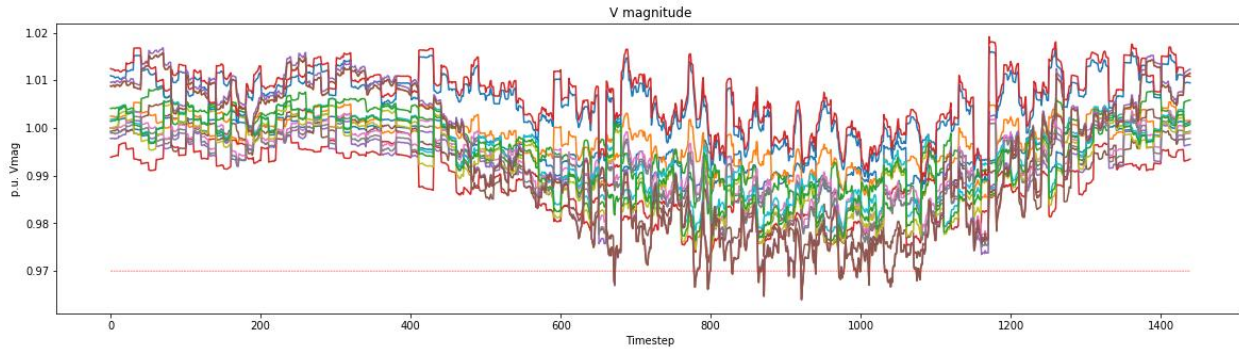
14 - Standard



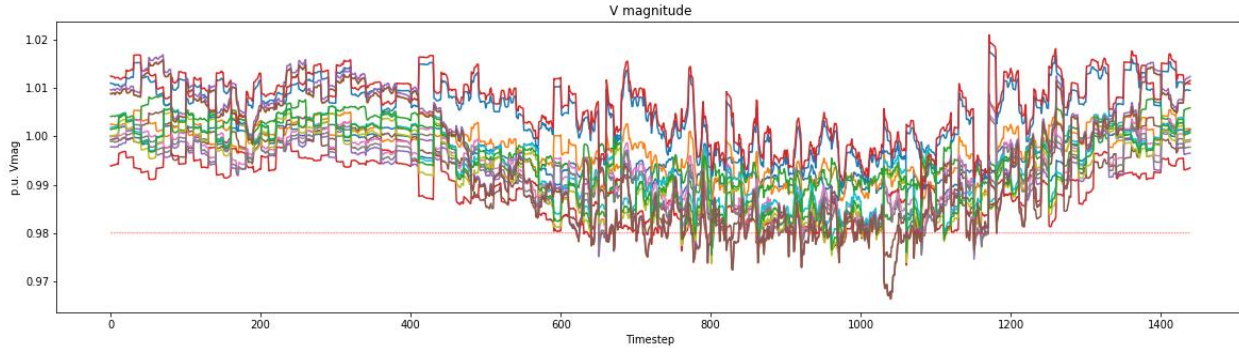
14 - Strict



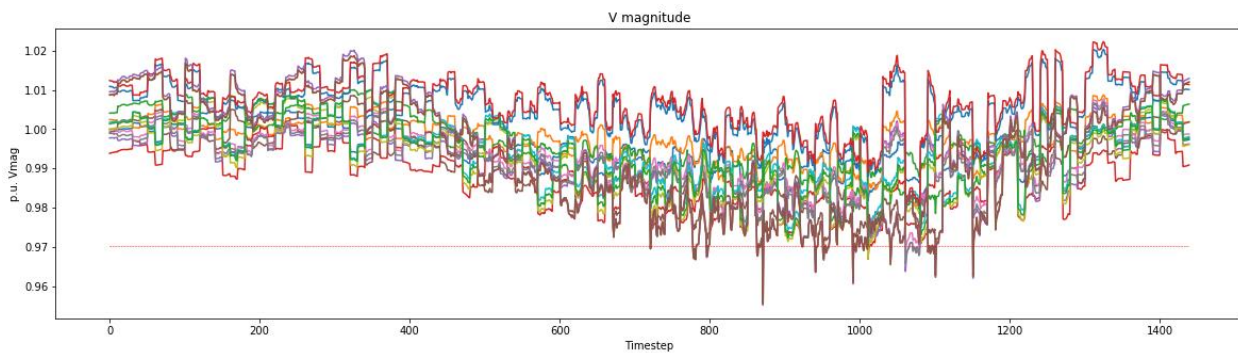
15 - Standard



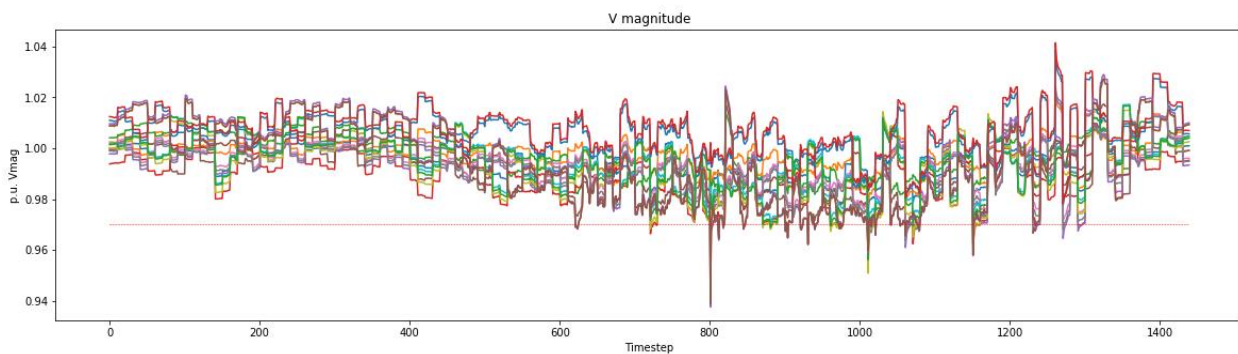
15 - Strict



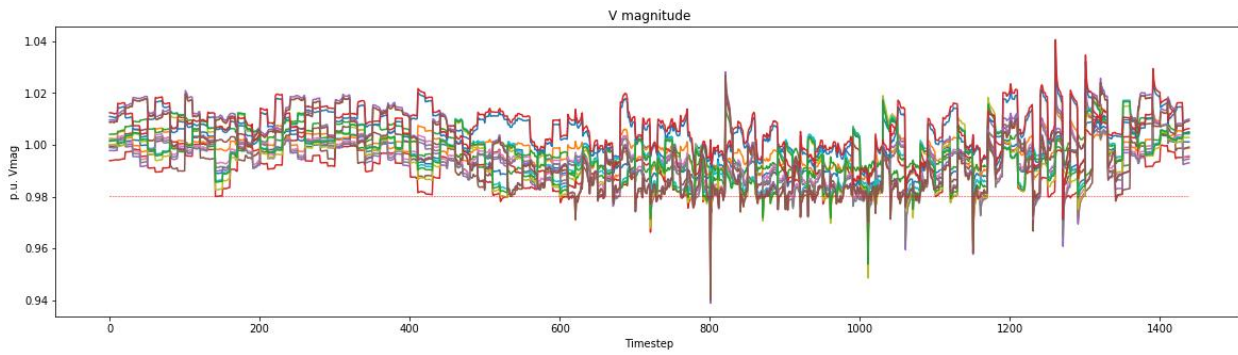
16 - Standard



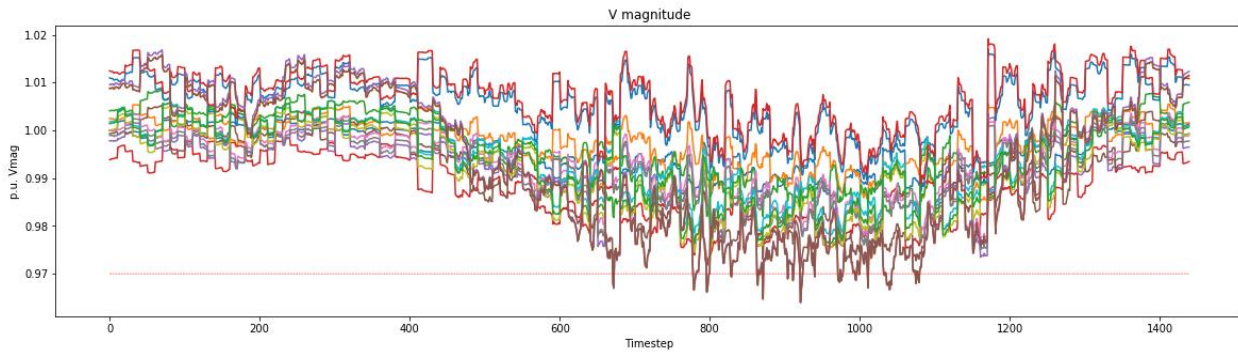
17 - Standard



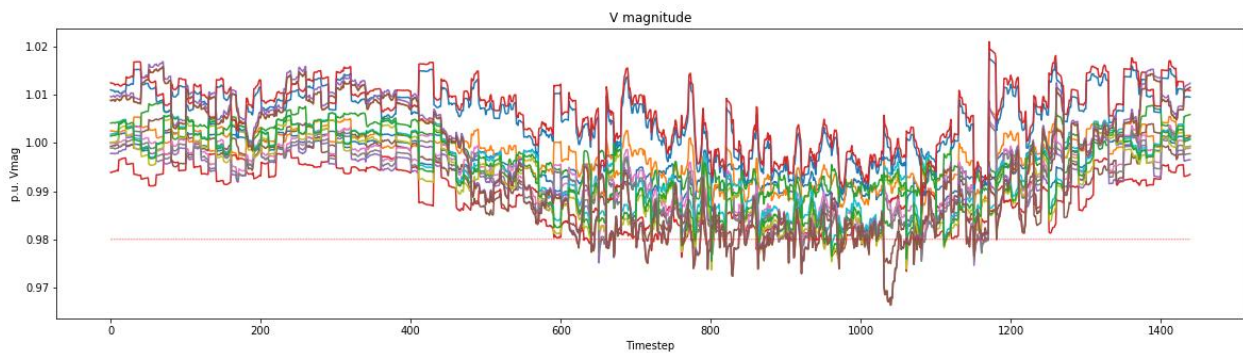
17 - Strict



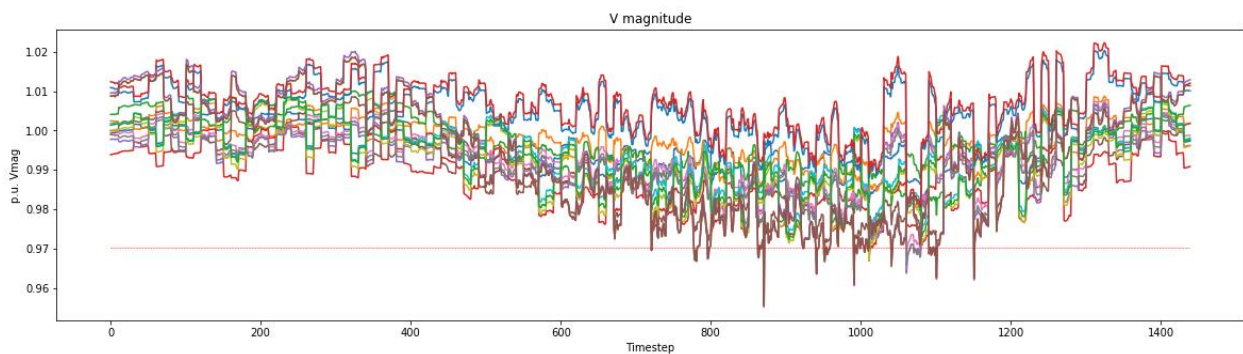
18 - Standard



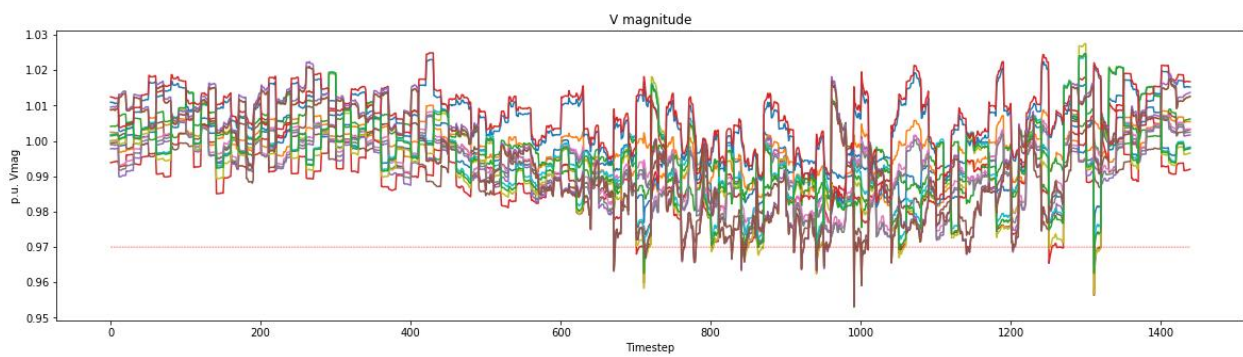
18 - Strict



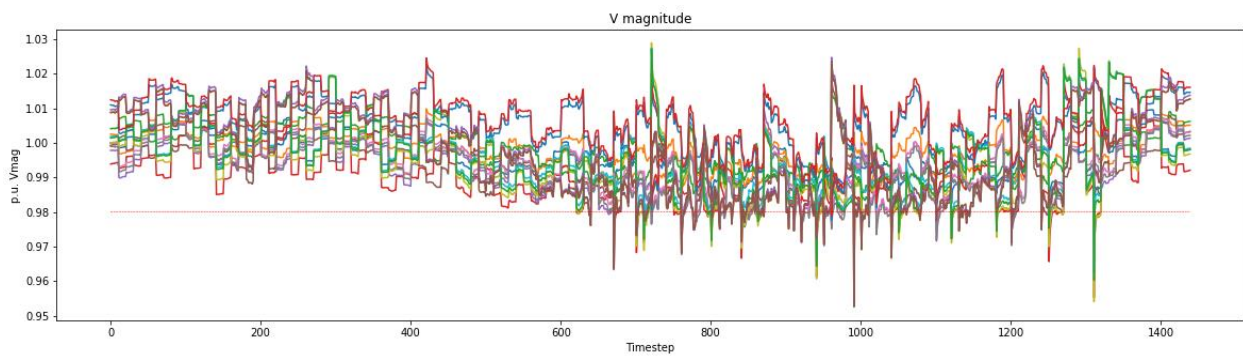
19 - Standard



20 - Standard

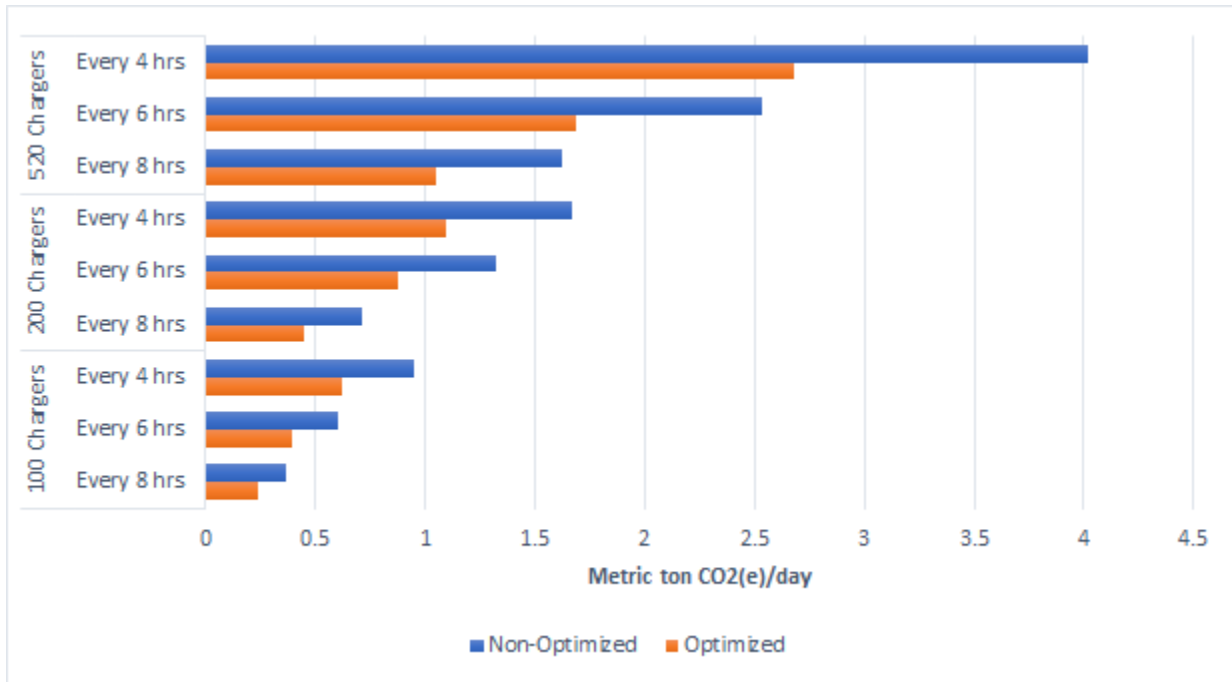


20 - Strict

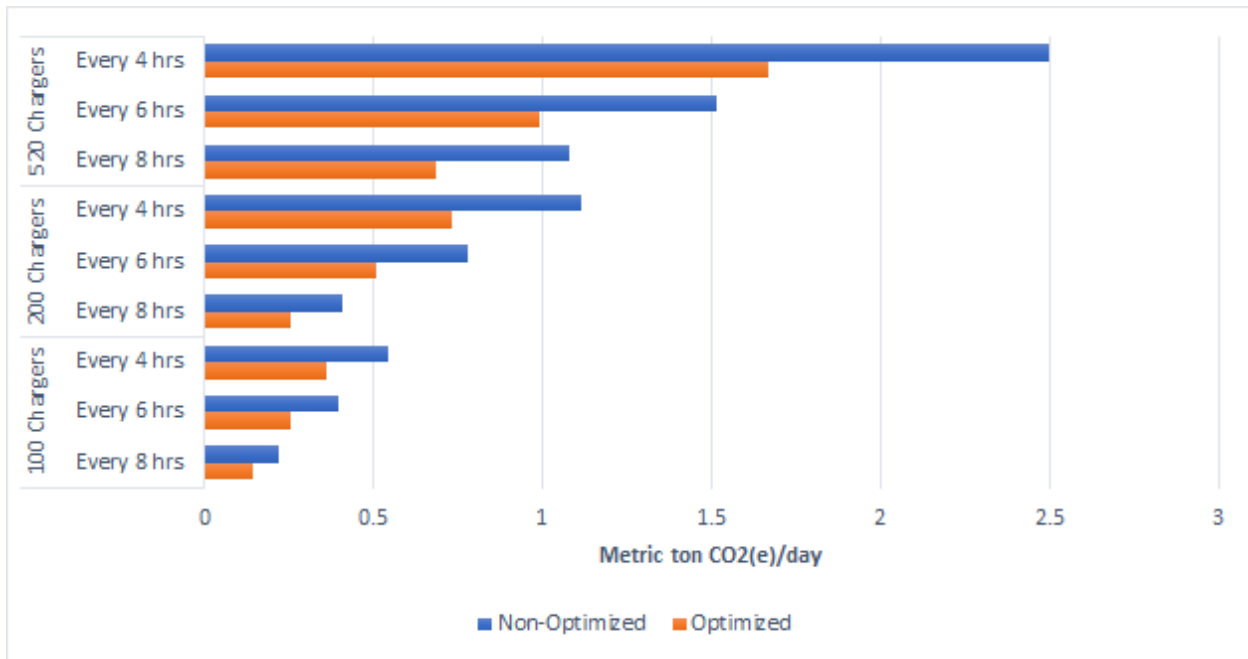


Appendix F: Graphs of Carbon Intensity for EV Penetration & Arrival Intensity Scenarios Excluding Discharge to the Grid

Winter Carbon Intensity of CA Electric Grid



Summer Carbon Intensity of CA Electric Grid



University of California, Berkeley
Civil and Environmental Engineering Department
CE 295 Energy Systems and Control

Final Project

Where to charge if not at home? Optimal Location of EV charging stations



Oscar Yllan Garza

Jonathan Kestelman

Arthur Labarre

Laetitia Moine

German Perea

Sena Soysal

Berkeley, Spring 2020

Abstract

As we are replacing Internal Combustion Engine (ICE) vehicles with electric vehicles (EVs) we are faced with the problem of how to properly charge them. An EV is very different from an ICE because an EV requires a lot more time to charge compared to just going to the gas station, and getting gasoline for ICE cars. Previous California governor Jerry Brown has set a goal of 1.5 million clean-energy vehicles on California's roads by 2025. Therefore, the development of electric vehicle infrastructure will be imperative to assure the feasibility of this goal. This project focuses on developing a Markov Chain model to analyze the best type of locations to implement charging stations. It will enable to reduce emissions deriving from ICE and increase the reliability of EV charging for the users. The model assesses the time spent by users commuting and parking in different types of locations throughout their daily routine. This allows us to decide the best locations to implement chargers and reduce the energy being consumed during times that solar and wind power aren't being generated.

Motivation & Background

As a group of concerned engineers, we care about reducing carbon emissions. There are many initiatives for replacing Internal Combustion Engines with Electric Vehicles, but there is not enough work done on where to install charging stations. According to the *Inventory of the U.S. Greenhouse Gas Emissions and Sinks 1990–2017*, transportation accounted for the largest portion (29%) of total U.S. GHG emissions in 2017 ([1] EPA, 2019). Therefore, electric vehicles offer a great chance to reduce GHG emissions from the transportation sector but necessitate the placement of optimal charging stations to satisfy their needs. The location of the EV charging stations must be designed in order to maintain high utilization rates and satisfy the needs of customers. However, the impact imposed on the local electrical grids distribution network should be considered as well. With the development of the Zero-Emission Vehicles in California - having 1.5 million clean-energy vehicles on California's roads by 2025 - the process of developing a smarter grid and planning for better electrical consumption patterns will be essential to allow the State of California to achieve these goals in an efficient way.

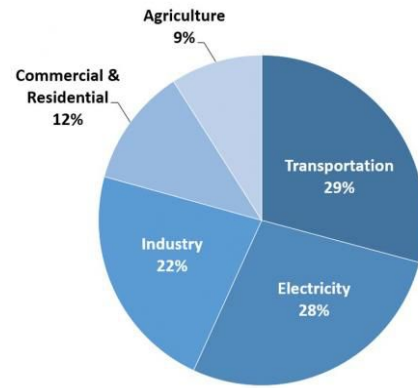


Figure 1. Total U.S. Greenhouse Gas Emissions by Economic Sectors in 2017 [1]

Relevant Literature

[2] Wang, Yue, and David Infield. "Markov Chain Monte Carlo simulation of electric vehicle use for network integration studies." *International Journal of Electrical Power & Energy Systems* 99 (2018): 85-94.

This paper explores EV's patterns of use for system and operation planning. Driving patterns were simulated using the UK 2000 time of use survey (referencing use of privately owned vehicles from 4am to 3:50am the next day with 10-min resolution) and a time-inhomogeneous Markov Chain method with 4 states

(driving, parking home, parking at work, parking at commercial area). The simulated patterns were used to assess the impact of EV charging on the network through two scenarios: home and work charging. In the case of uncontrolled charging at work, appropriate transformers can accommodate for the demand. For the home charging scenario, uncontrolled charging exceeds voltage tolerance at 99% confidence in both week and weekend charging scenarios (between 6-11pm). This paper demonstrates the need for controlled-charging which can be achieved by taking advantage of parking time at work to charge one's EV.

[3] Shepero, Mahmoud, and Joakim Munkhammar. "Spatial Markov chain model for electric vehicle charging in cities using geographical information system (GIS) data." *Applied Energy* 231 (2018): 1089-1099.

This paper focuses on modeling the charging load of EV's in cities by developing a time-dependent Markov Chain model based on three distinct charging profiles: home, work and other. To determine the charging profile of the charging stations, the paper explores geospatial data to spot certain types of buildings (parkings, housing, etc.). More specifically, charging stations are created according to building types locations. Then, the markov chain model estimates the current state of EVs which correspond to a parking type. Finally, the charging load of each station is evaluated based on the number of EVs allocated, and two scenarios: opportunistic charging or mostly home charging. Authors concluded several things: they noted that the higher the charging power, the higher variability in the charging load of the EVs. Indeed, they mostly highlight the challenge and potential danger of many EVs charging simultaneously. In their study case, if only 3% of EVs used fast chargers at the same time, this caused a sudden 1.2MW of charging load. All in all, this paper highlights the challenge of potential ramping up demand during peak hours if policies are not enforced to ensure opportunistic charging.

One can easily highlight recurrent trends from the above mentioned literature and more generally, from optimal EV charging stations placement publications. Obviously, the use of Markov chains is almost ubiquitous but more precisely, it is the combination of data and Markov chains models to predict human behaviors that is very widely used. From this first observation, one can also notice the dichotomy most publications make between home and work, and their effort to quantify potential charging time in each of these locations. Moreover, most publications raise questions from real-world data using either or both surveys and geographical data. More importantly, the literature is based on open-ended questions which are motivating our project, such as: how to distribute EV chargers to encourage opportunistic charging? How can we use our current infrastructures smartly for the increase in EVs adoption? In which locations would people be more inclined to charge their EV? Besides their home, are there any places in which people spend sufficient time during the day to allow for EV charging? How can we combine emissions reduction and EV charging?

Focus of this Study

The focus of this study is to model daily routes taken by different individuals in order to analyze the ideal locations for electric vehicles charging station placement. Using Markov Chains, it is possible to represent the different commutes and how much time people spend in specific locations throughout their days. It will enable to issue recommendations concerning preferable charging stations locations which encourage EV adoption and reduce GHG emissions deriving from the transportation sector.

Technical Description

1. Introduction to Markov Chains

This project focuses on developing a Markov Chain Model to analyze the best type of locations to implement charging stations and increase the reliability for users. A Markov Chain is a mathematical system in which probabilistic rules govern transitions from one state to another.

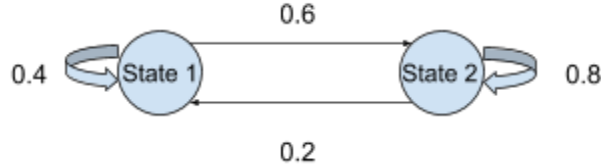


Figure 2: State transition diagram with two states: $X_k \in \{1,2\}$

One of the main characteristics of Markov Chains is that it is only the current state and time that rule the probability of transitioning to another state: this probability does not depend on previous states. This specific feature is often called the Markov Property and makes Markov Chains particular stochastic processes. In words, “The future is conditionally independent of the past, given the present.”. In mathematics:

$$\Pr [X_{k+1} = i_{k+1} \mid X_k = i_k, X_{k-1} = i_{k-1}, \dots, X_0 = i_0] = \Pr [X_{k+1} = i_{k+1} \mid X_k = i_k]$$

Our Markov chain is essentially a series of state transitions throughout a day on a 10-min basis and is constituted of four states: ‘driving’ (D), ‘parking at home’ (H), ‘parking at work-place’ (W), and ‘parking at other areas’ (exercise, shopping, medical activities, religious activities, bank activities, meals) (O). The transitions between any two different parking locations requires vehicle driving. The Markov Chain diagram shown in Figure 3, represents the vehicle state transition from time step t-1 to t, between the four illustrated states, {D, H, W, O}.

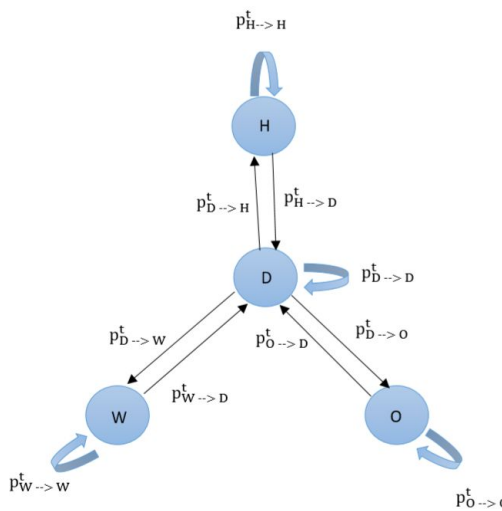


Figure 3: Markov Chain Diagram of possible vehicle state transitions at time t

A transition probability matrix enables to obtain the probability of the vehicle being in a certain state at step t, given his last state at time step t-1. For instance, element (2,1) in the transition probability matrix of Figure 4 indicates the probability of the vehicle being in state ‘W’ at t, given its precedent state ‘H’, at time t-1.

$$T^t = \begin{bmatrix} p_{W \rightarrow W}^t & p_{W \rightarrow H}^t & p_{W \rightarrow D}^t & p_{W \rightarrow O}^t \\ p_{H \rightarrow W}^t & p_{H \rightarrow H}^t & p_{H \rightarrow D}^t & p_{H \rightarrow O}^t \\ p_{D \rightarrow W}^t & p_{D \rightarrow H}^t & p_{D \rightarrow D}^t & p_{D \rightarrow O}^t \\ p_{O \rightarrow W}^t & p_{O \rightarrow H}^t & p_{O \rightarrow D}^t & p_{O \rightarrow O}^t \end{bmatrix}$$

Figure 4. Transition Probability Matrix at time step t

The sum of the transition probabilities along each row of the transition probability matrix must be equal to one. Therefore:

- $p_{W \rightarrow W}^t + p_{W \rightarrow H}^t + p_{W \rightarrow D}^t + p_{W \rightarrow O}^t = 1$
- $p_{H \rightarrow W}^t + p_{H \rightarrow H}^t + p_{H \rightarrow D}^t + p_{H \rightarrow O}^t = 1$
- $p_{D \rightarrow W}^t + p_{D \rightarrow H}^t + p_{D \rightarrow D}^t + p_{D \rightarrow O}^t = 1$
- $p_{O \rightarrow W}^t + p_{O \rightarrow H}^t + p_{O \rightarrow D}^t + p_{O \rightarrow O}^t = 1$

As we are making our study on a 24-hour period and on a 10-minute basis, there are 144 time steps of 10 minutes and therefore 144 transition matrices.

2. Data Set

In this project, we are using a data set from the National HouseHold Travel Survey (<https://nhts.ornl.gov/>), which provides us with information regarding household travel by car and SUV, from April 2016 to April 2017. This dataset covers the entire country, but we decided to focus on the states of California, New York and Maine.

We extracted different valuable variables for our project, from the "trippub.csv" file and used the information provided by the file into the format that would be the most useful for the Markov Chains in this project. The process involved transforming household trips into individual sessions and then for the same users, to build the dataframe with the different timesteps and locations for each step.

- **Variables allowing to identify each session:** *HOUSEID*, *PERSONID*
Apart from that, we created a **new variable** *SESSIONID*, which joins both *HOUSEID* and *PERSONID*. For example, if for the household *HOUSEID* = “3”, there are two drivers, with respectively the IDs *PERSONID* = “1” and *PERSONID* = “2”, these individuals will be respectively identified by *SESSIONID* = “3_1” and *SESSIONID* = “3_2”.
- **Variables allowing to know the start and end times of the trip:** *STRRTIME* (Trip Start Time), *ENDTIME* (Trip End Time)
- **Variable allowing to know how much time the trip takes:** *TRVLCMIN* (Trip Duration in Minutes)
- **Variable allowing to know how much time an individual remains in a location:** *DWELTIME* (Time at Destination)
- **Variables allowing to know from which location the individual comes from and where he/she is heading:** *WHYFROM* (Trip Origin Purpose), *WHYTO* (Trip Destination Purpose)

- **Variable which gives information on the trip mode:** *TRPTRANS* (Trip Mode Derived). We only deal with data for which the trip modes are “car” or “SUV”.

3. Data Processing

a) Formatting user data into states at time steps for Markov Chains

The first step of our technical work consisted in processing the above mentioned dataset. More generally, we aimed at formatting user data into Markov chain states and divide the dataset into different time steps, for us to develop a time-dependent Markov chain model. The process to preprocess the data can be described as transforming survey data based on household trips into a list with 144 locations (one for each 10 minutes of the day) for every user. The operations made on the original dataset can be detailed as:

- 1) Choosing relevant modes of transportation (cars, pickups, SUVs, etc.)
- 2) Filtering by states (in our case CA, NY and ME)
- 3) Transforming military time to time of the day
- 4) Creating states for Markov chains (from the numbers denoting home, work, etc. in the dataset)
- 5) Removing locations considered as not relevant for our study
- 6) Dividing dataset into 10mn time steps and creating markov chains states information for each (i.e. defining a user’s location at each time step)

	Session_ID	Start_Minute	End_Minute	WHYTRP1S	TRPMILES	WHYFROM	DWELTIME	WHYTO	TRAVDAY
0	30000492_1	645	690	Other	37.384	Home	60	Other	1
1	30000492_1	750	780	Other	3.891	Other	30	Other	1
2	30000492_1	810	816	Other	1.112	Other	69	Other	1
3	30000492_1	885	940	Home	33.889	Other	200	Home	1
4	30000492_2	605	645	Other	37.247	Other	105	Other	1

Figure 5: Dataset after step 5 and before step 6

b) Markov chains time-variant transition matrices probability calculations

Building on the definition of Markov chains given before and on some relevant literature’s process [2], let us detail the method we used in this project to build our transition matrices and obtain a time-dependent Markov chain model. As said before, our newly obtained dataset is made of 144 time steps of 10mn for which the locations of all users is provided. To put it differently, for a given 10mn time step t , all users are located in one of the four markov chain states: [Home, Work, Driving, Other]. Thus, for the same time step, the definition of the transition matrix yields:

$$T^t = \begin{bmatrix} p_{W \rightarrow W}^t & p_{W \rightarrow H}^t & p_{W \rightarrow D}^t & p_{W \rightarrow O}^t \\ p_{H \rightarrow W}^t & p_{H \rightarrow H}^t & p_{H \rightarrow D}^t & p_{H \rightarrow O}^t \\ p_{D \rightarrow W}^t & p_{D \rightarrow H}^t & p_{D \rightarrow D}^t & p_{D \rightarrow O}^t \\ p_{O \rightarrow W}^t & p_{O \rightarrow H}^t & p_{O \rightarrow D}^t & p_{O \rightarrow O}^t \end{bmatrix}$$

The definition of markov chains implies conditional probabilities which can be used to define the terms from the above matrix. For example:

$$p_{W \rightarrow W}^t = P[W^t | W^{t-1}] = \frac{N_{W \rightarrow W}}{\sum_{i=1}^4 N_{W \rightarrow i}}$$

$$p_{H \rightarrow O}^t = P[O^t | H^{t-1}] = \frac{N_{H \rightarrow O}}{\sum_{i=1}^4 N_{H \rightarrow i}}$$

Where $N_{W \rightarrow W}$ denotes the number of transitions from work at time step (t-1) to work at time step t, and $N_{H \rightarrow O}$ denotes the number of transitions from home at time step (t-1) to other at time step t.

For the initial definition of the Markov Chain, we first created a simple version that would take into account the probabilities of transitioning between two states by considering only the two states (the initial and end ones). In order to assess the correlation between the steps that influence the location a user is at time step t, we look at the correlation graphs (one for each location, since it depends on the data being used). Below is shown the correlation graphs from each state based on NY State data. The plots show the lag on the x-axis and the correlation values (from zero to one) on the y-axis. We tested the correlation for each specific location.

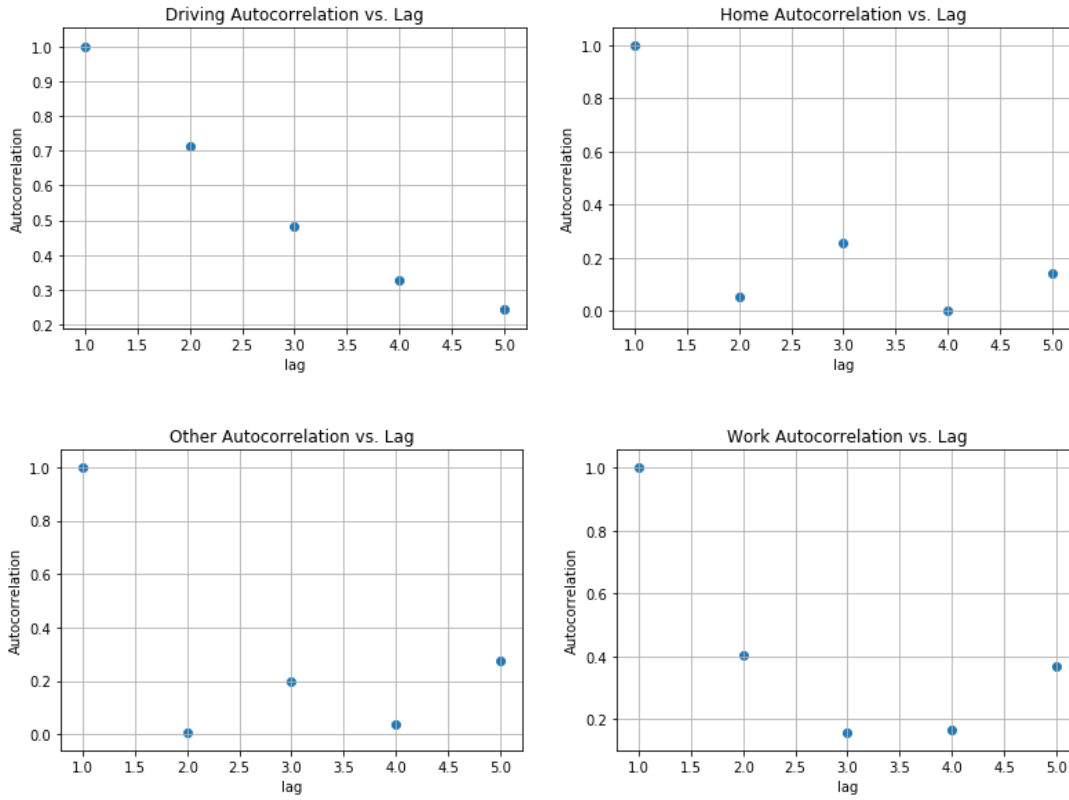


Figure 6: Autocorrelation vs. lag for each location/state.

The graphs above in Figure 6 show the correlation vs. lag plots for NY data. As the graphs show, there is some Driving has some significant correlation with previous steps. In addition, for the other three states, we can see that at least lag = 2 or lag = 3 has some significant impact and could be considered. This analysis led the team to consider two steps correlation for all the simulations and consequently the analysis after that.

c) Markov Chain Simulation and data generation.

We generated our data with some initial assumptions for the starting probability at a specific location. At first we assumed a 25% chance for a person to start at each location. We used the results of the first day simulation for the second day in order to further improve the simulation results. For example, in a simulation with 1,000 people, we had around 250 people at each location for $t = 0$ and by the end of the first day simulation the values reached the ‘asymptote’ for the end of the day. The distribution by time step $t = 142$ and $t = 143$ had: around 74.4% of our population at Home, 0.3% Driving, 22.5% at Work and 2.8% at Other locations. The stabilization on the first day was done to get more realistic results for the future days. The team recognizes that the process of updating the initial ratios for each location can change for a few iterations, but getting this measure very accurate was not a focus of the team.

4. Data Analysis

a) Overall time spent during one day

In order to choose optimal locations of the EV charger, we should analyze where people spend their time and how much time they spend at a certain type of location in a given day. For instance when we observe a peak at 13 hours for “Home” state, 3 and 11 hours for “Work” state, 0.75 hours for “Driving” state and 3.6 and 8 hours for “Other” state. When we look at the average values we observe that people spend 11.26 hours at home, 5.19 hours at work, 0.75 hours driving, 6.78 hours at other locations. From that we can conclude that people spend most of their time “home” and “work”. This analysis gives us insights on EVs possible plug-in duration depending on location and. However, we just calculate the total time they spend at each location in a given day. We don’t consider the consecutive time at each location. It will be considered in the next section.

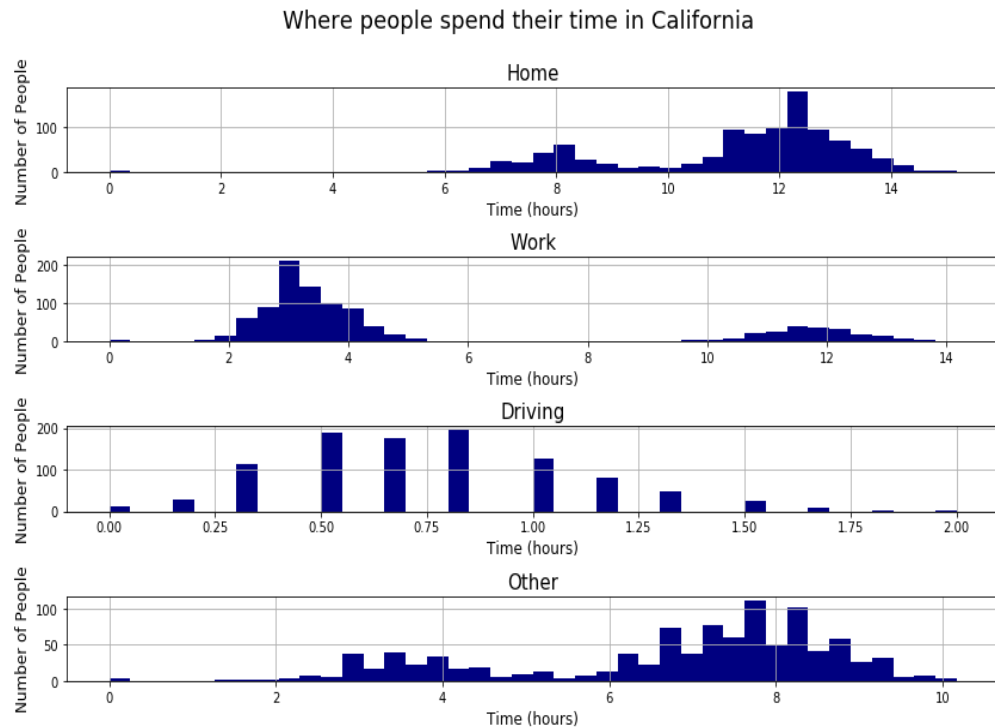


Figure 7: Where people spend their time in California

The figure below gives the average, min, max and standard deviation of time spent in each state/location for California.

AVERAGE - HOURS SPEND IN CA		MAX - HOURS SPEND IN CA	
Count_Home	11.264833	Count_Home	15.166667
Count_Work	5.195333	Count_Work	14.166667
Count_Driving	0.757500	Count_Driving	2.000000
Count_Other	6.782333	Count_Other	10.166667
dtype: float64		dtype: float64	
MIN - HOURS SPEND IN CA		STD - HOURS SPEND IN CA	
Count_Home	5.833333	Count_Home	1.979444
Count_Work	1.666667	Count_Work	3.586702
Count_Driving	0.000000	Count_Driving	0.334581
Count_Other	1.500000	Count_Other	1.920468
dtype: float64		dtype: float64	

Figure 8: [Average, Maximum, Minimum Hours of Time People spend in each state/location]

To obtain Figure 8 below, we used the simulation with 1,000 users from the markov chains and plotted the number of people at each state in a given time of the day. We start our analysis with the initial distribution probabilities of home: 0.7440, work: 0.2255, other: 0.0270 and driving: 0.0035 at midnight. For instance, in the results we obtain that the peak number of people at work is at 1:20 PM with 400 people while the people at home is lowest during that time. This model assesses the time spent by users commuting and parking in different types of locations throughout their daily routine.

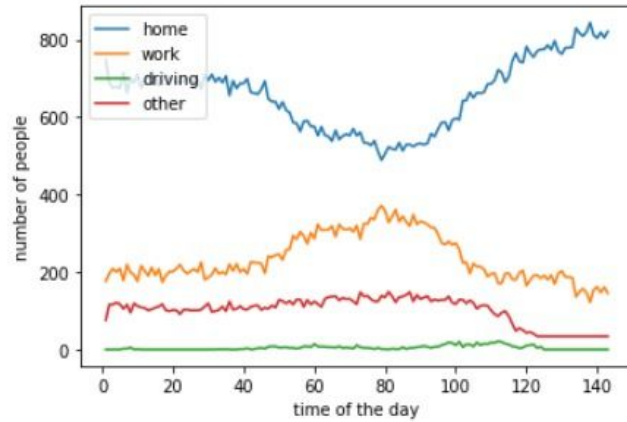


Figure 9: The number of people at each location during each 10-min time step of the day

With this analysis, we explained the overall time spent in each location in a given day. These results enabled us to have a general understanding of the locations/states in which people spend more time during the day. In the next section we will analyze the same data set considering consecutive times.

b) Consecutive time analysis (two days period)

In the previous section, we explained our results on the overall time spent in each location during one day. These results enabled us to have a general understanding of the locations in which people spend more time during the day. However, to be able to charge an EV, it is primordial to know the consecutive times spent in a location. Indeed, a vehicle that spends a total of 3 hours in a certain location but only with 10 minute intervals and a vehicle that spends 3 hours straight in a location, won't be able to use the charging station the same way. Therefore, obtaining consecutive times spent in each location is necessary. In our dataset, the first time step is at 00:00 am and the last one, at 11:50 pm. Therefore, to be able to take into account the entire consecutive times

spent during the night without having any cut between before and after midnight, we worked with a two-day period dataset, so with 288 time-steps. The different steps to get these consecutive times can be detailed as:

- 1) Read the dataset in which, for each user and time step the location is given.

0	1	2	3	4	5	6	7	8	9	...	278	279	280	281	282	283	284	285	286	287
0	Work	Work	Work	Home	Other	Work	Work	Work	Work	...	Home	Home	Home	Home	Other	Home	Home	Other	Home	Work
1	Work	Home	Work	Work	Work	Work	Work	Work	Home	Work	...	Home	Home	Home	Home	Home	Home	Home	Home	Home
2	Home	Other	Home	Home	Home	Other	Home	Other	Other	Work	...	Home	Home	Home	Home	Home	Home	Home	Home	Home
3	Home	Work	Work	Work	Work	Other	Work	Home	Work	Work	...	Home	Other	Home	Home	Home	Other	Home	Home	Home
4	Work	Work	Driving	Work	Home	Work	Work	Work	Work	Home	...	Home	Other	Home	Home	Home	Home	Home	Other	Home
...
995	Other	Home	Home	Home	Home	Home	Home	Other	Other	Home	...	Home	Work	Home	Home	Home	Home	Home	Other	Home
996	Home	Home	Other	Home	Other	Home	Home	Other	Other	Home	...	Home	Home	Home	Home	Home	Home	Home	Home	Home
997	Home	Home	Home	Work	Home	Home	Other	Other	Work	Home	...	Home	Home	Other	Home	Work	Other	Home	Home	Work
998	Home	Home	Home	Other	Home	Other	Home	Home	Work	Home	...	Other	Other	Home	Other	Home	Home	Home	Home	Home
999	Home	Home	Work	Home	Home	Home	Home	Home	Home	Home	...	Home	Other	Home	Home	Home	Driving	Home	Home	Other

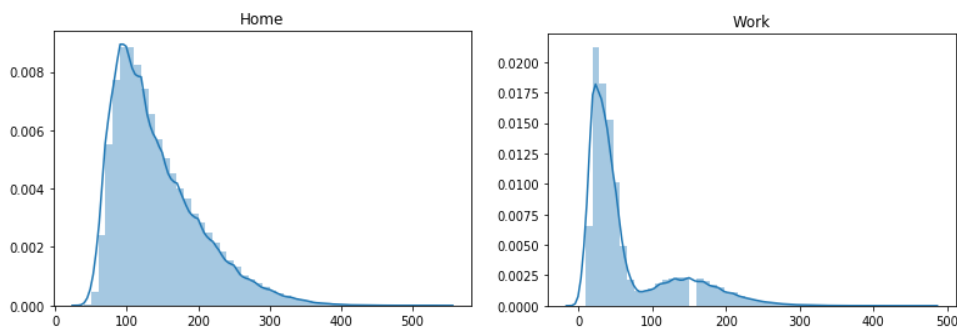
Figure 10: Used Dataset

- b) For each user, we first created four empty lists corresponding to the consecutive times lists of the four possible locations.
- c) Since each time step is equal to 10 minutes, we added 10 minutes to the corresponding location list each time the cursor was on this location.
- d) For each location and user, we took the maximum of the corresponding list, that we added to a new list, constituted by the maximum time spent in this location by each user.
- e) Therefore, in the end we had four lists - one for each location - of the maximum of consecutive times spent in the corresponding location by each user.

We did this same process for the three American states that we chose: California, Maine and New York. For the state of California, the plots below in Figure 11 show the distribution of the consecutive times spent in minutes, for the four locations:

X-axis: consecutive times spent in minutes

Y-axis: PDF



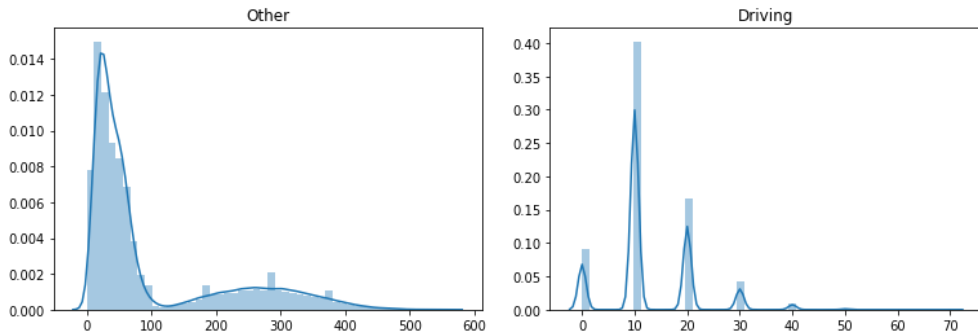


Figure 11: Distribution of the consecutive times spent in minutes, in California, for the four locations

The plots for Maine and New York can be found in Appendix 1. The values and plots obtained for the different American states were resulting in very similar distributions of time spent at each location. Therefore, as shown by the results, doing the same process for different American states might not be necessary to understand an overall behavior. This conclusion is only true for our simplified model with four possible states/locations. The results would maybe be different if we consider more states/locations. For example, new states could be created for shopping and school, instead of reuniting them respectively in “Other” and “Work”.

c) Emissions and time to charge

With the data generated by the simulation of Markov chains and the one available on the California ISO website on energy demand, supply and GHG Emissions, we have been able to calculate the total GHG emissions from a given number of ICEs and EVs, in California. GHG emissions depend on the amount of energy supplied by the grid at different times of the day and the source of energy used. This is why it is important to take into account the actual users’ behaviour.

Comparison between the GHG emissions from a sample of 1,000 EVs and 1,000 gasoline vehicles

On the California Independent Systems Operator (CAISO) website, data concerning the current and past supplied energy in California, along with the corresponding GHG emissions, actualized every 5 minutes, is provided.

Cleaning the Data

To determine the GHG emissions of one unique day we took an average of emissions in California, on seven days.

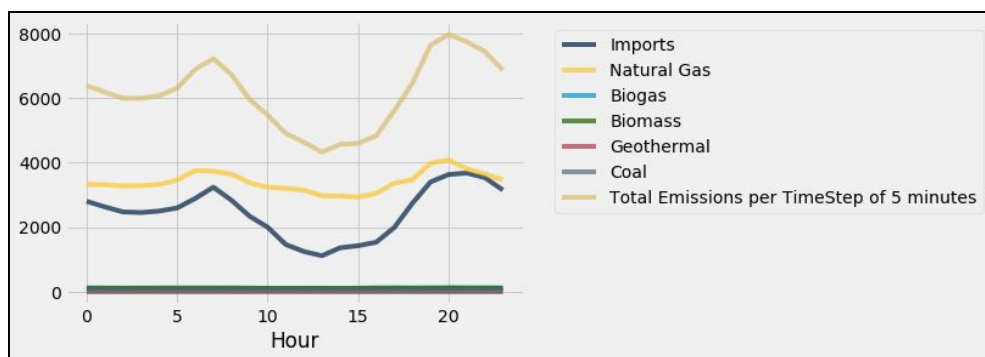


Figure 12: Emission in metric tons of CO₂/hour actualized every 5 min

Thanks to CAISO data, we have been able to generate the plot on Figure 12. According to this figure, the total emissions of CO₂ decrease between minutes 400 and 1100. This can be explained by the fact that, in California, renewable energies are massively used and generated during daytime. However, renewable energies also have their downsides since photovoltaic and wind energy are mainly produced during daytime. Also, during the day, users are generally at work which can reduce energy consumption since they are not using or charging their devices home.

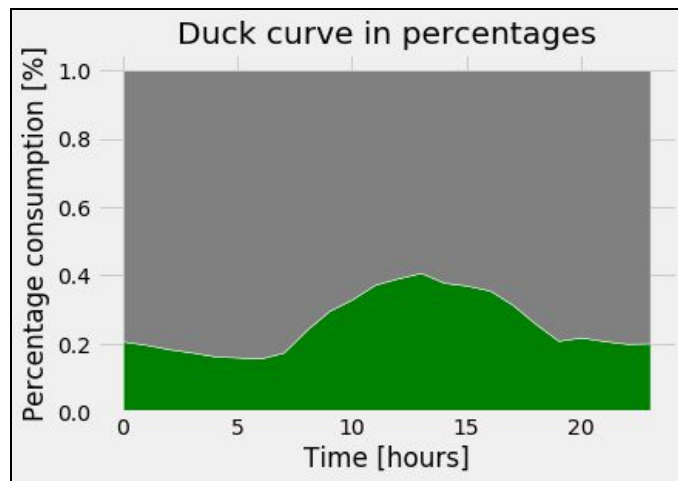


Figure 13: Percentage of consumption of renewable (in green) and non-renewable (in grey) energies

In Figure 13, the grey part represents the percentage of non renewable energy supplied to the grid and the green curve, the percentage of renewable energy supplied to the grid. We can observe that between minutes 400 and

1100, the percentage of green energy increases, which demonstrates that in California, daytime energy largely comes from ecological sources.

By taking the data generated by the Markov chain simulation, we have been able to determine, according to users' behaviour, the optimal time to charge their EV for each one of them. The different steps to determine the optimal time of the day for EV owners to charge their vehicle can be detailed as:

- 1.- Determine the consecutive times spent in each location for each user.
- 2.- With each user's driving time, we can determine the distance traveled by this user per day, since the average Californian traveler travels 0.4 mile per minute.
- 3.- With the distance traveled by the user, we can determine the power useful to the driver to charge the EV. Based on the consecutive times spent in each location for each user, we can determine what time of the day is optimal to charge their EV.

The histogram in Figure 14 represents the percentage of users who should be charging their EV at each time of the day, based on our study and their behaviour.

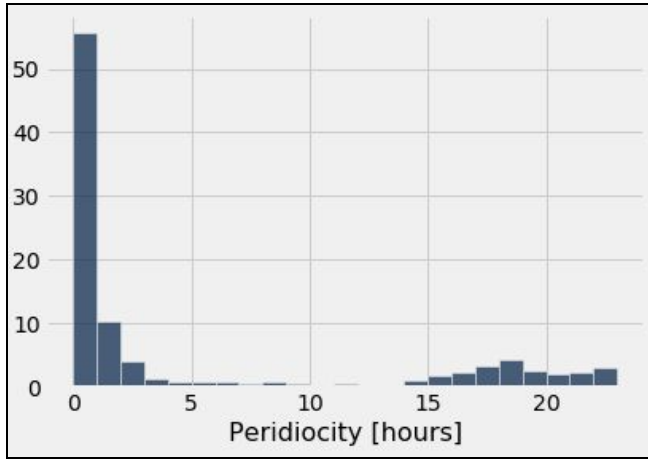


Figure 14. Percentage of users charging their vehicle throughout the day

Moreover, we have been able to compare the GHG emissions for the same user, when using an EV and an average ICE, thanks to the following information: Fuel consumption= 4.5 Liter/100km; Fuel type (Gasoline)= 2.3 kgCO₂/Liter. Figure 15 shows how many metric tons of CO₂ are emitted from the energy consumed to charge 1,000 EVs at each time step of the day. In this project for simplicity reasons, we based our study on an EV level 2 charger with a charging power of 19.2 kW.

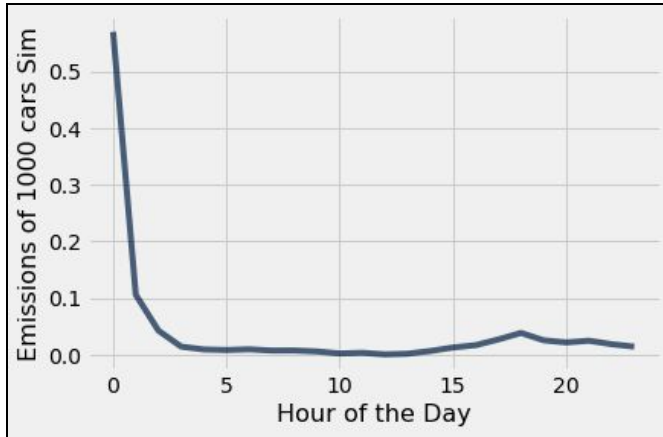


Figure 15: Emissions from the 1000 EVs, in tons of CO₂ (simulation)

Every 24h, the total emissions from 1,000 **EV charging are equal to 4.68 tons of CO₂** and for 1,000 **ICEs, they are equal to 7.61 tons of CO₂**. Therefore, there is a reduction of **2.93 tons of CO₂ per day, which results in a 38.5% reduction of emissions per day**. This shows us that even though the grid is not 100% clean in California the emissions are considerably lower when using electric vehicles.

Discussion

The results we obtained allowed the team to assess the overall process for this project. It is clear that this version 1.0 of the Markov Chain simulation and emission studies yielded a plausible result. This advances sustainability in energy systems because we can easily adapt this method to confirm to state officials and companies that the implementation of a certain amount of electric vehicles does indeed reduce the overall emissions. Even though the initial reduction comes from people charging their vehicles at night, the team was able to access the difference from internal combustion vehicles to the emissions from the electric grid. Systems and controls tools are uniquely positioned to help answer these questions and support the mathematical modelling, allowing for an effective and quick process.

Moreover, as explained in the Data Analysis section, our results would have maybe been more reliable if we had considered more states/locations. For example, new states could be created for shopping and school, instead of reuniting them respectively in “Other” and “Work”. Reducing the time-step from a 10-min basis to a 5 or 1-min basis could also allow to obtain more accurate results. This would be true since driving patterns would be better represented and less error would be brought from the original dataset. Another possible improvement for future CE295 that the team recommends is the implementation of an optimization program to further reduce the amount of emission generated by the simulated population. We believe that a program with an objective function to minimize the total amount of emission for a single individual will minimize the overall summation of emissions generated by the simulation. The program can be easily written by using constraints such as: total charging time should be greater or equal to the minimum energy necessary for the specified driving period divided by the charging rate, no negativity, and a constant power rate (for an initial optimization). Some complexity could be added by introducing the definition of emission being the SUM(Emission Value at each time step of the day * TRUE or FALSE): this would be an easy implementation but would lead to a non-convex program. Further thoughts could be put into developing this optimization program more carefully. However, this optimization program would add value to the confirmation of the methodology developed in this paper.

Table of Responsibilities

Team Members	Tasks	
Sena	Read Markov chain literature review Found data set Defined data set size	Data analysis on the overall time Data analysis on emissions
Jonathan	Read Markov chain literature review Found data set Defined data set size	Formated the data Modeled the Markov chains Data Processing
Laetitia	Read Markov chain literature review Found data set Defined data set size	Cleaned the data Modeled the Markov chains Data analysis on consecutive times
Arthur	Found Markov chain literature review Read Markov chain literature review Found data set	Defined data set size Modeled the Markov chains Data analysis on the consecutive times
German	Read Markov chain literature review Found data set Defined data set size	Simulated the Markov chains Generated Data
Oscar	Read Markov chain literature review Found data set Defined data set size	Data analysis on emissions Data analysis on the needed time to charge

Summary

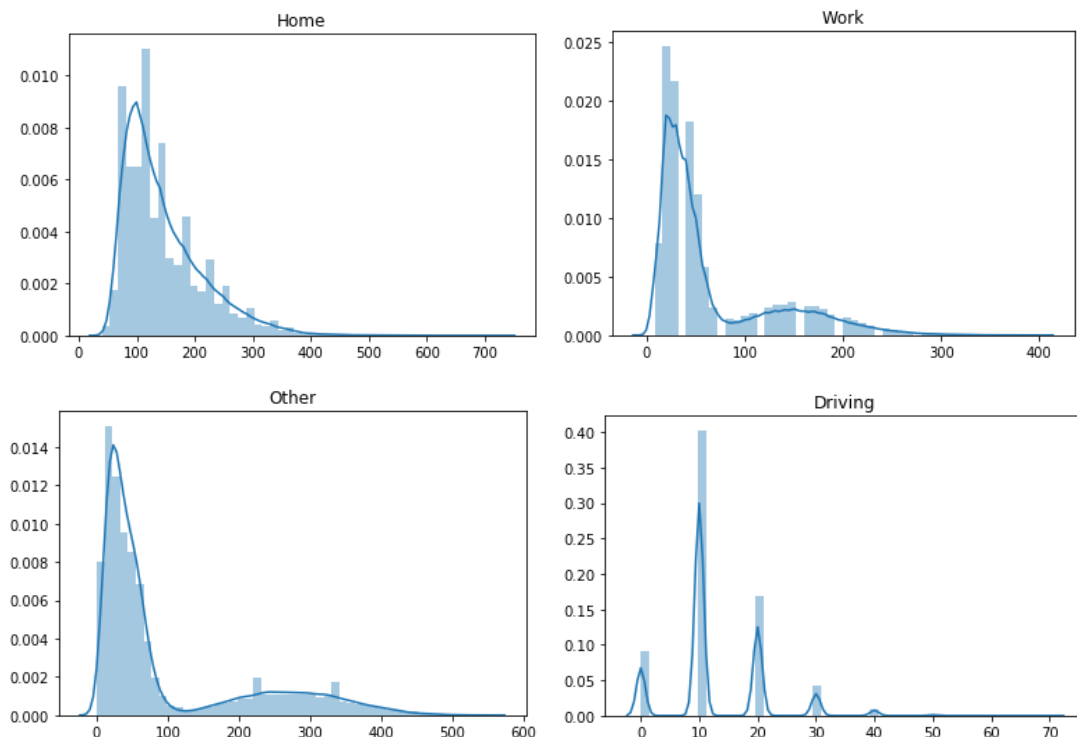
The project's aim was to decide the best locations to implement chargers and reduce the energy being consumed during times that solar and wind power aren't being generated. According to the different results obtained with the data analysis, the methodology implemented in this project sense and yields results that are plausible. Moreover, the team proved through the overall process that the implementation of electric vehicles reduces GHG emissions, even though the charging process that we found and which is the one being currently used (charging at night) is not the most environmentally friendly. However, to decrease even more GHG emissions, the utilization of renewable energies generated during daytime must be optimized: an improved EV charging pattern could lead the majority of EVs to charge during daytime instead of night-time. EVs would not be charged at home anymore, but for example, at 'Work' or at 'Other' locations. Therefore, the overall best locations to implement chargers are the ones that would enable EVs to charge at the time of the day allowing for a smaller amount of emissions. To determine precisely these different locations, a Markov chain composed of more specific states is needed, which has been mentioned as next steps for a future CE295 project team under the discussion part.

APPENDIX 1: The plots below show the distribution of the consecutive times spent in minutes, for the four locations, in the states of Maine and New York.

MAINE

X-axis: consecutive times spent in minutes

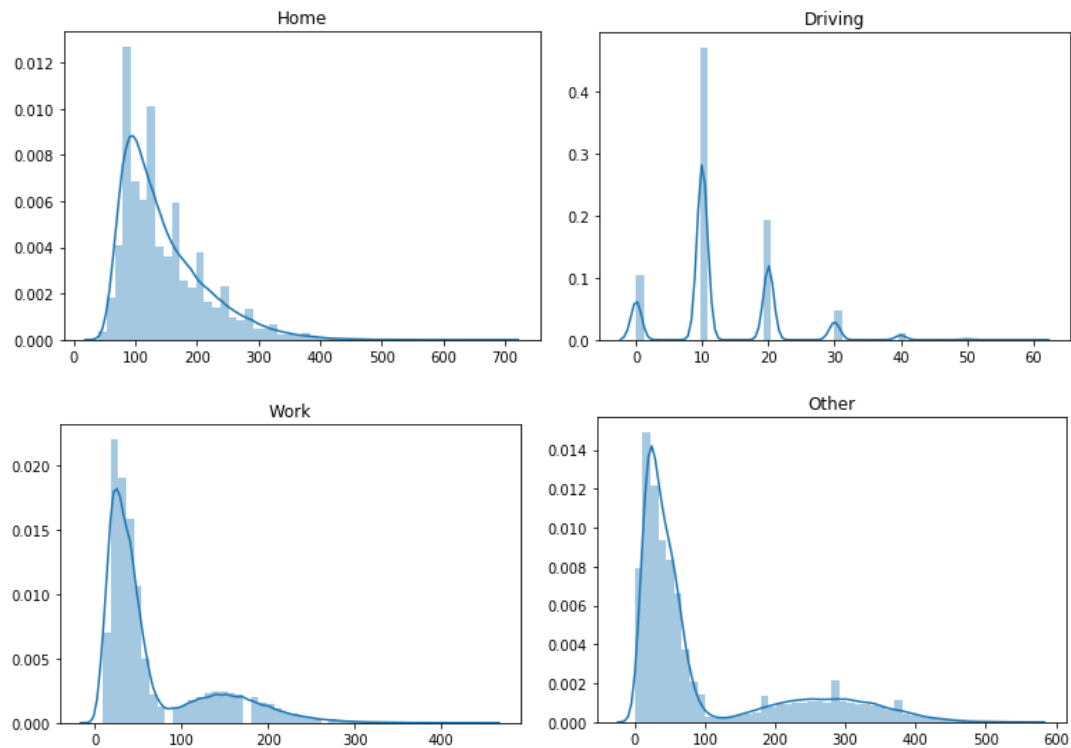
Y-axis: PDF



NEW YORK

X-axis: consecutive times spent in minutes

Y-axis: PDF



References

- [1] United States Environmental Protection Agency (2019), Sources of Greenhouse Gas Emissions, <https://www.epa.gov/ghgemissions/sources-greenhouse-gas-emissions>
- [2] Wang, Yue, and David Infield. "Markov Chain Monte Carlo simulation of electric vehicle use for network integration studies." *International Journal of Electrical Power & Energy Systems* 99 (2018): 85-94.
- [3] Shepero, Mahmoud, and Joakim Munkhammar. "Spatial Markov chain model for electric vehicle charging in cities using geographical information system (GIS) data." *Applied Energy* 231 (2018): 1089-1099.
- [4] TOLVER, Anders. An introduction to Markov chains. *Recuperado el*, 2016, vol. 15.

Appendix

May 4, 2020

0.1 CE 295 - Project

0.2 Time-Variant Markov Chain Transition Matrices

0.2.1 Imports and Dataset

```
[ ]: import pandas as pd
import numpy as np

# Update the name of the file changing the State:
```

0.3 New York

```
[ ]: Data = pd.read_csv("Markov_Dataset_NY_0429.csv")
Data = Data.drop(['Unnamed: 0'], axis=1)
#Data

[ ]: Data_NY = Data
Matrix = np.array(Data)

[ ]: np.unique(Matrix[:, 0], return_counts = True)

[ ]: index_ = ['Driving', 'Home', 'Other', 'Work']
array = np.array([0,0,0,0]).reshape(1,4)
Driving = list()
Home = list()
Work = list()
Other = list()

for j in range(0,144):
    B = np.unique(Matrix[:, j], return_counts = True)
    array = np.array([0,0,0,0]).reshape(1,4)

    length = len(B[0])
    #print(length)

    if length == 4:
```

```

array[0][0] = B[1][0]
array[0][1] = B[1][1]
array[0][2] = B[1][2]
array[0][3] = B[1][3]

elif length == 3:
    if B[0][0] == index_[0]:
        if B[0][1] == index_[1]:
            if B[0][2] == index_[2]:
                array[0][0] = B[1][0]
                array[0][1] = B[1][1]
                array[0][2] = B[1][2]
                array[0][3] = 0
            else:
                array[0][0] = B[1][0]
                array[0][1] = B[1][1]
                array[0][2] = 0
                array[0][3] = B[1][2]
        elif B[0][1] == index_[2]:
            array[0][0] = B[1][0]
            array[0][1] = 0
            array[0][2] = B[1][1]
            array[0][3] = B[1][2]

    elif B[0][1] == index_[1]:
        array[0][0] = 0
        array[0][1] = B[1][0]
        array[0][2] = B[1][1]
        array[0][3] = B[1][2]

elif length == 2:
    if B[0][0] == index_[0]:
        if B[0][1] == index_[1]:
            array[0][0] = B[1][0]
            array[0][1] = B[1][1]
            array[0][2] = 0
            array[0][3] = 0
        elif B[0][1] == index_[2]:
            array[0][0] = B[1][0]
            array[0][1] = 0

```

```

        array[0][2] = B[1][1]
        array[0][3] = 0

    elif B[0][1] == index_[3]:
        array[0][0] = B[1][0]
        array[0][1] = 0
        array[0][2] = 0
        array[0][3] = B[1][1]

    elif B[0][0] == index_[1]:
        if B[0][1] == index_[2]:
            array[0][0] = 0
            array[0][1] = B[1][0]
            array[0][2] = B[1][1]
            array[0][3] = 0

        elif B[0][1] == index_[3]:
            array[0][0] = 0
            array[0][1] = B[1][0]
            array[0][2] = 0
            array[0][3] = B[1][1]

        elif B[0][0] == index_[2]:
            array[0][0] = 0
            array[0][1] = 0
            array[0][2] = B[1][0]
            array[0][3] = B[1][1]

    elif length == 1:
        if B[0][0] == index_[0]:
            array[0][0] = B[1][0]
            array[0][1] = 0
            array[0][2] = 0
            array[0][3] = 0

        elif B[0][0] == index_[0]:
            array[0][0] = 0
            array[0][1] = B[1][0]
            array[0][2] = 0
            array[0][3] = 0

        elif B[0][0] == index_[0]:
            array[0][0] = 0
            array[0][1] = 0
            array[0][2] = B[1][0]
            array[0][3] = 0

```

```

        else:
            array[0][0] = 0
            array[0][1] = 0
            array[0][2] = 0
            array[0][3] = B[1][0]

List = list(array)
#print(List[0][0])

Driving.append(List[0][0])
Home.append(List[0][1])
Other.append(List[0][2])
Work.append(List[0][3])

```

```
[ ]: D = pd.Series(Driving)
H = pd.Series(Home)
O = pd.Series(Other)
W = pd.Series(Work)
```

```
[ ]: D_Series = np.zeros([1,5])
H_Series = np.zeros([1,5])
O_Series = np.zeros([1,5])
W_Series = np.zeros([1,5])

for i in range(0,5):
    D_Series[0][i] = D.autocorr(lag = i)
    H_Series[0][i] = H.autocorr(lag = i)
    O_Series[0][i] = O.autocorr(lag = i)
    W_Series[0][i] = W.autocorr(lag = i)
```

1 Correlation

1.1 New York

```
[ ]: import matplotlib
import matplotlib.pyplot as plt
```

```
[ ]: x = np.linspace(1,5,5)
x = x.reshape(1,5)
```

```
[ ]: fig, ax = plt.subplots()
ax.scatter(x, D_Series)
```

```

ax.set(xlabel='lag', ylabel='Autocorrelation',
       title='Driving Autocorrelation vs. Lag')
ax.grid()

plt.show()

```

```

[ ]: fig, ax = plt.subplots()
ax.scatter(x, H_Series)

ax.set(xlabel='lag', ylabel='Autocorrelation',
       title='Home Autocorrelation vs. Lag')
ax.grid()

plt.show()

```

```

[ ]: fig, ax = plt.subplots()
ax.scatter(x, O_Series)

ax.set(xlabel='lag', ylabel='Autocorrelation',
       title='Other Autocorrelation vs. Lag')
ax.grid()

plt.show()

```

```

[ ]: fig, ax = plt.subplots()
ax.scatter(x, W_Series)

ax.set(xlabel='lag', ylabel='Autocorrelation',
       title='Work Autocorrelation vs. Lag')
ax.grid()

plt.show()

```

2 Markov Chain Transition Functions

Transitions between two time steps

```

[ ]: ##### NEW 1

# Can't be Zero (from TWO to 142)

def Transitions_General(i,Data):

    W_Counter = 0
    H_Counter = 0
    D_Counter = 0
    O_Counter = 0

```

```

W_W = W_H = W_D = W_O = 0
H_W = H_H = H_D = H_O = 0
D_W = D_H = D_D = D_O = 0
O_W = O_H = O_D = O_O = 0

Col_Correlation2 = Data[Data.columns[i-2]]
Col_Correlation1 = Data[Data.columns[i-1]]
Col_A = Data[Data.columns[i]]
Col_B = Data[Data.columns[i+1]]

for k in range(0,len(Col_A)):
    if Col_A[k] == 'Work':
        W_Counter += 1
        if Col_B[k] == 'Work':
            W_W += 1
        if Col_B[k] == 'Home':
            W_H += 1
        if Col_B[k] == 'Driving':
            W_D += 1
        if Col_B[k] == 'Other':
            W_O += 1

        W_Counter += 1
        if Col_Correlation1[k] == 'Work':
            W_W += 1
        if Col_Correlation1[k] == 'Home':
            H_W += 1
        if Col_Correlation1[k] == 'Driving':
            D_W += 1
        if Col_Correlation1[k] == 'Other':
            O_W += 1

    if Col_A[k] == 'Home':
        H_Counter += 1
        if Col_B[k] == 'Work':
            H_W += 1
        if Col_B[k] == 'Home':
            H_H += 1
        if Col_B[k] == 'Driving':
            H_D += 1
        if Col_B[k] == 'Other':
            H_O += 1

        H_Counter += 1
        if Col_Correlation1[k] == 'Work':
            W_H += 1

```

```

if Col_Correlation1[k] == 'Home':
    H_H += 1
if Col_Correlation1[k] == 'Driving':
    D_H += 1
if Col_Correlation1[k] == 'Other':
    W_H += 1

if Col_A[k] == 'Driving':
    D_Counter += 1
    if Col_B[k] == 'Work':
        D_W += 1
    if Col_B[k] == 'Home':
        D_H += 1
    if Col_B[k] == 'Driving':
        D_D += 1
    if Col_B[k] == 'Other':
        D_O += 1

D_Counter += 1
if Col_Correlation1[k] == 'Work':
    W_D += 1
if Col_Correlation1[k] == 'Home':
    H_D += 1
if Col_Correlation1[k] == 'Driving':
    D_D += 1
if Col_Correlation1[k] == 'Other':
    O_D += 1

if Col_A[k] == 'Other':
    O_Counter += 1
    if Col_B[k] == 'Work':
        O_W += 1
    if Col_B[k] == 'Home':
        O_H += 1
    if Col_B[k] == 'Driving':
        O_D += 1
    if Col_B[k] == 'Other':
        O_O += 1

O_Counter += 1
if Col_Correlation1[k] == 'Work':
    W_O += 1
if Col_Correlation1[k] == 'Home':
    H_O += 1
if Col_Correlation1[k] == 'Driving':
    D_O += 1
if Col_Correlation1[k] == 'Other':

```

```

O_O += 1

#####
##### REPEAT #####
#####

if Col_Correlation1[k] == 'Work':
    W_Counter += 1
    if Col_Correlation2[k] == 'Work':
        W_W += 1
    if Col_Correlation2[k] == 'Home':
        H_W += 1
    if Col_Correlation2[k] == 'Driving':
        D_W += 1
    if Col_Correlation2[k] == 'Other':
        O_W += 1

if Col_Correlation1[k] == 'Home':
    H_Counter += 1
    if Col_Correlation2[k] == 'Work':
        W_H += 1
    if Col_Correlation2[k] == 'Home':
        H_H += 1
    if Col_Correlation2[k] == 'Driving':
        D_H += 1
    if Col_Correlation2[k] == 'Other':
        O_H += 1

if Col_Correlation1[k] == 'Driving':
    D_Counter += 1
    if Col_Correlation2[k] == 'Work':
        W_D += 1
    if Col_Correlation2[k] == 'Home':
        H_D += 1
    if Col_Correlation2[k] == 'Driving':
        D_D += 1
    if Col_Correlation2[k] == 'Other':
        O_D += 1

if Col_Correlation1[k] == 'Other':
    O_Counter += 1
    if Col_Correlation2[k] == 'Work':
        W_O += 1
    if Col_Correlation2[k] == 'Home':
        H_O += 1
    if Col_Correlation2[k] == 'Driving':

```

```

        D_O += 1
    if Col_Correlation2[k] == 'Other':
        O_O += 1

W_Counter = (W_W + W_H + W_D + W_O)
if W_Counter == 0:
    W_Counter += 1

H_Counter = (H_W + H_H + H_D + H_O)
if H_Counter == 0:
    H_Counter += 1

O_Counter = (O_W + O_H + O_D + O_O)
if O_Counter == 0:
    O_Counter += 1

D_Counter = (D_W + D_H + D_D + D_O)
if D_Counter == 0:
    D_Counter += 1

T_W_W = float(W_W/W_Counter)
T_W_H = float(W_H/W_Counter)
T_W_D = float(W_D/W_Counter)
T_W_O = float(W_O/W_Counter)

T_H_W = float(H_W/H_Counter)
T_H_H = float(H_H/H_Counter)
T_H_D = float(H_D/H_Counter)
T_H_O = float(H_O/H_Counter)

T_D_W = float(D_W/D_Counter)
T_D_H = float(D_H/D_Counter)
T_D_D = float(D_D/D_Counter)
T_D_O = float(D_O/D_Counter)

T_O_W = float(O_W/O_Counter)
T_O_H = float(O_H/O_Counter)
T_O_D = float(O_D/O_Counter)
T_O_O = float(O_O/O_Counter)

Work    = np.array([T_W_W , T_W_H, T_W_D , T_W_O])
Home    = np.array([T_H_W , T_H_H, T_H_D , T_H_O])
Driving = np.array([T_D_W , T_D_H, T_D_D , T_D_O])

```

```

Other    = np.array([T_0_W , T_0_H, T_0_D , T_0_O])

transition_matrix = np.array([Work , Home , Driving , Other])
transition_matrix = np.around(transition_matrix.reshape((4,4)),decimals = 4)

#np.set_printoptions(formatter={'float_kind':'{:f}'.format})

return transition_matrix

```

[]: *### NEW 2*

```

def Transitions_ONE(i_max,Data):

    W_Counter = 0
    H_Counter = 0
    D_Counter = 0
    O_Counter = 0

    W_W = W_H = W_D = W_O = 0
    H_W = H_H = H_D = H_O = 0
    D_W = D_H = D_D = D_O = 0
    O_W = O_H = O_D = O_O = 0

    Col_Correlation2 = Data[Data.columns[i_max]]
    Col_Correlation1 = Data[Data.columns[0]]
    Col_A = Data[Data.columns[1]]
    Col_B = Data[Data.columns[2]]

    for k in range(0,len(Col_A)):
        if Col_A[k] == 'Work':
            W_Counter += 1
            if Col_B[k] == 'Work':
                W_W += 1
            if Col_B[k] == 'Home':
                W_H += 1
            if Col_B[k] == 'Driving':
                W_D += 1
            if Col_B[k] == 'Other':
                W_O += 1

        W_Counter += 1
        if Col_Correlation1[k] == 'Work':
            W_W += 1
        if Col_Correlation1[k] == 'Home':
            H_W += 1
        if Col_Correlation1[k] == 'Driving':
            D_W += 1

```

```

if Col_Correlation1[k] == 'Other':
    O_W += 1

if Col_A[k] == 'Home':
    H_Counter += 1
    if Col_B[k] == 'Work':
        H_W += 1
    if Col_B[k] == 'Home':
        H_H += 1
    if Col_B[k] == 'Driving':
        H_D += 1
    if Col_B[k] == 'Other':
        H_O += 1

H_Counter += 1
if Col_Correlation1[k] == 'Work':
    W_H += 1
if Col_Correlation1[k] == 'Home':
    H_H += 1
if Col_Correlation1[k] == 'Driving':
    D_H += 1
if Col_Correlation1[k] == 'Other':
    W_H += 1

if Col_A[k] == 'Driving':
    D_Counter += 1
    if Col_B[k] == 'Work':
        D_W += 1
    if Col_B[k] == 'Home':
        D_H += 1
    if Col_B[k] == 'Driving':
        D_D += 1
    if Col_B[k] == 'Other':
        D_O += 1

D_Counter += 1
if Col_Correlation1[k] == 'Work':
    W_D += 1
if Col_Correlation1[k] == 'Home':
    H_D += 1
if Col_Correlation1[k] == 'Driving':
    D_D += 1
if Col_Correlation1[k] == 'Other':
    O_D += 1

if Col_A[k] == 'Other':
    O_Counter += 1

```

```

if Col_B[k] == 'Work':
    O_W += 1
if Col_B[k] == 'Home':
    O_H += 1
if Col_B[k] == 'Driving':
    O_D += 1
if Col_B[k] == 'Other':
    O_O += 1

O_Counter += 1
if Col_Correlation1[k] == 'Work':
    W_O += 1
if Col_Correlation1[k] == 'Home':
    H_O += 1
if Col_Correlation1[k] == 'Driving':
    D_O += 1
if Col_Correlation1[k] == 'Other':
    O_O += 1

#####
##### REPEAT #####
#####

if Col_Correlation1[k] == 'Work':
    W_Counter += 1
    if Col_Correlation2[k] == 'Work':
        W_W += 1
    if Col_Correlation2[k] == 'Home':
        H_W += 1
    if Col_Correlation2[k] == 'Driving':
        D_W += 1
    if Col_Correlation2[k] == 'Other':
        O_W += 1

if Col_Correlation1[k] == 'Home':
    H_Counter += 1
    if Col_Correlation2[k] == 'Work':
        W_H += 1
    if Col_Correlation2[k] == 'Home':
        H_H += 1
    if Col_Correlation2[k] == 'Driving':
        D_H += 1
    if Col_Correlation2[k] == 'Other':
        O_H += 1

if Col_Correlation1[k] == 'Driving':

```

```

D_Counter += 1
if Col_Correlation2[k] == 'Work':
    W_D += 1
if Col_Correlation2[k] == 'Home':
    H_D += 1
if Col_Correlation2[k] == 'Driving':
    D_D += 1
if Col_Correlation2[k] == 'Other':
    O_D += 1

if Col_Correlation1[k] == 'Other':
    O_Counter += 1
    if Col_Correlation2[k] == 'Work':
        W_O += 1
    if Col_Correlation2[k] == 'Home':
        H_O += 1
    if Col_Correlation2[k] == 'Driving':
        D_O += 1
    if Col_Correlation2[k] == 'Other':
        O_O += 1


W_Counter = (W_W + W_H + W_D + W_O)
if W_Counter == 0:
    W_Counter += 1

H_Counter = (H_W + H_H + H_D + H_O)
if H_Counter == 0:
    H_Counter += 1

O_Counter = (O_W + O_H + O_D + O_O)
if O_Counter == 0:
    O_Counter += 1

D_Counter = (D_W + D_H + D_D + D_O)
if D_Counter == 0:
    D_Counter += 1


T_W_W = float(W_W/W_Counter)
T_W_H = float(W_H/W_Counter)
T_W_D = float(W_D/W_Counter)
T_W_O = float(W_O/W_Counter)

T_H_W = float(H_W/H_Counter)

```

```

T_H_H = float(H_H/H_Counter)
T_H_D = float(H_D/H_Counter)
T_H_O = float(H_O/H_Counter)

T_D_W = float(D_W/D_Counter)
T_D_H = float(D_H/D_Counter)
T_D_D = float(D_D/D_Counter)
T_D_O = float(D_O/D_Counter)

T_O_W = float(O_W/O_Counter)
T_O_H = float(O_H/O_Counter)
T_O_D = float(O_D/O_Counter)
T_O_O = float(O_O/O_Counter)

Work      = np.array([T_W_W , T_W_H, T_W_D , T_W_O])
Home      = np.array([T_H_W , T_H_H, T_H_D , T_H_O])
Driving   = np.array([T_D_W , T_D_H, T_D_D , T_D_O])
Other     = np.array([T_O_W , T_O_H, T_O_D , T_O_O])

transition_matrix = np.array([Work , Home , Driving , Other])
transition_matrix = np.around(transition_matrix.reshape((4,4)),decimals = 4)

#np.set_printoptions(formatter={'float_kind':'{:f}'.format})

return transition_matrix

```

[]: *### NEW 3*

```

def Transitions_ZERO(i_max,Data):

    W_Counter = 0
    H_Counter = 0
    D_Counter = 0
    O_Counter = 0

    W_W = W_H = W_D = W_O = 0
    H_W = H_H = H_D = H_O = 0
    D_W = D_H = D_D = D_O = 0
    O_W = O_H = O_D = O_O = 0

    Col_Correlation2 = Data[Data.columns[i_max-1]]
    Col_Correlation1 = Data[Data.columns[i_max]]
    Col_A = Data[Data.columns[0]]
    Col_B = Data[Data.columns[1]]

```

```

for k in range(0,len(Col_A)):
    if Col_A[k] == 'Work':
        W_Counter += 1
        if Col_B[k] == 'Work':
            W_W += 1
        if Col_B[k] == 'Home':
            W_H += 1
        if Col_B[k] == 'Driving':
            W_D += 1
        if Col_B[k] == 'Other':
            W_O += 1

    W_Counter += 1
    if Col_Correlation1[k] == 'Work':
        W_W += 1
    if Col_Correlation1[k] == 'Home':
        H_W += 1
    if Col_Correlation1[k] == 'Driving':
        D_W += 1
    if Col_Correlation1[k] == 'Other':
        O_W += 1

    if Col_A[k] == 'Home':
        H_Counter += 1
        if Col_B[k] == 'Work':
            H_W += 1
        if Col_B[k] == 'Home':
            H_H += 1
        if Col_B[k] == 'Driving':
            H_D += 1
        if Col_B[k] == 'Other':
            H_O += 1

    H_Counter += 1
    if Col_Correlation1[k] == 'Work':
        W_H += 1
    if Col_Correlation1[k] == 'Home':
        H_H += 1
    if Col_Correlation1[k] == 'Driving':
        D_H += 1
    if Col_Correlation1[k] == 'Other':
        W_H += 1

    if Col_A[k] == 'Driving':
        D_Counter += 1
        if Col_B[k] == 'Work':
            D_W += 1

```

```

if Col_B[k] == 'Home':
    D_H += 1
if Col_B[k] == 'Driving':
    D_D += 1
if Col_B[k] == 'Other':
    D_O += 1

D_Counter += 1
if Col_Correlation1[k] == 'Work':
    W_D += 1
if Col_Correlation1[k] == 'Home':
    H_D += 1
if Col_Correlation1[k] == 'Driving':
    D_D += 1
if Col_Correlation1[k] == 'Other':
    O_D += 1

if Col_A[k] == 'Other':
    O_Counter += 1
    if Col_B[k] == 'Work':
        O_W += 1
    if Col_B[k] == 'Home':
        O_H += 1
    if Col_B[k] == 'Driving':
        O_D += 1
    if Col_B[k] == 'Other':
        O_O += 1

O_Counter += 1
if Col_Correlation1[k] == 'Work':
    W_O += 1
if Col_Correlation1[k] == 'Home':
    H_O += 1
if Col_Correlation1[k] == 'Driving':
    D_O += 1
if Col_Correlation1[k] == 'Other':
    O_O += 1


#####
# REPEAT ####

if Col_Correlation1[k] == 'Work':
    W_Counter += 1
    if Col_Correlation2[k] == 'Work':
        W_W += 1
    if Col_Correlation2[k] == 'Home':

```

```

        H_W += 1
    if Col_Correlation2[k] == 'Driving':
        D_W += 1
    if Col_Correlation2[k] == 'Other':
        O_W += 1

    if Col_Correlation1[k] == 'Home':
        H_Counter += 1
        if Col_Correlation2[k] == 'Work':
            W_H += 1
        if Col_Correlation2[k] == 'Home':
            H_H += 1
        if Col_Correlation2[k] == 'Driving':
            D_H += 1
        if Col_Correlation2[k] == 'Other':
            O_H += 1

    if Col_Correlation1[k] == 'Driving':
        D_Counter += 1
        if Col_Correlation2[k] == 'Work':
            W_D += 1
        if Col_Correlation2[k] == 'Home':
            H_D += 1
        if Col_Correlation2[k] == 'Driving':
            D_D += 1
        if Col_Correlation2[k] == 'Other':
            O_D += 1

    if Col_Correlation1[k] == 'Other':
        O_Counter += 1
        if Col_Correlation2[k] == 'Work':
            W_O += 1
        if Col_Correlation2[k] == 'Home':
            H_O += 1
        if Col_Correlation2[k] == 'Driving':
            D_O += 1
        if Col_Correlation2[k] == 'Other':
            O_O += 1

W_Counter = (W_W + W_H + W_D + W_O)
if W_Counter == 0:
    W_Counter += 1

```

```

H_Counter = (H_W + H_H + H_D + H_O)
if H_Counter == 0:
    H_Counter += 1

O_Counter = (O_W + O_H + O_D + O_O)
if O_Counter == 0:
    O_Counter += 1

D_Counter = (D_W + D_H + D_D + D_O)
if D_Counter == 0:
    D_Counter += 1

T_W_W = float(W_W/W_Counter)
T_W_H = float(W_H/W_Counter)
T_W_D = float(W_D/W_Counter)
T_W_O = float(W_O/W_Counter)

T_H_W = float(H_W/H_Counter)
T_H_H = float(H_H/H_Counter)
T_H_D = float(H_D/H_Counter)
T_H_O = float(H_O/H_Counter)

T_D_W = float(D_W/D_Counter)
T_D_H = float(D_H/D_Counter)
T_D_D = float(D_D/D_Counter)
T_D_O = float(D_O/D_Counter)

T_O_W = float(O_W/O_Counter)
T_O_H = float(O_H/O_Counter)
T_O_D = float(O_D/O_Counter)
T_O_O = float(O_O/O_Counter)

Work      = np.array([T_W_W , T_W_H, T_W_D , T_W_O])
Home      = np.array([T_H_W , T_H_H, T_H_D , T_H_O])
Driving   = np.array([T_D_W , T_D_H, T_D_D , T_D_O])
Other     = np.array([T_O_W , T_O_H, T_O_D , T_O_O])

transition_matrix = np.array([Work , Home , Driving , Other])
transition_matrix = np.around(transition_matrix.reshape((4,4)),decimals = 4)

#np.set_printoptions(formatter={'float_kind':'{:f}'.format})

return transition_matrix

```

```
[ ]: ### NEW 3

def Transitions_END(i_max,Data):

    W_Counter = 0
    H_Counter = 0
    D_Counter = 0
    O_Counter = 0

    W_W = W_H = W_D = W_O = 0
    H_W = H_H = H_D = H_O = 0
    D_W = D_H = D_D = D_O = 0
    O_W = O_H = O_D = O_O = 0

    Col_Correlation2 = Data[Data.columns[i_max-2]]
    Col_Correlation1 = Data[Data.columns[i_max-1]]
    Col_A = Data[Data.columns[i_max]]
    Col_B = Data[Data.columns[0]]

    for k in range(0,len(Col_A)):
        if Col_A[k] == 'Work':
            W_Counter += 1
            if Col_B[k] == 'Work':
                W_W += 1
            elif Col_B[k] == 'Home':
                W_H += 1
            elif Col_B[k] == 'Driving':
                W_D += 1
            elif Col_B[k] == 'Other':
                W_O += 1

            W_Counter += 1
            if Col_Correlation1[k] == 'Work':
                W_W += 1
            elif Col_Correlation1[k] == 'Home':
                H_W += 1
            elif Col_Correlation1[k] == 'Driving':
                D_W += 1
            elif Col_Correlation1[k] == 'Other':
                O_W += 1

        if Col_A[k] == 'Home':
            H_Counter += 1
            if Col_B[k] == 'Work':
                H_W += 1
            if Col_B[k] == 'Home':
                H_H += 1
```

```

if Col_B[k] == 'Driving':
    H_D += 1
if Col_B[k] == 'Other':
    H_O += 1

H_Counter += 1
if Col_Correlation1[k] == 'Work':
    W_H += 1
if Col_Correlation1[k] == 'Home':
    H_H += 1
if Col_Correlation1[k] == 'Driving':
    D_H += 1
if Col_Correlation1[k] == 'Other':
    W_H += 1

if Col_A[k] == 'Driving':
    D_Counter += 1
if Col_B[k] == 'Work':
    D_W += 1
if Col_B[k] == 'Home':
    D_H += 1
if Col_B[k] == 'Driving':
    D_D += 1
if Col_B[k] == 'Other':
    D_O += 1

D_Counter += 1
if Col_Correlation1[k] == 'Work':
    W_D += 1
if Col_Correlation1[k] == 'Home':
    H_D += 1
if Col_Correlation1[k] == 'Driving':
    D_D += 1
if Col_Correlation1[k] == 'Other':
    O_D += 1

if Col_A[k] == 'Other':
    O_Counter += 1
if Col_B[k] == 'Work':
    O_W += 1
if Col_B[k] == 'Home':
    O_H += 1
if Col_B[k] == 'Driving':
    O_D += 1
if Col_B[k] == 'Other':
    O_O += 1

```

```

O_Counter += 1
if Col_Correlation1[k] == 'Work':
    W_O += 1
if Col_Correlation1[k] == 'Home':
    H_O += 1
if Col_Correlation1[k] == 'Driving':
    D_O += 1
if Col_Correlation1[k] == 'Other':
    O_O += 1

#####
##### REPEAT #####
#####

if Col_Correlation1[k] == 'Work':
    W_Counter += 1
    if Col_Correlation2[k] == 'Work':
        W_W += 1
    if Col_Correlation2[k] == 'Home':
        H_W += 1
    if Col_Correlation2[k] == 'Driving':
        D_W += 1
    if Col_Correlation2[k] == 'Other':
        O_W += 1

if Col_Correlation1[k] == 'Home':
    H_Counter += 1
    if Col_Correlation2[k] == 'Work':
        W_H += 1
    if Col_Correlation2[k] == 'Home':
        H_H += 1
    if Col_Correlation2[k] == 'Driving':
        D_H += 1
    if Col_Correlation2[k] == 'Other':
        O_H += 1

if Col_Correlation1[k] == 'Driving':
    D_Counter += 1
    if Col_Correlation2[k] == 'Work':
        W_D += 1
    if Col_Correlation2[k] == 'Home':
        H_D += 1
    if Col_Correlation2[k] == 'Driving':
        D_D += 1
    if Col_Correlation2[k] == 'Other':
        O_D += 1

```

```

if Col_Correlation1[k] == 'Other':
    O_Counter += 1
    if Col_Correlation2[k] == 'Work':
        W_O += 1
    if Col_Correlation2[k] == 'Home':
        H_O += 1
    if Col_Correlation2[k] == 'Driving':
        D_O += 1
    if Col_Correlation2[k] == 'Other':
        O_O += 1

W_Counter = (W_W + W_H + W_D + W_O)
if W_Counter == 0:
    W_Counter += 1

H_Counter = (H_W + H_H + H_D + H_O)
if H_Counter == 0:
    H_Counter += 1

O_Counter = (O_W + O_H + O_D + O_O)
if O_Counter == 0:
    O_Counter += 1

D_Counter = (D_W + D_H + D_D + D_O)
if D_Counter == 0:
    D_Counter += 1

T_W_W = float(W_W/W_Counter)
T_W_H = float(W_H/W_Counter)
T_W_D = float(W_D/W_Counter)
T_W_O = float(W_O/W_Counter)

T_H_W = float(H_W/H_Counter)
T_H_H = float(H_H/H_Counter)
T_H_D = float(H_D/H_Counter)
T_H_O = float(H_O/H_Counter)

T_D_W = float(D_W/D_Counter)
T_D_H = float(D_H/D_Counter)
T_D_D = float(D_D/D_Counter)
T_D_O = float(D_O/D_Counter)

```

```

T_O_W = float(O_W/O_Counter)
T_O_H = float(O_H/O_Counter)
T_O_D = float(O_D/O_Counter)
T_O_O = float(O_O/O_Counter)

Work    = np.array([T_W_W , T_W_H, T_W_D , T_W_O])
Home    = np.array([T_H_W , T_H_H, T_H_D , T_H_O])
Driving = np.array([T_D_W , T_D_H, T_D_D , T_D_O])
Other   = np.array([T_O_W , T_O_H, T_O_D , T_O_O])

transition_matrix = np.array([Work , Home , Driving , Other])
transition_matrix = np.around(transition_matrix.reshape((4,4)),decimals = 4)

#np.set_printoptions(formatter={'float_kind':'{:f}'.format})

return transition_matrix

```

2.0.1 Markov Chain Generating Transition Matrices

when counter reaches 11:50 pm, it needs to create a transition between the last column of the dataset and the first one. For this, another function (very similar to the previous one was created).

```
[ ]: def Markov_Chain_Transition_Matrices(A,Data):

    Dataset = Data
    Transitions = []
    i = 0

    while i <= (A-1):

        if i == 0:
            T1 = Transitions_ZERO(A,Dataset)
            T1 = T1.reshape((16), order = 'C')
            Transitions.append(T1)

        elif i ==1:
            T1 = Transitions_ONE(A,Dataset)
            T1 = T1.reshape((16), order = 'C')
            Transitions.append(T1)

        else:
            T1 = Transitions_General(i,Dataset)
            T1 = T1.reshape((16), order = 'C')
            Transitions.append(T1)

    print(i)
```

```

    i += 1

T1 = Transitions_END(A, Dataset)
T1 = T1.reshape((16), order = 'C')
Transitions.append(T1)

return Transitions

```

```
[ ]: Data_NY[Data_NY.columns[0]]
```

```
[ ]: %%time
Transitions_NY = Markov_Chain_Transition_Matrices(143,Data_NY)
```

```
[ ]: %%time
Transitions_CA = Markov_Chain_Transition_Matrices(143,Data_CA)
```

```
[ ]: %%time
Transitions_ME = Markov_Chain_Transition_Matrices(143,Data_ME)
```

$$\begin{bmatrix} T_{W-W} & T_{W-H} & T_{W-D} & T_{W-O} \\ T_{H-W} & T_{H-H} & T_{H-D} & T_{H-O} \\ T_{D-W} & T_{D-H} & T_{D-D} & T_{D-O} \\ T_{O-W} & T_{O-H} & T_{O-D} & T_{O-O} \end{bmatrix}$$

```
[ ]: M = Transitions_NY[0].reshape(4,4)
M
```

```
[ ]: A = sum(M[0][:])
A
```

```
[ ]:
```

Saving and Exporting Matrices.

Make sure name of the CSV file is updated to match the State for which transitions are being generated

```
[ ]: from numpy import savetxt
```

```
[ ]: savetxt('Transitions_NY_0429.csv', Transitions_NY, delimiter=',')
```

```
[ ]: savetxt('Transitions_CA_0424.csv', Transitions_CA, delimiter=',')
```

```
[ ]: savetxt('Transitions_ME_0424.csv', Transitions_ME, delimiter=',')
```

```
[ ]:
```

Electrification Potential of Bus Routes in Boston

Final Report for CEE 295, Spring 2020



Gilbert Bahati, Line Osseiran, Marie Rajon Bernard,
Guillaume Varvoux, Upadhi Vijay, Jersey Wang Lee

Table of Contents

Abstract	2
Introduction	2
Motivation and Background	2
Relevant Literature	3
Scope of the Study	3
Technical Analysis and Data Collection	4
Model Formation	4
Modeling Objective	4
Sources of Power Consumption	4
Newton's Laws	4
Energy per Trip	5
Data Collection	6
Model Parameters	6
Ridership Data	7
GTFS Data	8
Choice of Scenarios	11
Results	11
Discussion	14
Conclusion	14
Version 2.0	14
Table of Responsibilities	15
Summary	16
References	17
Appendix	19

1. Abstract

U.S. cities mainly rely on diesel buses which present health, environmental and cost concerns (Casale et al., n.d.). Many transit agencies are thus planning to transition toward electric bus fleets (Tigue Kristoffer, 2019). Due to the range limitations and battery charging times, some routes are easier to electrify than others. This paper focuses on the Massachusetts Bay Transportation Authority that operates bus routes in the Greater Boston region. It aims at answering the following question: Which bus routes are the best candidates to be electrified in Boston? The first step was to develop a mathematical model to obtain the energy required per day per bus on a given line. We then collected and processed data on the bus routes and weather conditions in Boston, as well as characteristics of electric buses. We selected the worst-case scenario (i.e. HVAC on) in order to be conservative. After calculating the number of buses and the energy required on different lines at different times of the day, we obtained the energy required per day per bus for different lines. Considering an electric bus with a battery capacity of 460 kWh (Xcelsior CHARGE, n.d.), we found that 5 out of the 14 key routes in Boston can be electrified.

2. Introduction

2.1. Motivation and Background

As of 2018, the transportation sector in the US contributed to 28% of the overall greenhouse gas emissions, with public buses collectively burning over 430 million gallons of diesel in 2014 (US EPA, 2020 and Poulton, 2011). The transportation sector is also an important source of particulate matter emissions that have detrimental impacts on public health.

Electrification has been identified as a key contributor to the greenhouse gas abatement goal in road transport (International Energy Agency, 2016). The decline in battery costs and increase in battery range (up to 300 km) in recent years have contributed to make battery electric buses a good candidate to replace diesel vehicles. Furthermore, regenerative braking systems have led to energy saving benefits resulting in lower emissions over conventional vehicles.

These benefits have incentivised public transit agencies to deploy battery electric buses. Current decisions over fleet replacement are based on fuel economy standards and tailpipe regulations but public transit agencies lack a clear prioritization strategy for fleet electrification. Our project proposes a rigorous analysis of the energy consumption of buses to help identify the most relevant lines ready for electrification.

2.2. Relevant Literature

The most commonly used vehicle-activity based energy emissions model in the literature is the EPA's Motor Vehicle Emission Simulator (Xu et al., 2015). This model takes into account vehicle dynamics but relies on GPS based instantaneous velocity and acceleration data. Most of the transit agencies do not have access to this information and need an alternative model that can be applied on their existing datasets. Therefore, the alternative resources that we have used for our study are listed and described below:

- **Moura et al., 2010**

This paper exposes an equation for power demand, solely in terms of vehicle velocity and vehicle parameters. However, the inefficiencies were not taken into account.

- **Franca, 2015**

This thesis presents a battery electric bus energy consumption model coupled with an electrochemical battery capacity fade model. It also projects the operating costs of electric buses and the potential emission reductions compared to diesel vehicles for a given route, which could provide a starting point for further developments in a version 2.0 of our study (see Section 4.2).

- **Vahidi et al., 2018**

This paper also develops a model based on first principles of motion to highlight the energy saving potential of connected and automated vehicles. The authors integrated the power needed at the wheel and retrieved the energy required per trip, expressed in terms of initial and final conditions.

2.3. Scope of the Study

Our study aims to formulate a mathematical model that predicts the energy required per day per bus on a given line. We built it upon standard and publicly available data in order to make it easily scalable and broadly applicable. The General Transit Feed Specification (GTFS) is an industry standard which allows public transit agencies to publish their schedule, fare and geographic data. We therefore used GTFS data for our energy consumption study in order to assess the electrification potential of bus routes.

We applied our analysis on a case study focusing on the bus routes operated by the Massachusetts Bay Transportation Authority (MBTA), which is the fourth largest transit system in the US. It operates a fleet of 1008 heavy-duty transit buses which span 170 bus routes in the Greater Boston area. Currently, these routes are mostly served by diesel and compressed natural gas buses, as well as a few diesel-electric hybrid buses. A pilot testing for electric buses was initiated in late 2019 (Massachusetts Bay Transportation Authority, 2019).

3. Technical Analysis and Data Collection

3.1. Model Formation

Table 3.1 summarises the relevant parameters that are going to be useful for our model.

m	Mass of the vehicle	ρ	Air density
v	Forward velocity	A_{fr}	Vehicle front area
F_{prop}	Sum of the tractive force at the wheels	v_0	Velocity at origin
C_{rr}	Coefficient of rolling resistance	v_f	Velocity at destination
C_D	Aerodynamic drag coefficient	Δh	Total elevation change during the trip
α	Road slope	Δx	Horizontal distance covered
η_{conv}	Converter efficiency	\bar{v}	Average velocity over position
η_M	Motor efficiency	σ_v	Variance of the velocity

Table 3.1: Relevant parameters for our study.

3.1.1. Modeling Objective

In order to answer our problem statement, we want to formulate a mathematical model that predicts the energy required per day per bus on a given line. This model will be used to assess the electrification potential of bus routes in Boston.

3.1.2. Sources of Power Consumption

The vehicle's longitudinal motion represents the main power consumption for a bus. In addition, there exists another source of power consumption, which is commonly called the auxiliary load. This second source refers to the use of air conditioning, the opening of doors etc. Therefore, the instantaneous power consumption of the bus can be calculated as follows:

$$P_{inst}(t) = \frac{V(t)}{\eta_{conv} \eta_M} F_{prop} + \frac{P_{auxi}}{\eta_{conv}} \quad (3.1)$$

The motor efficiency η_M is given by the duty cycle of an electric bus and η_{conv} is the converter efficiency. The auxiliary load and the two efficiencies are values that can be found in the literature. V can be retrieved thanks to the GTFS data.

3.1.3. Newton's Laws

F_{prop} represents the force supplied by the motor to propel the vehicle by overcoming the external resistive forces. It is determined by applying Newton's second law of motion to vehicle as follows:

$$m \cdot \vec{a} = \sum \vec{F}_{ext}$$

The external forces correspond to the propulsion force, the gravitational force, the rolling resistance and the air drag, as illustrated in the free-body diagram in Figure 3.1. If we develop explicitly the right-hand side of the equation:

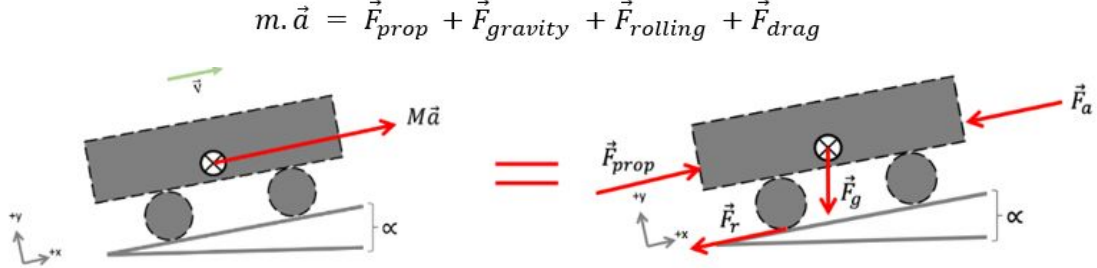


Figure 3.1: Free body diagram of the different forces.

Once the forces are projected on the x-axis, the vehicle must overcome the following external resistive forces:

$$F_{prop} = m \cdot a + F_{gravity} \sin(\alpha) + F_{rolling} + F_{drag}$$

Or equivalently,

$$F_{prop} = m \cdot \frac{dv}{dt} + m \cdot g \cdot \sin(\alpha) + m \cdot g \cdot C_{rr} + \frac{1}{2} \rho \cdot A_{fr} \cdot C_d \cdot v^2 \quad (3.2)$$

3.1.4. Energy per Trip

Since we are looking for the energy per trip, we need to integrate Equation 3.2, as power is the integral of energy over a given amount of time:

$$E_{trip} = \frac{E_{prop}}{\eta_{conv} \eta_M} + \frac{E_{auxi}}{\eta_{conv}} \quad (3.3)$$

Note that the auxiliary energy takes into account idling during the time t_f :

$$E_{auxi} = \int_0^{t_f} P_{auxi}(t) dt$$

The instantaneous power needed at the wheel is $V \cdot F_{prop}$. The energy needed at the wheel during the time t_f is given by:

$$E_{prop} = \int_0^{t_f} F_{prop}(t) \cdot v(t) dt$$

Changing the variable of integration from time to position, the net energy needed at the wheel to cover a distance s_f in the time t_f becomes:

$$E_{prop} = \int_0^{s_f} F_{prop}(s) ds$$

With the reasonable assumption that m , g , t_f , ρ , A_{fr} are constants during a trip, we can integrate Equation 3.2:

$$E_{prop} = \frac{1}{2}m(v_f^2 - v_0^2) + m.g.(\Delta h + C_{rr}\Delta x) + \frac{1}{2}\rho.A_{fr}\int_0^{s_f} C_D(s)v^2(s) ds$$

If C_D is considered constant, the last integral term becomes:

$$E_{prop} = \frac{1}{2}m(v_f^2 - v_0^2) + m.g.\Delta h + m.g.C_{rr}\Delta x + \frac{1}{2}\rho.A_{fr}.C_D(\bar{v}^2 + \sigma_v^2)s_f \quad (3.4)$$

The first and second terms of Equation 3.4 represent respectively the change in kinetic and potential energy. The third term refers to the irreversible frictional loss and it is a function of the horizontal trip distance Δx and C_{rr} . The last term is linked to the aerodynamic drag.

We can further simplify this expression. Indeed, the first and second terms are zero as we assume that the bus is doing a round-trip. Another assumption that we made is that there is no change in elevation along the routes considered in Boston, i.e $\Delta x = s_f$. In order to take into account the energy dissipated during braking at the numerous stops of the bus along the route, we add an extra term and the equation finally becomes:

$$E_{prop} = \frac{1}{2}n_{stop}m\bar{v}^2 + m.g.C_{rr}s_f + \frac{1}{2}\rho.A_{fr}.C_D(\bar{v}^2 + \sigma_v^2)s_f \quad (3.5)$$

Each term corresponds respectively to:

$$E_{prop} = E_{braking} + E_{rolling} + E_{drag} \quad (3.6)$$

Equation 3.6 refers to the energy for a round trip at a particular time of the day. We can compute the number of buses running on the line and since we assume overnight charging, the energy consumed per day per bus for a given line is thus given by:

$$E_{bus} = \sum_{day} \frac{E_{trip}}{\text{number of buses}} = \sum_{day} \frac{\frac{E_{prop}}{\eta_{conv} \eta_M} + \frac{E_{auxi}}{\eta_{conv}}}{\text{number of buses}} \quad (3.7)$$

3.2. Data Collection

3.2.1. Model Parameters

A pilot testing for electric buses was initiated in late 2019 in Boston using the XE60 battery electric bus. We decided to use in our report the XE40 model that comes from the same series of buses and is currently used by AC Transit. The numerical values of our model parameters with this choice of bus are listed in Table 3.2.

Data	Unit	Value	References
m_{bus} (empty mass of the bus)	kg	14 000	(A. Yulianto et al. 2017)
m_{pax} (avg mass of a passenger)	kg	70	(U.S. Department of Health and Human Services, 2016)
g	$\text{m} \cdot \text{s}^{-2}$	9.81	
C_{rr} (rolling coefficient)	n/a	0.00763	(A. Franca, 2015)
ρ	$\text{kg} \cdot \text{m}^{-3}$	1.225	
C_D (drag coefficient)	n/a	0.65	(Rasu et al., 2016)
A_{fr} (front area)	m^2	7.92	(xcelsoir CHARGE, n.d.)
η_{conv}	n/a	0.95	(C. Pan et al. 2018)
η_M	n/a	0.85	(C. Pan et al. 2018)
P_{auxi} (HVAC ON)	kW	12	(Göhlich et al., 2018)
P_{auxi} (HVAC OFF)	kW	4	(Jari Vepsäläinen et al., 2018)
B (battery capacity)	kWh	460	(xcelsoir CHARGE, n.d.)

Table 3.2: Numerical values of our model parameters.

Note that there is an observed 38% drop in range for battery electric buses from ambient temperatures of 10~15 degrees Celsius to -5~0 degrees Celsius (Kane, 2020), which reflects the temperature during the coldest part of the winter for the Boston area. There is a somewhat similar drop in efficiency for extreme heat (Margolis, 2019), however this is rare given Boston's relatively mild summers (d.o.o., 2020).

3.2.2. Ridership Data

Ridership has an impact on the energy required per trip in the energy balance, as shown in the Equation 3.5. Indeed, the number of passengers on the bus affects the overall weight of the vehicle. The energy required per trip thus increases with ridership.

We have found very granular data from the fall 2018 that gives us the ridership along all the lines operated by MBTA recorded at each bus stop at different times of the day and for different days of the week (MBTA Blue Book Open Data Portal, 2019). The aggregated ridership data for a given line and for a given day type (here, weekday) is shown in Figure 3.2. We used the moving average value (in orange) for our study.

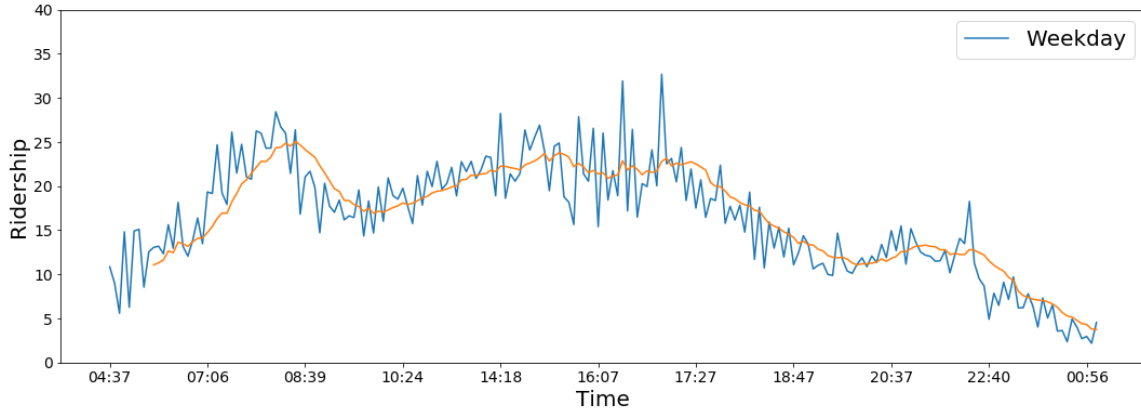


Figure 3.2: Ridership data for a given line on a weekday.

However, when the daily ridership data is not available, it can be retrieved thanks to mathematical models. Indeed, the literature (Yu et al., 2019) highlights that ridership presents two peaks on weekdays, while it follows a Gaussian curve on weekends. Accordingly, Figure A.1 (see Appendix) shows mathematical functions, namely either Gaussian functions or second-degree polynomials, used to model ridership on weekdays. It can be retrieved by taking the maximum of these functions as shown in Figure A.2 (see Appendix). Similarly, this process can be applied to model ridership on weekends.

3.2.3. GTFS Data

3.2.3.1. Speed Profile

The speed profiles of each bus trip are important in order to obtain average velocities and variance calculations of Equation 3.5. Therefore, in order to extract velocities from the scheduling data included in the GTFS reporting format, we calculated point velocities for each trip on a selected line as given by Equation 3.8. The results for one trip for a given time of the day and a given line is illustrated in Figure 3.3.

$$v = \frac{\text{distance between stops}}{\text{duration of bus ride between stops}} \quad (3.8)$$

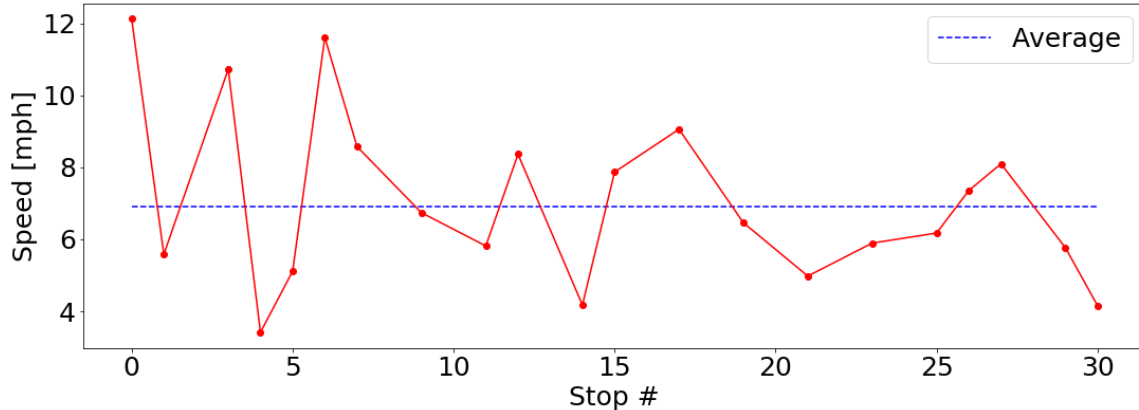


Figure 3.3: Point velocities between bus stops.

In order to obtain more accurate values for the variance of the speed, we need to account for stops. This means we need to disaggregate the data further by assuming constant velocities between stops and constant accelerations at the stops. We use these assumptions to create a more realistic velocity profile as shown in Figure 3.4.

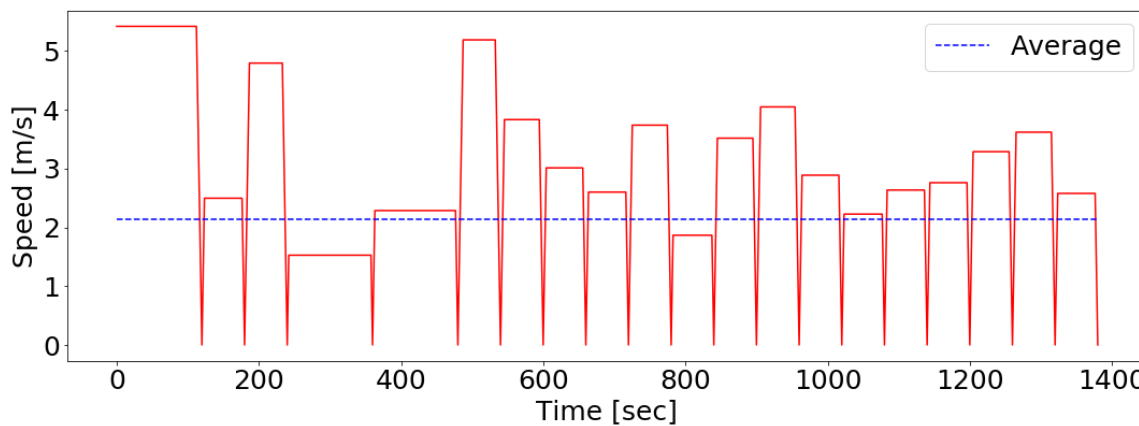


Figure 3.4: Extended velocity profile with stops.

We used acceleration values from the literature that suggests that they range from 0.9 to 1.1 m/s^2 for buses (Madison Area Transportation Planning Board, n.d.). Nevertheless this approach underestimates the variance of the speed. An example of a realistic speed profile from the Manhattan driving cycle is shown in Figure 3.5 (Emission Test Cycles: Manhattan Bus Cycle, n.d.). We have adjusted our variance values by a factor 4 in order to better match those realistic profiles that exhibit a standard deviation of 3.5 m/s .

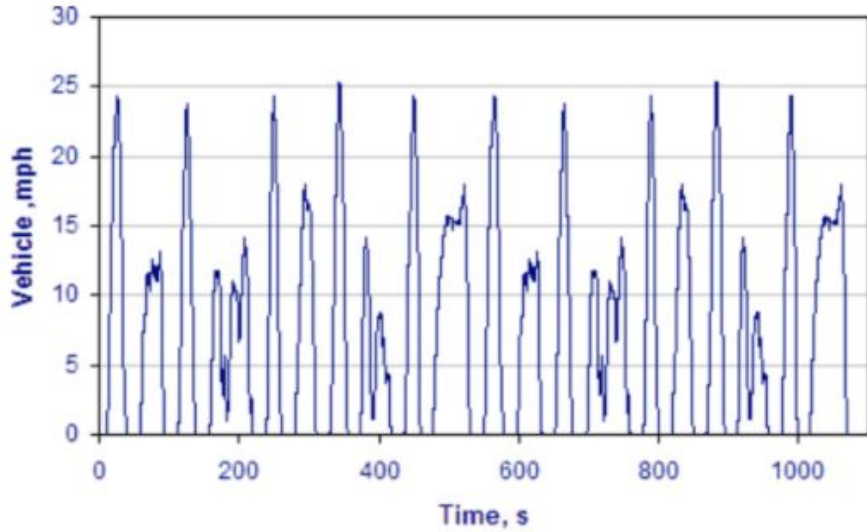


Figure 3.5: Manhattan driving cycle.

We then repeated this analysis for all trips along a given day (here, weekday) for a given line as illustrated in Figure 3.6. We can see how speed evolves along the day: buses travel slower during peak times (more traffic and more stops for pickup/dropoff) and similarly travel faster early in the day and later in the evening.

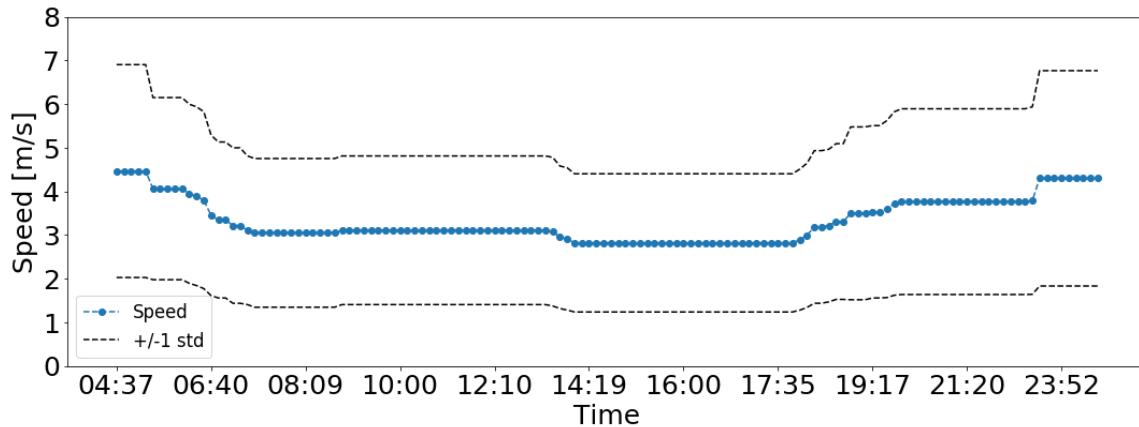


Figure 3.6: Average velocities for all bus trips along a day.

3.2.3.2. Stops Profile

Similar to the speed profiles of each bus trip, the number of bus stops is an extra variable that is important for the calculations of Equation 3.5. Therefore, we further computed the number of stops of each trip during the day. Note that we also see the trend of demand across the day: buses at peak hours stop more frequently than buses running early in the day and later in the evening.

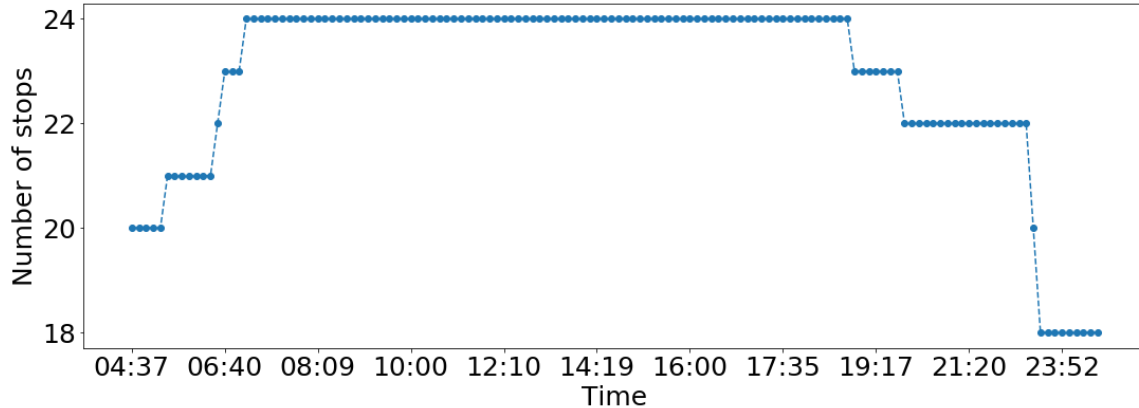


Figure 3.7: Number of stops for all bus trips along a day.

3.3. Choice of Scenarios

We have identified two main types of scenarios that affect the energy values in our model:

- HVAC on/off which affects the auxiliary load in Equation 3.3.
- Weekday/weekend which affects the ridership and hence the mass in Equation 3.5.

3.4. Results

We now have everything we need to compute energy values for round trips using Equation 3.5. We calculate those values for a given line and a given scenario (here HVAC off and weekday) and we do it for all trips along an entire day. We can see the energy values per km displayed in Figure 3.8 are in line with the literature at 1.2kWh/km (Osseiran, 2020). Note that E_{drag} remains around 10 times lower than E_{braking} and E_{rolling} while E_{prop} is around 2 times E_{auxi} .

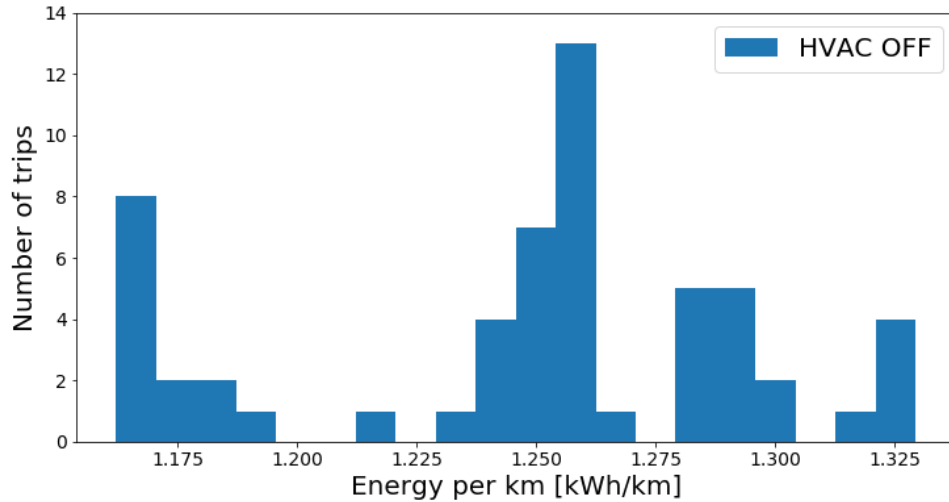


Figure 3.8: Distribution of energy per km values with HVAC off.

We repeat the same analysis for a different scenario (HVAC on and weekday). E_{auxi} is now around 2 times E_{prop} . We can see the energy values per km displayed in Figure 3.9 are around 1.9 kWh/km. We will use this conservative scenario to assess the electrification potential of bus routes. Note that additional HVAC loads required to maintain batteries and cabin temperatures during the winter can drastically reduce the range of battery electric buses as highlighted in Section 3.2.1.

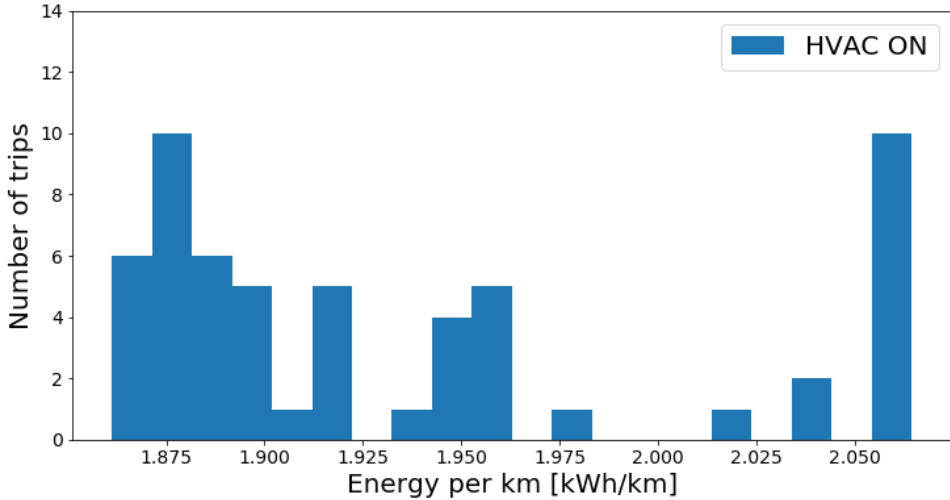


Figure 3.9: Distribution of energy per km values with HVAC on.

Figure 3.10 illustrates how the energy values we just calculated vary along one day. We have one data point for each bus departure. Since there is more than one bus per line, we need to compute the number of buses on the line in order to calculate E_{bus} given in Equation 3.7.

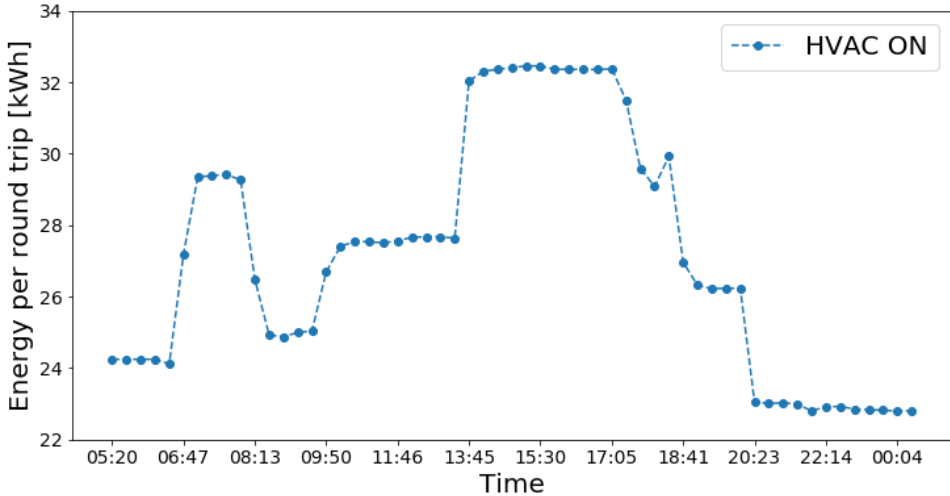


Figure 3.10: Evolution of energy per trip along one day with HVAC on.

We compute the number of buses using Equation 3.9. n_{bus} varies along the day: it increases at peak times when the cycle time goes up (more traffic and more stops for pickup/dropoff) and the headway goes down (i.e. frequency of buses goes up) as illustrated in Figure 3.11 for a weekday.

$$n_{bus} = \frac{\text{Cycle time}}{\text{Headway}} \quad (3.9)$$

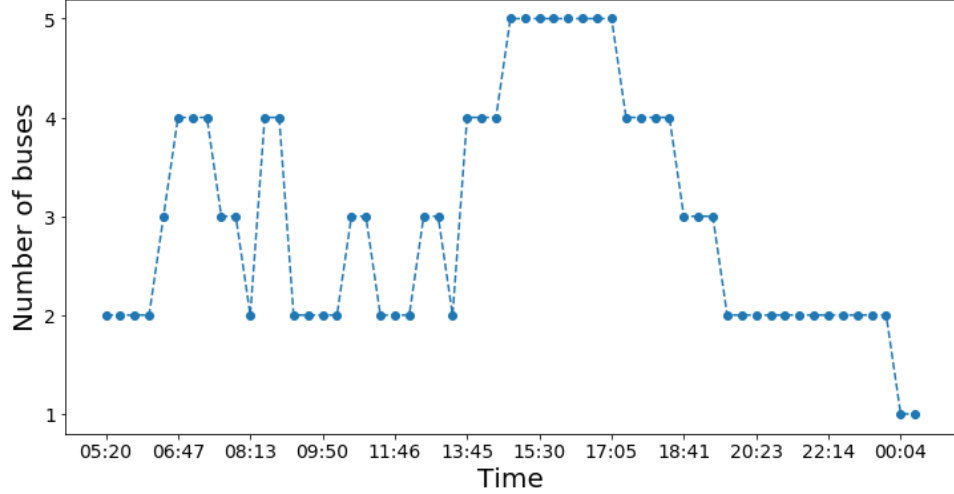


Figure 3.11: Evolution of number of buses along one day.

We computed E_{bus} using Equation 3.7 for 14 key routes in Boston using our conservative scenario (HVAC on and weekday). Those routes account for roughly 40% of the total bus ridership in Boston (Wikipedia, 2020). We found that 5 lines are ready for electrification as illustrated in Figure 3.12. E_{bus} is indeed less than the battery capacity of the bus for lines 15, 28, 66, 1 and 23 in ambient temperature conditions. Nevertheless, if the battery capacity is reduced by 38% to 285 kWh during the coldest part of the winter for the Boston area, no line can be electrified without further measures. Operational strategies that could be implemented to minimize the energy consumption in the winter involve pre-heating the buses or using small onboard diesel heaters.

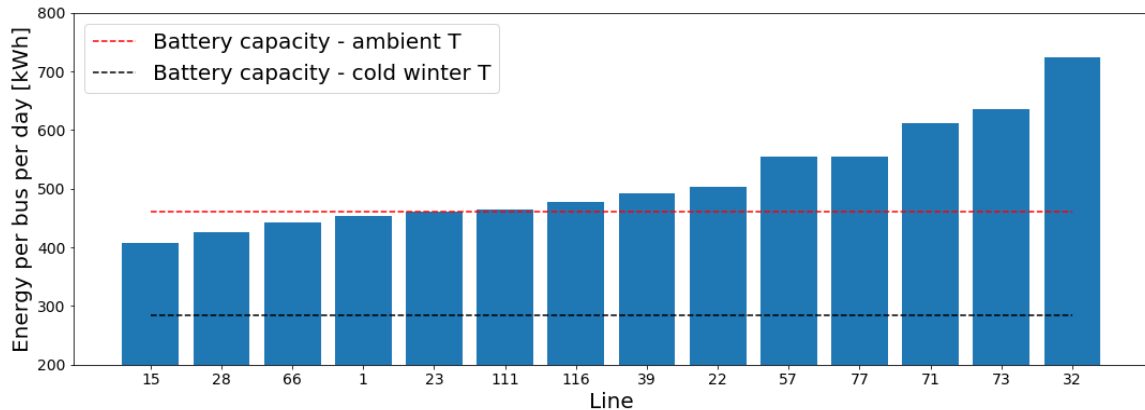


Figure 3.12: Energy per bus for key routes compared to battery capacity.

4. Discussion

4.1. Conclusion

Our project answers the following questions: Can we run an electric bus? Which lines can be electrified? When and where to deploy electric buses? After formulating a mathematical model, we gathered relevant data to compute the energy required per day per bus on a given line. For our calculations, we considered the worst-case scenario (i.e. HVAC on) in order to be conservative. Our case study focused on the MBTA bus routes in the Greater Boston region and our results show that 5 out of the 14 key routes are ready to be electrified. This analysis can easily be replicated for other cities that use the GTFS format to publish their schedule data.

4.2. Version 2.0

A future version of our study would seek to address the following limitations or extensions:

- It would be interesting to compare our results given by a white box model with some real data on bus energy consumption. It can be calculated based on the state-of-charge of the battery after charging and before charging. Such a comparison would help us assess the accuracy of our model. Besides, a sensitivity analysis should be performed on the key parameters of our model to further validate our conclusions.
- A cost analysis would be a crucial addition to our study in order to better guide public transit agencies that consider electrifying their fleets. Besides, an emission analysis could further support and quantify the positive impact of fleet electrification on greenhouse gas and particulate matter emissions, which are at the center of the project motivations.

- Our study is restricted to a scenario of overnight charging. In other words, we answered whether a bus can run for an entire day on a given line, given its battery capacity. A future version of this study should consider scenarios of charging during the day, which would unlock the electrification potential of a larger number of lines but would also come with additional operational constraints.
- Our study only takes into account simplified HVAC scenarios: HVAC is either on or off for an entire day. Instead, HVAC is likely to be on only for selected periods of time along a day. As a consequence, it would be relevant to refine our assumptions using granular weather data since HVAC is a major source of energy consumption.
- Finally, as highlighted in Section 3.2.1, bus battery capacities drop significantly in cold weather conditions. As a consequence, no lines can be electrified under such conditions in our case study in Section 3.4. Therefore, future work should investigate operational strategies that could be implemented to minimize the energy consumption of buses in extreme weather conditions as well as their cost and emission impacts.

5. Table of Responsibilities

Person	Responsibilities
Gilbert Bahati	Code analysis and development: produced velocity average and variance profiles from the MBTA raw data for model calculations. Prepared visuals for the presentation slides.
Line Osseiran	Technical analysis: model formulation. Literature review. Parameters and choices of scenarios. Ridership: mathematical model. Redaction of literature review, model formulation, choice of scenarios and discussion.
Marie Rajon Bernard	Technical analysis: model formulation. Literature review of existing models for electric buses and collection of parameter values. Slides on model formulation. Choices of scenarios. Redaction of the abstract and executive summary.
Guillaume Varvoux	Technical analysis: supported model formulation and led the code development for data collection and results. Coordinated work on deliverables (presentation and report).
Upadhi Vijay	Motivation, background and associated literature, GTFS data collection, MBTA ridership collection and analysis, code automation to estimate speed profiles for any number of routes, result discussion and application.
Jersey Wang Lee	Model parameters, selection of bus data, literature review and information gathering on winter battery changes.

6. Summary

An increase of public transit ridership can help reduce vehicle miles traveled and in turn decrease the environmental impact of the transportation sector. Yet, U.S. cities mainly rely on diesel buses which present health, environmental and cost concerns (Casale et al., n.d.). Many transit agencies are thus planning to transition toward electric bus fleets (Tigue, 2019). Due to the range limitations and battery charging times, some routes are easier to electrify than others. Their electrification potential depends on many factors including weather conditions, congestion and ridership levels, route length and number of buses per route.

This project focuses on the Massachusetts Bay Transportation Authority (MBTA) that operates bus routes in the Greater Boston region. It aims at answering the following question: Which bus routes are the best candidates to be electrified in Boston? It was assumed that MBTA would use XE40 non-articulated battery-electric buses that have a battery capacity of 460 kWh (Xcelsior CHARGE, n.d.).

The first step was to develop a mathematical model to obtain the energy required per day per bus on a given line assuming that buses are charged overnight. The model builds upon Newton's laws to express the energy required for a round trip. The energy per day per bus is then obtained by summing over an entire day the energy per trip divided by the number of buses operating on the line. We then collected and processed data on the bus routes (speed average and variance, ridership, route length, number of stops and number of buses) and weather conditions in Boston, as well as characteristics of electric buses. We selected the worst-case scenario (i.e. HVAC on) in order to be conservative.

We started with one route and came up with a distribution of energy per km values in order to validate our model. Our values are around 1.2kWh/km (with HVAC off) in line with the literature (Osseiran, 2020). After calculating the number of buses based on headways and the energy required on different lines at different times of the day, we obtained the energy required per day per bus for different lines. Considering our electric bus with a battery capacity of 460 kWh, we found that 5 out of the 14 key routes in Boston can be electrified in ambient temperature conditions: lines 15, 28, 66, 1 and 23. Nevertheless, if the battery capacity is reduced by 38% to 285 kWh during the coldest part of the winter for the Boston area (Kane, 2020), no line can be electrified without further measures.

References

- Casale, M., Fund, U. S. P. E., Folger, M. (n.d.). Electric Buses In America. Retrieved May 6, 2020, from <https://environmentamerica.org/feature/ame/electric-buses-america>
- d.o.o., Y. (2020). Boston, MA - Detailed climate information and monthly weather forecast | Weather Atlas. Retrieved 7 May 2020, from <https://www.weather-us.com/en/massachusetts-usa/boston-climate>
- Emission Test Cycles: Manhattan Bus Cycle. (n.d.). <https://dieselnet.com/standards/cycles/manhattan.php>
- Franca, A. (2015). Electricity consumption and battery lifespan estimation for transit electric buses: drivetrain simulations and electrochemical modelling. https://www.uvic.ca/research/centres/iesvic/assets/docs/dissertations/Dissertation_Franca.pdf
- Göhlich, D., Fay, T.-A., Jefferies, D., Lauth, E., Kunith, A., Zhang, X. (2018). Design of urban electric bus systems. *Design Science*, 4. <https://doi.org/10.1017/dsj.2018.10>
- International Energy Agency. (2016). Global EV Outlook 2016. https://www.iea.org/publications/freepublications/publication/Global_EV_Outlook_2016.pdf
- Kane, M. (2020). Study: Cold Weather Has Significant Impact On Electric Bus Range. Retrieved 7 May 2020, from <https://insideevs.com/news/390589/study-cold-weather-effects-electric-bus-range/>
- Madison Area Transportation Planning Board. (n.d.). <http://www.madisonareampo.org/documents/DBRTTravelTimeEstimationApproach.pdf>
- Marcor, A. et al. (2013). Fuel consumption reduction in urban buses by using power split transmissions. [10.1016/j.enconman.2013.03.019](https://doi.org/10.1016/j.enconman.2013.03.019)
- Margolis, J. (2019). China dominates the electric bus market, but the US is getting on board. Retrieved 18 December 2019, from <https://www.pri.org/stories/2019-10-08/china-dominates-electric-bus-market-us-getting-board>
- MBTA Blue Book Open Data Portal. (2019). MBTA Bus Ridership by Trip, Season, Route/Line and Stop. Retrieved May 7, 2020, from <https://mbta-massdot.opendata.arcgis.com/datasets/mbta-bus-ridership-by-trip-season-route-line-and-stop>
- Moura, S. et al. (2010). A Stochastic Optimal Control Approach for Power Management in Plug-In Hybrid Electric Vehicles. [10.1109/TCST.2010.2043736](https://doi.org/10.1109/TCST.2010.2043736)
- Osseiran, L. (2020) Data Analysis on Electric Bus Operating in Kolkata City, India

- Pan, C., et al. (2019). Optimal Control for Hybrid Energy Storage Electric Vehicle to Achieve Energy Saving Using Dynamic Programming Approach. 10.3390/en12040588
- Poulton, M. (2011). Electric buses.
- Rasu, N. G., Renil, A. M., Sachin, S. J. (2016). CFD analysis of commercial bus models for improvement of aerodynamic performance.
- Tigue, K. (2019, November 14). U.S. Electric Bus Demand Outpaces Production as Cities Add to Their Fleets. InsideClimate News.
<https://insideclimatenews.org/news/14112019/electric-bus-cost-savings-health-fuel-charging>
- U.S. Department of Health and Human Services. (2016). Anthropometric Reference Data for Children and Adults: United States, 2011–2014.
https://www.cdc.gov/nchs/data/series/sr_03/sr03_039.pdf
- US EPA. (2020). Sources of Greenhouse Gas Emissions. Retrieved May 7, 2020, from
<https://www.epa.gov/ghgemissions/sources-greenhouse-gas-emissions>
- Vahidi, A., Sciarretta, A. (2018). Energy Saving Potentials of Connected and Automated Vehicles. <https://doi.org/10.1016/j.trc.2018.09.001>
- Vepsäläinen, J., Otto, K., Lajunen, A., Tammi, K. (2018). Computationally efficient model for energy demand prediction of electric city bus in varying operating conditions. Elsevier Ltd.
- Wikipedia. (2020). MBTA key bus routes.
https://en.wikipedia.org/w/index.php?title=MBTA_key_bus_routes&oldid=951200561
- Xcelsior CHARGE. (n.d.). Xcelsior CHARGE, Our zero-emission battery-electric bus. Newflyer.com
- Xu, Y., Gboglah, F. E., Lee, D. Y., Liu, H., Rodgers, M. O., Guensler, R. L. (2015). Assessment of alternative fuel and powertrain transit bus options using real-world operations data: Life-cycle fuel and emissions modeling. Applied Energy, 154, 143–159.
<https://doi.org/10.1016/j.apenergy.2015.04.112>
- Yu, W., et al. (2019). Analysis of Space-Time Variation of Passenger Flow and Commuting Characteristics of Residents Using Smart Card Data of Nanjing Metro. 10.3390/su11184989
- Yulianto, A. et al. (2017). Modelling of full electric and hybrid electric fuel cells buses. 10.1016/j.procs.2017.08.036

Appendix

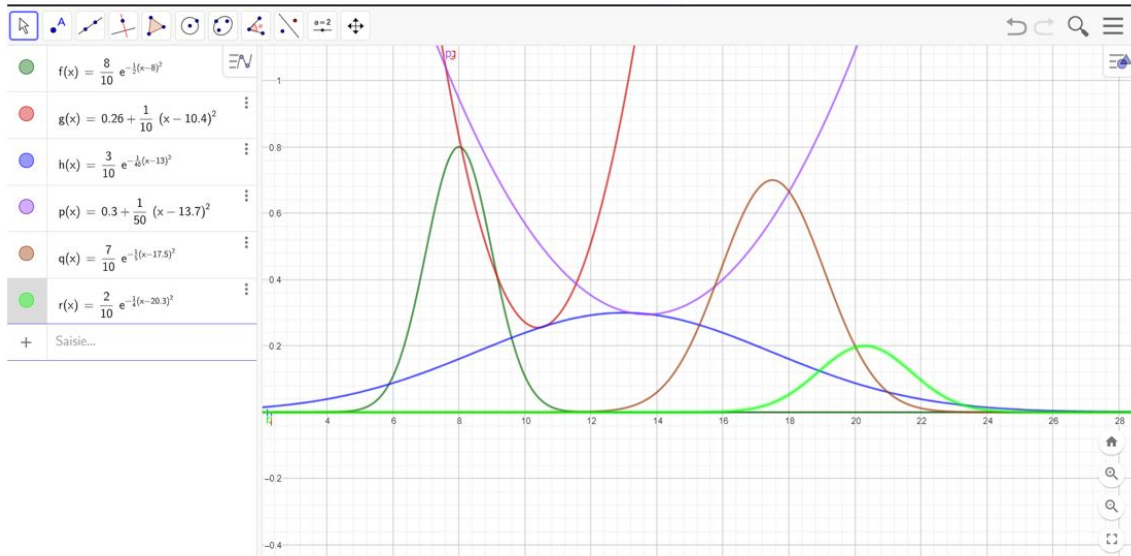


Figure A.1: Mathematical functions used to build the ridership function.

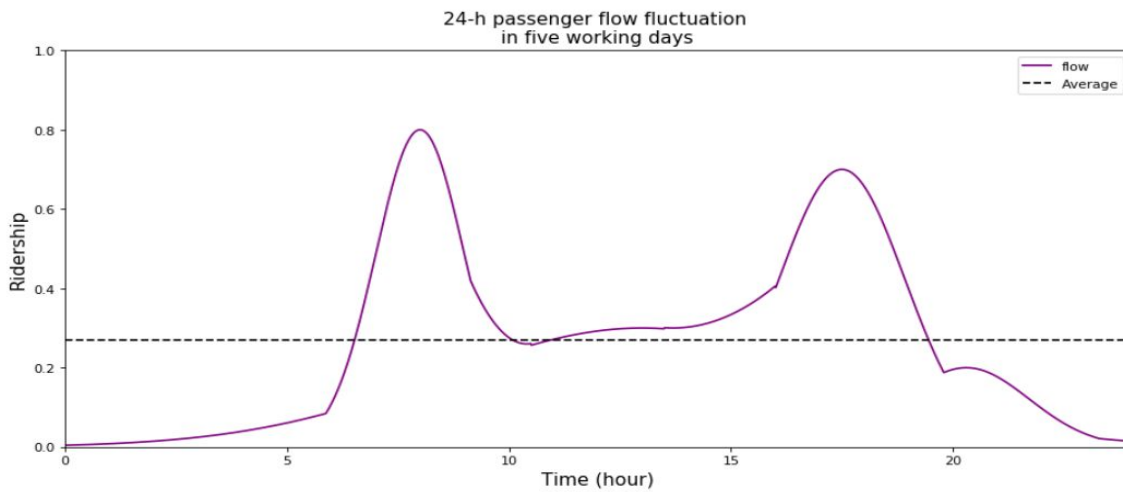


Figure A.2: Mathematical model for the percentage of ridership during a weekday.

Project Report

Total Cost of Ownership Optimization for Fleet Transformation from ICE to EV



Executive Summary

This project studies two types of vehicles, Internal Combustion Engine Vehicles (ICEVs) and Electric Vehicles (EVs). The project aims to calculate and compare the Total Cost of Ownership (TCO) for fleets of ICEVs and EVs. The motivation is that the global climate crisis has risen dramatically in recent years and increasing numbers of people are paying attention to the change of cost in switching from ICEVs to EVs.

For methodology, all cost sections will be converted to the Net Present Value (NPV) for TCO measurement. The size of the fleet is considered to be 5 vehicles, and TCO calculations use the most cost-effective manner which involves the optimization.

In the ICEV section, the diesel was chosen for analyzing. To calculate the total cost of ownership of baseline diesel vehicles, our team collected information to make assumptions like the baseline manufacturers suggested retail price, the annual insurance cost, the average fuel economy, and so on.

In the EV section, the report displays the inputs collection for the TCO calculation of the EVs, which mainly include the EVs price and infrastructure cost. The EVs part includes the cost of the EV in different weight classes, the data related to the battery, and the optimization of the battery. The infrastructure part includes the cost options for building a charger station based on the different charger levels and other costs, such as labor, material, and rebate. The final infrastructure is selected to be AC level 2.

For the result section, the report displays the result and analysis in tables and plots from the excel calculation model, all inputs and formulas are listed in the previous sections. The sensitivity analyses are also provided in the tables in this section.

In conclusion, under the ideal situation where battery in EVs only replaces once, annual mileage is constant 100,000 miles etc, TCO in different weight classes have the trend that TCO of EVs is slightly lower than that of ICEVs. As for sensitivity analysis, when the expected life of the battery is fixed, EVs have benefit for the large distance transport. Besides, the maximum allowable frequency of battery replacement when EVs have benefit in TCO comparison is once. One more battery replacement may eliminate the advantage of EVs in TCO.

Given that the research object is the trucks with large annual mileage, the results show that long-distance is preferable, and batteries may be replaced more than once. In this case, EV TCO outweighs ICE TCO.



Table of Contents

● Executive Summary.....	2
● Project Introduction.....	4
● Methodology.....	5
● Internal Combustion Engine Vehicles	7
○ Background.....	7
○ Assumptions Made for Project Comparison.....	7
○ Total Cost of Ownership Calculations for ICEVs.....	10
● Electric Vehicles	11
○ Background.....	11
○ Literature Review.....	11
○ EV Data Collection and Analysis.....	11
○ Additional Battery Data for Validation.....	14
○ EV Battery Optimization.....	17
○ EV Charging Infrastructure.....	21
○ Assumptions Made for Project Comparison.....	22
○ Total Cost of Ownership Calculations for EVs.....	24
● Result and Analysis.....	25
○ Comparison Between ICE and EV.....	25
○ Sensitivity Analysis.....	26
● Conclusion.....	28
● Reference	
● Appendix	



Project Introduction

This project aims to calculate and compare the TCO for fleets of ICEVs and EVs. To be consistent in TCO value comparison, all cost sections will be converted to the NPV for TCO measurement. The size of the fleet is considered to be 5 vehicles, and TCO calculations use the most cost-effective manner which involves the optimization.

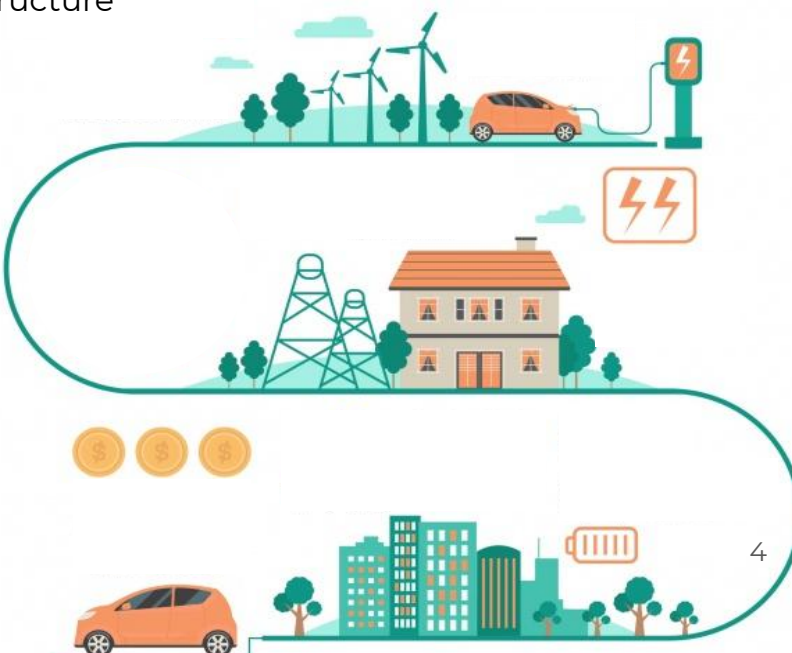
Over the last few decades, the global climate crisis has risen dramatically, and the need for the adoption of electric vehicles is higher than ever. At the same time, increasing numbers of people are now considering switching from their traditional ICE based vehicles, but the switch needs to be done in a considerate and cost-effective manner. In this case, more individuals and companies tend to know the different costs between ICEVs and EVs.

Due to the fact that ICEVs have a well-developed market and usage, the TCO of ICEVs has a negligible optimization space, our team tends to collect multiple online data and select the most fitting sources to the comparison scenarios, such as weight class, annual mileage and etc.

In this study, the challenges and opportunities especially EVs will be examined from several different angles with the objective of optimizing the TCO, which includes the battery storage of EVs.

With the ever-changing landscape of product availability, EV economics, infrastructure, regulatory policy and so on, the trade-offs between vehicle and infrastructure costs in different market scenarios will be evaluated.

The source of inputting data used are open-source, and our final result will also be open-source, allowing for flexible parameter changes later on.



Methodology

The first step of this project is preprocessing the information and data, including literature review and online source searching. There is massive data collected during this step, since the complexity of setting and the large range of this project topic. One type of setting parameters is the traffic scenarios, which contain urban or countryside road conditions and long-distance or short-distance transport. It is simplified in this study to the area of California and combines the transport model with the annual mileage. Since the system's complexity would increase as the size of the scenario increases, considering only 5 trucks for both ICEVs and EVs would be a good start of our project.

After preprocessing the information, the proper online source is selected to build up the TCO calculation model in excel. There are several reasons for using excel: The functions of it are enough for TCO calculation (maybe include optimization in the future, but it is not achieved by our team), and operations on calculation and regulations of features' values are convenient. Meanwhile, the sponsor of this project asked for this format. Other than that, the EVs are developing so fast that the input parameters need to be updated frequently, and many research directions are not covered in this project. Excel can easily allow other people to modify the TCO calculation model based on their own interests and data.

Optimization of this project is conducted in Python. Based on the collected information, the only part that can be optimized and is essential to consider is the battery of EVs. Other factors like ICEVs and infrastructure of EVs have negligible optimization space. The variables considered in this project are battery life length, energy efficiency, annual mileage, and etc.

In order to minimize the cost of the battery, the optimal variable is chosen to be battery life length (battery replacement timing) and all constraints are listed in subsection Battery Optimization. The optimal results will be presented in plots form.



As the report mentioned before, the NPV is used to calculate and compare TCO. NPV discounts the future benefits and costs into present-day numbers through the introduction of the inflation rate. NPV is generally calculated using formula:

$$NPV = -C_0 + \sum_{i=1}^T \frac{C_i}{(1+r)^i}$$

Where C is the cash flow during the given periods, C_0 is the upfront capital cost, T is the length of periods, and r is the inflation rate for the period.

Sensitivity analysis is applied towards the end of this research, the sensitivity of several factors is measured and listed to demonstrate the influence of changing those factors.

Total 3 factors are considered:

- Weight class
- Annual mileage
- Time of battery replacement

All results of each section or subsection will be presented in tables and figures.





Internal Combustion Engine Vehicles (ICEVs)

Background

Internal combustion engines (ICE) has served as the primary method to power different types of vehicles since the 1800s. However, because of the development of the electrical vehicles, gasoline and diesel station sales began to swell, with a slight dip following the recession, sales have been on the decline since 2012. However, they still have some advantages compared to electric vehicles, including vehicle costs and depreciation rate, in some cases. The purpose of this section is to find out the total cost of ownership for ICEVs given the same vehicle type and other conditions as that for EVs. Through this analysis, it would be easier to compare the two types of vehicles and come up with reliable conclusions.

Assumptions Made for Project Comparison

In this project, the type of baseline fuels that our team analyzed is diesel. To calculate the total cost of ownership of baseline diesel vehicles, a series of assumptions are made according to the information collected. The specific information for the value of different factors to calculate the total cost of ownership are listed in Table 1.



Symbols	Variables	Average Values
a	Expected Ownership Period (Years).	a=10
b	Number of Vehicles to compare (#)	b=1
c	Baseline Manufacturers Suggested Retail Price MSRP (\$).	\$120,000
d	Adjusted Price after rebates, etc. (\$).	\$118,000
e	Value of Trade-In (\$)	\$68,000
f	Projected Residual Value at end of ownership (% of baseline adjusted price after rebates etc)	20%
g	Annual Maintenance & Service Cost per Truck (\$)	\$1,000
h	Maintenance Cost Trend (% change per year)	8%
i	Annual Insurance Cost per Truck (\$)	\$1,300
j	Insurance Cost Trend (% change per year)	7%
k	Average fuel economy (MPG)	6 MPG
m	Current Fuel Price (\$/gal)	\$3.19
n	Fuel Price Trend (projected % change per year)	8%

Table 1. Values related to diesel Variables in our project

It is assumed the values for the expected ownership period and the number of vehicles to be 10 years and 1 vehicle. The average manufacturer's suggested retail price (MSRP) is found to be \$150,000 for the heavy duty truck. Also the rebate is approximately \$2,000 is assumed, which means that the adjusted price of a diesel vehicle would be \$148,000. The value of Trade-in should be between \$0 and the adjusted price after rebates. After consideration and investigation, the trade-in value is chosen to be around \$68,000.

The projected residual value at end of ownership should be between 15% to 85% per truck. The suggested value is 20% if owned over 10 years based on salvage value. So 20% is set to be the projected residual value at the end of ownership.

As for the annual maintenance and service cost per truck, it can also vary quite a bit and total up to several thousand dollars every year. On average, it could be \$1,000 per year [1].

Also, the maintenance cost trend is close to 8%. Of all the factors shown above, car insurance costs are one of the hardest things to determine because it relates not only to your credit score, age, marital status, but also to the city where you live and how often you drive your vehicle.

According to a study commissioned by Quadrant Information Services, the annual car insurance cost in the United States is around \$1,300 [1].

As for the current fuel price, the weekly California diesel price value is used which is around \$3.191 per gal in our project according to the latest update of the eia U.S. Energy Information Administration website. The true value of fuel prices of different locations in California are presented in Figure 1.

Show Data By: Product Area	<input type="button" value="Graph"/> <input type="button" value="Clear"/>	03/30/20	04/06/20	04/13/20	04/20/20	04/27/20	05/04/20	View History
U.S.	<input type="checkbox"/>	2.586	2.548	2.507	2.480	2.437	2.399	1994-2020
East Coast (PADD1)	<input type="checkbox"/>	2.671	2.634	2.599	2.576	2.545	2.510	1994-2020
New England (PADD 1A)	<input type="checkbox"/>	2.793	2.745	2.715	2.709	2.677	2.652	1997-2020
Central Atlantic (PADD 1B)	<input type="checkbox"/>	2.866	2.827	2.782	2.747	2.711	2.688	1997-2020
Lower Atlantic (PADD 1C)	<input type="checkbox"/>	2.514	2.480	2.450	2.434	2.406	2.360	1997-2020
Midwest (PADD 2)	<input type="checkbox"/>	2.432	2.394	2.353	2.326	2.287	2.248	1994-2020
Gulf Coast (PADD 3)	<input type="checkbox"/>	2.363	2.325	2.289	2.272	2.208	2.169	1994-2020
Rocky Mountain (PADD 4)	<input type="checkbox"/>	2.592	2.541	2.497	2.471	2.434	2.370	1994-2020
West Coast (PADD 5)	<input type="checkbox"/>	3.126	3.090	3.028	2.974	2.934	2.899	1994-2020
West Coast less California	<input type="checkbox"/>	2.798	2.754	2.695	2.640	2.593	2.545	2011-2020
States								
California	<input type="checkbox"/>	3.395	3.368	3.302	3.248	3.214	3.191	1995-2020

Figure 1. Weekly California Diesel Prices

Table 2. Truck Classes and Their Corresponding MPG

Truck Class	Miles Per Gallon (MPG)	MPG Range
3	13	12-14
4	10	9-11
5	9	8-10
6	7.5	7-8
7	6	5-7
8	5	<5

Total Cost of Ownership Calculations for ICEs

Using the previous assumptions and following equations, the total cost of ownership for one diesel vehicle over 10 years can be calculated:

- **Year 0:**
 - Initial Acquisition Cost: $-(d - e) \times b$
 - Total Cost of Year 0 = Initial Acquisition Cost = $-(d - e) \times b$

- **Year 1:**
 - Fuel Cost: $\left[\left(-\frac{\text{Annual Mileage}}{k} \right) \times m \times (1 + n)^1 \right] \times b$
 - Maintenance Cost: $-g \times (1 + h)^1 \times b$
 - Insurance Cost: $-i \times (1 + j)^1 \times b$
 - Total Cost of Year 1 = Fuel Cost + Maintenance Cost + Insurance Cost =

$$\left[\left(-\frac{\text{Annual Mileage}}{k} \right) \times m \times (1 + n)^1 \right] \times b + \left[-g \times (1 + h)^1 \times b \right] + \left[-i \times (1 + j)^1 \times b \right]$$

- **Year #:**
 - Fuel Cost: $\left[\left(-\frac{\text{Annual Mileage}}{k} \right) \times m \times (1 + n)^{\#} \right] \times b$
 - Maintenance Cost: $-g \times (1 + h)^{\#} \times b$
 - Insurance Cost: $-i \times (1 + j)^{\#} \times b$
 - Total Cost of Year # = Fuel Cost + Maintenance Cost + Insurance Cost =

$$\left[\left(-\frac{\text{Annual Mileage}}{k} \right) \times m \times (1 + n)^{\#} \right] \times b + \left[-g \times (1 + h)^{\#} \times b \right] + \left[-i \times (1 + j)^{\#} \times b \right]$$

- **TCO** = $\sum_0^{\#=10} (\text{Total Cost of Year } \#)$

The abbreviations can be found in Table 1. The total cost at year 0 is recorded, which is just the actual purchase cost times the number of vehicles bought. Then, each year the vehicles will have a certain Fuel Cost, Maintenance Cost, and Insurance Cost. It is assumed that these costs are not constant, which complicates the calculations. For the total cost at any given year after year 0, all of them are converted to net present values. Thus, the total cost of ownership would just be the sum of initial acquisition cost and of the annual costs. The predicted TCO for 1 vehicle (Class 5) over 10 years is calculated to be about \$407,000.

Electric Vehicles (EVs)



Background

EVs could bring economic and environmental benefits, such as increased job growth and reductions in GreenHouse Gas (GHG) emissions. Governments all over the world provide financial incentives to stimulate consumer behavior and support electric vehicle adoption. Battery plays a key role in the cost of EVs, so this project mainly focuses on the battery in the EVs part for both research and optimization.

Literature review

In order to conduct study on EVs, our team did lots of background research. Main takeaways include: Energy spending is the largest cost savings for electric vehicles compared to the traditional diesel vehicles, which is the opposite in reality due to the extreme low oil market price during the current pandemic. While driver compensation and fuel are the largest operational cost elements for conventional vehicles. Also, the battery is the largest cost element for EVs, and energy efficiency depends heavily on the weight class of the truck. Other than that, annual mileage and vehicle lifeline are main determinants of cost. Last but not least, uncertainty is a major barrier in optimization and TCO analysis.

EV Data Collection and Analysis

Based on the data from existing EVs companies, the capital cost of EVs is decreasing dramatically for the past decade, especially the energy storage that is the largest cost element for EVs. The battery costs are decreasing significantly year over year since 2010, the price of an average lithium-ion battery pack has dropped by over 80%. The tendency of future Battery Replacement Cost (\$/kWh) is gathered and predicted from figure 3 from an online article “Powering The EV Revolution” [9].



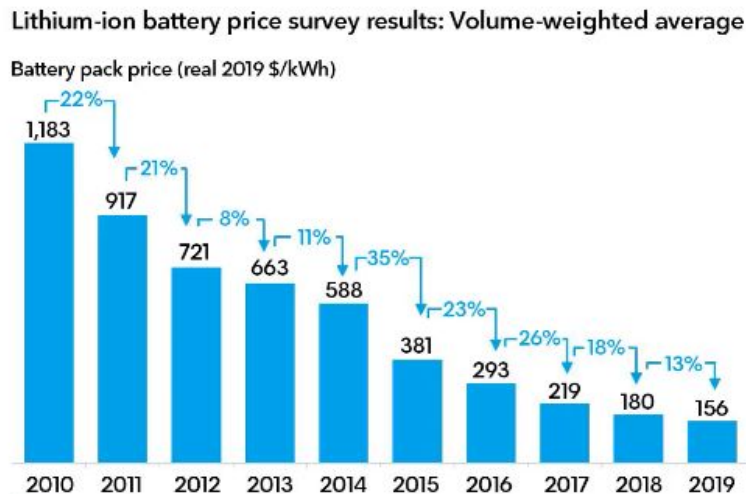


Figure 2. The past data of Battery Replacement Cost (\$/kWh)

Other than online sources, our team also contacted and discussed with expert Andrej Ivanco in the electric truck field, the lowest bound of Battery Replacement Cost should be around 80 \$/kWh were informed during the online meeting.

According to a 2017 report [6] of city transit electric buses (class 8), the average battery energy consumption is 1.89 kWh/mile. After doing deep research, our team figured out that the electric trucks have large differences in energy efficiency based on the weight class of the electric truck as the Table 3 demonstrates below.

Table 3. Electric Vehicle Weight Classification

ID	Description	Min Weight (lbs)	Max Weight (lbs)
1	Class 1	0	6,000
2	Class 2	6,001	10,000
3	Class 3	10,001	14,000
4	Class 4	14,001	16,000
5	Class 5	16,001	19,500
6	Class 6	19,501	26,000
7	Class 7	26,001	33,000
8	Class 8	33,001	100,000

From the paper “Medium- and Heavy-Duty Vehicle Electrification: An Assessment of Technology and Knowledge Gaps” [7] , the Figure 3 with multiple calculated energy efficiency of each weight class of electric trucks provides us with a more proper and accurate number of energy efficiency. According to this graph, higher weight class corresponds to more energy consumption.

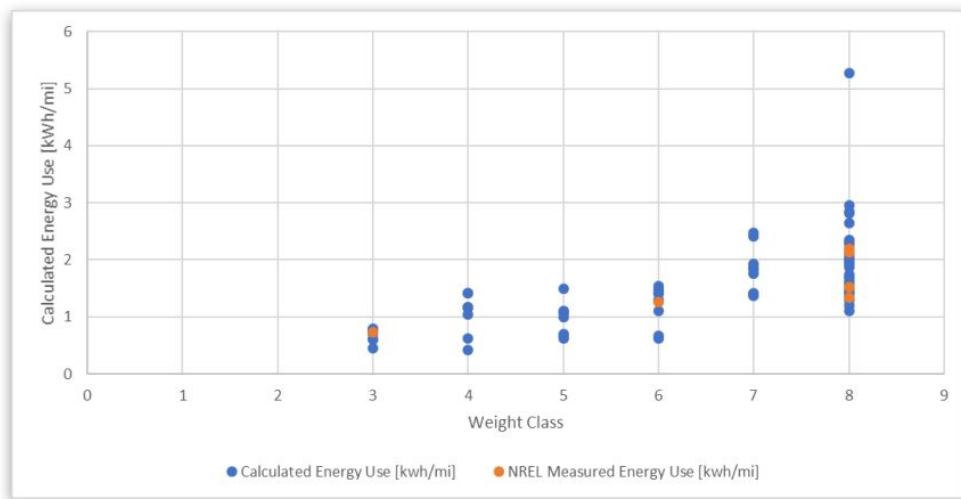


Figure 3. Energy Efficiency of Electric Vehicle with different weight class

Besides, annual mileage and vehicle lifeline are critical determinants of cost. Our team found the typical battery coverage of family use electric vehicles is 8 years or 100,000 miles, which varies by manufacturer and country. Due to the fact that food trucks from large manufacturers like whole food can drive more than 100,000 miles in just one year, so 8 year is considered as the constraint of maximum battery lifeline rather than 100,000 miles.

Uncertainty is the main issue in our TCO analysis, especially the rebate policy, essential charging data for different electric trucks. Therefore, lots of assumptions are made in this project to conduct the optimization and TCO analysis.

According to Table 4, the cost of vehicles consists of powertrain, vehicle assembly, and indirect cost. The price of diesel vehicles could be regarded as invariable. The electric vehicle powertrain includes battery pack, thermal management and powerdistribution, power distribution module, inverter/converter, electric drive module, DC converter, controller, control module, high voltage cables, on-board charger and charging cord. It should be mentioned that for electric vehicles.

The cost of the battery accounts for a large part of the cost of the vehicles. The costs of other parts of vehicles are relatively fixed. So, in the calculation of TCO, it is assumed that the costs of those are constants and mainly consider the price of the battery pack.

In addition, comparing the cost of diesel vehicles and electric vehicles, the other direct costs are the similar. For indirect cost, although electric vehicles have a higher cost in 2017, this expenditure decreases so much and is expected to drop to only 3,200 in 2025.

Table 4. Cost summary of Electric Vehicles

Type	Component	UBS (2017) costs			How UBS costs are adapted to determine electric vehicle costs for this analysis
		Gasoline	2017 electric	2025 electric	
Electric vehicle powertrain	Battery pack	-	\$11,500	\$8,000	The UBS estimate shown here is for \$133/kWh in 2025. This is updated to \$104/kWh in 2025 and \$72/kWh in 2030 for this analysis this by applying pack-level cost reduction of 7% per year based on research noted in the text. ^a
	Thermal management	-	\$250	\$225	Electric powertrain costs are based on UBS component costs for cars and crossover vehicles (150 kW) and scaled up by 47% (220 kW versus 150 kW) for SUVs. ^b
	Power distribution module	-	\$250	\$295	
	Inverter/converter	-	\$697	\$523	
	Electric drive module	-	\$1,200	\$1,080	
	DC converter	-	\$150	\$134	
	Controller	-	\$51	\$46	
	Control module	-	\$93	\$84	
	High voltage cables	-	\$335	\$302	
Conventional powertrain	On-board charger	-	\$273	\$205	UBS costs are scaled up to reflect the higher power of U.S. average cars and crossover vehicles by 18% (150 kW versus 127 kW) and SUVs by 74% (220 kW versus 127 kW) ^b
	Charging cord	-	\$150	\$135	
Other direct	Powertrain (engine, transmission, exhaust, etc.)	\$6,800	-	-	For vehicle assembly, UBS costs are scaled up to account for the larger footprint of average U.S. vehicles: 6% for cars, 5% for crossovers, and 21% for SUVs. ^b This also includes the incremental costs of vehicle improvements needed to meet efficiency standards.
Indirect cost	Vehicle assembly	\$12,700	\$12,600	\$11,900	Based on UBS, combustion vehicle indirect costs are fixed at 20.5% of direct costs. For electric vehicles, the same proportional R&D indirect cost reduction over time that UBS used for cars is assumed for all three vehicle classes.
Includes depreciation, amortization, research and development (R&D), and administration expenses	\$4,000	\$10,584	\$3,200		

Addition Battery Data for Validation

It should be mentioned that the resulting battery cell-level costs, averaged across the three EV cases, are \$78/kWh in 2025 and \$56/kWh in 2030, which largely match the trend mentioned before.

According to Figure 4, the highest-cost electric vehicle component is the battery pack, which declines from \$11,500 to \$8,000, based on UBS' estimate that the pack cost reaches \$133/kWh by 2025.

Currently, most electric vehicle batteries are designed for cars. These data were collected to calculate the cost of that for the truck.



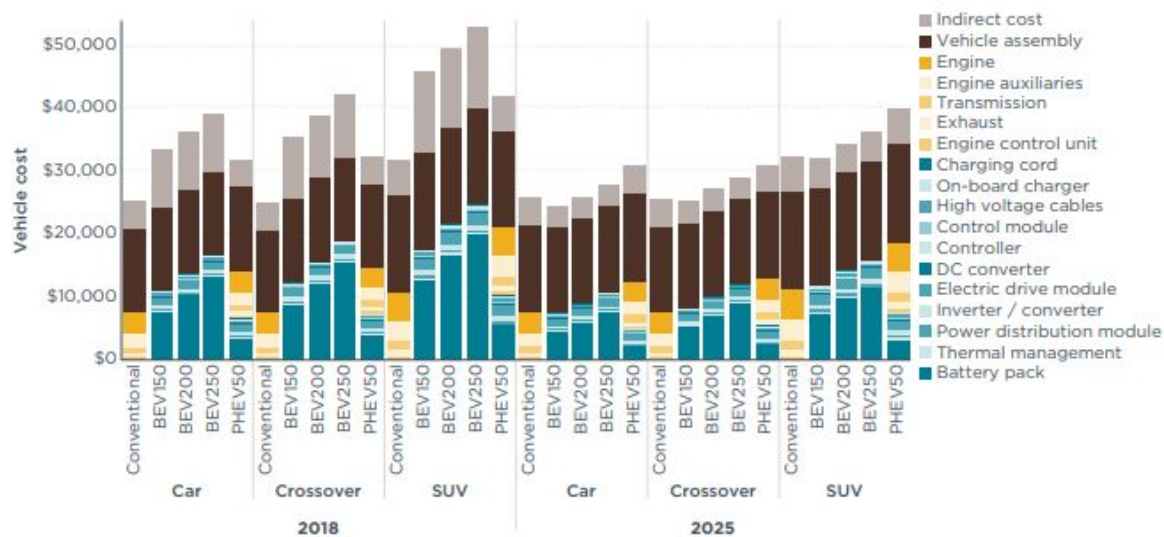


Figure 4. Vehicle technology costs for conventional and electric vehicles in 2008 and 2025 for cars, crossovers, and SUVs.

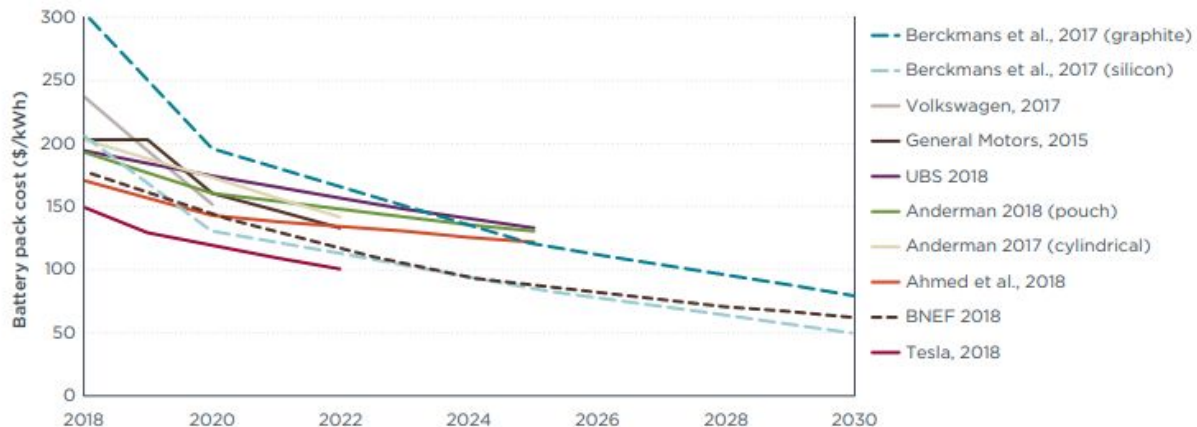
Table 5. Electric vehicle battery pack cost (\$/kWh) for 2020-2030.

Type	Report	2020	2022	2025	2030	Notes
Technical reports	Ahmed et al., 2018 ^a	143	134	122		Pouch NMC 6,2,2-graphite, production volume-based; includes total cost to automaker for material, process, overhead, depreciation, warranty
	Anderman, 2017 ^b		142			Cylindrical 21700, NCA 83,13,4, production volume-based; includes cost of material, capital, pack integration, labor, overhead, depreciation, R&D, administration, warranty, profit
	Anderman, 2018 ^c	160		128		Pouch NMC 8,1,1-graphite, production volume-based; includes cost of materials, capital, pack integration, labor, overhead, depreciation, R&D, administration, warranty, profit
	Berckmans et al., 2017 ^d	191	165	120	80	Pouch NMC 6,2,2-graphite anode, production volume-based; includes material, process, labor, overhead, depreciation, profit
	317	131	85	50		Pouch NMC 6,2,2-silicon alloy anode, production volume-based; includes material, process, labor, overhead, depreciation, profit
Automaker statements	UBS, 2017 ^e	184		133		Pouch NMC 6,2,2-graphite, production volume-based; includes material, process, labor, overhead, depreciation, profit
	Davies, 2017 ^f	152				Volkswagen statement. Associated with planned production volume of 100,000 per year by 2020 for I.D. series
	Lienert & White, 2018 ^g	160	133			General Motors statement related to Chevrolet Bolt (NMC 6,2,2), associated 2020-2022 production volume has not been stated
	Tesla, 2018 ^h	130	100			Tesla statement related to Model 3 production volume of 500,000 with Panasonic battery production in Nevada by 2020

Some estimates indicate that battery pack costs will decline to \$130–\$160/kWh by 2020–2022, and then to \$120–\$135/ kWh by 2025. However, Tesla states it will reach \$100/kWh by 2022, associated with its NCA-based battery pack technology and based on its earlier high-production volume. In Table 5, some factors are considered related to battery cost. The cost of the battery pack in this table can be approximately computed by mid pack cost multiply Battery pack from Table 6.

Table 6. Factors considered in the cost of car

	Conventional								Electric					
	Car		Crossover		SUV		Car		Crossover		SUV			
	2018	2030	2018	2030	2018	2030	2018	2030	2018	2030	2018	2030	2018	2030
Power (kW)	150	150	150	150	220	220	150	150	150	150	220	220		
Fuel economy (mpg)	30	37	26	33	20	25								
Range* (miles)	Short						150	150	150	150	150	150		
	Mid						200	200	200	200	200	200		
	Long						250	250	250	250	250	250		
Electric efficiency (kWh/mile)	Short						0.28	0.26	0.34	0.31	0.48	0.44		
	Mid						0.29	0.27	0.35	0.32	0.50	0.46		
	Long						0.30	0.28	0.36	0.33	0.51	0.47		
Battery pack (kWh)	Short						42	39	50	46	72	66		
	Mid						58	54	69	64	99	92		
	Long						75	69	90	83	128	119		
Utility factor	Short						0.93	0.93	0.93	0.93	0.93	0.93		
	Mid						0.95	0.95	0.95	0.95	0.95	0.95		
	Long						0.97	0.97	0.97	0.97	0.97	0.97		
Pack cost (\$/kWh)	Short						\$177	\$74	\$175	\$74	\$175	\$73		
	Mid						\$175	\$73	\$175	\$73	\$167	\$72		
	Long						\$175	\$73	\$172	\$73	\$154	\$64		

**Figure 5.** Electric vehicle battery pack costs from technical studies and automaker statements

Vehicle-to-Grid

V2G describes a system in which EVs connect to the power grid to charge and store electric energy at a relatively low price and sell electric energy back to the grid at high price in one day. The usage of V2G also involves storing and discharging electricity generated from renewable energy sources such as solar and wind, which reduces the wasting energy due to the weather or time of day. According to a report of potential earnings associated with V2G, the average earning of V2G is roughly \$400 per year [11].

In this project, V2G should only be considered during weekends when the EVs stop work for the daytime, so that EVs' battery storage is available for charging and discharging timing. Based on the data from chooseenergy.com [14], the value of the difference of electricity costs per day is \$0.009 as Figure 6 shown below.



Figure 6. Unit Electric Price Changes Over the Time (in one day)

EV Battery Optimization

Before going to battery optimization, here are some assumptions made for this project. The ownership period (N) is set to be 10 years in this study. And based on the inflation rate in California that was floating from 2% to 3% during the past few years, the inflation rate (i) is assumed to be constant 2.5% throughout this project. The conversion of present value from future value and annual value used the online equations listed below [10]:

$$\text{From future to present } (P/F, i, N) = 1/(1+i)^N$$

$$\text{From future to present } (P/A, i, N) = ((1+i)^N - 1)/(i(1+i)^N)$$

In consideration of battery charging, battery replacement only happens one time during the ownership period (year of replacement $\gg 5$) to simplify the optimization and TCO analysis.

Also, Vehicle-to-Grid (V2G) is used to benefit the TCO of EVs in this study, and it is assumed that battery life will not be affected by V2G which is only used during the weekend.

As for the vehicle usage part, our team considered the average daily mileage as a constant in calculation, and EVs are only used during weekdays. The Objective Function is to minimize the TCO with Net Present Value of Battery cost and the battery usage life is chosen as the optimal variable.

All constraints are listed below:

- Battery replacement cost = Battery capacity (kWh) * Unit replacement cost (\$/kWh);
- Ownership Period = 10 years;
- The size of the fleet is 5;
- Battery usage length \geq 5 (yrs) (only replace battery once);
- Unit cost for first battery \geq 156 (\$/kWh);
- Unit replacement cost $\geq \max(80, 156 \cdot 0.9^n)$ (\$/kWh)
- Battery Efficiency = a range based on weight class (kWh/mi);
- Battery Capacity Margin for aging = $25\% \cdot \text{Battery usage length} / 8 \text{ year}$ (% of new full capacity);
- Battery Capacity Margin for design = $5\% \cdot \text{Battery usage length} / 8 \text{ year}$;
- Battery Capacity Margin for agine = $5\% \cdot \text{Battery usage length} / 8 \text{ year}$;
- Battery Capacity Margin for Cold/Hot Weather Operation = 3% (% of full capacity);
- Battery Capacity Margin for Driver Efficiency = 3% (% of full capacity);
- Battery Low Cutoff = 3% (% of full capacity);
- Total Battery Capacity Margin = Battery Capacity Margin for aging + Battery Capacity Margin for design + Battery Capacity Margin for Cold/Hot Weather Operation + Battery Capacity Margin for Driver Efficiency + Battery Capacity Margin for Low Cutoff (% of full capacity)
- Battery capacity = Average daily mileage * Battery Efficiency * (1 + Total Battery Capacity Margin) (\$/kwh)
- Profit of V2G = Reduced Efficiency due to the charge/discharge time(%) * 2 days (weekends) * 52 weeks * Battery capacity * Value of Changes of electricity costs per day

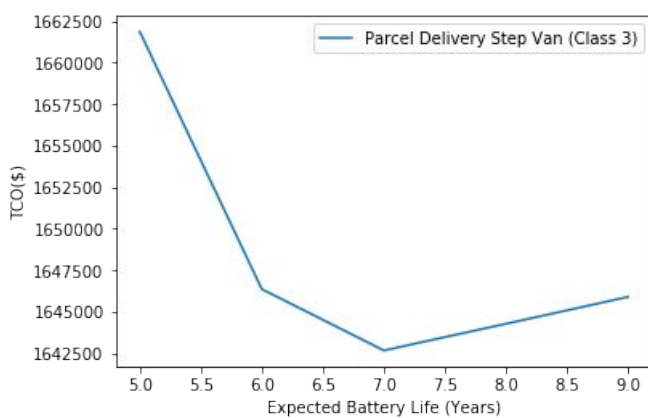
Precisely, the TCO is only considered in 10 years and replaces the battery once. So, the expected life of the first battery should be larger than 5 years. Battery cost is from the multiplication of Battery capacity (kWh) and Unit replacement cost (\$/kWh). From data collected before, unit cost for first battery is \$156/kWh and based on previous data, the future unit replacement cost is predicted to be \$ $156 \cdot 0.9^n / \text{kWh}$ but not less than \$80/kWh. Based on the article "Design and Optimization of Lithium-Ion Batteries for Electric-Vehicle Applications" [12], battery capacity margin and battery low cutoff are also put into consideration to design the battery. Particularly, the rate of battery capacity margin for aging and design vary as the expected usage length. For the V2G calculation, it is assumed that vehicles do not work on weekends and there are 52 weeks per year and 2 weekends as rest days per week. Then an efficiency reduction is added to the V2G equation to control the results and integrate all factors which affect V2G.

Cases Calculation

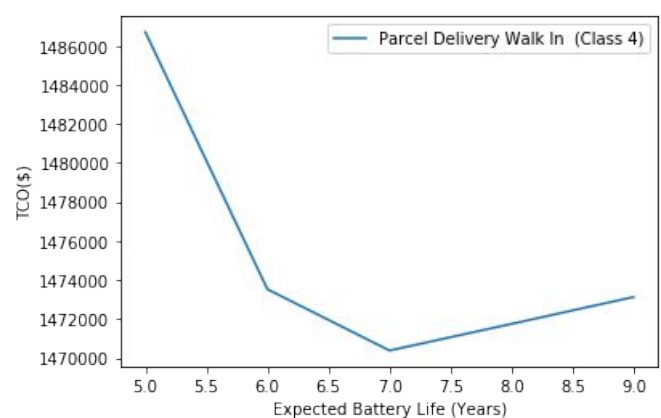
The data from National Renewable energy Lab [13] are listed below. These data are used to calculate TCO in each case. Particularly, the team focuses on its weight class and vocation type as well as mileage. For each case, annual mileage is a constant.

Table 7. Commercial Fleet Vehicle Operating Data. [13]

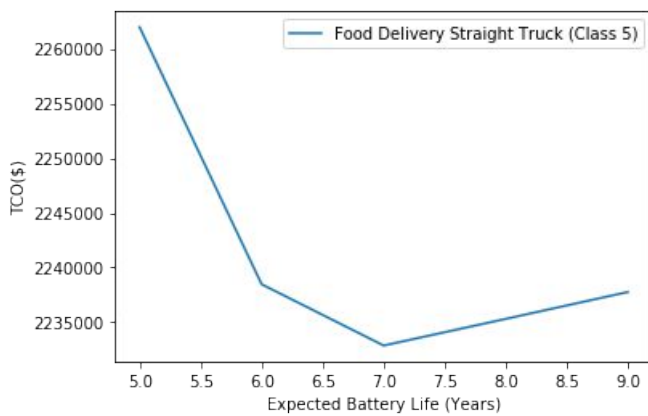
class_id	voc_id	type_id	vocation	type	duration_hrs	driving_hrs	rate	distance_total	total_ave_speed	ave_speed	Mileage_per_day	Mileage_per_year
6	6	39	Linen Delivery	Walk In	501.793889	258.306389	0.514766	8776.592749	17.490434	33.977451	475.684318	123677.922737
5	14	32	Food Delivery	Straight Truck	727.321389	288.740556	0.396992	9678.659162	13.307266	33.520262	469.283672	122013.754812
7	3	32	Warehouse Delivery	Straight Truck	260.398056	168.088889	0.645507	5581.027633	21.432678	33.202835	464.839689	120858.319189
3	14	32	Food Delivery	Straight Truck	180.455000	126.397222	0.700436	4195.351812	23.248742	33.191804	464.685254	120818.166138
7	6	32	Linen Delivery	Straight Truck	119.014722	36.733333	0.308645	1183.345201	9.942847	32.214479	451.002708	117260.704135
6	6	31	Linen Delivery	Step Van	875.245278	383.406944	0.438057	11830.005685	13.516218	30.854959	431.969431	112312.052031
6	5	26	School Bus	School Bus	2539.101944	1790.397778	0.705130	51917.580084	20.447222	28.997791	405.969070	105551.958258
5	6	31	Linen Delivery	Step Van	661.009444	258.727222	0.391412	7033.276359	10.640206	27.184137	380.577924	98950.260144
7	4	32	Parcel Delivery	Straight Truck	249.608333	131.670278	0.527508	3303.264023	13.233789	25.087393	351.223504	91318.111014
4	4	39	Parcel Delivery	Walk In	438.242778	190.233333	0.434082	4292.220089	9.794160	22.562923	315.880925	82129.040429
3	4	31	Parcel Delivery	Step Van	499.336667	258.203056	0.517092	5335.972856	10.686123	20.665801	289.321208	75223.514120
8	10	5	Mass Transit	City Transit Bus	887.975000	514.773611	0.579716	10431.027170	11.746983	20.263329	283.686609	73758.518464
7	10	5	Mass Transit	City Transit Bus	3617.023889	2004.649722	0.554226	40552.443316	11.211550	20.229192	283.208682	73634.257412
4	4	31	Parcel Delivery	Step Van	1263.064722	499.745556	0.395661	9764.714355	7.730969	19.539372	273.551209	71123.314371
5	4	39	Parcel Delivery	Walk In	546.642222	296.095833	0.541663	5499.483516	10.060481	18.573323	260.026520	67606.895284
6	4	39	Parcel Delivery	Walk In	311.626389	177.472222	0.569503	3008.670888	9.654737	16.952912	237.340762	61708.598095



(a)



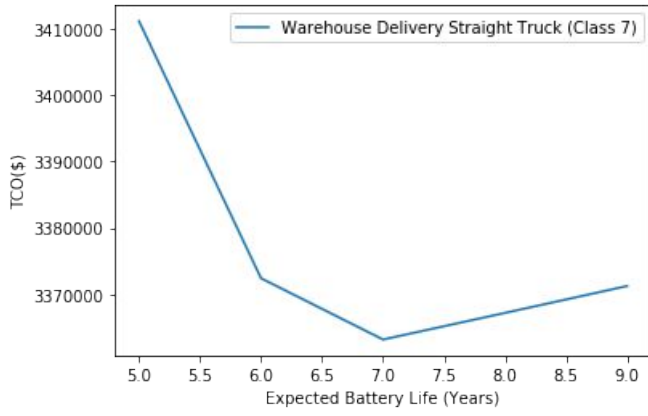
(b)



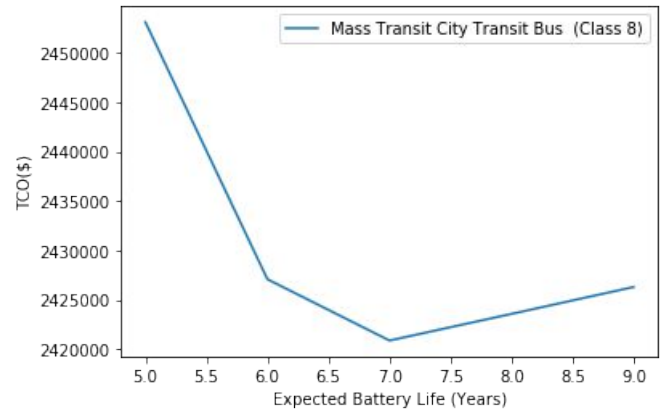
(c)



(d)



(e)



(f)

Figure 7. TCO values for: (a) weight class 3; (b) weight class 4; (c) weight class 5; (d) weight class 6; (e) weight class 7; (f) weight class 8 EV with different expected battery life.

From the results, 7 years is the optimal value. If Expected Battery Life is less than 5 years, the battery has to replace more than once. If the battery is replaced after 5 to 9 years, the longer battery life is, the lower replacement battery cost is. Battery cost (\$/kWh) decreases fast, so longer battery life will result in a lower replacement battery cost. But too long lifeline means improving the capital cost (first battery).

EV Charging Infrastructure

According to the report related to the infrastructure cost from the US department of energy, there are three types of charging levels, which are AC level 1, AC level 2 and DC Fast Charging, here is the table showing the three charging levels:

Table 8. Characteristics of different charging levels

Charging Level	Vehicle Range Added per Charging Time and Power	Supply Power
AC (Alternating Current) Level 1	4 mi/hour @ 1.4kW 6 mi/hour @ 1.9kW	120VAC/20A (12-16A continuous)
AC Level 2	10 mi/hour @ 3.4kW 20 mi/hour @ 6.6kW 60 mi/hour @ 19.2kW	208/240VAC/20-100A (16-80A continuous)
DC Fast Charging	24 mi/hour @ 24kW 50 mi/hour @ 50kW 90 mi/hour @ 90kW	208/480VAC 3-phase (input current proportional to output power; ~20-400A AC)

And here is the estimated range of the cost for every type of charger unit:

Table 9. Costs for different charger units

EVSE Type (single port)	EVSE Unit Cost Range
Level 1	\$ 300 - \$ 1,500
Level 2	\$ 400 - \$ 6,500
DCFC (Direct-current fast charger)	\$ 10,000 - \$ 40,000

Common Cost Factors to consider for Workplace Charging:

Charging level

Workplace charging stations are typically Level 1 or Level 2 single or dual port units. For level 2, it decreases the vehicle charge time, but requires a higher power circuit for operation. As the quantity of charging units at a workplace increases, electrical upgrades may be required, which could increase costs. So it is better to talk with an electrical contractor to determine how much power is available from your electrical service. The amount of available power will affect the quantity and type of charging units that can be installed at your location without the need for extensive electrical upgrades.

Charging Station Features

While some employers will choose the most basic system, others may want networking, access control, point of sale, and energy monitoring/management. Employers can minimize their costs by not paying for features that they do not need or are unlikely to use.

Location Selection

Choosing a wall-mounted unit close to an existing electrical panel will typically be the lowest cost installation option. If the prime location is far from the electrical service, there will be a significant cost to connect the charging units to the electrical service. Choosing a less prominent, but easier to install location will minimize costs.

Installation

Workplace charging sites frequently involve the installation of two or more charging units, which lowers the installation cost per unit. Workplace installations typically cost less than public installations because they have a higher percentage of stations with wall-mounted units and there is more flexibility to place charging units close to the electrical service panel.

Assumptions Made for Project Comparison

After analyzing, it is concluded that using the AC Level 2 is the best choice for our project, since DC fast charging costs much higher and even though DC fast charging has the fastest charging speed, it isn't suitable for our scenario, since our troop would return to the company everyday and the truck could be fully charged during the whole night, therefore the fastest charging speed is not the most important, the highest cost performance is what the team is looking for.

For AC level 1, according to the low charging speed, it cannot ensure that our trucks could be fully charged. Based on the reasons above, the DC fast charging and the AC Level 1 aren't suitable for our scenario.

Table 10 shows the cost of Level 2 AC charger related to the network and number of the port on the pedestal. The charger with the network provides a way to connect the charger with the mobile through Wifi.

Table 10. Hardware costs per charger for level 2 charging ports with network options

	Network (\$)	Non-Network (\$)
AC Level 2 Single Port	2,793	938
AC Level 2 Dual Port	3,127	938

Table 11 displays other cost includes labor cost, material cost, tax cost and permit cost for the Level 2 AC chargers, the cost change based on the change of the number of charger installation of the station.

Table 11. Installation Costs Per Charger

Number of installations	Labor cost per charger (\$)	Material cost per charger (\$)	Tax cost per charger (\$)	Permit cost per charger (\$)
1	2,471	1,235	283	186
2	1,786	958	172	121
3-5	1,491	1,014	110	128
> 5	1,747	908	65	115

Total Cost of Ownership Calculations for EVs

- TCO for charging structure = Hardware cost + Installation cost
- Hardware cost = f (Level, Type, Chargers per pedestal)
 - Level: level 2
 - Type: Networked, Non-networked
 - Chargers per pedestal: One, Two
- Installation cost = Labor + Materials + Permit + 70% * Tax + Rebate
 - Factors like labor, materials, permit, and tax are affected by the chargers per site
 - According to California policy, the tax for installation has a 30% credit refund

In the following part, a cost table based on the different truck numbers in our troop is displayed, our troop includes 5 to 10 trucks, the number of charger stations depends on the number of trucks. The cost table includes the lowest cost which has the largest number of the dual port charger without network and the highest cost represents the largest number of the single port charger with network.

Table 12. Total costs of charging stations

Numbers of installation	Charger Cost Min (\$)	Charger Cost Max (\$)	Other cost (\$)	Total Instal. Cost min (\$)	Total Instal. Cost Max (\$)
5	3,197	14,299	10,523	13,720	24,822
6	3,576	16,758	13,803	17,379	30,561
7	4,389	19,885	16,603.5	20,992.5	36,488.5
8	4,758	22,344	19,404	24,162	41,748
9	5,581	23,157	22,204.5	27,785.5	45,361.5
10	5,960	27,930	25,005	30,965	52,935

For the maintenance cost, it is assumed that most of the charger station's repair and replacement fee would be covered in the warranties. Therefore, it is not considered in this project.



Result and Analysis

In this Section, ICE TCO and EV TCO in different scenarios are calculated and compared. In the comparison about weight class and annual mileage, it is assumed that the battery replacement only occurs once in the study period. The size of the fleet is 5. From the subsection Battery Optimization, the team figured out the best battery replacement timing is the 7th year. So, in this part the battery is replaced at the 7th year and annual mileage is assumed as 100,000 miles. Although one time replacement of batteries is too ideal, it represents a trend in TCO calculation. The effect of replacement times are discussed in the last section.

Comparison between ICE and EV

Table 13. TCO outputs with different weight class

Class	ICE TCO	EV TCO	Delta %
3	-\$1,536,352	-\$1,445,130	6%
4	-\$1,876,173	-\$1,682,347	10%
5	-\$2,039,790	-\$1,919,564	6%
6	-\$2,367,025	-\$2,275,390	4%
7	-\$2,857,878	-\$2,868,432	0%
8	-\$3,348,731	-\$3,105,649	7%

* Delta % = $(ICE\ TCO - EV\ TCO) / ICE\ TCO * 100\%$ (positive = EV is better choice, negative = ICE is better choice)

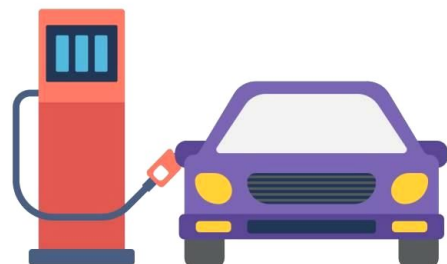


Table 13 shows that as the class increases with the fixed mileage, the change of delta is slight and unstable. It is because both battery efficiency (EVs) and MPG (ICEVs) decrease as the increase of weight class and share a similar rate of change. Therefore, due to similar change between battery efficiency and MPG, the weight class could have only a slight effect on relative TCO. It should be mentioned the technology of ICE is mature while the development of EVs is fast. So, technological breakthroughs in EVs could change its effect and provide EVs with much economic value.

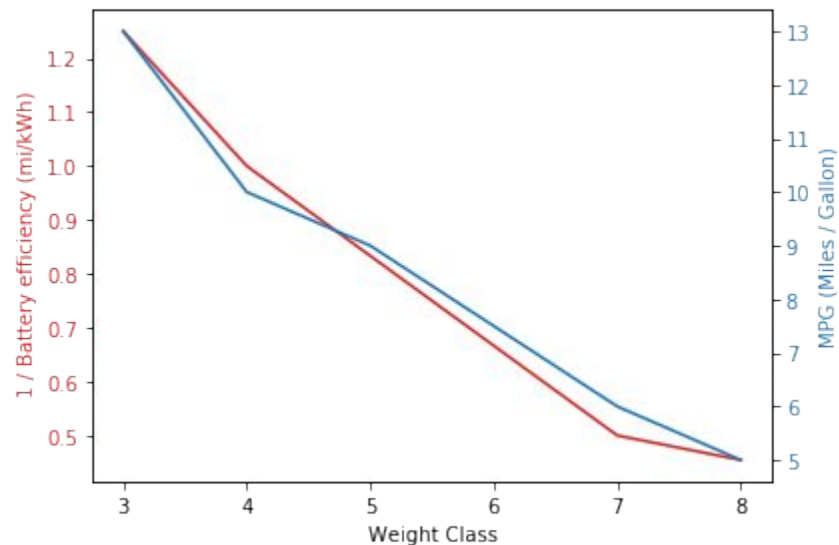


Figure 8. Battery efficiency and MPG change with weight class

Sensitivity Analysis

Annual mileage

The weight class 5 is taken as an example, and the battery replacement timing at the 7th year is replaced. In this part, the team explored the effect of annual mileage on TCO. The small distance (5000 miles per year), medium distance(25000 miles, 50000 miles) and large distance (100000 miles) are put into consideration. From results listed in table 13, it is clear that as the increase of the distance, the EVs gradually shows advantage in TCO. In the case of short distance, the TCO of EVs is largely outweighed that of ICE. However, as the distance increases, the gap decreases and when distance per year is 25000 miles, both TCOs are similar and for the long distance, ICE TCO is larger than EV TCO. This trend denotes that popularization of electric trunks is promising although now the use of electric trunks is rare compared with that of electric cars.

Considering that electric vehicles are still in its infancy, research costs and production costs are high. Increasing the distance is a way to improve economic efficiency.

Table 14. TCO outputs with different weight class

Distance	ICE TCO	EV TCO	Delta %
5000 miles	-\$485,424	-\$567,427	-17%
25000 miles	-\$812,659	-\$852,087	-5%
50000 miles	-\$1,221,703	-\$1,207,913	1%
100000 miles	-\$2,039,790	-\$1,919,564	6%

* $\text{Delta \%} = (\text{ICE TCO} - \text{EV TCO}) / \text{ICE TCO} * 100\%$ (positive = EV is better choice, negative = ICE is better choice)

Battery Replacement

The discussion above ignores the effect of the times of battery replacement. Because the cost of the battery makes up a large part of the total cost, its effect is explored in this part.

First, the vehicle life extends to be 12 years for convenience and the annual mileage keeps 100,000 miles. The cost of replacement battery each time is from the multiplication of Battery capacity (kWh) and Unit replacement cost (\$/kWh) at that year. Table 14 shows a dramatic change and the short expected life means more times of replacement. For example, when expected battery life is 3 year, the battery needs to be replaced in the fourth, seventh, and 10th year. And, while expected battery life is 6 year, the battery only needs to be replaced in the 7th year.

The results show that the times of battery replacement have a significant effect on TCO. The big frequency of battery replacement results in a considerable increase of EVs TCO. So, in the case of high frequency of battery replacement, ICE TCO has a huge advantage.

Table 15. TCO outputs with different weight class

Expected Battery Life (Year)	Replacement Times	ICE TCO	EV TCO	Delta %
2	5	-\$2,378,905	-\$3,095,566	-30%
3	3	-\$2,378,905	-\$2,585,444	-9%
4	2	-\$2,378,905	-\$2,384,304	0%
6	1	-\$2,378,905	-\$2,174,298	9%

* $\text{Delta \%} = (\text{ICE TCO} - \text{EV TCO}) / \text{ICE TCO} * 100\%$ (positive = EV is better choice, negative = ICE is better choice)



Conclusion

From the result tables presented above, it is clear that under the ideal situation (battery in EVs only replaces once), annual mileage is constant 100,000 miles and etc, TCO in different weight classes have the trend that TCO of EVs is relatively lower than that of ICEVs with small difference.

In reality, the battery of an EVs may not have a long lifeline like 7 years, and the annual mileage can be a vast range. Therefore, two sensitivity analyses were conducted in this study.

Once the weight class is set to be class 5, and the battery in EVs still replaces one time. The results suggest that TCO of ICE is relatively small when annual mileage is small, and TCO of EVs is relatively small when annual mileage is large, which corresponds to one of the main takeaways in EVs literature review: energy spending is the largest cost savings for electric vehicles compared to the traditional diesel vehicles. In other words, when the expected life of the battery is fixed, EVs have benefit for the large distance transport.

The other sensitivity analysis is to change the frequency of battery replacement. In this case, the only TCO affected is EVs TCO, so the goal of this part is to find the maximum allowable frequency of battery replacement when EVs have benefit in TCO comparison. The study period is tuned to be 12 years for better frequency setting, and results demonstrate that once the EVs replace the battery more than one time, EV TCO will exceed the ICE TCO. It also matches one of the main takeaways in EVs literature review: the battery is the largest cost element for EVs, and one more battery replacement may eliminate the advantage of EVs in TCO.

Given that the research object is the trunks with large annual mileage, the result shows that long distance is preferable, in the real world, batteries may be replaced more than once. So in general, EV TCO slightly outweighs ICE TCO.

On the other hand, with the development of technology, the costs of unit battery and research are decreasing obviously. Therefore, in the future, the advancement of technology is conducive to the popularization of EVs.





Reference

- [1] Delbridge, Emily. "What is the True Cost of Owning a Car?." *The Balance Small Business*. February 28, 2019.
- [2] http://www.cngprices.com/station_map.php
- [3] <https://www.fueleconomy.gov/feg/label/learn-more-gasoline-label.shtml>
- [4] https://www.eia.gov/dnav/pet/pet_pri_gnd_a_epd2d_pte_dpgal_w.htm
- [5] <https://www.clippercreek.com/evse-rebates-and-tax-credits-by-state/>
- [6] Gao, Zhiming, Lin, Zhenhong, LaClair, Tim J., Liu, Changzheng, Li, Jan-Mou, Birky, Alicia K., & Ward, Jacob. *Battery capacity and recharging needs for electric buses in city transit service*. United States. doi:10.1016/j.energy.2017.01.101.
- [7] Smith, David, et al. *Medium-and Heavy-Duty Vehicle Electrification: An Assessment of Technology and Knowledge Gaps*. No. ORNL/SPR-2020/7. Oak Ridge National Lab.(ORNL), Oak Ridge, TN (United States), 2020.
- [8] Nicholas, Michael. "Estimating electric vehicle charging infrastructure costs across major US metropolitan areas." (2019).
- [9] <https://cleantechnica.com/2019/12/04/powering-the-ev-revolution-battery-packs-now-at-156-kwh-13-lower-than-2018-finds-bnef/>
- [10] https://www.me.utexas.edu/~me353/lessons/S2_Evaluation/L02_Equivalence/factor_formulas.html
- [11] He, Y.; Bhavsar, P.; Chowdhury, M.; Li, Z. (2015-10-01). "Optimizing the performance of vehicle-to-grid (V2G) enabled battery electric vehicles through a smart charge scheduling model". *International Journal of Automotive Technology*. 16 (5): 827–837.
- [12] Xue, Nansi. Design and Optimization of Lithium-Ion Batteries for Electric-Vehicle Applications. Diss. 2014.
- [13] <https://www.nrel.gov/transportation/fleettlest-fleet-dna.html>
- [14] <https://www.chooseenergy.com/shop/residential/electricity/CA/94704/pge-ca-electricity/>



Appendix

[1] TCO Calculator Excel

https://drive.google.com/file/d/1vvaTqrLxZFCZSumsqZ-LaFvF-IL_KGJ/view?usp=sharing

[2] Jupyter notebook and Excel files for calculating cost of charging infrastructure

<https://drive.google.com/drive/folders/1XZoy2UO8FoLWiVOE2ij1KF95BQ7lq6ra?usp=sharing>



Battery Electric Vehicle VS Diesel Vehicle TCO Calculator User Inputs

User Inputs	Program Value	TCO Calculator Results
Dependents Values		Diesel -\$2,804,951
Calculations		Electric -\$2,530,441
		% Delta 10%
Duty Cycle Factors	Value from Online Source and Reasonable Assumptions	Citation
Duty Cycle	Food Delivery Straight Truck (Class 5)	2 Pick duty cycle to class closest to yours
Average Daily Mileage	469	469 Pulled from Duty Cycles Tab.
Annual Mileage	122,013	122,013 Pulled from Duty Cycles Tab.
Type	Trunk	5 Vehicle Class
Baseline Diesel vehicle Information	Value from Online Source and Reasonable Assumptions	Citation
Expected Ownership Period (Years)	12	12 Number between 1 to 30 years.
Number of Vehicles to compare (#)	5	5 Number between 1 to 1,000 trucks.
Baseline Manufacturers Suggested Retail Price MSRP (\$)	\$120,000	\$120,000 Between \$80,000 to \$160,000 per truck. Suggest \$100k for Class 3 baseline, higher for other classes.
Adjusted Price after rebates, etc. (\$)	\$118,000	\$118,000 Should be less than MSRP in Cell C21.
Value of Trade-in (\$)	\$47,200	\$47,200 Between \$0 and Adjusted Price after Rebates
Projected Residual Value at end of ownership (% of baseline adjusted price after	20%	20% Between 15% to 85% per truck. Suggest 20% if owned over 10 years based
Annual Maintenance & Service Cost per Truck (\$)	\$1,000	\$1,000 Between \$600 to \$1200 per truck.
Maintenance Cost Trend (% change per year)	8%	8% Between -1,000% to +1,000% per truck.
Annual Insurance Cost per Truck (\$)	\$1,300	\$1,300 Between \$0 to \$1000 per truck per year.
Insurance Cost Trend (% change per year)	5%	5% Between -1,000% to +1,000% per truck.
Average fuel economy (MPG - Miles Per Gallon)	9.0	9 Between 5 to 14 mpg per truck, depending on the class
Fuel Type	Diesel	1 Diesel
Current Fuel Price (\$/gal)	\$3.19	\$3.19 Between \$2.4 to \$4 per gallon. Suggest \$2.9.
Fuel Price Trend (projected % change per year)	1%	1% Between -15% to +15% per truck.
Electric Vehicle vehicle Information	Value from Online Source and Reasonable Assumptions	Citation
Max Battery Life (Years to 80% of capacity)	0.8	10.00 Default assumption: battery can be used for 8 years/100,000 miles
New Battery Efficiency (kWh/mi)	1.2	1.20 Refer the online resource. Use 1.89 kWh/mi.
Expected Battery Life (Years to 80% of capacity)	6.0	6 Total mileage less than 100,000 miles or less than 8 years
Battery Capacity Margin for aging (% of new full capacity)	4%	4% Linear increase from 0 to 25% based on time (max. 8 yrs)
Battery Capacity Margin for design (% of new full capacity)	4%	4% Linear increase from 10% to 25% based on time (max. 8 yrs)
Battery Capacity Margin for Cold/Hot Weather Operation (% of full capacity)	3%	3% Between 0% to 100%. Suggest 10%.
Battery Capacity Margin for Driver Efficiency (% of full capacity)	3%	3% Between 0% to 100%. Suggest 5%.
Battery Low Cutoff (% of full capacity)	3%	3% Between 0% to 50%. Suggest 20%.
Estimated Battery Capacity Required (kWh)	656	656 Calculation
First Battery Replacement Cost (\$/kWh)	\$83	\$83 In recent 10 years, the annual decrease rate of battery replacement is
Percent of battery pack to replace at end of life	100%	100% Between 0% to 100%. Suggest 100%.
Cost of Replacement Battery Pack (\$)	\$54,390	\$54,390 Calculation
Current Electricity Price (\$/kWh)	\$0.12	\$0.12 Between \$0.01 to \$1.00/kWh. Suggest \$0.12 kWh.
Electricity Price Trend (% change per year)	5.0%	5% Between -1,000% to +1,000%. Suggest 5%.
Manufacturers Suggested Retail Price MSRP (\$)	\$180,000	\$180,000 Price from Tesla Semi (class 8).
Grants, Incentives, Rebates, etc (% of MSRP)	0	0% Between 0% to 100%. Suggest 50%.
Second Battery Replacement Cost (\$/kWh)	\$80	\$80
Third Battery Replacement Cost (\$/kWh)	\$80	\$80
Forth Battery Replacement Cost (\$/kWh)	\$80	\$80
Fifth Battery Replacement Cost (\$/kWh)	\$80	\$80
Initial Batter Cost (\$/kWh)	\$156	\$156
Estimated Initial Battery Capacity Required (kWh)	656	656
Adjusted Vehicle Acquisition Actual Cost (\$)	\$80,000	\$80,000 Calculation
Value of Trade-In (\$)	\$12,000	\$12,000 Already keyed in at Cell C23
Projected Residual Value at end of ownership (% of Adjusted Vehicle Acquisition	5%	5% Between 0% to 100% per truck. Suggest 5% if owned over 10 years based
Expected Annual Maintenance Cost (% of Baseline)	100%	100% Between 0% to +1,000% of Baseline Maintenance Cost. Suggest 100%
Annual Insurance Cost per Truck (\$)	\$3,000	\$3,000 Between \$0 to \$1M per truck. Suggest 2X baseline cost.
Insurance Cost Trend (% change per year)	5%	5% Between -1,000% to +1,000% per truck. Suggest 5%.
Include Equivalent Highway Trust Fund fuel tax?	Exclude	2 Include or Exclude. Suggest "Exclude" today, (assumes 18.4 cents/gal for Considering every weekend (2days * 52weeks) - recommend 100% improvement over ownership period.
V2G	0.8	2 Between -100% to +100% of Electric Truck MSRP. Suggest 2%
Value of Changes to Driver Retention Costs (% of MSRP)	2%	2% Between -100% to +100% of Electric Truck MSRP. Suggest 2%
Value of Changes to Technician Retention Costs (% of MSRP)	2%	2% Between -100% to +100% of Electric Truck MSRP. Suggest 2%
Value of Changes to Emissions Compliance Costs (% of MSRP)	2%	2% Between -100% to +100% of Electric Truck MSRP. Suggest 2%
Value of Changes to Brand Image (% of MSRP)	2%	2% Between -100% to +100% of Electric Truck MSRP. Suggest 2%
Value of Changes to Other Overhead Factors (% of MSRP)	2%	2% Between -100% to +100% of Electric Truck MSRP. Suggest 2%
Charging Infrastructure	Value from Online Source and Reasonable Assumptions	Citation
Charging System Cost Recovery Method	Amortized Over Ownership Period	2 Paid up front or amortized over ownership period. Suggest paid up front.
Cost of Charging Infrastructure per Truck (% of MSRP)	7%	7% Between 0% and 15%00% of electric truck MSRP. Suggest 5% of electric
Number of Trucks Per Charge Station	5	5 Between 1 to 10 trucks per charging station. Suggest 1.
AC Labor per charger (over 5 chargers): \$1747	5%	https://afdc.energy.gov/files/u/publication/eve_cost_report_2015.pdf
AC Materials per charger (5 chargers): \$98	3%	https://redwoodenergy.org/wp-content/uploads/2019/02/Electric-Vehicle-Charger-Selection-Guide.pdf
AC Permit per charger (5 chargers): \$115	0.32%	https://atlasevhub.com/resource/estimating-electric-vehicle-charging-infrastructure-costs-across-major-u-s-metropolitan-areas/
AC Tax per charger (5 chargers): \$65 rebate(1000)	0.18%	
Value of difference of electricity costs per day (\$)	0.009	
Finance Information	Value from Online Source and Reasonable Assumptions	Citation
Type of Purchase	Cash	1 Cash, Lease or Loan
Discount Rate	2.50%	0.025 Between 2% and 3%. Suggest 2.5%
Down Payment % per Truck	5%	5% Between 0% and 100% of MSRP. Use 100% if cash purchase, if lease or

Battery Electric Vehicle VS Diesel Vehicle **TCO Calculator Outputs**

Battery Electric Vehicle VS Diesel Vehicle

TCO Calculator Duty Cycles

Duty Cycle Factor			
	Weight & Class	Average Daily Distantce (mile/day)	Annual Travel Mileagea (mile)
1	Linen Delivery Walk In (Class 6)	476	123,677
2	Food Delivery Straight Truck (Class 5)	469	122,013
3	Warehouse Delivery Straight Truck (Class 7)	465	120,856
4	Food Delivery Straight Truck (Class 3)	465	120,817
5	Linen Delivery Straight Truck (Class 7)	451	117,260
6	Linen Delivery Step Van (Class 6)	432	112,310
7	School Bus School Bus (Class 6)	406	105,552
8	Linen Delivery Step Van (Class 5)	381	98,951
9	Parcel Delivery Straight Truck (Class 7)	351	91,317
10	Parcel Delivery Walk In (Class 4)	316	82,129
11	Parcel Delivery Step Van (Class 3)	289	75,223
12	Mass Transit City Transit Bus (Class 8)	284	73,757
13	Mass Transit City Transit Bus (Class 7)	283	73,632
14	Parcel Delivery Step Van (Class 4)	274	71,123
15	Parcel Delivery Walk In (Class 5)	260	67,608
16	Parcel Delivery Walk In (Class 6)	237	61,708

Battery Electric Vehicle VS Diesel Vehicle
TCO Calculator Look Up Values

TCO Comparison Scope	
Pump to Wheel	1
Well to Wheel	2

Baseline Diesel Truck Information	
Duty Cycle	
Linen Delivery Walk In (Class 6)	1
Food Delivery Straight Truck (Class 5)	2
Warehouse Delivery Straight Truck (Class 7)	3
Food Delivery Straight Truck (Class 3)	4
Linen Delivery Straight Truck (Class 7)	5
Linen Delivery Step Van (Class 6)	6
School Bus School Bus (Class 6)	7
Linen Delivery Step Van (Class 5)	8
Parcel Delivery Straight Truck (Class 7)	9
Parcel Delivery Walk In (Class 4)	10
Parcel Delivery Step Van (Class 3)	11
Mass Transit City Transit Bus (Class 8)	12
Mass Transit City Transit Bus (Class 7)	13
Parcel Delivery Step Van (Class 4)	14
Parcel Delivery Walk In (Class 5)	15
Parcel Delivery Walk In (Class 6)	16
	6

Keyed Baseline Details

Duty Cycle
 Expected Vehicle Life (yr)
 Expected Ownership Period (yr)
 Number of Vehicles to compare (#)
 Baseline Purchase Cost (\$)
 Annual Maintenance & Service Cost per Truck (\$)
 Annual Insurance Cost per Truck (\$)
 Average fuel economy (MPG)

Baseline Fuel Type	
Diesel	1
Current Cost Per Gallon	

Charging System Cost Recovery Method	
Paid Upfront Lump Cost	1
Amortized Over Ownership Period	2

Type of Vehicle Purchase	
Cash	1
Lease	2
Loan	3

Highway Trust Fund Equivalent Tax	
Include	1
Exclude	2

New Battery Efficiency		(kWh/mi)
3		0.8
4		1
5		1.2
6		1.5
7		2
8		2.2

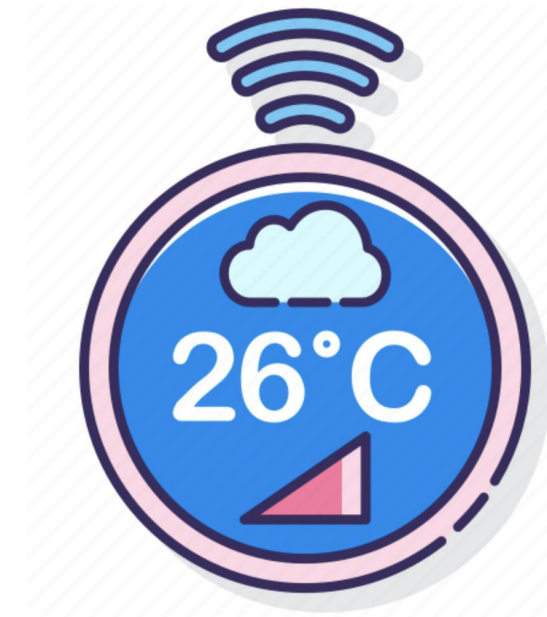
Truck Class	Miles Per	MPG
3	13	12-14
4	10	9-11
5	9	8-10
6	7.5	7-8
7	6	5-7
8	5	<5

Reference: <https://rentar.com/diesel-truck-miles-per-gallon-mpg/>



UNIVERSITY OF CALIFORNIA, BERKELEY
DEPARTMENT OF CIVIL AND ENVIRONMENTAL ENGINEERING
ENERGY SYSTEMS AND CONTROLS

The Design of a Model Predictive Control Algorithm for Smart Thermostats in Residential Buildings



Ronggen Chen, Mingxin Jia, Xiaotian Wang, Yuming Xu

Professor Scott Moura

Berkeley, May 2020

Abstract

Improving building energy efficiency is among the many energy challenges that our society faces today. In the US, one of the most significant contributing factors that cause excessive building energy consumption is inefficient HVAC systems. Traditional HVAC thermostats only function to maintain the room temperature at a preset value, and they lack sophistication in adjusting room temperature based on climate and user behavior. Therefore, developing a smart thermostat controller for more energy-efficient heating and cooling and for maintaining indoor thermal comfort is direly needed. In this work, we combine building thermal modeling and optimization to develop a model predictive control algorithm for a smart thermostat controller. The control algorithm will wisely adjust the heating or cooling power of the HVAC system based on outdoor temperature, relative humidity, occupancy, and electricity price. We tested our model in three days that represent three different scenarios: extreme cooling-need, extreme heating-need and both heating and cooling needs. In any scenario, the control algorithm could always maintain the temperature within the thermal comfort zone with adaptation to the changing upper/lower bound. The control algorithm could also adapt to the change in occupancy and reduce electricity costs by improving energy efficiency.

1. Introduction

1.1 Motivation & Background

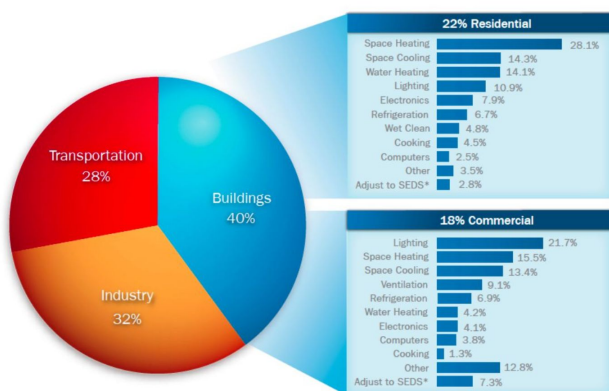


Fig 1.1 Energy Consumption by Ends in U.S.

Building consumes a substantial portion of energy in the United States, which accounts for 40% of total energy consumption. Moreover, 22% from the residential sector and 18% from the commercial sector. Figure 1.1 shows that spacing heating, space cooling and lighting account for more than 50% of building energy consumption [1].

Air conditioning is one of the leading contributors to peak electricity demand. Furthermore, electricity used for air conditioning is rapidly increasing due to population growth and greater demand for comfort. Hence, immediate reductions to these consumptions are required to combat high energy consumption in building energy systems.

A smart thermostat can provide opportunities for building occupants to improve thermal comfort conditions while simultaneously reducing space conditioning energy responding to grid reliability signals, and reducing maintenance compared to legacy systems. One of the core

features of smart thermostats to achieve the above advantages is automated operations. Smart thermostats are known for automatically responding to occupancy, behavior patterns and weather conditions. They can improve thermal comfort by pre-cooling and preheating and reduce energy cost by eliminating overheating and overcooling. According to the ACEEE report about the energy impacts of smart home technologies [2], smart thermostats can save up to 10% cooling energy and 8% heating energy.

Technology	Description	Affected end use	Retail cost (\$US)	Estimated energy savings as % of affected end-use consumption
Smart thermostat	Connected thermostat	HVAC	\$150–250/thermostat	7–10% cooling 6–8% heating

Fig 1.2 Energy Savings for Smart Thermostats

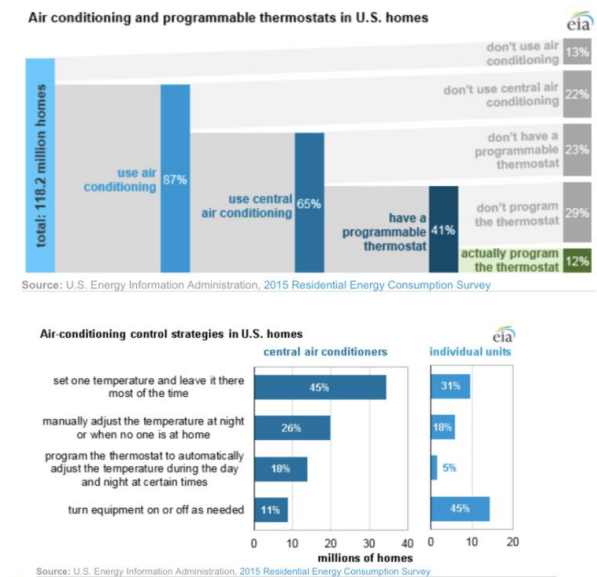


Figure 1.3 Air-conditioning Control Strategies in U.S. Homes

Previously, some of the main challenges faced by building energy researchers include difficulty in developing a universal building thermal model for all types of buildings and difficulty in gathering enough data to train and verify the thermal control algorithm. With reasonable simplifications and by fully utilizing available data from open databases, we believe that these challenges can be overcome in this project. Our team consists of members with building science and mechanical engineering backgrounds. With expertise in heat transfer, control theory, structural engineering and architecture, we believe that we are about to find a satisfactory solution that overcomes the above mentioned challenges.

1.2 Relevant Literature

Therese Peffer et al carefully review the current state of smart thermostats. A smart thermostat is based on the same principle of operation as a conventional thermostat, but also

has a series of sensors and functionalities that allow the thermostat to make decisions on its own to provide greater comfort at home and save on heating costs [4].

Burger et al proposed a control system that is capable of maintaining a given comfortable temperature range in a space while optimizing electricity consumption given weather forecasts and price data [5]. The predictive control algorithm is a mixed integer linear program (MILP) which predicts the temperature in the place 6 hours into the future, minimizes the cost of electricity and keeps the indoor temperature above a minimum setpoint.

Rajendra Adhikari et al presented a novel linear-time algorithm to find the maximum load reduction potential for an aggregation of houses such that their comfort requirements are not violated and an associated algorithm to optimally control the HVACs in those houses such that the aggregated power is kept at the minimum value [6].

1.3 Focus of this Study

This study focuses on developing a model predictive control algorithm for smart thermostats that can reduce building energy consumption while still maintaining thermal comfort. The control algorithm should be able to vary the heating or cooling power of the HVAC system based on indoor temperature, humidity, occupancy, occupant schedule and electricity price. Given the large percentage of building energy consumption within the total energy consumption, the smart thermostat control algorithm has the potential to help reduce the high heating and cooling energy demand of conventional HVAC systems.

2. Technical Description

2.1 Key Assumptions

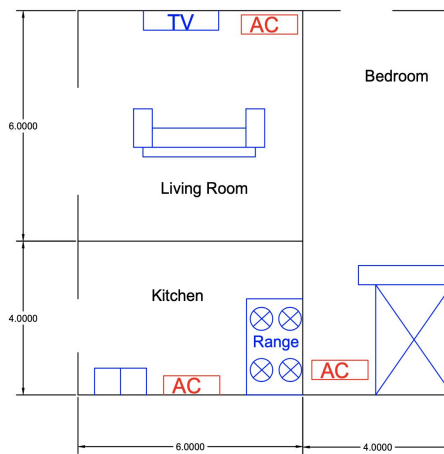


Fig 2.1 House Model Floor Plan

Fig 2.1 represents the floor plan of the house that we modeled. To simplify our model, the house is assumed as a one-story house. The house is 10 meters in both length and width. Three representative rooms in a typical house are chosen for our modeling purpose. They are

the living room where daytime activities are held, the kitchen which is a significant heat source, and the bedroom for nighttime activities. The openings on the wall represent the windows. In the kitchen and bedroom, the area of each window is 1 m^2 . In the living room, the area of window is 2 m^2 . AC represents the air conditioning units.

To simplify our heat transfer model, four assumptions were made. First, there is no solar gain and ventilation through windows. Second, all the floors are adiabatic. Third, internal heat sources only include TV and cooking equipment. Last, only conduction happens through walls, windows and ceilings and heat loss or gain due to radiation and convection are neglected.

For the thermostat, three built-in sensors are set in each room. They are temperature sensors, humidity sensors and occupancy detectors. We assume that the temperature is uniform in each of these three rooms. Meanwhile, humidity sensors directly read data from outdoor humidity, and the indoor humidity is assumed to be always equal to the outdoor humidity. And for the host's schedule, the system has already finished the learning procedure. Usually, this process will be conducted for three weeks after the thermostat is installed to learn the behavior patterns of the host.

2.2 Smart Thermostat Operation Diagram

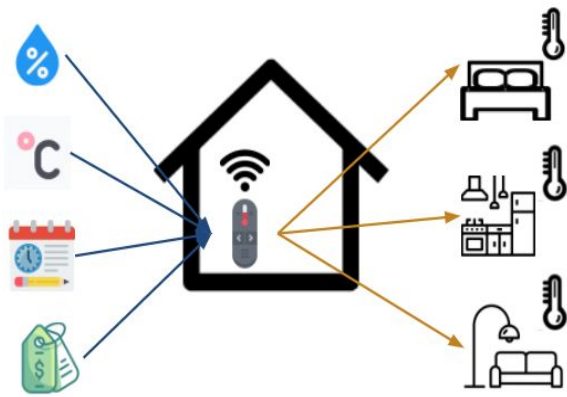


Fig 2.2 Smart Thermostat Operation Diagram

Fig 2.2 is the schematic diagram of our thermostat's working process. The input of the thermostat includes humidity (measured and forecast), temperature (measured and forecast), occupant's schedule and electricity price. These are all read automatically from sensors and from online real time data. After the operation of the smart thermostat, it implements the outputs, which are the powers for the heating or cooling in the three rooms to maintain the room temperature within the thermal comfort range.

2.3 Data Sets

The assumed location of this project is chosen to be New York City because it has a relatively large temperature difference between summer and winter and there is a larger demand for heating and cooling. The weather data is collected from Weather Underground for January 31st, July 1st and July 20th in 2019 [7]. January 31st and July 20th are the coldest and hottest days in 2019, respectively. They have been chosen as a candidate to test how the model predictive algorithm works in such extreme conditions. July 1st was chosen to test the control algorithm on a day when both heating and cooling is needed. The plots of the weather

data (temperature and relative humidity) and weather forecast data (temperature and relative humidity) are shown in Fig. A1 to A3 in the appendix of this report. It is important to note that New York is selected only as a test case for our control algorithm. The control algorithm is general and versatile enough so that it can easily be used on households in other cities around the world.



Fig 2.3 Weather Station Location

The occupant's daily schedule can be seen in the Gantt Chart below. The host wakes up at 8 am in the morning and spends one hour each in the living room and kitchen and leaves the house at 10 am. The host comes home at 6 pm and spends two hours each in the living room and kitchen and goes to bed at 22 pm. Only one occupant presents in the house for this project.

Table 2.1 Occupancy Daily Schedule

Room	0	1	2	3	4	5	6	7	8	9	10	11	12	13	14	15	16	17	18	19	20	21	22	23
Bedroom																								
Kitchen																								
Living Room																								

The hourly electricity price shown below is based on NYISO Day-Ahead Prices [8]. The data is from Con Edison, the primary electric and gas provider in New York City. It reaches its peak in the late afternoon and remains low during the nighttime.

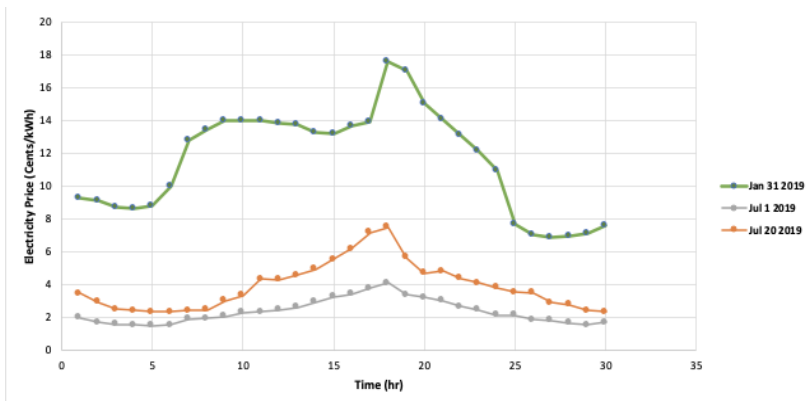


Fig 2.4 Hourly Electricity Price in Cents Per kWh

2.4 Thermal Comfort

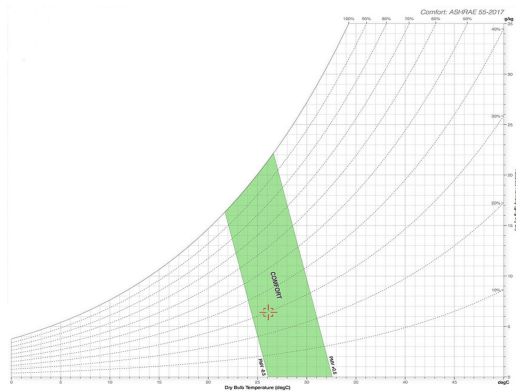


Fig. 2.5 Temperature and Relative Humidity

Thermal comfort zone refers to the combinations of air temperature, mean radiant temperature, and humidity that are predicted to be an acceptable thermal environment at particular values of air speed, metabolic rate, and clothing insulation. For simplicity, in our case, only the effects of temperature and relative humidity on thermal comfort are explored. In the psychrometric chart as shown in Fig. 2.5, the thermal comfort zone is represented by the green region highlighted in the figure. For each relative humidity (the curve lines), there is an upper and a lower temperature limit in the comfort zone area. The job of our smart thermostat controller is then to maintain the room temperature for the occupied room within the upper and lower limit given the relative humidity.

2.5 Modeling

2.5.1 Wall Thermal Modeling

We divide the walls into exterior walls and interior walls. The configuration of these two walls are shown in Fig. 2.6. The exterior wall consists of two $\frac{1}{2}$ -inch Drywall and a $3\frac{1}{2}$ -inch framing. The interior wall consists of a $\frac{3}{4}$ -inch siding, a $\frac{3}{8}$ -inch sheathing, a $3\frac{1}{2}$ -inch framing and a $\frac{1}{2}$ -inch Drywall. The corresponding thermal circuits for exterior and interior walls are also shown in Fig. 2.7. It is important to note that in the framing section of the wall, there is air in between the frames, therefore the thermal resistance of the wooden frame is in parallel with the thermal resistance of the air between the frames. We neglect the wall thermal capacitance and the wall materials are considered as follows: oak (framing), plaster (drywall), plywood (sheathing), vinyl siding (siding), double-pane glass with Ar interlayer (window).



Fig. 2.6 Wall Thickness for Interior (Left) and Exterior (Right) Walls

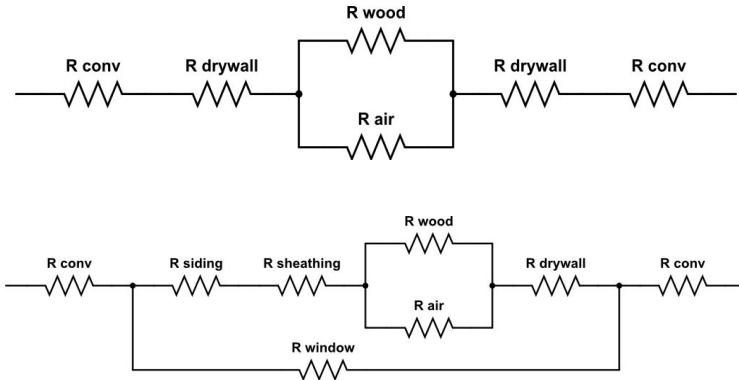


Fig. 2.7 Thermal models of Interior (upper) and Exterior (lower) Walls

2.5.2 Thermal System Modeling

According to our floor plan, the thermal circuit of the entire house is shown below in Fig. 2.8. The states of the system are the temperatures in living room (T_l), in bedroom (T_b) and in kitchen (T_k). The controllable inputs are HVAC powers in three zones (P_l , P_b , P_k). The uncontrollable output is ambient temperature ($T_{ambient}$). We are using smart thermostat to detect temperatures in three zones, so the measurable outputs of the system are also T_l , T_b and T_k . The parameters are thermal resistances and capacitances (R_{lb} , R_{lk} , R_{bk} , R_{ba} , R_{la} , T_{ka} , C_l , C_b , C_k). The corresponding state equations in State-Space Form are shown as follows:

$$\frac{d}{dt} \begin{bmatrix} T_l \\ T_b \\ T_k \end{bmatrix} = \underbrace{\begin{bmatrix} -\frac{1}{R_{lb}C_l} - \frac{1}{R_{lk}C_l} - \frac{1}{R_{la}C_l} & \frac{1}{R_{lb}C_l} & \frac{1}{R_{lk}C_l} \\ \frac{1}{R_{lb}C_b} & -\frac{1}{R_{lb}C_b} - \frac{1}{R_{bk}C_b} - \frac{1}{R_{ba}C_b} & \frac{1}{R_{bk}C_b} \\ \frac{1}{R_{lk}C_k} & \frac{1}{R_{bk}C_k} & -\frac{1}{R_{lk}C_k} - \frac{1}{R_{bk}C_k} - \frac{1}{R_{ka}C_k} \end{bmatrix}}_A \begin{bmatrix} T_l \\ T_b \\ T_k \end{bmatrix} + \underbrace{\begin{bmatrix} \frac{1}{C_l} & 0 & 0 & \frac{1}{R_{la}C_l} \\ 0 & \frac{1}{C_b} & 0 & \frac{1}{R_{ba}C_b} \\ 0 & 0 & \frac{1}{C_k} & \frac{1}{R_{ka}C_k} \end{bmatrix}}_B \begin{bmatrix} P_l \\ P_b \\ P_k \\ T_{amb} \end{bmatrix} \quad (1)$$

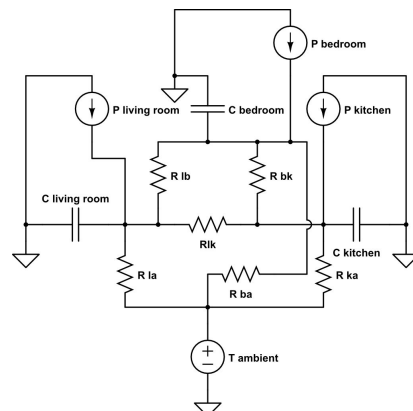


Fig. 2.8 Thermal Circuit of the Entire House

Based on the wall materials and dimension of house, thermal resistance calculation results are shown in Table 2.2.

Table 2.2 Thermal Resistance in K/W

Unit: K/W	Living Room	Bedroom	Kitchen	Ambient
Living Room	N/A	0.0811	0.0811	0.0333
Bedroom	0.0811	N/A	0.1216	0.0370
Kitchen	0.0811	0.1216	N/A	0.0374
Ambient	0.0333	0.0370	0.0374	N/A

2.6 Optimization

2.6.1 Discretization

The model above is time-continuous, it is not likely for the thermostat to do the optimization in a continuous time domain. Hence, the model is transformed into the discrete time domain with a time step of five minutes. By applying the transformation of matrix A and B from equation (1),

$$A_d = e^{A\Delta t} \quad (2)$$

$$B_d = \left(\int_0^{\Delta t} e^{A\tau} d\tau \right) B \quad (3)$$

the discrete state-space equation is given as

$$\begin{bmatrix} T_l(k+1) \\ T_b(k+1) \\ T_k(k+1) \end{bmatrix} = A_d \begin{bmatrix} T_l(k) \\ T_b(k) \\ T_k(k) \end{bmatrix} + B_d \begin{bmatrix} P_l(k) \\ P_b(k) \\ P_k(k) \\ T_{amb}(k) \end{bmatrix} \quad (4)$$

2.6.2 Optimization Function

The objective function is formulated as

$$J = \min \sum_{k=1}^{N-1} c(k) \frac{P(k)\Delta t}{3,600,000} \cdot \frac{1}{COP} \quad (5)$$

Subject to

$$\begin{bmatrix} T_l(k+1) \\ T_b(k+1) \\ T_k(k+1) \end{bmatrix} = A_d \begin{bmatrix} T_l(k) \\ T_b(k) \\ T_k(k) \end{bmatrix} + B_d \begin{bmatrix} P_l(k) \\ P_b(k) \\ P_k(k) \\ T_{amb}(k) \end{bmatrix} \quad (6)$$

$$T_{high}(k+1) \geq T(k+1) \geq T_{low}(k+1) \quad (7)$$

$$P_{\max}(k) \geq P(k) \geq P_{\min}(k) \quad (8)$$

This optimization program aims to minimize the cost of electricity while maintaining the indoor temperature within a range determined by humidity. The minimization is shown by the objective function in (5), where $c(k)$ is the electricity price shown in Fig 2.4 and COP is the coefficient of performance whose value is 3.8. The thermal comfort constraint (7) is only valid for a given room at time steps when there is an occupant in the room. It is relaxed at time steps when there is no occupant. Constraints (6) and (8), the physical constraint and the power constraint, should be satisfied for all the time steps and for all the rooms.

2.7 Control Algorithm

This optimization control algorithm follows the following steps:

- (1) Set the current temperature measurement as the initial state, $T(0) = T_0$.
- (2) Solve optimization equations to get optimal powers for the next six hours.
- (3) Execute the first values of P_l, P_b, P_k to advance to the next time step.
- (4) Repeat the algorithm at the next time step.

In order to predictively control the system to save energy expenses, the algorithm makes its decision by applying the temperature and humidity predictions and finding the best heating or cooling strategy in the next six hours. The whole process repeats itself every five minutes to regenerate the optimal powers for the next six hours. Therefore the control system operates on a model predictive control algorithm that looks 6 hours ahead into the future.

3. Results and Discussion

By using the methodology described in the previous sections, a simulation can be done to determine the smart thermostat controlled room temperatures within the 24-hour period. The simulation result for Jul 20th, 2019 the warmest day in New York City in 2019 is shown below in Fig. 3.1. For comparison, we have also performed the room temperature response simulation for a HVAC system with a constant cooling power of 300W whenever there is an occupant in the house. The result is plotted in the same graph. The purple lines in these subplots represent the ambient temperature; the blue and green dashed lines represent the upper and lower limits of the humidity-dependent thermal comfort zone, respectively. The two vertical dotted lines represent the time instant when the occupant leaves for work and returns back home. By comparing these room temperature plots, we can conclude that the smart thermostat controlled system has three key advantages compared to the traditional fixed-power HVAC system. First of all, the smart thermostat always maintains the room temperature within thermal comfort zone when there is an occupant in the room. It is worth noting that in this case, the occupied room temperature is maintained at the upper limit of the thermal comfort zone because when the exterior temperature is higher than indoor temperature, this is the most efficient cooling strategy without compromising thermal comfort. The fixed-power HVAC system, on the other hand, has limited capability in always maintaining thermal comfort. In the afternoon when the occupant returns home, it takes time for the constant-power HVAC system to cool the rooms back to

thermal comfort again. Secondly, the smart thermostat system is adaptive to the change in room occupancy. As evident in the temperature plot, when the occupant is moving from one room to another, the smart thermostat system will automatically turn off cooling in the previous room and will precool the next room to thermal comfort zone prior to the arrival of the occupant. This is why with the smart system, the room temperatures are more independent (though not fully independent, since there is heat transfer between rooms through the walls). In the conventional fixed-power system, all the rooms have to be cooled in order to guarantee that the occupant will always be in thermal comfort during room changing. As a result, the room temperatures are more synchronized. Finally, the smart thermostat system is adaptive to the varying upper and lower limits of the thermal comfort range. Unlike many commercially available automatic AC systems that maintain the room at a fixed temperature within the thermal comfort range, the smart thermostat can adjust the room temperature of the occupied room as the thermal comfort range changes with changing relative humidity.

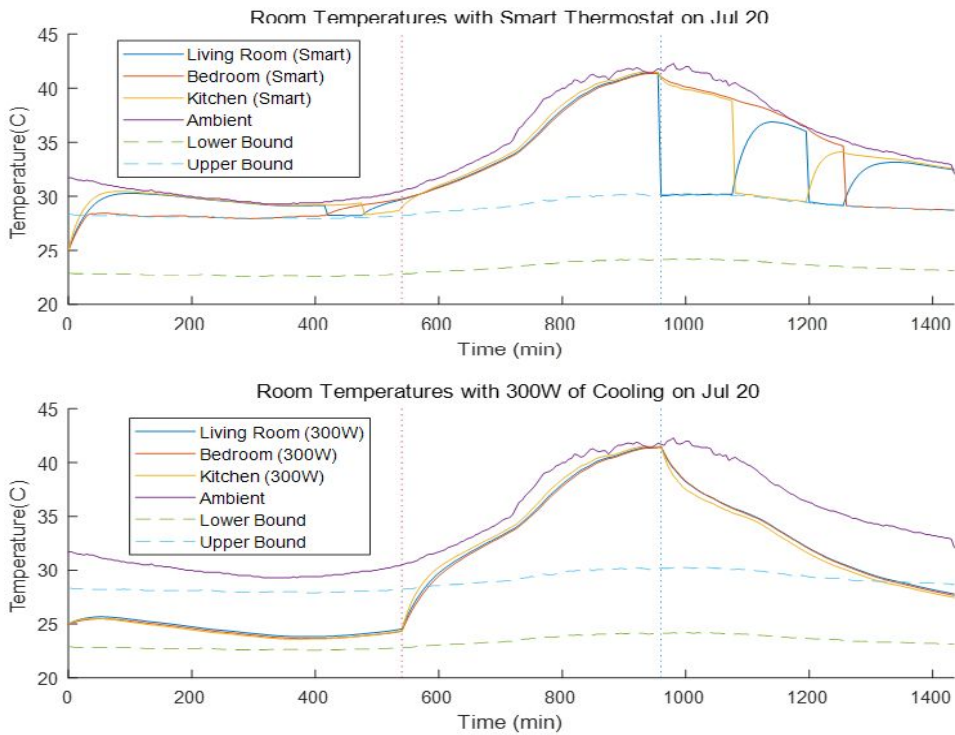


Fig. 3.1 Room Temperature Variation for the Smart Thermostat System (Top) and a Fixed 300W Power HVAC Cooling System (Bottom) on Jul 20th, 2019

The simulation results for Jan 31st, the coldest day in New York City in 2019, is shown in Fig. 3.2. For comparison, the room temperature response of a 2kW constant-power HVAC heating system is also shown. In this case, the smart thermostat maintains the temperature of the occupied room at the lower limit of the thermal comfort zone, which is the optimal heating strategy in winter without compromising thermal comfort. From the plots, the conclusions that the smart thermostat system is always able to maintain the room temperature within the thermal

comfort zone, is adaptive to the change in room occupancy and is adaptive to the varying upper and lower limits of the thermal comfort range can still be reached.

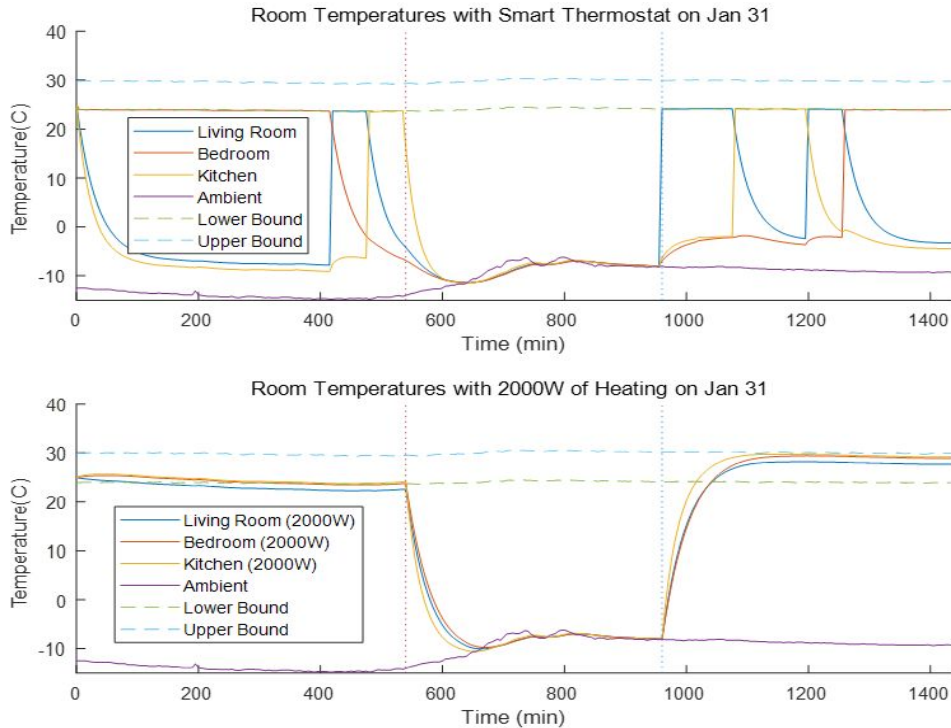


Fig. 3.2 Room Temperature Variation for the Smart Thermostat System (Top) and a Fixed 2kW Power HVAC Heating System (Bottom) on Jan 31st, 2019

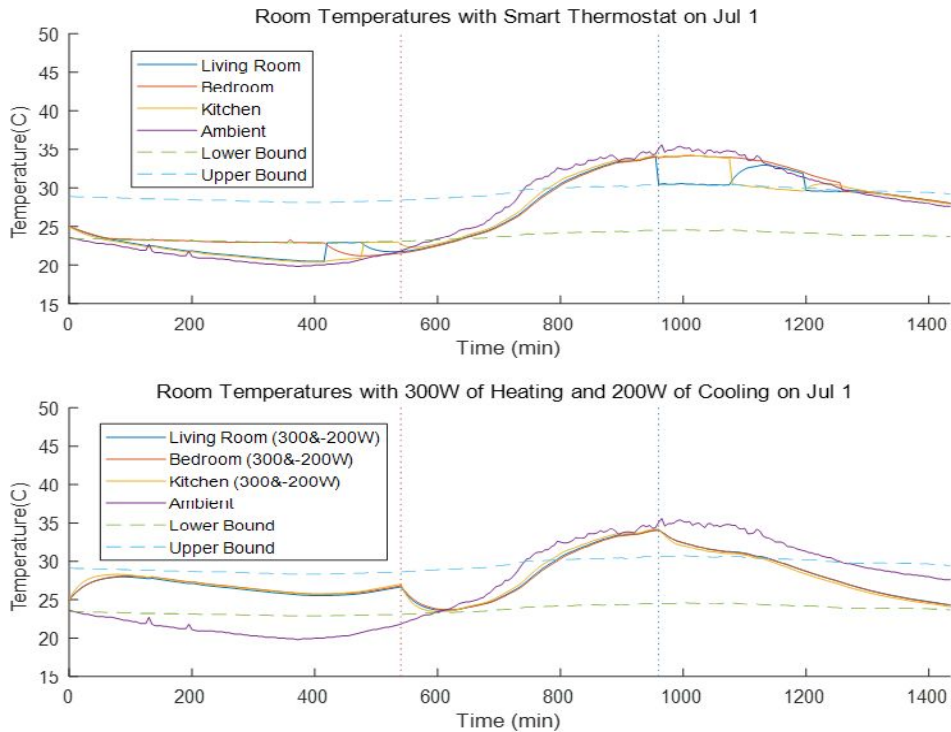


Fig. 3.3 Room Temperature Variation for the Smart Thermostat System (Top) and a Fixed Power (300W Heating in the Morning and 200W Cooling in the Evening) System (Bottom) on Jul 1st, 2019

Finally, the simulation results for Jul 1st, 2019 are shown in Fig. 3.3. As mentioned previously, this day is chosen because it has a large day-to-night temperature difference and both heating and cooling (heating in the morning and cooling in the evening) are needed to maintain thermal comfort within the rooms. As a baseline for comparison, the room temperature variation for a fixed-power HVAC system with 300W of heating in the morning and 200W of cooling in the evening is also shown. Once again, it can be confirmed that the smart thermostat system is always able to maintain the room temperature within the thermal comfort zone, is adaptive to the change in room occupancy and is adaptive to the varying upper and lower limits of the thermal comfort range. The system takes full advantage of the thermal comfort range to save energy. In the morning the occupied room temperature sticks to the lower comfort limit, and in the evening, the temperature sticks to the upper limit. With all three test cases, we can conclude that from the temperature response perspective, the smart thermostat system is superior to the conventional fixed-power HVAC system in most scenarios.

After comparing the temperature responses of the smart thermostat system with conventional HVAC systems, and confirming that the smart thermostat system has an outstanding temperature control performance, since the main objective of the project is to minimize electricity expenses while maintaining thermal comfort, the next thing that needs to be examined is the electricity cost generated when using the smart thermostat system. The comparisons of the hourly electricity costs for the smart thermostat system and the hourly costs of the fixed-power systems on Jul 20th, Jan 31st and Jul 1st are shown in Fig. 3.4 to 3.6, respectively. It can be observed that the total and hourly electricity costs of the smart system are lower than those of the constant-power systems. Thus, from an energy perspective, the smart thermostat system is also superior to the conventional fixed-power HVAC system.

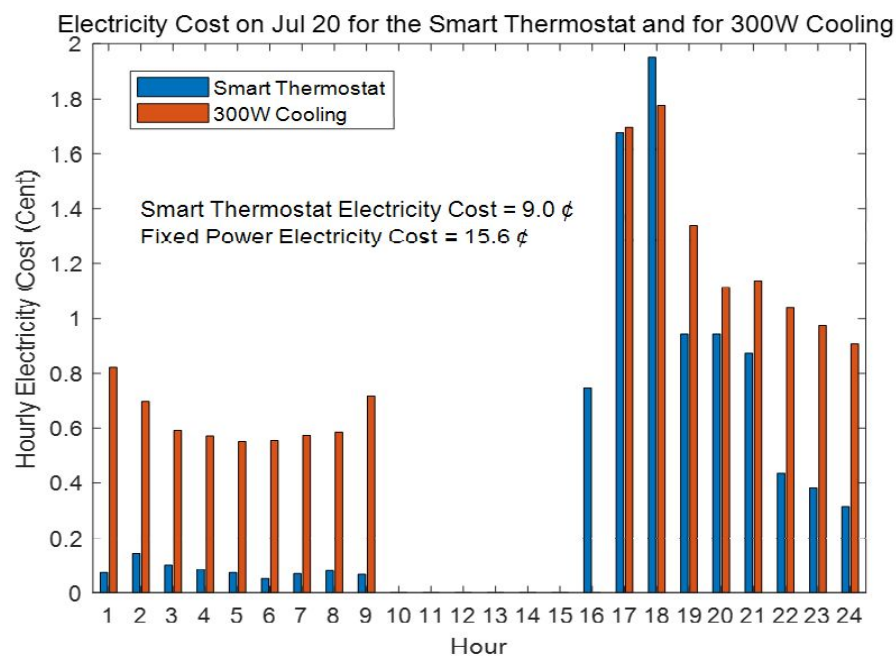


Fig. 3.4 Comparison of Hourly Electricity Price of the Smart Thermostat System and the Constant Power HVAC System on Jul 20th, 2019

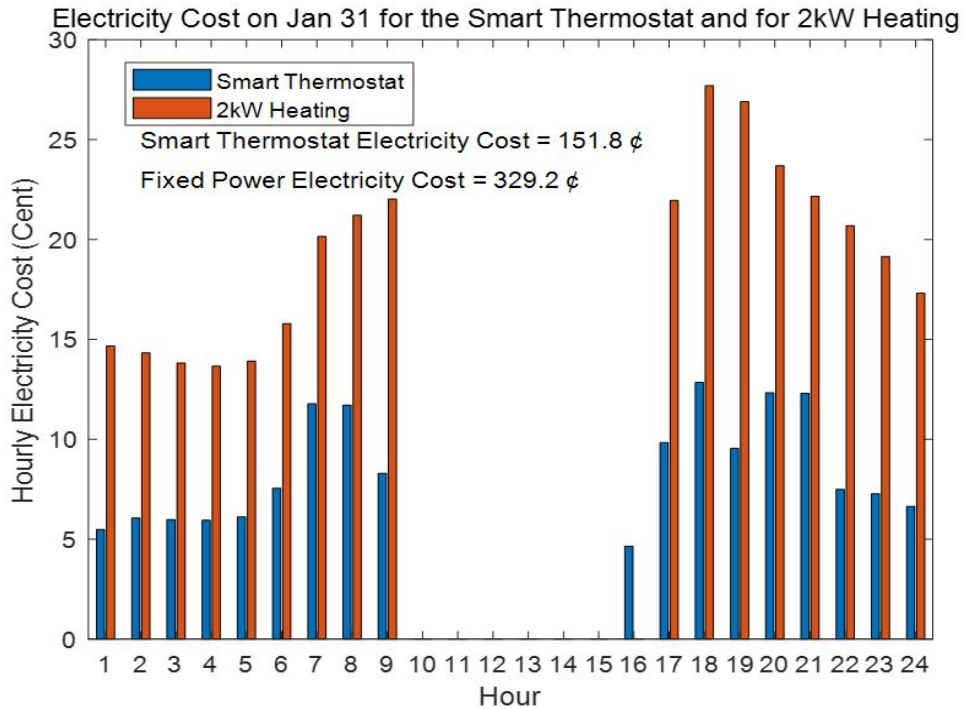


Fig. 3.5 Comparison of Hourly Electricity Price of the Smart Thermostat System and the Constant Power HVAC System on Jan 31st, 2019

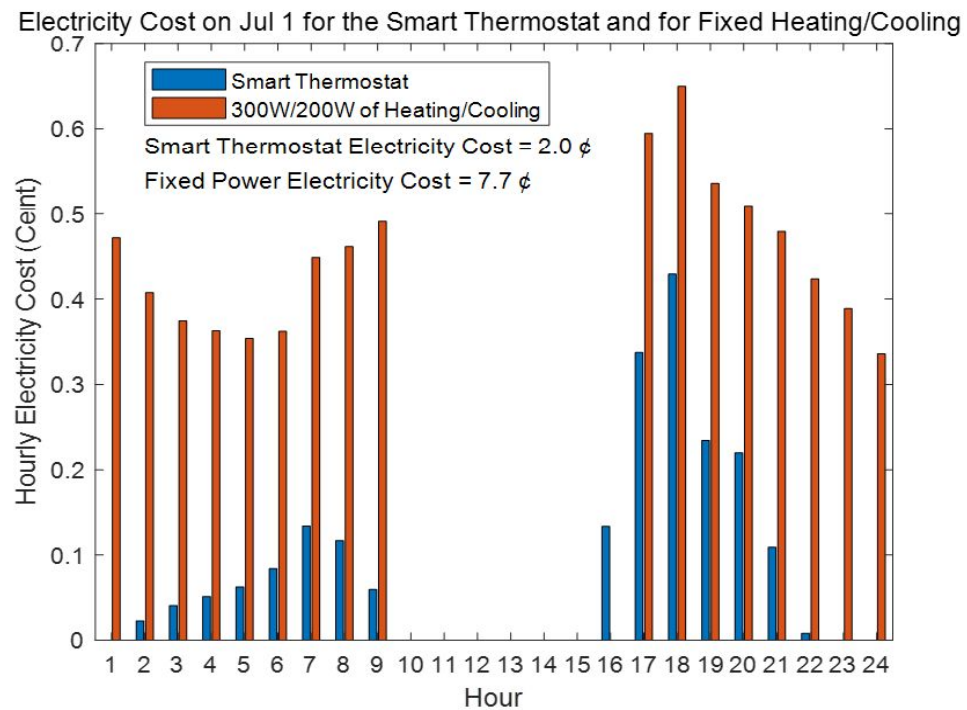


Fig. 3.6 Comparison of Hourly Electricity Price of the Smart Thermostat System and the Constant Power HVAC System on Jul 1st, 2019

4. Table of Responsibilities

Our tasks are distributed as follows:

1. Initial brainstorming and idea formulation
2. Thermal modeling of residential buildings
3. Collection of historical data (weather, electricity price, daily schedule, etc.)
4. Design of optimization and model predictive control algorithm
5. Comparison between our design and traditional HVAC systems
6. Presentation and final report

The responsibility of work is divided in the following way:

	Task 1	Task 2	Task 3	Task 4	Task 5	Task 6
Ronggen Chen	X			X		X
Mingxin Jia	X	X	X	X	X	X
Xiaotian Wang	X			X		X
Yuming Xu	X		X	X		X

5. Summary

In this work, we have developed an optimization algorithm for a smart thermostat controller to control an energy-efficient heating and cooling system, to maximize indoor thermal comfort and to minimize electricity expenses. The smart thermostat control algorithm is implemented using an iterative optimization approach that optimizes the heating/cooling power to minimize the total electricity cost in the next 6-hour period. The results of our work show that the system is capable of (a) maintaining room temperatures within thermal comfort range, (b) being adaptive to the changes of occupancy (occupant moving from one room to another), (c) being adaptive to change the lower and upper bounds of thermal comfort zone according to real-time humidity and (d) improving energy efficiency and reducing electricity cost. Since heating and cooling of buildings accounts for a relatively large percentage of the world's total energy consumption, the more reliable and more energy efficient smart thermostat system has the potential to greatly reduce the HVAC energy demand in the global society and make HVAC systems more sustainable.

References:

- [1] Energy Consumption by Ends <https://www.eia.gov/consumption/>
- [2] J. King, "Energy Impacts of Smart Home Technologies," American Council for an Energy-Efficient Economy, April 2018.
- [3] C. Lawrence, M. Woodward and C. Berry, "One in eight U.S. homes uses a programmed thermostat with a central air conditioning unit," U.S. Energy Information Administration, July 2017. [Online]. Available: <https://www.eia.gov/todayinenergy/detail.php?id=32112>. [Accessed April. 20, 2020].
- [4] T. Peffer, et al. "How people use thermostats in homes: A review," *Building and Environment*, vol. 46, no. 12, pp: 2529-2541, Dec. 2011.
- [5] E. M. Burger, H. E. Perez, and S. J. Moura, "Model Predictive Control of Residential Baseboard Heaters with Distributed System Architecture," 2014. [Online]. Available: <https://escholarship.org/uc/item/0g98j84k>. [Accessed April. 3, 2020].
- [6] R. Adhikari, et al. "An algorithm for optimal management of aggregated HVAC power demand using smart thermostats," *Applied Energy*, vol. 217, pp: 166-177, May 2018.
- [7] New York City Weather Data
<https://www.wunderground.com/weather/us/ny/upper-west-side/10024>
- [8] Electricity Price Data from Con Edison
<https://apps.coned.com/CEMyAccount/csol/MscDayAheadCC.aspx>

Appendix

Figures:

Comparison between true and forecast temperature and relative humidity on Jan 31, July 1 and July 20

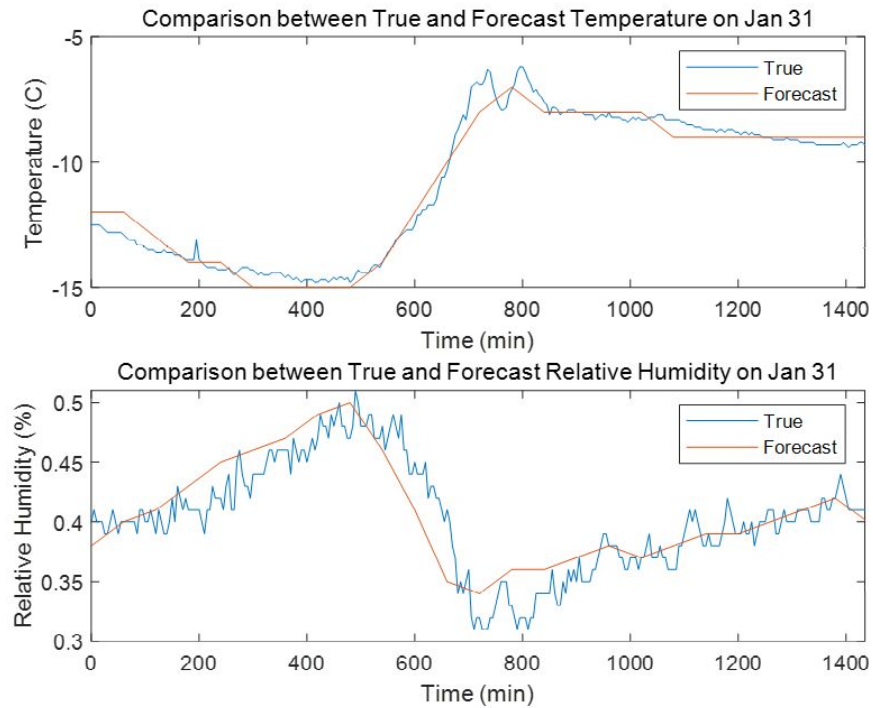


Fig A1 Comparison between True and Forecast Data on Jan 31st

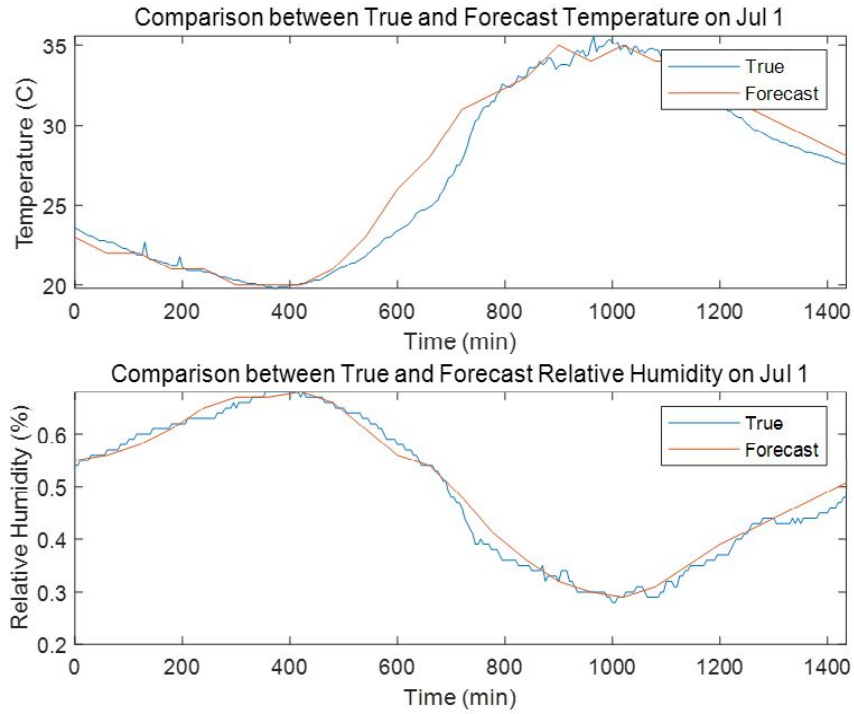


Fig A2 Comparison between True and Forecast Data on Jul 1st

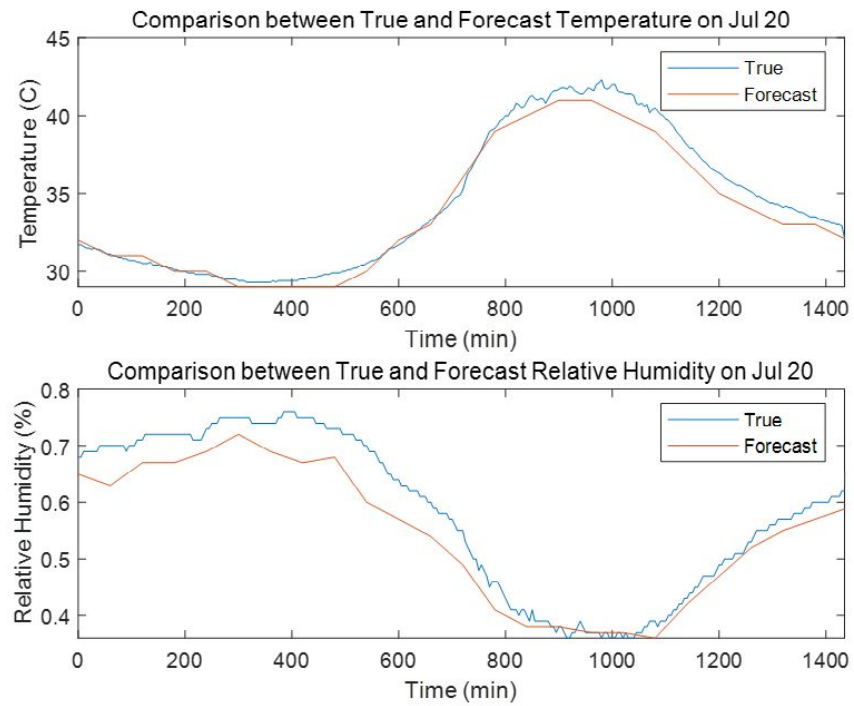


Fig A3 Comparison between True and Forecast Data on Jul 20th

MATLAB Code:

```
%% Main Function
clear;
close all;
%% Material Properties and Dimensions
Nu = 2; k_oak = 0.17; k_air = Nu*0.026; k_ply = 0.13; k_plaster = 0.5;
k_siding = 0.96; k_window = 0.016; A_window = 1; d_plaster = 12.7/1000;
d_oak = 88.8/1000; d_air = 88.8/1000; d_ply = 0.525/1000; d_siding =
1.905/1000;
d_window = 5/1000; f_oak = 38/406.4; f_air = 1 - f_oak; A_la = 36+12*3 -
2*A_window;
A_ka = 24+10*3 - A_window; A_ba = 40+18*3 - A_window; A_lb = 6*3; A_bk = 4*3;
A_lk = 6*3;

%% Parameter Calculation
R_la_f =
(d_oak/(k_oak*A_la*f_oak)*d_air/(k_air*A_la*f_air))/(d_oak/(k_oak*A_la*f_oak)
+d_air/(k_air*A_la*f_air));
R_la =
d_siding/(k_siding*A_la)+d_ply/(k_ply*A_la)+R_la_f+d_plaster/(k_plaster*A_la)
;
R_la_t =
(R_la*d_window/(k_window*2*A_window))/(R_la+d_window/(k_window*2*A_window));
R_ka_f =
(d_oak/(k_oak*A_ka*f_oak)*d_air/(k_air*A_ka*f_air))/(d_oak/(k_oak*A_ka*f_oak)
+d_air/(k_air*A_ka*f_air));
R_ka =
d_siding/(k_siding*A_ka)+d_ply/(k_ply*A_ka)+R_la_f+d_plaster/(k_plaster*A_ka)
;
R_ka_t =
(R_ka*d_window/(k_window*A_window))/(R_ka+d_window/(k_window*A_window));
R_ba_f =
(d_oak/(k_oak*A_ba*f_oak)*d_air/(k_air*A_ba*f_air))/(d_oak/(k_oak*A_ba*f_oak)
+d_air/(k_air*A_ba*f_air));
R_ba =
d_siding/(k_siding*A_ba)+d_ply/(k_ply*A_ba)+R_la_f+d_plaster/(k_plaster*A_ba)
;
R_ba_t =
(R_ba*d_window/(k_window*A_window))/(R_ba+d_window/(k_window*A_window));
R_lb_f =
(d_oak/(k_oak*A_lb*f_oak)*d_air/(k_air*A_lb*f_air))/(d_oak/(k_oak*A_lb*f_oak)
+d_air/(k_air*A_lb*f_air));
R_lb_t = R_lb_f+2*d_plaster/(k_plaster*A_lb);
R_bk_f =
(d_oak/(k_oak*A_bk*f_oak)*d_air/(k_air*A_bk*f_air))/(d_oak/(k_oak*A_bk*f_oak)
+d_air/(k_air*A_bk*f_air));
R_bk_t = R_bk_f+2*d_plaster/(k_plaster*A_bk);
R_lk_f =
(d_oak/(k_oak*A_lk*f_oak)*d_air/(k_air*A_lk*f_air))/(d_oak/(k_oak*A_lk*f_oak)
+d_air/(k_air*A_lk*f_air));
R_lk_t = R_lk_f+2*d_plaster/(k_plaster*A_lk);
rho_air = 1.225;
cp_air = 1005;
```

```

C_b = rho_air*4*10*3*cp_air;
C_l = rho_air*6*6*3*cp_air;
C_k = rho_air*4*6*3*cp_air;

%% State Space Form (Both Continuous and Discrete)
delta_t = 5*60;
A_mat = [-1/(R_lb_t*C_l)-1/(R_lk_t*C_l)-1/(R_la_t*C_l) 1/(R_lb_t*C_l)
1/(R_lk_t*C_l);...
1/(R_lb_t*C_b) -1/(R_lb_t*C_b)-1/(R_bk_t*C_b)-1/(R_ba_t*C_b)
1/(R_bk_t*C_b);...
1/(R_lk_t*C_k) 1/(R_bk_t*C_k) -1/(R_lk_t*C_k)-1/(R_bk_t*C_k)-
1/(R_ka_t*C_k)];
B_mat = [1/C_l 0 0 1/(R_la_t*C_l); 0 1/C_b 0 1/(R_ba_t*C_b); 0 0 1/C_k
1/(R_ka_t*C_k)];
A_mat_d = expm(A_mat*delta_t);
B_mat_d = inv(A_mat)*(A_mat_d-eye(length(A_mat)))*B_mat;

%% Import Data
actual_matrix_cold = csvread('Jan_31_Cleaned_Data_5min_Interval.csv',1,0);
actual_matrix_hot = csvread('Jul_20_Cleaned_Data_5min_Interval.csv',1,0);
actual_matrix_mid = csvread('Jul_1_Cleaned_Data_5min_Interval.csv',1,0);
time = actual_matrix_cold(:,1);
Jan31_Temp = actual_matrix_cold(:,2); Jan31_Hum = actual_matrix_cold(:,3);
Jul20_Temp = actual_matrix_hot(:,2); Jul20_Hum = actual_matrix_hot(:,3);
Jul1_Temp = actual_matrix_mid(:,2); Jul1_Hum = actual_matrix_mid(:,3);

Jul20_forecast_matrix = csvread('Hourly Forecast for Jul 20 2019.csv',1,0);
Jul20_Temp_F = interp1(0:60:60*30,Jul20_forecast_matrix(:,1),0:5:60*30)';
Jul20_Temp_F(end) = [];
Jul20_Hum_F = interp1(0:60:60*30,Jul20_forecast_matrix(:,2),0:5:60*30)';
Jul20_Hum_F(end) = [];

Jan31_forecast_matrix = csvread('Hourly Forecast for Jan 31 2019.csv',1,0);
Jan31_Temp_F = interp1(0:60:60*30,Jan31_forecast_matrix(:,1),0:5:60*30)';
Jan31_Temp_F(end) = [];
Jan31_Hum_F = interp1(0:60:60*30,Jan31_forecast_matrix(:,2),0:5:60*30)';
Jan31_Hum_F(end) = [];

Jul1_forecast_matrix = csvread('Hourly Forecast for Jul 1 2019.csv',1,0);
Jul1_Temp_F = interp1(0:60:60*30,Jul1_forecast_matrix(:,1),0:5:60*30)';
Jul1_Temp_F(end) = [];
Jul1_Hum_F = interp1(0:60:60*30,Jul1_forecast_matrix(:,2),0:5:60*30)';
Jul1_Hum_F(end) = [];

Jul20_Price_matrix = csvread('Hourly Electricity Price in Cents Per kWh for
Jul 20 2019.csv',0,1);
Jul20_Price = zeros(12*30,1);
for i = 1:30
    Jul20_Price(1+(i-1)*12:12+(i-1)*12) = Jul20_Price_matrix(i);
end

Jan31_Price_matrix = csvread('Hourly Electricity Price in Cents Per kWh for
Jan 31 2019.csv',0,1);
Jan31_Price = zeros(12*30,1);

```

```

for i = 1:30
    Jan31_Price(1+(i-1)*12:12+1+(i-1)*12) = Jan31_Price_matrix(i);
end

Jul1_Price_matrix = csvread('Hourly Electricity Price in Cents Per kWh for
Jul 1 2019.csv',0,1);
Jul1_Price = zeros(12*30,1);
for i = 1:30
    Jul1_Price(1+(i-1)*12:12+1+(i-1)*12) = Jul1_Price_matrix(i);
end

schedule_matrix = csvread('Occupant Schedule.csv',1,1);
schedule = zeros(12*30,3);
for i = 1:30
    for j = 1:3
        schedule(1+(i-1)*12:12+1+(i-1)*12,j) = schedule_matrix(i,j);
    end
end
living_room_schedule = schedule(:,1); kitchen_schedule = schedule(:,2);
bedroom_schedule = schedule(:,3);
Jan31_T_comfort = zeros(12*30,2); Jan31_T_comfort_F = zeros(12*30,2);
Jul20_T_comfort = zeros(12*30,2); Jul20_T_comfort_F = zeros(12*30,2);
Jul1_T_comfort = zeros(12*30,2); Jul1_T_comfort_F = zeros(12*30,2);
for i = 1:12*30
    [Jan31_temp_low,Jan31_temp_high] = comfort(Jan31_Hum(i));
    Jan31_T_comfort(i,1) = Jan31_temp_low;
    Jan31_T_comfort(i,2) = Jan31_temp_high;
    [Jan31_temp_low_F,Jan31_temp_high_F] = comfort(Jan31_Hum_F(i));
    Jan31_T_comfort_F(i,1) = Jan31_temp_low_F;
    Jan31_T_comfort_F(i,2) = Jan31_temp_high_F;
    [Jul20_temp_low,Jul20_temp_high] = comfort(Jul20_Hum(i));
    Jul20_T_comfort(i,1) = Jul20_temp_low;
    Jul20_T_comfort(i,2) = Jul20_temp_high;
    [Jul20_temp_low_F,Jul20_temp_high_F] = comfort(Jul20_Hum_F(i));
    Jul20_T_comfort_F(i,1) = Jul20_temp_low_F;
    Jul20_T_comfort_F(i,2) = Jul20_temp_high_F;
    [Jul1_temp_low,Jul1_temp_high] = comfort(Jul1_Hum(i));
    Jul1_T_comfort(i,1) = Jul1_temp_low;
    Jul1_T_comfort(i,2) = Jul1_temp_high;
    [Jul1_temp_low_F,Jul1_temp_high_F] = comfort(Jul1_Hum_F(i));
    Jul1_T_comfort_F(i,1) = Jul1_temp_low_F;
    Jul1_T_comfort_F(i,2) = Jul1_temp_high_F;
end
Jan31_T_constrt_l = [-999*ones(12*30,1),999*ones(12*30,1)];
Jan31_T_constrt_l_F = [-999*ones(12*30,1),999*ones(12*30,1)];
Jul20_T_constrt_l = [-999*ones(12*30,1),999*ones(12*30,1)];
Jul20_T_constrt_l_F = [-999*ones(12*30,1),999*ones(12*30,1)];
Jul1_T_constrt_l = [-999*ones(12*30,1),999*ones(12*30,1)];
Jul1_T_constrt_l_F = [-999*ones(12*30,1),999*ones(12*30,1)];
Jan31_T_constrt_k = [-999*ones(12*30,1),999*ones(12*30,1)];
Jan31_T_constrt_k_F = [-999*ones(12*30,1),999*ones(12*30,1)];
Jul20_T_constrt_k = [-999*ones(12*30,1),999*ones(12*30,1)];
Jul20_T_constrt_k_F = [-999*ones(12*30,1),999*ones(12*30,1)];
Jul1_T_constrt_k = [-999*ones(12*30,1),999*ones(12*30,1)];
Jul1_T_constrt_k_F = [-999*ones(12*30,1),999*ones(12*30,1)];
Jan31_T_constrt_b = [-999*ones(12*30,1),999*ones(12*30,1)];

```

```

Jan31_T_constrt_b_F = [-999*ones(12*30,1),999*ones(12*30,1)];
Jul20_T_constrt_b = [-999*ones(12*30,1),999*ones(12*30,1)];
Jul20_T_constrt_b_F = [-999*ones(12*30,1),999*ones(12*30,1)];
Jul1_T_constrt_b = [-999*ones(12*30,1),999*ones(12*30,1)];
Jul1_T_constrt_b_F = [-999*ones(12*30,1),999*ones(12*30,1)];

for i = 1:12*30
    if living_room_schedule(i) == 1
        Jan31_T_constrt_l(i,1) = Jan31_T_comfort(i,1);
        Jan31_T_constrt_l(i,2) = Jan31_T_comfort(i,2);
        Jan31_T_constrt_l_F(i,1) = Jan31_T_comfort_F(i,1);
        Jan31_T_constrt_l_F(i,2) = Jan31_T_comfort_F(i,2);
    end
end
for i = 1:12*30
    if kitchen_schedule(i) == 1
        Jan31_T_constrt_k(i,1) = Jan31_T_comfort(i,1);
        Jan31_T_constrt_k(i,2) = Jan31_T_comfort(i,2);
        Jan31_T_constrt_k_F(i,1) = Jan31_T_comfort_F(i,1);
        Jan31_T_constrt_k_F(i,2) = Jan31_T_comfort_F(i,2);
    end
end
for i = 1:12*30
    if bedroom_schedule(i) == 1
        Jan31_T_constrt_b(i,1) = Jan31_T_comfort(i,1);
        Jan31_T_constrt_b(i,2) = Jan31_T_comfort(i,2);
        Jan31_T_constrt_b_F(i,1) = Jan31_T_comfort_F(i,1);
        Jan31_T_constrt_b_F(i,2) = Jan31_T_comfort_F(i,2);
    end
end
for i = 1:12*30
    if living_room_schedule(i) == 1
        disp(Jul20_T_comfort(i,1))
        Jul20_T_constrt_l(i,1) = Jul20_T_comfort(i,1);
        Jul20_T_constrt_l(i,2) = Jul20_T_comfort(i,2);
        Jul20_T_constrt_l_F(i,1) = Jul20_T_comfort_F(i,1);
        Jul20_T_constrt_l_F(i,2) = Jul20_T_comfort_F(i,2);
    end
end
for i = 1:12*30
    if kitchen_schedule(i) == 1
        Jul20_T_constrt_k(i,1) = Jul20_T_comfort(i,1);
        Jul20_T_constrt_k(i,2) = Jul20_T_comfort(i,2);
        Jul20_T_constrt_k_F(i,1) = Jul20_T_comfort_F(i,1);
        Jul20_T_constrt_k_F(i,2) = Jul20_T_comfort_F(i,2);
    end
end
for i = 1:12*30
    if bedroom_schedule(i) == 1
        Jul20_T_constrt_b(i,1) = Jul20_T_comfort(i,1);
        Jul20_T_constrt_b(i,2) = Jul20_T_comfort(i,2);
        Jul20_T_constrt_b_F(i,1) = Jul20_T_comfort_F(i,1);
        Jul20_T_constrt_b_F(i,2) = Jul20_T_comfort_F(i,2);
    end
end
for i = 1:12*30
    if living_room_schedule(i) == 1

```

```

        disp(Jull_T_comfort(i,1))
    Jull_T_constrt_l(i,1) = Jull_T_comfort(i,1);
    Jull_T_constrt_l(i,2) = Jull_T_comfort(i,2);
    Jull_T_constrt_l_F(i,1) = Jull_T_comfort_F(i,1);
    Jull_T_constrt_l_F(i,2) = Jull_T_comfort_F(i,2);
    end
end
for i = 1:12*30
    if kitchen_schedule(i) == 1
        Jull_T_constrt_k(i,1) = Jull_T_comfort(i,1);
        Jull_T_constrt_k(i,2) = Jull_T_comfort(i,2);
        Jull_T_constrt_k_F(i,1) = Jull_T_comfort_F(i,1);
        Jull_T_constrt_k_F(i,2) = Jull_T_comfort_F(i,2);
    end
end
for i = 1:12*30
    if bedroom_schedule(i) == 1
        Jull_T_constrt_b(i,1) = Jull_T_comfort(i,1);
        Jull_T_constrt_b(i,2) = Jull_T_comfort(i,2);
        Jull_T_constrt_b_F(i,1) = Jull_T_comfort_F(i,1);
        Jull_T_constrt_b_F(i,2) = Jull_T_comfort_F(i,2);
    end
end

%% Data Visualization
figure; subplot(2,1,1); plot(time,Jul20_Temp); hold on;
plot(time,Jul20_Temp_F); hold off;
xlabel('Time (min)'); ylabel('Temperature (C)'); xlim([0 1435]);
title('Comparison between True and Forecast Temperature on Jul 20');
legend('True','Forecast');
subplot(2,1,2); plot(time,Jul20_Hum); hold on; plot(time,Jul20_Hum_F); hold off;
xlabel('Time (min)'); ylabel('Relative Humidity (%)'); xlim([0 1435]);
title('Comparison between True and Forecast Relative Humidity on Jul 20');
legend('True','Forecast');

figure; subplot(2,1,1); plot(time,Jan31_Temp); hold on;
plot(time,Jan31_Temp_F); hold off;
xlabel('Time (min)'); ylabel('Temperature (C)'); xlim([0 1435]);
title('Comparison between True and Forecast Temperature on Jan 31');
legend('True','Forecast');
subplot(2,1,2); plot(time,Jan31_Hum); hold on; plot(time,Jan31_Hum_F); hold off;
xlabel('Time (min)'); ylabel('Relative Humidity (%)'); xlim([0 1435]);
title('Comparison between True and Forecast Relative Humidity on Jan 31');
legend('True','Forecast');

figure; subplot(2,1,1); plot(time,Jull_Temp); hold on;
plot(time,Jull_Temp_F); hold off;
xlabel('Time (min)'); ylabel('Temperature (C)'); xlim([0 1435]);
title('Comparison between True and Forecast Temperature on Jul 1');
legend('True','Forecast');
subplot(2,1,2); plot(time,Jull_Hum); hold on; plot(time,Jull_Hum_F); hold off;
xlabel('Time (min)'); ylabel('Relative Humidity (%)'); xlim([0 1435]);
title('Comparison between True and Forecast Relative Humidity on Jul 1');

```

```

legend('True','Forecast');

%% Optimization 1
dt = 5*60; COP = 3.8;
P_max = 6000; P_min = -5000;
power_matrix = zeros(12*24,3); T_matrix = zeros(12*24,3);
Tl0 = 25; Tb0 = 25; Tk0 = 25;

for k = 1:12*24
    summation = 0;
    T_inf = Jul20_Temp(k:k+71);
    T_inf_F = Jul20_Temp_F(k:k+71);
    T_high_l_F = Jul20_T_constrt_l_F(k:k+71,2);
    T_low_l_F = Jul20_T_constrt_l_F(k:k+71,1);
    T_high_b_F = Jul20_T_constrt_b_F(k:k+71,2);
    T_low_b_F = Jul20_T_constrt_b_F(k:k+71,1);
    T_high_k_F = Jul20_T_constrt_k_F(k:k+71,2);
    T_low_k_F = Jul20_T_constrt_k_F(k:k+71,1);
    T_matrix(k,1) = Tl0; T_matrix(k,2) = Tb0; T_matrix(k,3) = Tk0;

    cvx_begin
        variables P_l(72) P_b(72) P_k(72) T(72,3)
        for i = 1:72
            summation = summation+Jul20_Price(k+i-
1)*(abs(P_l(i))+abs(P_b(i))+abs(P_k(i)))*dt/3600000/100/COP;
        end
        minimize(summation)
        subject to
            T(1,1) == Tl0;
            T(1,2) == Tb0;
            T(1,3) == Tk0;
            for j = 1:71
                T(j+1,1) ==
A_mat_d(1,:)*[T(j,1);T(j,2);T(j,3)]+B_mat_d(1,:)*[P_l(j);P_b(j);P_k(j);T_inf_
F(j)];
                T(j+1,2) ==
A_mat_d(2,:)*[T(j,1);T(j,2);T(j,3)]+B_mat_d(2,:)*[P_l(j);P_b(j);P_k(j);T_inf_
F(j)];
                T(j+1,3) ==
A_mat_d(3,:)*[T(j,1);T(j,2);T(j,3)]+B_mat_d(3,:)*[P_l(j);P_b(j);P_k(j);T_inf_
F(j)];
                T(j+1,1) >= T_low_l_F(j+1); T(j+1,1) <= T_high_l_F(j+1);
                T(j+1,2) >= T_low_b_F(j+1); T(j+1,2) <= T_high_b_F(j+1);
                T(j+1,3) >= T_low_k_F(j+1); T(j+1,3) <= T_high_k_F(j+1);
                P_l(j) >= P_min; P_l(j) <= P_max;
                P_b(j) >= P_min; P_b(j) <= P_max;
                P_k(j) >= P_min; P_k(j) <= P_max;
            end
    cvx_end
    power_matrix(k,1) = P_l(1)/COP; power_matrix(k,2) = P_b(1)/COP;
    power_matrix(k,3) = P_k(1)/COP;
    Tl0 =
A_mat_d(1,:)*[Tl0;Tb0;Tk0]+B_mat_d(1,:)*[P_l(1);P_b(1);P_k(1);T_inf(1)];
    Tb0 =
A_mat_d(2,:)*[Tl0;Tb0;Tk0]+B_mat_d(2,:)*[P_l(1);P_b(1);P_k(1);T_inf(1)];

```

```

Tk0 =
A_mat_d(3,:)*[Tl0;Tb0;Tk0]+B_mat_d(3,:)*[P_l(1);P_b(1);P_k(1);T_inf(1)];
disp(k);

end

%% Optimization 2

power_matrix_1 = zeros(12*24,3); T_matrix_1 = zeros(12*24,3);
Tl0 = 25; Tb0 = 25; Tk0 = 25;

for k = 1:12*24
    summation = 0;
    T_inf = Jan31_Temp(k:k+71);
    T_inf_F = Jan31_Temp_F(k:k+71);
    T_high_l_F = Jan31_T_constrt_l_F(k:k+71,2);
    T_low_l_F = Jan31_T_constrt_l_F(k:k+71,1);
    T_high_b_F = Jan31_T_constrt_b_F(k:k+71,2);
    T_low_b_F = Jan31_T_constrt_b_F(k:k+71,1);
    T_high_k_F = Jan31_T_constrt_k_F(k:k+71,2);
    T_low_k_F = Jan31_T_constrt_k_F(k:k+71,1);
    T_matrix_1(k,1) = Tl0; T_matrix_1(k,2) = Tb0; T_matrix_1(k,3) = Tk0;

    cvx_begin
        variables P_l(72) P_b(72) P_k(72) T(72,3)
        for i = 1:72
            summation = summation+Jan31_Price(k+i-
1)*(abs(P_l(i))+abs(P_b(i))+abs(P_k(i)))*dt/3600000/100/COP;
        end
        minimize(summation)
        subject to
        T(1,1) == Tl0;
        T(1,2) == Tb0;
        T(1,3) == Tk0;
        for j = 1:71
            T(j+1,1) ==
            A_mat_d(1,:)*[T(j,1);T(j,2);T(j,3)]+B_mat_d(1,:)*[P_l(j);P_b(j);P_k(j);T_inf_
F(j)];
            T(j+1,2) ==
            A_mat_d(2,:)*[T(j,1);T(j,2);T(j,3)]+B_mat_d(2,:)*[P_l(j);P_b(j);P_k(j);T_inf_
F(j)];
            T(j+1,3) ==
            A_mat_d(3,:)*[T(j,1);T(j,2);T(j,3)]+B_mat_d(3,:)*[P_l(j);P_b(j);P_k(j);T_inf_
F(j)];
            T(j+1,1) >= T_low_l_F(j+1); T(j+1,1) <= T_high_l_F(j+1);
            T(j+1,2) >= T_low_b_F(j+1); T(j+1,2) <= T_high_b_F(j+1);
            T(j+1,3) >= T_low_k_F(j+1); T(j+1,3) <= T_high_k_F(j+1);
            P_l(j) >= P_min; P_l(j) <= P_max;
            P_b(j) >= P_min; P_b(j) <= P_max;
            P_k(j) >= P_min; P_k(j) <= P_max;
        end
    cvx_end
    power_matrix_1(k,1) = P_l(1)/COP; power_matrix_1(k,2) = P_b(1)/COP;
    power_matrix_1(k,3) = P_k(1)/COP;
    Tl0 =
A_mat_d(1,:)*[Tl0;Tb0;Tk0]+B_mat_d(1,:)*[P_l(1);P_b(1);P_k(1);T_inf(1)];

```

```

Tb0 =
A_mat_d(2,:) * [Tl0; Tb0; Tk0] + B_mat_d(2,:) * [P_l(1); P_b(1); P_k(1); T_inf(1)];
Tk0 =
A_mat_d(3,:) * [Tl0; Tb0; Tk0] + B_mat_d(3,:) * [P_l(1); P_b(1); P_k(1); T_inf(1)];
disp(k);

end

%% Optimization 3
power_matrix_2 = zeros(12*24,3); T_matrix_2 = zeros(12*24,3);
Tl0 = 25; Tb0 = 25; Tk0 = 25;

for k = 1:12*24
    summation = 0;
    T_inf = Jul1_Temp(k:k+71);
    T_inf_F = Jul1_Temp_F(k:k+71);
    T_high_l_F = Jul1_T_constrt_l_F(k:k+71,2);
    T_low_l_F = Jul1_T_constrt_l_F(k:k+71,1);
    T_high_b_F = Jul1_T_constrt_b_F(k:k+71,2);
    T_low_b_F = Jul1_T_constrt_b_F(k:k+71,1);
    T_high_k_F = Jul1_T_constrt_k_F(k:k+71,2);
    T_low_k_F = Jul1_T_constrt_k_F(k:k+71,1);
    T_matrix_2(k,1) = Tl0; T_matrix_2(k,2) = Tb0; T_matrix_2(k,3) = Tk0;

    cvx_begin
        variables P_l(72) P_b(72) P_k(72) T(72,3)
        for i = 1:72
            summation = summation+Jul1_Price(k+i-
1)*(abs(P_l(i))+abs(P_b(i))+abs(P_k(i)))*dt/3600000/100/COP;
        end
        minimize(summation)
        subject to
        T(1,1) == Tl0;
        T(1,2) == Tb0;
        T(1,3) == Tk0;
        for j = 1:71
            T(j+1,1) ==
A_mat_d(1,:)*[T(j,1);T(j,2);T(j,3)]+B_mat_d(1,:)*[P_l(j);P_b(j);P_k(j);T_inf_
F(j)];
            T(j+1,2) ==
A_mat_d(2,:)*[T(j,1);T(j,2);T(j,3)]+B_mat_d(2,:)*[P_l(j);P_b(j);P_k(j);T_inf_
F(j)];
            T(j+1,3) ==
A_mat_d(3,:)*[T(j,1);T(j,2);T(j,3)]+B_mat_d(3,:)*[P_l(j);P_b(j);P_k(j);T_inf_
F(j)];
            T(j+1,1) >= T_low_l_F(j+1); T(j+1,1) <= T_high_l_F(j+1);
            T(j+1,2) >= T_low_b_F(j+1); T(j+1,2) <= T_high_b_F(j+1);
            T(j+1,3) >= T_low_k_F(j+1); T(j+1,3) <= T_high_k_F(j+1);
            P_l(j) >= P_min; P_l(j) <= P_max;
            P_b(j) >= P_min; P_b(j) <= P_max;
            P_k(j) >= P_min; P_k(j) <= P_max;
        end
    cvx_end
    power_matrix_2(k,1) = P_l(1)/COP; power_matrix_2(k,2) = P_b(1)/COP;
    power_matrix_2(k,3) = P_k(1)/COP;

```

```

Tl0 =
A_mat_d(1,:) * [Tl0; Tb0; Tk0] + B_mat_d(1,:) * [P_l(1); P_b(1); P_k(1); T_inf(1)];
Tb0 =
A_mat_d(2,:) * [Tl0; Tb0; Tk0] + B_mat_d(2,:) * [P_l(1); P_b(1); P_k(1); T_inf(1)];
Tk0 =
A_mat_d(3,:) * [Tl0; Tb0; Tk0] + B_mat_d(3,:) * [P_l(1); P_b(1); P_k(1); T_inf(1)];
disp(k);

end

%% Comparison
P_cool = -300; % Cooling Power
P_fixed = P_cool*max((schedule(1:12*24,:))')';
Tl_fixed = 25; Tb_fixed = 25; Tk_fixed = 25;
T_matirx_fixed = zeros(12*24:3);
for m = 1:12*24
    T_matrix_fixed(m,1) = Tl_fixed; T_matrix_fixed(m,2) = Tb_fixed;
    T_matrix_fixed(m,3) = Tk_fixed;
    Tl_fixed = A_mat_d(1,:)*[Tl_fixed; Tb_fixed; Tk_fixed]+B_mat_d(1,:) ...
        *[P_fixed(m); P_fixed(m); P_fixed(m); Jul20_Temp(m)];
    Tb_fixed = A_mat_d(2,:)*[Tl_fixed; Tb_fixed; Tk_fixed]+B_mat_d(2,:) ...
        *[P_fixed(m); P_fixed(m); P_fixed(m); Jul20_Temp(m)];
    Tk_fixed = A_mat_d(3,:)*[Tl_fixed; Tb_fixed; Tk_fixed]+B_mat_d(3,:) ...
        *[P_fixed(m); P_fixed(m); P_fixed(m); Jul20_Temp(m)];
end

P_heat = 2000; % Heating Power
P_fixed_1 = P_heat*max((schedule(1:12*24,:))')';
Tl_fixed_1 = 25; Tb_fixed_1 = 25; Tk_fixed_1 = 25;
T_matirx_fixed_1 = zeros(12*24:3);
for m = 1:12*24
    T_matrix_fixed_1(m,1) = Tl_fixed_1; T_matrix_fixed_1(m,2) = Tb_fixed_1;
    T_matrix_fixed_1(m,3) = Tk_fixed_1;
    Tl_fixed_1 =
    A_mat_d(1,:)*[Tl_fixed_1; Tb_fixed_1; Tk_fixed_1]+B_mat_d(1,:) ...
        *[P_fixed_1(m); P_fixed_1(m); P_fixed_1(m); Jan31_Temp(m)];
    Tb_fixed_1 =
    A_mat_d(2,:)*[Tl_fixed_1; Tb_fixed_1; Tk_fixed_1]+B_mat_d(2,:) ...
        *[P_fixed_1(m); P_fixed_1(m); P_fixed_1(m); Jan31_Temp(m)];
    Tk_fixed_1 =
    A_mat_d(3,:)*[Tl_fixed_1; Tb_fixed_1; Tk_fixed_1]+B_mat_d(3,:) ...
        *[P_fixed_1(m); P_fixed_1(m); P_fixed_1(m); Jan31_Temp(m)];
end

P_hot = 300; P_cold = -200;
P_fixed_2 = [P_hot*ones(1,540/5),zeros(1,420/5),P_cold*ones(1,480/5)]';
Tl_fixed_2 = 25; Tb_fixed_2 = 25; Tk_fixed_2 = 25;
T_matirx_fixed_2 = zeros(12*24:3);
for m = 1:12*24
    T_matrix_fixed_2(m,1) = Tl_fixed_2; T_matrix_fixed_2(m,2) = Tb_fixed_2;
    T_matrix_fixed_2(m,3) = Tk_fixed_2;
    Tl_fixed_2 =
    A_mat_d(1,:)*[Tl_fixed_2; Tb_fixed_2; Tk_fixed_2]+B_mat_d(1,:) ...
        *[P_fixed_2(m); P_fixed_2(m); P_fixed_2(m); Jul11_Temp(m)];

```

```

Tb_fixed_2 =
A_mat_d(2,:)*[Tl_fixed_2;Tb_fixed_2;Tk_fixed_2]+B_mat_d(2,:)*...
    *[P_fixed_2(m);P_fixed_2(m);P_fixed_2(m);Jul1_Temp(m)];
Tk_fixed_2 =
A_mat_d(3,:)*[Tl_fixed_2;Tb_fixed_2;Tk_fixed_2]+B_mat_d(3,:)*...
    *[P_fixed_2(m);P_fixed_2(m);P_fixed_2(m);Jul1_Temp(m)];
end

%% Result Analysis 1
figure
subplot(2,1,1)
hold on;
plot(0:5:1435,T_matrix(:,1)'); plot(0:5:1435,T_matrix(:,2)');
plot(0:5:1435,T_matrix(:,3)');
plot(0:5:1435,Jul20_Temp(1:288));
plot(0:5:1435,Jul20_T_comfort(1:288,1), '--');
plot(0:5:1435,Jul20_T_comfort(1:288,2)+0.2, '--');
plot([540 540],[20 45],':'); plot([960 960],[20 45],':');
hold off; xlabel('Time (min)'); ylabel('Temperature(C)'); xlim([0 1435]);
ylim([20 45]);
legend('Living Room (Smart)', 'Bedroom (Smart)', 'Kitchen
(Smart)', 'Ambient', 'Lower Bound',...
    'Upper Bound'); title('Room Temperatures with Smart Thermostat on Jul
20');

subplot(2,1,2)
hold on;
plot(0:5:1435,T_matrix_fixed(:,1)'); plot(0:5:1435,T_matrix_fixed(:,2)');
plot(0:5:1435,T_matrix_fixed(:,3)');
plot(0:5:1435,Jul20_Temp(1:288));
plot(0:5:1435,Jul20_T_comfort(1:288,1), '--');
plot(0:5:1435,Jul20_T_comfort(1:288,2)+0.2, '--');
plot([540 540],[20 45],':'); plot([960 960],[20 45],':');
hold off; xlabel('Time (min)'); ylabel('Temperature(C)'); xlim([0 1435]);
ylim([20 45]);
legend('Living Room (300W)', 'Bedroom (300W)', 'Kitchen (300W)', 'Ambient',...
    'Lower Bound', 'Upper Bound');
title('Room Temperatures with 300W of Cooling on Jul 20');

figure
subplot(2,1,1)
hold on;
plot(0:5:1435,T_matrix_1(:,1)'); plot(0:5:1435,T_matrix_1(:,2)');
plot(0:5:1435,T_matrix_1(:,3)');
plot(0:5:1435,Jan31_Temp(1:288));
plot(0:5:1435,Jan31_T_comfort(1:288,1), '--');
plot(0:5:1435,Jan31_T_comfort(1:288,2), '--');
plot([540 540],[-15 40],':'); plot([960 960],[-15 40],':');
hold off; xlabel('Time (min)'); ylabel('Temperature(C)'); xlim([0 1435]);
ylim([-15 40]);
legend('Living Room', 'Bedroom', 'Kitchen', 'Ambient', 'Lower Bound',...
    'Upper Bound');
title('Room Temperatures with Smart Thermostat on Jan 31');

subplot(2,1,2)
hold on;
plot(0:5:1435,T_matrix_fixed_1(:,1)'); plot(0:5:1435,T_matrix_fixed_1(:,2)');


```

```

plot(0:5:1435,T_matrix_fixed_1(:,3)');
plot(0:5:1435,Jan31_Temp(1:288));
plot(0:5:1435,Jan31_T_comfort(1:288,1), '--');
plot(0:5:1435,Jan31_T_comfort(1:288,2)+0.2, '--');
plot([540 540], [-15 40], ':'); plot([960 960], [-15 40], ':');
hold off; xlabel('Time (min)'); ylabel('Temperature(C)'); xlim([0 1435]);
ylim([-15 40]);
legend('Living Room (2000W)', 'Bedroom (2000W)', 'Kitchen
(2000W)', 'Ambient',...
    'Lower Bound', 'Upper Bound');
title('Room Temperatures with 2000W of Heating on Jan 31');

figure
subplot(2,1,1)
hold on;
plot(0:5:1435,T_matrix_2(:,1)); plot(0:5:1435,T_matrix_2(:,2));
plot(0:5:1435,T_matrix_2(:,3));
plot(0:5:1435,Jull_Temp(1:288));
plot(0:5:1435,Jull_T_comfort(1:288,1), '--');
plot(0:5:1435,Jull_T_comfort(1:288,2), '--');
plot([540 540], [15 50], ':'); plot([960 960], [15 50], ':');
hold off; xlabel('Time (min)'); ylabel('Temperature(C)'); xlim([0 1435]);
ylim([15 50]);
legend('Living Room', 'Bedroom', 'Kitchen', 'Ambient', 'Lower Bound',...
    'Upper Bound');
title('Room Temperatures with Smart Thermostat on Jul 1');

subplot(2,1,2)
hold on;
plot(0:5:1435,T_matrix_fixed_2(:,1));plot(0:5:1435,T_matrix_fixed_2(:,2));
plot(0:5:1435,T_matrix_fixed_2(:,3));
plot(0:5:1435,Jull_Temp(1:288));
plot(0:5:1435,Jull_T_comfort(1:288,1), '--');
plot(0:5:1435,Jull_T_comfort(1:288,2)+0.2, '--');
plot([540 540], [15 50], ':'); plot([960 960], [15 50], ':');
hold off; xlabel('Time (min)'); ylabel('Temperature(C)'); xlim([0 1435]);
ylim([15 50]);
legend('Living Room (300&-200W)', 'Bedroom (300&-200W)', 'Kitchen (300&-
200W)', 'Ambient',...
    'Lower Bound', 'Upper Bound');
title('Room Temperatures with 300W of Heating and 200W of Cooling on Jul 1');

%% Result Analysis 2

bill_list = zeros(24,1);
total_bill = 0;
for m = 1:24
    cost = 0;
    for n = (m-1)*12+1:12*m
        cost =
Jul20_Price(n)*(abs(power_matrix(n,1))+abs(power_matrix(n,2))+...
                abs(power_matrix(n,3)))*dt/3600000+cost;
    end
    bill_list(m) = cost;
    total_bill = total_bill+cost;
end

```

```

bill_list_fixed = zeros(24,1);
total_bill_fixed = 0;
for m = 1:24
    cost = 0;
    for n = (m-1)*12+1:12*m
        cost = Jul20_Price(n)*(abs(P_fixed(n))*3/COP)*dt/3600000+cost;
    end
    bill_list_fixed(m) = cost;
    total_bill_fixed = total_bill_fixed+cost;
end
bill_matrix = [bill_list,bill_list_fixed];
figure;
bar(bill_matrix);
text(2,1.4,'Smart Thermostat Electricity Cost = 9.0 ?');
text(2,1.3,'Fixed Power Electricity Cost = 15.6 ?');
set(gca,'XTick',1:24)
ax = gca;
xlabel('Hour'); ylabel('Hourly Electricity Cost (Cent)');
legend('Smart Thermostat','300W Cooling')
title('Electricity Cost on Jul 20 for the Smart Thermostat and for 300W Cooling')

bill_list_1 = zeros(24,1);
total_bill_1 = 0;
for m = 1:24
    cost = 0;
    for n = (m-1)*12+1:12*m
        cost =
Jan31_Price(n)*(abs(power_matrix_1(n,1))+abs(power_matrix_1(n,2))+...
                abs(power_matrix_1(n,3)))*dt/3600000+cost;
    end
    bill_list_1(m) = cost;
    total_bill_1 = total_bill_1+cost;
end

bill_list_fixed_1 = zeros(24,1);
total_bill_fixed_1 = 0;
for m = 1:24
    cost = 0;
    for n = (m-1)*12+1:12*m
        cost = Jan31_Price(n)*(abs(P_fixed_1(n))*3/COP)*dt/3600000+cost;
    end
    bill_list_fixed_1(m) = cost;
    total_bill_fixed_1 = total_bill_fixed_1+cost;
end
bill_matrix_1 = [bill_list_1,bill_list_fixed_1];
figure;
bar(bill_matrix_1);
text(2,25,'Smart Thermostat Electricity Cost = 151.8 ?');
text(2,23,'Fixed Power Electricity Cost = 329.2 ?');
set(gca,'XTick',1:24)
ax = gca;
xlabel('Hour'); ylabel('Hourly Electricity Cost (Cent)');
legend('Smart Thermostat','2kW Heating')

```

```

title('Electricity Cost on Jan 31 for the Smart Thermostat and for 2kW
Heating')

bill_list_1 = zeros(24,1);
total_bill_1 = 0;
for m = 1:24
    cost = 0;
    for n = (m-1)*12+1:12*m
        cost =
Jan31_Price(n)*(abs(power_matrix_1(n,1))+abs(power_matrix_1(n,2))+...
                abs(power_matrix_1(n,3)))*dt/3600000+cost;
    end
    bill_list_1(m) = cost;
    total_bill_1 = total_bill_1+cost;
end

bill_list_fixed_1 = zeros(24,1);
total_bill_fixed_1 = 0;
for m = 1:24
    cost = 0;
    for n = (m-1)*12+1:12*m
        cost = Jan31_Price(n)*(abs(P_fixed_1(n))*3/COP)*dt/3600000+cost;
    end
    bill_list_fixed_1(m) = cost;
    total_bill_fixed_1 = total_bill_fixed_1+cost;
end
bill_matrix_1 = [bill_list_1,bill_list_fixed_1];
figure;
bar(bill_matrix_1);
text(2,25,'Smart Thermostat Electricity Cost = 151.8 ?');
text(2,23,'Fixed Power Electricity Cost = 329.2 ?');
set(gca,'XTick',1:24)
ax = gca;
xlabel('Hour'); ylabel('Hourly Electricity Cost (Cent)');
legend('Smart Thermostat','2kW Heating')
title('Electricity Cost on Jan 31 for the Smart Thermostat and for 2kW
Heating')

bill_list_2 = zeros(24,1);
total_bill_2 = 0;
for m = 1:24
    cost = 0;
    for n = (m-1)*12+1:12*m
        cost =
Jull_Price(n)*(abs(power_matrix_2(n,1))+abs(power_matrix_2(n,2))+...
                abs(power_matrix_2(n,3)))*dt/3600000+cost;
    end
    bill_list_2(m) = cost;
    total_bill_2 = total_bill_2+cost;
end

bill_list_fixed_2 = zeros(24,1);
total_bill_fixed_2 = 0;
for m = 1:24
    cost = 0;
    for n = (m-1)*12+1:12*m

```

```

    cost = Jul1_Price(n) * (abs(P_fixed_2(n)) * 3/COP) * dt / 3600000 + cost;
end
bill_list_fixed_2(m) = cost;
total_bill_fixed_2 = total_bill_fixed_2 + cost;
end
bill_matrix_2 = [bill_list_2, bill_list_fixed_2];
figure;
bar(bill_matrix_2);
text(2, 0.58, 'Smart Thermostat Electricity Cost = 2.0 ?');
text(2, 0.54, 'Fixed Power Electricity Cost = 7.7 ?');
set(gca, 'XTick', 1:24)
ax = gca;
xlabel('Hour'); ylabel('Hourly Electricity Cost (Cent)');
legend('Smart Thermostat', '300W/200W of Heating/Cooling')
title('Electricity Cost on Jul 1 for the Smart Thermostat and for Fixed
Heating/Cooling')

%% Define Function
function [T_low, T_high] = comfort(Hum)
RH = [0.1, 0.2, 0.3, 0.4, 0.5, 0.6, 0.7, 0.8, 0.9, 1];
T_top = [31.8, 31.0, 30.4, 29.8, 29.1, 28.6, 28.0, 27.5, 27.1, 26.5];
T_low = [25.5, 25.0, 24.5, 24.0, 23.6, 23.2, 22.8, 22.4, 22.1, 21.8];
RHi = 0.1:0.01:1;
vq1 = interp1(RH, T_top, RHi);
vq2 = interp1(RH, T_low, RHi);
t = [RHi; vq1; vq2];
indx = round(1 + (Hum - 0.1) / 0.01);
T_high = t(2, indx);
T_low = t(3, indx);
end

```

Energy Modeling for Early-stage Net Zero Energy House

CE295 Energy Systems and Control, Professor Moura Scott

Team 15: Jiaqi Cui, Jieyu Cui, Ruinan Xu, Yanis Pradeau

System Engineering, Department of Civil and Environmental Engineering

Jing Yuan, Zhirong Lin

Center of Built Environment, Department of Architecture

Abstract

While global warming threatens the future of Humanity, the key could be the emergence of energy-efficient strategies in buildings. This project will build a simplified model of Net Zero Energy Buildings (NZEBS) to determine suitable net zero design strategy in the early design phase of a studied building. Our work will be based on a simplified house model with an electricity, heating, and cooling system. A single room will be analyzed with solar panel, radiant system, and heat pump. For the solar panel, nonlinear equation systems will be solved to determine the voltage cell maximizing the power generated. Optimization using CVXY package will be conducted to find the minimum areas of solar panel for our zero-energy system. Hourly Analysis Program (HAP) will generate annual energy consumption for our validation process. The result of this study will provide guidance about net zero design strategy in the early design phase of our simplified model.

Table of Contents

<i>Abstract</i>	- 2 -
<i>1. Motivation & Background</i>	- 4 -
<i>2. Literature Review</i>	- 4 -
2.1 Building energy modelling	- 4 -
2.2 Photovoltaic power generation modelling.....	- 5 -
2.3 Heat Pump model	- 5 -
2.4 HVAC system Modelling	- 6 -
<i>3. Focus of this Study</i>	- 7 -
<i>4. Technical Description</i>	- 7 -
4.1 System determination	- 7 -
4.2 House model.....	- 8 -
4.3 Weather data	- 10 -
4.4 Solar Panel.....	- 11 -
4.5 Thermal model.....	- 12 -
4.6 Optimization	- 12 -
<i>5. Result</i>	- 13 -
5.1 Annual Solar Power Generation	- 13 -
5.2 Total Area of PV Panel	- 13 -
5.3 Validation.....	- 14 -
<i>6. Discussion & Limitation</i>	- 15 -
6.1 Generalizability/Application.....	- 15 -
6.2 Limitations	- 15 -
<i>7. Table of Responsibilities</i>	- 16 -
<i>8. Summary</i>	- 17 -
<i>Reference</i>	- 18 -
<i>Appendix</i>	- 20 -
Appendix 1: Variable list.....	- 20 -
Appendix 2: Code for Solar Panel.....	- 23 -
Appendix 3: Code for Optimization	- 25 -
Appendix 4: Feedback from Presentation	- 28 -

1. Motivation & Background

Nowadays, global warming has become one of the most important challenges of our society. Based on the Intergovernmental Panel on Climate Change (IPCC), if the production of greenhouse gas is maintained, the global temperature would rise by 2°C (Mann, 2018). If it happens, we would pass a “tipping point” that we could not compensate even by reducing our emission afterward, and global changes would happen (Hoegh-Guldberg, 2018). As 40% of greenhouse gas comes from buildings, we understand the necessity to implement energy-efficient strategies (WGBC, 2018). A concept, known as Net Zero Energy Building (NZEB), has evolved from research to reality for this purpose. NZEB is a building producing as much energy as it uses over the course of the year (Torcellini, et al., 2016).

Net Zero Energy Buildings (NZEB) is becoming more and more feasible with the ameliorations of construction technologies and renewable energies. However, modeling NZEB is complex, costly, and tedious. NZEBs need a performance-based design process including passive building design, energy installations, and HVAC solutions considered during the early phase design. Evaluating different design combinations and parameters based on their performance creates high complexity. High uncertainty of decision-making, complexity of combining passive and active systems, and lack of high-level software package make NZEB modeling even more challenging. We want to build a simplified model to balance energy consumption with on-site energy generation, and find the adequate net zero design strategy in the early design phase of a building.

Our team is comprised of students from system engineering, who are capable of designing and managing complex systems over their life cycles, and students from building science as well, who could offer insightful knowledge of building system operation and design strategies. Even though the diverse background between team members, we share the interests of applying sustainable strategies to improve the performances of building through the way of both system controlling and designing.

2. Literature Review

2.1 Building energy modelling

Many researches have been conducted in the past few decades in terms of mathematical models for intelligent buildings, and physical and empirical are two types of building modeling approaches that are commonly used (Estrada-Flores et al., 2006). Physical model is also wildly defied as white box model based on known principles and equations to predict the whole building behaviors. All component characteristics namely building facilities, structural details and building systems will be considered as inputs to generate outputs such as energy consumption or indoor comfort (Li and Wen, 2014). Many software in the market have already been well developed in terms of predict and analysis energy flow for building control purpose, and Energy Plus, ESP-r and TRNSYS are those which are commonly used (Crawley, et al., 2008). However, detailed structure specification and time-consuming calculation are two main considerations for doing white box model analysis (Li and Wen, 2014). Using data driven model to build relationship between data and energy consumption could be more time efficient compared to pure physical model. In the study of Yun et al.(2012), they develop a fourth order Autoregressive with exogenous model (ARX) to simulate the overall building thermal load. However, black box model is more sensitive to provided data,

meaning significant error might occur with inadequate training data. A third model, Gray box model, therefore, has been introduced, combining simplified physical demonstration of building components with coefficients obtained from the training data to predict building behavior (Li and Wen, 2014). For example, Braun (1990) proposed a Resistance and capacitance network (RC) in his study in 1990 to capture the thermal network for a whole building. In his model, thermal capacitance and thermal resistance between building envelope and indoor objects are represented by capacitors and resistors between each node. 3R2C model (3 resistances and 2 capacitances) is used for envelope while 2R2C (2 resistances and 2 capacitances) is used for indoor mass (Wang and Xu, 2006) due to different sensitivities on external climate changes of these two components.

An entire building system is consisted of different subsystems, such as photovoltaic system to generate power required, HPAC system and Heat Pump System to control indoor temperatures in a comfort range.

2.2 Photovoltaic power generation modelling

Multiple studies are focusing the PV panel model, aiming at maximizing the power generation efficiency to reduce the power consumption and costs. The key principles for the current generated are Kirchhoffs Voltage and Current Law which is mostly cited in the field.

King, Boyson and Kratochvil (2003) summarized a model to capture the behavior of solar panel and in their study, the output current was expressed as

$$I_p = MI_I - MI_o \left[\exp\left(\frac{q(NV + (I_p R_s N/M))}{NAK T_p}\right) - 1 \right] - \left[\frac{NV + (I_p R_s N/M)}{NR_s N/M} \right]$$

Showing the final output depends on the number of modules in both parallel and series string, diode properties and properties for the existing system condition.

Scott and Chang (2013) used a more accurate model taking the solar radiation and outside temperature into consideration, and in their model, the output current is expressed as

$$I = I_{sc} - I_0 \left[\exp\left(\frac{qV_d}{AkT}\right) - 1 \right] - \frac{V_d}{R_p}$$

$$I_0 = I_{0,r} \left(\frac{T}{T_r} \right)^3 \exp\left[\frac{qE_{Si}}{Ak} \left(\frac{1}{T_r} - \frac{1}{T} \right)\right]$$

2.3 Heat Pump model

Heat pump is an energy-efficient method to manage and control the inner building temperature with respect to the adjusting outside environmental climates. In general, there are three types of heat pump: air source heat pump, ground source heat pump and geothermal heat pump. After comparing these three types, we decide to focus on the ground source heat pump.

There are two qualitative models of the system in question exemplifying two different levels of complexity (Madani, et al., 2011). In the first level of complexity, all the component models are black box models inter-connected via certain inputs and outputs, e.g., fluid flow, or energy flow. We do not need to know what happens inside of any of the system components. Our only concern is how the system behaves due to a change in input/output. A typical black box model of the heat pump system could be based on test data expressed as polynomials based on EN14511 (BSI, 2007)

or other test standards, for example, the COP formulas. COP is the ratio of the output heat and the work done by the heat pump (Dincer and Rosen, 2013) as shown in the equation below

$$COP = \frac{Q_{output}}{W}$$

which captures the heat pump efficiency well. This coefficient varies with different heat pump sources, and for ground water heat pump, the coefficients is normally between 3-5.

Using such a model together with an elaborate calibration with test data may be quite good at predicting performance of a well-defined system. The model could be as simple as a constant temperature or an equation describing how the temperature in the ground changes over the year, for example on an hourly basis.

In the second level of complexity, the more detailed model of the heat pump unit includes new submodels of the condenser, evaporator, compressor, and expansion valve systems taking the thermo-physical behavior of the working fluid into consideration. For example, the evaporator part can be modeled as:

$$\begin{aligned}\dot{Q}_{total,evap} &= \dot{Q}_{evap} + \dot{Q}_{superheat} \\ \dot{Q}_{evaporation} &= \dot{Q}_{water} = \dot{m}_{water} \times c_{water} \times (T_{water,mid} - T_{water,out}) \\ \dot{Q}_{ref} &= \dot{m}_{ref} \times c_{ref} \times (T_{ref,dew} - T_{ref,bubble}) \\ \dot{Q}_{superheat} &= \dot{Q}_{water} = \dot{m}_{water} \times c_{water} \times (T_{water,in} - T_{water,mid}) \\ \dot{Q}_{ref} &= \dot{m}_{ref} \times c_{ref} \times (T_{ref,out} - T_{ref,dew}) \\ W_{comp} &= \frac{\dot{m}_{ref}}{\eta_{comp}} \left[\frac{k}{k-1} \right] \frac{P+s}{\rho_{ref,s}} \left[\left(\frac{P_d}{P_s} \right)^{k-1/k} - 1 \right] \\ \dot{m}_{ref} &= V_{dis} \rho_{ref,s} Hz \times \eta_{vol} / 10^6 \text{ (kg/s)}\end{aligned}$$

Although the mathematical models are quite accurate, those equations are extremely complicated and require a deep understanding on the mechanical working principles. Additionally, based on these formulas shown above, to solve the heat pump system problem becomes more difficult, because the system objective function is not convex. Therefore, instead of white box, treating the while heat pump system as a black box is more appropriate in this project.

2.4 HVAC system Modelling

HVAC is a model to simulate the heating, ventilation and air conditioning process in a building system. To understand the model of HVAC is a key for building designers and constructors. Foundation of the HVAV system is the heat conduction equation, which is been mostly referred, showing the relationship between change in heat and temperature (Homod, 2013). To alleviate the complexity of the whole HVAV model, sub-model is always needed (Agachi. et al., 2006) by separate the system into different heat generation and transformation processes. The most commonly used model is to balance the heats through labs, the opaque fabric, and the heat transfer between internal surfaces and the room air. And in 1970s, Stephenson and Mitalas (1971) develop a new response factor method, improve the accuracy of the model. And in 1980s, more complicated and rigorous methods were developed such as transient models. Based on the research done by

Woolley and Dennis (2016), the HVAC system are divided into 4 processed as Wall isolation, AC duct, Air inlet and the impact of indoor residents, balancing heats form room air, component surfaces, and outsides, which is the key reference in this project to model this system.

For our Net Zero Energy Building, empirical models may be the better choice as these models are dynamic, uncertainty and time dependent. In order to represent human behavior, models such as neural networks, expert systems, genetic algorithm and fuzzy logic are efficient (Lu, Derek and Martti, 2009). Considering the complexity of Net Zero Energy Building, our model is most likely to be non-linear instead of linear. As for non-linear models, the equations that describe the system are sensitive to the initial starting behavior conditions. For two slightly different initial sets, their states may quickly diverge (Howe and Lewis, 2005). Ríos-Moreno et al. (2007) identified non-linear behaviors of indoor temperature variations for intelligent buildings, using outside air temperature, global solar radiation flux, outside air relative humidity and air velocity as the input variables, and predict the output (indoor temperature) efficiently.

3. Focus of this Study

In this project, our primary focus will be building up a simplified model for balancing the energy consumption and onsite energy generation of net zero energy buildings under the dynamic climate and consumption situation. We aim to use this model to determine the appropriate net zero design strategy in the early design phase of a target building.

4. Technical Description

4.1 System determination

For this project we used a simplified house modeling with electricity system as well as heating and cooling system. Given the fact that heating and cooling is the largest energy consumption units, we only model heat transfer and ignore other systems, such as lighting and plug-in equipment load. Detailed information of the system refers to **Figure 0-1**.

Electricity system includes solar panel. Moreover, we also used the public power grid to balance the electricity generation of solar panel. Because, solar panel can only generate electricity during the daytime and extra electricity might be generated under higher solar radiance, under this circumstance, grid will offer power during night or cloudy day and take in extra electricity generated from the solar panel. Heating and cooling system of our model includes the ground source heat pump and radiant heating and cooling system. In our system, we used vertical heat pump, which will use the phase change of refrigerant to transfer heat from the groundwater. And we only used floor radiant systems for both heating and cooling, the floor system will heat up the room during cold days and take in heats during hot weather by changing the temperature of the water inside the under-floor pipes. However, heat pump cannot always satisfy residents' heating and cooling demand under extreme weather, we also considered other source of electrical heating in our system.

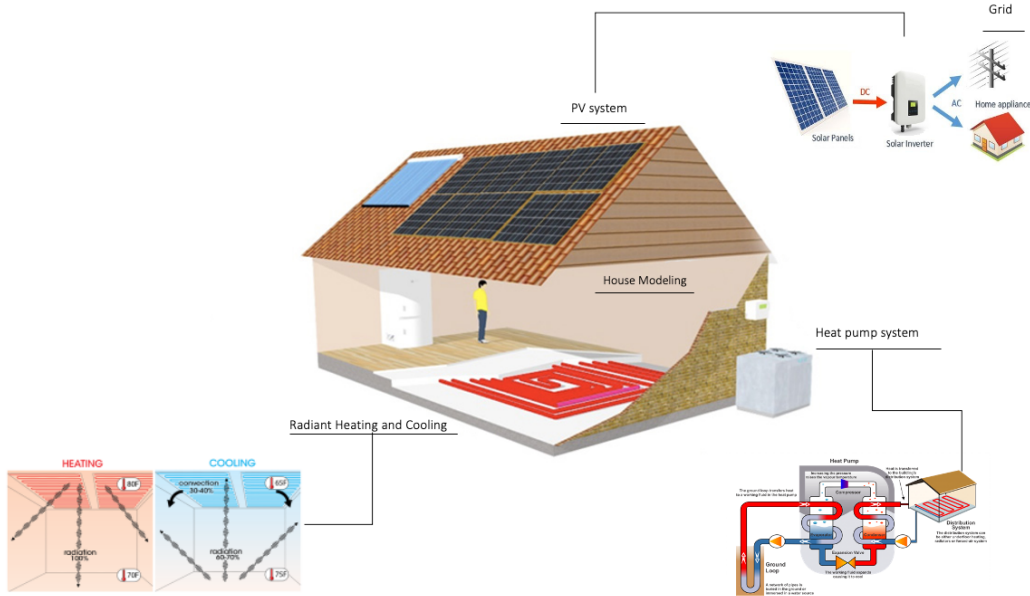


Figure 0-1: System Composition

4.2 House model

A single room house is used for mathematical modeling. Room geometry and material property can be found in **Figure 0-2** and **Table 1**. The house is 8 meters by 6 meters large with the height of 3 meters. There are two windows on the north and south wall in the dimension of 3 meters by 2 meters. Solar power systems located on the top of the roof, radiant system in the slab under the floor and heat pump mounted outside of the house.

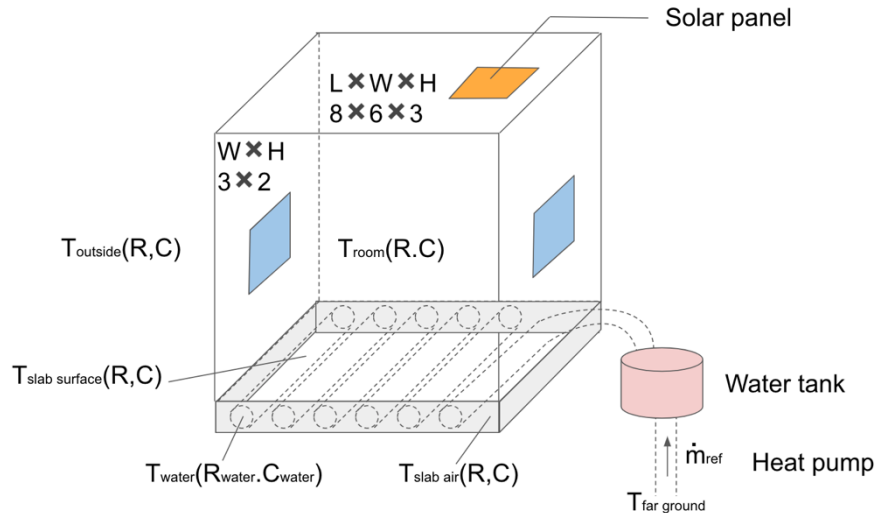


Figure 0-2:House Model

Table 1: House Model Parameter

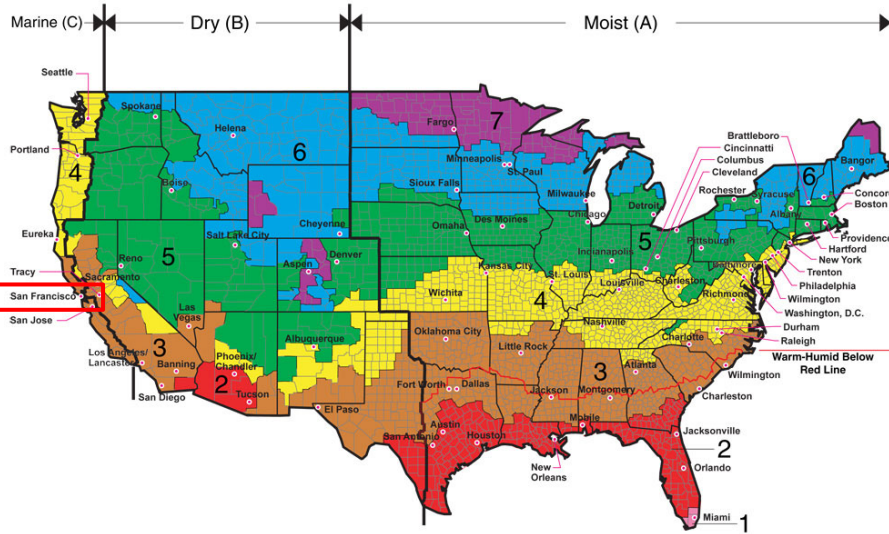


Figure 0-3: ASHRAE 90.1 Climate Zone Classification

Variable	Value	Unit	Description
L	8	meter	Length of the house
W	6	meter	Width of the house
H	3	meter	Height from ceiling to floor
L_w	3	meter	Window-width
W_w	2	meter	Window-length
N_w	2	count	Number of windows
H_s	0.3	meter	Height of the slab

This house locates in San Francisco, CA, which is classified by ASHARE as Zone 3, Marine Climate (C) (Figure 0-3).

To improve the credibility of our mathematic model, material is carefully selected to meet the minimum requirement of ASHRAE 90.1 and Title 24. In our simplified model, we consider exterior wall, window, slab on grade with radiant floor and radiant tubing. The parameter can be found in **Table 2**.

Table 2: Material Parameter

Type of Material	Thickness (mm)	Radius (mm)	R-Value (m ² ·°K/W)	U-Value (W/m ² ·°K)	SHGC	Thermal Conductivity (W/m·°K)
Wood stud wall, R-13 batt	146.0500	-	2.2964	0.4355	-	-
Window (Double Low E)	21.59	-	-	1.393	0.469	-
Slab on Grade with Radiant Floor	153.4	-	2.6416	0.3786	-	-

Roof (R-30)	-	-	5.2833	0.189	-	-
Tubing (PEX) @ 60 C	-	31.75	0.010567	94.634	-	0.429

4.3 Weather data

Geothermal resources in California are diverse in character and distributed and the state possesses the nation's largest high temperature geothermal resource base. California also can maximize its low temperature geothermal resources which can be used by geothermal heat pump (GHP) systems to heat and cool building spaces. The ground temperature of San Francisco maintains a nearly constant temperature around 56°F year-round.

Besides, San Francisco has an average monthly Global Horizontal Irradiance (GHI) of 4.35 kilowatt hours per square meter per day (kWh/m²/day), which is approximately 7% greater than the average monthly Direct Normal Irradiance (DNI) of 4.05 kWh/m²/day (**Figure x**). Moreover, the renewable energy policy is positive in Californian. And California became the first state to require all new homes to have solar power.

All the evidence shows that San Francisco should be a perfect location to build up a zero energy house from both weather and policy aspects.

In our modeling, we will use weather data downloaded from the United States Environmental Protection Agency (EPA). The monthly average diurnal global horizontal radiance and diurnal direct radiance are shown in **Figure 0-4**. Radiance value will be used for solar panel calculation and window heat loss calculation.

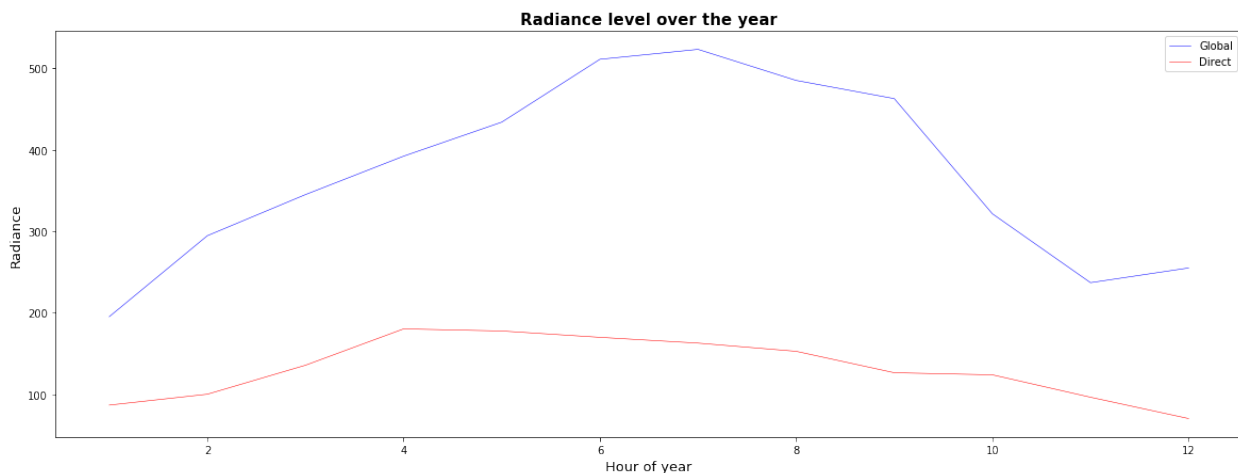


Figure 0-4: Monthly Solar Radiance

The hourly average ambient dry bulb temperature is shown in the **Figure 0-5**. We will use the outside temperature for the heat transfer modeling. The monthly average temperature of San Francisco ranges between 5°C ~ 25°C.

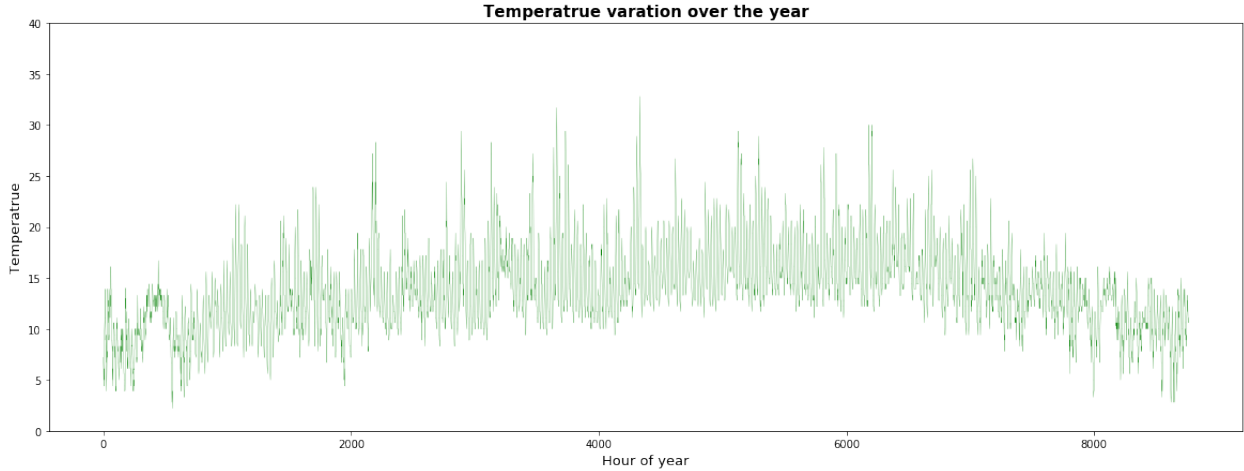


Figure 0-5: Annual Temperature level in San Francisco(°C)

4.4 Solar Panel

$$V_d = V_{cell} + IR_s \quad (1)$$

$$I = I_{sc} - I_0 \left[\exp\left(\frac{qV_d}{AkT}\right) - 1 \right] - \frac{V_d}{R_p} \quad (2)$$

$$I_{sc} = [I_{sc,r} + k_I(T - T_r)] \frac{S}{1000} \quad (3)$$

$$I_0 = I_{0,r} \left(\frac{T}{T_r} \right)^3 \exp\left[\frac{qE_{Si}}{Ak} \left(\frac{1}{T_r} - \frac{1}{T} \right)\right] \quad (4)$$

$$V_{pv} = n_{cell} V_{cell} \quad (5)$$

The first two equations are Kirchhoffs Voltage Law and Kirchhoffs Current Law.

The third equation implies that the current source is a function of temperature T and solar irradiance S.

The fourth equation is to model diode. The current flowing through the diode is related to the temperature.

By plugging the third and fourth equations into the first two equations, and controlling input V_{cell} we can solve this nonlinear equation systems to find voltage of cell that maximize power generated by that cell. This model is parameterized by temperature T and solar irradiance S.

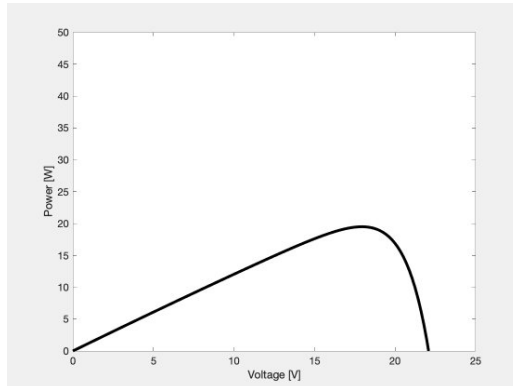


Figure 0-6: Power generate by one cell by controlling voltage

Figure above shows how we control V_{cell} to maximize power of that cell, for given temperature and solar irradiance. And once we know the maximum power, we can assume that the power of this cell is the maximum power. Since we have voltage and current of one cell, we can compute power generated by that cell. And the total power generated by the solar panel is just the number of cells times power generated by one cell.

4.5 Thermal model

Our thermal was made based on the Newton Cooling Law and Energy Conservation law:

$$Q_{water} = \frac{1}{R_{slabair-water}}(T_{slabair} - T_{water}) - COP \times P_{heatpump} \quad (6)$$

$$Q_{slabair} = \frac{1}{R_{slabsurface-slabair}}(T_{slabsurface} - T_{slabair}) - \frac{1}{R_{slabair-water}}(T_{water} - T_{slabair}) \quad (7)$$

$$Q_{slabsurface} = \frac{1}{R_{room-slabsurface}}(T_{room} - T_{slabsurface}) - \frac{1}{R_{slabsurface-slabair}}(T_{slabsurface} - T_{slabair}) \quad (8)$$

$$\begin{aligned} Q_{room} = & \frac{1}{R_{outside-room}}(T_{outside} - T_{room}) \times \frac{A_{wall}}{A_{all}} - \frac{1}{R_{room-slabsurface}}(T_{room} - T_{slabsurface}) \\ & + \frac{A_{window}}{A_{all}} \times U(T_{outside} - T_{room}) + F_{solar-room} Q_{solar_HG} + P_{ele-need} \times \eta \end{aligned} \quad (9)$$

$$Q_i = C_i \times \frac{T_i - T_{i-1}}{dt} \quad (10)$$

4.6 Optimization

In order to achieve zero energy, we need to make sure that the power generated by the PV panel can supply the house by offering electricity for heat pump compressor and the electrical heating/cooling system. The goal of this optimization is to determine the number of square meter (n) solar panel we need for this system. objective function and constraints are listed below. In the meantime, we limited the maximum power operation of heat pump and room temperature.

The objective function is linear as well as constraint. We will use CVXPY package to solve the problem and get the minimum areas of solar panel we need for this zero-energy house system. This problem is considered as a time series problem, because current temperature is highly related to the past hours' temperature. We use 1 hour lag-effect during the optimization.

1) Objective function: *Minimize (n)*

2) Constraints:

◊ Inequality constrains:

$$n \geq 0$$

$$nP_{electricityPV} \geq \sum(P_{ele-need}) + \sum(P_{heat-pump})$$

$$P_{max} \geq P_{heat-pump} \geq 0$$

$$22 \geq T_{room} \geq 19$$

$$n \geq 0$$

$$MSE = \frac{1}{n} \sum_{i=1}^n (y_i - \hat{y}_i)^2$$

◊ Equality constrains:

1) Thermal energy model

$$\begin{aligned}
 Q_{water} &= \frac{1}{R_{slabair-water}}(T_{slabair} - T_{water}) - COP \times P_{heatpump} \\
 Q_{slabair} &= \frac{1}{R_{slabsurface-slabair}}(T_{slabsurface} - T_{slabair}) - \frac{1}{R_{slabair-water}}(T_{water} - T_{slabair}) \\
 Q_{slabsurface} &= \frac{1}{R_{room-slabsurface}}(T_{room} - T_{slabssurface}) - \frac{1}{R_{slabsurface-slabair}}(T_{slabsurface} - T_{slabair}) \\
 Q_{room} &= \frac{1}{R_{outside-room}}(T_{outside} - T_{room}) \times \frac{A_{wall}}{A_{all}} - \frac{1}{R_{room-slabsurface}}(T_{room} - T_{slabsurface}) \\
 &\quad + \frac{A_{window}}{A_{all}} \times U(T_{outside} - T_{room}) + F_{solar-room}Q_{solar_HG} + P_{ele-need} \times \eta \\
 Q_i &= C_i \times \frac{T_i - T_{i-1}}{dt}
 \end{aligned}$$

2) Solar PV model

$$\begin{aligned}
 V_d &= V_{cell} + IR_s \\
 I &= I_{sc} - I_0[\exp(\frac{qV_d}{AkT}) - 1] - \frac{V_d}{R_p} \\
 I_{sc} &= [I_{sc,r} + k_I(T - T_r)]\frac{S}{1000} \\
 I_0 &= I_{0,r}(\frac{T}{T_r})^3 \exp[\frac{qE_{Si}}{Ak}(\frac{1}{T_r} - \frac{1}{T})] \\
 V_{pv} &= n_{cell}V_{cell}
 \end{aligned}$$

5. Result

5.1 Annual Solar Power Generation

After calculation using MATLAB and whole year weather data of San Francisco, we found that one cell can produce 1.79KW·h electricity per year.

5.2 Total Area of PV Panel

After optimization, the final area needed for Solar panel is 38 m² which is smaller than the total roof area, 48 m². Then we also visualized the hourly temperature changes over the year for water temperature, slab air temperature, room temperature and outside temperature (Figure 0-7).

First of all, we could read that cooling is merely needed for this house, only a short period of time during September need cooling. Moreover, at the beginning of the year and the end of the year, the outdoor temperature is lower than the indoor set point, thus heating is needed during these time period. In this system, water in the pipe has the highest temperature followed with slab air temperature, slab surface temperature and room temperature.

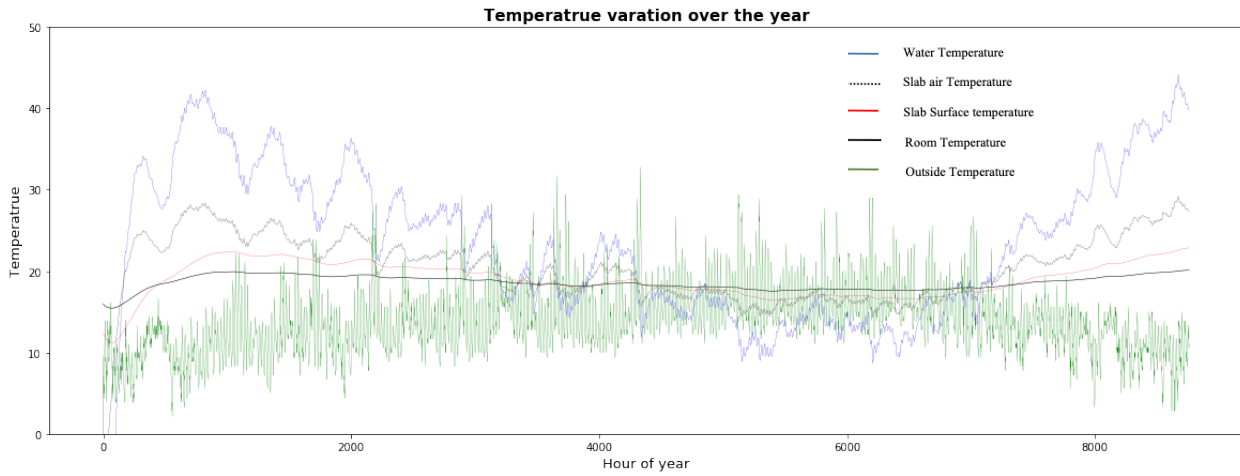


Figure 0-7: Medium Temperature Variation over the Year

5.3 Validation

Hourly Analysis Program (HAP) is an energy simulation tool widely used in North America. It is designed for consulting engineers, design/build contractors, HVAC contractors, facility engineers and other professionals involved in the design and analysis of building HVAC systems. It has capability to design system and size system component.

We use HAP to generate annual energy consumption for our validation process with the limitation that we do not have real data in world. The HAP model has the same parameter as our simplified house model, weather data, system and sizing. **Figure 0-8** Below is the visualized hourly energy consumption over the year for both HAP modeling and our mathematic model.

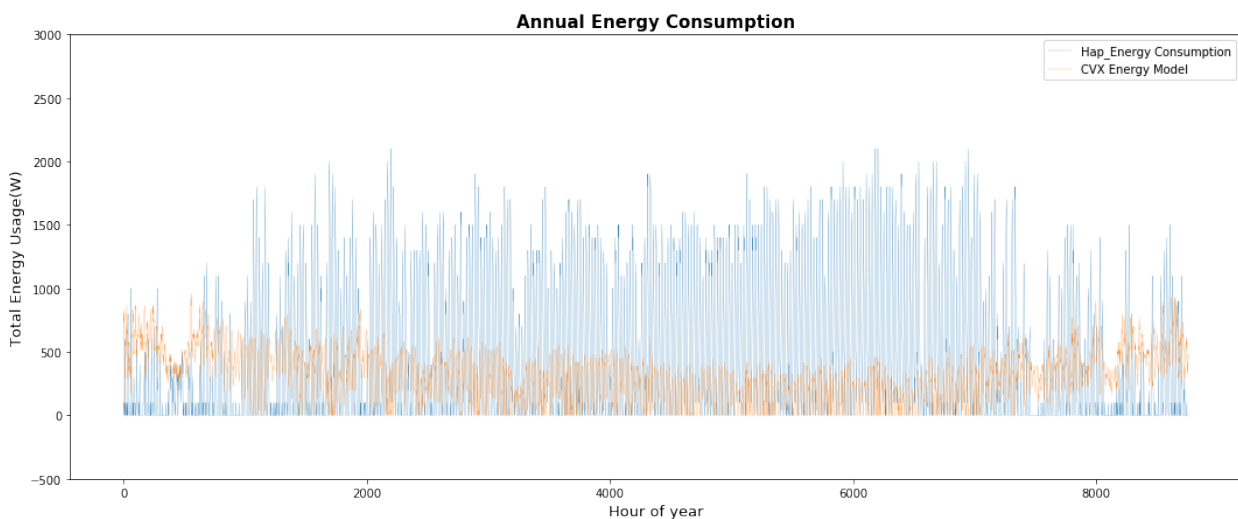


Figure 0-8: Annual Energy Consumption - HAP & Mathematic model

The output from HAP is considered as actual value. Mean Square Error(MSE) is the metric that we used for evaluation as the result of 680(W).

$$MSE = \frac{1}{n} \sum_{i=1}^n (y_i - \hat{y}_i)^2$$

Several possibilities can lead to the error:

- HAP is an energy simulation normally used for commercial building. Normally, commercial building has a large energy consumption per square foot than residential. With the extreme sizing offset, heat pump system used in HAP can utilize a larger scale energy than in residential house.
- We use $COP \times P_{heatpump}$ to conduct the heat pump energy consumption which may underestimate heap pump system
- The heat flow rate is assumed still within a unit hour in our mathematic model
- The HAP cannot implement radiant floor system which would increase energy usage.

6. Discussion & Limitation

Using the skills acquired in this class, our project helps to better understand how to build net zero buildings in the future. Given the limited time that we have, we adjusted the model to simplify the reality while keeping a good scope of the problem. We successfully optimized our model to minimize solar panel used. This work could be further improved by adding optimization variables for reducing the size, cost, and number of energy systems such as the heat pump.

6.1 Generalizability/Application

In current energy simulation market, there does not have an application is designed for residential building due to sizing. However, the residential community is a large-scope. One of our model applications it to build a residential housing energy simulation software after finalize our model and do further-step study on site data collecting. Secondly, our project motivation is using this mathematic model for engineers and designers on early-stage system selection. With the optimization result turned out, decision maker can easily determine whether or not the heat pump with radiant floor system could be an approach to achieve their Net Zero Energy goal.

6.2 Limitations

We do not include all the variables and phenomena that affect a real-world system. For the heating system, we do not take into account people and electronics. We also overlook the heating loss inside the water tank and consider an average temperature for the temperature from the ground. Additionally, in our mathematic model, we consider the energy loss between each direction of heat loos, such as between outdoor air and indoor air, and between group source and indoor air. Furthermore, we will think of applying actual heat pump model instead of simplifying it in Coefficient of Performance (COP). To make it more concise, loss between the convention solar energy to electricity need to be included.

Furthermore, our study was focus on a simplified model. A real-world house with multiple floors and rooms would have more complex heat transfer and convection, depending on the position of the heating and cooling source. In reality, houses have often multiple layers for the walls, slab, and roof. For more accuracy, we should also consider the orientation of the house, solar panels, and windows.

In addition, our model does not take into account economic factors. For example, we did not consider the cost of solar panels, since to generate more electricity we need more cells, which means higher costs. Furthermore, the cost of heat pump mainly depends on how deep we dig, which is positively correlated with how much heat we can get. And if the costs of solar panels and heat pump are extremely high, designing and maintaining a Net Zero Building may not be a wise choice.

With more time, we would have measured the sensitivity of our model for different scenarios taking into account the category of inhabitants (large family, single), and the period of the year (holidays). An interesting work for the future would be to consider various set-up with different energy production (wind, hydraulic, solar power), heating generation (wood heating, geothermal), cooling systems.

In general, our model can be applied to different sizes and locations of houses, with just simple changes of parameters such as numbers of solar panel cells and the size of the house. Based on the climate data of the location, we can use this model to tell if houses located there are able to be built as zero energy buildings.

7. Table of Responsibilities

Project Timeline					
Week	Phase	Task		Responsibility	Due Date
Week 1 2/1-2/7	Project Proposal	Project Topic Discussion		All Members	2/7/20
Week 2 2/8-2/14		Literature Review and Project Proposal		All Members	2/14/20
Week 3 2/15-2/21 to Week 6 3/7-3/13	Progress Report	Fundamental Model Build-up	HVAC System	Zhirong Lin & Jing Yuan	3/6/20
			Heat Pump System	Jiaqi Cui & Jieyu Cui	3/6/20
			Solar Radiation	Ruinan Xu & Yanis Pradeau	3/6/20
		Progress Report	Complete the report	All Members	3/13/20
		Optimization	Meet with Professor for comments	Zhirong Lin & Jingyuan	3/20/20
Week7 3/14-3/20			Group Updates and Discussion	All Members	
Week8 3/21-3/27			Battery Model Study	All Members	3/27/20
Week9 3/28-4/3			Union all systems together	All Members	4/4/20
Week10 3/24-4/10			Optimization strategies upon discussion	All Members	4/17/20
Week11 4/11-4/17					
Week12 4/18-4/24	Result Visualization	Conduct result visualized diagram & presentation material			4/24/20
Week12 4/25-5/1	In-Class Presentation	Conduct Presentation Materials		All Members	4/24/20
Week14 5/1-5/8	Final Report	Write final report		All Members	5/8/20

8. Summary

This project aimed at finding appropriate net zero design strategies in the early design phase of a simplified model. The model considered solar panel on the roof, radiant system in the slab under the floor, and heat pump outside. For a more accurate model, materials were chosen to fulfill the minimum requirement of ASHRAE 90.1 and Title 24. Weather data from the United States Environmental Protection Agency (EPA) was used for solar panel calculation, window heat loss calculation, and heat transfer modeling. Nonlinear equation systems determined the voltage of cell maximizing the generated power. A thermal model was defined as well. With CVXPY package, we optimized the number of square meter solar panel necessary. We found that one cell generated 1.79 KW.h electricity per year, and that a solar panel area of 38 m² was needed. We also found that the cooling system was only needed for September. Hourly Analysis Program (HAP) was used to simulate actual value of our model and compare it with our mathematical model.

Reference

- Agachi, Paul Ţerban. *Model Based Control : Case Studies in Process Engineering*. Wiley-VCH, 2006. *EBSCOhost*, search.ebscohost.com/login.aspx?direct=true&db=cat04202a&AN=ucb.b15334676&site=eds-live.
- Dincer, I. and Roson, M.A. "Chapter 7 - Exergy Analysis of Heat Pump Systems." *Exergy*, (2013): 101–113. *EBSCOhost*, doi:10.1016/B978-0-08-097089-9.00007-3.
- Drury B.Crawley , et al. "Contrasting the capabilities of building energy performance simulation programs" *Build and Environment* 43.4 (2008): 661-673
- EN14511, B. S. I. B. S. "Air conditioners, liquid chilling packages and heat pumps with electrically driven compressors for space heating and cooling" London: BSI (2007).
- Estrada-Flores, Silvia, et al. "Development and validation of "grey-box" models for refrigeration applications: A review of key concepts." *International Journal of Refrigeration* 29.6 (2006): 931-946.
- Hoegh-Guldberg, O.; Jacob, D.; Taylor, M.; Bind, M.; et al. "Chapter 3: Impacts of 1.5°C Global Warming on Natural and Human Systems"(PDF). *IPCC SR15 2018*. (2018):175–311
- Homod, Raad.Z. "Review on the HVAC System Modeling Types and the Shortcomings of Their Application". *Journal of Energy*, 2013(2013), *EBSCOhost*, doi:10.1155/2013/768632.
- Howe, Mark L., and Marc D. Lewis. "The importance of dynamic systems approaches for understanding development." *Developmental Review* 25.3-4 (2005): 247-251.
- James E. Braun "Reducing energy costs and peak electrical demand through optimal control of building thermal storage" *ASHRAE Trans*, 96.2 (1990): 876-888
- King, W.E., Botson, W.E. and Kratochcil J.A. "Photovoltaic Array Performance Model" *Sandia National Laboratories*. Albuquerque, New Mexico (2003)
- Kyungtae. Yun, et al. "Building hourly thermal load prediction using an indexed ARX model" *Energy and Buildings* 54.0 (2012): 225-233
- Lu, Xiaoshu, Derek Clements-Croome, and Martti Viljanen. "Past, present and future mathematical models for buildings: focus on intelligent buildings (part 1)." *Intelligent Buildings International* 1.1 (2009): 23-38.
- Madani, Hatef, Joachim Claesson, and Per Lundqvist. "Capacity control in ground source heat pump systems: Part I: modeling and simulation." *International Journal of Refrigeration* 34.6 (2011): 1338-1347.
- Mann, M.E.. "Earth Will Cross the Climate Danger Threshold by 2036." *Scientific American*, Scientific American, 1 Apr. 2014, www.scientificamerican.com/article/earth-will-cross-the-climate-danger-threshold-by-2036/.
- Moura, S. J., and Y. A. Chang. "Lyapunov-Based Switched Extremum Seeking for Photovoltaic Power Maximization." *Control Engineering Practice*, 21.7(2013): 971-980 *EBSCOhost*, doi:DOI: 10.1016/j.conengprac.2013.02.009.
- Torcellini,P. et al.(2016) "Zero Energy Buildings: A Critical Look at the Definition" *National Renewable Energy Laboratory Report* June, (2006).
- Ríos-Moreno, G. J., et al. "Modelling temperature in intelligent buildings by means of autoregressive models." *Automation in construction* 16.5 (2007): 713-722.
- Shengwei. Wang and Xinhua. Xu "Simplified building model for transient thermal performance estimation using GA-based parameter identification" *International Journal Thermal Science*, 45.4 (2006): 419-432
- Wang, X. Li and Jin, Wen. "Review of building energy modeling for control and operation." *Renewable and Sustainable Energy Reviews*, 37 (2014):517-537

WGBC. "World Green Building Council Calls on Companies Across the World to Make Their Buildings Net Zero Carbon." *World Green Building Council*: (2018),
www.worldgbc.org/news-media/world-green-building-council-calls-companies-across-world-make-their-buildings-net-zero.

Woolley, J. and Dennis,A. "Control of Radiant Cooling Systems for the Honda Smart Home"
Unpublished CE295 report (2016)

Appendix

Appendix 1: Variable list

The definition of variables/parameters were used in the optimization process shown in **Table x**.

Table x: Variable and Parameter used in Mathematical Model

Variable/Parameter	Value	Unit	Description
Q_{water}	Optimize	W	Heat loss of water
$Q_{slabair}$	Optimize	W	Heat loss of the air in the slab
$Q_{slabsurface}$	Optimize	W	Heat loss of slab surface
Q_{room}	Optimize	W	Heat loss of air in the room
T_{water}	Optimize	°C	Water temperature
$T_{slabair}$	Optimize	°C	Slab air temperature
$T_{slabsurface}$	Optimize	°C	Slab surface temperature
T_{room}	Optimize	°C	Water temperature
$T_{outside}$	Data provided	°C	Ambient temperature
C_{water}	1.2×10^7	J/K	Thermal capacity of water in the pipe
$C_{slabair}$	1.9×10^4	J/K	Thermal capacity of air in the slab
$C_{slabsurface}$	3.0×10^7	J/K	Thermal capacity of slabsurface
C_{room}	1.9×10^5	J/K	Thermal capacity of water in the pipe
$R_{water-slabair}$	0.0106	(m ² • °K/W)	Thermal resistance between the water inside the pip and the air in the slab
$R_{slabair-slabsurface}$	2.6416	(m ² • °K/W)	Thermal resistance between the air in the slab and the surface of the slab
$R_{slabsurface-room}$	3.0000	(m ² • °K/W)	Thermal resistance between the air on the surface of the slab and the air in the room
$R_{room-outside}$	2.2964	(m ² • °K/W)	Thermal resistance between the indoor and outdoor air
A_{wall}	58	m ²	Total surface area of the wall
A_{window}	12	m ²	Total surface area of the window
A_{roof}	48	m ²	Total surface area of the roof

Variable/Parameter	Value	Unit	Description
A_{all}	132	m ²	Total surface area of the house
$V_{water-pip}$	2.88	m ³	Total volume of the water pip
$V_{slabair}$	14.4	m ³	Total volume of the air within the slab
$V_{slabsurface}$	7.2	m ³	Total volume of the slab
V_{room}	144	m ³	Total volume of the room
$P_{ele-need}$	Optimize	W	Extra heating or cooling needed to compensate for the heat pump
Q_{solar}	Data provided	W	Global Solar radiance
$F_{soalr-room}$	0.8	%	The efficiency of transfer solar heat into the room through window.
η	0.8	%	The efficiency of transfer electricity to heat
COP _{heating}	3.5	constant	The Coefficient of performance or COP of a heat pump is a ratio of useful heating or cooling provided to work required.
COP _{cooling}	2.5	constant	The Coefficient of performance or COP of a heat pump is a ratio of useful heating or cooling provided to work required.
V_d	Unknown	V	Voltage of diode
V_{cell}	Controlable input	V	Voltage of cell
I	Unknown	A	Current in cell
I_{sc}	Unknown	A	Ideal current source
R_s	0.0009	Ω	Resistance of resistor
R_p	9	Ω	Resistance of diode
I_0	Unknown	A	Cell reverse saturation current
q	1.6e-19	C	Coulomb's constant
A	1.92	constant	Identity factor
k	1.38e-23	constant	Boltzmann's constant
$I_{sc,r}$	2.52	A	Cell short-circuit current at 28°C and 100mW/cm ²
k_I	0.0017	°C	Short-circuit current temperature coefficient at $I_{sc,r}$

Variable/Parameter	Value	Unit	Description
T_r	301.18	°K	Reference temperature
$I_{0,r}$	20e-6	A	Reverse saturation current at T_r
E_{Si}	1.11	eV	Band gap for silicon
n_{cell}	36	constant	Number of cells of single solar panel
V_{pv}	Unknown	V	Voltage of solar panel
T	Parameter	°K	Cell temperature
S	Parameter	W/ m ²	Solar irradiance

Appendix 2: Code for Solar Panel

Part 1: Function

```

%% I-V Characteristic Curve for PV Cell
% Created by Scott Moura on April 8, 2009

%Given V_cell determine V_d and I
function I = pv_iv(V,alpha,T)

x0 = [0.6; 1];
options = optimset('Display','off');
x = fsolve(@(x) pv_nonlin(x,V,alpha,T),x0,options);

I = x(2);

function F = pv_nonlin(x,V,alpha,T)

% Parameters
I_0r = 20e-6;
q = 1.6e-19;
k = 1.38e-23;
R_p = 9;
R_s = 0.0009;

T_r = 301.18;
A = 1.92;
E_Si = 1.11; %[eV]
I_sc = 2.52;
K_I = 0.0017;

lambda = alpha * 1e3;

%parameter in T;Two extra function
I_0s = I_0r * (T/T_r)^3 * exp((q*E_Si)/(A*k)*(1/T_r - 1/T));
I_lg = (I_sc + K_I * (T - T_r)) * lambda / 1000;
V_d = x(1);
I = x(2);

%V is V_cell; I_lg is I_sc; I_0s is I_0
F = zeros(2,1);
F(1) = V + I*R_s - V_d;
F(2) = I_lg - I_0s * (exp((q*V_d)/(A*k*T)) - 1) - V_d/R_p - I;

```

Part 2: Prediction

```

%%%
close;clear;clc;
% [month,day,hour,temp,irrad,a,b,c]= xlsread('hourly_solar.csv');
M=readtable('hourly_solar_new.csv');
M_data=table2array(M);
temp=M_data(:,4);
rad=M_data(:,6)*0.001;

V = (0:0.005:0.64)';
I = zeros(length(V),1);

% Operating Conditions
T_vec = 273 + temp;
alpha_vec = rad;

I_ = zeros(length(V),length(alpha_vec));
P_ = zeros(length(V),length(alpha_vec));
for idx = 1:length(alpha_vec)

    for k = 1:length(V)

        I_(k,idx) = pv_iv(V(k),alpha_vec(idx),T_vec(idx));
    end
end

```

```
end  
P(:,idx) = 36*V.*I(:,idx);  
end  
  
P_max=max(P_);  
%  
P_max=P_max';  
P_sum=sum(P_max);
```

Appendix 3: Code for Optimization

```

#!/usr/bin/env python
# coding: utf-8

## Zero Energy Building-CE 295 Final Project

# In[1]:


#CE295-Zero energy building-team 15
import numpy as np
import matplotlib.pyplot as plt
from cvxpy import *
get_ipython().run_line_magic('matplotlib', 'inline')
import pandas as pd
import math
from tqdm import tqdm_notebook as tqdm

#Read in Weather Data
weather = pd.read_csv("hourly_solar.csv")
weather.head(10)
#print(len(weather))

time=[]
for i in range(8760):time.append(i)
weather['Thour']=time
weather.head(10)

#constant value
P=1.7*1000/0.024 #156 mm * 156 mm=0.024m2
P_hp_max=1000
COP_h=3.5
COP_c=2.5
yita=0.8

#Thermal Resistance
R_wa=0.010567
R_as=2.6416
R_sr=3
R_ro=2.2964
R_roof=5.2833
C=1003 #J/kg.C
C_w=4186
pho=1.29#Kg/m3
pho_water=997 #kg/m3

Ca_w=C_w*pho_water*0.25*(0.31**2)*6*20
Ca_a=C*pho*6*8*0.3
Ca_s=C_w*pho_water*6*8*0.15
Ca_r=C*pho*6*8*3

>window
U=1.393
F=0.49*0.89*0.6

#AREA
V=3*6*8
A=6*3*2+8*3*2+6*8
A_roof=6*8
A_slab=A_roof
A_window=3*2*2
A_pip=0.31*3.1415*6*20

#Temperattrue
T_r=20
T_r_c=20
T_r_h=20

```

```

T_far=15.6
T_o=weather.iloc[:,3].tolist()
T_o_h=weather[weather["Dry Bulb Temp"]<T_r].iloc[:,3].tolist()
N_h=weather[weather["Dry Bulb Temp"]<T_r].iloc[:,1].tolist()
Q_solar_h=weather[weather["Dry Bulb Temp"]<T_r].iloc[:,4].tolist()
T_o_c=weather[weather["Dry Bulb Temp"]>T_r].iloc[:,3].tolist()
N_c=weather[weather["Dry Bulb Temp"]>T_r].iloc[:,1].tolist()
Q_solar_c=weather[weather["Dry Bulb Temp"]>T_r].iloc[:,4].tolist()

# Solve with CVXPY

# Define optimization vars
n = Variable(1)

P_need_h = Variable(len(T_o_h))
P_hp_h = Variable(len(T_o_h))
Q_hp_h = Variable(len(T_o_h))
Q_w_h = Variable(len(T_o_h))
Q_a_h = Variable(len(T_o_h))
Q_s_h = Variable(len(T_o_h))
Q_r_h = Variable(len(T_o_h))
T_w_h = Variable(len(T_o_h))
T_a_h = Variable(len(T_o_h))
T_s_h = Variable(len(T_o_h))
T_r_h = Variable(len(T_o_h))

P_need_c = Variable(len(T_o_c))
P_hp_c = Variable(len(T_o_c))
Q_hp_c = Variable(len(T_o_c))
Q_w_c = Variable(len(T_o_c))
Q_a_c = Variable(len(T_o_c))
Q_s_c = Variable(len(T_o_c))
Q_r_c = Variable(len(T_o_c))
T_w_c = Variable(len(T_o_c))
T_a_c = Variable(len(T_o_c))
T_s_c = Variable(len(T_o_c))
T_r_c = Variable(len(T_o_c))

# Define objective function
objective = Minimize(n)

# Define constraints
# Apparent Power Limits
constraints = [n>=0,n*p>=sum(P_need_h)+sum(P_need_c)+sum(P_hp_h)+sum(P_hp_c)]
# Balance power generation with power consumption
#constraints += [P_hp_h>=0,P_hp_h<=P_hp_max]
#constraints += [P_hp_c>=0,P_hp_c<=P_hp_max]
constraints += [P_need_h>=0,P_hp_h<=P_hp_max,Q_w_h>=0,Q_a_h>=0,Q_s_h>=0,Q_r_h>=0]
constraints += [P_need_c>=0,P_hp_c>=0,P_hp_c<=P_hp_max,Q_w_c>=0,Q_a_c>=0,Q_s_c>=0,Q_r_c>=0]
#constraints += [T_w_h>=30,T_w_h<=52]
#constraints += [T_w_c>=13,T_w_c<=21]
#constraints += [T_r_c>=19,T_r_c<=22,T_r_h>=22,T_r_h<=25]
#constraints += [T_w_h>=T_a_h,T_a_h>=T_s_h,T_s_h>=T_r_h]
#constraints += [T_w_c<=T_a_c,T_a_c<=T_s_c,T_s_c<=T_r_c]

# Loop over each node
for i in tqdm(range(len(T_o_h))):
    constraints +=[Q_hp_h[i]==COP_h*p_hp_h[i]]
    constraints +=[Q_w_h[i]==Q_hp_h[i]-R_wa*(T_w_h[i]-T_a_h[i])*A_pip]
    constraints +=[Q_a_h[i]==1/R_wa*(T_w_h[i]-T_a_h[i])*A_pip-1/R_as*(T_a_h[i]-T_s_h[i])*8*6]
    constraints +=[Q_s_h[i]==1/R_as*(T_a_h[i]-T_s_h[i])*8*6-1/R_sr*(T_s_h[i]-T_r_h)*8*6]
    #constraints +=[Q_r_h[i]==C*pho*8*6*3*(T_r_h-T_o_h[i])/3600]
    constraints +=[P_need_h[i]==Q_r_h[i]-1/R_as*(T_a_h[i]-T_s_h[i])*8*6-F*Q_solar_h[i]*A_window+1/R_ro*(T_r_h[i]-T_o_h[i])*(A_A_window-A_roof)+1/R_roof*(T_r_h-T_o_h[i])*(A_roof)+U*(T_r_h-T_o_h[i])*A_window]
    print("Constraint for heating: Loading finished")

for i in tqdm(range(len(T_o_c))):
    constraints +=[Q_hp_c[i]==COP_c*p_hp_c[i]]

```

```

constraints +=[Q_w_c[i]==Q_hp_c+1/R_wa*(T_w_c[i]-T_a_c[i])*A_pip]
constraints +=[Q_a_c[i]==-1/R_wa*(T_w_c[i]-T_a_c[i])*A_pip+1/R_as*(T_a_c[i]-T_s_c[i])*8*6]
constraints +=[Q_s_c[i]==-1/R_as*(T_a_c[i]-T_s_c[i])*8*6+1/R_sr*(T_s_c[i]-T_r_c)*8*6]
#constraints +=[Q_r_c[i]==-C*pho*8*6*3*(T_r_c-T_o_c[i])/3600]
constraints +=[P_need_c[i]==Q_r_c[i]+1/R_as*(T_a_h[i]-T_s_h[i])*8*6+F*Q_solar_c[i]*A_window-1/R_ro*(T_r_c[i]-T_o_c[i))*(A_A_window-A_roof)-1/R_roof*(T_r_c-T_o_c[i])*(A_roof)-U*(T_r_c-T_o_c[i])*A_window]
print("Constraint for cooling: Loading finished")

# Define problem and solve
prob = Problem(objective, constraints)
prob.solve(solver=SCS, verbose=True)

print(installed_solvers())

print("The number of solar panel needed:",n.value)

print(sum(P_need_h).value)
print(sum(P_need_c).value)
print(sum(P_hp_h).value)
print(sum(P_hp_c).value)
print(Q_r_c[i].value)
print(F*Q_solar_c[i]*A_window)

fig, ax = plt.subplots(figsize=(15,7))
T_a=np.full(len(weather),np.nan)
T_w=np.full(len(weather),np.nan)
T_s=np.full(len(weather),np.nan)
T_r=np.full(len(weather),np.nan)
for idx,i in enumerate(N_h):
    T_a[i]=T_a_h[idx].value
    T_w[i]=T_w_h[idx].value
    T_s[i]=T_s_h[idx].value
    T_r[i]=T_r_h[idx].value
for idx,i in enumerate(N_c):
    T_a[i]=T_a_c[idx].value
    T_w[i]=T_w_c[idx].value
    T_s[i]=T_s_c[idx].value
    T_r[i]=T_r_c[idx].value
#ax.plot(time,T_w,linewidth = 0.5,color="blue")
#ax.plot(time,T_a,linewidth = 0.5,color="red")
#ax.plot(time,T_s,linewidth = 0.5,color="green")
ax.plot(time,T_r,linewidth = 0,marker=".",color="black")
ax.plot(time,T_o,linewidth = 0,marker=".",color="green")
plt.xlabel('Hour of year',fontsize=13)
plt.ylabel('Temperattrue',fontsize=13)
plt.ylim((-50, 50))
plt.title('Temperattrue varation over the year',fontsize=15,fontweight='bold')
plt.show()

#weather
weather_summer=weather[(weather["month"]>=11)|(weather["month"]<=4)]
weather_winter=weather[(weather["month"]<11) & (weather["month"]>4)]
weather_winter.head(10)
T_r_w=20
T_r_s=25
T_o_h_s=weather[weather["Dry Bulb Temp"]<T_r_s].iloc[:,3].tolist()
N_h_s=weather[weather["Dry Bulb Temp"]<T_r_s].iloc[:,1].tolist()
Q_solar_h_s=weather[weather["Dry Bulb Temp"]<T_r_s].iloc[:,4].tolist()
T_o_c_s=weather[weather["Dry Bulb Temp"]>T_r_s].iloc[:,3].tolist()
N_c_s=weather[weather["Dry Bulb Temp"]>T_r_s].iloc[:,1].tolist()
Q_solar_c_s=weather[weather["Dry Bulb Temp"]>T_r_s].iloc[:,4].tolist()

```

Appendix 4: Feedback from Presentation

SM:

- Super-detailed modeling. It was difficult for the audience to absorb all the modeling details. It would have been wise to dedicate more time to the results and impact.

Audience:

- A good scope for a class project, simple enough for the time allowed and easy to follow.
- Impressive modeling!
- Good job! Just the model seems to be too ideal and doesn't consider the energy loss.
- Interesting modelling - If I understood correctly, the objective function aims at minimising solar panel used, I wonder if it could also take into account other optimization variables, like reducing size/cost/number (in MILP formulation) of other appliances/heat pump
- Great house model and well explained functions that been used
- Interested where you obtained Solar Irradiance data – if you get from, for example, PVWatts.com, the irradiance time series will account for avg weather/climate of some location. I think there is also an option to include shading/other effects
- Excellent presentation!
- Sounds like you have a good plan for next steps. Would really like to see some of this analysis bolstered by economic analysis and maybe cost minimization. Some sensitivity showing ranges of results would also be really interesting to see!
- Very specific setup, how does this apply more broadly? Generalizability? Nice job including limitations and discussion
- Very creative way of using CE 295 skills, this project left me pondering about how we could build net zero buildings in the future
- Motivation was explained well.
- Orientation of house/windows/solar generally plays a role in net-zero buildings to minimize heating/cooling and lighting needs, maximize solar- it would be interesting to look at that for a scenario analysis

- Interesting results and motivation, but presentation at times was getting too into the details.
- How sensitive is your model to the assumed demand of the home? I would guess that in real life it would be much more variable than what you assume here.
- Simple, concise slides - easy to follow
- Detailed physics!